Clinical Connections

Tapering TNFi to Withdrawal Compared With Continued TNFi Among Patients With RA

CORRESPONDENCE
Kaja E. Kjørholt, MD: kajakristianeeriksrud.kjorholt@diakonsyk.no

RA remission 12 months on stable treatment

M0 — M12 — M24 — M36

Stable dose TNFi

4-month half-dose TNFi, thereafter withdrawal of TNFi

Flare-free survival (%) vs Months

Time of withdrawal

Stable TNFi
Tapering TNFi

Hazard ratio (95% CI): 9.4 (3.9–22.8)
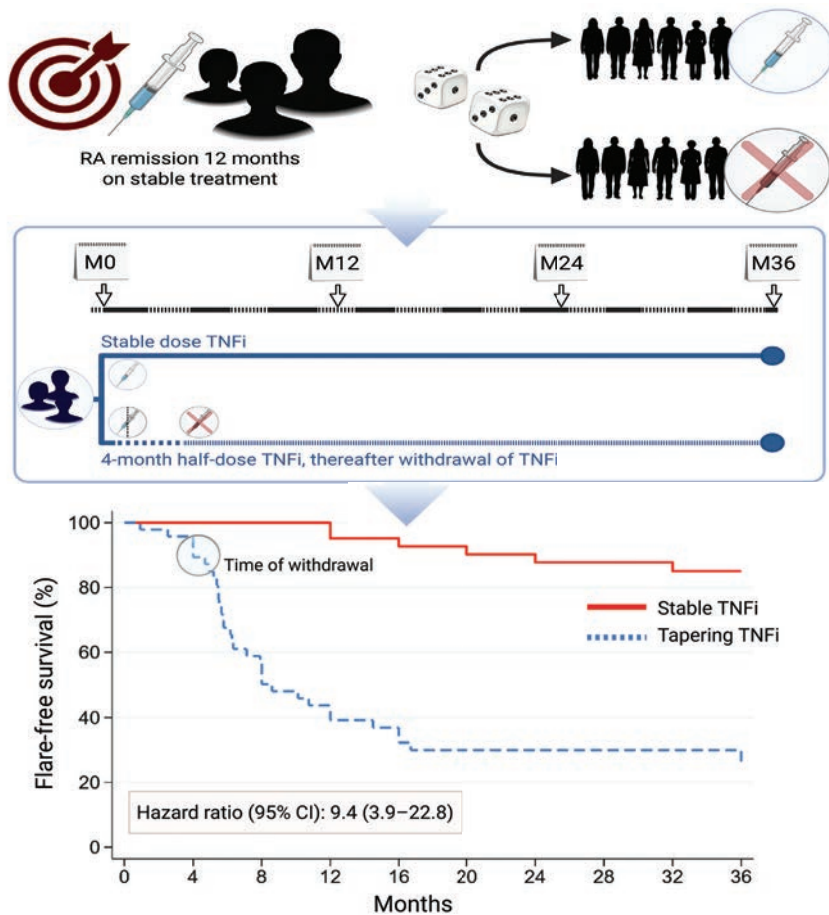
SUMMARY

The ARCTIC REWIND study investigated whether patients with rheumatoid arthritis (RA) in sustained remission for at least 12 months could safely taper and discontinue tumor necrosis factor inhibitor (TNFi) therapy compared with continuing stable TNFi therapy. The main outcomes were disease flares and radiographic joint damage evaluated over 3 years. Among the 99 enrolled patients, 90% received concomitant, conventional synthetic disease-modifying antirheumatic drugs (DMARDs), which were maintained throughout the study.

During follow-up, 25% of patients successfully tapered and discontinued TNFi without experiencing a flare. In contrast, 85% of patients who continued stable TNFi treatment remained flare-free during the same period. There was no statistically significant difference in radiographic progression between the groups, and most patients who experienced a flare were able to regain remission after restarting TNFi. The two treatment strategies were not associated with differences in adverse events or DMARD intensification, but a lower rate of ACR/EULAR Boolean 2.0 remission was observed in the tapering group. These findings support shared decision making and prompt recognition and treatment of flares.

KEY POINTS

- It is debated whether biologic therapy should be tapered or not in patients with RA who have achieved remission.

- The 3-year results from the ARCTIC REWIND study do not support routine tapering of TNFi among patients with RA in sustained remission because a majority experienced flare when tapering.

- Tapering attempts were associated with a lower rate of Boolean 2.0 remission, but no differences in radiographic progression, adverse events, or DMARD intensification were observed compared to stable treatment.

Longitudinal Associations Between Sarcopenia and Knee Osteoarthritis Progression

CORRESPONDENCE
Jia Li, PhD: nylijia5@smu.edu.cn

SUMMARY

Sarcopenia and knee osteoarthritis (KOA) are both chronic diseases of the musculoskeletal system. However, their causal relationship remains controversial. Wu et al used a multicenter, propensity score–matched cohort from the Osteoarthritis Initiative to investigate the longitudinal associations of baseline sarcopenia with radiographic and symptomatic KOA progression and subsequent knee replacement (KR).

Participants who screened positive for sarcopenia using the SARC-F questionnaire scale were classified as screened sarcopenia (Scre-S), and those with an additional positive chair-stand test were defined as probable sarcopenia (Prob-S). Results showed that Scre-S and Prob-S groups were positively associated with both radiographic and symptomatic KOA progression over 24- and 48-month follow-up. The risks of KR among individuals with Scre-S and Prob-S were 3.8-fold and 2.3-fold higher, respectively, than in those without sarcopenia. These associations remained significant after propensity score matching. These findings highlight that sarcopenia screening and management in middle-aged and older adults may slow KOA progression and aid in reducing the risk of subsequent KR.
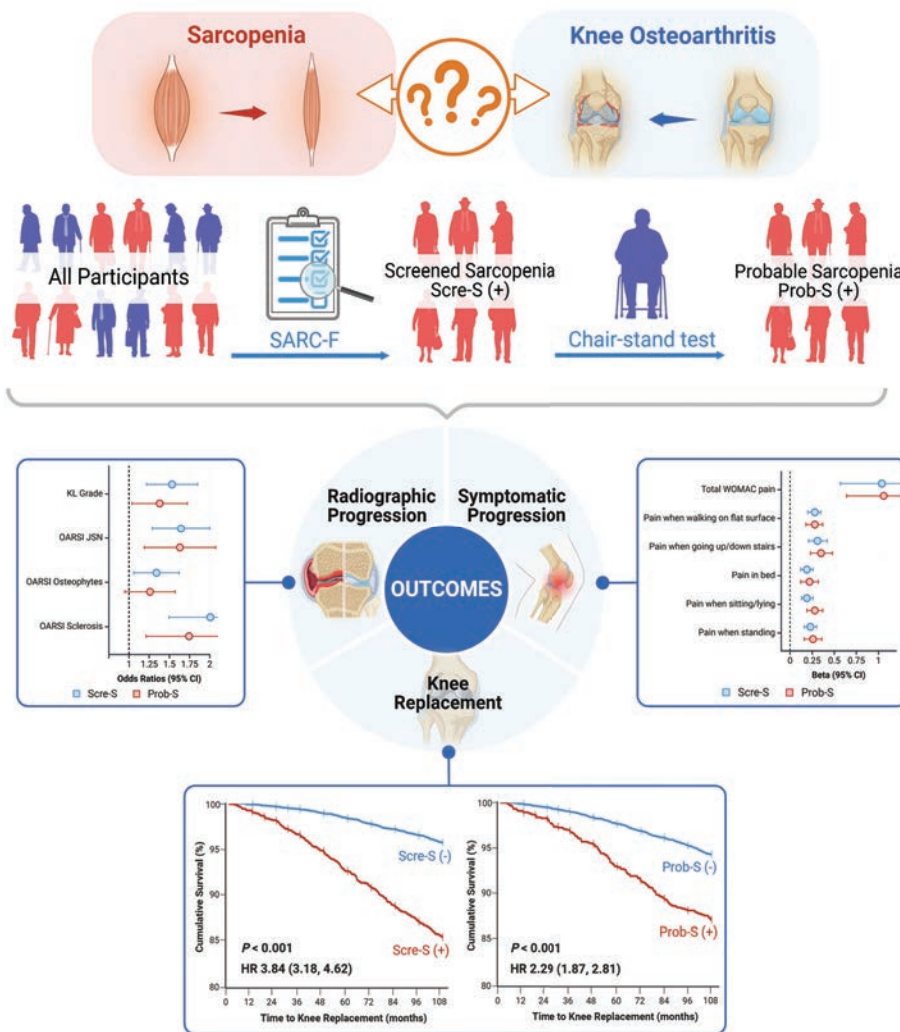
KEY POINTS

- Sarcopenia is longitudinally associated with both radiographic and symptomatic progression in KOA and subsequent KR.

- Such temporal relationships highlight the need for more attention to sarcopenia screening and potential treatment in KOA management.

- Simple and accessible sarcopenia screening tools, such as the SARC-F and chair-stand test, could aid in widespread prevention of KOA progression.

Long-Term Voclosporin for Lupus Nephritis Safe for Kidneys

The AURORA clinical program evaluated a voclosporin-based triple therapy regimen including mycophenolate mofetil (MMF) and low-dose glucocorticoids (GCs) for lupus nephritis (LN). In this issue, Rovin et al (p. 1387) report results from a substudy of the AURORA trials that assessed histologic changes in the kidneys of patients with active LN.

p.1387

AURORA 1 randomly assigned patients to voclosporin (or placebo) plus MMF and GCs. AURORA 2 was a 2-year continuation study in which enrolled patients continued on the same study drug assigned in AURORA 1. Patients could elect for kidney biopsy to be performed 6 months into AURORA 2 as part of a repeat kidney biopsy substudy.

The outcomes at 18 months from the 26-patient subgroup revealed that exposure to the study treatment was not associated with nephrotoxicity as determined by histopathologic evaluation.

Chronicity indices (CI), as measured by histologic findings of chronic kidney injury, remained stable at follow-up in both treatment groups. For most patients, activity indices, a histologic measure of kidney inflammation, decreased or remained unchanged between baseline and repeated biopsies. Of the 14 patients with an activity index of 0, however, 8 had moderate to severe kidney damage (as indicated by CI scores), which could have contributed to the clinically relevant levels of proteinuria at trial entry. The authors concluded their paper by stating that the data are reassuring and further contribute to the understanding of the safety profile of voclosporin for the treatment of adults with active LN.

Journal Club

A monthly feature designed to facilitate discussion on research methods in rheumatology.

Three-Year Outcomes and Latent Class Trajectory Analysis of the CARRA Polyarticular JIA Consensus Treatment Plans Study

Ringold et al, *Arthritis Rheumatol.* 2025;77:1433-1441.

The availability of multiple conventional synthetic disease-modifying antirheumatic drugs (csDMARDs) and biologic DMARDs (bDMARDs) for polyarticular juvenile idiopathic arthritis (pJIA) has improved patient outcomes. However, optimal DMARD initiation strategies have not been established. The objective of the STOP-JIA study was to compare effectiveness of three Childhood Arthritis and Rheumatology Research Alliance (CARRA) consensus treatment plans (CTPs) for untreated pJIA. These three CTPs differ in timing of bDMARD introduction: Step-Up (SU: initial csDMARD monotherapy, adding bDMARD 3 months later if needed); Early Combination (EC: csDMARD and bDMARD together); and Biologic First (BF: bDMARD monotherapy).

STOP-JIA used an observational comparative effectiveness design nested within the CARRA registry. At the 12-month endpoint, no significant differences were seen among CTPs in achieving American College of Rheumatology (ACR) clinical inactive disease (CID). However, secondary analyses suggested that the EC group had improved patient outcomes. Additionally, latent class trajectory analyses (LCTA) demonstrated that starting bDMARD by 3 months predicted likelihood of rapid improvement.

The present study assessed effects of initial CTP and timing of bDMARD introduction on disease outcomes across 3 years. Although there were no differences among treatment groups in achieving either ACR-CID or cJADAS-10 (clinical Juvenile Arthritis Disease Activity Score using 10 joints [cJADAS-10 ≤2.5]) at the 3-year registry visit, patients started on the EC CTP spent significantly more time in inactive disease states (ACR-CID and cJADAS-10), than patients on the SU CTP. The EC group also achieved clinical remission on medication significantly more frequently than the SU group. LCTA of cJADAS-10 scores again found rapid, moderate, and slow improvement trajectories. Patients starting a bDMARD within 2 months of enrollment were again more likely to be in the rapid improvement trajectory.

Questions

1. What are the pros and cons of using an observational, pragmatic study design compared to a randomized design? What statistical methods can be used to overcome the disadvantages?

2. What is the usefulness of nesting shorter-term effectiveness studies within larger, longer-term chronic disease registries capturing real-world outcomes?

3. Why was LCTA used in this study, and what insights did this method provide?

4. Why might a summative measure such as percentage of time spent in Clinical Inactive Disease (CID) show a significant difference between groups when that same CID outcome measured at a single timepoint may not?

5. Do the study's findings have potential practice change implications for new-onset untreated pJIA patients?

In this Issue

Highlights from this issue of *A&R* | **By Lara C. Pullen, PhD**

Prophylactic TMP-SMX Associated With Reduced Risk of Infections in AAV

Patients with antineutrophil cytoplasmic antibody–associated vasculitis (AAV) experience disease-specific organ damage and widespread inflammation. In addition, exposure to immunosuppressant medications makes them more susceptible to serious infections. Unfortunately, few studies have examined the optimal management of AAV to minimize the risk for infection.

p.1407

In this issue, Kim et al (p. 1407) report the results of a retrospective study that found that prophylactic trimethoprim–sulfamethoxazole (TMP-SMX) significantly reduced the risk for serious infections in patients with AAV. The effect was particularly pronounced during the first 6 months of induction therapy with rituximab or cyclophosphamide. The protection, which reduced incidence of infections beyond protection against *Pneumocystis jirovecii* pneumonia (PJP), was more evident in patients with additional risk factors for serious infections.

During the 252.1 person–years of observation, the investigators identified 77 cases of serious infections in 65 patients. The infections had a fatality rate of 18.5%. The majority (85.7%) of serious infections occurred within the first 180 days of observation.

The researchers found that the prophylaxis group experienced a significantly lower incidence of serious infections than the control group (hazard ratio [HR] 0.48 [95% confidence interval (CI) 0.32-0.72]). The beneficial effect of TMP-SMX was only significant, however, during the first 180 days (HR 0.41 [95% CI 0.22-0.76]) and not thereafter (HR 3.67 [95% CI 0.46-29.43]) (interaction $P = 0.044$) — a finding that was reinforced by the results of their time-varying analysis. There was one case of severe adverse drug reaction related to TMP-SMX; based on that, the number of
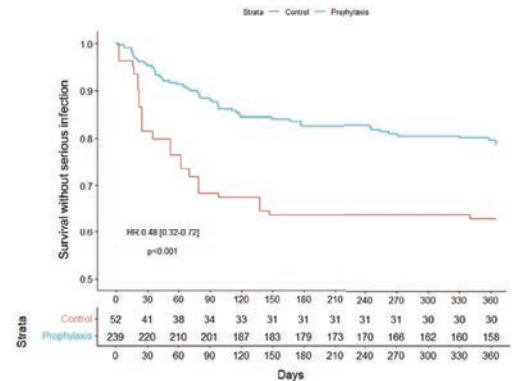

Figure 1. Kaplan–Meier curve showing one-year incidence of serious infection based on ITT analysis. HR, hazard ratio; ITT, intention-to-treat; TMP/SMX, trimethoprim–sulfamethoxazole.

treated patients needed to harm was 127.4. The number needed to treat to prevent one serious infection was 8.0. The researchers note that although they have demonstrated the beneficial effects of prophylactic TMP-SMX in reducing the risk for severe infection, the optimal duration of treatment needs to be further validated in future studies.

Predictive Biomarkers Identified for NHL in Primary Sjögren Disease

One of the central questions in primary Sjögren disease (pSD) is whether the CD11c⁺ FcRL5⁺ tissue-like memory (TLM) B cell population represents the prelymphomatous B cell source that contributes to the development of non-Hodgkin lymphoma (NHL). In this issue, Marques et al (p. 1394) describe their use of integrative analysis, coupling deep immunophenotyping findings with clinical, biological, and histopathologic data, to identify novel biomarkers of NHL in pSD. They report that CD11c⁺ FcRL5⁺ TLMs and IFNγ⁺ TNFα⁺ conventional T cells can be used to identify patients with pSD who are at higher risk of developing lymphoma.

p.1394

Their cross-sectional study included demographic, clinical, biological, histopathological, and immunological data from 206 patients with pSD (19 of whom had NHL-pSD). After immunophenotyping of blood samples from the patients, the investigators combined an unsupervised approach, data normalization, and deep cluster analysis to identify two clusters of NHL-pSD. They then characterized their shared and specific cell and biological/clinical parameters.

The investigators found that the combination of number of cells in the two clusters (CD11c⁺ FcRL5⁺ TLMs and IFNγ⁺ TNFα⁺ T cells) discriminates patients with NHL-pSD with a sensitivity of 78.9% and a specificity

of 76.8%. The combination thus exceeded the performance of the traditionally used combination of clinical and biologic markers, including cryoglobulinemia vasculitis and parotid enlargement. The new data refine the phenotype of CD21⁻ cells in pSD by identifying them as TLMs that express CD11c and FcRL5. The results also highlight the correlation between lymphoproliferation and a CD4⁺ T cell population with a phenotype similar to that of Th1 lymphocytes. The authors propose that eventually flow cytometry might be used by clinicians to quantify these cell populations, thereby enabling the identification of patients at risk of developing NHL-pSD.

Long-Term Voclosporin for Lupus Nephritis Safe for Kidneys

p.1387 The AURORA clinical program evaluated a voclosporin-based triple therapy regimen including mycophenolate mofetil (MMF) and low-dose glucocorticoids (GCs) for lupus nephritis (LN). In this issue, Rovin et al (p. 1387) report results from a substudy of the AURORA trials that assessed histologic changes in the kidneys of patients with active LN.

AURORA 1 randomly assigned patients to voclosporin (or placebo) plus MMF and GCs. AURORA 2 was a 2-year continuation study in which enrolled patients continued on the same study drug assigned in AURORA 1. Patients could elect for kidney biopsy to be performed 6 months into AURORA 2 as part of a repeat kidney biopsy substudy.

The outcomes at 18 months from the 26-patient subgroup revealed that exposure to the study treatment was not associated with nephrotoxicity as determined by histopathologic evaluation.

Chronicity indices (CI), as measured by histologic findings of chronic kidney injury, remained stable at follow-up in both treatment groups. For most patients, activity indices, a histologic measure of kidney inflammation, decreased or remained unchanged between baseline and repeated biopsies. Of the 14 patients with an activity index of 0, however, 8 had moderate to severe kidney damage (as indicated by CI scores), which could have contributed to the clinically relevant levels of proteinuria at trial entry. The authors concluded their paper by stating that the data are reassuring and further contribute to the understanding of the safety profile of voclosporin for the treatment of adults with active LN.

Journal Club

A monthly feature designed to facilitate discussion on research methods in rheumatology.

Three-Year Outcomes and Latent Class Trajectory Analysis of the CARRA Polyarticular JIA Consensus Treatment Plans Study

Ringold et al, *Arthritis Rheumatol.* 2025;77:1433-1441.

The availability of multiple conventional synthetic disease-modifying antirheumatic drugs (csDMARDs) and biologic DMARDs (bDMARDs) for polyarticular juvenile idiopathic arthritis (pJIA) has improved patient outcomes. However, optimal DMARD initiation strategies have not been established. The objective of the STOP-JIA study was to compare effectiveness of three Childhood Arthritis and Rheumatology Research Alliance (CARRA) consensus treatment plans (CTPs) for untreated pJIA. These three CTPs differ in timing of bDMARD introduction: Step-Up (SU: initial csDMARD monotherapy, adding bDMARD 3 months later if needed); Early Combination (EC: csDMARD and bDMARD together); and Biologic First (BF: bDMARD monotherapy).

STOP-JIA used an observational comparative effectiveness design nested within the CARRA registry. At the 12-month endpoint, no significant differences were seen among CTPs in achieving American College of Rheumatology (ACR) clinical inactive disease (CID). However, secondary analyses suggested that the EC group had improved patient outcomes. Additionally, latent class trajectory analyses (LCTA) demonstrated that starting bDMARD by 3 months predicted likelihood of rapid improvement.

The present study assessed effects of initial CTP and timing of bDMARD introduction on disease outcomes across 3 years. Although there were no differences among treatment groups in achieving either ACR-CID or cJADAS-10 (clinical Juvenile Arthritis Disease Activity Score using 10 joints [cJADAS-10 ≤2.5]) at the 3-year registry visit, patients started on the EC CTP spent significantly more time in inactive disease states (ACR-CID and cJADAS-10), than patients on the SU CTP. The EC group also achieved clinical remission on medication significantly more frequently than the SU group. LCTA of cJADAS-10 scores again found rapid, moderate, and slow improvement trajectories. Patients starting a bDMARD within 2 months of enrollment were again more likely to be in the rapid improvement trajectory.

Questions

1. What are the pros and cons of using an observational, pragmatic study design compared to a randomized design? What statistical methods can be used to overcome the disadvantages?

2. What is the usefulness of nesting shorter-term effectiveness studies within larger, longer-term chronic disease registries capturing real-world outcomes?

3. Why was LCTA used in this study, and what insights did this method provide?

4. Why might a summative measure such as percentage of time spent in Clinical Inactive Disease (CID) show a significant difference between groups when that same CID outcome measured at a single timepoint may not?

5. Do the study's findings have potential practice change implications for new-onset untreated pJIA patients?

Arthritis & Rheumatology

An Official Journal of the American College of Rheumatology
www.arthritisrheum.org and wileyonlinelibrary.com

Arthritis & Rheumatology

An Official Journal of the American College of Rheumatology
www.arthritisrheum.org and wileyonlinelibrary.com

VOLUME 77 • October 2025 • NO. 10

Cover image: The image on the cover (Bhargava et al; pages 1421–1432) features immunofluorescence staining of nephrin (green) and F-actin (red) in cultured human podocytes after exposure to IgG derived from individuals with lupus nephritis before and after deglycosylation. This image captures the cytoskeletal defects and change in nephrin expression during lupus nephritis in podocytes modulated by IgG glycosylation.

AMERICAN COLLEGE
of RHEUMATOLOGY
Empowering Rheumatology Professionals

EDITORIAL

Voclosporin Nephrotoxicity: A Myth Debunked?

Anthony Chang (iD)

Gary Hill, a prominent nephropathologist, quipped more than five decades ago that "if you are only going to do one biopsy, do the second."[1] In practice, the second kidney biopsy may be obtained when there is a relapse or flare, often months to years later. However, the most desired second kidney biopsy would be when the patient has improved or stabilized after a clinical intervention, and that can only occur within a clinical trial.

Voclosporin is a second-generation calcineurin inhibitor (CNI) that has demonstrated efficacy in lupus nephritis with the allure of less nephrotoxicity.[2] In this issue of *Arthritis and Rheumatology*, Rovin and colleagues conducted a substudy of AURORA patients with lupus nephritis focusing on whether voclosporin treatment demonstrated histopathologic features of CNI toxicity (CNIT).[3] Repeat kidney biopsies with a mean separation time of 18 months were obtained, and there were no significant differences in the vascular or tubular compartments regarding the recognized features of CNIT. The voclosporin-treated group demonstrated worse arteriolar hyalinosis in 1 of 16 patients compared with 3 of 10 patients in the placebo group.

These data potentially support the tantalizing narrative that voclosporin is less nephrotoxic than first-generation CNIs, cyclosporine and tacrolimus. However, it would be premature to conclude that voclosporin does not cause any nephrotoxicity. This was a small cohort with limited racial diversity. In reality, complete arteriolar cross-sections are infrequent in tissue sections and may be less frequent than glomerular cross-sections. The four slides that were examined for this study are one-third to one-half of the number of slides that are routinely evaluated by most nephropathology laboratories. As a result, focal lesions of CNIT may have been missed, or alternatively an arteriolar mechanism of injury, if present, may be low grade such that significant changes may not be identifiable by the human eye within 18 to 24 months. Thus, we are reminded that the absence of proof is not proof of absence.

Despite these limitations, these data represent an important step forward and could only have been obtained because the study design required repeat kidney biopsies. These findings may also allay some concerns about voclosporin nephrotoxicity with long-term treatment given that the 2024 American College of Rheumatology practice guidelines for active lupus nephritis flares recommend considering CNIs along with triple immunosuppressive regimens (intravenous glucocorticoids, methylprednisolone, and steroid taper) and mycophenolic acid analogues, especially with protein levels in the urine (proteinuria)[4] ≥3 g/g.

My skepticism regarding our tendency to blame any arteriolar alterations on CNIT has steadily increased over my two decades of experience given that arteriolar hyalinosis is not a specific feature and is often observed in diabetic or hypertensive patients who have never been exposed to CNIs. Perhaps, hyalinosis represents a low-grade or smoldering microangiopathic injury, of which there are several culprits in lupus nephritis. Newer therapies that are better suppressors of the adaptive and/or innate immune system may also have the added benefit of dampening such a microangiopathic injury. In other words, we might consider that arteriolar hyalinosis reflects inadequate treatment of lupus nephritis rather than direct injury solely by CNIs. The three patients in the control group with worse arteriolar hyalinosis in their repeat kidney biopsies and no CNI therapy would support this notion.

Other arteriolar alterations, such as vessel wall thickness, luminal reduction, and endothelial cell enlargement or swelling, are not recognized features of CNIT, but these may be important pathologic parameters for future investigations that will require automated and precise measurements involving image analysis and/or machine learning. Perhaps these quantitative methods could detect subtle changes that are not apparent to the human eye so that we would not have to wait five years or longer before a statistically significant difference can be seen.

Anthony Chang, MD: The University of Chicago, Chicago, Illinois.
Author disclosures are available at https://onlinelibrary.wiley.com/doi/10.1002/art.43208.
Address correspondence via email to Anthony Chang, MD, at anthony.chang@bsd.uchicago.edu.

The kidney biopsy still remains the gold standard, and the investigators of this AURORA substudy should be applauded for reminding us of the important knowledge that sequential kidney biopsies can provide. I hope that future investigators are inspired to conduct more studies with repeat kidney biopsies in clinical settings beyond lupus nephritis and kidney allografts, which will advance our understanding of other complex kidney diseases as my favorite mantra of Gary Hill continues to remain relevant.

AUTHOR CONTRIBUTIONS

The author contributed to at least one of the following manuscript preparation roles: conceptualization AND/OR methodology, software, investigation, formal analysis, data curation, visualization, and validation AND drafting or reviewing/editing the final draft. As corresponding author, Dr Chang confirms that he has provided the final approval of the version to be published and takes responsibility for the affirmations regarding article submission (eg, not under consideration by another journal), the integrity of the data presented, and the statements regarding compliance with institutional review board/Declaration of Helsinki requirements.

REFERENCES

1. Hill GS, Delahousse M, Nochy D, et al. Predictive power of the second renal biopsy in lupus nephritis: significance of macrophages. Kidney Int 2001;59(1):304–316.
2. Kale A, Shelke V, Lei Y, et al. Voclosporin: unique chemistry, pharmacology and toxicity profile, and possible options for implementation into the management of lupus nephritis. Cells 2023;12(20): 2440.
3. Rovin BH, Cassol C, Parikh SV, et al. Effect of long-term voclosporin treatment on renal histology in patients with active lupus nephritis with repeat renal biopsies. Arthritis Rheumatol 2025;77(10):1387–1393.
4. American College of Rheumatology. New ACR guideline summary provides guidance to screen, treat, and manage lupus nephritis. November 18, 2024. Accessed April 12, 2025. https://rheumatology. org/press-releases/new-acr-guideline-summary-provides-guidance-to-screen-treat-and-manage-lupus-nephritis

AMERICAN COLLEGE
of RHEUMATOLOGY
Empowering Rheumatology Professionals

EDITORIAL

Tapering in Rheumatoid Arthritis: A Path to Predict Flares

Elise van Mulligen,[1] (iD) Jon T. Giles,[2] (iD) and Angelique E. A. M. Weel[3]

For patients with rheumatoid arthritis (RA) who achieve sustained remission, the question of tapering biologic therapies, especially anti–tumor necrosis factor (anti-TNF) drugs, is increasingly relevant. Although dose reduction may decrease treatment costs and adverse effects, the looming threat of disease flares, reported in up to 66% of patients within 6 to 12 months of tapering, presents a significant clinical and economic challenge.[1]

To address this, Kjørholt and colleagues report three-year data from the TNF inhibitor arm of the ARCTIC REWIND trial in this issue of *Arthritis & Rheumatology*.[2] The trial was powered on the primary end point of flare at 12 months among patients with RA in sustained remission who were randomized to taper off their TNF inhibitor over four months versus continue stable TNF inhibitor therapy. The primary analyses of the primary end point were published previously.[3] All patients continued to take stable background conventional synthetic disease-modifying antirheumatic drugs (DMARDs). The trial was open label for the patients and investigators but blinded to the assessors. At 12 months, there were 47 patients in the taper group in the intent-to-treat analysis, compared with 43 patients in the stable therapy group. By three years, this had dropped to 44 patients in the taper group and 43 patients in the stable group, with the losses to follow-up in the taper group due to a non–study-related death and loss to follow-up. Similar to the 12-month findings, the flare rate was higher in the taper group compared with the stable group, with only 25% in the taper group remaining flare free compared with 85% in the stable TNF inhibitor group, which was highly statistically significant. Notably, in the taper group, there were very few flares past 12 to 16 months. There was no significant difference in radiographic progression between the groups, although the rate of radiographic progression for those in the tapering group was almost double that of the stable group (15% vs 8%), and most, but not all, of the patients who restarted their original TNF inhibitor in the taper group regained remission or low disease activity. There was no meaningful difference in adverse events between the groups.

Although none of the three-year findings were part of the trial's statistical powering, these extended findings provide valuable information that providers and patients can use when contemplating TNF inhibitor tapering in the setting of sustained remission. An important element missing from this report is whether specific patient characteristics could predict those who could successfully taper. However, we assume that this is being explored in separate analyses because it is key information needed to inform shared decision-making when patients and providers contemplate tapering.

The trial's open-label design introduces the possibility of reporting bias, particularly in flare detection. The composite flare definition, which includes formal clinical criteria as well as patient and physician judgment, may lead to more subjective flare reporting in patients tapering therapy. Given that no difference was found in Disease Activity Score (DAS) remission or ultrasound synovitis, but a significant difference existed in American College of Rheumatology/EULAR Boolean remission, the potential influence of subjective components merits further exploration.[4] A breakdown of flares by definition type would improve transparency and contextualize the findings more fully.

Flares in RA are far more than brief setbacks. They result in worsened joint pain, functional decline, increased health care use, and reduced work productivity. The TARA trial highlighted this burden, showing greater indirect costs linked to work productivity loss in patients who experienced flares during tapering.[5] Such findings make it clear: the cost of a flare can easily negate the savings from reduced drug use.

International guidelines cautiously support tapering for patients in sustained remission, typically defined by stringent DAS remission lasting at least six months. However, focusing solely on disease activity overlooks broader patient characteristics and experiences, including pain, fatigue, and disability. This shift toward a dual-target approach, treating both inflammation

[1]Elise van Mulligen, MSc, PhD: Rheumatology, Leiden University Medical Center, Leiden, The Netherlands, and Rheumatology, Erasmus Medical Center, Rotterdam, The Netherlands; [2]Jon T. Giles, MD, MPH: Kao Autoimmunity Institute, Cedars-Sinai Medical Center, Los Angeles, California; [3]Angelique E. A. M. Weel, MD: Rheumatology, Maasstad Hospital and Erasmus School of Health Policy and Management, Erasmus University, Rotterdam, The Netherlands.

and other domains that result in poorer quality of life, marks a significant evolution of the traditional treat-to-target paradigm.[6,7] Yet, approximately 19% to 50% of patients remain outside remission, often because of discordance between clinical assessments and patient-reported symptoms such as pain and fatigue.

To taper wisely, we need to predict flares with precision, specifically in remote monitoring. Cohort studies have identified some risk factors.[8] Also, tapering studies such as OPTTIRA and DRESS have begun to illuminate risk factors, including DAS-related radiologic progression, impaired physical function, and fatigue.[9,10] These findings, alongside gradual tapering strategies (eg, dose reduction or interval extension),[11] show promise: up to 43% of patients tapered TNF inhibitors successfully without major setbacks. Imaging and biomarker studies also contribute; magnetic resonance imaging features such as synovitis and bone edema and serum markers such as soluble tumor necrosis factor receptor type I and interleukin-2 can help flag patients at higher risk.[12] Moreover, innovative tools are emerging. The RETRO study demonstrated how machine learning,[13] combined with patient-reported data, achieved a predictive accuracy of an area under the receiver operating characteristic curve of 0.81. Artificial intelligence–driven decision-support systems are now being developed to integrate clinical, biologic, and imaging data, pointing toward a future in which individualized flare prediction is both feasible and actionable. Furthermore, results from the PATIO trial are awaited, in which a dynamic flare prediction model is used as a decision aid during stepwise tapering of biologic DMARDs.[14]

The objective of treatment tapering should be clearly defined in advance: is the intention to reduce the dosage or to eventually discontinue medication altogether? Recent trials exploring the tapering of biologic DMARDs to half-doses have generally reported favorable outcomes. However, when the ultimate goal is complete cessation, results become more variable, particularly across different risk groups. Notably, the risk of disease flare before tapering varies significantly. For instance, DMARD-free remission was achieved in 40% of anti–citrullinated protein antibody (ACPA)–negative patients, compared to 5% to 10% of those who were ACPA-positive.[15] Interestingly, patients in remission while taking conventional DMARDs appear more likely to successfully discontinue treatment than those taking biologic agents. Supporting this, data from the separate nonbiologic DMARD tapering companion trial of ARCTIC REWIND showed that among patients taking conventional DMARDs, 80% of those taking a stable dose remained flare free, compared to 57% in the half-dose group and just 38% in the complete withdrawal group.[16] These findings underscore the importance of accurate risk prediction and patient stratification before initiating DMARD tapering or withdrawal.

The conclusion by Kjørholt et al that tapering should not be done "on a regular basis" may be interpreted as more restrictive than necessary. Although their study demonstrates an increased risk of flares with TNF inhibitor tapering, it also shows that these flares are largely reversible and not associated with radiographic progression over a three-year period. This suggests that tapering remains a viable option for selected patients, especially when guided by patient preferences, accompanied by close monitoring, and supported by a clear plan for rapid reintroduction of therapy if needed. Central to this process is shared decision-making, in which clinicians and patients must engage in open discussions, weighing the benefits of reduced medication against the risk of flares, with plans for close monitoring in place. A gradual stepwise approach is preferred to minimize risk. The path forward lies in building robust, multidimensional prediction models through prospective studies and interdisciplinary collaboration. Identifying predictors of successful tapering, refining the definition of flares, and optimizing monitoring strategies will be essential to enabling safe and effective de-escalation. With precision tapering informed by reliable predictors, we can strike the right balance, reducing treatment burden while safeguarding quality of life. In doing so, RA care can shift from reactive to proactive, ensuring that remission remains not just a milestone but a sustainable reality.

AUTHOR CONTRIBUTIONS

All authors contributed to at least one of the following manuscript preparation roles: conceptualization AND/OR methodology, software, investigation, formal analysis, data curation, visualization, and validation AND drafting or reviewing/editing the final draft. As corresponding author, Dr van Mulligen confirms that all authors have provided the final approval of the version to be published and takes responsibility for the affirmations regarding article submission (eg, not under consideration by another journal), the integrity of the data presented, and the statements regarding compliance with institutional review board/Declaration of Helsinki requirements.

REFERENCES

1. Ahmad HA, Baker JF, Conaghan PG, et al. Prediction of flare following remission and treatment withdrawal in early rheumatoid arthritis: post hoc analysis of a phase IIIb trial with abatacept. Arthritis Res Ther 2022;24(1):47.

2. Kjørholt KE, Paulshus Sundlisæter N, Aga AB, et al. Three-year results of tapering tumor necrosis factor inhibitor to withdrawal compared to stable tumor necrosis factor inhibitor among patients with rheumatoid arthritis in sustained remission: a multicenter randomized trial. Arthritis Rheumatol 2025;77(10):1327–1336.

3. Lillegraven S, Paulshus Sundlisæter N, Aga AB, et al. Effect of tapered versus stable treatment with tumour necrosis factor inhibitors on disease flares in patients with rheumatoid arthritis in remission: a randomised, open label, non-inferiority trial. Ann Rheum Dis 2023; 82(11):1394–1403.

4. Studenic P, Aletaha D, de Wit M, et al. American College of Rheumatology/EULAR remission criteria for rheumatoid arthritis: 2022 revision. Arthritis Rheumatol 2022;75(1):15–22.

5. van Mulligen E, Weel AE, Kuijper TM, et al. Two-year cost effectiveness between two gradual tapering strategies in rheumatoid arthritis: cost-utility analysis of the TARA trial. Ann Rheum Dis 2020;79(12): 1550–1556.

6. Ferreira RJO, Ndosi M, de Wit M, et al. Dual target strategy: a proposal to mitigate the risk of overtreatment and enhance patient satisfaction in rheumatoid arthritis. Ann Rheum Dis 2019;78(10):e109–e110.

7. van den Dikkenberg M, Luurssen-Masurel N, Kuijper TM, et al. Meta-analyses on the effects of disease-modifying antirheumatic drugs on the most relevant patient-reported outcome domains in rheumatoid arthritis. Arthritis Care Res (Hoboken) 2023;75(8):1659–1672.

8. Oh YJ, Moon KW. Predictors of flares in patients with rheumatoid arthritis who exhibit low disease activity: a nationwide cohort study. J Clin Med 2020;9(10):3219.

9. Bouman CA, den Broeder AA, van der Maas A, et al. What causes a small increase in radiographic progression in rheumatoid arthritis patients tapering TNF inhibitors? RMD Open 2017;3(1):e000327.

10. Bechman K, Sin FE, Ibrahim F, et al. Mental health, fatigue and function are associated with increased risk of disease flare following TNF inhibitor tapering in patients with rheumatoid arthritis: an exploratory analysis of data from the Optimizing TNF Tapering in RA (OPTTIRA) trial. RMD Open 2018;4(1):e000676.

11. van Esveld L, Cox JM, Kuijper TM, et al. Cost-utility analysis of tapering strategies of biologicals in rheumatoid arthritis patients in the Netherlands. Ann Rheum Dis 2023;82(10):1296–1306.

12. Kameda H, Hirata A, Katagiri T, et al. Prediction of disease flare by biomarkers after discontinuing biologics in patients with rheumatoid arthritis achieving stringent remission. Sci Rep 2021;11(1):6865.

13. Vodencarevic A, Tascilar K, Hartmann F, et al; RETRO study group. Advanced machine learning for predicting individual risk of flares in rheumatoid arthritis patients tapering biologic drugs. Arthritis Res Ther 2021;23(1):67.

14. Messelink MA, van der Leeuw MS, den Broeder AA, et al. Prediction Aided Tapering In rheumatoid arthritis patients treated with biOlogicals (PATIO): protocol for a randomized controlled trial. Trials 2022; 23(1):494.

15. Verstappen M, van Mulligen E, de Jong PHP, et al. DMARD-free remission as novel treatment target in rheumatoid arthritis: a systematic literature review of achievability and sustainability. RMD Open 2020;6(1): e001220.

16. Kjørholt KE, Sundlisæter NP, Aga AB, et al. Effects of tapering conventional synthetic disease-modifying antirheumatic drugs to drug-free remission versus stable treatment in rheumatoid arthritis (ARCTIC REWIND): 3-year results from an open-label, randomised controlled, non-inferiority trial. Lancet Rheumatol 2024;6(5):e268–e278.

EXPERT PERSPECTIVES ON CLINICAL CHALLENGES

Expert Perspective: How, When, and Why to Potentially Stop Antiresorptive Drugs in Osteoporosis

Giovanni Adami[1] and Kenneth G. Saag[2] iD

Osteoporosis is a chronic disease, and antiresorptive treatments are often continued for many years. Despite their established efficacy in reducing fracture risk, the most commonly used antiresorptive treatments, bisphosphonates and denosumab, have short- and long-term risks that, coupled with their benefits and other unique characteristics, influence consideration for at least periodic discontinuation. Bisphosphonates retain their effects even after discontinuation due to their prolonged skeletal retention, whereas denosumab discontinuation is associated with a rapid rebound in bone turnover and increased fracture risk. There is controversy about how, when, and why to potentially stop these agents. We discuss both permanent and temporary discontinuation of long-term treatment with bisphosphonates and denosumab. We focus on the reasons and timing for discontinuation as well as strategies to mitigate future fracture risk.

Clinical challenge

Two 70-year-old postmenopausal identical twins (Ms DMS and Ms BPS) were seen for a second opinion about their severe osteoporosis. Ms DMS had a vertebral fracture 12 years ago and experienced a wrist fracture in her fifties. She has been treated for nine years with denosumab at 60 mg subcutaneously every six months. Her twin sister has a history of two vertebral fractures 9 and 13 years ago, and she has been taking alendronate at 70 mg orally once a week for the past 15 years. Beyond age, menopausal status, and a family history of an early hip fracture in their mother, neither sister has additional major risk factors for fractures. They have both been reading about adverse effects related to long-term osteoporosis treatment and are concerned about continuing their medications.

Osteoporosis treatment considerations and why to consider stopping certain drugs. Effective management of osteoporosis is critical to reducing the risk of fractures, which significantly impact the quality of life in older adults. Several pharmacologic treatments are available for the management of osteoporosis, each with distinct mechanisms of action and long-term effects on bone metabolism. This perspective will be limited to issues surrounding the longer-term use of the two most commonly used types of antiresorptive osteoporosis drugs: bisphosphonates and denosumab.

Bisphosphonates and denosumab have been the cornerstone of osteoporosis management because of their wide availability and efficacy in reducing bone resorption by inhibiting osteoclast activity, leading to improved bone mineral density (BMD) and reduced fracture risk.[1–6] Bisphosphonates, such as alendronate, bind to hydroxyapatite crystals and are incorporated directly into the bone hydroxyapatite matrix. They inhibit osteoclast activity by targeting the enzyme farnesyl diphosphate synthase in the osteoclast mevalonate pathway and limit production of a ruffled border necessary for bone resorption. They have a very extended activity because as the bone is resorbed, they are progressively uncovered and become reactivated.[7] Based on this rather unique depot mechanism of action, bisphosphonates provide a prolonged antifracture benefit and have drug effects that may persist months or years even after their discontinuation. On the other hand, denosumab, a monoclonal antibody that inhibits the RANKL, a key factor in osteoclast activation differentiation, activation, and survival, has biologic effects that are sustained for only six months after a single subcutaneous dose. If denosumab is discontinued, there is a rapid "rebound" in bone turnover associated with an increased fracture risk.[8–12] Suppression of bone turnover is a key mechanism by which these drugs reduce fracture risk. However, prolonged suppression of bone turnover can cause the bone to become more highly mineralized and lose its ability to repair microdamage.[13,14] This can lead to bone fragility. Potential "oversuppression" of bone

[1]Giovanni Adami, MD, PhD: Rheumatology Section, Department of Medicine, University of Verona, Verona, Italy; [2]Kenneth G. Saag, MD, MSc: University of Alabama at Birmingham.
Author disclosures and graphical abstract are available at https://onlinelibrary.wiley.com/doi/10.1002/art.43179.

Address correspondence via email to Kenneth G. Saag, MD, MSc, at ksaag@uab.edu.

remodeling has been associated with rare adverse events with both classes of agents.

The most concerning adverse events associated with both bisphosphonates and denosumab are atypical femoral fractures (AFFs) and osteonecrosis of the jaw (ONJ). These adverse events are believed to stem, at least in part, from the profound and longer-term suppression of bone remodeling. Although both conditions share a common pathophysiology related to the suppression of bone turnover, each has unique characteristics and potential mechanisms.[15]

ONJ is characterized by exposed necrotic bone in the maxillofacial region, often following dental extractions or other invasive dental procedures. It is believed that prolonged suppression of bone turnover compromises the ability of the jawbone to repair microdamage and maintain vascularity, leading to localized necrosis. Additionally, factors such as local infection, reduced angiogenesis, and microbial biofilms play significant roles in the pathogenesis of ONJ.[16]

AFFs occur along the subtrochanteric or diaphyseal regions of the femur and occur with minimal trauma. The pathogenesis involves oversuppression of bone turnover leading to reduced bone remodeling capacity, accumulation of microdamage, and altered bone material properties.[17]

Both events are estimated to have an overall incidence of 1 of 1,000 to 1 of 10,000 in patients treated for osteoporosis.[18,19] Despite the overall rarity and the typical modest severity of most cases of ONJ in osteoporosis, it occasionally can be very serious and lead to morbidity and even death. Further establishing causality of these events with bisphosphonates, ONJ rates approach 1% to 10% when potent intravenous bisphosphonates are administered as frequently as every month in the setting of malignancy.[19] Because of the unusual depot effects of bisphosphonates, the risk of these longer-term adverse effects with both treatments, and/or achievement of successful bone health outcomes, some clinicians and patients, such as the twins, will consider stopping these treatments after variable periods of use.

In the complex clinical challenge we described, the approach to care for Ms DMS and Ms BPS varies greatly, based on their specific bone treatment history, even if the two sisters present with a somewhat similar health history and identical genetic background.

A detailed bone medication history is essential in evaluating and managing osteoporosis. For Ms DMS, questions should focus on her adherence to denosumab, including whether she has missed or delayed any doses, given the rebound risk. For Ms BPS, the medical history should explore her adherence to alendronate over the years. Indeed, oral bisphosphonates, although effective, are well known for poor long-term adherence due to their strict dosing requirements and potential gastrointestinal side effects. In addition to adherence, another challenge with oral bisphosphonates, particularly in older adult patients, is reduced gastrointestinal absorption. Bisphosphonates have inherently low bioavailability (∼1%), and their absorption is further impaired by common factors in older adults, such as concurrent medication use (eg, proton pump inhibitors). Medical history should also include the evaluation of the need for future invasive dental procedures, particularly tooth extraction and intended dental implants, that might affect use and/or timing of antiresorptives due to risk of ONJ.

How and when to discontinue antiresorptives

Given their different mechanisms of action, we will discuss separately denosumab discontinuation and bisphosphonate drug holidays. The evidence supporting the decision-making in continuing or stopping these therapies is summarized in Tables 1 and 2.

Bisphosphonates. Bisphosphonates can be classified based on the route of administration and, more importantly, based on their relative osteoclast inhibition potency, mostly determined by their affinity to the bone. Among the commonly used bisphosphonates—alendronate, risedronate, zoledronic acid, and ibandronate—there are significant differences in their bone affinity, with zoledronic acid having the most affinity to bone and ibandronate and risedronate having the lowest.[20]

Long-term extension to the clinical trials of bisphosphonates, such as alendronate, have provided critical insights into their efficacy and the effects on treatment discontinuation. In the pivotal study of alendronate for postmenopausal participants with osteoporosis who continued alendronate treatment for up to 10 years showed significant and sustained increases in BMD. This was most notable at the lumbar spine, where after approximately five years of therapy, BMD essentially plateaued and persisted even after the drug was stopped for five years.[21] In contrast, BMD at

Table 1. Bisphosphonate discontinuation: benefits, risks, and competing evidence*

Benefits/rationale to discontinue	Risks to discontinue/ rationale to continue
Protracted efficacy even after discontinuation (especially with alendronate or zoledronic acid–prolonged skeletal retention)[21–23,26]	Residual fracture risk in high-risk patients[22,33]
Plateauing of BMD benefit after prolonged therapy (≈3–5 years) and similar fracture risk[21,22]	Refracture risk during drug holiday[23,32,36]
Risk of adverse effects related to treatment duration[18,32]	Secondary mineralization might offer benefit beyond BMD increase[76,77]
Reduced adverse effects upon stopping (ONJ, AFF)[18,19,33]	–
Temporary discontinuation (holiday)[23,33,36]	–

* AFF, atypical femoral fracture; BMD, bone mineral density; ONJ, osteonecrosis of the jaw.

Table 2. Denosumab discontinuation: benefits, risks, and competing evidence*

Benefits/rationale to discontinue	Risks to discontinue/rationale to continue
No further risk reduction after achieving T score greater than[78] −1.5/−2.0	Rebound in bone turnover markers and loss of BMD[8,10,12,40]
Successful exit strategies to attenuate rebound exist: transition to zoledronic acid or alendronate[41]	Increased risk of fractures and multiple vertebral fractures after discontinuation[40,42–44,50,54]
Adverse effects (eg, ONJ, AFF)[15,18,19]	Risk of fracture higher than expected from BMD loss[45,51]
–	Efficacy and safety tested through 10 years[39]
–	Bisphosphonates (especially with less potent bisphosphonates such as risedronate), SERMs, or romosozumab after discontinuation still associate with bone loss[52,53,55,70,79,80]

* AFF, atypical femoral fracture; BMD, bone mineral density; ONJ, osteonecrosis of the jaw; SERM, selective estrogen receptor modulator.

the hip and bone turnover returned toward baseline over approximately five years. The impact of alendronate discontinuation after five years on fracture risk is somewhat nuanced. Overall, there was no significant difference in the incidence of morphometric vertebral, nonvertebral, and hip fractures between those who continued treatment for 10 years and those who discontinued after only 5 years. However, there was a 55% reduction in the risk of clinical vertebral fractures in those who continued alendronate therapy for 10 years, and the subgroup of women who were at highest fracture risk also saw a preferential benefit to continuing therapy.[22] Notably, the study was considerably underpowered to detect differences in fracture risk among those who persisted with therapy and patients who remain in extensions to clinical trials have low generalizability to the general population.

Risedronate, another oral bisphosphonate given weekly or monthly, exhibits a comparatively much shorter "tail effect" than alendronate. Specifically, although bone turnover and BMD in patients treated with alendronate returns to baseline levels over approximately five years, those treated with risedronate revert to baseline within approximately one year after stopping the medication, regardless of the treatment duration.[23,24]

Zoledronic acid (also known as zoledronate), is another common bisphosphonate administered intravenously once a year. It also has an even longer tail effect, and participants who discontinued treatment after years still exhibited some residual benefits.[25] Notably, a single infusion of zoledronic acid can sustain BMD gains over baseline for up to 10 years and reduce clinical fracture risk,[26] supporting that its very prolonged effects may offer bone benefits even after discontinuation. Beyond its well-established role in fracture prevention, zoledronate has also been associated

with a reduction in overall death in older adults with osteoporosis and after hip fractures. The Health Outcomes and Reduced Incidence with Zoledronic Acid Once Yearly Recurrent Fracture Trial showed a 28% reduction in all-cause deaths in patients receiving zoledronate following a hip fracture.[27]

Although AFFs and ONJ have generated the greatest concerns, the most common bisphosphonate adverse events are gastrointestinal issues with oral administration and acute flu-like symptoms (acute-phase reaction) with intravenous administration.[15] However, gastrointestinal intolerance to oral bisphosphonates is usually rapidly reversible on discontinuation, not related to the duration of the treatment, and more likely to occur within weeks of the first dose. Acute-phase reactions (APR)s are usually limited to a few days and wane with subsequent administrations of bisphosphonates. Moreover, a short course of dexamethasone before the first infusion reduces APR severity.[28] Renal toxicity with zoledronic acid is also seen and primarily associated with rapid infusion rates in patients with impaired renal function.[29] Although concerns have been raised about esophageal cancer and atrial fibrillation being associated with bisphosphonates, causality has not been firmly established.[30,31]

The risk–benefit balance of bisphosphonates can be evaluated by the number needed to treat (NNT) and number needed to harm (NNH). Although the NNT for preventing typical osteoporosis fractures is largely favorable in the early years of treatment, the NNH for serious adverse events such as AFF increases with extended therapy. In White women, bisphosphonate use corresponded to a NNT for preventing a typical fragility hip fractures of approximately 350 and 170 at 5 and 10 years, respectively.[32] In contrast, in Asian women, the NNT was greater at 575 and 278 at 5 and 10 years, respectively. After five years of treatment, the NNH to cause an AFF was 12,500 for all women. However, The NNH decreased after 10 years of continuous treatment to 2,630. Of note, the NNH at 10 year was disproportionately lower among Asian women at only 424, thus indicating a higher rate of AFF compared to the overall population. The study also identified other risk factors for AFF, beside Asian ethnicity, including reduced height, weight, and glucocorticoid use. Importantly, the risk of AFF decreased rapidly after discontinuation of bisphosphonates, highlighting the importance of considering so called drug holidays. These therapy transitions to other types of medications are intended to mitigate long-term risks while maintaining the therapeutic benefits of fracture prevention. This balance in risk and benefit among different ethnic groups of women, in particular, necessitates careful consideration on the selective timing and duration of bisphosphonate therapy.

The 2016 American Society of Bone and Mineral Research (ASBMR) guidance on drug holidays for patients on long-term bisphosphonates offers emphasizes the balance between the benefits of fracture prevention with bisphosphonate and the need to reassess fracture risk over time[33] (see Figure 1). High-risk patients, such as persons age >70 years, those with a low hip T

score (less than –2.5), those who have had a major osteoporotic fracture, or those who continue to fracture while on therapy, may benefit from extended treatment for up to 10 years with oral bisphosphonates or 6 years with intravenous zoledronic acid. For patients deemed to be at low or moderate fracture risk after the initial treatment period, a drug holiday of two to three years may be considered. During this period, patients should undergo periodic reassessment of their fracture risk, including monitoring BMD and possibly bone turnover markers (BTMs). This reassessment helps determine the appropriate time to reinitiate therapy if the patient's fracture risk increases. A decrease in BMD of >3% (usually more than the least significant change on dual x-ray absorptiometry [DXA]) is considered significant at an individual patient level.[34]

BTMs, such as C-terminal telopeptide (CTX), also can be used in monitoring the effectiveness of osteoporosis therapy and guiding decisions about drug holidays or treatment reinitiation. CTX reflects the rate of bone resorption, and its levels typically decrease with effective antiresorptive treatment, such as bisphosphonates. A significant drop in CTX from pretreatment levels, defined as more than the least significant change of 30%, suggests that an antiresorptive therapy is effective in suppressing bone turnover. CTX levels also can be used to monitor drug holidays. A common approach involves comparing baseline (predrug holiday) levels with those during the drug holiday. Two potential thresholds for interpretation include a return to baseline levels (pretreatment) or an increase of more than 30% from the end-of-treatment levels. Our approach to these two thresholds can be summarized as follows: (1) a return to pretreatment baseline levels or higher (ie, before any bone active drug has been started), indicating complete loss of antiresorptive effect or (2) an increase of more than 30% (above the least significant change of most BTMs) from end-of-treatment levels, suggesting excessive bone loss. Measuring BTMs at 6 to 12 months after stopping bisphosphonates might allow clinicians to determine whether therapy should be restarted earlier than BMD alone would suggest, particularly in high-risk patients. Other BTMs, including urinary N-telopeptide, can be used in similar ways, albeit urinary turnover markers are more subject to diurnal variations.[35]

A corollary concern is that once bisphosphonates are discontinued for an extended period, fragility fractures may recur. US Medicare data were used to examine the fracture risk associated with various lengths of drug holidays among 81,427 women aged 65 years and older who had been adherent to
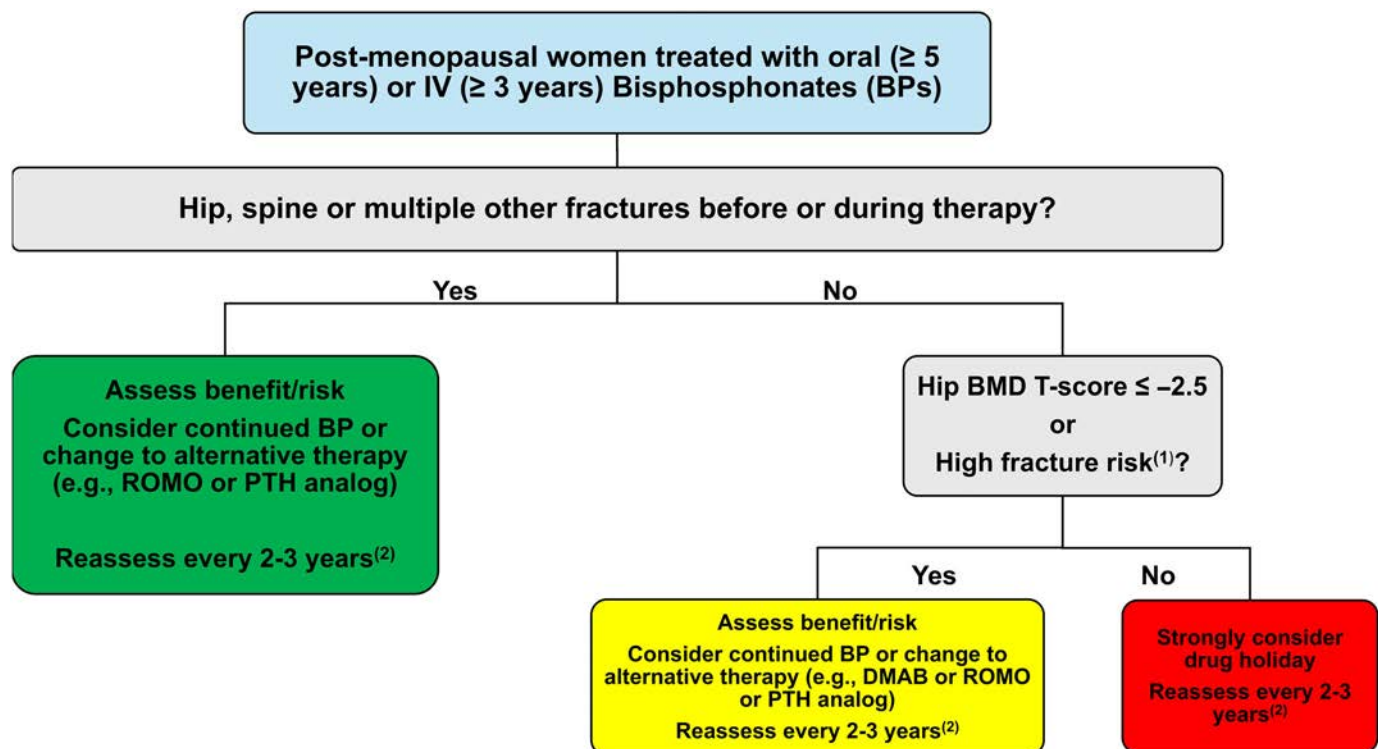
Figure 1. Approach to the management of postmenopausal women undergoing long-term bisphosphonate therapy (adapted from Adler et al[33]). (1) High fracture risk: defined by older age (70–75 years), other strong risk factors for fracture, or a validated fracture risk assessment tool fracture risk score above country specific thresholds. (2) Reassessment includes clinical evaluation and risk assessment including risk factors and may include bone density measurement by dual x-ray absorptiometry (DXA). The monitoring interval with DXA should be based on changes that are detectable and clinically significant. Reassessment may be necessary at <2 years in patients with a new fracture, or in light of anticipated accelerated bone loss (eg, institution of aromatase inhibitor or glucocorticoid therapy). BMD, bone mineral density; DMAB, denosumab; PTH, parathyroid hormone; ROMO, romosozumab.

bisphosphonate therapy (alendronate, risedronate, or zoledronate) for at least three years.[36] Discontinuing alendronate therapy for more than two years in more than a quarter of these women was associated with a significantly increased 30% greater risk of fractures compared to those who continued therapy (adjusted hazard ratio [HR] 1.3, 95% confidence interval [CI] 1.1–1.4). These findings suggest that extending the duration of a drug holiday beyond two years may significantly increase the risk of hip, humerus, and vertebral fractures. Among 25,000 matched pairs of older adults who had undergone long-term bisphosphonate therapy (either alendronate or risedronate) followed by a drug holiday (1.8 years on average), hip fracture rates were approximately 18% higher in the group of patients who discontinued risedronate compared to those who discontinued alendronate (12.4 vs 10.6 per 1,000 patient years, HR 1.18, 95% CI 1.04–1.34). Although risedronate and alendronate provide significant protection against fractures during active treatment, the shorter tail effect of risedronate may lead to a slightly higher risk of fractures, particularly hip fractures, during extended drug holidays.[36]

Many consider a slightly longer drug holiday duration for zoledronic acid (18–24 months) compared to oral bisphosphonates (no more than 12–24 months for alendronate and perhaps even less for risedronate).[23,24] Indeed, risedronate drug holidays may pose similar risk to alendronate drug holidays for most patients at up to two years, but over three years the risk was 18% higher. However, decisions should be individualized based on the patient's duration of bisphosphonates therapy, fracture risk profile, and overall health status. Regular monitoring and bone health reassessment are crucial to determining the appropriate time to resume therapy to balance the benefits of fracture prevention with the potential adverse event risks of continued bisphosphonate exposure.

Denosumab. Denosumab exhibits distinct effects on bone modeling and remodeling that may contribute to its unique safety profile. Unlike bisphosphonates, denosumab effects on bone remodeling are rapidly reversible, and a partial "escape" of remodeling occurs at the end of denosumab's pharmacologic effect, just before the next dose is due.[37] Moreover, denosumab's effect on BMD may not reach a plateau as seen with bisphosphonates, possibly due to an effect on modeling based bone formation.[38,39] These unique aspects of denosumab's action highlight the complexity of its impact on bone health and underscore the importance of careful timing and monitoring in its long-term use to optimize outcomes while minimizing potential adverse effects.

The problem of rebound following denosumab discontinuation is a significant concern in the management of osteoporosis. On denosumab discontinuation the beneficial effects of this agent are rapidly reversed, leading to a marked increase in bone turnover, that can surpass pretreatment levels. This corresponds to significant loss of BMD and a substantial increase in the risk of fractures, particularly multiple vertebral fractures.[8,40]

At six months after the last denosumab injection, CTX rises rapidly, often exceeding baseline values.[10–12] BMD typically returns to pretreatment levels within one to two years after stopping denosumab, and in some cases, the BMD can even drop below baseline, especially at the hip.[12,40] Those who took denosumab for three or more years and then discontinued had a heightened rate of fractures. The incidence of multiple vertebral fractures was as high as 10% to 15% within the first year after stopping denosumab, even in patients who are subsequently treated with oral bisphosphonates.[40–43] Beyond duration of previous denosumab use, other risk factors for developing vertebral fractures after denosumab discontinuation include a history of prevalent vertebral fractures, a greater gain in BMD during denosumab therapy, and a greater loss of hip BMD after stopping the drug.[41,44] Patients with chronic kidney disease are also at higher risk.[41] The rebound may be caused by an exaggerated hyperactivation of a pool of dormant preosteoclasts and osteomorphs that accumulate during the treatment.[45–48] Additional mechanisms have been proposed to explain this phenomenon, including the depletion of osteoprotegerin-producing osteoblasts and osteocytes, which leaves RANKL activity unopposed on denosumab cessation, leading to excessive osteoclast activation. Furthermore, the mechanostatic reset hypothesis suggests that bone mass accumulated during denosumab treatment exceeds mechanical strain demands, triggering a compensatory loss of bone on discontinuation.[45] Regardless of the risk factors that contribute to the overshoot, a different potent antiresorptive, such as an intravenous bisphosphonate, is recommended after the discontinuation of denosumab.[41] Previous treatment with bisphosphonates also offers some protection against the rebound effect observed on discontinuation of denosumab.[49,50] As noted, bisphosphonates, which remain embedded into the bone matrix for years, continue to inhibit osteoclast activity and very likely dampen the excessive bone resorption typically seen after stopping denosumab.

The rapid and profound rebound in bone turnover could lead to such excessive and uncoordinated remodeling that it results in the perforation of trabeculae, in addition to just their thinning.[51] This mechanism could help explain the observation that multiple vertebral fractures can occur within just a few months of the last denosumab dose, even in patients who had previously achieved substantial gains in BMD. The hypothesis that fracture risk is driven more by the quality of bone microarchitecture, specifically, the preservation of trabecular connectivity, rather than by BMD alone, underscores the importance of stabilizing bone turnover after discontinuing potent antiresorptive therapies such as denosumab. Monitoring BTMs may be as or more important than monitoring BMD in predicting and preventing fractures. If the rebound in turnover could be controlled or mitigated, it might be possible to prevent the catastrophic structural failures that lead to fractures, particularly multiple vertebral fractures. Bisphosphonate treatment before or after denosumab does not always reduce

the BMD loss over the time,[52,53] but it strongly reduces the incidence of multiple vertebral fractures by attenuating the rebound in BTMs.[54–56] Moreover, the Denosumab Adherence Preference Satisfaction trial demonstrated that switching to alendronate after one year of denosumab discontinuation successfully maintained bone mass in 80% to 90% of patients.[57] Furthermore, administering zoledronic acid after two years of denosumab can be effective in mitigating bone loss and maintaining bone density.[58]

The European Calcified Tissue Society (ECTS) provided guidance on managing the discontinuation of denosumab to mitigate the rebound effect.[41] The ECTS strongly recommended initiating an alternative antiresorptive treatment at the time the patient is due for the next denosumab injection. Moreover, in patients who have been taking denosumab for only one year, switching to alendronate has been demonstrated to be effective in preventing rebound bone loss.[57] The most commonly recommended approach is to administer a potent bisphosphonate such as zoledronate six months after the final dose of denosumab. This timing is crucial because it coincides with the period when denosumab's effects start to wane and the risk of rebound increases. The exact timing of bisphosphonate administration following denosumab discontinuation is still an open question.[49] For example, if bisphosphonates are administered too late (ie, more than nine months after the last denosumab injection), the maximum rebound in bone turnover might have already occurred, reducing the efficacy of bisphosphonates in preventing BMD loss and fractures.[52,59] Administration of a pulsatile bisphosphonate too early also might not be maximally effective. Indeed, six months after the last dose of denosumab, many patients still have a closed remodeling phase with less exposed bone available for binding by a bisphosphonate. In patients with prolonged denosumab use, the rebound effect is more pronounced,[40] and a single dose of bisphosphonate might not be sufficient, potentially necessitating additional doses or alternative strategies.

If clinically available, monitoring of BTMs after denosumab discontinuation can help tailor subsequent therapy more effectively. For patients showing significant increases in these markers, rapid BMD loss or not responding to a single dose of zoledronic acid, additional doses may be required. If BTMs are not available, then redosing as soon as three months or as late as six months after the first zoledronic acid dose is prudent. Moreover, the ECTS guidance on denosumab discontinuation may present challenges for implementation in the United States and other health systems due to payment concerns. Specifically, the recommendation for BMD assessment at six months after discontinuation, followed by a zoledronic acid infusion at the same time, is often not covered or reimbursed by some health plans. As an alternative approach, if BTMs remain elevated at 6 months, clinicians could consider adding alendronate for 6 months before administering a second dose of zoledronic acid 12 months after denosumab discontinuation.

An alternative preliminarily tested approach to managing denosumab discontinuation involves gradual dose reduction.[60] Tapering the dose of denosumab (to 30 mg and then 15 mg) could prevent the significant bone loss observed after stopping the standard 60-mg treatment. A combined approach with reduced dose of denosumab paralleled by the administration of a potent antiresorptive such as zoledronic acid could eventually be proven to attenuate rebound.

Beyond ONJ and AFF, denosumab potential adverse events include an increased risk of infections, seen in some but not all denosumab studies and in one metanalysis showing more mostly minor respiratory tract infections.[61,62] Although some studies have suggested a potential increased risk of infections with denosumab, other evidence provides more reassurance. In one population-based cohort, denosumab was not associated with higher rates of hospitalized infections in patients with rheumatoid arthritis receiving a biologic compared to those treated with zoledronic acid.[63]

There is an argument for continuing denosumab in patients who are responding well to treatment, particularly in terms of maintaining or improving BMD and reducing fracture risk. In contrast to bisphosphonates, there is no compelling evidence that denosumab becomes less effective or more dangerous with extended use. Therefore, continuing treatment can be a reasonable and effective strategy for long-term management of osteoporosis. The decision to discontinue denosumab can be considered particularly when the patient's clinical status changes. For example, if a patient experiences a new fracture or if their BMD does not improve despite ongoing denosumab therapy, this could indicate that the treatment is no longer effective. For cases in which denosumab is no longer sufficient to prevent fractures, the best strategy might not be discontinuation or switching but rather the addition of another treatment, such as an osteoanabolic medication, on top of denosumab to increase bone strength and reduce fracture risk.[64–66]

Adding romosozumab to ongoing denosumab treatment in postmenopausal women with severe osteoporosis led to a significant increase in lumbar spine BMD and the bone formation marker procollagen type 1 N-terminal propeptide, compared to continuing denosumab alone.[66] This approach is particularly relevant for patients who had a fracture despite being on long-term denosumab. However, this additive approach to managing osteoporosis in high-risk patients may be constrained in some health care systems by financial barriers to the concomitant use of two expensive antiosteoporotic drugs. The concept of adding treatment rather than discontinuing is further supported by findings showing that combining teriparatide (a parathyroid hormone analog) with denosumab in treatment-naïve patients led to greater increases in BMD than either treatment alone.[67] To date, no study has explored the combination of parathyroid hormone (PTH) analog in patients with ongoing long-term denosumab. A small observational study investigated the addition of teriparatide to ongoing denosumab; however, in that study, teriparatide was

introduced just three months after the initiation of denosumab. This time frame may be insufficient to ensure complete closure of the remodeling surface.[68] Nonetheless, a combination therapy approach could be effective in patients already receiving denosumab, especially those not responding adequately.

In contrast to adding, switching from denosumab to a PTH analog is not recommended. The rebound effect could be amplified by the stimulation of bone remodeling induced by bone anabolic agents, with negative effects on BTMs and BMD.[64] Although switching from denosumab to romosozumab has been shown to partially attenuate the rebound, there have been reports of vertebral fractures after this sequential treatment.[69–73] However, when the treatment duration with denosumab is limited, switching to romosozumab can increase lumbar spine BMD to a greater extent than continuing denosumab alone and CTX rebound was evident as soon as three months after the transition.[74] Figure 2 proposes an algorithm for osteoporosis management in patients on longer-term denosumab, adapted from the ECTS guidance.

Discussion

As the data on bisphosphonate and denosumab efficacy, adverse effects, and the risks and benefits of stopping indicate,

the clinical management of Ms DMS and Ms BPS presents a nuanced challenge. It underscores the importance of individualized osteoporosis therapy, especially concerning long-term antiresorptive treatments.

For Ms DMS, who has been on denosumab for more than eight years, the primary concern revolves around the potential rebound she will experience on discontinuation. A complete clinical evaluation should also assess for any signs of new fractures, height loss, or kyphosis, which may indicate undiagnosed vertebral fractures. Diagnostic testing should include a current BMD assessment via DXA, with comparisons to previous results to evaluate BMD trends. Additionally, measuring bone turnover makers can provide insights into her bone resorption status and treatment adherence. For many patients, particularly those at a higher risk of future fracture, denosumab discontinuation is not encouraged in patients with long-term treatment (>2 years) given the potential for bone loss and the risk of multiple vertebral fractures.

Given her history of vertebral and wrist fractures, and assuming her fracture risk remains high by DXA, the continuation of denosumab may be the most prudent course. If discontinuation is chosen, likely due to her strong preference, transitioning to a potent bisphosphonate such as zoledronic acid is recommended
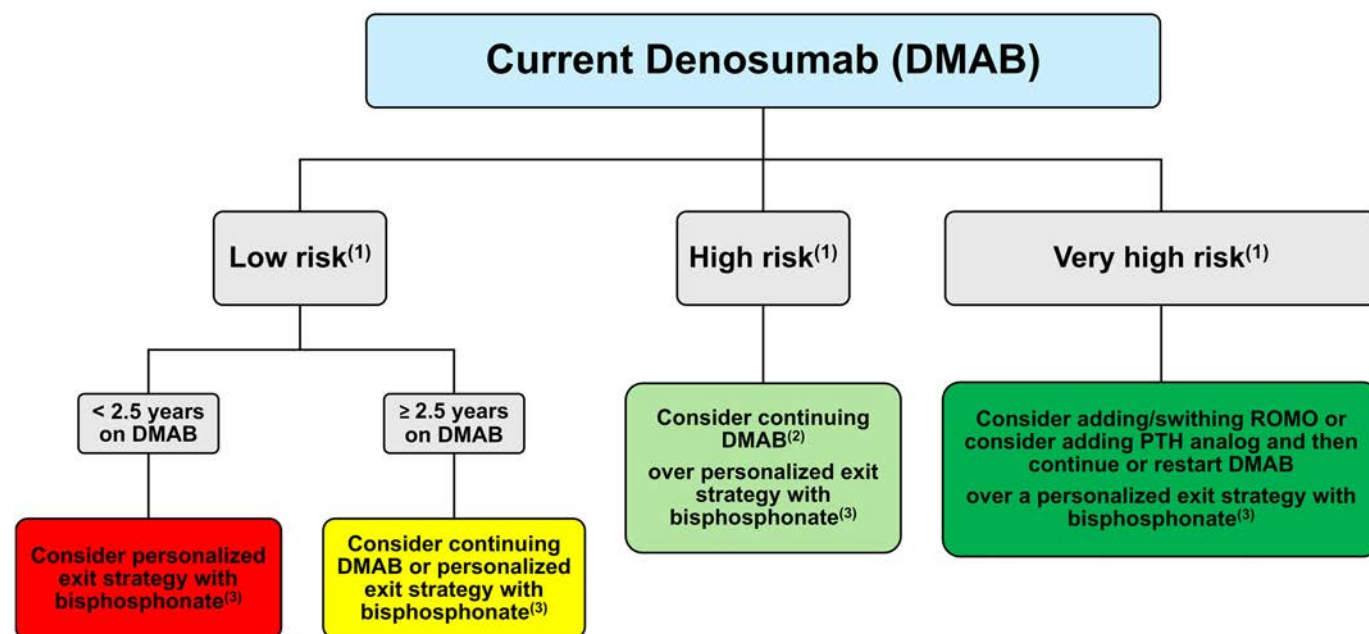
Figure 2. Approach to considering DMAB discontinuation (adapted from Tsourdi et al[41]). (1) Risk–benefit balance should account for the risk for rebound multiple vertebral fractures on DMAB discontinuation. High fracture risk: defined by older age (70–75 years), other strong risk factors for fracture, or validated fracture risk assessment tool fracture risk score that is above country specific thresholds. Very high or imminent fracture risk: defined by recent (within two years) fracture while taking DMAB. (2) DMAB can be used indefinitely but only has been studied for up to 10 years. (3) Exit strategy: usually a potent intravenous bisphosphonate (eg, zoledronic acid) administered when the next dose of DMAB would have been due. A pulsatile bisphosphonate can be repeated based on bone turnover markers or if there is a high risk of rebound associated vertebral fractures. Other exit strategies include oral bisphosphonates or DMAB dose reduction ± bisphosphonates. Combination could be considered based on the results of the Denosumab and Teriparatide Administration study and other observational studies.[64,66,68] DMAB, denosumab; PTH, parathyroid hormone; ROMO, romosozumab. Color figure can be viewed in the online issue, which is available at http://onlinelibrary.wiley.com/doi/10.1002/art.43179/abstract.

to prevent postdenosumab rebound bone loss. Zoledronic acid should initially be administered at the time she is due for her next dose of denosumab. She should optimally have monitoring of BTMs three to six months after this first dose of zoledronic to guide the timing of the need for additional doses. If her BTMs remain elevated or if BTMs are not clinically available, it is reasonable to administer a second dose of zoledronic acid three to six months after her first dose. However, the effectiveness of even this potent bisphosphonate to fully prevent the rebound phenomenon is variable, and she should be counseled about these residual risks. Lastly, an alternative, but arguably minimally tested, approach might be to reduce the dosage of denosumab to 30 mg every 6 months and continue this dosage indefinitely of further reducing the dose to 15 mg and combining with zoledronic acid and then stopping the treatment within 18 months. However, little is known about potential adverse effects of reduced doses and their ability to control the rebound overshoot.

Ms BPS has been taking alendronate for 15 years, a duration of treatment that should be generally discouraged due to the cumulative efficacy of bisphosphonates and concern of rare adverse effects, albeit ones that are more strongly associated with very prolonged bisphosphonate use. A detailed history should explore any previous drug holidays or temporary discontinuation (prescribed or self-administered). This could help to tailor the length of a new, possible drug holiday. Clinical evaluation should include assessment for thigh or groin pain indicative of prodromal symptoms of AFF and oral examination for dental health status that might affect ONJ risk.

Diagnostic evaluation should include a current DXA scan to assess BMD changes over time. If her BMD has remained stable or improved, and her fracture risk is now moderate to low, initiating a drug holiday might be considered. In addition, DXA images sometimes (if the window of interest is slightly lowered) can be used to screen for AFF and may add value. During her drug holiday, she should be under regular monitoring of BMD and BTMs. A significant decline in BMD or a significant increase in BTMs toward baseline levels may indicate the need to resume therapy. The duration of her drug holiday might vary but is typically less than one year.

However, given her history of two vertebral fractures, Ms BPS would be considered by the ASBMR task force to be at higher risk for future fractures. Moreover, the ASBMR guidance suggests that all patients aged >70 to 75 years should be considered at high risk, independently from T score improvement. Thus, continuing bisphosphonate or switching to an alternate bone therapy could be justified despite her very prolonged duration of bisphosphonates. If she is agreeable to transitioning to a nonbisphosphonate therapy, options would include osteoanabolic agents such as teriparatide, abaloparatide, or romosozumab. Romosozumab, in particular, demonstrated significantly greater increases in bone mass and bone strength, as assessed by finite element analysis, compared to teriparatide.[75] We would not

generally favor a selective estrogen receptor modulator in this circumstance after alendronate. If a PTH analog is chosen, she should know that there may be a period of slight and temporary bone loss at cortical sites such as the hip. Of note, an antiresorptive agent would again be recommended at the end of any anabolic treatment. It is important to note that osteoanabolic agents may be less effective after 15 years of bisphosphonate therapy compared to a treatment-naïve patient. Long-term bisphosphonate use significantly suppresses bone turnover and leads to reduced remodeling surfaces, which are necessary for an optimal anabolic response.

Both patients require comprehensive fracture risk assessments incorporating clinical factors, BMD results, and using validated fracture risk calculators or algorithms. This assessment should consider the limitations of these expert panel generated recommendations for drug holidays and should be heavily guided by shared decision-making. It is critical to discuss with these sisters the known benefits of fracture prevention against the risks of longer-term risks of therapy with alendronate and the rebound risk when discontinuing denosumab. The sisters' preferences are paramount, especially when concerns about adverse effects influence their willingness to continue treatment and when the evidence available is not of the highest level.

Conclusions

In conclusion, the management of Ms DMS and Ms BPS should be individualized. The treating clinician must consider their fracture histories, treatment responses, and individual concerns to devise a personalized treatment plan informed by the best available evidence and understanding of the biology of these two effective therapies that, like all drugs and biologics, are not without risk. Close monitoring through clinical evaluations, imaging, and laboratory tests are essential in optimizing osteoporosis care and minimizing the risks associated with osteoporosis therapy modifications.

AUTHOR CONTRIBUTIONS

REFERENCES

1. Black DM, Rosen CJ. Clinical practice. Postmenopausal osteoporosis. N Engl J Med 2016;374(3):254–262.

2. Adami G, Fassio A, Gatti D, et al. Osteoporosis in 10 years time: a glimpse into the future of osteoporosis. Ther Adv Musculoskelet Dis 2022;14:1759720X221083541.

3. Black DM, Cummings SR, Karpf DB, et al; Fracture Intervention Trial Research Group. Randomised trial of effect of alendronate on risk of fracture in women with existing vertebral fractures. Lancet 1996; 348(9041):1535–1541.

4. Harris ST, Watts NB, Genant HK, et al; Vertebral Efficacy With Risedronate Therapy (VERT) Study Group. Effects of risedronate treatment on vertebral and nonvertebral fractures in women with postmenopausal osteoporosis: a randomized controlled trial. JAMA 1999;282(14):1344–1352.

5. Black DM, Delmas PD, Eastell R, et al; HORIZON Pivotal Fracture Trial. Once-yearly zoledronic acid for treatment of postmenopausal osteoporosis. N Engl J Med 2007;356(18):1809–1822.

6. Cummings SR, San Martin J, McClung MR, et al; FREEDOM Trial. Denosumab for prevention of fractures in postmenopausal women with osteoporosis. N Engl J Med 2009;361(8):756–765.

7. Reszka AA, Rodan GA. Mechanism of action of bisphosphonates. Curr Osteoporos Rep 2003;1(2):45–52.

8. Cummings SR, Ferrari S, Eastell R, et al. Vertebral fractures after discontinuation of denosumab: a post hoc analysis of the randomized placebo-controlled FREEDOM trial and its extension. J Bone Miner Res 2018;33(2):190–198.

9. Zanchetta MB, Boailchuk J, Massari F, et al. Significant bone loss after stopping long-term denosumab treatment: a post FREEDOM study. Osteoporos Int 2018;29(1):41–47.

10. Fassio A, Adami G, Benini C, et al. Changes in Dkk-1, sclerostin, and RANKL serum levels following discontinuation of long-term denosumab treatment in postmenopausal women. Bone 2019;123: 191–195.

11. Miller PD, Bolognese MA, Lewiecki EM, et al. Effect of denosumab on bone density and turnover in postmenopausal women with low bone mass after long-term continued, discontinued, and restarting of therapy: a randomized blinded phase 2 clinical trial. Bone 2008;43(2): 222–229.

12. Bone HG, Bolognese MA, Yuen CK, et al. Effects of denosumab treatment and discontinuation on bone mineral density and bone turnover markers in postmenopausal women with low bone mass. J Clin Endocrinol Metab 2011;96(4):972–980.

13. Ahn J, Kim CH, Kim JW. Comparison of bone turnover suppression in atypical femoral fractures and osteoporotic hip fractures. Sci Rep 2024;14(1):19974.

14. Odvina CV, Zerwekh JE, Rao DS, et al. Severely suppressed bone turnover: a potential complication of alendronate therapy. J Clin Endocrinol Metab 2005;90(3):1294–1301.

15. Rossini M, Adami G, Adami S, et al. Safety issues and adverse reactions with osteoporosis management. Expert Opin Drug Saf 2016; 15(3):321–332.

16. Lee K, Kim K, Kim JY, et al. Mechanisms underlying medication-related osteonecrosis of the jaw. Oral Dis 2024. https://doi.org/10.1111/odi.15198.

17. Ural A. Biomechanical mechanisms of atypical femoral fracture. J Mech Behav Biomed Mater 2021;124:104803.

18. Shane E, Burr D, Ebeling PR, et al; American Society for Bone and Mineral Research. Atypical subtrochanteric and diaphyseal femoral fractures: report of a task force of the American Society for Bone and Mineral Research. J Bone Miner Res 2010;25(11):2267–2294.

19. Khan AA, Morrison A, Hanley DA, et al; International Task Force on Osteonecrosis of the Jaw. Diagnosis and management of osteonecrosis of the jaw: a systematic review and international consensus. J Bone Miner Res 2015;30(1):3–23.

20. Leu CT, Luegmayr E, Freedman LP, et al. Relative binding affinities of bisphosphonates for human bone and relationship to antiresorptive efficacy. Bone 2006;38(5):628–636.

21. Black DM, Schwartz AV, Ensrud KE, et al; FLEX Research Group. Effects of continuing or stopping alendronate after 5 years of treatment: the Fracture Intervention Trial Long-term Extension (FLEX): a randomized trial. JAMA 2006;296(24):2927–2938.

22. Schwartz AV, Bauer DC, Cummings SR, et al; FLEX Research Group. Efficacy of continued alendronate for fractures in women with and without prevalent vertebral fracture: the FLEX trial. J Bone Miner Res 2010;25(5):976–982.

23. Hayes KN, Brown KA, Cheung AM, et al. Comparative fracture risk during osteoporosis drug holidays after long-term risedronate versus alendronate therapy: a propensity score-matched cohort study. Ann Intern Med 2022;175(3):335–343.

24. Eastell R, Hannon RA, Wenderoth D, et al. Effect of stopping risedronate after long-term treatment on bone turnover. J Clin Endocrinol Metab 2011;96(11):3367–3373.

25. Black DM, Reid IR, Boonen S, et al. The effect of 3 versus 6 years of zoledronic acid treatment of osteoporosis: a randomized extension to the HORIZON-Pivotal Fracture Trial (PFT). J Bone Miner Res 2012;27(2):243–254.

26. Grey A, Horne A, Gamble G, et al. Ten years of very infrequent zoledronate therapy in older women: an open-label extension of a randomized trial. J Clin Endocrinol Metab 2020;105(4):dgaa062.

27. Lyles KW, Colón-Emeric CS, Magaziner JS, et al; HORIZON Recurrent Fracture Trial. Zoledronic acid and clinical fractures and mortality after hip fracture. N Engl J Med 2007;357(18):1799–1809.

28. Murdoch R, Mellar A, Horne AM, et al. Effect of a three-day course of dexamethasone on acute phase response following treatment with zoledronate: a randomized controlled trial. J Bone Miner Res 2023; 38(5):631–638.

29. Perazella MA, Markowitz GS. Bisphosphonate nephrotoxicity. Kidney Int 2008;74(11):1385–1393.

30. Dixon WG, Solomon DH. Bisphosphonates and esophageal cancer--a pathway through the confusion. Nat Rev Rheumatol 2011; 7(6):369–372.

31. Fazmin IT, Huang CLH, Jeevaratnam K. Bisphosphonates and atrial fibrillation: revisiting the controversy. Ann N Y Acad Sci 2020; 1474(1):15–26.

32. Black DM, Geiger EJ, Eastell R, et al. Atypical femur fracture risk versus fragility fracture prevention with bisphosphonates. N Engl J Med 2020;383(8):743–753.

33. Adler RA, El-Hajj Fuleihan G, et al. Managing osteoporosis in patients on long-term bisphosphonate treatment: report of a task force of the American Society for Bone and Mineral Research. J Bone Miner Res 2016;31(1):16–35.

34. Lewiecki EM, Binkley N, Morgan SL, et al; International Society for Clinical Densitometry. Best practices for dual-energy x-ray absorptiometry measurement and reporting: International Society for Clinical Densitometry guidance. J Clin Densitom 2016;19(2):127–140.

35. Woitge HW, Pecherstorfer M, Li Y, et al. Novel serum markers of bone resorption: clinical assessment and comparison with established urinary indices. J Bone Miner Res 1999;14(5):792–801.

36. Curtis JR, Saag KG, Arora T, et al. Duration of bisphosphonate drug holidays and associated fracture risk. Med Care 2020;58(5):419–426.

37. Bekker PJ, Holloway DL, Rasmussen AS, et al. A single-dose placebo-controlled study of AMG 162, a fully human monoclonal antibody to RANKL, in postmenopausal women. J Bone Miner Res 2004; 19(7):1059–1066.

38. Ikebuchi Y, Aoki S, Honma M, et al. Coupling of bone resorption and formation by RANKL reverse signalling. Nature 2018;561(7722): 195–200.

39. Bone HG, Wagman RB, Brandi ML, et al. 10 years of denosumab treatment in postmenopausal women with osteoporosis: results from the phase 3 randomised FREEDOM trial and open-label extension. Lancet Diabetes Endocrinol 2017;5(7):513–523.

40. Cosman F, Huang S, McDermott M, et al. Multiple vertebral fractures after denosumab discontinuation: FREEDOM and FREEDOM extension trials additional post hoc analyses. J Bone Miner Res 2022; 37(11):2112–2120.

41. Tsourdi E, Zillikens MC, Meier C, et al. Fracture risk and management of discontinuation of denosumab therapy: a systematic review and position statement by ECTS. J Clin Endocrinol Metab 2020. dgaa756.

42. Clifton Goldney D, Pelegrin C, Jerkovich F, et al. Twenty-four months of follow-up in women with rebound-associated vertebral fractures after discontinuation of denosumab: a single-centre case series. Osteoporos Int 2024;35(1):165–171.

43. Florez H, Ramírez J, Monegal A, et al. Spontaneous vertebral fractures after denosumab discontinuation: a case collection and review of the literature. Semin Arthritis Rheum 2019;49(2):197–203.

44. Everts-Graber J, Reichenbach S, Gahl B, et al. Risk factors for vertebral fractures and bone loss after denosumab discontinuation: a real-world observational study. Bone 2021;144:115830.

45. Ferrari S, Langdahl B. Mechanisms underlying the long-term and withdrawal effects of denosumab therapy on bone. Nat Rev Rheumatol 2023;19(5):307–317.

46. Schini M, Gossiel F, Saini T, et al. The effects of denosumab on osteoclast precursors in postmenopausal women: a possible explanation for the overshoot phenomenon after discontinuation. J Bone Miner Res 2025;40(3):301–306.

47. McDonald MM, Khoo WH, Ng PY, et al. Osteoclasts recycle via osteomorphs during RANKL-stimulated bone resorption. Cell 2021;184(5): 1330–1347.e13.

48. Kim AS, Girgis CM, McDonald MM. Osteoclast recycling and the rebound phenomenon following denosumab discontinuation. Curr Osteoporos Rep 2022;20(6):505–515.

49. Chapurlat R. Effects and management of denosumab discontinuation. Joint Bone Spine 2018;85(5):515–517.

50. Burckhardt P, Faouzi M, Buclin T, et al; The Swiss Denosumab Study Group. Fractures after denosumab discontinuation: a retrospective study of 797 cases. J Bone Miner Res 2021;36(9):1717–1728.

51. Drejer LA, El-Masri BM, Ejersted C, et al. Trabecular bone deterioration in a postmenopausal female suffering multiple spontaneous vertebral fractures due to a delayed denosumab injection - a post-treatment re-initiation bone biopsy-based case study. Bone Rep 2023;19:101703.

52. Reid IR, Horne AM, Mihov B, et al. Bone loss after denosumab: only partial protection with zoledronate. Calcif Tissue Int 2017;101(4): 371–374.

53. Lee CC, Wang CY, Yen HK, et al. Zoledronate sequential therapy after denosumab discontinuation to prevent bone mineral density reduction: a randomized clinical trial. JAMA Netw Open 2024;7(11):e2443899.

54. McClung MR, Wagman RB, Miller PD, et al. Observations following discontinuation of long-term denosumab therapy. Osteoporos Int 2017;28(5):1723–1732.

55. Laroche M, Couture G, Ruyssen-Witrand A, et al. Effect of risedronate on bone loss at discontinuation of denosumab. Bone Rep 2020;13: 100290.

56. Sølling AS, Harsløf T, Langdahl B. Treatment with zoledronate subsequent to denosumab in osteoporosis: a 2-year randomized study. J Bone Miner Res 2021;36(7):1245–1254.

57. Kendler DL, McClung MR, Freemantle N, et al; DAPS Investigators. Adherence, preference, and satisfaction of postmenopausal women taking denosumab or alendronate. Osteoporos Int 2011;22(6):1725–1735.

58. Anastasilakis AD, Papapoulos SE, Polyzos SA, et al. Zoledronate for the prevention of bone loss in women discontinuing denosumab treatment. A prospective 2-year clinical trial. J Bone Miner Res 2019; 34(12):2220–2228.

59. Leder BZ, Tsai JN, Jiang LA, et al. Importance of prompt antiresorptive therapy in postmenopausal women discontinuing teriparatide or denosumab: the Denosumab and Teriparatide Follow-up study (DATA-Follow-up). Bone 2017;98:54–58.

60. Laroche M, Couture G, Degboé Y. Discontinuation of denosumab: gradual decrease in doses preserves half of the bone mineral density gain at the lumbar spine. JBMR Plus 2023;7(7):e10731.

61. Huang ST, Chiu TF, Chiu CW, et al. Denosumab treatment and infection risks in patients with osteoporosis: propensity score matching analysis of a national-wide population-based cohort study. Front Endocrinol (Lausanne) 2023;14:1182753.

62. Catton B, Surangiwala S, Towheed T. Is denosumab associated with an increased risk for infection in patients with low bone mineral density? A systematic review and meta-analysis of randomized controlled trials. Int J Rheum Dis 2021;24(7):869–879.

63. Curtis JR, Xie F, Yun H, et al. Risk of hospitalized infection among rheumatoid arthritis patients concurrently treated with a biologic agent and denosumab. Arthritis Rheumatol 2015;67(6):1456–1464.

64. Tsai JN, Uihlein AV, Lee H, et al. Teriparatide and denosumab, alone or combined, in women with postmenopausal osteoporosis: the DATA study randomised trial. Lancet 2013;382(9886):50–56.

65. Kumar S, Gild ML, McDonald MM, et al. A novel sequential treatment approach between denosumab and romosozumab in patients with severe osteoporosis. Osteoporos Int 2024;35(9):1669–1675.

66. Adami G, Pedrollo E, Rossini M, et al. Romosozumab added to ongoing denosumab in postmenopausal osteoporosis, a prospective observational study. JBMR Plus 2024;8(4):ziae016.

67. Leder BZ, Tsai JN, Uihlein AV, et al. Denosumab and teriparatide transitions in postmenopausal osteoporosis (the DATA-Switch study): extension of a randomised controlled trial. Lancet 2015;386(9999): 1147–1155.

68. Idolazzi L, Rossini M, Viapiana O, et al. Teriparatide and denosumab combination therapy and skeletal metabolism. Osteoporos Int 2016; 27(11):3301–3307.

69. Cosman F, Kendler DL, Langdahl BL, et al. Romosozumab and antiresorptive treatment: the importance of treatment sequence. Osteoporos Int 2022;33(6):1243–1256.

70. Kashii M, Ebina K, Kitaguchi K, et al. Romosozumab was not effective in preventing multiple spontaneous clinical vertebral fractures after denosumab discontinuation: a case report. Bone Rep 2020;13: 100288.

71. Miyauchi A, Hamaya E, Shimauchi J, et al. Effectiveness of romosozumab in patients with osteoporosis at high fracture risk: a Japanese real-world study. J Bone Miner Metab 2024;42(1):77–89.

72. Ebina K, Tsuboi H, Nagayama Y, et al. Effects of prior osteoporosis treatment on 12-month treatment response of romosozumab in patients with postmenopausal osteoporosis. Joint Bone Spine 2021; 88(5):105219.

73. Ebina K, Etani Y, Tsuboi H, et al. Effects of prior osteoporosis treatment on the treatment response of romosozumab followed by denosumab in patients with postmenopausal osteoporosis. Osteoporos Int 2022;33(8):1807–1813.

74. Hong N, Shin S, Kim H, et al. Romosozumab following denosumab improves lumbar spine bone mineral density and trabecular bone score greater than denosumab continuation in postmenopausal women. J Bone Miner Res 2025;40(2):184–192.

75. Langdahl BL, Libanati C, Crittenden DB, et al. Romosozumab (sclerostin monoclonal antibody) versus teriparatide in postmenopausal women with osteoporosis transitioning from oral bisphosphonate

therapy: a randomised, open-label, phase 3 trial. Lancet 2017; 390(10102):1585–1594.

76. Roschger P, Lombardi A, Misof BM, et al. Mineralization density distribution of postmenopausal osteoporotic bone is restored to normal after long-term alendronate treatment: qBEI and sSAXS data from the fracture intervention trial long-term extension (FLEX). J Bone Miner Res 2010;25(1):48–55.

77. Bala Y, Farlay D, Chapurlat RD, et al. Modifications of bone material properties in postmenopausal osteoporotic women long-term treated with alendronate. Eur J Endocrinol 2011;165(4):647–655.

78. Ferrari S, Libanati C, Lin CJF, et al. Relationship between bone mineral density T-score and nonvertebral fracture risk over 10 years of denosumab treatment. J Bone Miner Res 2019;34(6):1033–1040.

79. Hong N, Shin S, Lee S, et al. Raloxifene use after denosumab discontinuation partially attenuates bone loss in the lumbar spine in postmenopausal osteoporosis. Calcif Tissue Int 2022;111(1):47–55.

80. Ramchand SK, Tsai JN, Lee H, et al. The Comparison of Alendronate and Raloxifene After Denosumab (CARD) study: a comparative efficacy trial. Osteoporos Int 2024;35(2):255–263.

AMERICAN COLLEGE
of RHEUMATOLOGY
Empowering Rheumatology Professionals

EXPERT PERSPECTIVES ON CLINICAL CHALLENGES

Expert Perspective: Hematologic Malignancies and Vasculitis

Michelle L. Robinette[1] and Hetty E. Carraway[2] (iD)

CLINICAL CHALLENGE

The patient, a 69-year-old man, presents to the emergency department with four days of left pleuritic chest and mid-epigastric abdominal pain associated with low-grade fever and night sweats. He has no cranial or polymyalgia rheumatica symptoms. Computed tomography (CT) of the abdomen and pelvis raises concern for aortitis (Figure 1A). ^{18}F-labeled fluorodeoxyglucose (FDG) positron emission tomography (PET) CT demonstrates increased FDG uptake in the abdominal aorta with surrounding fat stranding and diffuse bone marrow uptake (Figure 1B). Laboratory evaluation finds elevated markers of inflammation, normocytic anemia, monocytosis (2,700 monocytes/μL, 33%), and otherwise unrevealing serologic and infectious studies (Supplemental Table 1). Fifty milligrams of oral prednisone daily is initiated for idiopathic aortitis, with complete resolution of symptoms over weeks and normalization of computed tomography angiogram after the end of the steroid taper five months later. However, after discontinuation of steroid treatment, low-grade fevers and chest pain return with a negative ischemia evaluation. Repeat PET CT demonstrates resolution of prior abdominal FDG uptake but a new focus of uptake in the lower thoracic aorta with associated fat stranding. Laboratory evaluation again reveals monocytosis (2,800 monocytes/μL, 37.8%) and anemia with new thrombocytopenia (Supplemental Table 1). Sixty milligrams of prednisone and interleukin-6 receptor inhibition (IL-6Ri) with 8 mg/kg of intravenous monthly tocilizumab (TCZ) are initiated for large vessel vasculitis (LVV), with symptom resolution.

The patient is referred to a hematology oncologist for bicytopenia and persistent monocytosis. A bone marrow biopsy is performed. Core biopsy and aspirate findings demonstrate markedly hypercellular marrow with left-shifted maturation, erythroid and megakaryocytic dysplasia, and no increase in blasts (<5%)

(Figure 1C and D). A next-generation sequencing (NGS) panel for hematologic malignancy identifies two *TET2* mutations in *trans* as well as *PHF6* and *ASXL1* mutations. Cytogenetics shows normal male karyotype without fusions or rearrangements detected. In the setting of persistently elevated monocyte levels >500 × 10^9/L greater than three months, a diagnosis of chronic myelomonocytic leukemia (CMML) is made, with a plan to monitor given mild cytopenia and no bleeding.[1,2]

BACKGROUND

Systemic vasculitis describes a collection of rare diseases each caused by inflammation of blood vessel walls that can cause severe systemic complications.[3,4] The pattern of vascular inflammation and resultant damage is frequently variable and may be mimicked or directly triggered by infection or malignancy. Myeloid and lymphoid hematologic malignancy have long been recognized in association with vasculitis and were recognized by the 2012 Consensus Conference on the Nomenclature of Systemic Vasculitis as vasculitis associated with probable etiology (cancer-associated).[4] We will refer to this as vasculitis with concomitant hematologic malignancy (VCHM). This is a rapidly evolving field with a limited but growing evidence base. Because of increased use of molecular diagnostics in hematologic clinical practice, rheumatologists should be aware of the diagnostic and treatment complexity in rare patients with VCHM, who often have refractory disease and are at risk of comorbidity from both hematologic and inflammatory disease and their treatments.

Here, we discuss our collaborative approach to diagnosis and management of VCHM shared between rheumatology and hematology/oncology in the context of relatively limited literature. We focus on myeloid neoplasia as a clinically relevant model of

Figure 1. (A) CT abdomen pelvis coronal section shows fat stranding along the suprarenal and infrarenal abdominal aorta (arrowheads) out of proportion to degree of atherosclerosis. (B) PET CT transverse section shows corresponding FDG uptake in circumferential abdominal aorta (arrowhead). (C and D) Hematoxylin and eosin stained bone marrow core biopsy specimen demonstrates hypercellular marrow with limited fat due to granulocytic and monocytic hyperplasia with (D) dysplastic megakaryocytes (black arrows) and peripheral monocytosis consistent with chronic myelomonocytic leukemia. CT, computed tomography; FDG, fluorodeoxyglucose; PET, positron emission tomography.

the emerging recognition of overlap between our fields, with more limited discussion of associations with lymphoid forms of VCHM, such as cryoglobulinemic vasculitis, which have been previously discussed in the literature.[5]

APPROACH

Rheumatology approach to hematologic diagnostic testing in patients with new or suspected vasculitis. *When to consider hematologic malignancy.* We consider hematologic malignancy as part of the broader differential diagnosis in all patients with new imaging or pathologic findings suggestive of vasculitis as a concurrent and potentially underlying diagnosis or a diagnostic mimic, especially when unusual clinical features are present (Table 1). Vasculitis can occur as a "hematoinflammatory" feature across a wide variety of hematologic malignancy and often co-occurs with indolent and lower-risk disease stages monitored in clinic with or without specific disease-modifying treatment.[6] For example, giant cell arteritis (GCA) and Beçhet disease can be associated with myeloid neoplasms such as myelodysplastic syndrome (MDS) or CMML. Furthermore, leukocytoclastic vasculitis (LCV) with chronic monoclonal antibody–producing lymphoid malignancies can be associated with chronic lymphocytic leukemia and/or Waldenström macroglobulinemia. Additionally, polyarteritis nodosa (PAN) and LCV can occur in both myeloid and lymphoid malignancies, with an enrichment of PAN in hairy cell leukemia[7–10] (Supplemental Figure 1).

Patients with hematologic malignancy, especially myeloid neoplasia, can also have other significant inflammatory features. For example, 10% to 45% of individuals with MDS and CMML have concurrent inflammation, with common categories including vasculitis, neutrophilic dermatosis, inflammatory arthritis, and connective tissue disease; nonspecific inflammation, fever, chondritis, crystalline arthritis, inflammatory eye diseases, autoimmune cytopenia, and acquired bleeding diatheses, among others, have also been described.[11–16] Suggesting bidirectional interactions and/or shared risk, antecedent autoimmune disease was likewise found more frequently in patients with MDS (odds ratio [OR] 1.5 and 2.1, respectively) and acute myeloid leukemia (AML) (OR 1.29 and 1.7, respectively) in two large case-control studies using registry data from the United States and Sweden; systemic vasculitis had particularly high effect sizes (OR 6.23–23.8).[17,18]

The pathogenesis of VCHM and other inflammatory features of hematologic malignancy remains an active area of research. Recent genomic mutational analyses have identified some hematopoietic somatic mutations that may determine collective biologic pathways.[6] For example, novel somatic mutations in *UBA1* have been identified as a shared robust monogenic driver of the adult-onset systemic inflammatory syndrome VEXAS which is an acronym for the defining features of the disorder, namely **v**acuoles, **E**1 enzyme, **X**-linked, **a**utoinflammatory, **s**omatic syndrome. Organ manifestations of VEXAS include vasculitis as well as hematologic malignancies such as MDS or plasma cell dyscrasias.[19–21] Additionally, somatic mutations in hematologic malignancy driver genes have recently been identified and associated with forms of vasculitis and worse clinical trajectories, including cryoglobulinemic

Table 1. Examples of hematologic malignancies that may mimic specific forms of vasculitis[*]

Vasculitis	Malignancy	Suggestive features	
		Diagnostic	Clinical
GCA Cranial symptoms: headache, vision changes, high ESR	Hyperviscosity syndrome, Waldenström macroglobulinemia more frequently seen than multiple myeloma	High globulin gap, rouleaux on peripheral smear; very elevated M-spike SPEP, elevated serum viscosity	Mucosal bleeding, central retinal vein occlusion
Temporal arteritis	Myeloproliferative neoplasms, PV, essential thrombocythemia Temporal artery involvement from amyloidosis	Erythrocytosis (PV) Congo red stain of temporal artery biopsy, M-spike SPEP, highly skewed FLC	Pruritus, other clinical clotting, erythromelalgia Macroglossia, carpal tunnel syndrome
IgG4-related disease/ aortitis	Erdheim–Chester disease: periaortic infiltration and sheathing of aortic branches	Biopsy of affected tissue with histiocytic inflammation, bony uptake on bone scintigraphy or FDG-PET, $BRAF^{V600E}$ or $MAPK$ mutations	Bone pain, splenomegaly
			Imaging findings of "hairy kidneys"
Sinonasal granulomatosis with polyangiitis	Extranodal NK/T cell lymphoma (nasal type)	Nasal biopsy, ANCA negative, EBV PCR positive	Perforation of hard palate, hemophagocytic lymphohistiocytosis (HLH)
Eosinophilic granulomatosis with polyangiitis	Myeloproliferative hypereosinophilic syndrome, chronic eosinophilic leukemia, chronic myeloid leukemia, chronic monomyelocytic leukemia with eosinophilia	ANCA negative, increased serum tryptase and B_{12}, cytopenia, absence of vasculitis on tissue biopsy	Splenomegaly
		Diagnosis distinguished by NGS, cytogenetics, FISH, and multiplex PCR	
CNS vasculitis	Primary CNS lymphoma	Brain biopsy	Nonresponse to standard treatment
Retinal vasculitis	Primary intraocular CNS lymphoma	Vitreous or chorioretinal biopsy	
		Both: CSF cytology, β_2-microglobulin, lactose dehydrogenase, IgH rearrangement, and flow cytometry	
Small vessel vasculitis	Intravascular B cell lymphoma	Affected tissue more frequently diagnostic than random skin or cherry angioma biopsy	Unusual pattern of disease, neurologic symptoms may be prominent but not limited to CNS

* ANCA, antineutrophil cytoplasmic antibody; CNS, central nervous system; CSF, cerebrospinal fluid; EBV, Epstein-Barr virus; ESR, erythrocyte sedimentation rate; FDG-PET, fluorodeoxyglucose–positron emission tomography; FISH, fluorescence in situ hybridization; FLC, free light chains; GCA, giant cell arteritis; NGS, next-generation sequencing; NK, natural killer; PCR, polymerase chain reaction; PV, polycythemia vera; SPEP, serum protein electrophoresis.

vasculitis and GCA.[22–26] For the purposes of this review, we will discuss VEXAS separately from MDS, with the recognition that there is a lack of distinction between VEXAS and other hematologic malignancies in the pre-2021 literature.

Approach to diagnostic testing when considering VCHM. <u>Laboratory testing.</u> Because most patients with vasculitis do not have hematologic malignancy, we do not exhaustively test all patients with a new diagnosis of vasculitis with a bone marrow biopsy and flow cytometry, for example. However, we always consider the presteroid complete blood cell count (CBC) with differential and, if available, the historic CBC with differential trend as a vital

piece of diagnostic information to integrate with other diagnostic testing that, from our hematologic evaluation minimally, includes erythrocyte sedimentation rate, C-reactive protein, lactate dehydrogenase (LDH), serum protein electrophoresis (SPEP), serum-free light chains (SFLC), cryoglobulins, C3, and C4 (Figure 2).

Some laboratory abnormalities in patients with vasculitis significantly raise our suspicion for underlying hematologic malignancy and lead us to initiate hematology consultation or referral (Figure 2). Inflammatory diseases such as vasculitis often cause anemia, neutrophil-dominant leukocytosis, and thrombocytosis. In contrast, erythrocytosis, neutropenia, persistent monocytosis or

Figure 2. Flowchart showing evaluation of hematologic abnormalities in patients with known or suspected vasculitis starting with laboratory tests obtained in rheumatology clinical practice. Some hematologic abnormalities, such as anemia and thrombocytosis, are common in patients with vasculitis. Other abnormalities are uncommon and should lead to hematology consultation, with relative level of urgency here depicted by degree of darker shade. ALC, absolute lymphocyte count; AMC, absolute monocyte count; AML, acute myeloid leukemia; ANA, antinuclear antibody; ANC, absolute neutrophil count, APLS, antiphospholipid syndrome; CBC, complete blood cell count; CMP, comprehensive metabolic panel; CMV, cytomegalovirus; CRP, C-reactive protein; CT, computed tomography; EBV, Epstein-Barr virus; EPO, erythropoietin; ESR, erythrocyte sedimentation rate; EtOH, ethanol; FISH, fluorescence in situ hybridization; FLC, free light chains; GC, glucocorticoid; HBV, hepatitis B virus; HCV, hepatitis C virus; Hgb, hemoglobin; HTLV-1, human T lymphotropic virus type 1; INR, international normalized ratio; KIR, killer cell immunoglobulin-like receptor; LDH, lactate dehydrogenase; LFTs, liver function tests; LGL, large granular lymphocyte; MCV, mean cell volume; MMA, methylmalonic acid; NGS, next-generation sequencing; NK, natural killer; PET, positron emission tomography; PLT, platelet count; PNH, paroxysmal nocturnal hemoglobinuria; PT, prothrombin time; PTT, partial thromboplastin time; RBC, red blood cell; RDW, red cell distribution width; RPR, rapid plasma reagin; SFLC, serum free light chain; SPEP, serum protein electrophoresis; TCR, T cell receptor; TSH, thyroid-stimulating hormone; UA, urinalysis; Vit, vitamin. Color figure can be viewed in the online issue, which is available at http://onlinelibrary.wiley.com/doi/10.1002/art.43195/abstract.

lymphocytosis, thrombocytopenia, and especially bicytopenia or pancytopenia are uncommon and merit further evaluation.[23] Eosinophilia is commonly recognized by rheumatologists and has its own broad differential diagnosis, including eosinophilic granulomatosis with polyangiitis, IgG4-related disease, and hematologic mimics (Table 1), as has previously been described.[27] In the absence of lymphocytosis, elevated SPEP and SFLC are more likely to reveal monoclonal gammopathy of uncertain significance (MGUS) than plasma cell dyscrasia. Both these diagnoses increase in prevalence with age and can be followed annually in clinic in the absence of clinical features of hypercalcemia, bone pain, and renal dysfunction. However, together with elevated LDH and cryoglobulin levels and hypocomplementemia, especially of C4 or consistent clinical phenotype (Table 1), these may also support consideration of MGUS- or lymphoid malignancy–associated cryoglobulinemia or amyloidosis (Figure 2). In patients developing vasculitis or perivascular inflammation during treatment of solid tumors, especially with neutrophilia and possibly circulating blasts on CBC, we look for antecedent granulocyte colony stimulating factor (G-CSF) exposure.

Imaging. We approach vasculitis imaging somewhat differently in individuals with known hematologic malignancy or suspicious hematologic laboratory abnormalities. In individuals who have known or suspected LVV or fever of unknown origin phenotype, our diagnostic test of choice is PET CT. PET can be useful to diagnose large and medium vessel vasculitis as well as some forms of hematologic malignancy, particularly lymphomas, and can identify lymphadenopathy or tissue level uptake to guide biopsy.[28,29] Prominent bone marrow uptake is often seen in hematologic malignancy, but this is also a common and nonspecific finding in nonmalignant inflammatory disease and must be considered together with other clinical and laboratory features.[29] In patients with periaortic FDG-avid sheathing that may be reminiscent of IgG4-related disease, imaging features such as "hairy kidneys," bony uptake, or splenomegaly should raise concern for the histiocytic disease Erdheim–Chester disease, caused by somatic mutations in the BRAF/MAPK pathway in myeloid progenitor cells; we have rarely also observed this phenotype in individuals with CMML. Tissue biopsy and hematologic evaluation, including molecular genetic testing, is required to reach diagnosis (Table 1). Based on our experience (as described in our index patient above), we additionally consider hematologic malignancy phenotypically in individuals with LVV and atypical patterns of

vessel involvement such as older adults with abdominal aortitis, waxing and waning perivascular and patchy vascular uptake, or prominent lower extremity disease. In all patients undergoing PET for question of LVV, atherosclerosis is an important LVV mimic; expert radiology review is key.[30] Although we do not initiate hematology referral in the absence of hematologic abnormalities by vascular pattern, we do monitor the CBC with differential with more scrutiny.

Histopathology. We preferentially obtain tissue diagnoses, even if an imaging or clinical diagnosis would have otherwise been accepted in a provider's practice, if evaluation is suggestive of hematologic malignancy or the pattern of disease includes a mimic (Table 1). We consider additional diagnostic testing such as flow cytometry from peripheral blood or lymph node biopsy if lymphadenopathy is prominent, especially if steroid exposure is necessary to treat vasculitis and may obscure a concurrent lymphoid malignancy diagnosis. Of note, the negative predictive value of flow cytometry in the diagnosis of diffuse large B cell lymphoma from peripheral blood is highly limited.[31] For patients who do not respond to therapy as expected and hematologic malignancy was not originally considered, we reconsider a broader differential diagnosis that includes malignancy and often requires a tissue biopsy to pursue definitive diagnosis (Table 1).

When to consider and how to test for VEXAS. Initially described in late 2020, the literature surrounding VEXAS has rapidly evolved and has been extensively reviewed.[6,32] Briefly, VEXAS is caused by somatic hematopoietic mutations in X-linked *UBA1*, encoding the primary ubiquitin-activating enzyme upstream of most cellular ubiquitin conjugation.[19,33] Mutations are enriched at an M41 hotspot and lead to highly penetrant syndromic but variable autoinflammatory and hematologic disease.[19,20,34,35] More recent extension of whole-gene sequencing has demonstrated several mutations across the gene, including recurrent non-M41 mutations in patients with MDS and autoinflammatory phenotype.[33,36–38] Typically affecting men, VEXAS can rarely impact women who have congenital or somatic monosomy X.

The most common forms of vasculitis in VEXAS are PAN and LCV, though other forms of vasculitis have been described in a small retrospective cases series and review of the literature.[21] Other common inflammatory features of disease include fever, chondritis, rash (especially neutrophilic dermatoses), ocular inflammation, pulmonary infiltrates, renal dysfunction, and inflammatory arthritis.[19,34,35] These systemic features are responsive to high-dose steroids but often nonresponsive to most disease-modifying antirheumatic drugs (DMARDs) and biologic therapies.[19,34,35] Common hematologic manifestations include macrocytic anemia, thrombosis, thrombocytopenia, lymphopenia, monocytopenia, vacuoles in erythroid and myeloid progenitors, and incident MDS (∼30%–50%) or plasma cell dyscrasia (∼25%), including MGUS and, less frequently, myeloma.[19,20,39] In a large population-based cohort study of individuals with MDS, 1% had *UBA1* variants (n = 26 of 2,027), of which 44%

were known or likely pathogenic and the remaining were of uncertain significance.[38] In comparison, pathogenic *UBA1* variants were detected in 8% of individuals in a cohort with relapsing polychondritis (n = 7 of 92) and in 0% of men with GCA (n = 0 of 612).

Collectively, we consider VEXAS in patients with robust adult-onset multisystem inflammation with or without vasculitis, especially, though not universally, if cytopenia or macrocytosis is present and the patient is male, with a broader differential diagnosis including myeloid neoplasia with inflammatory features. LVV appears to be an uncommon phenotype. Testing should ideally include whole-gene *UBA1* sequencing, not limited amplicon testing at M41, and is commercially available from companies such as the Genomic Testing Cooperative and Blueprint Genetics. This can currently be performed by rheumatology or hematology/oncology, but in the future, it is most likely to be incorporated into hematologic clinical NGS mutation panels for hematologic malignancy.

Hematology approach to diagnosis and management of suspected VCHM. Hematology consultation should be pursued in patients with vasculitis and cytopenia if counts are severe or trending down despite treatment (Figure 2) or associated with symptoms such as difficult-to-treat or chronic infections, presence of bleeding or bruising, worsening fatigue, and/or B symptoms. Persistent overproduction of cells such as lymphocytosis, erythrocytosis, or, as in this case, monocytosis should also lead to hematology consultation, especially when cytopenia coexists. Hematologists will consider a wide differential diagnosis that includes various hematologic malignancies and a multitude of alternative and potentially reversible diagnoses (Figure 2). For example, monocytosis is most commonly reactive to acute or chronic infection. If no reversible cause is identified or if cytopenia or cytoses persists despite their treatment, further tests are needed, including bone marrow aspirate and biopsy and various context-dependent functional and molecular clonal analyses that may include flow cytometry, NGS, cytogenetics, T cell receptor clonality, and fluorescence in situ hybridization. In our practices, these tests are typically ordered and interpreted by the hematologist or oncologist, given their expertise.

Various forms of myeloid neoplasia can display persistent monocytosis, which may phenotypically overlap histopathology, and are differentiated by molecular diagnostics and, in this case, yield a diagnosis of CMML.[40] NGS has been particularly transformational in diagnosis, risk stratification, and etiologic understanding of hematologic malignancy. Prognostic scoring systems use clinically obtained variables such as NGS mutations, blast percentage, blood cell counts, and transfusion dependency to predict risk of progression of disease to AML and overall survival to help guide clinical interventions.[41,42] Importantly, as our understanding of mutations evolves, clinically obtained NGS panels are often not comprehensive. Thus, it is essential to review what was tested when considering "negative" test results. For example, no panel genetic testing before 2021 included *UBA1* testing. Although not obtained in this case, flow cytometry of peripheral

blood from patients with CMML also often demonstrates an immunophenotypic skew toward CD14^{++}CD16^{+} classical monocytes reaching a threshold of ≥94%, highly suggestive against reactive monocytosis.[2,43,44]

Curative treatment for CMML requires hematopoietic stem cell transplantation (HSCT), which carries its own significant risks of morbidity and mortality.[40] This patient has intermediate-risk CMML by multiple scoring systems. Therapy for lower-risk disease generally includes supportive measures such as transfusions and medications that improve cytopenias, whereas individuals with high symptom burden are increasingly managed with off-label Janus kinase inhibitors (JAKi), especially ruxolitinib (RUX). For higher-risk and/or progressive disease, DNA methyltransferase inhibitors (DNMTi) and HSCT can also be used (Supplemental Table 2).[40] Notably, the clinical presence of autoimmune or inflammatory diseases is not included in risk stratification, and whether autoimmune features of MDS or CMML impacts prognosis is controversial.[14,40,45] Because manifestations are variable, these do not have a standardized treatment approach and are often treated according to type and severity of disease in collaboration with rheumatology.

Our patient. Fevers and chest pain resolve with immunosuppression. At the third infusion of TCZ, cytopenias are noted to worsen, with a white blood cell count of 6,600/μL, a hemoglobin level of 7.8 g/dL, and a platelet count of 80,000/μL, leading to TCZ discontinuation. Prednisone is tapered off over the next several months. Erythroid-stimulating agent therapy is prescribed for persistent macrocytic anemia after a repeat bone marrow aspirate and biopsy confirms no increase in blasts concerning for progression, the erythropoietin level is noted to be 17 mU/mL, and other nutritional test results are normal (Supplemental Table 2).

Use of immunomodulators and chemotherapy in the treatment of VCHM. *What data exist to support the use of immunosuppression or chemotherapy in VCHM?.* The data driving the treatment of patients with inflammatory features of heterogenous hematologic malignancy, including VCHM, are highly limited. Response, as well as lack of response, of vasculitis to either leukemic-focused therapies or immunosuppressive therapies has been described. Furthermore, patients with noncutaneous active or recent prior malignancies were deliberately excluded from transformational vasculitis clinical trials.[46–49] From retrospective case series focused on VCHM, observational data suggest that patients with underlying hematologic malignancy may have more prolonged refractory treatment courses than individuals without known or established hematologic malignancy, especially in patients with small vessel vasculitis.[9,10]

Some therapies, such as cyclophosphamide or B cell depletion with rituximab (RTX), may have shared use in the management of vasculitis and underlying hematologic malignancy, particularly in B cell lymphoproliferative diseases. Standard practice is to treat underlying symptomatic cryoglobulinemia with or without vasculitis by treating the underlying cause, such as hematologic malignancy or any underlying infection (such as hepatitis C virus), as has been described.[5,50] In a single-center retrospective study of 64 patients with cryoglobulinemic vasculitis treated with RTX, 50% of all patients had underlying B cell lymphoproliferative disease. Interestingly, CD20 depletion with both RTX and obinutuzumab has been recognized to trigger vasculitis flares, and 12 of 14 patients with a flare in this study also had underlying malignancy. However, none of these events were of sufficient severity to lead to therapy discontinuation, though additional steroid therapy or chemotherapy was added in some cases.[51]

In myeloid neoplasia, innate immune dysregulation has long been recognized, and some pathways have been targeted for this primary indication. For example, proinflammatory cytokines, including tumor necrosis factor (TNF), IL-1b, and IL-6, are increased in the serum of patients with MDS, AML, and chronic myeloid leukemia and may have prognostic significance because higher TNF levels are associated with inferior prognosis, and lower IL-1b levels are associated with longer survival in MDS.[52–54] Initial small open-label studies (n =2–15) in the early 2000s studying short-term TNF inhibition in MDS had mixed clinical results, with improvements of cytopenia in some patients and worsening in others.[55–57] However, three months of TNF inhibition was overall well tolerated, with the notable finding of high levels of clinically significant infections in neutropenic patients. More recently, identification of recurrently up-regulated inflammatory pathways in high-resolution analyses of patient samples has reinvigorated interest in immunomodulation in myeloid neoplasias and its genetically defined clonal precursors[14] (Supplemental Figure 1), though these immunomodulatory agents are not used therapeutically outside of clinical trials. Exceptions are that some forms of myeloproliferative neoplasms (MPN), including polycythemia vera (PV), essential thrombocytosis (ET), and myelofibrosis, carry US Food and Drug Administration–labeled indications for use of RUX. Therapeutic use has also been described in early-phase trials for symptomatic CMML and VEXAS observational data.[58–61] Similarly, short-term use of IL-6Ri has a labeled indication in cytokine release syndrome (CRS) in the setting of chimeric antigen receptor T cell use and is used off-label for CRS in haploidentical HSCT, with observational data described in VEXAS.

Data describing the use of biologic therapies or chemotherapy to specifically treat myeloid neoplasia–associated VCHM are sparse, with most data from retrospective case series and case-control series from France. In a retrospective MDS/CMML VCHM cohort (n = 70), patients were most often treated with steroids, followed by DMARDs, biologics, and the DNMTi azacytidine (5AC). Relapse of vasculitis was high, near 60%, and was higher for those treated with DMARDs only, though the small number of patients per group limits analyses.[62] Other retrospective data

suggest 5AC may have benefit in treating inflammatory features of MDS/CMML and VEXAS, recently reproduced in a prospective phase 2 trial in which 41% of patients were found post hoc to have VEXAS.[63] However, only a small portion of these patients had vasculitis; seven of eight patients in the retrospective study and two of three patients in the prospective study showed at least a partial response. Of note, molecular clearance of the UBA1-mutated clone has been described with 5AC but not RUX in limited patients with VEXAS.[60,64]

Worsening of cytopenia, infection, and thrombosis are all significant concerns with immunosuppressive treatment, especially with underlying hematologic malignancy. As in allcomers treated with RUX and IL-6Ri, cytopenia, especially thrombocytopenia and neutropenia, is an expected toxicity but can be managed with close monitoring. Myelosuppression is likewise an expected toxicity with the use of DNMTi (Supplemental Table 2). For example, 57% to 91% of patients with MDS treated with 5AC in the AZA-001 study experienced myelosuppression.[65] 5AC and RUX have the most real-world retrospective data in myeloid neoplasia, and both have been associated with clinically significant but manageable infections.[66,67] The comparative effect size of specific medications on infection is difficult to discern given immense heterogeneity. In a more homogenous but smaller population of patients diagnosed with VEXAS in a retrospective multicenter registry from France (n = 74), patients with serious infections had a higher rate of RUX use compared to those using biologics and 5AC. Finally, thrombosis is increased in many patients with VCHM, especially in VEXAS and MPN, such as ET/PV. From the same retrospective French VEXAS registry, thrombosis did occur in patients treated with both JAKi (n = 5 of 78) and IL-6Ri (n = 12 of 51) more often than in patients treated with other biologics (n = 3 of 65). Notably, patients continued therapy significantly longer with IL-6Ri, and especially JAKi, than with other drugs owing to perceived clinical efficacy.[61] Interestingly, in a phase 2 trial evaluating RUX in MPN, RUX treatment surprisingly had no increased risk of the most common thrombotic complication, splanchnic thrombosis.[68] Similarly, in meta-analyses of patients with MPN treated with RUX, there were no increased or decreased rates of thrombosis.[69,70] Mouse models of JAK2-mutated MPN have similarly found reduced NETosis and thrombosis in JAK2^{V617F} mice treated with RUX.[71] Because most patients with VCHM have MDS or CMML rather than other MPN, the relationship between thrombosis and RUX or other immunosuppressive therapies in these conditions, as well as VEXAS, and optimal prophylaxis remains unclear and requires further investigation.

What is our clinical practice? Clinical practice requires collaborative care and shared decision-making between rheumatology and hematology/oncology providers and the patient based on factors such as vasculitis and malignant risks, comorbid diseases, fitness for therapy, and personal preferences. For patients in the community, we recommend referral to tertiary care to facilitate coordinated care. There is considerable evidence that VCHMs

are interconnected and may mutually drive worsening disease states. The challenge for clinicians is to determine which disease to "treat first," with the hope that control of one may mitigate the other with lowest toxicity. It is essential to determine and discuss prognosis of each diagnosis with patients and their loved ones to help them make decisions that impact both clinical outcome and quality of life.

We treat patients with VCHM proportionately to severity of organ manifestations, clarity of diagnosis, and effective therapies available for the type of vasculitis and malignant diagnosis. We aggressively pursue and exonerate infection in patients who may have previously been immunosuppressed from treatment or immune dysfunction related to malignancy, often with support from infectious disease colleagues with expertise in immunocompromised hosts. We do not consider atypical patterns of vascular inflammation to be definitive of infection without evidence thereof.

If vasculitis treatment is required, we use steroids as a backbone of induction therapy and attempt to taper to the lowest tolerated dose (Figure 3). In some individuals with VCHM and current treatment of VEXAS, some maintenance doses of steroids may be required. Although the data are limited, we use pneumocystis prophylaxis in all patients with VCHM taking steroids greater than 20 mg for more than one month. We immunize patients with influenza, COVID-19, pneumococcal, and recombinant zoster vaccines, ideally before treatment. In patients for whom recombinant zoster vaccine has not been given before steroids, we strongly consider valacyclovir prophylaxis, especially if they have had prior episodes of varicella-zoster virus. Given expected neutropenic states with use of JAKi or chemotherapy, we recommend valacyclovir or acyclovir prophylaxis, though data are limited. We screen all patients for tuberculosis and hepatitis B and C serologic tests and initiate appropriate treatment or prophylaxis for positive results.

For patients with B cell malignancies and especially those with cryoglobulinemic vasculitis, we strongly favor using therapies that could treat both malignancy and vasculitis, such as RTX. However, we consider the addition of other immunomodulatory treatments if RTX is ineffective in treating vasculitis despite effective treatment of malignancy, commensurate with degree and phenotype of disease involvement. If neither malignancy nor vasculitis is treated, we favor enhanced malignancy-directed therapy (Figure 3).

Due to significant risks of myelosuppression, infection and negative impact on quality of life from an infusion schedule of DNMTi, steroids or other rheumatic steroid-sparing agents are strongly considered for the treatment of VCHM with concurrent diagnosis of myeloid neoplasia. Importantly, therapeutic decisions in this context will depend on malignancy type and risk of progression (Figure 3). Depending on clinical phenotype, we prefer steroid-sparing agents that have some evidence of safety and mutual benefit in myeloid neoplasia as well as vasculitis, while recognizing comparative data regarding progression of each condition, and adverse events are highly limited. We and others disfavor the use of conventional DMARDs given limited evidence
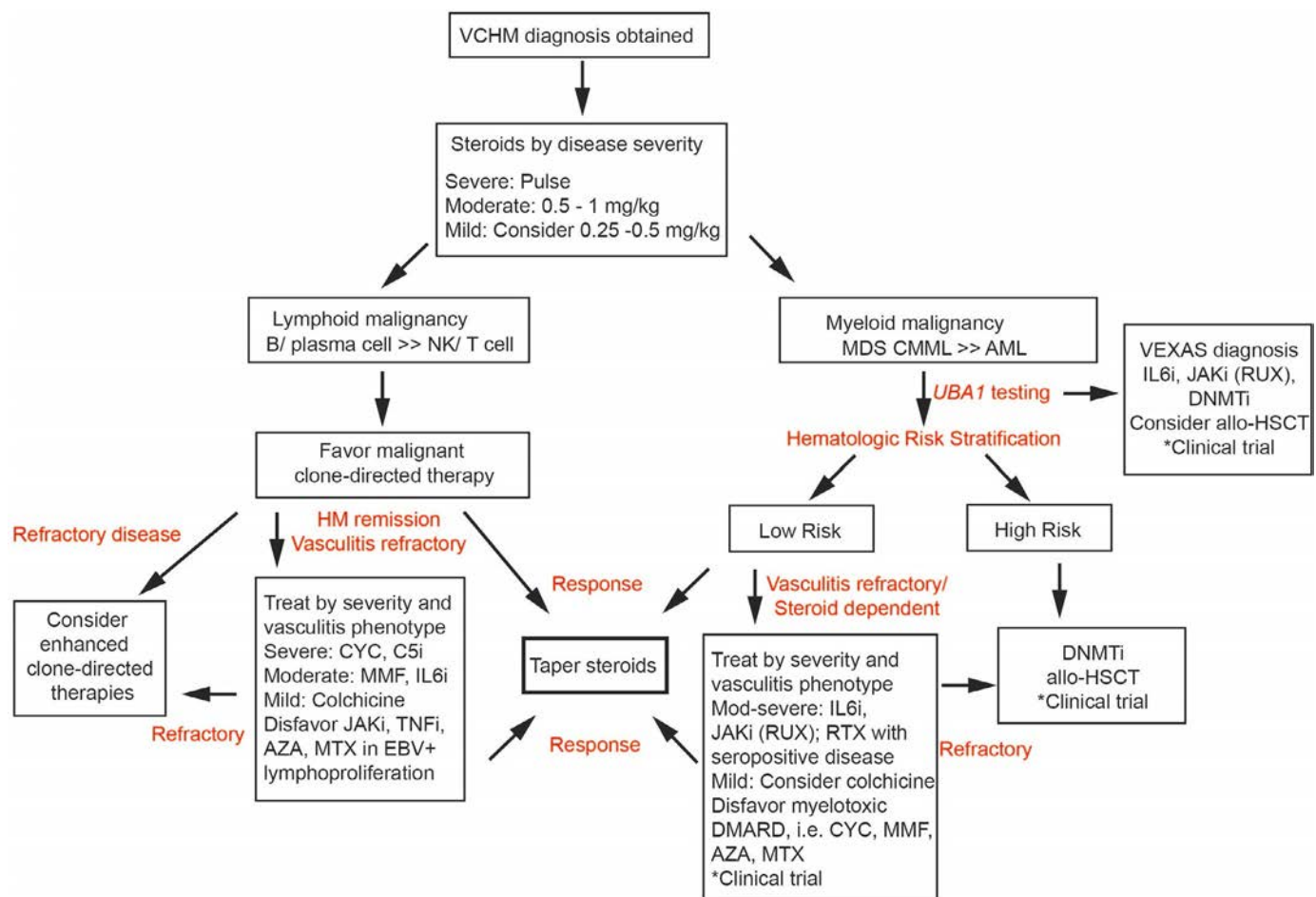
Figure 3. Treatment algorithm of VCHM. Clinical trial availability and patient eligibility are variable but clinical trials are preferred if possible. AML, acute myeloid leukemia; AZA, azathioprine; C5i, complement five inhibitor; CMML, chronic myelomonocytic leukemia; CYC, cyclophosphamide; DMARD, disease-modifying antirheumatic drug; DNMTi, DNA methyltransferase inhibitor; EBV, Epstein-Barr virus; HM, hematologic malignancy; HSCT, hematopoietic stem cell transplantation; IL-6Ri, interleukin-6 receptor inhibition; JAKi, JAK inhibitor; MDS, myelodysplastic syndrome; MMF, mycophenolate mofetil; MTX, methotrexate; NK, natural killer; RTX, rituximab; RUX, ruxolitinib; TNFi, tumor necrosis factor inhibitor; VCHM, vasculitis with concomitant hematologic malignancy; VEXAS, vacuoles, E1 enzyme, X-linked, autoinflammatory, somatic syndrome. Color figure can be viewed in the online issue, which is available at http://onlinelibrary.wiley.com/doi/10.1002/art.43195/abstract.

of efficacy and risk of myelotoxicity.[45] The presence of AML or high-risk disease typically drives the imminent addition of chemotherapy, and VCHM may be bridged with steroid monotherapy, if needed. However, many individuals with VCHM have lower-risk disease and will not meet hematologic criteria for treatment.

In rheumatic treatments, we have the most experience with effective IL-6Ri use in LVV across a host of underlying myeloid neoplasia. We often see progression of thrombocytopenia and neutropenia with IL-6Ri but not typically to a severe range. Rheumatology is reluctant to initiate immunosuppressive medications when the platelet count is approximately <75,000 or absolute neutrophil count (ANC) is approximately <1,000 given the risk of bleeding or infection, though the exclusion criteria for a phase 2 trial of RUX in CMML[59] were a platelet count <35,000 and ANC <250. Hematologists monitor CBC with differential more frequently, such as weekly or bimonthly, in these cases. We may collaboratively tolerate some

thrombocytopenia or neutropenia depending on degree of cytopenia, transfusion needs, response of vasculitis (if there are flares with vascular damage during periods of treatment discontinuation), and availability of alternate treatment options. Reminiscent of the approach to manage other paraneoplastic syndromes with treatment of the underlying disorder, we consider treatment of MDS, CMML, and VEXAS with DNMTi therapy in patients with severe or significant refractory and/or progressive inflammatory manifestations, even in lower-risk patients in whom its use is off-label (Figure 3).

Our patient: continued treatment and testing. Fevers and chest pain return one month after discontinuing steroids. In anticipation of starting 5AC for new transfusion-dependent anemia and relapsing CMML-associated LVV refractory to steroid taper, repeat marrow and NGS mutation panel testing are performed, without substantial changes in atypia, blast

count, or new mutations compared to before. He begins intravenous 5AC infusions (Supplemental Table 2). Initial leukopenia (white blood cell count between 2,000 and 3,000 per μL) is tolerated, and at the end of 10 cycles, he achieves steroid and transfusion independence. A PET CT at one year shows no evidence of LVV, and he has no further vasculitis symptoms. Preferring to avoid upfront HSCT, he eventually transitions to oral decitabine/cedazuridine for the next 2.5 years. Ultimately, his cytopenia progresses, though blasts remain <5%, and he proceeds to curative HSCT.

Longitudinal management in patients with VCHM.

Multidisciplinary care for patients with VCHM. Longitudinal care for patients with VCHM is often complex and poses unique clinical challenges. Patients may develop multiple autoimmune and/or inflammatory features as well as toxicity from disease and/or treatment. Additionally, patients with VCHM tend to be older, and individuals with MDS or CMML additionally have higher population risks for common diseases of aging, including cardiovascular, pulmonary, and metabolic diseases.[72] For patients with new symptoms, we consider a broad differential diagnosis that includes common age-related diseases, as well as uncommon infections, inflammation, and progression of malignancy, and we attempt to obtain objective evidence to differentiate these in a timely matter. For example, patients with CMML have hypersensitivity to granulocyte–macrophage colony-stimulating factor (GM-CSF) and may exhibit leukemoid reactions with infection that can mimic disease progression. Similarly, they may experience robust response to vaccinations, with often self-limited significant arm swelling, erythema, and pain, which can be associated with increased risk for thrombosis. Collaborative care teams beyond rheumatology and hematology/oncology from other disciplines with clinical interest and expertise in sicker patients with unusual manifestations of disease are helpful and may include infectious disease, vascular medicine, neurology, dermatology, pulmonology, nephrology, and radiology, among others. Depending on severity, these may require inpatient admission for expedited multidisciplinary evaluation. Given the complexity of care for patients with VCHM, evaluation in tertiary referral centers to provide multidisciplinary care is recommended.

Rheumatologic role in monitoring and longitudinal management of VCHM. We guide diagnostics to monitor known vasculitis and help evaluate possible multisystem inflammatory disease, which rheumatology is well experienced to diagnose as a specialty focused on systemic disease. We typically observe patients through allogeneic HSCT at clinical visits approximately every one to two months early in the diagnosis, every three months once the disease has stabilized, and at least annually in periods of prolonged remission. For patients with LVV, we favor PET CT to monitor response to therapy and to test for symptomatic flare. Laboratory testing and frequency depends on the pattern of vasculitis and organ system involved but should minimally

include CBC with differential, a complete metabolic panel, and monitoring of affected or symptomatic organ systems. We obtain yearly Ig levels, which, when low, have been associated with increased risk of infection in both myeloid neoplasia and some forms of vasculitis, especially when treated with RTX.[73–75] We anticipate, test, and manage bone mineral density in patients with steroid use.

Hematology/oncology pearls for a rheumatologist in monitoring and longitudinal management of VCHM. The natural history of myeloid neoplasia is eventual progression of disease without treatment. Notably, VEXAS behaves differently from forms of MDS without *UBA1* mutation and rarely progresses to AML.[38] When used, DNMTi are given monthly in repeated cycles, continuing until progression of disease or toxicities prevent continuation (Supplemental Table 2). The benefit of treatment is that about 40% to 50% of patients will have some hematologic response, including ~17% complete remission when the disease is controlled for some time, but progression will eventually occur unless HSCT is feasible. DNMTi treatment requires CBC monitoring, with the expectation that blood cell counts will reach nadir around day 14 after the first day of treatment and will improve around days 21 to 28 just before the subsequent cycle. With this count recovery, some of the symptoms from the VCHM or other inflammatory condition can flare, and it is important to consider steroid-based therapy to manage the symptoms at this cyclical time point until disease control is optimized, typically after cycles three to four.[63] We recommended patients stay on monthly treatment cycles irrespective of count recovery because phase 3 studies have repeatedly shown better response rates with demonstrated adherence to the schedule.[76] For HSCT-eligible patients with inflammatory complications, such as VCHM and VEXAS, the hope is that transplantation can control both disease processes, although specific data around this question are currently limited, with a prospective clinical trial underway in VEXAS.[77]

Implications of the bidirectional relationship in VCHM and future directions.

We hope that as research progresses, we will have more data-driven options to safely, effectively, and perhaps mutually treat VCHM. For example, clinical trials investigating anti-GM-CSF in CMML are ongoing, and a phase 2 trial has also suggested therapeutic effect in GCA.[78] In myeloid neoplasia, it is not clear whether malignancy-directed or vasculitis-directed therapy is superior, especially given the paucity of available agents. Further refinement of the genotype–phenotype patterns of these entities may also guide optimal upfront therapies for patients and likewise generate genetic models to dissect development of vasculitis as well as hematologic malignancy. For example, beyond *UBA1*, the mutations of *TET2* and *IDH1/2* have emerged in association with various inflammatory diseases across the spectrum of precursor clonal genetic lesions to myeloid neoplasia.[12,14,23,79–81] With the increasing development of well-tolerated oral targeted therapies for specific mutations, such as *IDH* inhibitors, these novel agents may

be effective in mutually managing disease, though this currently represents a small portion of patients. Furthermore, there is emerging interest in prevention therapies whereby therapies can be delivered to hematologic precursor lesions, which may be more amenable to immunomodulation or other molecular targeted approaches (Supplemental Figure 1).

Here, we have focused primarily on VCHM, but we know there are other clinical presentations that extend the paradigm that inflammatory disease can overlap, with hematologic malignancies as common presentations of uncommon disease.[14] Accurate identification of the primary malignancy is essential, especially as multiple distinct clones, including in different lineages, are increasingly identified in patients via high-resolution analyses available in clinic (Supplemental Figure 1). For example, patients with rheumatoid arthritis and Felty syndrome can have either a concurrent overlapping diagnosis of MDS, large granular lymphocytic (LGL) leukemia, or MGUS. In this case, determining which clone may be driving disease and symptomatology may change choice of therapy, from DNMTi for MDS to methotrexate or cyclophosphamide for LGL. As new immunomodulatory agents are introduced in solid and hematologic malignancies and cellular therapies likewise transition into clinical trial for rheumatic disease, we anticipate the dual possibility of new inflammatory toxicities and, hopefully, also transformative treatments. Further prospective research is needed to investigate these known and yet unrecognized relationships between NGS mutations, clinical response, toxicity, and inflammatory phenomena in this new era of increasing recognition of interconnection between our fields.

CONCLUSIONS

Hematologic malignancy and systemic vasculitis are uncommon diseases, of which rare subtypes have strong associations. Hematologic malignancy should always be considered in the differential diagnosis of systemic vasculitis as a mimic, concomitant diagnosis, or possible adverse outcome. CBC with differential, PET scan, tissue biopsy, and clonal analyses, especially with NGS, are helpful to discriminate diagnoses and delineate risks. Some somatic mutations, such as UBA1 mutated in VEXAS, are shared drivers of vasculitis and hematologic malignancy. Data regarding treatment of VCHM are limited. Vasculitis-directed therapy and neoplasia-directed therapies may each be effective, and risk of infection is high with both approaches. Care of overlap syndromes benefits from proactive collaboration across multiple disciplines. The underlying etiology of how these disorders are connected remains an area of active research, with the goal to inform best therapies and practices for management. Prospective research focused on the integration of NGS testing into the diagnostic workup of vasculitis and other adult-onset inflammatory diseases will likely lead to advances in the field. Further study may generate mechanistic insights into vasculitis pathogenesis and refine treatment paradigms.

AUTHOR CONTRIBUTIONS

All authors contributed to at least one of the following manuscript preparation roles: conceptualization AND/OR methodology, software, investigation, formal analysis, data curation, visualization, and validation AND drafting or reviewing/editing the final draft. As corresponding author, Dr. Carraway confirms that all authors have provided the final approval of the version to be published and takes responsibility for the affirmations regarding article submission (eg, not under consideration by another journal), the integrity of the data presented, and the statements regarding compliance with institutional review board/Declaration of Helsinki requirements.

REFERENCES

1. Arber DA, Orazi A, Hasserjian RP, et al. International consensus classification of myeloid neoplasms and acute leukemias: integrating morphologic, clinical, and genomic data. Blood 2022;140(11):1200–1228.

2. Khoury JD, Solary E, Abla O, et al. The 5th edition of the World Health Organization classification of haematolymphoid tumours: myeloid and histiocytic/dendritic neoplasms. Leukemia 2022;36(7):1703–1719.

3. Zeek PM. Periarteritis nodosa and other forms of necrotizing angiitis. N Engl J Med 1953;248(18):764–772.

4. Jennette JC, Falk RJ, Bacon PA, et al. 2012 revised International Chapel Hill Consensus Conference Nomenclature of Vasculitides. Arthritis Rheum 2013;65(1):1–11.

5. Muchtar E, Magen H, Gertz MA. How I treat cryoglobulinemia. Blood 2017;129(3):289–298.

6. Grayson PC, Beck DB, Ferrada MA, et al. VEXAS syndrome and disease taxonomy in rheumatology. Arthritis Rheumatol 2022;74(11):1733–1736.

7. Vitale C, Montalbano MC, Salvetti C, et al. Autoimmune complications in chronic lymphocytic leukemia in the era of targeted drugs. Cancers (Basel) 2020;12(2):282.

8. Wooten MD, Jasin HE. Vasculitis and lymphoproliferative diseases. Semin Arthritis Rheum 1996;26(2):564–574.

9. Fain O, Hamidou M, Cacoub P, et al. Vasculitides associated with malignancies: analysis of sixty patients. Arthritis Rheum 2007;57(8):1473–1480.

10. Greer JM, Longley S, Edwards NL, et al. Vasculitis associated with malignancy. Experience with 13 patients and literature review. Medicine (Baltimore) 1988;67(4):220–230.

11. Mekinian A, Grignano E, Braun T, et al. Systemic inflammatory and autoimmune manifestations associated with myelodysplastic syndromes and chronic myelomonocytic leukaemia: a French multicentre retrospective study. Rheumatology (Oxford) 2016;55(2):291–300.

12. Hong LE, Wechalekar MD, Kutyna M, et al. IDH-mutant myeloid neoplasms are associated with seronegative rheumatoid arthritis and innate immune activation. Blood 2024;143(18):1873–1877.

13. Watad A, Kacar M, Bragazzi NL, et al. Somatic mutations and the risk of undifferentiated autoinflammatory disease in MDS: an under-

recognized but prognostically important complication. Front Immunol 2021;12:610019.

14. Belizaire R, Wong WJ, Robinette ML, et al. Clonal haematopoiesis and dysregulation of the immune system. Nat Rev Immunol 2023; 23(9):595–610.

15. Zahid MF, Barraco D, Lasho TL, et al. Spectrum of autoimmune diseases and systemic inflammatory syndromes in patients with chronic myelomonocytic leukemia. Leuk Lymphoma 2017;58(6):1488–1493.

16. Peker D, Padron E, Bennett JM, et al. A close association of autoimmune-mediated processes and autoimmune disorders with chronic myelomonocytic leukemia: observation from a single institution. Acta Haematol 2015;133(2):249–256.

17. Kristinsson SY, Björkholm M, Hultcrantz M, et al. Chronic immune stimulation might act as a trigger for the development of acute myeloid leukemia or myelodysplastic syndromes. J Clin Oncol 2011;29(21): 2897–2903.

18. Anderson LA, Pfeiffer RM, Landgren O, et al. Risks of myeloid malignancies in patients with autoimmune conditions. Br J Cancer 2009; 100(5):822–828.

19. Beck DB, Ferrada MA, Sikora KA, et al. Somatic mutations in *UBA1* and severe adult-onset autoinflammatory disease. N Engl J Med 2020;383(27):2628–2638.

20. Patel N, Dulau-Florea A, Calvo KR. Characteristic bone marrow findings in patients with UBA1 somatic mutations and VEXAS syndrome. Semin Hematol 2021;58(4):204–211.

21. Watanabe R, Kiji M, Hashimoto M. Vasculitis associated with VEXAS syndrome: a literature review. Front Med (Lausanne) 2022;9:983939.

22. Singh M, Jackson KJL, Wang JJ, et al. Lymphoma driver mutations in the pathogenic evolution of an iconic human autoantibody. Cell 2020; 180(5):878–894.e19.

23. Robinette ML, Weeks LD, Kramer RJ, et al; Association of somatic TET2 mutations with giant cell arteritis. Association of somatic TET2 mutations with giant cell arteritis. Arthritis Rheumatol 2024;76(3): 438–443.

24. Gutierrez-Rodrigues F, Wells KV, Jones AI, et al. Clonal haematopoiesis across the age spectrum of vasculitis patients with Takayasu's arteritis, ANCA-associated vasculitis and giant cell arteritis. Ann Rheum Dis 2024;83(4):508–517.

25. Arends CM, Weiss M, Christen F, et al. Clonal hematopoiesis in patients with anti-neutrophil cytoplasmic antibody-associated vasculitis. Haematologica 2020;105(6):e264–e267.

26. Guedon AF, Ouafdi A, Belfeki N, et al. Higher risk profile among patients with TET2-mutated giant cell arteritis: a cluster analysis. RMD Open 2024;10(4):e004694.

27. Klion AD. Approach to the patient with suspected hypereosinophilic syndrome. Hematology Am Soc Hematol Educ Program 2022; 2022(1):47–54.

28. Dejaco C, Ramiro S, Duftner C, et al. EULAR recommendations for the use of imaging in large vessel vasculitis in clinical practice. Ann Rheum Dis 2018;77(5):636–643.

29. Kouijzer IJE, Mulders-Manders CM, Bleeker-Rovers CP, et al. Fever of unknown origin: the value of FDG-PET/CT. Semin Nucl Med 2018; 48(2):100–107.

30. Robinette ML, Rao DA, Monach PA. The immunopathology of giant cell arteritis across disease spectra. Front Immunol 2021;12:623716.

31. Bertram HC, Check IJ, Milano MA. Immunophenotyping large B-cell lymphomas. Flow cytometric pitfalls and pathologic correlation. Am J Clin Pathol 2001;116(2):191–203.

32. Beck DB, Werner A, Kastner DL, et al. Disorders of ubiquitylation: unchained inflammation. Nat Rev Rheumatol 2022;18(8):435–447.

33. Collins JC, Magaziner SJ, English M, et al. Shared and distinct mechanisms of UBA1 inactivation across different diseases. EMBO J 2024; 43(10):1919–1946.

34. Georgin-Lavialle S, Terrier B, Guedon AF, et al; French VEXAS group; GFEV; GFM; CEREMAIA; MINHEMON. Further characterization of clinical and laboratory features in VEXAS syndrome: large-scale analysis of a multicentre case series of 116 French patients. Br J Dermatol 2022;186(3):564–574.

35. Ferrada MA, Savic S, Cardona DO, et al. Translation of cytoplasmic UBA1 contributes to VEXAS syndrome pathogenesis. Blood 2022; 140(13):1496–1506.

36. Sakuma M, Blombery P, Meggendorfer M, et al. Novel causative variants of VEXAS in UBA1 detected through whole genome transcriptome sequencing in a large cohort of hematological malignancies. Leukemia 2023;37(5):1080–1091.

37. Faurel A, Heiblig M, Kosmider O, et al. Recurrent mutations of the active adenylation domain of UBA1 in atypical form of VEXAS syndrome. HemaSphere 2023;7(4):e868.

38. Sirenko M, Bernard E, Creignou M, et al. Molecular and clinical presentation of UBA1-mutated myelodysplastic syndromes. Blood 2024;144(11):1221–1229.

39. Olteanu H, Patnaik M, Koster MJ, et al. Comprehensive morphologic characterization of bone marrow biopsy findings in a large cohort of patients with VEXAS syndrome: a single-institution longitudinal study of 111 bone marrow samples from 52 patients. Am J Clin Pathol 2024;161(6):609–624.

40. Patnaik MM, Tefferi A. Chronic myelomonocytic leukemia: 2024 update on diagnosis, risk stratification and management. Am J Hematol 2024;99(6):1142–1165.

41. Elena C, Gallì A, Such E, et al. Integrating clinical features and genetic lesions in the risk assessment of patients with chronic myelomonocytic leukemia. Blood 2016;128(10):1408–1417.

42. Wassie EA, Itzykson R, Lasho TL, et al. Molecular and prognostic correlates of cytogenetic abnormalities in chronic myelomonocytic leukemia: a Mayo Clinic-French Consortium Study. Am J Hematol 2014; 89(12):1111–1115.

43. Tarfi S, Harrivel V, Dumezy F, et al; Groupe Francophone des Myélodysplasies (GFM). Multicenter validation of the flow measurement of classical monocyte fraction for chronic myelomonocytic leukemia diagnosis. Blood Cancer J 2018;8(11):114.

44. Jestin M, Tarfi S, Duchmann M, et al; Groupe Francophone des Myélodysplasies (GFM). Prognostic value of monocyte subset distribution in chronic myelomonocytic leukemia: results of a multicenter study. Leukemia 2021;35(3):893–896.

45. Zhao LP, Sébert M, Mékinian A, et al. What role for somatic mutations in systemic inflammatory and autoimmune diseases associated with myelodysplastic neoplasms and chronic myelomonocytic leukemias? Leukemia 2023;37(6):1186–1190.

46. Stone JH, Tuckwell K, Dimonaco S, et al. Trial of tocilizumab in giant-cell arteritis. N Engl J Med 2017;377(4):317–328.

47. Stone JH, Merkel PA, Spiera R, et al; RAVE-ITN Research Group. Rituximab versus cyclophosphamide for ANCA-associated vasculitis. N Engl J Med 2010;363(3):221–232.

48. Jones RB, Tervaert JW, Hauser T, et al; European Vasculitis Study Group. Rituximab versus cyclophosphamide in ANCA-associated renal vasculitis. N Engl J Med 2010;363(3):211–220.

49. Wechsler ME, Akuthota P, Jayne D, et al; EGPA Mepolizumab Study Team. Mepolizumab or placebo for eosinophilic granulomatosis with polyangiitis. N Engl J Med 2017;376(20):1921–1932.

50. Dammacco F, Lauletta G, Vacca A. The wide spectrum of cryoglobulinemic vasculitis and an overview of therapeutic advancements. Clin Exp Med 2023;23(2):255–272.

51. Martin de Fremont G, Chiron A, Krzysiek R, et al. Flare of a mixed cryoglobulinaemic vasculitis after obinutuzumab infusion. Clin Exp Rheumatol 2021;39(2 suppl 129):52–55.

52. Kitagawa M, Saito I, Kuwata T, et al. Overexpression of tumor necrosis factor (TNF)-α and interferon (IFN)-γ by bone marrow cells from patients with myelodysplastic syndromes. Leukemia 1997;11(12): 2049–2054.

53. Wetzler M, Kurzrock R, Estrov Z, et al. Altered levels of interleukin-1 beta and interleukin-1 receptor antagonist in chronic myelogenous leukemia: clinical and prognostic correlates. Blood 1994;84(9):3142–3147.

54. Nievergall E, Reynolds J, Kok CH, et al. TGF-α and IL-6 plasma levels selectively identify CML patients who fail to achieve an early molecular response or progress in the first year of therapy. Leukemia 2016; 30(6):1263–1272.

55. Maciejewski JP, Risitano AM, Sloand EM, et al. A pilot study of the recombinant soluble human tumour necrosis factor receptor (p75)-Fc fusion protein in patients with myelodysplastic syndrome. Br J Haematol 2002;117(1):119–126.

56. Deeg HJ, Gotlib J, Beckham C, et al. Soluble TNF receptor fusion protein (etanercept) for the treatment of myelodysplastic syndrome: a pilot study. Leukemia 2002;16(2):162–164.

57. Stasi R, Amadori S. Infliximab chimaeric anti-tumour necrosis factor alpha monoclonal antibody treatment for patients with myelodysplastic syndromes. Br J Haematol 2002;116(2):334–337.

58. Padron E, Dezern A, Andrade-Campos M, et al; Myelodysplastic Syndrome Clinical Research Consortium. A multi-institution phase I trial of ruxolitinib in patients with chronic myelomonocytic leukemia (CMML). Clin Cancer Res 2016;22(15):3746–3754.

59. Hunter AM, Newman H, Dezern AE, et al. Integrated human and murine clinical study establishes clinical efficacy of ruxolitinib in chronic myelomonocytic leukemia. Clin Cancer Res 2021;27(22): 6095–6105.

60. Heiblig M, Ferrada MA, Koster MJ, et al. Ruxolitinib is more effective than other JAK inhibitors to treat VEXAS syndrome: a retrospective multicenter study. Blood 2022;140(8):927–931.

61. Hadjadj J, Nguyen Y, Mouloudj D, et al; FRENVEX. Efficacy and safety of targeted therapies in VEXAS syndrome: retrospective study from the FRENVEX. Ann Rheum Dis 2024;83(10):1358–1367.

62. Roupie AL, Guedon A, Terrier B, et al; On behalf MINHEMON (French Network of dysimmune disorders associated with hemopathies) and SNFMI. Vasculitis associated with myelodysplastic syndrome and chronic myelomonocytic leukemia: French multicenter case-control study. Semin Arthritis Rheum 2020;50(5):879–884.

63. Mekinian A, Zhao LP, Chevret S, et al. A phase II prospective trial of azacitidine in steroid-dependent or refractory systemic autoimmune/inflammatory disorders and VEXAS syndrome associated with MDS and CMML. Leukemia 2022;36(11):2739–2742.

64. Sockel K, Götze K, Ganster C, et al. VEXAS syndrome: complete molecular remission after hypomethylating therapy. Ann Hematol 2024;103(3):993–997.

65. Fenaux P, Mufti GJ, Hellstrom-Lindberg E, et al; International Vidaza High-Risk MDS Survival Study Group. Efficacy of azacitidine compared with that of conventional care regimens in the treatment of higher-risk myelodysplastic syndromes: a randomised, open-label, phase III study. Lancet Oncol 2009;10(3):223–232.

66. Mądry K, Lis K, Biecek P, et al. Predictive model for infection risk in myelodysplastic syndromes, acute myeloid leukemia, and chronic myelomonocytic leukemia patients treated with azacitidine; azacitidine infection risk model: the Polish Adult Leukemia Group Study. Clin Lymphoma Myeloma Leuk 2019;19(5):264–274.e4.

67. Sadjadian P, Wille K, Griesshammer M. Ruxolitinib-associated infections in polycythemia vera: review of the literature, clinical significance, and recommendations. Cancers (Basel) 2020;12(11):3132.

68. Pieri L, Paoli C, Arena U, et al. Safety and efficacy of ruxolitinib in splanchnic vein thrombosis associated with myeloproliferative neoplasms. Am J Hematol 2017;92(2):187–195.

69. Samuelson BT, Vesely SK, Chai-Adisaksopha C, et al. The impact of ruxolitinib on thrombosis in patients with polycythemia vera and myelofibrosis: a meta-analysis. Blood Coagul Fibrinolysis 2016;27(6): 648–652.

70. Masciulli A, Ferrari A, Carobbio A, et al. Ruxolitinib for the prevention of thrombosis in polycythemia vera: a systematic review and meta-analysis. Blood Adv 2020;4(2):380–386.

71. Wolach O, Sellar RS, Martinod K, et al. Increased neutrophil extracellular trap formation promotes thrombosis in myeloproliferative neoplasms. Sci Transl Med 2018;10(436):eaan8292.

72. Weeks LD, Marinac CR, Redd R, et al. Age-related diseases of inflammation in myelodysplastic syndrome and chronic myelomonocytic leukemia. Blood 2022;139(8):1246–1250.

73. Toma A, Fenaux P, Dreyfus F, et al. Infections in myelodysplastic syndromes. Haematologica 2012;97(10):1459–1470.

74. Liberatore J, Nguyen Y, Hadjadj J, et al. Risk factors for hypogammaglobulinemia and association with relapse and severe infections in ANCA-associated vasculitis: a cohort study. J Autoimmun 2024; 142:103130.

75. Barmettler S, Ong MS, Farmer JR, et al. Association of immunoglobulin levels, infectious risk, and mortality with rituximab and hypogammaglobulinemia. JAMA Netw Open 2018;1(7):e184169.

76. Adès L, Girshova L, Doronin VA, et al. Pevonedistat plus azacitidine vs azacitidine alone in higher-risk MDS/chronic myelomonocytic leukemia or low-blast-percentage AML. Blood Adv 2022;6(17):5132–5145.

77. Mohty R, Reljic T, Abdel-Razeq N, et al. Assessing the efficacy of allogeneic hematopoietic cell transplantation in VEXAS syndrome: results of a systematic review and meta-analysis. Bone Marrow Transplant 2024;59(10):1423–1427.

78. Cid MC, Unizony SH, Blockmans D, et al; KPL-301-C001 Investigators. Efficacy and safety of mavrilimumab in giant cell arteritis: a phase 2, randomised, double-blind, placebo-controlled trial. Ann Rheum Dis 2022;81(5):653–661.

79. Zhao LP, Boy M, Azoulay C, et al. Genomic landscape of MDS/CMML associated with systemic inflammatory and autoimmune disease. Leukemia 2021;35(9):2720–2724.

80. Agrawal M, Niroula A, Cunin P, et al. TET2-mutant clonal hematopoiesis and risk of gout. Blood 2022;140(10):1094–1103.

81. Jaiswal S, Natarajan P, Silver AJ, et al. Clonal hematopoiesis and risk of atherosclerotic cardiovascular disease. N Engl J Med 2017;377(2): 111–121.

AMERICAN COLLEGE
of RHEUMATOLOGY
Empowering Rheumatology Professionals

R E V I E W

Gout and NLRP3 Inflammasome Biology

Raewyn Poulsen[1] and Nicola Dalbeth[2] iD

This review describes the three broad stages of acute inflammation in the context of gout: initiation, leucocyte mobilization, and self-resolution. A typical case of a gout flare is presented. The role of the NLRP3 inflammasome in acute monosodium urate crystal–induced inflammation is reviewed in detail. Treatment strategies for gout are outlined in the context of the mechanisms of NLRP3 inflammasome–mediated acute inflammation.

Clinical case

The patient, a 60-year-old man, presents with a six-hour history of right big toe pain and swelling. He awoke overnight with a throbbing sensation in the toe and, over one hour, developed intense pain, redness, heat, and swelling of the first metatarsophalangeal joint. He describes the pain as the worst pain he has ever experienced (9 of 10 in severity). He is unable to move the joint, take weight on his foot, or put on a shoe. The day before, he celebrated his 60th birthday with a round of golf and a large meal. He had an episode of joint pain and swelling in the left ankle six months ago, which was treated with naproxen and resolved after one week. He usually has no joint pain. He has a history of hypertension, hyperlipidemia, and impaired glucose tolerance.

Examination shows that he is distressed with the pain. There is exquisite tenderness, swelling, warmth, and erythema of the right first metatarsophalangeal joint. He is unable to bear weight on the right foot. The other joints examine normally. There is a small white nodule (tophus) on the helix of the left ear.

Laboratory test findings show a C-reactive protein level of 68 mg/L (reference range <5 mg/L) and a neutrophil count of 12.3×10^9/L (reference range $1.9–7.5 \times 10^9$/L). The serum urate level measures 8.0 mg/dL (reference range 3.3–7.0 mg/dL).

Point-of-care ultrasound shows a double contour sign, together with grade 3 synovial hypertrophy and color Doppler signal at the right first metatarsophalangeal joint. At the left first metatarsophalangeal joint, a double contour sign is also present, together with a tophus and adjacent bone erosion at the medial metatarsal head.

[1]Raewyn Poulsen, PhD: Department of Pharmacology, University of Auckland, Auckland, New Zealand; [2]Nicola Dalbeth, MBChB, MD, FRACP, FRSNZ: Department of Medicine, University of Auckland, Auckland, New Zealand.

Histopathology of gout flare

The gout flare represents the prototypical acute inflammatory response. At high concentrations, urate precipitates and is deposited in joints and soft tissues, where it forms crystals of monosodium urate (MSU).[1] Deposition of MSU crystals alone may not cause any symptoms, but these crystals can induce intermittent episodes of acute inflammation (gout flares).[2,3] Hence, the first presentation of gout is often intense pain and inflammation in a joint that persists for several days before self-resolving over one to two weeks.[4] Symptoms of gout flare occur in parallel with a rapid increase in leucocyte numbers in synovial fluid.[3] In the synovial membrane, there is prominent neutrophilic infiltration as well as perivascular infiltration of macrophages, lymphocytes, and small amounts of plasma cells.[5] MSU crystals are often evident within neutrophils and synovial lining cells in synovial fluid,[5] and cell fragments as well as intact neutrophils are present within macrophage phagosomes.[5]

Immune mechanisms of gout flare

Like all acute inflammatory responses, there are three broad stages of gout flare: initiation, leucocyte mobilization, and self-resolution.

Initiation: The central role of NLRP3 inflammasome activation. Activation of the NLRP3 inflammasome and release of mature interleukin-1β (IL-1β) from monocytes and macrophages is central to initiation of gout flare.[6,7] The NLRP3

Address correspondence via email to Nicola Dalbeth, MBChB, MD, FRACP, FRSNZ, at n.dalbeth@auckland.ac.nz.

inflammasome is normally activated in response to tissue damage or pathogen attack. However, MSU crystals can act on some or all of the mechanisms driving NLRP3 inflammasome activation, and this underlies the reason why MSU crystal deposition predisposes to gout flare.[8,9] The NLRP3 inflammasome has been implicated in numerous health conditions. In rheumatology practice, a direct pathogenic role for NLRP3 inflammasome activation has been most convincingly demonstrated in inflammation related to gout,[6] calcium pyrophosphate deposition disease,[6] and cryopyrin-associated periodic syndromes[10] and has been implicated in a range of chronic rheumatic diseases.[7]

The NLRP3 inflammasome is a large multiprotein complex made up of three proteins: NLRP3, which is a cytosolic receptor sensing internal cell stress; ASC, an adapter protein; and caspase 1, the effector protein of the inflammasome. The NLRP3 inflammasome directly drives maturation (activation) and secretion of the inflammatory cytokines IL-1β and IL-18.[6,11]

NLRP3 inflammasome formation is a sequential process involving oligomerization of NLRP3, followed by recruitment of ASC and caspase 1, resulting in formation of a wheel-like structure with caspase 1 at the center[12] (Figure 1A). Mitochondria have a critical role in inflammasome assembly.[13,14] For instance, NLRP3 uses a microtubule-dependent process to translocate from the endoplasmic reticulum toward the mitochondria, where ASC is localized.[13] NLRP3 and ASC assemble together on mitochondria-associated endoplasmic reticulum membranes.[13] Similarly, both caspase 1 and NLRP3 interact with phospholipids in the mitochondrial outer membrane, and this facilitates caspase 1 recruitment to the inflammasome.[14] Caspase 1 is produced in an inactive "pro" form. Incorporation of caspase 1 into the inflammasome results in its activation by self-cleavage.[15]

Both IL-1β and IL-18 are also first produced as inactive proproteins.[16] Caspase 1 is required to produce the biologically active mature cytokines.[16] For instance, caspase 1 specifically cleaves the 31kDa pro-IL-1β protein at Tyr-Val-His-Asp116/Ala117, releasing the 17.5kDa mature IL-1β cytokine.[16] Mature IL-1β and IL-18 are released from monocytes and/or macrophages through membrane pores.[17] These pores are formed by insertion of cleavage products of the protein gasdermin D into the plasma membrane.[17] Gasdermin D pore formation triggers a form of inflammatory cell death called pyroptosis, resulting in the release of cellular contents, including proinflammatory factors as well as factors that promote the eventual resolution of inflammation.[18] Caspase 1 is also the enzyme responsible for cleavage of gasdermin D.[17,19]. Therefore caspase 1 promotes both the maturation and the secretion of IL-1β and IL-18.[12,13,15]

Inflammasome formation and activation is highly regulated. It involves two steps, and in most cases, stimulation by two distinct signals (known as signal 1 and signal 2) is required to initiate both steps, enabling full inflammasome activation.[20]

NLRP3 inflammasome priming. Step 1 involves priming the inflammasome and readying it for activation. During step 1, the production of new inflammasome components is up-regulated because of the activation of NF-κB. NF-κB promotes both *NLRP3*, as well as *pro-IL-1β* transcription.[21] It can be activated by a variety of pathways, including pattern recognition receptors such as toll-like receptors (TLRs) and inflammatory cytokine receptors such as tumor necrosis factor (TNF) receptor and IL-1 receptor.[22]

Aside from increased production of inflammasome components, signal 1 stimuli also promote conditions that facilitate inflammasome assembly and an inflammatory state. For instance, TLR activation leads to a change in energy metabolism pathway usage in macrophages, promoting use of glycolysis, disrupting mitochondrial energy metabolism, and inhibiting the removal of damaged mitochondria, leading to accumulation of mitochondrial reactive oxygen species (mtROS).[23–25] The balance of pathways used for energy metabolism is a critical determinant of macrophage polarization, and high glycolysis usage is required for M1 polarization and an inflammatory response.[26] Priming stimuli also induce pathways, controlling the posttranslational modification of inflammasome components. For instance, TLR activation promotes deubiquitination of NLRP3 by a pathway independent of NF-κB but dependent on mtROS. Deubiquitination alone is insufficient to promote full inflammasome assembly but is essential for enabling NLRP3 oligomerization in the first step of NLRP3 inflammasome assembly.[27]

Normally, NLRP3 inflammasome priming is induced in response to pathogen attack, tissue damage, or inflammatory cytokines in the extracellular environment. TLRs are important for sensing pathogens and tissue damage, and members of the TLR family are activated by stimuli such as the bacterial endotoxin lipopolysaccharide (LPS), single-stranded RNA (present in some viruses), and tissue debris, such as remnants of extracellular matrix components. In the case of gout, MSU crystals can activate TLR (specifically TLR-2 and TLR-4),[8] promote metabolic reprogramming in macrophages leading to increased glycolysis,[28] and induce inflammasome priming.[8] However, their ability to prime the inflammasome is dependent on several factors, including the amount, size, and shape of the crystals.[29] Clinically, both increased MSU crystal deposition due to high urate concentrations and increased crystal dissolution (eg following initiation of urate-lowering therapy) are associated with increased risk of gout flare.[30,31] One of the mechanisms for this increased flare risk may be due to increased availability of MSU crystals in the right form to induce NLRP3 inflammasome priming. Other factors may also facilitate the inflammasome priming ability of MSU crystals. For example, reactive oxygen species (ROS) generation, inflammasome, and IL-1β levels were found to be substantially reduced in germ-free mice following MSU crystal exposure but restored following treatment with acetate, a short-chain fatty acid normally produced by gut microbiota, implicating a potential role of fermentation products of gut microbiota in modulating the proinflammatory effects of MSU crystals.[32] Aside from MSU crystals, various other factors associated with increased risk of gout flare can also induce inflammasome priming. For instance,
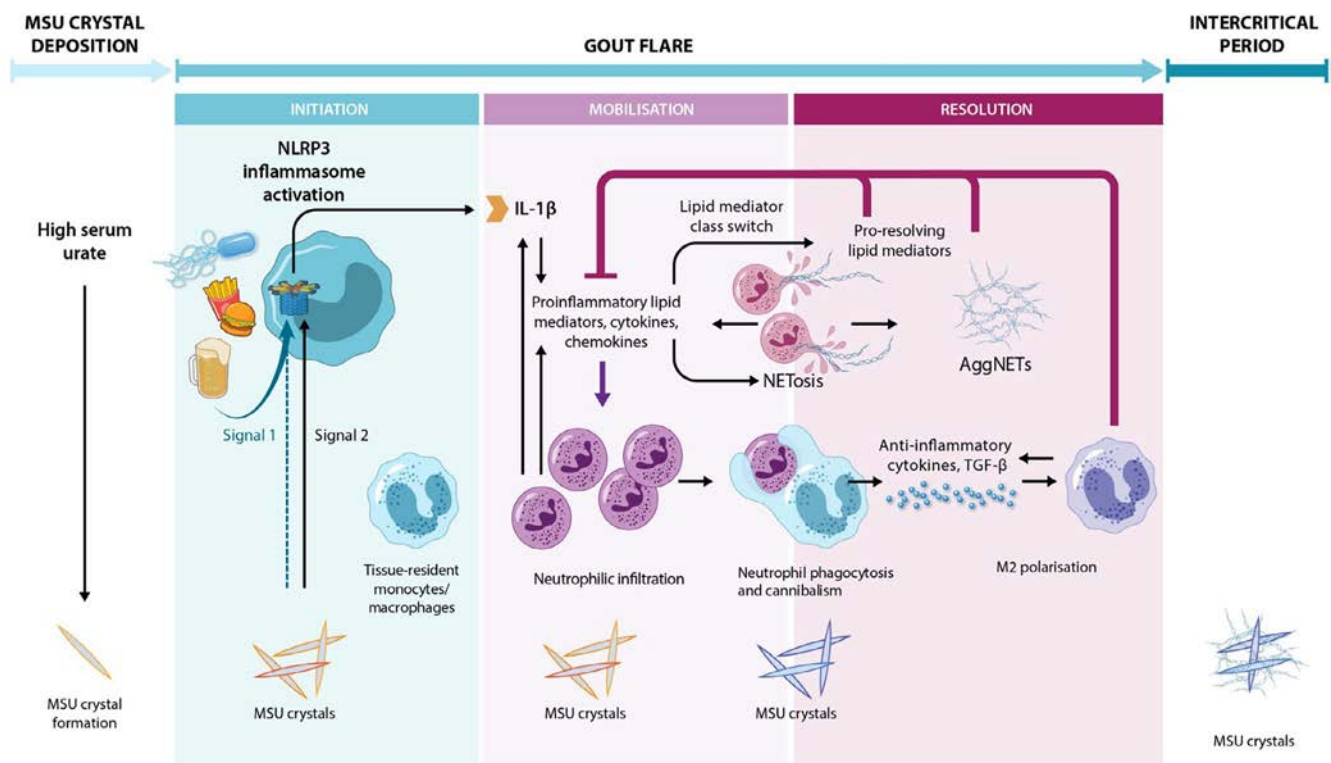
Figure 1. Development and self-resolution of the gout flare. A high urate level leads to deposition of MSU crystals in joints and soft tissues. Gout flares initiate as a result of activation of the NLRP3 inflammasome within tissue-resident monocytes and macrophages. Inflammasome activation requires two signals (signal 1 and signal 2). MSU crystals can serve as both signals; however, they usually act as signal 2 and another factor (eg, alcohol, saturated fatty acids) serves as signal 1. NLRP3 inflammasome activation results in the production of IL-1β, the major inflammatory cytokine driving the gout flare. IL-1β promotes the production of chemokines and other inflammatory mediators promoting mobilization of immune cells, particularly neutrophils, which are recruited to the affected joint. Neutrophils also produce IL-1β as well as other inflammatory cytokines and contribute to the inflammatory response. Neutrophils undergo NETosis, which results in the release of NETs and increased inflammatory cytokine levels. With increasing NET production, NETs form aggregates (AggNETs). AggNETs sequester and degrade inflammatory cytokines, inhibiting the inflammatory response and contributing to resolution of the gout flare. Apoptotic neutrophils are phagocytosed by macrophages and other neutrophils. This also leads to production of anti-inflammatory mediators as well as TGF-β. TGF-β promotes a switch in macrophage polarization to the pro-resolving M2 state. M2 macrophages also produce anti-inflammatory and pro-resolving mediators, contributing to gout flare resolution. High levels of proinflammatory lipid mediators (for instance produced by neutrophils) trigger a class switch in lipid mediator production, resulting in production of pro-resolving rather than proinflammatory mediators. These inhibit further neutrophil recruitment to the joint. During resolution of the gout flare, the composition of the coating of biologic material on MSU crystals within joints alters, and this is likely crucial for maintenance of the intercritical period. IL-1β, interleukin-1β; MSU, monosodium urate; NET, neutrophil elastase trap; TGF-β, transforming growth factor β Color figure can be viewed in the online issue, which is available at http://onlinelibrary.wiley.com/doi/10.1002/art.43215/abstract.

both alcohol and saturated fatty acids activate NF-κB by mechanisms dependent on TLR.[33–36] High urate levels can also promote NF-κB activation.[37] The ability of these factors to prime the inflammasome is likely central to their association with gout flare risk.

NLRP3 inflammasome activation. In most cases, signal 1 alone is insufficient to promote full inflammasome activation, and a second signal is also required. Signal 2 promotes full assembly and activation of the NLRP3 inflammasome. At least part of the mechanism by which this occurs is through further posttranslational modification of inflammasome components.[27] In the case of gout, MSU crystal phagocytosis has been implicated as a major trigger driving step 2 of the NLRP3 inflammasome activation process.[38] However, how this leads to transmission of a signal to promote assembly and activation of the inflammasome componentry is only just beginning to be

understood. In this respect, studies that have examined the processes driving inflammasome activation in response to other stimuli, such as pathogen attack or cell damage, have been instrumental in providing insight into the mechanisms involved in inflammasome assembly and activation in the context of gout. These studies have demonstrated that mtROS generation, cellular ionic imbalance, and extracellular ATP signaling through purinergic receptors drive NLRP3 inflammasome assembly and caspase 1 activation, and this is likely through an interconnected mechanism.[39–42]

Cell damage (particularly mitochondrial dysfunction and mtROS), lysosomal damage, and plasma membrane damage result in perturbation of cellular ion levels, for example, reduced intracellular potassium or chloride or intracellular calcium flux.[39,43] In LPS-primed macrophages, caspase 1 activation and IL-1β

secretion were shown to be induced by the addition of a stimulus, which caused a change in cell osmolarity, indicating that cellular ion imbalance can provide signal 2 for inflammasome activation. A change in cellular ion balance also causes mitochondrial damage and mtROS production[41] and results in compensatory activation of ion channels to restore normal ion balance and maintain cell volume.[44] Activity of these ion channels results in activation of a signaling cascade, which promotes extracellular ATP production and purinergic receptor activation, leading to a calcium-dependent signaling cascade that promotes inflammasome assembly.[44] mtROS also activate calcium signaling to promote NLRP3 inflammasome assembly.[41] Recent evidence indicates that cell volume–regulating ion channels are also activated following MSU crystal exposure, and this contributes to the mechanism by which MSU crystals promote step 2 of the inflammasome activation process.[9] Specifically, MSU crystals were shown to activate leucine-rich repeat–containing 8 (LRRC8) anion channels, which in turn stimulated release of extracellular ATP and purinergic receptor activation, leading to calcium signaling–dependent inflammasome activation as evidenced by IL-1β secretion. Although yet to be demonstrated, it is likely that MSU crystal–induced LRRC8 activation occurs as a consequence of MSU crystal phagocytosis because MSU crystal dissolution within phagosomes is believed to increase intracellular ion load.[9] MSU crystal phagocytosis can also induce lysosomal damage as a result of incomplete breakdown of phagocytosed crystals, leading to cellular ion imbalance.[45] Although ion imbalance has been clearly shown to have a major role in promoting inflammasome assembly and activation in response to MSU crystals, other mechanisms may also contribute, and this remains an evolving area of research.

Rather than just acting in an additive manner, it seems likely that there is synergism between signal 1 and signal 2, and hence the effects of both signals together is more pronounced than the effects of either signal alone. For instance, TLR activation in signal 1 inhibits mitophagy,[24] the normal process by which damaged mitochondria are removed from a cell.[24] This may amplify mtROS generation by signal 2 stimuli by allowing damaged mitochondria to accumulate. Conversely, signal 2 may also enhance sensitivity to priming signals. As an example, some TLRs, such as TLR-2, have been shown to localize to the phagosome in macrophages, are activated by triggers present in the contents of the phagosome, and initiate inflammatory signaling from the internalized phagosome.[46] This raises the possibility that MSU crystal phagocytosis not only provides signal 2 for inflammasome activation but may also sensitize to priming by TLR.

The potential synergism between signal 1 and signal 2 may be particularly relevant in the context of gout flares. MSU crystals are believed to predominantly provide signal 2 for NLRP3 inflammasome activation in gout flare, whereas often another factor (eg, a dietary factor) is believed to serve as signal 1. It is possible that the presence of MSU crystals and/or the gout disease environment may sensitize to priming signals such that a factor that is normally only a weak priming signal for the inflammasome is a stronger stimuli in the context of gout. Several factors relevant to the gout disease environment have been shown to contribute to controlling the propensity for NLRP3 inflammasome activation as well as the extent of inflammation generated. For instance, high urate levels can amplify IL-1 signaling by reducing expression of the endogenous IL-1 receptor antagonist.[47] Therefore, high urate levels may exacerbate the NLRP3 inflammasome–mediated inflammatory response. Low n-3 long-chain polyunsaturated fatty acid (LCPUFA) intake is associated with increased frequency of gout flares,[48] and n-3 LCPUFAs have been shown to suppress the ability of MSU crystals to activate the NLRP3 inflammasome in macrophages.[49] High-density lipoproteins (HDLs) have also been shown to repress MSU crystal–induced inflammation in mice.[50] Whether n-3 LCPUFAs and HDLs act to inhibit signal 1 or 2 specifically or whether they have broader effects on the inflammatory cascade is unclear.

The involvement of mtROS in inflammasome regulation also means that factors that promote mitochondrial damage and ROS generation facilitate inflammasome activation. Of potential relevance to gout, high-calorie consumption causes mitochondrial stress and increased mtROS production.[19,20] Mitochondrial dysfunction and increased mtROS are also inherent features of metabolic syndrome disorders.[51–55] Additionally, increased activity of AMP-activated protein kinase (AMPK), which drives the autophagic clearance of damaged mitochondria,[56] has been shown to repress NLRP3 inflammasome activity and inflammation in in vitro and in vivo models of gouty inflammation.[57,58] AMPK also inhibits glycolysis,[56,59,60], promotes autophagy-mediated degradation of inflammasomes,[61] and promotes M2 macrophage polarization.[57] Therefore, AMPK may act in multiple ways to repress the inflammatory response.

Inflammasome activation results in rapid induction of an inflammatory response, which escalates over time. The initial inflammatory response is due to signal 1 and signal 2 controlling posttranslational modification of pre-existing inflammasome components present within the cell.[17] Escalation of the inflammatory response occurs because of increased production of inflammasome components and hence increased NLRP3 inflammasome activity stimulated by signal 1.[17] This inflammatory response is further amplified during the mobilization phase.[62]

Mobilization: Neutrophilic infiltration. IL-1β has a major role in facilitating the recruitment of other immune cells, particularly neutrophils, to the joint during gout fare.[62] IL-1β triggers production of other inflammatory mediators, for example, IL-6, prostaglandins, and leukotrienes, which together with chemokines promote proliferation and migration of immune cells. Consequently, neutrophils as well as monocytes accumulate within the joint. Like monocytes and macrophages, neutrophils are capable of phagocytosis, including phagocytosis of MSU crystals.[63] They

can also produce IL-1β via the NLRP3 inflammasome. Additionally, neutrophils can produce proteases that can activate IL-1β independent of caspase 1,[64] and this is also important for gout flare inflammation. Inhibition of neutrophil IL-1β–activating proteases by α_1-antitrypsin has been shown to substantially repress inflammation in a murine gout model.[65]

Neutrophils produce high amounts of other inflammatory cytokines, for example, TNFα, IL-6, and IL-8,[63] and high amounts of ROS.[66] Both IL-1β and ROS promote a type of neutrophil cell death termed NETosis. As MSU crystals promote ROS and IL-1β formation, they also promote NETosis.[67,68] NETosis leads to the formation of neutrophil elastase traps (NETs),[69] which are extracellular fiber-like structures made up of components of neutrophil granules, including enzymes, biocidal proteins, and nuclear material.[70] Normally NETs trap and incapacitate pathogens. In gout, NETs trap MSU crystals.[63] Initially, NETosis is proinflammatory, resulting in increased release of proinflammatory mediators.[70] As the inflammatory response progresses, neutrophil numbers and the extent of NET production become so great that the NETs form aggregates (aggNETs).[63] aggNET formation contributes to flare resolution.[63]

Self-resolution. Inflammation is designed to be self-limiting, and even without treatment, gout flares will self-resolve. Many of the mechanisms that stimulate the inflammatory response also activate pathways to resolve it. For instance, caspase 1 self-cleavage activates caspase 1 but also destabilizes it, resulting in its rapid degradation.[15] TLR signaling promotes inflammasome activation but also promotes production of anti-inflammatory cytokines, for example, IL-37. These anti-inflammatory cytokines act by a feedback mechanism to inhibit inflammasome activity.[71] Although MSU crystals can induce NF-κB activation, they also up-regulate expression of peroxisome proliferator–activated receptor γ (PPARγ),[72] a ligand-dependent transcription factor that strongly represses NF-κB target genes.[73]

Neutrophil influx into the joint exacerbates the inflammatory response in gout flare but also promotes resolution. As neutrophils undergo apoptosis at the end of their life cycle, they are phagocytosed by macrophages[74] and other neutrophils,[75] triggering production of anti-inflammatory cytokines and transforming growth factor β1 (TGFβ1).[75] TGFβ1 represses ROS and IL-1β production[75] and up-regulates IL-37, dampening the inflammatory response.[71] TGFβ1 also promotes a switch in macrophage polarization from proinflammatory M1-like macrophages to anti-inflammatory or pro-resolving M2-like macrophages.[76] M2-like macrophages have greater phagocytotic activity, produce lower levels of inflammatory cytokines, and secrete high amounts of anti-inflammatory or pro-repair mediators, such as IL-10 and TGFβ, than M1-like macrophages.[77] M2 macrophages also fail to up-regulate NLRP3 inflammasome expression following stimulation with LPS, a classic TLR activator, indicating that M2 macrophages do not activate the NLRP3 inflammasome in response to stimuli.[78]

aggNET formation also contributes to gout flare resolution. aggNETs sequester and inactivate proinflammatory chemokines and cytokines (including IL-1β), thereby removing the signals that drive further immune cell recruitment to the joint.[63] A class switch in lipid mediator production by cyclooxygenase (COX) and lipoxygenase (LOX) also contributes to reducing signals, promoting immune cell recruitment. Instead of producing proinflammatory prostaglandins and leukotrienes, LOX and COX switch to producing anti-inflammatory lipoxins[79] as well as n-3 LCPUFA–derived anti-inflammatory or pro-resolving lipid mediators, for example, maresins and resolvins.[80,81] Both maresins and resolvins are potent inhibitors of neutrophil migration,[80,81] and synovial fluid levels of pro-resolving lipid mediators are negatively correlated with extent of joint inflammation in gout.[82]

Maintenance of MSU crystals in a noninflammatory state during intercritical gout

Although the symptoms of the flare fully dissipate on resolution, MSU crystals persist in the joint.[83,84] MSU crystal deposits within joints attract a coating of biologic material, at least some of which is due to the trapping of MSU crystals in aggNETs.[63,85] The composition of the MSU crystal coating has been shown to differ considerably during the inflammatory phase of gout flare compared to during flare resolution.[85] The composition of this coating likely influences whether crystals are proinflammatory. In support, type II collagen has been found to be associated with MSU crystals in synovial fluid in individuals with gout following joint injury. This collagen coating promoted MSU crystal–mediated activation of NF-κB by TLR-2.[86] Similarly, coating MSU crystals with serum proteins such as albumin was shown to reduce their ability to induce IL-1β secretion and to cause mitochondrial dysfunction and extracellular ATP secretion.[87] The composition of the coating on MSU crystals therefore may influence their ability to serve as signal 1 and potentially also signal 2 for NLRP3 inflammasome activation. The role of MSU crystals during development, progression, and self-resolution of gout flare, as well as during the intercritical period, is summarized in Figure 1.

Maintenance of MSU crystals in the clinically uninflamed tophus

The tophus presents clinically as a "draining or chalk-like subcutaneous nodule under transparent skin, often with overlying vascularity."[88] In contrast to gout flare, tophi appear clinically uninflamed and nontender. Histopathologically, tophi are organized chronic granulomatous lesions with islands of tightly packed MSU crystals surrounded by a cellular "corona zone," which is in turn encased by an outer fibrovascular zone. In the corona zone, mononucleated and multinucleated macrophages

predominate. Although numerous IL-1β–positive cells are present within the corona zone,[89] it seems likely that other factors contribute to the lack of clinically evident inflammation within these lesions; this may be due to lack of IL-1β released into the extracellular compartment, increased production of anti-inflammatory cytokines or IL-1 inhibitors in vivo, or rapid degradation of IL-1β following its release by aggNETs. The architecture of the tophus, with its collagen-rich fibrovascular zone, may also play a role in separating MSU crystals from other cells and tissues, allowing the crystals to remain in a relatively uninflamed state.

Targeted treatment and prevention of gout flare?

Traditional treatment options for gout flare include colchicine, glucocorticoids, and nonsteroidal anti-inflammatory drugs (NSAIDs). The mechanisms of action of these medications are summarized in Table 1. Despite the different mechanisms of action, in head-to-head clinical trials, traditional therapies have similar clinical efficacy for treatment of gout flare.[90,91]

Colchicine inhibits NLRP3 inflammasome activity and neutrophil mobilization.[92,93] One of the major mechanisms by which it acts is by inhibiting microtubules, which are essential for the transport of NLRP3 components within a cell during inflammasome assembly as well as for cell migration.[93] Colchicine also acts by a wide range of other mechanisms to suppress inflammation, including promoting AMPK activation,[57] inhibiting ROS production by neutrophils, and inhibiting NET formation.[94,95]

Glucocorticoids have wide-ranging effects, acting by both receptor-dependent and receptor-independent mechanisms to inhibit proliferation, migration, and maturation of immune cells and promote their apoptotic death.[96] The glucocorticoid receptor physically associates with NF-κB, inhibiting its activity,[97] and represses transcription of inflammatory pathway genes.[98] Glucocorticoids also regulate energy metabolism, promoting metabolic rewiring in immune cells such as macrophages in favor of mitochondrial energy metabolism pathway use, and this is also a major contributor to their anti-inflammatory effects.[99]

NSAIDs act downstream of NLRP3 inflammasome activation, inhibiting the activity of COX and therefore the production of proinflammatory lipid mediators such as prostaglandin E_2.[100] At high concentrations, various NSAIDs also act as PPARγ agonists, and this may contribute to some of their anti-inflammatory effects.[101,102]

Informed by understanding about the central role of the NLRP3 inflammasome in the pathogenesis of gout flare, IL-1 inhibitors have been tested for treatment of gout flare.[93] Two randomized clinical trials of anakinra (a short-acting IL-1 receptor antagonist) reported clinical efficacy that was similar to the traditional oral therapies for treatment of gout flare.[103,104] In contrast, subcutaneous canakinumab 150 mg, a long-acting human anti–IL-1β monoclonal antibody, had greater efficacy than intramuscular triamcinolone 40 mg in reducing joint pain, swelling, and tenderness during a gout flare.[105] These findings support the importance of IL-1β as the key inflammatory mediator of the initiation and maintenance of gout flare. Although NLRP3 inflammasome inhibitors have been investigated for gout flare treatment in early-phase development,[106] the clinical efficacy and safety of these agents is not yet established.

Once gout flare has been effectively treated in the acute setting, long-term gout management is also required. For people with frequent gout flares (two or more over 12 months), tophaceous gout, or joint damage related to gout, long-term urate-lowering therapy is strongly recommended to maintain a serum

Table 1. Anti-inflammatory mechanisms of medications used to treat gout flares*

Therapeutic class	Anti-inflammatory mechanisms
Colchicine	Inhibits NLRP3 inflammasome activity and neutrophil mobilization[92,93]
	Inhibits microtubule formation (essential for the transport of NLRP3 components during inflammasome assembly and for cell migration[93])
	Promotes AMPK activation[57]
	Reduces expression of adhesion molecules on neutrophils and inhibits neutrophil chemotaxis[108,109]
	Inhibits ROS production by neutrophils[94]
	Inhibits NET formation[95]
Glucocorticoids	Inhibit proliferation, migration, and maturation of immune cells and promote their apoptotic death by numerous mechanisms[96]
	Inhibit NF-κB[97]
	Repress transcription of inflammatory pathway genes[98]
	Promote mitochondrial energy metabolism pathway use[99]
NSAIDs	Inhibit COX and proinflammatory lipid mediator production[100]
	At high concentrations, some NSAIDs act as PPARγ agonists[101,102]
IL-1 inhibitors	Block IL-1 activity by blocking IL-1 from interacting with its receptor (either by binding to the receptor in place of IL-1 [anakinra, a recombinant version of human IL-1 receptor antagonist] or by binding to IL-1β, preventing it from then binding to the receptor [canakinumab, a humanized anti–IL-1β antibody])[110]
	Prevents IL-1 proinflammatory effects (eg, production of other inflammatory mediators such as IL-6 and proinflammatory lipid mediators), reduces signals to promote neutrophilic infiltration[111]

* AMPK, AMP-activated protein kinase; COX, cyclooxygenase; IL, interleukin; NET, neutrophil elastase trap; NSAID, nonsteroidal anti-inflammatory drug; PPARγ, peroxisome proliferator–activated receptor γ; ROS, reactive oxygen species.

urate level below 6 mg/dL and dissolve deposited MSU crystals, which ultimately treats the underlying cause of gout flare and prevents ongoing NLRP3 inflammasome activation.[107] In the first months of initiating urate-lowering therapy, gout flares are common, and these flares can be prevented by low doses of oral colchicine or other anti-inflammatory medications.[31] Consistent with the central role of IL-1β in the initiation of acute MSU crystal–induced inflammation, canakinumab significantly prevented recurrent gout flares over 24 weeks in a randomized controlled trial.[105]

Clinical case follow-up

The diagnosis of a gout flare is made, and the patient is prescribed prednisone 40 mg daily for one week. This treatment results in clinical improvement and full resolution of symptoms over 10 days. In view of his recurrent gout flares and clinical evidence of tophus, urate-lowering therapy is recommended, and allopurinol is started at 100 mg daily and gradually increased to 400 mg daily, which reduces the serum urate level to 5.2 mg/dL. Low-dose colchicine (0.6 mg daily) is also prescribed in the first six months of allopurinol treatment to prevent recurrent gout flares.

The patient continues to experience mild gout flares over the first year of allopurinol treatment, which are rapidly treated by a home supply of prednisone. After three years of allopurinol treatment, he has been free of gout flares for more than a year, and the nodule on his ear has disappeared. He can exercise regularly and enjoys his 63rd birthday without pain!

ACKNOWLEDGMENT

AUTHOR CONTRIBUTIONS

All authors contributed to at least one of the following manuscript preparation roles: conceptualization AND/OR methodology, software, investigation, formal analysis, data curation, visualization, and validation AND drafting or reviewing/editing the final draft. As corresponding author, Dr Dalbeth confirms that all authors have provided the final approval of the version to be published and takes responsibility for the affirmations regarding article submission (eg, not under consideration by another journal), the integrity of the data presented, and the statements regarding compliance with institutional review board/Declaration of Helsinki requirements.

REFERENCES

1. McCarty DJ, Hollander JL. Identification of urate crystals in gouty synovial fluid. Ann Intern Med 1961;54(3):452–460.

2. Dalbeth N, House ME, Aati O, et al. Urate crystal deposition in asymptomatic hyperuricaemia and symptomatic gout: a dual energy CT study. Ann Rheum Dis 2015;74(5):908–911.

3. Faires J, McCarty D Jr. Acute arthritis in man and dog after intrasynovial injection of sodium urate crystals. Lancet 1962;280(7258):682–685.

4. Hench PS. Diagnosis and treatment of gout and gouty arthritis. JAMA 1941;116(6):453–459.

5. Agudelo CA, Schumacher HR. The synovitis of acute gouty arthritis. A light and electron microscopic study. Hum Pathol 1973;4(2):265–279.

6. Martinon F, Pétrilli V, Mayor A, et al. Gout-associated uric acid crystals activate the NALP3 inflammasome. Nature 2006;440(7081):237–241.

7. Hoffman HM, Mueller JL, Broide DH, et al. Mutation of a new gene encoding a putative pyrin-like protein causes familial cold autoinflammatory syndrome and Muckle-Wells syndrome. Nat Genet 2001;29(3):301–305.

8. Liu-Bryan R, Scott P, Sydlaske A, et al. Innate immunity conferred by Toll-like receptors 2 and 4 and myeloid differentiation factor 88 expression is pivotal to monosodium urate monohydrate crystal-induced inflammation. Arthritis Rheum 2005;52(9):2936–2946.

9. Chirayath TW, Ollivier M, Kayatekin M, et al. Activation of osmosensitive LRRC8 anion channels in macrophages is important for micro-crystallin joint inflammation. Nat Commun 2024;15(1):8179.

10. Putnam CD, Broderick L, Hoffman HM. The discovery of NLRP3 and its function in cryopyrin-associated periodic syndromes and innate immunity. Immunol Rev 2024;322(1):259–282.

11. Martinon F, Burns K, Tschopp J. The inflammasome: a molecular platform triggering activation of inflammatory caspases and processing of proIL-β. Mol Cell 2002;10(2):417–426.

12. Lu A, Magupalli VG, Ruan J, et al. Unified polymerization mechanism for the assembly of ASC-dependent inflammasomes. Cell 2014;156(6):1193–1206.

13. Subramanian N, Natarajan K, Clatworthy MR, et al. The adaptor MAVS promotes NLRP3 mitochondrial localization and inflammasome activation. Cell 2013;153(2):348–361.

14. Cassel SL, Elliott E, Iyer SS, et al. Cardiolipin provides a platform for caspase-1 activation and NLRP3 inflammasome assembly [abstract]. J Allergy Clin Immunol 2016;137(2):AB72.

15. Boucher D, Monteleone M, Coll RC, et al. Caspase-1 self-cleavage is an intrinsic mechanism to terminate inflammasome activity. J Exp Med 2018;215(3):827–840.

16. Thornberry NA, Bull HG, Calaycay JR, et al. A novel heterodimeric cysteine protease is required for interleukin-1β processing in monocytes. Nature 1992;356(6372):768–774.

17. Evavold CL, Ruan J, Tan Y, et al. The Pore-forming protein gasdermin d regulates interleukin-1 secretion from living macrophages. Immunity 2018;48(1):35–44.e6.

18. Fink SL, Cookson BT. Caspase-1-dependent pore formation during pyroptosis leads to osmotic lysis of infected host macrophages. Cell Microbiol 2006;8(11):1812–1825.

19. Shi J, Zhao Y, Wang K, et al. Cleavage of GSDMD by inflammatory caspases determines pyroptotic cell death. Nature 2015;526(7575):660–665.

20. Paik S, Kim JK, Silwal P, et al. An update on the regulatory mechanisms of NLRP3 inflammasome activation. Cell Mol Immunol 2021;18(5):1141–1160.

21. Bauernfeind FG, Horvath G, Stutz A, et al. Cutting edge: NF-κB activating pattern recognition and cytokine receptors license NLRP3 inflammasome activation by regulating NLRP3 expression. J Immunol 2009;183(2):787–791.

22. Swanson KV, Deng M, Ting JP. The NLRP3 inflammasome: molecular activation and regulation to therapeutics. Nat Rev Immunol 2019; 19(8):477–489.

23. Balic JJ, Albargy H, Luu K, et al. STAT3 serine phosphorylation is required for TLR4 metabolic reprogramming and IL-1β expression. Nat Commun 2020;11(1):3816.

24. Piao Y, Gwon DH, Kang DW, et al. TLR4-mediated autophagic impairment contributes to neuropathic pain in chronic constriction injury mice. Mol Brain 2018;11(1):11.

25. Zhang H, He F, Zhou L, et al. Activation of TLR4 induces inflammatory muscle injury via mTOR and NF-κB pathways in experimental autoimmune myositis mice. Biochem Biophys Res Commun 2022; 603:29–34.

26. Cheng SC, Quintin J, Cramer RA, et al. mTOR- and HIF-1α-mediated aerobic glycolysis as metabolic basis for trained immunity. Science 2014;345(6204):1250684.

27. Juliana C, Fernandes-Alnemri T, Kang S, et al. Non-transcriptional priming and deubiquitination regulate NLRP3 inflammasome activation. J Biol Chem 2012;287(43):36617–36622.

28. Renaudin F, Orliaguet L, Castelli F, et al. Gout and pseudo-gout-related crystals promote GLUT1-mediated glycolysis that governs NLRP3 and interleukin-1β activation on macrophages. Ann Rheum Dis 2020;79(11):1506–1514.

29. Chen C, Wang J, Liang Z, et al. Monosodium urate crystals with controlled shape and aspect ratio for elucidating the pathological progress of acute gout. Biomater Adv 2022;139:213005.

30. Pascart T, Grandjean A, Capon B, et al. Monosodium urate burden assessed with dual-energy computed tomography predicts the risk of flares in gout: a 12-month observational study: MSU burden and risk of gout flare. Arthritis Res Ther 2018;20(1):210.

31. Stamp L, Horne A, Mihov B, et al. Is colchicine prophylaxis required with start-low go-slow allopurinol dose escalation in gout? A non-inferiority randomised double-blind placebo-controlled trial. Ann Rheum Dis 2023;82(12):1626–1634.

32. Vieira AT, Macia L, Galvão I, et al. A role for gut microbiota and the metabolite-sensing receptor GPR43 in a murine model of gout. Arthritis Rheumatol 2015;67(6):1646–1656.

33. Kong EQZ, Subramaniyan V, Lubau NSA. Uncovering the impact of alcohol on internal organs and reproductive health: exploring TLR4/NF-kB and CYP2E1/ROS/Nrf2 pathways. Animal Model Exp Med 2024;7(4):444–459.

34. Expression of concern: Wang F, Yang JL, Yu KK, et al. Activation of the NF-κB pathway as a mechanism of alcohol enhanced progression and metastasis of human hepatocellular carcinoma. Mol Cancer 2015;14(1):10. *Mol Cancer* 2022;21(1):222. doi: 10.1186/s12943-022-01693-8.

35. Hall CJ, Sanderson LE, Lawrence LM, et al. Blocking fatty acid-fueled mROS production within macrophages alleviates acute gouty inflammation. J Clin Invest 2018;128(5):1752–1771.

36. Joosten LA, Netea MG, Mylona E, et al. Engagement of fatty acids with Toll-like receptor 2 drives interleukin-1β production via the ASC/caspase 1 pathway in monosodium urate monohydrate crystal-induced gouty arthritis. Arthritis Rheum 2010;62(11):3237–3248.

37. Crişan TO, Cleophas MCP, Novakovic B, et al. Uric acid priming in human monocytes is driven by the AKT-PRAS40 autophagy pathway. Proc Natl Acad Sci USA 2017;114(21):5485–5490.

38. Hornung V, Bauernfeind F, Halle A, et al. Silica crystals and aluminum salts activate the NALP3 inflammasome through phagosomal destabilization. Nat Immunol 2008;9(8):847–856.

39. Triantafilou K, Hughes TR, Triantafilou M, et al. The complement membrane attack complex triggers intracellular Ca^{2+} fluxes leading to NLRP3 inflammasome activation. J Cell Sci 2013;126(Pt 13): 2903–2913.

40. Zhou R, Yazdi AS, Menu P, et al. A role for mitochondria in NLRP3 inflammasome activation. Nature 2011;469(7329):221–225.

41. Yang Y, Wang H, Kouadir M, et al. Recent advances in the mechanisms of NLRP3 inflammasome activation and its inhibitors. Cell Death Dis 2019;10(2):128.

42. Beckwith KS, Beckwith MS, Ullmann S, et al. Plasma membrane damage causes NLRP3 activation and pyroptosis during *Mycobacterium tuberculosis* infection. Nat Commun 2020;11(1):2270.

43. Deng M, Guo H, Tam JW, et al. Platelet-activating factor (PAF) mediates NLRP3-NEK7 inflammasome induction independently of PAFR. J Exp Med 2019;216(12):2838–2853.

44. Compan V, Baroja-Mazo A, López-Castejón G, et al. Cell volume regulation modulates NLRP3 inflammasome activation. Immunity 2012;37(3):487–500.

45. Maejima I, Takahashi A, Omori H, et al. Autophagy sequesters damaged lysosomes to control lysosomal biogenesis and kidney injury. EMBO J 2013;32(17):2336–2347.

46. Underhill DM, Ozinsky A, Hajjar AM, et al. The Toll-like receptor 2 is recruited to macrophage phagosomes and discriminates between pathogens. Nature 1999;401(6755):811–815.

47. Crişan TO, Cleophas MC, Oosting M, et al. Soluble uric acid primes TLR-induced proinflammatory cytokine production by human primary cells via inhibition of IL-1Ra. Ann Rheum Dis 2016;75(4): 755–762.

48. Abhishek A, Valdes AM, Doherty M. Low omega-3 fatty acid levels associate with frequent gout attacks: a case control study. Ann Rheum Dis 2016;75(4):784–785.

49. Yan Y, Jiang W, Spinetti T, et al. Omega-3 fatty acids prevent inflammation and metabolic disorder through inhibition of NLRP3 inflammasome activation. Immunity 2013;38(6):1154–1163.

50. Scanu A, Luisetto R, Oliviero F, et al. High-density lipoproteins inhibit urate crystal-induced inflammation in mice. Ann Rheum Dis 2015; 74(3):587–594.

51. Kelley DE, He J, Menshikova EV, et al. Dysfunction of mitochondria in human skeletal muscle in type 2 diabetes. Diabetes 2002;51(10): 2944–2950.

52. Heilbronn LK, Gan SK, Turner N, et al. Markers of mitochondrial biogenesis and metabolism are lower in overweight and obese insulin-resistant subjects. J Clin Endocrinol Metab 2007;92(4):1467–1473.

53. Xia W, Veeragandham P, Cao Y, et al. Obesity causes mitochondrial fragmentation and dysfunction in white adipocytes due to RalA activation. Nat Metab 2024;6(2):273–289.

54. Eirin A, Lerman A, Lerman LO. Mitochondrial injury and dysfunction in hypertension-induced cardiac damage. Eur Heart J 2014;35(46): 3258–3266.

55. Yao YS, Li TD, Zeng ZH. Mechanisms underlying direct actions of hyperlipidemia on myocardium: an updated review. Lipids Health Dis 2020;19(1):23.

56. Herzig S, Shaw RJ. AMPK: guardian of metabolism and mitochondrial homeostasis. Nat Rev Mol Cell Biol 2018;19(2):121–135.

57. Wang Y, Viollet B, Terkeltaub R, et al. AMP-activated protein kinase suppresses urate crystal-induced inflammation and transduces colchicine effects in macrophages. Ann Rheum Dis 2016;75(1): 286–294.

58. McWherter C, Choi YJ, Serrano RL, et al. Arhalofenate acid inhibits monosodium urate crystal-induced inflammatory responses through activation of AMP-activated protein kinase (AMPK) signaling. Arthritis Res Ther 2018;20(1):204.

59. Kishton RJ, Barnes CE, Nichols AG, et al. AMPK is essential to balance glycolysis and mitochondrial metabolism to control T-ALL cell stress and survival. Cell Metab 2016;23(4):649–662.

60. Egan DF, Shackelford DB, Mihaylova MM, et al. Phosphorylation of ULK1 (hATG1) by AMP-activated protein kinase connects energy sensing to mitophagy. Science 2011;331(6016):456–461.

61. Zhao B, Qiang L, Joseph J, et al. Mitochondrial dysfunction activates the AMPK signaling and autophagy to promote cell survival. Genes Dis 2016;3(1):82–87.

62. Amaral FA, Costa VV, Tavares LD, et al. NLRP3 inflammasome-mediated neutrophil recruitment and hypernociception depend on leukotriene B$_4$ in a murine model of gout. Arthritis Rheum 2012; 64(2):474–484.

63. Schauer C, Janko C, Munoz LE, et al. Aggregated neutrophil extracellular traps limit inflammation by degrading cytokines and chemokines. Nat Med 2014;20(5):511–517.

64. Coeshott C, Ohnemus C, Pilyavskaya A, et al. Converting enzyme-independent release of tumor necrosis factor α and IL-1β from a stimulated human monocytic cell line in the presence of activated neutrophils or purified proteinase 3. Proc Natl Acad Sci USA 1999; 96(11):6261–6266.

65. Joosten LA, Crişan TO, Azam T, et al. Alpha-1-anti-trypsin-Fc fusion protein ameliorates gouty arthritis by reducing release and extracellular processing of IL-1β and by the induction of endogenous IL-1Ra. Ann Rheum Dis 2016;75(6):1219–1227.

66. Bylund J, Samuelsson M, Collins LV, et al. NADPH-oxidase activation in murine neutrophils via formyl peptide receptors. Exp Cell Res 2003;282(2):70–77.

67. Schorn C, Janko C, Krenn V, et al. Bonding the foe - NETting neutrophils immobilize the pro-inflammatory monosodium urate crystals. Front Immunol 2012;3:376.

68. Sil P, Wicklum H, Surell C, et al. Macrophage-derived IL-1β enhances monosodium urate crystal-triggered NET formation. Inflamm Res 2017;66(3):227–237.

69. Lin S, Zhu P, Jiang L, et al. Neutrophil extracellular traps induced by IL-1β promote endothelial dysfunction and aggravate limb ischemia. Hypertens Res 2024;47(6):1654–1667.

70. Brinkmann V, Reichard U, Goosmann C, et al. Neutrophil extracellular traps kill bacteria. Science 2004;303(5663):1532–1535.

71. Nold MF, Nold-Petry CA, Zepp JA, et al. IL-37 is a fundamental inhibitor of innate immunity. Nat Immunol 2010;11(11):1014–1022.

72. Akahoshi T, Namai R, Murakami Y, et al. Rapid induction of peroxisome proliferator-activated receptor γ expression in human monocytes by monosodium urate monohydrate crystals. Arthritis Rheum 2003;48(1):231–239.

73. Pascual G, Fong AL, Ogawa S, et al. A SUMOylation-dependent pathway mediates transrepression of inflammatory response genes by PPAR-γ. Nature 2005;437(7059):759–763.

74. Savill JS, Wyllie AH, Henson JE, et al. Macrophage phagocytosis of aging neutrophils in inflammation. Programmed cell death in the neutrophil leads to its recognition by macrophages. J Clin Invest 1989; 83(3):865–875.

75. Steiger S, Harper JL. Neutrophil cannibalism triggers transforming growth factor β1 production and self regulation of neutrophil inflammatory function in monosodium urate monohydrate crystal-induced inflammation in mice. Arthritis Rheum 2013;65(3):815–823.

76. Zhang F, Wang H, Wang X, et al. TGF-β induces M2-like macrophage polarization via SNAIL-mediated suppression of a pro-inflammatory phenotype. Oncotarget 2016;7(32):52294–52306.

77. Shapouri-Moghaddam A, Mohammadian S, Vazini H, et al. Macrophage plasticity, polarization, and function in health and disease. J Cell Physiol 2018;233(9):6425–6440.

78. Awad F, Assrawi E, Jumeau C, et al. Impact of human monocyte and macrophage polarization on NLR expression and NLRP3 inflammasome activation. PLoS One 2017;12(4):e0175336.

79. Levy BD, Clish CB, Schmidt B, et al. Lipid mediator class switching during acute inflammation: signals in resolution. Nat Immunol 2001; 2(7):612–619.

80. Serhan CN, Clish CB, Brannon J, et al. Novel functional sets of lipid-derived mediators with antiinflammatory actions generated from omega-3 fatty acids via cyclooxygenase 2-nonsteroidal antiinflammatory drugs and transcellular processing. J Exp Med 2000;192(8): 1197–1204.

81. Serhan CN, Yang R, Martinod K, et al. Maresins: novel macrophage mediators with potent antiinflammatory and proresolving actions. J Exp Med 2009;206(1):15–23.

82. Barden AE, Moghaddami M, Mas E, et al. Specialised pro-resolving mediators of inflammation in inflammatory arthritis. Prostaglandins Leukot Essent Fatty Acids 2016;107:24–29.

83. Bomalaski JS, Lluberas G, Schumacher HR Jr. Monosodium urate crystals in the knee joints of patients with asymptomatic nontophaceous gout. Arthritis Rheum 1986;29(12):1480–1484.

84. Pascual E. Persistence of monosodium urate crystals and low-grade inflammation in the synovial fluid of patients with untreated gout. Arthritis Rheum 1991;34(2):141–145.

85. Ortiz-Bravo E, Sieck MS, Schumacher HR Jr. Changes in the proteins coating monosodium urate crystals during active and subsiding inflammation. Immunogold studies of synovial fluid from patients with gout and of fluid obtained using the rat subcutaneous air pouch model. Arthritis Rheum 1993;36(9):1274–1285.

86. Xu H, Zhang B, Chen Y, et al. Type II collagen facilitates gouty arthritis by regulating MSU crystallisation and inflammatory cell recruitment. Ann Rheum Dis 2023;82(3):416–427.

87. Renaudin F, Sarda S, Campillo-Gimenez L, et al. Adsorption of proteins on m-CPPD and urate crystals inhibits crystal-induced cell responses: study on albumin-crystal interaction. J Funct Biomater 2019;10(2):18.

88. Neogi T, Jansen TL, Dalbeth N, et al. 2015 Gout classification criteria: an American College of Rheumatology/European League Against Rheumatism collaborative initiative. Arthritis Rheumatol 2015;67(10):2557–2568.

89. Dalbeth N, Pool B, Gamble GD, et al. Cellular characterization of the gouty tophus: a quantitative analysis. Arthritis Rheum 2010;62(5): 1549–1556.

90. Rainer TH, Cheng CH, Janssens HJ, et al. Oral prednisolone in the treatment of acute gout: a pragmatic, multicenter, double-blind, randomized trial. Ann Intern Med 2016;164(7):464–471.

91. Roddy E, Clarkson K, Blagojevic-Bucknall M, et al. Open-label randomised pragmatic trial (CONTACT) comparing naproxen and low-dose colchicine for the treatment of gout flares in primary care. Ann Rheum Dis 2020;79(2):276–284.

92. Phelps P. Polymorphonuclear leukocyte motility in vitro: IV. Colchicine inhibition of chemotactic activity formation after phagocytosis of urate crystals. Arthritis Rheum 2008;58(2 suppl): S25–S33.

93. Misawa T, Takahama M, Kozaki T, et al. Microtubule-driven spatial arrangement of mitochondria promotes activation of the NLRP3 inflammasome. Nat Immunol 2013;14(5):454–460.

94. Chia EW, Grainger R, Harper JL. Colchicine suppresses neutrophil superoxide production in a murine model of gouty arthritis: a rationale for use of low-dose colchicine. Br J Pharmacol 2008;153(6): 1288–1295.

95. Vaidya K, Tucker B, Kurup R, et al. Colchicine inhibits neutrophil extracellular trap formation in patients with acute coronary syndrome after percutaneous coronary intervention. J Am Heart Assoc 2021; 10(1):e018993.

96. Quatrini L, Ugolini S. New insights into the cell- and tissue-specificity of glucocorticoid actions. Cell Mol Immunol 2021;18(2):269–278.

97. Ray A, Prefontaine KE. Physical association and functional antagonism between the p65 subunit of transcription factor NF-kappa B and the glucocorticoid receptor. Proc Natl Acad Sci USA 1994; 91(2):752–756.

98. King EM, Chivers JE, Rider CF, et al. Glucocorticoid repression of inflammatory gene expression shows differential responsiveness by transactivation- and transrepression-dependent mechanisms. PLoS One 2013;8(1):e53936.

99. Auger JP, Zimmermann M, Faas M, et al. Metabolic rewiring promotes anti-inflammatory effects of glucocorticoids. Nature 2024; 629(8010):184–192.

100. Vane JR. Inhibition of prostaglandin synthesis as a mechanism of action for aspirin-like drugs. Nat New Biol 1971;231(25):232–235.

101. Lehmann JM, Lenhard JM, Oliver BB, et al. Peroxisome proliferator-activated receptors α and γ are activated by indomethacin and other non-steroidal anti-inflammatory drugs. J Biol Chem 1997;272(6): 3406–3410.

102. Jiang C, Ting AT, Seed B. PPAR-gamma agonists inhibit production of monocyte inflammatory cytokines. Nature 1998;391(6662): 82–86.

103. Janssen CA, Oude Voshaar MAH, Vonkeman HE, et al. Anakinra for the treatment of acute gout flares: a randomized, double-blind, placebo-controlled, active-comparator, non-inferiority trial. Rheumatology (Oxford) 2019;58(8):1344–1352.

104. Saag KG, Khanna PP, Keenan RT, et al. A randomized, phase II study evaluating the efficacy and safety of anakinra in the treatment of gout flares. Arthritis Rheumatol 2021;73(8):1533–1542.

105. Schlesinger N, Alten RE, Bardin T, et al. Canakinumab for acute gouty arthritis in patients with limited treatment options: results from two randomised, multicentre, active-controlled, double-blind trials and their initial extensions. Ann Rheum Dis 2012;71(11):1839–1848.

106. Klück V, Jansen TLTA, Janssen M, et al. Dapansutrile, an oral selective NLRP3 inflammasome inhibitor, for treatment of gout flares: an open-label, dose-adaptive, proof-of-concept, phase 2a trial. Lancet Rheumatol 2020;2(5):e270–e280.

107. FitzGerald JD, Dalbeth N, Mikuls T, et al. 2020 American College of Rheumatology guideline for the management of gout. Arthritis Care Res (Hoboken) 2020;72(6):744–760.

108. Cronstein BN, Molad Y, Reibman J, et al. Colchicine alters the quantitative and qualitative display of selectins on endothelial cells and neutrophils. J Clin Invest 1995;96(2):994–1002.

109. Paschke S, Weidner AF, Paust T, et al. Technical advance: inhibition of neutrophil chemotaxis by colchicine is modulated through viscoelastic properties of subcellular compartments. J Leukoc Biol 2013; 94(5):1091–1096.

110. So A, Dumusc A, Nasi S. The role of IL-1 in gout: from bench to bedside. Rheumatology (Oxford) 2018;57(suppl 1):i12–i19.

111. So AK, Martinon F. Inflammation in gout: mechanisms and therapeutic targets. Nat Rev Rheumatol 2017;13(11):639–647.

Three-Year Results of Tapering Tumor Necrosis Factor Inhibitor to Withdrawal Compared to Stable Tumor Necrosis Factor Inhibitor Among Patients With Rheumatoid Arthritis in Sustained Remission: A Multicenter Randomized Trial

Kaja E. Kjørholt,[1] Nina Paulshus Sundlisæter,[2] Anna-Birgitte Aga,[2] Joseph Sexton,[2] Inge C. Olsen,[3] Åse S. Lexberg,[4] Tor M. Madland,[5] Hallvard Fremstad,[6] Christian A. Høili,[7] Gunnstein Bakland,[8] Cristina Spada,[9] Hilde Haukeland,[10] Inger M. Hansen,[11] Ellen Moholt,[2] Karen Holten,[2] Till Uhlig,[1] Tore K. Kvien,[1] Daniel H. Solomon,[12] Désirée van der Heijde,[13] Espen A. Haavardsholm,[1] and Siri Lillegraven[2]

Objective. Tapering of tumor necrosis factor inhibitor (TNFi) treatment in rheumatoid arthritis (RA) remission is debated. We assessed the effect of tapering TNFi to withdrawal versus continued stable TNFi on flare-free survival and joint damage progression over three years.

Methods. ARCTIC REWIND was a multicenter open-label, noninferiority trial that included patients with RA in remission for ≥12 months taking stable TNFi therapy. Patients were randomized 1:1 to taper TNFi to withdrawal or continue stable treatment. The primary end points of the current study were flare-free survival and radiographic progression over three years. Flare-free survival was analyzed by Kaplan-Meier methods, flare rates were analyzed by Cox regression, and radiographic progression was analyzed by logistic mixed-effects models.

Results. Of 99 randomized patients, 92 received the allocated therapy, and 80 completed the three-year follow-up. The mean baseline Disease Activity Score based on the 44 joint count was 0.8, and conventional synthetic disease-modifying antirheumatic drug comedication was used by 90% of patients. After three years, 25% (95% confidence interval [CI] 13%–38%) remained flare free in the tapering TNFi group, compared to 85% (95% CI 70%–93%) in the stable group, and the corresponding hazard ratio for flare was 9.4 (95% CI 3.9–22.8, $P < 0.0001$). In the tapering group, 6 of 41 (15%) experienced radiographic progression, compared with 3 of 38 (8%) in the stable group (risk difference 6.7%, 95% CI –7.1% to 20.5%, $P = 0.3$). Adverse events occurred in 81% of the patients in the tapering group and 89% of the patients in the stable group.

Conclusion. In contrast to those receiving stable TNFi treatment, a minority of patients with RA in remission tapering TNFi to withdrawal remained flare free over three years. There was no statistically significant difference in radiographic progression between the groups.

INTRODUCTION

Patients with rheumatoid arthritis (RA) are increasingly achieving remission with early and aggressive treatment strategies.[1] If first-line therapy with conventional synthetic disease-modifying antirheumatic drugs (csDMARDs) fails to provide sufficient response, a tumor necrosis factor inhibitor (TNFi) is commonly added to the treatment regimen.[2,3] In patients who achieve

---

[1]Kaja E. Kjørholt, MD, Till Uhlig, MD, PhD, Tore K. Kvien, MD, PhD, Espen A. Haavardsholm, MD, PhD: Center for Treatment of Rheumatic and Musculoskeletal Diseases (REMEDY), Diakonhjemmet Hospital and Faculty of Medicine, University of Oslo, Oslo, Norway; [2]Nina Paulshus Sundlisæter, MD, PhD, Anna-Birgitte Aga, MD, PhD, Joseph Sexton, PhD, Ellen Moholt, RN, MSc, Karen Holten, RN, MSc, PhD, Siri Lillegraven, MD, MPH, PhD: Center for Treatment of Rheumatic and Musculoskeletal Diseases (REMEDY), Diakonhjemmet Hospital, Oslo, Norway; [3]Inge C. Olsen, PhD: Department of Research Support for Clinical Trials, Oslo University Hospital, Oslo, Norway; [4]Åse S. Lexberg, MD: Department of Rheumatology, Vestre Viken Hospital Trust, Drammen, Norway; [5]Tor M. Madland, MD: Department of Rheumatology, Haukeland University Hospital, Bergen, Norway; [6]Hallvard Fremstad, MD: Department of Rheumatology, Møre og Romsdal Hospital Trust, Ålesund, Norway; [7]Christian A. Høili, MD: Department of Rheumatology, Østfold Hospital Trust, Moss, Norway; [8]Gunnstein Bakland, MD, PhD: Department of Rheumatology, University Hospital of North Norway, Tromsø, Norway; [9]Cristina Spada, MD: Department of Rheumatology, Revmatismesykehuset AS, Lillehammer, Norway; [10]Hilde Haukeland, MD: Department of Rheumatology, Martina Hansens Hospital, Sandvika, Norway; [11]Inger M. Hansen, MD: Department of Rheumatology, Helgelandssykehuset, Mo i Rana, Norway; [12]Daniel H. Solomon, MD, MPH: Brigham and Women's Hospital, Boston, Massachusetts; [13]Désirée van der Heijde, MD, PhD: Department of Rheumatology, Leiden University Medical Center, Leiden, The Netherlands and Center

sustained remission, it is debated whether TNFi could be tapered.[2,3] Tapering or discontinuing TNFi might be beneficial regarding potential adverse events, unnecessary health care costs, and burden of taking medication.[4–7] Many patients with well-controlled disease have a desire to reduce their biologic DMARDs, but the potential for disease flare and joint damage causes concerns.[2,3,8]

The American College of Rheumatology (ACR) and The European Alliance of Associations for Rheumatology (EULAR) recommend that dose reduction of DMARDs should only be considered among patients with RA in whom the disease activity target has been met for at least six months,[2,3] with the latter recommendations emphasizing that this target should be fulfillment of the stringent ACR/EULAR remission criteria.[9,10] However, one-year results from the ARCTIC REWIND trial showed that in a population in remission for at least a year (of which 86% were in Simplified Disease Activity Index [SDAI] remission), significantly more flares occurred after tapering TNFi to withdrawal compared to stable TNFi treatment.[11] Other randomized trials evaluating tapering strategies among patients with RA in sustained remission six or more months who needed TNFi to achieve this state also show an overall increased risk of flare in those tapering or withdrawing their TNFi.[12,13]

Before implementing or discarding a treatment strategy, long-term consequences should be addressed. In a previous study assessing dose reduction versus usual care with maintenance of low disease activity as the treatment goal, patients were observed over an 18- to 36-month observational extension phase. The difference between the two strategies regarding remission rates, physical function, radiographic progression, and adverse events was statistically nonsignificant during this nonrandomized period.[14] Long-term data on tapering strategies and outcomes for patients in sustained remission are otherwise sparse, and more data would provide valuable information for clinicians and patients when discussing treatment options. The objective of this study was to assess the three-year effects of tapering and withdrawal of TNFi versus continuing stable TNFi on disease activity flare and radiographic joint damage among patients with RA in sustained remission.

PATIENTS AND METHODS

Study design. This multicenter randomized, open-label, noninferiority trial assessed the three-year clinical and radiographic effects of tapering TNFi among patients with RA in sustained remission. The ARCTIC REWIND (Remission in Rheumatoid Arthritis - Assessing Withdrawal of Disease-Modifying Antirheumatic Drugs in a Non-Inferiority Design) project contained two separate randomized trials for patients in sustained remission: one enrolling patients using TNFi therapy (the current trial)[11] and the other enrolling patients using only csDMARD therapy at inclusion, for which results are previously published.[15–17] The patients were recruited and observed at nine rheumatology departments in Norway. The trial was performed in compliance with the Declaration of Helsinki and International Council of Harmonisation Guidelines for Good Clinical Practice and Norwegian regulations and was approved by the South-Eastern Norway Regional Ethics Committee (approval number 2012/2285) and the Norwegian Medical Products Agency (Supplement 1). Patients provided written informed consent to participate in the study before taking part.

A deidentified patient data set can be made available to researchers upon reasonable request. The data will only be made available after submission of a project plan outlining the reason for the request and any proposed analyses and will have to be approved by the ARCTIC REWIND project group. Project proposals can be submitted to the corresponding author. Data sharing will have to follow appropriate regulations. The study protocol and statistical analysis plan are available in Supplement 1.

Participants. Participants aged between 18 and 80 years were eligible if they fulfilled the ACR/EULAR classification criteria[18] for RA and had documented remission status according to established criteria for at least 12 months, with no swollen joints (of 44 assessed) and fulfillment of Disease Activity Score (DAS) remission criteria at inclusion. The DAS is a composite measure of disease activity (range 0–10) based on the 44 swollen joint count, the Ritchie Articular Index, the erythrocyte sedimentation rate, and the patient's global assessment of disease activity.[19,20] DAS remission is defined as a score <1.6, and higher scores indicate more disease activity. All patients had to use unchanged dosages of TNFi therapy during the last 12 months. csDMARD comedication was allowed if kept stable over the same period. The patients had been treated according to current recommendations at the time of diagnosis with initial csDMARD treatment. The initial inclusion criteria required the patient to have less than five years of symptom duration. However, this requirement could be difficult to determine and was removed in a protocol update, which also increased the number of eligible patients. The inclusion and exclusion criteria are listed in Supplementary Table 1 (Supplement 2). All patients provided written consent before inclusion.

Randomization and masking. Patients were randomly assigned 1:1 to either tapering to withdrawal of TNFi or continuing stable TNFi. Randomization was stratified by study center using an electronic case report form system (version 3; Viedoc Technologies AB) with a computer-based block randomization with a block size of four. Study personnel at each study center enrolled and confirmed eligibility of the patients, and the allocated treatment group was revealed to the study personnel and participants after randomization. Radiographic outcomes were scored centrally by two readers blinded to the allocated treatment group and clinical information.

Procedures. At baseline, the patients used either TNFi (etanercept, adalimumab, infliximab, certolizumab pegol, golimumab) in monotherapy or TNFi in combination with csDMARDs. In the tapering group, TNFi therapy was reduced by 50% for four months by either doubling the time between injections or reduced dosages (Protocol, Supplement 1), followed by withdrawal of TNFi if no flare had occurred. If a patient experienced a flare, full-dose TNFi treatment was reinstated, with no further scheduled tapering attempts. In the stable group, patients who experienced a flare were treated in accordance with current treatment recommendations. In addition to DMARDs, a flare could be treated with intramuscular, intraarticular, or oral glucocorticoids regardless of randomization group. Comedication with csDMARDs should be kept stable throughout the study in both randomization groups. Patients were examined every four months, including additional visits within a week if patients experienced disease worsening, with a total follow-up period of 36 months (ie, 10 standard visits). Patients who experienced a flare were to continue to attend visits until the end of the study.

Outcomes. The primary end points of the three-year analyses (Statistical analysis plan, Supplement 1) were absence of disease activity flare and radiographic joint damage over the study period. A flare was defined as a combination of a DAS >1.6 (ie, loss of remission), an increase in the DAS ≥0.6 units since the previous visit (ie, change larger than the measurement error), and ≥2 swollen joints of 44 examined, with all components having to be present to fulfill the definition. If these criteria were not fulfilled, a flare could also be recorded if the physician and patient agreed that a clinically significant flare had occurred. Radiographs of hands and feet (baseline and yearly) were scored in chronological order by two readers unaware of clinical data and treatment information using the van der Heijde modified Sharp score (vdHSS), ranging from 0 to 448, with higher scores indicating greater joint damage.[21] Progression of joint damage (compared to baseline) was assessed on a continuous scale and defined as a change of ≥1 unit yearly ie, a change of ≥3 units after three years, using the average score of the readers.

Secondary clinical outcomes included ACR/EULAR Boolean 2.0 remission (defined as a combination of a C-reactive protein [CRP] level ≤1 mg/dL, a swollen joint count ≤1, a tender joint count ≤1, and patient global assessment of disease activity ≤2 on a 0–10 visual analog scale) and DAS remission (score <1.6).[19,9] Additionally, continuous clinical outcomes consisted of the DAS, swollen joint count (0–44), and CRP level (mg/dL), collected at every visit. Ultrasound examinations (at baseline, flare visits, and yearly) were scored based on assessment of 32 joints (scored 0–3 for both gray scale synovitis and power Doppler signal using an atlas for reference).[22] The 32 assessed joints were metacarpophalangeal joints I–V, the radiocarpal joint, the distal radioulnar joint, the intercarpal joint, the elbow, the knee, the talocrural joint, and metatarsophalangeal joints I–V bilaterally. A secondary radiographic outcome was joint damage progression above the smallest detectable change after three years. Physical function was assessed by the Patient-Reported Outcomes Measurement Information System (PROMIS) 20-item short form (translated to a T score with a mean of 50 and SD of 10).[23] Information about DMARD use (type, dose, and frequency) and glucocorticoid treatment (intraarticular injections and systemic use, yes or no) was collected at every visit. Potential clinical and laboratory adverse events were monitored at each visit.

Statistical analysis. The sample size was determined, and the noninferiority margin of 20% was set with respect to the initial comparison after one year.[11] The outcomes were analyzed in a per protocol population, excluding patients with major protocol deviations potentially affecting the treatment efficacy. In cases with major protocol deviations or cases lost to follow-up, the patients were included in the analyses up to the date of deviation. Baseline characteristics were described by frequency (percentage), mean (SD), and median (interquartile range [IQR]) as appropriate. Flare-free survival curves and the corresponding center-adjusted hazard ratio of flare were estimated by the Kaplan-Meier method and Cox proportional hazard regression. Radiographic joint damage was analyzed on a continuous scale and as a dichotomous outcome (radiographic joint progression) and compared after three years using logistic mixed-effects models (average risk difference estimator) and the Mann-Whitney U test. Missing values for radiographic scoring of single joints, for example, due to surgery during the study, were handled by using the last observation carried forward at the joint level. The radiographic progression in patients who experienced a flare versus those who did not was assessed using logistic mixed-effects models, adjusted for treatment group.

Yearly differences in remission rates were estimated using logistic mixed models with treatment group, time (categorical), and their interaction as fixed effects and patient and study center as random intercepts. The differences in remission status between the two treatment groups from baseline to 36 months were analyzed by generalized estimating equations for logistic regression using subject-level bootstrapping, with adjustment for baseline status in analyses of ACR/EULAR Boolean 2.0 remission (due to unbalanced status between the two groups at baseline). The percentage of patients with absence of ultrasound power Doppler signal throughout the study was compared using Fisher's exact test.

Among patients who experienced a flare, differences in DAS, CRP level, swollen joint count, and PROMIS score before, at, and after a flare within each treatment group were compared by the Wilcoxon matched-paired singed rank test.

Sensitivity analyses of the primary outcomes and remission status were repeated in a modified intention-to-treat population, which included all patients receiving the intervention until the end of the study or loss to follow-up. In addition, the outcome of disease activity flare was analyzed by a nonresponder imputation, that is, imputing dropouts (major protocol violations or lost to follow-up) as a flare (worst-case analysis), and finally by using a flare definition based on the DAS and swollen joint count only.

In post hoc analyses, we repeated the testing of noninferiority of the tapering strategy with a similar approach as applied in the one-year analyses and with the same noninferiority margin of 20%. This was done using logistic mixed-effects models and the adjusted risk difference estimator to compare the risk of any flare during three years of follow-up. In this model, treatment group was the only fixed factor, and center was entered as a random intercept to account for the center stratification. The 95% confidence interval (CI) for the difference in flare risk was computed using the delta method. Furthermore, in post hoc analyses, we assessed hazards of flare over time and calculated the hazard ratio of flare adjusted for Boolean 2.0 baseline status.

Statistical analyses were performed in Stata version 16.0 (StataCorp) and R Statistical Software version 4.0.3. The trial registration number was 2012-005275-14 in EudraCT and NCT01881308 in ClinicalTrials.gov.

RESULTS

Patients. Between June 17, 2013, and January 4, 2019, 99 patients were randomized in the study. Ninety-two received the allocated therapy and were included in the per protocol set: 47 in the tapering group and 45 in the stable group (Figure 1). Of these, 89% (42 of 47) in the tapering group and 84% (38 of 45) in the stable group completed the three-year follow-up without major protocol violations. Patient characteristics were overall well balanced between the TNFi tapering group and the stable TNFi group: mean age 57.6 (SD 12.6) versus 57.4 (SD 10.7) years, 53% (25 of 47) versus 67% (30 of 45) female, and 77% (36 of 47) versus 78% (35 of 45) anti–citrullinated peptide positive, respectively (Supplementary Table 2 in Supplement 2). At baseline, the mean DAS was 0.8 (SD 0.3) in the tapering TNFi group and 0.9 (SD 0.4) in the stable group (Supplementary Table 2 in Supplement 2); 94% (44 of 47) in the tapering group had absence of ultrasound power Doppler signal, compared with 95% (42 of 44) in the stable group. The majority of patients were in ACR/EULAR remission at baseline; ACR/EULAR Boolean 2.0 criteria were fulfilled by 91% (43 of 47) in the tapering group and 67% (30 of 45) in the stable group, and ACR/EULAR SDAI

remission were fulfilled by 96% (45 of 47) and 76% (34 of 45) of the patients, respectively. The mean time since the first swollen joint was 11.9 (SD 6.9) years in the tapering group and 10.0 (SD 7.2) years in the stable group. csDMARD comedication was used by 89% in the tapering group and 91% in the stable group, mainly methotrexate monotherapy.

Primary outcomes. After three years, 25% (95% CI 13%–38%) remained flare free in the tapering TNFi group, compared to 85% (95% CI 70%–93%) in the stable dose TNFi group (Figure 2A). Thirty-four patients experienced a flare in the tapering group, compared to six patients in the stable group, with an estimated adjusted risk difference of 59% (95% CI 43%–75%, $P < 0.0001$) over the three-year study period. The lower CI limit exceeded the noninferiority margin of 20% defined for the one-year analyses, confirming that the tapering strategy was not noninferior to stable treatment in the long term. The corresponding center-adjusted hazard ratio of flare in the tapering group was 9.4 (95% CI 3.9–22.8, $P < 0.0001$).

The mean and median radiographic change in total vdHSS over three years were 1.4 (SD 2.4) and 0.5 (IQR 0.0–2.0) units in the tapering group, compared to 1.0 (SD 1.1) and 0.5 (IQR 0.0–1.5) units in the stable group (P value of comparison = 0.9) (Figure 3). In the tapering TNFi group, 15% (6 of 41) experienced radiographic progression ≥3 units, compared with 8% (3 of 38) in the stable TNFi group (risk difference 6.7%, 95% CI –7.1% to 20.5%, $P = 0.3$). Analyses of flare and radiographic joint damage repeated in the intention-to-treat population gave similar results (Figure 2B and Supplementary Tables 3 and 4 in Supplement 2).

Disease activity. ACR/EULAR Boolean 2.0 remission rates were significantly lower in the tapering TNFi group than the stable TNFi group throughout the 36-month study period (Figure 4), with an adjusted risk difference of –24% (95% CI –33% to –15%, $P < 0.0001$). Rates of ACR/EULAR Boolean 1.0 remission and analyses in the intention-to-treat population revealed similar results, whereas no significant difference was observed for DAS remission (Supplementary Figure 1 in Supplement 2). A difference regarding inflammation assessed by ultrasound was observed; 45% (21 of 47) of patients had no power Doppler signal at any of the visits where ultrasound was performed in the tapering group, compared to 76% (34 of 45) in the stable group ($P = 0.003$).

At the time of flare, the mean DAS was 2.2 (SD 0.7) in the tapering group and 2.0 (SD 0.3) in the stable group, corresponding to low disease activity in both groups (Supplementary Figure 2 in Supplement 2). A moderate or high DAS at the time of flare was observed in 34% (11 of 32) of the patients in the tapering group, compared to 17% (1 of 6) in the stable group. Within the first visit after a flare, 84% (26 of 31) in the tapering group and 67% (4 of 6) in the stable group regained DAS remission. In the tapering group,
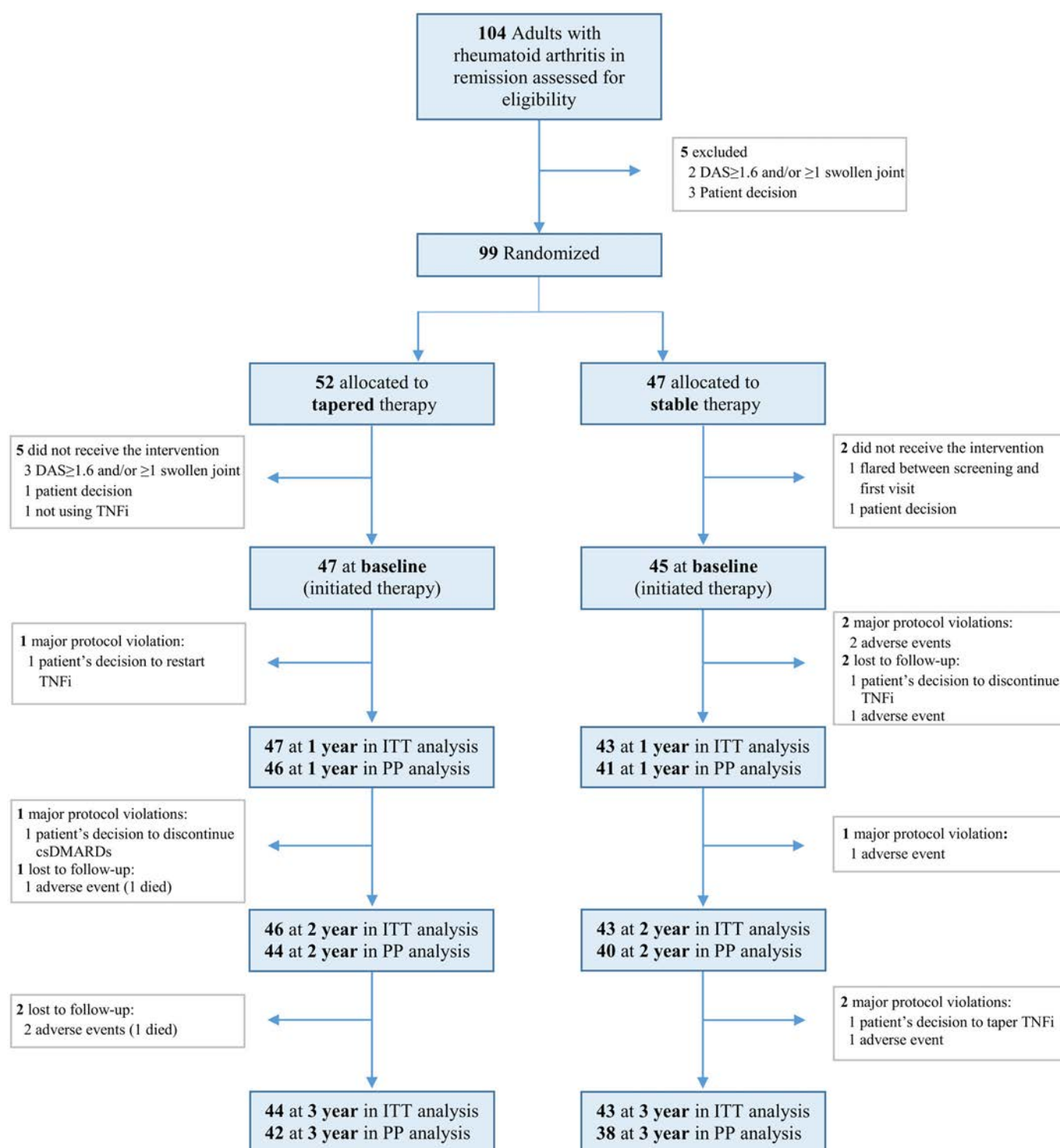
Figure 1. Flowchart of patients in the ARCTIC REWIND TNFi trial with three years of follow-up. csDMARD, conventional synthetic disease-modifying antirheumatic drug; DAS, Disease Activity Score; ITT, intention to treat; PP, per protocol; TNFi, tumor necrosis factor inhibitor.

the CRP level, 44 swollen joint count, DAS, and PROMIS physical function were significantly worse at the time of flare compared to the visit before and after a flare ($P \leq 0.0001$) (Supplementary Figure 2 in Supplement 2; statistical testing was not performed in the stable group owing to small numbers).

Additional radiographic outcomes. Radiographic progression above the smallest detectable change after three years was 2.44 units, and was experienced by 22% (9 of 41) in the tapering group, compared to 13% (5 of 38) in the stable group (risk difference 9%, 95% CI –8% to 25%, $P = 0.3$). Of patients
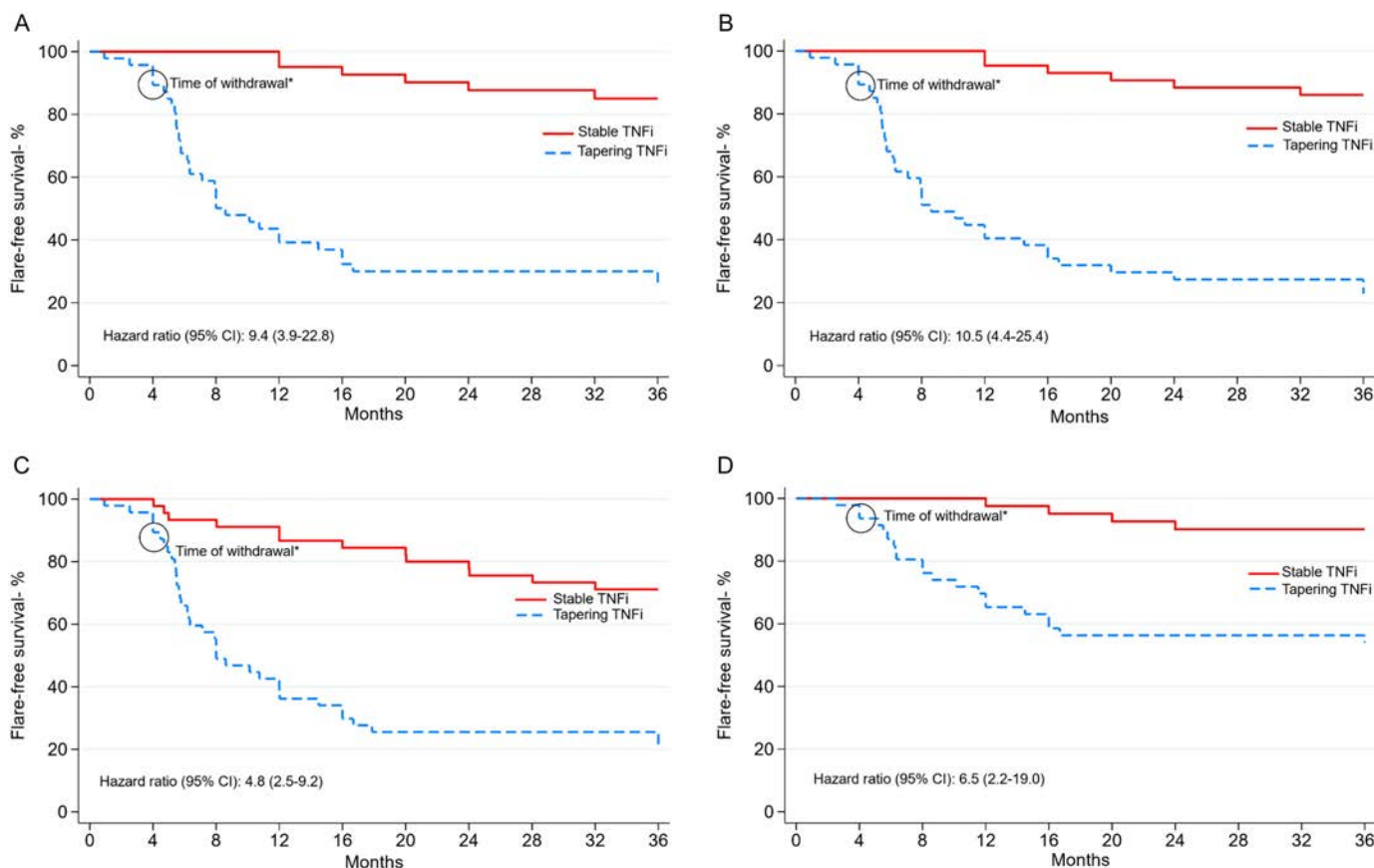
Figure 2. Proportions of patients without a flare over the study period. Flare was defined as a combination of DAS above the cutoff for remission (1.6), a change in DAS of at least 0.6, and at least two swollen joints or that both the treating physician and the patient agreed that a clinically significant flare had occurred. The risk of flare was analyzed by Cox proportional hazard regression with 95% CI, adjusted for study center. *TNFi was reduced to a half dose for four months, followed by withdrawal at the four-month visit if no flare had occurred. (A) Primary outcome: any flare, analyzed in a PP population. (B) Sensitivity analysis: any flare, analyzed in a modified ITT population. (C) Sensitivity analysis: nonresponder imputation, that is, imputing dropouts (the date of major protocol violation or lost to follow-up) as flare, analyzed in a PP population. (D) Sensitivity analysis: using flare by definition criteria only (combination of DAS >1.6, a change in DAS off at least 0.6, and at least two swollen joins), analyzed in a PP population. CI, confidence interval; DAS, Disease Activity Score; ITT, intention to treat; PP, per protocol; TNFi, tumor necrosis factor inhibitor.

who experienced a flare during follow-up who had radiographs available, 16% (6 of 37) had progression of joint damage over three years, compared to 7% (3 of 42) among patients without a flare (risk difference 7.7%, 95% CI –9.9% to 25.4%, $P = 0.4$). In patients who experienced a flare, the mean/median change in vdHSS after three years was 1.5 (SD 2.4)/0.5 (IQR 0.0–2.0), compared to 0.9 (SD 1.1)/0.5 (IQR 0.0–1.5) in patients without a flare (P value for comparison = 0.2).

Medication. Among patients who completed three years of follow-up, 29% (12 of 42) in the tapering group were not treated with any TNFi or other biologic DMARDs at the last visit (Table 1). Compared to baseline treatment, 10% (4 of 42) in the tapering group and 11% (4 of 38) in the stable group had switched to other types of TNFi or started JAK inhibitor treatment by the end of the study. Systemic glucocorticoids (one or more treatment periods during the three-year follow-up) were used by

23% (11 of 47) in the tapering TNFi group and 13% (6 of 45) in the stable TNFi group (Table 1).

Adverse events. Adverse events occurred in 81% of the patients in the tapering group and 89% of the patients in the stable group, with corresponding percentages for serious adverse events of 21% in the tapering group and 11% in the stable group (Table 2). Infection was the most common adverse event in both groups, mostly affecting the respiratory tract. Adverse events led to study discontinuation or major protocol violations in 4% (2 of 47) of the patients in the tapering group and 11% (5 of 45) of the patients in the stable group. Two deaths considered unrelated to treatment occurred among patients in the tapering group. Analyses of adverse events in the intention-to-treat population were almost identical (Supplementary Table 5 in Supplement 2).

Sensitivity and post hoc analyses. Of the flares in the tapering group, 53% (18 of 34) were detected by the formal
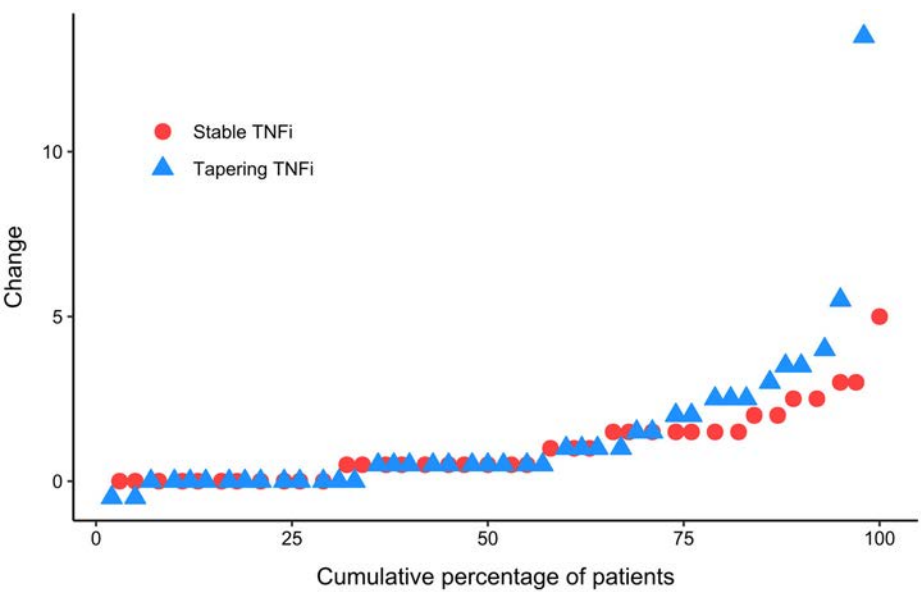
Figure 3. Change in van der Heijde modified Sharp score at 36 months compared to baseline. The van der Heijde modified Sharp scoring method assesses erosions in 16 joints of each hand and 6 joints of each foot, and the erosions are given a score of 1 to 5. Joint space narrowing is assessed in 15 joints for each hand and 6 joints for each foot. This gives scores for erosions on a scale from 0 to 280 and for joint space narrowing on a scale from 0 to 168; thus, the total van der Heijde modified Sharp score ranges from 0 to 448, with higher scores indicating greater joint damage. The analyses were performed in a per protocol population. TNFi, tumor necrosis factor inhibitor.

definition based on the DAS and swollen joint count, compared to 67% (4 of 6) of the flares in the stable group. Sensitivity analyses of disease activity flares by nonresponder imputation gave consistent results (Figure 2C and Supplementary Table 3 in

Supplement 2). When excluding flares by consensus and thus only taking flares that met the definition based on the DAS and swollen joint count into account, we consistently found that the tapering group had a higher risk of flare compared to the
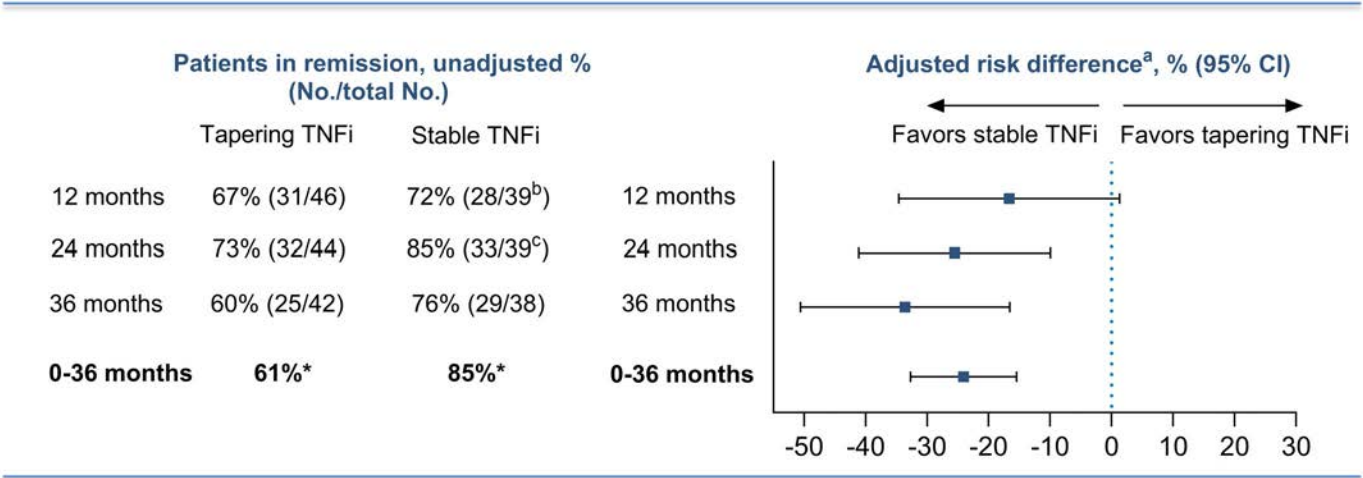
Figure 4. ACR/EULAR Boolean 2.0 remission status. ACR/EULAR remission is defined as tender joint count ≤1, swollen joint count ≤1, CRP level ≤1 mg/dL, and patient's global assessment ≤2 (on a 0–10 scale). The analyses were performed in a per protocol population. [a] Absolute risk difference analyzed by logistic regression with patient and study center as random intercepts, adjusted for Boolean 2.0 baseline status, and computed with 95% CI based on the delta method. Combined remission at 0 to 36 months was analyzed by generalized estimated equations, with subject-level bootstrapping. [b] Two patients did not take blood samples and are excluded from the denominator. [c] One patient did not take blood samples and is excluded from the denominator. * Not applicable to measure no./total no. because the result is an average estimate of remission status during the complete study period. ACR, American College of Rheumatology; CI, confidence interval; CRP, C-reactive protein; EULAR, The European Alliance of Associations for Rheumatology; TNFi, tumor necrosis factor inhibitor.

Table 1. Medication use[*]

	Tapering TNFi, % (no./total no.)	Stable TNFi, % (no./total no.)
bDMARD/tsDMARD treatment at 3-y follow-up[a]		
No bDMARD/JAKi	29 (12/42)	0 (0/38)
Same TNFi as baseline	62 (26/42)	89 (34/38)
Other TNFi	10 (4/42)	5 (2/38)
JAKi	0 (0/42)	5 (2/38)
csDMARD comedication increase at 3-y follow-up compared to baseline[a]	7 (3/42)	3 (1/38)
Glucocorticoids during the study[b]		
≥1 treatment period with systemic glucocorticoids	23 (11/47)	13 (6/45)
≥1 intraarticular glucocorticoids injections	47 (22/47)	24 (11/45)

[*] bDMARD, biologic disease-modifying antirheumatic drug; csDMARD, conventional synthetic DMARD; JAKi, JAK inhibitor; TNFi, tumor necrosis factor inhibitor; tsDMARD, targeted synthetic DMARD.
[a] The analyses were performed in patients who completed 3 years of follow-up in a per protocol population.
[b] In addition to DMARDs, a flare could be treated with intramuscular, intraarticular, or oral glucocorticoids.

Table 2. Adverse events from 0 to 36 months[*]

	Tapering TNFi (n = 47)	Stable TNFi (n = 45)
Total number of adverse events	162	133
Patients with ≥1 adverse event, % (n)	81 (38)	89 (40)
Patients with ≥3 adverse events, % (n)	47 (22)	53 (24)
Patients with serious adverse events,[a] % (n)	21 (10)	11 (5)
Patients with adverse events of special interest,[b] % (n)		
Leading to study discontinuation or major protocol violation	4 (2)	11 (5)
Any type of infection	60 (28)	62 (28)
Cancer	9 (4)	4 (2)
Death	4 (2)	0 (0)

[*] The analyses were performed in a per protocol population. TNFi, tumor necrosis factor inhibitor.
[a] Serious adverse events in the tapering group consisted of the following: lung carcinoma (adenocarcinoma) resulting in death, breast cancer, acute myocardial infarction, sudden death, cancer vesicae with transurethral resection of the bladder and cystoprostatektomi, traumatic fractures after traffic accident with hospitalization, toe amputation with hospitalization followed by postoperative infection, acute kidney failure with hospitalization (2 events), fall leading to hospitalization, and infection leading to hospitalization (3 events). Serious adverse events in the stable group consisted of the following: third-degree atrioventricular block, cancer vesicae, hysterectomy, rheumatoid vasculitis, and keratitis with hospitalization.
[b] Adverse events occurring at a minimum frequency of 5% in at least one group are listed. Additionally, the number of deaths is listed.

stable group, with a risk difference of 36% (95% CI 19%–52%, $P < 0.0001$) (Figure 2D and Supplementary Table 3 in Supplement 2). Post hoc analysis indicated that the flare rate varied over time in the tapering group, with the highest hazard the first three months after discontinuation of TNFi, whereas the stable treatment group had an approximately constant flare rate across the three-year study period. The hazard ratio of any flare after adjusting for Boolean 2.0 status was 9.9 (95% CI 3.9–25.1, $P < 0.0001$).

DISCUSSION

A minority of patients with RA who were in remission and tapering TNFi to withdrawal remained flare free over three years, whereas the majority of patients receiving stable treatment were flare free during the same time period. Although most patients regained remission after reinstatement of TNFi with minimal radiographic joint damage progression, TNFi tapering was associated with significantly lower ACR/EULAR Boolean 2.0 remission rates throughout the study.

We show that in patients who needed to add TNFi treatment to achieve sustained remission, only 25% could taper their TNFi to withdrawal without experiencing a flare over three years of follow-up, even though 90% were using stable csDMARD comedication. The study population and results are relevant when discussing current recommendations and

guidelines regarding tapering,[2,3] as the patients had been in remission for ≥12 months and had no signs of clinical disease activity at inclusion (no clinical arthritis, 96% of those tapering TNFi were in SDAI remission, and only 6% had any power Doppler signal when assessing 32 joints).

In previous randomized trials that either required shorter duration of remission or less stringent remission criteria for inclusion, 20% to 55% remained flare free within a maximum of 18 months after TNFi withdrawal.[24–27] Additionally, differences in TNFi tapering strategies and flare definition may impact the flare rate and complicate the comparison of these studies. In the ARCTIC REWIND trial, patients reduced their TNFi by 50% for four months, followed by complete withdrawal of TNFi. In contrast, patients in the SEAM-RA trial (Study of Etanercept and Methotrexate in Combination or as Monotherapy in Subjects with Rheumatoid Arthritis) withdrew TNFi without an initial tapering phase, and the STRASS trial (Spacing of TNF-blocker injections in Rheumatoid ArthritiS Study) had a more stepwise tapering strategy in which TNFi spacing was augmented by approximately 50% every three months in a five-step algorithm.[24,27] However regardless of tapering strategy, the risk of flare was significantly higher in the tapering/withdrawal group compared to the stable TNFi group in all of these studies.

In the current long-term study, most of the patients who remained flare free during the first 16 months after tapering TNFi

to withdrawal continued to remain flare free throughout the study. This means that the flare rate in the tapering group was close to stable during the last 20 months of our study, but whether the risk of flare differed from stable treatment in this time period is not feasible to investigate. However, it indicates that close follow-up is of greatest importance the first year after discontinuation of TNFi and that there is a potential for identification of a relevant subgroup in which tapering might be successful. If these patients share prognostic characteristics, further insight about biomarkers related to disease activity flare could provide important information for more personalized treatment decisions in RA remission.

Few tapering strategy trials in RA remission have been powered to compare radiographic joint damage, as is also the case of our study.[28] Systematic literature reviews of studies assessing the consequences of tapered treatment favor dose reduction over withdrawal regarding minimal joint damage progression.[13,29] We did not find any significant difference in radiographic progression between the two groups or between those who experienced a flare and those who did not. The rapid reintroduction of TNFi upon a flare might have prevented affection of bone and cartilage. However, the lower rate of ACR/EULAR Boolean 2.0 remission in the tapering group might be a concern because being in ACR/EULAR remission is associated with better long-term outcomes regarding joint damage and functional capacity compared to not being in remission.[9,10] No difference was found for DAS remission, reflecting that the ACR/EULAR Boolean criteria are more sensitive to isolated elevation in one of the parameters.

The absence of any difference in adverse events favoring tapering may be due to the fact that a large proportion of the patients had reintroduced their TNFi in the first half of the follow-up period so that any benefit of less treatment was reduced. Additionally, our findings are in line with previous observations in populations of patients who likely tolerated TNFi well, as they had used the medication over time before inclusion.[12,13] We observed a similar number of treatment intensifications between the groups, although patients in the tapering group received numerically more glucocorticoids during the study, reflecting the higher flare rate. The prescription of glucocorticoids might also contribute to dilute potential differences in adverse events between the two groups.

Our study addresses several aspects that should be considered when deciding on a treatment strategy in remission and provide information to discuss with the patients. It is important to continue monitoring patients who decide to taper off their TNFi, as a rapid reintroduction of the therapy is likely beneficial to prevent adverse consequences of a disease activity flare.

This study has some limitations. First, the power calculation was based on a one-year risk difference of flare. However, because we observed an overwhelming statistically significant risk difference of flare between the two treatment groups after three years, the potential lack of power did not influence our conclusion on disease activity flare. Secondly, because this was an open-label design, the disease flare recording could potentially

be affected by detection bias. To counteract this, study personnel were repeatedly instructed to record flares in the same manner regardless of treatment group. Furthermore, sensitivity analyses of flare solely based on the DAS and swollen joint count yielded consistent results with the primary analyses. Additionally, CRP level, swollen joint count, and PROMIS physical function were worse at the time of flare compared to the visit before and after. Because radiographic joint damage was scored by central blinded readers, these results could not be affected by potential detection bias. Thirdly, there was heterogeneity in TNFi treatment regimens and csDMARD comedication. Fourth, the initial inclusion criterion of less than five years of symptom duration was removed in a protocol update, but post hoc analyses did not find any association between time since first swollen joint and flare (data not shown). However, the generalizability to patients in an early phase of disease might be limited.

In conclusion, these three-year results do not support tapering of treatment in RA remission on a regular basis, as a majority of patients experienced a flare when tapering TNFi to withdrawal, and there was a low risk of flare if stable TNFi therapy was continued. Although a lower rate of ACR/EULAR Boolean 2.0 remission was observed in the tapering group, the two treatment strategies were not associated with differences regarding progression of radiographic joint damage, adverse events, or DMARD intensification. This information is important for shared decisions between the patients and physicians and highlights the value of detecting a flare with reinstatement of treatment without delay.

ACKNOWLEDGMENTS

AUTHOR CONTRIBUTIONS

All authors contributed to at least one of the following manuscript preparation roles: conceptualization AND/OR methodology, software, investigation, formal analysis, data curation, visualization, and validation AND drafting or reviewing/editing the final draft. As corresponding author, Dr Kjørholt confirms that all authors have provided the final approval of the version to be published and takes responsibility for the affirmations regarding article submission (eg, not under consideration by another journal), the integrity of the data presented, and the statements regarding compliance with institutional review board/Declaration of Helsinki requirements.

REFERENCES

1. Di Matteo A, Bathon JM, Emery P. Rheumatoid arthritis. Lancet 2023; 402(10416):2019–2033.

2. Fraenkel L, Bathon JM, England BR, et al. 2021 American College of Rheumatology guideline for the treatment of rheumatoid arthritis. Arthritis Care Res (Hoboken) 2021;73(7):924–939.

3. Smolen JS, Landewé RBM, Bergstra SA, et al. EULAR recommendations for the management of rheumatoid arthritis with synthetic and biological disease-modifying antirheumatic drugs: 2022 update. Ann Rheum Dis 2023;82(1):3–18.

4. Singh JA, Cameron C, Noorbaloochi S, et al. Risk of serious infection in biological treatment of patients with rheumatoid arthritis: a systematic review and meta-analysis. Lancet 2015;386(9990):258–265.

5. Verhoef LM, Bos D, van den Ende C, et al. Cost-effectiveness of five different anti-tumour necrosis factor tapering strategies in rheumatoid arthritis: a modelling study. Scand J Rheumatol 2019;48(6):439–447.

6. Baker KF, Isaacs JD, Thompson B. "Living a normal life": a qualitative study of patients' views of medication withdrawal in rheumatoid arthritis. BMC Rheumatol 2019;3(1):2.

7. Fautrel B, Den Broeder AA. De-intensifying treatment in established rheumatoid arthritis (RA): why, how, when and in whom can DMARDs be tapered? Best Pract Res Clin Rheumatol 2015;29(4–5):550–565.

8. Wiemer N, Webster P, Attur M, et al. Patient perspectives on tapering biologic or targeted synthetic therapy in well-controlled rheumatoid arthritis and comparison with providers' perspectives. Rheumatology (Oxford) 2023;62(suppl 4):iv3–iv7.

9. Studenic P, Aletaha D, de Wit M, et al. American College of Rheumatology/EULAR remission criteria for rheumatoid arthritis: 2022 revision. Arthritis Rheumatol 2023;75(1):15–22.

10. Felson DT, Smolen JS, Wells G, et al; American College of Rheumatology; European League Against Rheumatism. American College of Rheumatology/European League Against Rheumatism provisional definition of remission in rheumatoid arthritis for clinical trials. Arthritis Rheum 2011;63(3):573–586.

11. Lillegraven S, Paulshus Sundlisæter N, Aga AB, et al. Effect of tapered versus stable treatment with tumour necrosis factor inhibitors on disease flares in patients with rheumatoid arthritis in remission: a randomised, open label, non-inferiority trial. Ann Rheum Dis 2023; 82(11):1394–1403.

12. Uhrenholt L, Christensen R, Dinesen WKH, et al. Risk of flare after tapering or withdrawal of biologic/targeted synthetic disease-modifying anti-rheumatic drugs in patients with rheumatoid arthritis or axial spondyloarthritis: a systematic review and meta-analysis. Rheumatology (Oxford) 2022;61(8):3107–3122.

13. Verhoef LM, Tweehuysen L, Hulscher ME, et al. bDMARD dose reduction in rheumatoid arthritis: a narrative review with systematic literature search. Rheumatol Ther 2017;4(1):1–24.

14. Bouman CA, van Herwaarden N, van den Hoogen FH, et al. Long-term outcomes after disease activity-guided dose reduction of TNF inhibition in rheumatoid arthritis: 3-year data of the DRESS study - a randomised controlled pragmatic non-inferiority strategy trial. Ann Rheum Dis 2017;76(10):1716–1722.

15. Lillegraven S, Paulshus Sundlisæter N, Aga AB, et al. Effect of half-dose vs stable-dose conventional synthetic disease-modifying antirheumatic drugs on disease flares in patients with rheumatoid arthritis in remission: the ARCTIC REWIND randomized clinical trial. JAMA 2021;325(17):1755–1764.

16. Lillegraven S, Paulshus Sundlisæter N, Aga AB, et al. Discontinuation of conventional synthetic disease-modifying antirheumatic drugs in patients with rheumatoid arthritis and excellent disease control. JAMA 2023;329(12):1024–1026.

17. Kjørholt KE, Sundlisæter NP, Aga AB, et al. Effects of tapering conventional synthetic disease-modifying antirheumatic drugs to drug-free remission versus stable treatment in rheumatoid arthritis (ARCTIC REWIND): 3-year results from an open-label, randomised controlled, non-inferiority trial. Lancet Rheumatol 2024;6(5):e268–e278.

18. Aletaha, D., Neogi, T., Silman, A. J., et al. Rheumatoid arthritis classification criteria: an American College of Rheumatology/European League Against Rheumatism collaborative initiative. Ann Rheum Dis 2010;69(9):1580–1588.

19. van der Heijde DM, van 't Hof MA, van Riel PL, et al. Judging disease activity in clinical practice in rheumatoid arthritis: first step in the development of a disease activity score. Ann Rheum Dis 1990;49(11):916–920.

20. Ritchie DM, Boyle JA, McInnes JM, et al. Clinical studies with an articular index for the assessment of joint tenderness in patients with rheumatoid arthritis. Q J Med 1968;37(147):393–406.

21. van der Heijde D. How to read radiographs according to the Sharp/van der Heijde method. J Rheumatol 1999;26(3):743–745.

22. Hammer HB, Bolton-King P, Bakkeheim V, et al. Examination of intra and interrater reliability with a new ultrasonographic reference atlas for scoring of synovitis in patients with rheumatoid arthritis. Ann Rheum Dis 2011;70(11):1995–1998.

23. Fries JF, Cella D, Rose M, et al. Progress in assessing physical function in arthritis: PROMIS short forms and computerized adaptive testing. J Rheumatol 2009;36(9):2061–2066.

24. Fautrel B, Pham T, Alfaiate T, et al. Step-down strategy of spacing TNF-blocker injections for established rheumatoid arthritis in remission: results of the multicentre non-inferiority randomised open-label controlled trial (STRASS: Spacing of TNF-blocker injections in Rheumatoid ArthritiS Study). Ann Rheum Dis 2016;75(1):59–67.

25. Emery P, Burmester GR, Naredo E, et al. Adalimumab dose tapering in patients with rheumatoid arthritis who are in long-standing clinical remission: results of the phase IV PREDICTRA study. Ann Rheum Dis 2020;79(8):1023–1030.

26. Chatzidionysiou K, Turesson C, Teleman A, et al. A multicentre, randomised, controlled, open-label pilot study on the feasibility of discontinuation of adalimumab in established patients with rheumatoid arthritis in stable clinical remission. RMD Open 2016;2(1):e000133.

27. Curtis JR, Emery P, Karis E, et al. Etanercept or methotrexate withdrawal in rheumatoid arthritis patients in sustained remission. Arthritis Rheumatol 2021;73(5):759–768.

28. Kuijper TM, Lamers-Karnebeek FB, Jacobs JW, et al. Flare rate in patients with rheumatoid arthritis in low disease activity or remission when tapering or stopping synthetic or biologic DMARD: a systematic review. J Rheumatol 2015;42(11):2012–2022.

29. Henaux S, Ruyssen-Witrand A, Cantagrel A, et al. Risk of losing remission, low disease activity or radiographic progression in case of bDMARD discontinuation or tapering in rheumatoid arthritis: systematic analysis of the literature and meta-analysis. Ann Rheum Dis 2018;77(4):515–522.

AMERICAN COLLEGE
of RHEUMATOLOGY
Empowering Rheumatology Professionals

Efficacy and Safety of Zimlovisertib, Ritlecitinib, and Tofacitinib, Alone and in Combination, in Patients With Moderate to Severe Rheumatoid Arthritis and an Inadequate Response to Methotrexate

Spencer I. Danto,[1] Mikhail Salganik,[1] Anindita Banerjee,[1] Pawel Hrycaj,[2] Irina Jashi,[3] Negin Shojaee,[1] Ravi Shankar P. Singh,[1] Steven A. Gilbert,[1] Karen Page,[1] Elena Peeva,[1] Michael S. Vincent,[1] and Jean S. Beebe[1]

Objective. We aimed to evaluate the efficacy and safety of zimlovisertib (interleukin-1 receptor–associated kinase 4 inhibitor) in combination with ritlecitinib (a JAK3 and tyrosine kinase expressed in hepatocellular carcinoma [TEC] kinase family inhibitors) or tofacitinib (a JAK inhibitor) versus tofacitinib alone.

Methods. This phase 2 study randomized patients with moderate to severe active rheumatoid arthritis to zimlovisertib 400 mg + tofacitinib 11 mg, zimlovisertib 400 mg + ritlecitinib 100 mg, zimlovisertib 400 mg, ritlecitinib 100 mg, or tofacitinib 11 mg (4:4:3:3:4) for 24 weeks. The primary endpoint was change from baseline (CFB) in Disease Activity Score in 28 joints, C-reactive protein (DAS28-CRP) at week 12. Treatment-emergent adverse events (TEAEs) were monitored.

Results. Overall, 460 patients were randomized. At week 12, zimlovisertib + tofacitinib demonstrated a greater magnitude of mean CFB in DAS28-CRP (–2.65; 90% confidence interval [CI], –2.84 to –2.46) versus tofacitinib (–2.30; 90% CI, –2.49 to –2.11; $P = 0.032$); mean CFB with zimlovisertib + ritlecitinib (–2.35; 90% CI, –2.54 to –2.15) was similar to tofacitinib. TEAEs were reported in 246 patients (53.5%), with the highest aggregate incidence of TEAEs in the tofacitinib group (n = 60 [58.8%]). Most TEAEs were mild; severe TEAEs were reported by 9 patients (2.0%) and 10 patients reported serious AEs. One patient receiving tofacitinib died because of severe COVID-19 infection. Safety profiles were similar across all treatment groups, with no evidence of additive/synergistic issues.

Conclusion. Zimlovisertib + tofacitinib was more effective than tofacitinib for the primary endpoint, whereas the efficacy of zimlovisertib + ritlecitinib did not achieve statistical significance versus tofacitinib. All treatments were well tolerated.

INTRODUCTION

Rheumatoid arthritis (RA) is a chronic autoimmune disease characterized by joint inflammation and progressive disability.[1] The global prevalence of RA is estimated at 208.8 per 100,000 individuals, and the prevalence is generally higher in developed countries.[2] Several therapeutic options are available for RA; however, many patients cannot attain or sustain remission.[3,4] The treat-to-target strategy, endorsed by the American College of Rheumatology (ACR) and EULAR, represents a core therapeutic approach for RA to achieve the goal of remission or low disease activity.[5,6]

Methotrexate (MTX), a conventional synthetic disease-modifying antirheumatic drug (csDMARD), is recommended by EULAR and ACR as the first-line treatment for RA[5,6] and can be used alone or in combination with other csDMARDs or with

biologic DMARDs (bDMARDs) or targeted synthetic DMARDs (tsDMARDs).[7] Some patients with RA are treatment-refractory and fail to respond to multiple targeted therapies owing to a lack of efficacy or adverse events (AEs).[8] There is a potential need for new treatment combinations with different mechanisms of action, which are effective and well tolerated, to offer alternative strategies for patients who have failed targeted therapies.

tsDMARDs, such as tofacitinib, are attractive therapeutic strategies for the treatment of RA[9] that have the potential for superior efficacy to bDMARDs.[10,11] Tofacitinib inhibits signaling by heterodimeric receptors associated with JAK1 and/or JAK3 and has functional selectivity over JAK2;[12] it is approved for the treatment of RA.[13] Zimlovisertib is the first inhibitor of interleukin-1 receptor–associated kinase 4 to enter phase 2 clinical trials. It has demonstrated efficacy as a monotherapy in preclinical models of rheumatic disease and has been shown to modify inflammatory biomarkers in healthy individuals.[14] Zimlovisertib also demonstrated dose-dependent improvements in clinical disease scores of RA in a phase 2 study in patients with moderate to severe active RA.[15] Ritlecitinib is a selective, small molecule inhibitor of JAK3 and tyrosine kinase expressed in hepatocellular carcinoma (TEC) kinases[16] that is approved for the treatment of severe alopecia areata.[17] It has also demonstrated efficacy versus placebo in a small 8-week phase 2 clinical trial in patients with moderate to severe active RA.[18]

Because zimlovisertib targets different proinflammatory immune signaling pathways compared with either tofacitinib or ritlecitinib it was hypothesized that a combination of zimlovisertib with tofacitinib or ritlecitinib could improve RA symptoms superior to that achievable by any of the individual components, thereby driving more patients closer to the goal of clinical remission while maintaining an acceptable safety profile consistent with a favorable benefit-risk relationship. The aim of this study was to test this hypothesis. Specifically, the study was designed to evaluate the efficacy, safety, and pharmacokinetic (PK) profiles of zimlovisertib in combination with ritlecitinib, and zimlovisertib in combination with tofacitinib, compared with tofacitinib alone.

PATIENTS AND METHODS

Study design. This was a 24-week, phase 2, multicenter, randomized, double-blind, five-arm, parallel-group, active comparator study conducted in patients with moderate to severe active RA across 77 centers in 10 countries (Supplementary Table 1) between July 2020 and February 2022 (ClinicalTrials. gov identifier: NCT04413617). The study comprised a screening period of ≤28 days, a 24-week active treatment period, and a 4-week drug-free follow-up period (Supplementary Figure 1). Patients were randomized (4:4:3:3:4) to one of five treatment groups: zimlovisertib 400 mg modified release (MR) + tofacitinib 11 mg MR, zimlovisertib 400 mg MR + ritlecitinib 100 mg, tofacitinib 11 mg MR, zimlovisertib 400 mg MR, or ritlecitinib 100 mg.

All doses were administered orally once daily in a fasted state (approximately 4 hours after the last meal and 1.5 hours before the next meal). MTX was discontinued by patients during the week before randomization and washed out during the treatment period. Patients who had not achieved at least an ACR criteria for 20% improvement (ACR20) clinical response[19] by weeks 12, 16, and 20 were programmatically discontinued from the study.

The study was conducted in accordance with the protocol and ethical principles derived from the Declaration of Helsinki Council and International Council for Harmonisation Good Clinical Practice guidelines. The study protocol was reviewed and approved by the institutional review board and/or independent ethics committee at each participating center. All patients provided written informed consent.

Patients. Eligible patients were aged 18–70 years and had a body weight >40 kg. Patients were required to have a diagnosis of RA that met the 2010 ACR/EULAR classification criteria[20] with a total score ≥6/10; moderate to severe active disease at screening and randomization, defined by at least six tender/painful joints and at least six swollen joints; a high-sensitivity C-reactive protein (CRP) concentration >7 mg/L or erythrocyte sedimentation rate (ESR) >28 mm/h at or before randomization; to meet class I, II, or III of the ACR 1991 Revised Criteria for Global Functional Status in RA;[21] and to be seropositive for anticitrullinated protein antibodies or rheumatoid factor at the time of randomization. Patients must have been taking oral MTX at an adequate dose (15–25 mg weekly unless documented to be intolerant to these doses) for a sufficient duration before screening (generally ≥3 months but could be as short as 8 weeks if consistent with local standard of care treatment guidelines) to be considered an inadequate responder according to local practice guidelines. Patients receiving nonprohibited concomitant medications were required to be on a stable regimen, defined as not starting a new drug or changing a dosage, within 7 days or five half-lives before the first study dose.

Patients were excluded if they had active or latent infections, including tuberculosis, a history of deep vein thrombosis and pulmonary embolism, or if they had previously been treated with any of the study drugs in the context of a clinical trial. The exclusion criteria were amended on July 7, 2021, to minimize the potential risk of patients developing major adverse cardiovascular events to reflect the emerging data on cardiovascular risk associated with tofacitinib. Additional exclusion criteria are described in the Supplementary Materials.

Endpoints. *Efficacy.* The primary endpoint was the change from baseline in the four-component Disease Activity Score in 28 joints using CRP (DAS28-CRP) at week 12, and the key secondary endpoint was the proportion of patients achieving DAS28-CRP remission (<2.6) at week 24. Exploratory analyses

to evaluate treatment effects for these endpoints over time, assessed at all postrandomization time points (except weeks 12 and 24 for DAS28-CRP and ACR response rates and week 24 for DAS28-CRP remission rate), included the change from baseline in DAS28-CRP and DAS28-ESR rate; DAS28-CRP and DAS28-ESR remission rates; and ACR20, ACR50, ACR70, and ACR90 response rates.

Multiple prespecified continuous clinical and patient-reported outcomes are also reported, including the change from baseline in Tender/Painful Joint Counts among 28 and 68 joints (TJC28 and TJC68, respectively), Swollen Joint Counts among 28 and 66 joints (SJC28 and SJC66, respectively), Physician Global Assessment Score, Health Assessment Questionnaire – Disability Index, Patient's Assessment of Arthritis Pain, Patient's Global Assessment of Arthritis, Physical Component Summary (PCS) and Mental Component Summary (MCS) scores within the Short Form-36 (SF-36) questionnaire, European Quality of Life-visual analog scale (EQ-VAS) score within the European Quality of Life-5 Dimensions-5 level questionnaire, and Functional Assessment of Chronic Illness Therapy-Fatigue (FACIT-F). Outcomes based on composite scores included the change from baseline in the Clinical Disease Activity Index (CDAI) and Simplified Disease Activity Index (SDAI) as well as CDAI, SDAI, and ACR-EULAR remission rates. Prespecified responder definitions included low disease activity score based on DAS28-CRP, DAS28-ESR, CDAI, and SDAI.

The change from baseline of individual components of the DAS28-CRP and DAS28-ESR scores was also analyzed to provide additional insight into the magnitude of the contributions of individual components to the observed treatment effects on DAS28-CRP and DAS28-ESR scores. For most continuous efficacy outcomes (except EQ-VAS, SF-36 PCS, SF-36 MCS, and FACIT-F scores), lower scores indicate the lower level of disability so that a decrease in the baseline score during the treatment period (increases in EQ-VAS, SF-36 PCS, SF-36 MCS, and FACIT-F scores) is desirable.

Safety. The incidence and severity of treatment-emergent AEs (TEAEs), laboratory abnormalities, changes in vital signs, and electrocardiogram findings were assessed from the time each patient provided informed consent up to and including a minimum of 28 days after the last administration of the study drug. AEs were classified according to Medical Dictionary for Regulatory Activities, version 24.1.

PKs. Blood samples to measure plasma concentrations of zimlovisertib (and its two major metabolites PF-06787899 and PF-06787900) and ritlecitinib were collected at baseline and weeks 2, 4, 8, 12, 16, 20, and 24. For PK analysis of tofacitinib, blood samples were collected at baseline and weeks 4, 12, 16, and 24; samples were analyzed using validated high-performance liquid chromatography–mass spectrometry methods.

Statistical analyses. The primary objective was to evaluate whether either of the combination treatments (zimlovisertib + ritlecitinib or zimlovisertib + tofacitinib) produced superior efficacy compared with tofacitinib monotherapy. The declaration of superior treatment efficacy required the rejection of the null hypothesis of no difference in mean changes from baseline of DAS28-CRP at week 12 in the corresponding treatment groups at the two-sided significance level of 0.10. No adjustment for the multiplicity of comparisons (n = 2) between the combination treatment groups and the tofacitinib treatment group was applied. The observations for all patients who took at least one dose of investigational treatment were included into efficacy analyses regardless of their compliance to the randomized treatments or exposure to the concomitant medications. The dropout rate of 18% and an SD of baseline-adjusted change from baseline DAS28-CRP score of 1.20 at week 12 were assumed.

A sample size of approximately 100 patients in each of the zimlovisertib + ritlecitinib and zimlovisertib + tofacitinib combination groups and the tofacitinib monotherapy group, and up to 75 patients in the zimlovisertib and ritlecitinib monotherapy groups, was selected. A pairwise comparison of a combination group contrasted with the tofacitinib monotherapy group using a two-sided $\alpha = 0.10$ significance level had approximately 84% power to detect the assumed between-arm difference of means of 0.5.

Continuous endpoints were analyzed using a mixed model for repeated measures[22,23] and descriptive statistics. A change from the baseline value of the continuous variable was used as an outcome. Treatment, scheduled study visit, baseline value of the variable of interest, treatment-by-visit interaction, and baseline-by-visit interaction were used as fixed effects. The model used an unstructured covariance matrix. Missing data were not imputed.

All binary endpoints were analyzed using the Blyth and Still[24] and Casella[25] methods for the estimation of the probability of response at a given visit and in a given treatment group, and the Chan and Zhang method[26] was used for comparison of the probabilities of response across the treatment groups. A nonresponder imputation method was used for imputation of missing observations. A missing value was treated as a nonresponse except in two special cases: missingness related to COVID-19 infection (patient illness or a COVID-19–related reason for being unable to attend the visit) and missingness when the patient attended the visit but had missing components for calculating outcomes. The observations that were missing for these reasons were excluded from the calculation of the response rate at a given visit. The two-sided *P* values and 90% confidence intervals (CIs) were not adjusted for multiplicity.

Safety data were summarized based on observed case data by treatment group. Plasma concentrations of zimlovisertib, ritlecitinib, and tofacitinib were summarized and presented with descriptive statistics.

RESULTS

Patients. Of 626 patients who were screened, 460 met the eligibility criteria, were enrolled in the study, and received at least one dose of study treatment (Figure 1). Most patients (88.7% at week 12 and 69.8% at week 24) did not discontinue treatment before the corresponding study visit. The main reason for discontinuation after week 12 was a failure to achieve at least an ACR20 response at week 12 (70 patients [15.2%]), which was a protocol-specific requirement for the continuation of treatment per protocol. Most ACR20 nonresponders discontinued treatment at weeks 16 and 20.

Demographic and baseline disease characteristics for each treatment group are shown in Table 1. A total of 70 patients (15.2%) received prior tumor necrosis factor (TNF) inhibitors, with adalimumab being the most commonly used (38 patients [8.3%]). No patients had previously received a non-TNF bDMARD. Characteristics were generally similar across treatment groups.

Efficacy. The estimated mean changes from baseline in DAS28-CRP scores at week 12 were −2.65 (90% CI, −2.83 to −2.46) in the zimlovisertib + tofacitinib group, −2.35 (90% CI, −2.54 to −2.15) in the zimlovisertib + ritlecitinib group, −2.30 (90% CI, −2.49 to −2.11) in the tofacitinib group, −2.21 (90% CI, −2.44 to −1.99) in the ritlecitinib group, and −1.82 (90% CI, −2.04 to −1.61) in the zimlovisertib group (Figure 2A; Table 2).

The difference in the estimated mean values between the combination groups and tofacitinib monotherapy was statistically significant for the zimlovisertib + tofacitinib group ($P = 0.032$) but was not statistically significant for the zimlovisertib + ritlecitinib group ($P = 0.787$).

At week 12, all treatment groups had clinically meaningful and statistically significant decreases in DAS28-CRP mean values. The zimlovisertib monotherapy group had the smallest decrease from baseline in DAS28-CRP.

The estimated mean changes from baseline in DAS28-ESR scores at week 12 were −2.94 (90% CI, −3.13 to −2.75) in the zimlovisertib + tofacitinib group, −2.77 (90% CI, −2.96 to −2.57) in the zimlovisertib + ritlecitinib group, −2.54 (90% CI, −2.73 to −2.34) in the tofacitinib group, −2.48 (90% CI, −2.71 to −2.25) in the ritlecitinib group, and −2.44 (90% CI, −2.66 to −2.21) in the zimlovisertib group (Figure 2B; Table 2). The difference in the estimated mean values observed in the combination treatment group and the tofacitinib treatment group was marginally statistically significant for zimlovisertib + tofacitinib and was not statistically significant for the zimlovisertib + ritlecitinib treatment group.

In the zimlovisertib + tofacitinib and zimlovisertib + ritlecitinib groups, the proportion of patients achieving DAS28-CRP remission at week 24 was higher (40.8% [90% CI, 32.6%–48.7%] and 31.3% [90% CI, 24.1%–39.8%], respectively) compared with the tofacitinib monotherapy group (24.0% [90% CI, 17.1%–31.8%]) (Figure 2C; Table 2). The difference in the estimated proportion

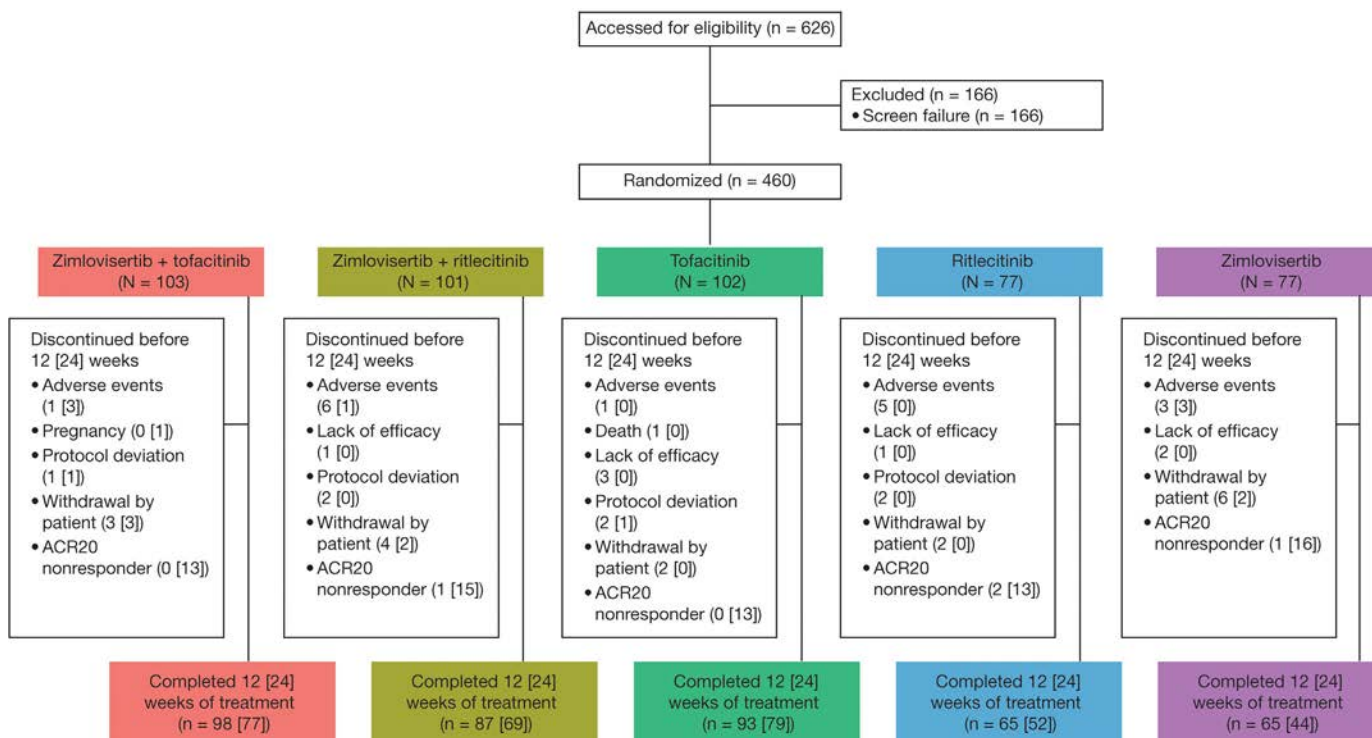**Figure 1.** Patient disposition. A study discontinuation event during the treatment period was defined as an event in which the patient discontinued study treatment and did not complete the 4-week follow-up period. ACR20, American College of Rheumatology criteria for 20% improvement in disease activity; N, number of patients randomized to each cohort; n, number of patients completing treatment.

Table 1. Demographics and baseline disease characteristics*

Characteristics	Tofacitinib 11 mg QD (n = 102)	Ritlecitinib 100 mg QD (n = 77)	Zimlovisertib 400 mg QD (n = 77)	Zimlovisertib 400 mg + tofacitinib 11 mg QD (n = 103)	Zimlovisertib 400 mg + ritlecitinib 100 mg QD (n = 101)
Age, mean (SD), y	51.2 (10.6)	52.8 (10.9)	53.6 (9.9)	54.0 (10.4)	53.0 (10.4)
Female, n (%)	82 (80.4)	62 (80.5)	61 (79.2)	78 (75.7)	73 (72.3)
Race, n (%)					
White	101 (99.0)	76 (98.7)	77 (100.0)	102 (99.0)	101 (100.0)
Other[a]	1 (1.0)	1 (1.3)	0 (0.0)	1 (1.0)	0 (0.0)
Ethnicity, n (%)					
Hispanic or Latino	14 (13.7)	6 (7.8)	6 (7.8)	14 (13.6)	9 (8.9)
Not Hispanic or Latino	87 (85.3)	71 (92.2)	71 (92.2)	89 (86.4)	92 (91.1)
Not reported	1 (1.0)	0 (0.0)	0 (0.0)	0 (0.0)	0 (0.0)
Tobacco use, n (%)					
Never	66 (64.7)	45 (58.4)	50 (64.9)	62 (60.2)	64 (63.4)
Former	14 (13.7)	13 (16.9)	10 (13.0)	21 (20.4)	14 (13.9)
Current	22 (21.6)	19 (24.7)	17 (22.1)	20 (19.4)	23 (22.8)
Alcohol use, n (%)					
Never	65 (63.7)	48 (62.3)	56 (72.7)	64 (62.1)	58 (57.4)
Former	4 (3.9)	6 (7.8)	3 (3.9)	5 (4.9)	3 (3.0)
Current	33 (32.4)	23 (29.9)	18 (23.4)	34 (33.0)	40 (39.6)
Duration since onset of RA, mean (SD), y	8.0 (7.6)	8.5 (6.7)	7.9 (8.1)	7.6 (7.4)	8.4 (6.9)
TJC28, mean (SD)	15.0 (6.3)	13.6 (5.6)	15.2 (5.9)	15.0 (6.3)	13.5 (5.8)
SJC28, mean (SD)	10.5 (5.1)	10.5 (5.5)	11.6 (5.3)	10.8 (4.8)	10.2 (4.9)
TJC68, mean (SD)	23.5 (11.8)	19.6 (10.2)	22.1 (12.2)	23.8 (13.0)	20.9 (10.7)
SJC66, mean (SD)	14.2 (7.5)	13.3 (7.1)	14.5 (7.9)	14.0 (6.5)	13.4 (6.4)
PhGA, mean (SD), mm	67.5 (14.1)	60.6 (13.6)	63.3 (14.6)	67.7 (13.8)	64.2 (15.3)
PAAP, mean (SD), mm	65.0 (19.6)	57.8 (20.7)	63.0 (21.1)	64.2 (20.3)	61.0 (22.2)
PtGA, mean (SD), mm	66.1 (18.8)	59.6 (19.3)	63.4 (19.5)	65.6 (19.7)	60.8 (22.3)
HAQ-DI score, mean (SD)	1.6 (0.5)	1.4 (0.6)	1.5 (0.6)	1.6 (0.6)	1.5 (0.6)
hsCRP, mean (SD), mg/dL	9.9 (16.3)	11.4 (18.1)	9.4 (11.4)	14.4 (22.4)	13.5 (24.1)
ESR, mean (SD), mm/h	39.9 (17.2)	44.3 (20.5)	39.9 (13.5)	42.6 (16.0)	39.8 (16.2)
DAS28-CRP, mean (SD)	6.3 (1.0)	6.1 (1.0)	6.3 (0.8)	6.4 (1.0)	6.1 (1.1)
Prior TNF inhibitor use, n (%)	14 (13.7)	14 (18.2)	11 (14.3)	17 (16.5)	14 (13.9)

* CRP, C-reactive protein; DAS28, Disease Activity Score in 28 joints; ESR, erythrocyte sedimentation rate; HAQ-DI, Health Assessment Questionnaire–Disability Index; hsCRP, high-sensitivity C-reactive protein; N, number of patients randomized to each treatment group; n, number of patients within each category; PAAP, Patient's Assessment of Arthritis Pain; PhGA, Physician Global Assessment; PtGA, Patient's Global Assessment of Arthritis; QD, once daily; RA, rheumatoid arthritis; SJC, Swollen Joint Count; TJC, Tender/Painful Joint Count; TNF, tumor necrosis factor.
[a] Includes Asian, Native Hawaiian or other Pacific Islander, and multiracial.

of patients with DAS28-CRP remission at week 24 was marginally statistically significant for zimlovisertib + tofacitinib versus tofacitinib monotherapy but was not significant for zimlovisertib + ritlecitinib versus tofacitinib monotherapy.

A rapid decrease in the mean value of DAS28-CRP in comparison to baseline occurred by week 12, which was maintained to week 24 and followed by a rapid increase approaching baseline levels during the drug-free follow-up period (Figure 2A; Table 2). Similarly, DAS28-CRP remission rates increased nearly linearly in all treatment groups during the treatment period and decreased during the drug-free follow-up period (Figure 2C; Table 2).

In the zimlovisertib + tofacitinib and zimlovisertib + ritlecitinib groups, the proportion of patients achieving DAS28-ESR remission at week 24 was higher (37.9% [90% CI, 29.9%–45.8%] and 32.3% [90% CI, 24.6%–40.8%], respectively) compared with the tofacitinib monotherapy group (23.0% [90% CI, 16.3%–30.8%]) (Figure 2D; Table 2). The difference in the estimated proportion of participants with the DAS28-ESR remission observed in the

combination treatment group and the tofacitinib treatment group was marginally statistically significant at weeks 12 and 24 for the zimlovisertib + tofacitinib treatment group and was not statistically significant for the zimlovisertib + ritlecitinib treatment group.

The proportion of ACR20 responders increased to week 12 and then declined; an increase in ACR50/70 responders over treatment time was observed for all the treatment groups (Figure 3). At week 12, the proportions of patients achieving an ACR20 response were 86.4%, 79.2%, 83.2%, 72.7%, and 75.0% in the zimlovisertib + tofacitinib, zimlovisertib + ritlecitinib, tofacitinib, ritlecitinib, and zimlovisertib treatment groups, respectively. At week 24, the proportions of patients achieving an ACR20 response were 75.7%, 70.0%, 75.3%, 67.5%, and 55.3% in the zimlovisertib + tofacitinib, zimlovisertib + ritlecitinib, tofacitinib, ritlecitinib, and zimlovisertib treatment groups, respectively. ACR50 response rates at weeks 12 and 24 were 62.8% and 65.1% (zimlovisertib + tofacitinib), 54.5% and 65.0% (zimlovisertib + ritlecitinib), 46.5% and 65.4% (tofacitinib), 44.2% and 54.6% (ritlecitinib), and 38.2% and 43.4% (zimlovisertib). ACR70
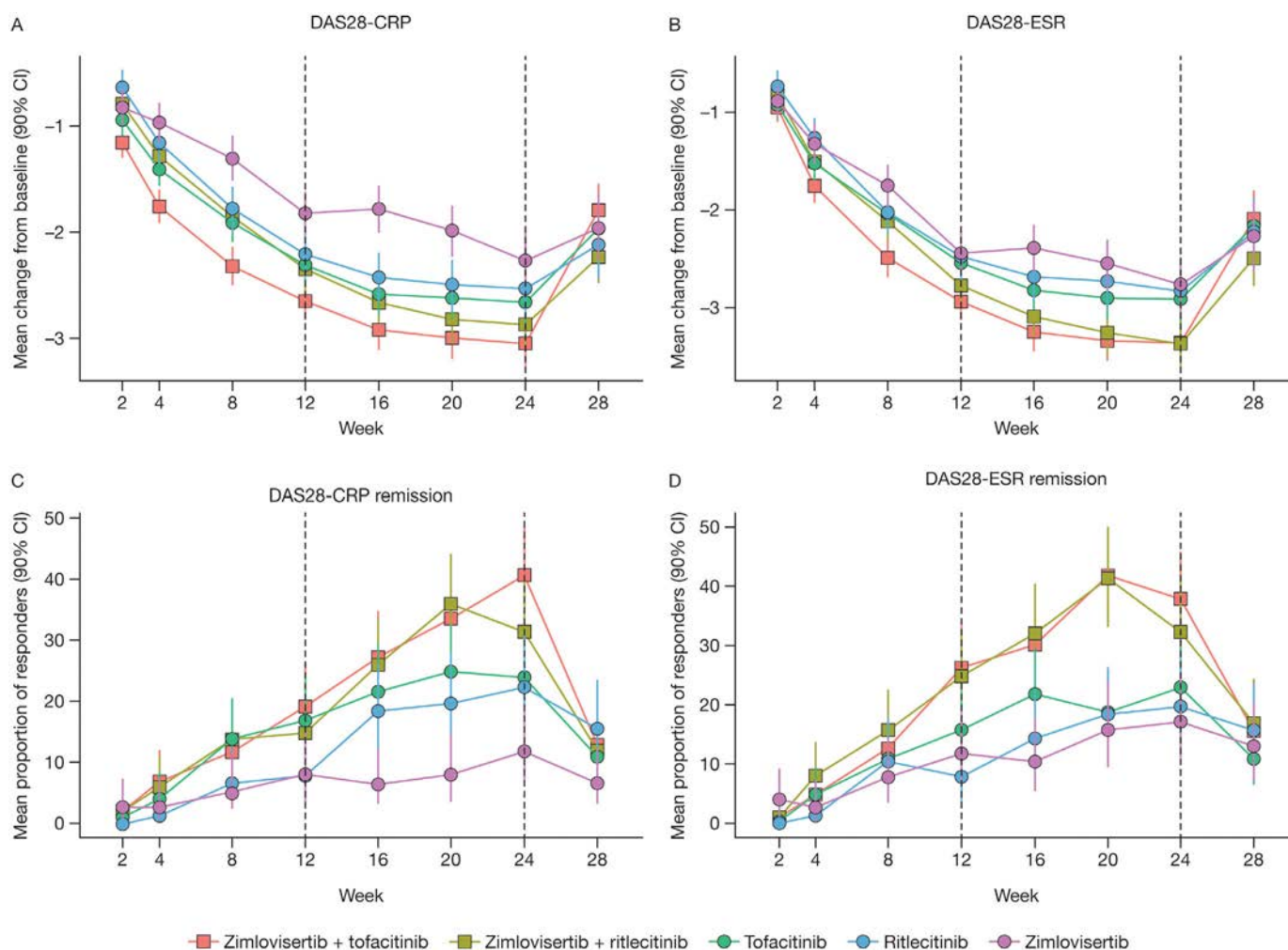
Figure 2. Mean change from baseline (90% CI) in (A) DAS28-CRP and (B) DAS28-ESR, and the proportion of patients with (C) DAS28-CRP remission and (D) DAS28-ESR remission for each treatment group over time. Vertical solid lines show CIs with 90% coverage. Dashed vertical lines show the timing of the primary analysis (week 12) and the last dose of treatment (week 24). CI, confidence interval; CRP, C-reactive protein; DAS28, Disease Activity Score in 28 joints; ESR, erythrocyte sedimentation rate.

response rates were 21.4% and 45.6% (zimlovisertib + tofacitinib), 25.7% and 44.0% (zimlovisertib + ritlecitinib), 23.8% and 44.6% (tofacitinib), 18.2% and 31.2% (ritlecitinib), and 10.5% and 27.6% (zimlovisertib). The proportion of ACR90 responders increased over the treatment time for both combination treatment groups as well as tofacitinib monotherapy, but this was not observed for the zimlovisertib and ritlecitinib monotherapy groups (Figure 3; Supplementary Table 2). A reduction in the proportion of ACR20/50/70 responders was observed after completion of treatment at week 24. The estimated proportions of responders in the zimlovisertib monotherapy group were lower than in the tofacitinib monotherapy group, with the difference being marginally statistically significant at week 24 (Supplementary Table 2).

The estimated means of multiple secondary and exploratory outcomes are presented in Supplementary Table 2. The differences between the mean values of outcomes between the combination treatment groups and tofacitinib did not reach statistical

significance. The zimlovisertib monotherapy group appeared to have lower efficacy for many outcomes.

Improvements in multiple components of DAS28-CRP and DAS28-ESR scores were observed in all treatment groups (Supplementary Figure 2A–E). A large decrease in the level of biomarker-related components (CRP and ESR) was observed in the zimlovisertib + tofacitinib treatment group (Supplementary Figure 2A and B).

Safety. Overall, 246 patients (53.5%) reported a total of 469 all-causality TEAEs. The tofacitinib monotherapy treatment group had the highest aggregate incidence of TEAEs (n = 60 [58.8%]). The incidence of specific TEAEs was similar across all treatment groups (Table 3), and most TEAEs were mild in severity (mild: n = 329 [70.1%]; moderate: n = 129 [27.5%]; and severe: n = 11 [2.3%]). Infections and infestations were the most common TEAEs (by system organ class), with the highest proportion of

Table 2. Change from baseline in DAS28-CRP and DAS28-ESR and DAS28-CRP and DAS28-ESR remission rates at weeks 12 and 24*

Outcome	Week	Tofacitinib 11 mg QD (n = 102)	Ritlecitinib 100 mg QD (n = 77)	Zimlovisertib 400 mg QD (n = 77)	Zimlovisertib 400 mg + tofacitinib 11 mg QD (n = 103)	Zimlovisertib 400 mg + ritlecitinib 100 mg QD (n = 101)
DAS28-CRP						
Mean (90% CI)	12	−2.30 (−2.49 to −2.11)	−2.21 (−2.44 to −1.99)	−1.82 (−2.04 to −1.61)	−2.65 (−2.83 to −2.46)	−2.35 (−2.54 to −2.15)
Difference from tofacitinib (90% CI)	12	–	0.09 (−0.21 to 0.38)	**0.48 (0.19 to 0.77)**	**−0.34 (−0.61 to −0.08)**	−0.04 (−0.32 to 0.23)
Mean (90% CI)	24	−2.66 (−2.88 to −2.45)	−2.53 (−2.78 to −2.28)	−2.26 (−2.51 to −2.00)	−3.05 (−3.26 to −2.85)	−2.87 (−3.08 to −2.65)
Difference from tofacitinib (90% CI)	24	–	0.13 (−0.19 to 0.46)	**0.41 (0.08 to 0.74)**	**−0.39 (−0.69 to −0.09)**	−0.20 (−0.51 to 0.10)
DAS28-ESR						
Mean (90% CI)	12	−2.54 (−2.73 to −2.34)	−2.48 (−2.71 to −2.25)	−2.44 (−2.66 to −2.21)	−2.94 (−3.13 to −2.75)	−2.77 (−2.96 to −2.57)
Difference from tofacitinib (90% CI)	12	–	0.05 (−0.25 to 0.35)	0.10 (−0.20 to 0.40)	**−0.40 (−0.68 to −0.13)**	−0.23 (−0.51 to 0.05)
Mean (90% CI)	24	−2.91 (−3.14 to −2.67)	−2.83 (−3.10 to −2.55)	−2.76 (−3.04 to −2.48)	−3.36 (−3.59 to −3.14)	−3.36 (−3.60 to −3.12)
Difference from tofacitinib (90% CI)	24	–	0.08 (−0.28 to 0.44)	0.14 (−0.22 to 0.51)	**−0.46 (−0.78 to −0.13)**	**−0.46 (−0.79 to −0.12)**
DAS28-CRP remission						
Responder rate, % (90% CI)	12	16.83 (11.02 to 24.06)	7.79 (3.45 to 14.58)	8.00 (3.54 to 14.99)	19.19 (13.20 to 26.43)	14.85 (9.66 to 21.36)
Difference from tofacitinib (90% CI)	12	–	**−9.04 (−17.45 to −0.32)**	−8.83 (−17.23 to 0.09)	2.36 (−6.88 to 11.61)	−1.98 (−10.84 to 6.79)
Responder rate, % (90% CI)	24	24.00 (17.13 to 31.75)	22.37 (14.78 to 31.27)	11.84 (6.68 to 19.32)	40.78 (32.61 to 48.70)	31.31 (24.11 to 39.77)
Difference from tofacitinib (90% CI)	24	–	−1.63 (−12.16 to 9.50)	**−12.16 (−21.61 to −1.44)**	**16.78 (3.82 to 27.43)**	7.31 (−3.41 to 17.84)
DAS28-ESR remission rate						
Responder rate, % (90% CI)	12	15.84 (10.41 to 22.52)	7.79 (3.45 to 14.58)	11.84 (6.68 to 19.32)	26.21 (19.19 to 33.64)	24.75 (17.89 to 32.36)
Difference from tofacitinib (90% CI)	12	–	−8.05 (−16.40 to 0.57)	−4.00 (−12.80 to 5.21)	**10.37 (0.46 to 19.84)**	8.91 (−0.53 to 18.54)
Responder rate, % (90% CI)	24	23.00 (16.26 to 30.81)	19.74 (12.58 to 28.23)	17.11 (11.10 to 25.20)	37.86 (29.86 to 45.80)	32.32 (24.57 to 40.82)
Difference from tofacitinib (90% CI)	24	–	−3.26 (−13.47 to 7.64)	−5.89 (−15.85 to 4.66)	**14.86 (3.06 to 25.51)**	9.32 (−1.36 to 20.06)

* Values in bold indicate the 90% CI of the difference from tofacitinib for which the difference is marginally statistically significant. CI, confidence interval; CRP, C-reactive protein; DAS28, Disease Activity Score in 28 joints; ESR, erythrocyte sedimentation rate; QD, once daily.
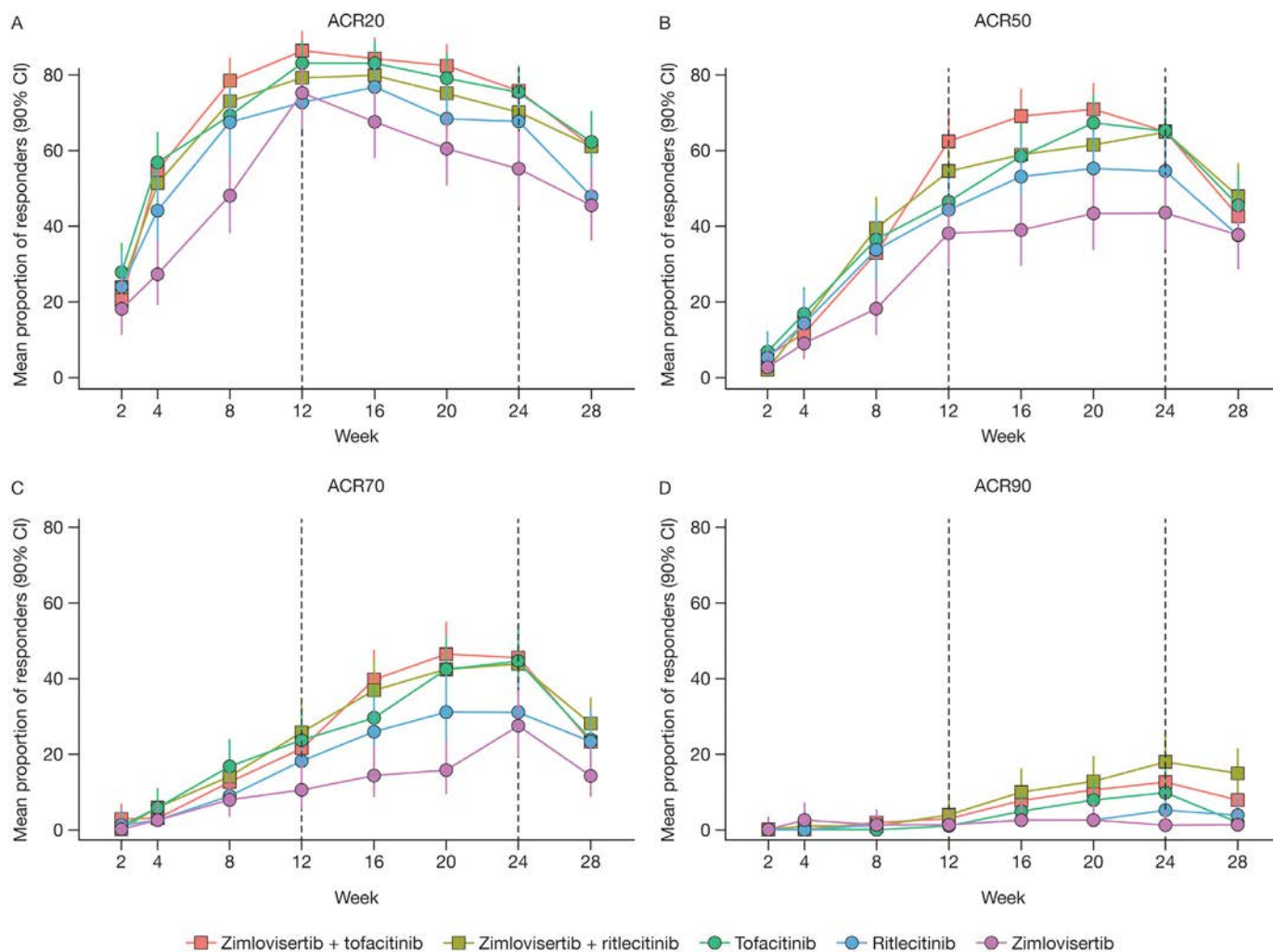
Figure 3. Mean proportion (90% CI) of (A) ACR20, (B) ACR50, (C) ACR70, and (D) ACR90 responders for each treatment group over time. Vertical solid lines show CIs with 90% coverage. Dashed vertical lines show the timing of the primary analysis (week 12) and the last dose of treatment (week 24). ACR20/50/70/90, American College of Rheumatology criteria for 20%/50%/70%/90% improvement in disease activity; CI, confidence interval.

patients experiencing infections and infestations in the zimloviser-tib + tofacitinib group (n = 13 [12.6%]; Table 3). Eight patients (1.7%) experienced eight all-causality TEAEs of herpes infection (zimlovisertib + ritlecitinib: n = 2 [2.0%]; zimlovisertib + tofacitinib: n = 3 [2.9%]; tofacitinib: n = 2 [2.0%]; ritlecitinib: n = 1 [1.3%]; and zimlovisertib: n = 0). Severe TEAEs were reported by nine (2.0%) patients, and 10 patients had serious AEs: one in the zim-lovisertib + ritlecitinib group, three in the zimlovisertib group, three in the ritlecitinib group, and three in the tofacitinib group (Table 3). Four patients permanently discontinued from the study because of TEAEs (of which two [50%] were in the tofacitinib monotherapy group) (Table 3). Twenty-two patients (4.8%) discontinued treatment owing to TEAEs, and 44 patients (9.6%) had a temporary discontinuation owing to TEAEs. In addition, two patients (0.4%) in the zimlovisertib + tofacitinib combination group discontinued the treatment but continued the study because of herpes infection. One participant in the tofacitinib monotherapy group died

because of a severe AE of COVID-19 infection that was considered unrelated to the study intervention.

One patient in the zimlovisertib group had elevated transaminases that were recorded as moderate liver injury, which was considered to be treatment related. This patient had normal alanine aminotransferase (ALT) and aspartate aminotransferase (AST) at baseline; between days 57 and 100, ALT and AST levels ranged between 93–197 U/L and 49–115 U/L, respectively, before returning to normal on day 126. Increases in ALT were reported by five patients (1.1%): three in the zimlovisertib group and two in the zim-lovisertib + tofacitinib group. Four patients (0.9%) (two each in the zimlovisertib and zimlovisertib + tofacitinib groups) had increased AST. All AEs of ALT and AST increases were of mild or moderate severity. One patient in the tofacitinib group reported mild hyperbi-lirubinemia, and one patient each in the zimlovisertib group reported increased hepatic enzyme and increased transaminases; all were considered to be treatment related.

Table 3. Overview of TEAEs (all-causality) occurring in ≥2% of patients in any group by MedDRA system organ class and preferred term[*]

Patients	Tofacitinib 11 mg QD (n = 102), n (%)	Ritlecitinib 100 mg QD (n = 77), n (%)	Zimlovisertib 400 mg QD (n = 77), n (%)	Zimlovisertib 400 mg + tofacitinib 11 mg QD (n = 103), n (%)	Zimlovisertib 400 mg + ritlecitinib 100 mg QD (n = 101), n (%)
TEAEs	60 (58.8)	42 (54.5)	38 (49.4)	51 (49.5)	55 (54.5)
Serious AEs[a]	3 (2.9)	3 (3.9)	3 (3.9)	0	1 (1.0)
Severe AEs	3 (2.9)	1 (1.3)	0	3 (2.9)	2 (2.0)
Discontinued from study owing to AEs	2 (2.0)	0	0	1 (1.0)	1 (1.0)
Discontinued study drug owing to AEs and continued study	0	6 (7.8)	6 (7.8)	4 (3.9)	6 (5.9)
Temporary discontinuation or dose reduction owing to AEs	6 (5.9)	9 (11.7)	4 (5.2)	9 (8.7)	16 (15.8)
Infections and infestations	11 (10.8)	4 (5.2)	4 (5.2)	13 (12.6)	12 (11.9)
Urinary tract infection	5 (4.9)	1 (1.3)	1 (1.3)	7 (6.8)	3 (3.0)
Nasopharyngitis	3 (2.9)	2 (2.6)	1 (1.3)	3 (2.9)	6 (5.9)
Upper respiratory tract infection	2 (2.0)	1 (1.3)	1 (1.3)	3 (2.9)	2 (2.0)
Pharyngitis	2 (2.0)	0 (0.0)	2 (2.6)	1 (1.0)	1 (1.0)
Musculoskeletal and connective tissue disorders	6 (5.9)	9 (11.7)	7 (9.1)	7 (6.8)	7 (6.9)
Arthralgia	3 (2.9)	5 (6.5)	1 (1.3)	2 (1.9)	2 (2.0)
RA	3 (2.9)	4 (5.2)	4 (5.2)	1 (1.0)	1 (1.0)
Arthritis	0 (0.0)	0 (0.0)	2 (2.6)	1 (1.0)	3 (3.0)
Back pain	0 (0.0)	1 (1.3)	0 (0.0)	3 (2.9)	2 (2.0)
Myalgia	0 (0.0)	2 (2.6)	0 (0.0)	0 (0.0)	0 (0.0)
Gastrointestinal disorders	9 (8.8)	8 (10.4)	3 (3.9)	3 (2.9)	10 (9.9)
Nausea	4 (3.9)	5 (6.5)	2 (2.6)	1 (1.0)	3 (3.0)
Vomiting	3 (2.9)	1 (1.3)	2 (2.6)	2 (1.9)	3 (3.0)
Diarrhea	2 (2.0)	2 (2.6)	0 (0.0)	1 (1.0)	2 (2.0)
Dyspepsia	2 (2.0)	0 (0.0)	0 (0.0)	0 (0.0)	4 (4.0)
Investigations	7 (6.9)	1 (1.3)	5 (6.5)	6 (5.8)	8 (7.9)
SARS-CoV-2 test positive	7 (6.9)	1 (1.3)	2 (2.6)	4 (3.9)	8 (7.9)
ALT increased	0 (0.0)	0 (0.0)	3 (3.9)	2 (1.9)	0 (0.0)
AST increased	0 (0.0)	0 (0.0)	2 (2.6)	2 (1.9)	0 (0.0)
Nervous system disorders	4 (3.9)	7 (9.1)	3 (3.9)	5 (4.9)	7 (6.9)
Headache	4 (3.9)	4 (5.2)	2 (2.6)	3 (2.9)	7 (6.9)
Dizziness	0 (0.0)	3 (3.9)	1 (1.3)	2 (1.9)	0 (0.0)
General disorders and administration site conditions	1 (1.0)	3 (3.9)	3 (3.9)	2 (1.9)	1 (1.0)
Fatigue	1 (1.0)	2 (2.6)	1 (1.3)	1 (1.0)	1 (1.0)
Pyrexia	0 (0.0)	1 (1.3)	2 (2.6)	1 (1.0)	0 (0.0)
Metabolism and nutrition disorders	3 (2.9)	3 (3.9)	2 (2.6)	0 (0.0)	2 (2.0)
Hyperlipidemia	2 (2.0)	2 (2.6)	0 (0.0)	0 (0.0)	1 (1.0)
Dyslipidemia	1 (1.0)	0 (0.0)	2 (2.6)	0 (0.0)	1 (1.0)
Hyperglycemia	0 (0.0)	2 (2.6)	0 (0.0)	0 (0.0)	0 (0.0)
Vascular disorders	2 (2.0)	0 (0.0)	0 (0.0)	3 (2.9)	2 (2.0)
Hypertension	2 (2.0)	0 (0.0)	0 (0.0)	3 (2.9)	2 (2.0)
Blood and lymphatic system disorders	0 (0.0)	4 (5.2)	0 (0.0)	0 (0.0)	2 (2.0)
Lymphopenia	0 (0.0)	3 (3.9)	0 (0.0)	0 (0.0)	2 (2.0)

(Continued)

Table 3. (Cont'd)

Patients	Tofacitinib 11 mg QD (n = 102), n (%)	Ritlecitinib 100 mg QD (n = 77), n (%)	Zimlovisertib 400 mg QD (n = 77), n (%)	Zimlovisertib 400 mg + tofacitinib 11 mg QD (n = 103), n (%)	Zimlovisertib 400 mg + ritlecitinib 100 mg QD (n = 101), n (%)
Leukopenia	0 (0.0)	2 (2.6)	0 (0.0)	0 (0.0)	0 (0.0)
Ear and labyrinth disorders	4 (3.9)	0 (0.0)	0 (0.0)	1 (1.0)	0 (0.0)
Tinnitus	4 (3.9)	0 (0.0)	0 (0.0)	1 (1.0)	0 (0.0)
Renal and urinary disorders	2 (2.0)	2 (2.6)	1 (1.3)	0 (0.0)	0 (0.0)
Leukocyturia	2 (2.0)	2 (2.6)	1 (1.3)	0 (0.0)	0 (0.0)

* AE, adverse event; ALT, alanine aminotransferase; AST, aspartate aminotransferase; MedDRA, Medical Dictionary for Regulatory Activities, version 24.1; QD, once daily; RA, rheumatoid arthritis; TEAE, treatment-emergent adverse event.
[a] A total of 10 patients reported 11 serious AEs. Serious AEs include the following preferred terms: tofacitinib (uterine leiomyoma [n = 1], skin squamous cell carcinoma recurrent [n = 1], and coronavirus infection [n = 1]); ritlecitinib (diabetic ketoacidosis [n = 1], uterine leiomyoma [n = 1], and femur fracture [n = 1]); zimlovisertib (renal colic [n = 1], endometrial hyperplasia [n = 1], uterine polyp [n = 1], and spinal stenosis [n = 1]); and zimlovisertib + ritlecitinib (COVID-19 pneumonia [n = 1]).

Changes in hematology parameters (reticulocytes/erythrocytes, hemoglobin, hematocrit, and leukocytes) were consistent between all treatment groups. Decreases from baseline in platelets through week 24 were observed in the zimlovisertib + ritlecitinib and ritlecitinib monotherapy groups. Additional safety results, as well as PK results, are described in the Supplementary Results.

DISCUSSION

This phase 2 study evaluated the efficacy, safety, and PK profiles of two different drug combinations (zimlovisertib + tofacitinib and zimlovisertib + ritlecitinib) versus tofacitinib monotherapy to test the hypothesis that a combination of drugs with nonoverlapping mechanisms of action could provide improvements in efficacy compared with currently available treatments in patients with moderate to severe active RA. The effects of zimlovisertib and ritlecitinib monotherapies were also evaluated. Improvements in all endpoints, across all treatment groups, were observed over time, with most improvements occurring by the middle of the active treatment period. The proportion of ACR20 responders declined after week 12; a potential reason for this could be the per protocol removal of nonresponders at weeks 12, 16, and 20 from the study and treating them as nonresponders at subsequent visits.

A larger decrease in mean DAS28-CRP at week 12 (primary endpoint) was observed in patients receiving the zimlovisertib + tofacitinib combination treatment, but not zimlovisertib + ritlecitinib, versus those receiving tofacitinib monotherapy; the difference between zimlovisertib + tofacitinib and the tofacitinib monotherapy group was statistically significant. A differentiation between the efficacy of the zimlovisertib + tofacitinib combination treatment and tofacitinib monotherapy was also observed for some of the secondary outcomes, including DAS28-CRP remission rate and mean change from baseline in DAS28-CRP at week 24. Improvements were noted in both the DAS28-CRP and DAS28-ESR scores. An exploratory analysis demonstrated a nearly immediate and substantial reduction in both acute-phase reactant components (CRP and ESR) for the zimlovisertib + tofacitinib combination. This suggests a potential anti-inflammatory effect of this treatment combination in RA. No meaningful differences in the 28 joint count outcomes (TJC28 and SJC28) at week 24 were observed between tofacitinib monotherapy and the combination treatment groups. This suggests that the differences noted in DAS28-CRP and DAS28-ESR were driven by the effects on the acute-phase reactants (Supplementary Figure 2). Furthermore, no meaningful differences in the steady-state predose exposure of tofacitinib, ritlecitinib, or zimlovisertib were observed when dosed in combination versus when dosed as monotherapy. This suggests that the differentiation in efficacy was not driven by exposure; rather, it could be an additive pharmacological effect.

Zimlovisertib, tofacitinib, and ritlecitinib have different mechanisms of action. Specifically, zimlovisertib predominantly inhibits toll-like receptor signaling pathways[27] and, unlike tofacitinib and ritlecitinib, does not directly inhibit JAK/STAT signaling.[18,28] A combination of zimlovisertib and a JAK or JAK3/TEC inhibitor theoretically has a broader anti-inflammatory profile that could improve clinical efficacy without an inferior safety profile. The current study supports this hypothesis for the combination of zimlovisertib + tofacitinib but not for zimlovisertib + ritlecitinib, although the latter did exhibit encouraging trends that may become more prominent with further prolonged dosing.

The safety profiles of all treatment groups in the current study were consistent with a potentially favorable benefit-risk profile without evidence of increased TEAEs in the combination groups, although it should be recognized that sample sizes were relatively small. Both combination therapies had safety profiles that were similar to those of the monotherapies with no evidence of treatment-dependent differences. Importantly, although improvements in clinical efficacy were seen with the combination groups versus monotherapies, there did not appear to be any increase in incidence, type, and severity of TEAEs. In addition, MTX is associated with AEs, such as gastrointestinal disorders[29,30]; thus, some patients with RA discontinue MTX.[31,32] Therefore, withdrawal of MTX may be beneficial in improving safety and reducing

AEs. The safety profiles of the monotherapy treatments were consistent with those previously reported.[15,33,34]

Sporadic increases in ALT and AST were reported following treatment with zimlovisertib in the combination and monotherapy groups, similar to those seen in earlier phase 1 studies with this molecule. One patient had elevations in ALT and AST that were reported as an AE of "liver injury" without elevation in total bilirubin or other evidence of hepatic synthetic dysfunction. There were no clinically relevant changes in organ function, including renal function, confirming observations in previous trials with these study interventions.[14,35,36] Laboratory changes were consistent with those previously described for the individual drugs without evidence of enhanced effects in the combination groups.[14,37,38]

This study demonstrates the utility of the multiple-arm umbrella study design, whereby the efficacy of multiple treatments is explored in a single study.[39] The study was successfully conducted during the COVID-19 pandemic; the overall impact of COVID-19 on the study was small, with only 10 patients (2.2%) missing a visit and 21 patients (4.6%) having a study visit outside of allowable visit windows. Furthermore, a relatively small number of patients (5.2%) experienced TEAEs related to COVID-19, most of which were mild in severity.

The limitations of the study include the relatively small sample size, which may limit the generalizability of our findings and make it difficult to draw meaningful conclusions regarding treatment efficacy. Additionally, statistical analyses of the 6-month data for nonbinary endpoints were complicated by the programmatic discontinuation of patients who did not achieve at least an ACR20 response by week 12. This design element was included to preclude continuing patients who were nonresponders. Furthermore, the study was not placebo-controlled, which has the potential for increased bias and efficacy inflation.

In conclusion, treatment with zimlovisertib + tofacitinib was more effective than tofacitinib monotherapy for the treatment of patients with moderate to severe active RA. The differentiation from the tofacitinib monotherapy group was not established for the zimlovisertib + ritlecitinib combination group. Both combination treatments were well tolerated with acceptable safety profiles.

ACKNOWLEDGMENT

AUTHOR CONTRIBUTIONS

All authors contributed to at least one of the following manuscript preparation roles: conceptualization AND/OR methodology, software, investigation, formal analysis, data curation, visualization, and validation AND drafting or reviewing/editing the final draft. As corresponding author, Dr Danto confirms that all authors have provided the final approval of the version to be published and takes responsibility for the affirmations regarding article submission (eg, not under consideration by another journal), the integrity of the data presented, and the statements regarding compliance with institutional review board/Declaration Helsinki requirements.

ROLE OF THE STUDY SPONSOR

REFERENCES

1. Guo Q, Wang Y, Xu D, et al. Rheumatoid arthritis: pathological mechanisms and modern pharmacologic therapies. Bone Res 2018;6:15.

2. Rheumatoid Arthritis Collaborators GBD; GBD 2021 Rheumatoid Arthritis Collaborators. Global, regional, and national burden of rheumatoid arthritis, 1990-2020, and projections to 2050: a systematic analysis of the Global Burden of Disease Study 2021. Lancet Rheumatol 2023;5(10):e594–e610.

3. Einarsson JT, Willim M, Ernestam S, et al. Prevalence of sustained remission in rheumatoid arthritis: impact of criteria sets and disease duration, a nationwide study in Sweden. Rheumatology (Oxford) 2019;58(2):227–236.

4. Sun X, Li R, Cai Y, et al; APLAR RA SIG group. Clinical remission of rheumatoid arthritis in a multicenter real-world study in Asia-Pacific region. Lancet Reg Health West Pac 2021;15:100240.

5. Fraenkel L, Bathon JM, England BR, et al. 2021 American College of Rheumatology guideline for the treatment of rheumatoid arthritis. Arthritis Care Res (Hoboken) 2021;73(7):924–939.

6. Smolen JS, Landewé RBM, Bergstra SA, et al. EULAR recommendations for the management of rheumatoid arthritis with synthetic and biological disease-modifying antirheumatic drugs: 2022 update. Ann Rheum Dis 2023;82(1):3–18.

7. Smolen JS, Landewé RBM, Bijlsma JWJ, et al. EULAR recommendations for the management of rheumatoid arthritis with synthetic and biological disease-modifying antirheumatic drugs: 2019 update. Ann Rheum Dis 2020;79(6):685–699.

8. Fitton J, Melville A, Naraghi K, et al. Single-centre experience of refractory rheumatoid arthritis. Rheumatol Adv Pract 2022;6(2):rkac057.

9. Holdsworth EA, Donaghy B, Fox KM, et al. Biologic and targeted synthetic DMARD utilization in the United States: Adelphi Real World Disease Specific Programme for rheumatoid arthritis. Rheumatol Ther 2021;8(4):1637–1649.

10. Fleischmann R, Pangan AL, Song IH, et al. Upadacitinib versus placebo or adalimumab in patients with rheumatoid arthritis and an inadequate response to methotrexate: results of a phase III, double-blind, randomized controlled trial. Arthritis Rheumatol 2019;71(11):1788–1800.

11. Rubbert-Roth A, Enejosa J, Pangan AL, et al. Trial of upadacitinib or abatacept in rheumatoid arthritis. N Engl J Med 2020;383(16):1511–1521.

12. Meyer DM, Jesson MI, Li X, et al. Anti-inflammatory activity and neutrophil reductions mediated by the JAK1/JAK3 inhibitor, CP-690,550, in rat adjuvant-induced arthritis. J Inflamm (Lond) 2010;7:41.

13. Xeljanz. Prescribing information. Pfizer; 2018. Accessed June 5, 2023. https://www.accessdata.fda.gov/drugsatfda_docs/label/2018/203214s018lbl.pdf

14. Danto SI, Shojaee N, Singh RSP, et al. Safety, tolerability, pharmacokinetics, and pharmacodynamics of PF-06650833, a selective interleukin-1 receptor-associated kinase 4 (IRAK4) inhibitor, in single and multiple ascending dose randomized phase 1 studies in healthy subjects. Arthritis Res Ther 2019;21(1):269.

15. Danto SI, Shojaee N, Singh RSP, et al. Efficacy and safety of the selective interleukin-1 receptor associated kinase 4 inhibitor, PF-06650833, in patients with active rheumatoid arthritis and inadequate response to methotrexate. *Arthritis* Rheumatol 2019;71(Suppl 10). https://acrabstracts.org/abstract/efficacy-and-safety-of-the-selective-interleukin-1-receptor-associated-kinase-4-inhibitor-pf-06650833-in-patients-with-active-rheumatoid-arthritis-and-inadequate-response-to-methotrexate/

16. Xu H, Jesson MI, Seneviratne UI, et al. PF-06651600, a dual JAK3/TEC family kinase inhibitor. ACS Chem Biol 2019;14(6):1235–1242.

17. LITFULO. Prescribing information. Pfizer; 2023. Accessed June 17, 2024. https://www.accessdata.fda.gov/drugsatfda_docs/label/2023/215830s000lbl.pdf

18. Robinson MF, Damjanov N, Stamenkovic B, et al. Efficacy and safety of PF-06651600 (ritlecitinib), a novel JAK3/TEC inhibitor, in patients with moderate-to-severe rheumatoid arthritis and an inadequate response to methotrexate. Arthritis Rheumatol 2020;72(10): 1621–1631.

19. Felson DT, Anderson JJ, Boers M, et al. American College of Rheumatology. Preliminary definition of improvement in rheumatoid arthritis. Arthritis Rheum 1995;38(6):727–735.

20. Aletaha D, Neogi T, Silman AJ, et al. Rheumatoid arthritis classification criteria: An American College of Rheumatology/European League Against Rheumatism collaborative initiative. Arthritis Rheum 2010;62 (9):2569–2581.

21. Hochberg MC, Chang RW, Dwosh I, et al. The American College of Rheumatology 1991 revised criteria for the classification of global functional status in rheumatoid arthritis. Arthritis Rheum 1992;35(5): 498–502.

22. Fitzmaurice GM, Laird NM, Ware JH. Applied Longitudinal Analysis. 2nd ed. John Wiley & Sons, Inc; 2011.

23. Mallinckrodt C, Lipkovich I. Analyzing Longitudinal Clinical Trial Data: A Practical Guide. Chapman & Hall; 2017.

24. Blyth CR, Still H. Binomial confidence intervals. J Am Stat Assoc 1983;78:108–116.

25. Casella G. Refining binomial confidence intervals. Can J Stat 1986;14: 113–129.

26. Chan IS, Zhang Z. Test-based exact confidence intervals for the difference of two binomial proportions. Biometrics 1999;55(4):1202–1209.

27. Winkler A, Sun W, De S, et al. The interleukin-1 receptor-associated kinase 4 inhibitor PF-06650833 blocks inflammation in preclinical models of rheumatic disease and in humans enrolled in a randomized clinical trial. Arthritis Rheumatol 2021;73(12):2206–2218.

28. Boyle DL, Soma K, Hodge J, et al. The JAK inhibitor tofacitinib suppresses synovial JAK1-STAT signalling in rheumatoid arthritis. Ann Rheum Dis 2015;74(6):1311–1316.

29. Asai S, Nagai K, Takahashi N, et al. Influence of methotrexate on gastrointestinal symptoms in patients with rheumatoid arthritis. Int J Rheum Dis 2019;22(2):207–213.

30. Salliot C, van der Heijde D. Long-term safety of methotrexate monotherapy in patients with rheumatoid arthritis: a systematic literature research. Ann Rheum Dis 2009;68(7):1100–1104.

31. Nikiphorou E, Negoescu A, Fitzpatrick JD, et al. Indispensable or intolerable? Methotrexate in patients with rheumatoid and psoriatic arthritis: a retrospective review of discontinuation rates from a large UK cohort. Clin Rheumatol 2014;33(5):609–614.

32. Gomides APM, de Albuquerque CP, Santos ABV, et al. Causes of synthetic disease-modifying drug discontinuation in rheumatoid arthritis: data from a large real-life cohort. PLoS One 2019;14(3): e0213219.

33. Cohen SB, Pope J, Haraoui B, et al. Efficacy and safety of tofacitinib modified-release 11 mg once daily plus methotrexate in adult patients with rheumatoid arthritis: 24-week open-label phase results from a phase 3b/4 methotrexate withdrawal non-inferiority study (ORAL Shift). RMD Open 2021;7(2):e001673.

34. Sandborn WJ, Danese S, Leszczyszyn J, et al. Oral ritlecitinib and brepocitinib for moderate-to-severe ulcerative colitis: results from a randomized, phase 2b study. Clin Gastroenterol Hepatol 2023; 21(10):2616–2628.e7.

35. King B, Soung J, Tziotzios C, et al. Integrated safety analysis of ritlecitinib, an oral JAK3/TEC family kinase inhibitor, for the treatment of alopecia areata from the ALLEGRO clinical trial program. Am J Clin Dermatol 2024;25(2):299–314.

36. Wollenhaupt J, Silverfield J, Lee EB, et al. Safety and efficacy of tofacitinib, an oral Janus kinase inhibitor, for the treatment of rheumatoid arthritis in open-label, longterm extension studies. J Rheumatol 2014;41(5):837–852.

37. King B, Guttman-Yassky E, Peeva E, et al. Safety and efficacy of ritlecitinib and brepocitinib in alopecia areata: results from the crossover open-label extension of the ALLEGRO phase 2a trial. JID Innov 2022;2(6):100156.

38. Tanaka Y, Suzuki M, Nakamura H, et al; Tofacitinib Study Investigators. Phase II study of tofacitinib (CP-690,550) combined with methotrexate in patients with rheumatoid arthritis and an inadequate response to methotrexate. Arthritis Care Res (Hoboken) 2011;63(8): 1150–1158.

39. Peeva E, Banerjee A, Banfield C, et al. Master protocols and other innovative trial designs in inflammation and immunology to expedite clinical drug development. Drug Discov Today 2024;29(5):103948.

AMERICAN COLLEGE
of RHEUMATOLOGY
Empowering Rheumatology Professionals

Comparative Analysis of Circulating and Synovial Immune Cells in Early Untreated Rheumatoid Arthritis and Their Relationship With Molecular Pathology and Disease Outcomes

Felice Rivellese,[1] [iD] Elena Pontarini,[2] [iD] Liliane Fossati-Jimack,[2] Rita A. Moura,[3] Vasco C. Romão,[4] [iD] João Eurico Fonseca,[4] [iD] Alessandra Nerviani,[1] Cankut Çubuk,[2] [iD] Katriona Goldmann,[2] Giovanni Giorli,[2] Myles Lewis,[1] [iD] Michele Bombardieri,[1] and Costantino Pitzalis,[5] [iD] on behalf of the Pathobiology of Early Arthritis Cohort (PEAC) investigators

Objective. To assess the relationship of circulating and synovial immune cells with synovial molecular pathology and disease outcomes in patients with early rheumatoid arthritis (RA).

Methods. Patients with early (<12 months) treatment-naive RA (n = 144) from the Pathobiology of Early Arthritis Cohort were included in this post hoc analysis. Following ultrasound (US)-guided synovial biopsy of the most active joint, patients received standard of care treatment and were observed for 12 months. Synovial biopsies were analyzed by immunohistochemistry and classified into synovial pathotypes. Peripheral blood (PB) samples (n = 70) underwent flow cytometry, whereas RNA sequencing from synovial tissue (n = 144) and matched PB (n = 55) were analyzed using signature-based deconvolution.

Results. T peripheral helper cells (Tph) cells, identified by flow cytometry, were the only circulating immune cell subset positively correlated with both systemic markers of inflammation (erythrocyte sedimentation rate and C-reactive protein) and local inflammation (US synovial thickening and synovitis score). Circulating Tph cells were also significantly higher in patients who were seropositive and patients with lymphomyeloid synovitis. Conversely, circulating B cells showed a significant inverse correlation with markers of inflammation, US scores, and disease activity. Signature-based deconvolution of matched synovial and PB identified divergent immune cell signatures. Although PB signatures showed no associations with longitudinal outcomes, synovium signatures were linked to clinical outcomes. In particular, patients achieving remission at six months (Disease Activity Score in 28 joints < 2.6) had higher baseline synovial Tph signatures and a greater posttreatment reduction of the Tph signature.

Conclusion. Patients with early untreated RA showed divergent immune cell signatures between synovia and PB. Tph cells, in both compartments, emerged as key markers for inflammation, disease activity, and treatment response.

INTRODUCTION

Rheumatoid arthritis (RA) is characterized by clinical heterogeneity, mirrored by the diverse infiltration of immune cells within the synovial tissue.[1] Alterations of immune cells T and B cells,[2] monocytes,[3] dendritic cells,[4,5] and natural killer (NK) cells[6–8] have been observed in the peripheral blood (PB) of patients with RA. Although circulating immune cells have been associated with

[1]Felice Rivellese, MD, PhD, Alessandra Nerviani, MD, PhD, Myles Lewis, MD, PhD, Michele Bombardieri, MD, PhD: Centre for Experimental Medicine and Rheumatology, William Harvey Research Institute, Queen Mary University of London and Barts Health NHS Trust and Barts Biomedical Research Centre, NIHR, London, United Kingdom; [2]Elena Pontarini, PhD, Liliane Fossati-Jimack, PhD, Cankut Çubuk, PhD, Katriona Goldmann, PhD, Giovanni Giorli, PhD: Centre for Experimental Medicine and Rheumatology, William Harvey Research Institute, Queen Mary University of London, London, United Kingdom; [3]Rita A. Moura, MD, PhD: Instituto de Medicina Molecular João Lobo Antunes, Faculdade de Medicina, Universidade de Lisboa, Lisbon Academic Medical Center, Lisbon, Portugal; [4]Vasco C. Romão, MD, PhD, João Eurico Fonseca, MD, PhD: Instituto de Medicina Molecular João Lobo Antunes,

disease activity and disease outcomes, including treatment response, their usage as biomarkers remains unvalidated. For example, an expansion of PB memory B cells has been noted in patients with RA, even in early disease stages.[9,10] Increased pre-treatment PB memory B cells have been identified in patients responding to B cell-depleting therapies.[11] However, consistent B cell depletion after rituximab, regardless of treatment response, limits the predictive value of B cell assessment before and after treatment.[12] Similarly, other circulating immune cell patterns, including monocytes, dendritic cells, and T cells, fail to predict treatment response. Thus, despite the established role of immune cells in RA pathogenesis, the relationship between their circulating levels and disease outcomes remains uncertain. In some cases, changes in circulating immune cell frequency may reflect a general inflammatory response rather than disease-specific immunophenotypes. Conversely, the direct study of the synovial membrane has revealed distinct cellular and molecular signatures linked to disease activity and response to conventional synthetic disease modifying antirheumatic drugs (csDMARDs).[13,14] Similarly, in patients with established RA, synovial B cell lineage signatures have been identified as a promising marker of disease progression and treatment response,[15,16] and, more recently, in-depth histologic and molecular analyses of synovial biopsies identified immune response gene signatures associated with response to rituximab and tocilizumab, and a stromal and fibroblast signature in patients refractory to all medications.[17] The analysis of the synovial tissue by mass cytometry and single-cell transcriptomics led to the identification of a T helper cell subpopulation, named T peripheral helper (Tph) cells.[18] These cells were found to be expanded in the PB of patients with active seropositive RA and reduced by treatment.[19] However, because of the small sample size, their precise association with treatment response remains unclear. Furthermore, mass cytometry analyses have revealed 18 unique cell populations in the synovia of patients with RA, including subsets of monocytes, fibroblasts, and B and T cells.[20] However, the association of these subsets with clinical outcomes remains to be elucidated.

Therefore, in this study, we aim to establish the relationship between circulating immune cells and infiltrating synovial immune cells through in-depth cellular and molecular analyses of matched PB and synovial tissue in a unique cohort of patients with early treatment-naive RA. The study incorporated matched blood and synovial tissue biopsies obtained before any potential treatment modification of the disease. Our findings underscore Tph cells as clinically relevant cellular signatures linked to lymphomyeloid synovitis and are indicative of disease progression and treatment response.

PATIENTS AND METHODS

Patients. 144 patients fulfilling the 2010 American College of Rheumatology/EULAR classification criteria for RA[21] consecutively recruited in the Pathobiology of Early Arthritis Cohort (PEAC) at Barts Health NHS Trust[22] between 2009 and 2019 were selected for this post hoc analysis (see Supplementary Table 1 for patient demographics and baseline characteristics). Inclusion criteria for the PEAC study were: (1) the presence of at least one swollen joint amenable to synovial biopsy (ultrasound [US] synovial thickening >1); (2) symptoms duration less than 12 months; (3) naive to csDMARD or steroid treatments. Following a baseline synovial biopsy (see below for details), patients were observed for 12 months and underwent quarterly assessments performed by clinical research fellows (rheumatologist trainees) or rheumatology consultants, with the treatment given according to the standard of care following a treat-to-target approach, that is, all patients started methotrexate unless contra-indicated, were escalated to a second csDMARD if the target was not met at follow-up and to a biologic DMARD as per UK National Institute for Health and Clinical Excellence guidelines in place at the time of the study (after treatment with two csDMARDs and Disease Activity Score in 28 joints [DAS28] >5.1). Routine blood was processed by an NHS laboratory, whereas study blood taken in parallel was processed for peripheral blood mononuclear cell (PBMC) isolation and flow cytometry by the Centre for Experimental Medicine and Rheumatology laboratory. Plain radiographs of the hands and feet performed at baseline and 12-month follow-up were scored in a time sequential order according to the van der Heijde-modified total Sharp score (mTSS) by a single reader blinded to all clinical or histologic data. Progression at 12 months was defined as any increase in the mTSS (delta mTSS ≥1). All patients gave written informed consent, and the study received local ethics approval (REC ref 05/Q0703/198).

Synovial biopsy. All patients underwent US-guided synovial biopsies of a clinically active joint selected according to a previously reported algorithm defining the level of synovial tissue thickness aimed at confirming localized synovitis while ensuring good synovial tissue retrieval.[23] From each procedure, a minimum

Faculdade de Medicina, Universidade de Lisboa and Department of Rheumatology, Hospital de Santa Maria, Centro Hospitalar Universitário Lisboa Norte, Lisbon Academic Medical Center, Lisbon, Portugal; [5]Costantino Pitzalis, MD, PhD: Centre for Experimental Medicine and Rheumatology, William Harvey Research Institute, Queen Mary University of London and Barts Health NHS Trust and Barts Biomedical Research Centre, NIHR, London, United Kingdom, and Department of Biomedical Sciences Humanitas University and IRCCS Humanitas Research Hospital, Milan, Italy.

Drs Rivellese and Pontarini contributed equally to this work.

of six synovial samples were retained for subsequent histologic analysis and six for RNA extraction. In parallel, blood samples were collected, and PBMCs were isolated using gradient separation with Lymphoprep (StemCell Tecnologies).

Histopathological scoring. Formalin-fixed, paraffin embedded sections (3μm) underwent standard hematoxylin and eosin and immunohistochemistry staining (CD20, CD68, CD3, CD138). Following semiquantitative assessment (0–4), according to previously validated score,[24] biopsies were then stratified into one of the three synovial pathotypes, as previously described[13]: (1) lymphomyeloid presence of grades 2–3—CD20+ aggregates, (CD20 ≥2) and/or CD138 ≥2; (2) diffuse-myeloid—CD68 sublining (SL) ≥2, CD20 ≤1 and/or CD3 ≥1, CD138 ≤2; and (3) pauci-immune-fibroid—CD68 SL <2 and CD3, CD20, CD138 <1.

Flow cytometry. Flow cytometry was performed on cryopreserved PBMCs (n = 70 patients). Cells were thawed by adding dropwise warm medium (RPMI-10% FCS), washed once and resuspended in phosphate buffered saline. Upon thawing, cells were counted, and viability was verified using trypan blue staining (median viability 86%, with 82% of the samples showing viability >70%).

Dead cells were excluded by live-dead exclusion dye (Aqua Zombie, BioLegend); FcReceptors were blocked using an Fc receptor-blocking solution (TruStain, BioLegend). Cells were stained with four different panels (Supplementary Table 2, also indicating the number of samples analyzed for each panel), according to standard procedures. Samples were acquired on an LSRII Fortessa cytometer (BD Biosciences) equipped with 405, 488, 561, and 640 nm lasers, and analyzed using FlowJo version 10 (FlowJo LLC).

RNA extraction and RNA sequencing. RNA extraction and RNA sequencing were performed as previously described.[22] Briefly, RNA was extracted from synovial tissue homogenized at 4°C in Trizol (ThermoFisher Scientific), observed a phenol/chloroform extraction. 1μg of total RNA was used as input material for library preparation using TruSeq RNA Sample Preparation Kit version 2 (Illumina). Generated libraries were amplified with 10 cycles of polymerase chain reaction. The libraries were first multiplexed (five per lane) and then sequenced on Illumina HiSeq2500 (Illumina) to generate 50 million paired ends with 75 base pair reads. As for blood, whole blood samples were preserved in RNALater solution (ThermoFisher Scientific) at 500 mL whole blood to 1.3 mL RNALater solution and stored at 80°C before extraction. Blood samples in RNALater solution were thawed on ice and RNA was prepared using the Ambion Ribo-Pure Blood kit (ThermoFisher Scientific), as per the manufacturer's instructions. The concentration and purity of RNA samples was measured using the NanoDrop 2000C (Lab Tech) and RNA

quality (RIN) was assessed by Agilent 2100 Bioanalyser (Agilent Technologies) and 2200 TapeStation (Agilent Technologies).

RNA sequencing analysis and deconvolution. RNA sequencing was analyzed as previously described.[14] Following the identification of outliers using principal component analysis (3 patients for synovium, 0 for blood as described in Cell Report), the remaining samples were deconvoluted using ImmuneDeconv.[25] Publicly available single-cell expression data with cell subset annotations were downloaded from ImmPort (https://www.immport.org/shared/study/SDY998). For each cell subset, we collapsed normalized single-cell expression profiles into artificial-bulk count matrices by summing the counts for each gene using bulk_construct function of the MuSiC R package, and then the bulk dataset was subjected to quantile normalization using preprocessCore (https://github.com/bmbolstad/preprocessCore). The normalized artificial-bulk data was deconvoluted with five different deconvolution tools (xCell, MCP-counter, quanTIseq, EPIC, and Cibersort) for their performance comparison. The cell fractions estimated by these tools were visualized by heatmap plots. The concordance between cell subset annotations and in silico cell type predictions was explored manually to assess their performance.

For the enrichment of single cell states, we scored each subtype using a modular approach that integrates gene signatures[26] obtained from differential gene expression analysis and known markers that are previously described by scRNA-Seq study.[20] Module scores for each subtype were calculated using *AddGeneSetScore*,[27] a repurposing of the AddModuleScore function from the R package Seurat,[28] adapted for bulk RNA sequencing data processed with DESeq2 (https://doi.org/10.1186/s13059-014-0550-8). After comparing module scores using top five, top 10, and top 20 differentially expressed genes, we used the top five exclusively differentially expressed genes (based on area under the curve scores) as subtype-specific gene sets because this allowed us to differentiate a higher number of subsets. Module scores between responders and nonresponders were compared using the Wilcoxon test. ComplexHeatmap was used for clustering.[29]

Statistical analysis. Measures of central tendency, dispersion, and statistical tests are indicated in each figure legend. Unless stated otherwise, the following statistical tests have been used: Mann-Whitney U test for comparison between two groups; Kruskal-Wallis test with Dunn's post hoc test for multiple group comparison; chi-square test for proportions; Spearman's test for correlations. Statistical analyses were performed using R (version 4.2.1 or later). $P < 0.05$ was considered statistically significant. Correction for multiplicity was applied using the false discovery rate method in correlation matrices involving multiple comparisons between cell subsets and various clinical/biologic

parameters. Figure legends specify when multiple testing correction was applied.

RESULTS

Relationship of circulating immune cells with systemic inflammation and disease activity. To explore the association of circulating immune cells with clinical phenotypes and histologic and molecular profiles, we used flow cytometry to analyze the frequency of immune cell subsets to include B cells, T cells, monocytes, NK cells, and regulatory T cells in the PB of patients with early treatment-naive RA recruited to the PEAC study, thus with available matched synovial tissue, as shown in Figure 1A. Details of the gating strategy are provided in Supplementary Figure 1.

First, we examined the correlation of circulating immune cells with systemic inflammation and disease activity. B cells and their subsets showed significant inverse correlations, persisting after correction for multiple testing, with markers of inflammation (erythrocyte sedimentation rate [ESR], C-reactive protein [CRP]), swollen joint count, DAS28 scores, and US scores (Figure 1B and C). As for T cells, $CD8^+GNZB^+CD69B^+$ T cells showed positive correlations with markers of inflammation and disease activity scores (Supplementary Figure 2A). Conversely, monocytes, NK cells, and Treg cells did not exhibit any significant correlations (Supplementary Figure 2B and C). Next, we looked at CXC chemokine receptor (CXCR) 5^-PD1^{hi} inducible costimulator positive $CD4^+$ T peripheral helper cells (Tph) cells, a subset known to be expanded in the PB of patients with RA.[19] Accordingly, Tph showed a significant positive correlation with markers of inflammation (ESR and CRP, R = 0.49, $P < 0.001$ and R = 0.51, adjusted $P < 0.001$, respectively) and US scores (synovial thickening, R = 0.43, adjusted $P = 0.015$) (Supplementary Figure 2D). Importantly, this correlation was not evident for the $CXCR5^+$ counterpart, T follicular helper cells (Tfh) (Supplementary Figure 2D).

Next, we investigated the relationship of circulating immune cells with synovial immune cell infiltration in matched PB and synovial biopsies (Figure 1A). Although the majority of the circulating subsets did not show any correlation with synovial histology scores (Supplementary Figure 2E–H), a notable exception was observed for Tph cells, displaying significant positive correlations with immune cell infiltration in synovia (Figure 2A). This association was not observed for Tfh (Figure 2B). Additionally, circulating Tph cells were significantly higher in patients with positive anti–citrullinated protein antibody or rheumatoid factor, and, in line with their correlation with immune cell infiltration in synovia, were significantly higher in patients with a lymphomyeloid pathotype, characterized by the infiltration of T and B cells (Figure 2C and D). Accordingly, circulating Tph cells were significantly correlated with key genes for Tph cell biology and known to be involved in the formation of ectopic lymphoid structures (ELS), such as CXC

chemokine ligand (CXCL) 13, interleukin (IL) 21 and IL21R, and lymphotoxin β (Figure 2E and F).

Benchmarking transcriptome deconvolution in PB and synovial tissue against flow cytometry and histopathology. Next, we aimed to use bulk transcriptome deconvolution to dissect the characteristics of immune cells infiltrating the synovial tissue. To this aim, we benchmarked the performance of five commonly used tools, primarily developed in cancer research, in the blood and synovial tissue of patients with RA. In the PB, the tools showed various degrees of correlation with their counterparts measured by flow cytometry, which served as our gold standard. Interestingly, all tools performed quite poorly for certain cell types, such as CD4 T cells, with MCPcounter and xCell showing the most favorable correlations across multiple subsets (Supplementary Figure 3A).

Next, we applied deconvolution to the synovial transcriptome, using semiquantitative scores by immunohistochemistry as a surrogate gold standard (Supplementary Figure 3B). As seen for PB, MCPcounter and xCell showed the highest correlation rates.

Taking into account these results, our analyses continued with xCell because this tool can identify up to 39 immune cells, providing a significant advantage over traditional histology, although with the caveat of poor performance for certain cell populations, as shown for CD4 T cells.

Matched PB and synovial transcriptome deconvolution identify divergent associations with histopathological and clinical features. To further explore the presence and relevance of immune cells in matched PB and synovial tissue, we used xCell to deconvolute blood and synovia bulk transcriptome available from the same patients (see Figure 1A for an overview of the samples used). In synovia, signatures for B cells, plasma cells, T cells, and macrophages showed significant positive correlations with histologic semiquantitative scores (Figure 3A), whereas fibroblasts, hematopoietic stem cells, and stromal scores had negative correlations with synovial immune cell infiltration assessed by histology (Figure 3A). Synovial macrophage/monocyte signatures were the only cell signatures to show a significant correlation with disease activity scores (Figure 3A). When comparing immune cell signatures in matched PB and synovial samples, although no significant correlations were found, most cells showed a clear trend toward negative correlations, which suggests the same cell types might have opposing trends in the two compartments (Figure 3B).

Upon stratifying patients by synovial pathotypes, synovial B and T cell signatures were higher in patients with a lymphomyeloid pathotype, as expected for a pathotype characterized by the infiltration of B and T cells. On the contrary, circulating B cells and total CD4+ and CD8+ T cell signatures were lower in patients with synovial lymphomyeloid pathotypes. On the other hand,
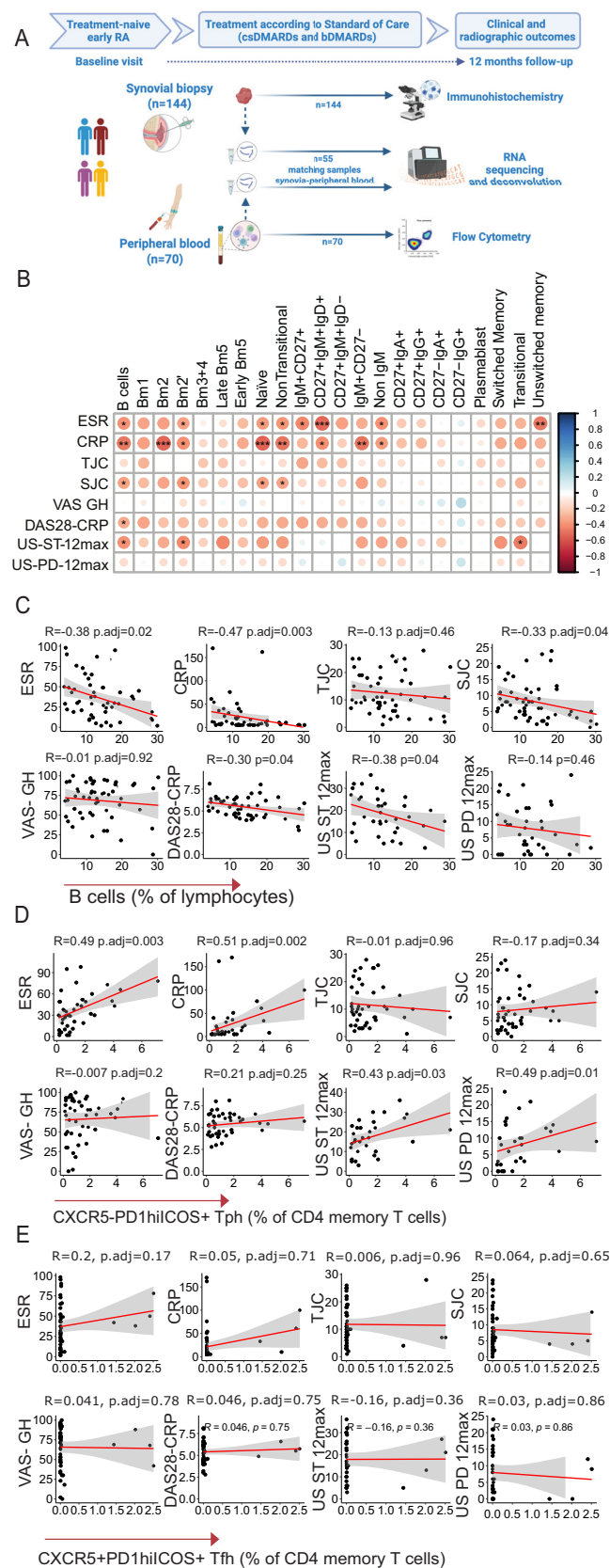
lymphomyeloid and diffuse-myeloid pathotypes, both characterized by the infiltration of macrophages, showed higher myeloid signatures in both PB and synovial tissue.

Overall, we observed a potential divergence of immune cell signatures between PB and diseased tissue, emphasizing how the PB may not always accurately reflect synovial inflammation, thus reinforcing the relevance of studying the diseased tissue.

Module signatures of synovial single cell states define diverse disease phenotypes. Next, as we aimed to investigate synovium-specific immune cell subsets described by mass cytometry and single cell transcriptomic,[20] we used their top five expressed genes as a proxy to assess their presence in the matched bulk synovial and peripheral transcriptome h (Supplementary Figure 4A). Tissue-resident cells, such as fibroblast and macrophages subsets were significantly higher in synovia, while most T and B cell subsets were higher in PB (Supplementary Figure 5B). Notably, however, PD1+ Tph/Tfh cells, granzyme K (GZMK) positive/GNZMB+ T cells, and plasmablast signatures were higher in synovia, aligning with their known role in driving synovial inflammation in patients with RA (Supplementary Figure 5B). We then examined the correlations of these signatures with synovial inflammation. Unsurprisingly, given the divergence we observed between synovial and blood

Figure 1. Correlation of circulating immune cell subsets with disease activity. Pictured are correlations between immune cell subsets assessed by flow cytometry and markers of inflammation, DAS28s and their components, and US scores. (A) Overview of samples included in the analysis, including synovial biopsies (n = 144) and matched peripheral blood (n = 70), undergoing immunohistochemistry and flow cytometry. RNA extracted from synovial tissue (n = 144) and peripheral blood mononuclear cells (n = 55) underwent RNA sequencing. (B) Correlation matrix for B cell subsets identified by flow cytometry and markers of disease activity; dot size and color intensity corresponding to the correlation coefficient R, with positive correlations in blue and negative correlations in red, using Spearman correlation, with correction for multiple comparisons by false discovery rate. (C–E) Individual correlation plots for B cells, Tph cells, and Tfh cells, with Spearman correlation coefficients (R) and adjusted *P* values (Spearman correlation with false discovery rate correction). *P < 0.05; **P < 0.01; ***P < 0.001. adj, adjusted; bDMARD, biologic disease-modifying antirheumatic drug; Bm, mature B cells; CRP, C-reactive protein; csDMARD, conventional synthetic disease-modifying antirheumatic drug; CXCR, CXC chemokine receptors; DAS28, Disease Activity Score in 28 joints; ESR, erythrocyte sedimentation rate; RA, rheumatoid arthritis; SJC, swollen joint count; TJC, tender joint count; Tfh, T follicular helper; Tph, T peripheral helper; US, ultrasound; US-ST 12, ultrasound synovial thickening score in 12 joints; US-PD 12, ultrasound power doppler score in 12 joints; VAS-GH, visual analog scale global health (patient-reported).
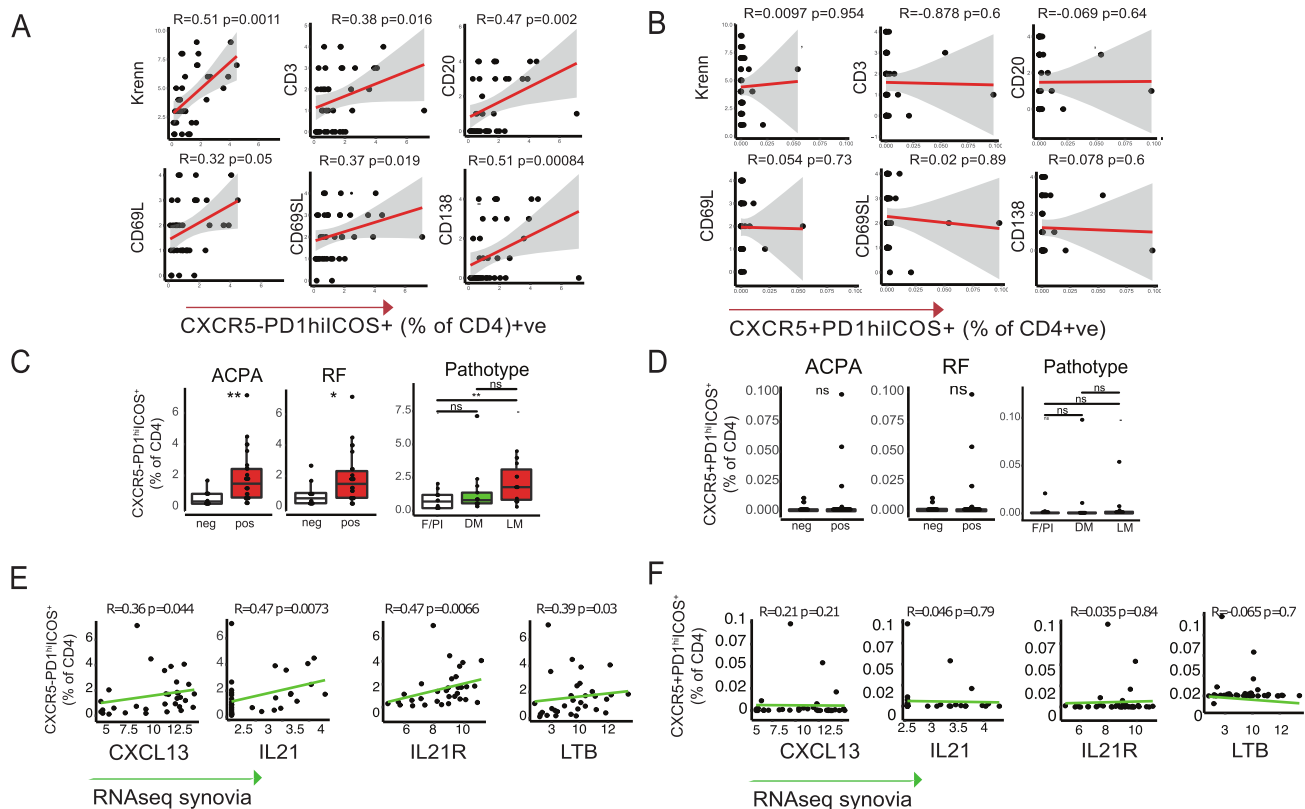
Figure 2. Circulating Tph and Tfh cells. Correlation plots of circulating (A) Tph and (B) Tfh cells with synovial semiquantitative immune scores Krenn total synovitis score (0–9 semiquantitative scores measured with hematoxylin and eosin), CD3 T cells, CD20 B cells, CD68 lining and sublining macrophages, and CD138 plasma cells (0–4 semiquantitative scores by immunohistochemistry). R = Spearman's rank correlation coefficient, with exact (nominal) *P* values. n = 51 samples measured in Figure 2A and B. (C) Tph and (D) Tfh cells, measured by flow cytometry, in patients stratified according to the positivity of ACPA, RF, and according to synovial pathotypes. Mann-Whitney test was used. n = 48 for ACPA and RF (antibody status missing for three patients); n = 50 for histology (1 sample ungraded). Correlation plots of circulating (E) Tph and (F) Tfh cells with representative lymphoid genes measured by RNA sequencing (seq). R = Spearman's rank correlation coefficient, with exact (nominal) *P* values. n = 32 samples measured in Figure 2E and F. *P < 0.05; **P < 0.01. ACPA, anti–citrullinated protein antibody; CXCL, CXC chemokine ligands; CXCR, CXC chemokine receptors; IL, interleukin; LTB, lymphotoxin β; RF, rheumatoid factor; Tfh, T follicular helper; Tph, T peripheral helper. Color figure can be viewed in the online issue, which is available at http://onlinelibrary.wiley.com/doi/10.1002/art.43194/abstract.

signatures, none of the synovial single cell signatures showed any correlation with either synovial inflammation (data not shown) On the contrary, in synovia, CD34+ sublining fibroblasts, Dickkopf-related protein 3 (DKK3)-positive sublining fibroblasts, and IL-1B+ pro-inflammatory macrophages inversely correlated with immune cell scores, whereas other subsets showed positive correlations (Figure 4A). When stratifying patients by synovial pathotypes, specific signatures were associated with each pathotype (Figure 4B). Specifically, CD34+ sublining fibroblasts, DKK3+ sublining fibroblasts and CD55+ lining fibroblasts were significantly higher in patients with a pauci-immune pathotype, supporting the idea that stromal cells might drive inflammation in this subset of patients. Macrophage signatures were higher in both myeloid and lymphomyeloid pathotypes, except for IL-1B+ macrophages, which were up-regulated in patients classified with fibroid or pauci-immune pathotypes. Finally, most T and B cell subsets were up-regulated in patients with lymphomyeloid pathotypes, consistent with the

pathotype's characteristic abundance of B and T cells. Next, we assessed the associations of single cell signatures with clinical disease activity (Figure 5A and B). Synovial signatures for CD34+ sublining fibroblasts, DKK3+ sublining fibroblasts, and IL-1B+ pro-inflammatory macrophages negatively correlated with markers of inflammation and disease activity, whereas C1QA+ macrophages, PD1+ Tph T cells GZMK+CD8+ T cells and all B cells had positive correlations. In contrast, in circulation, a positive correlation was only observed for PD1+ Tph/Tfh cells (Figure 5B), in line with the flow cytometry results in which circulating CXCR5– Tph cells emerged as markers of inflammation and disease activity.

To explore the impact of these signatures on disease outcomes, we assessed baseline synovial single cell modules in association with different outcomes: (1) remission as determined by DAS28 (score < 2.6) at six months; (2) progression to biologic DMARDs within one year; and (3) any worsening of radiographic scores at one year (mTSS ≥1) (Figure 5C).
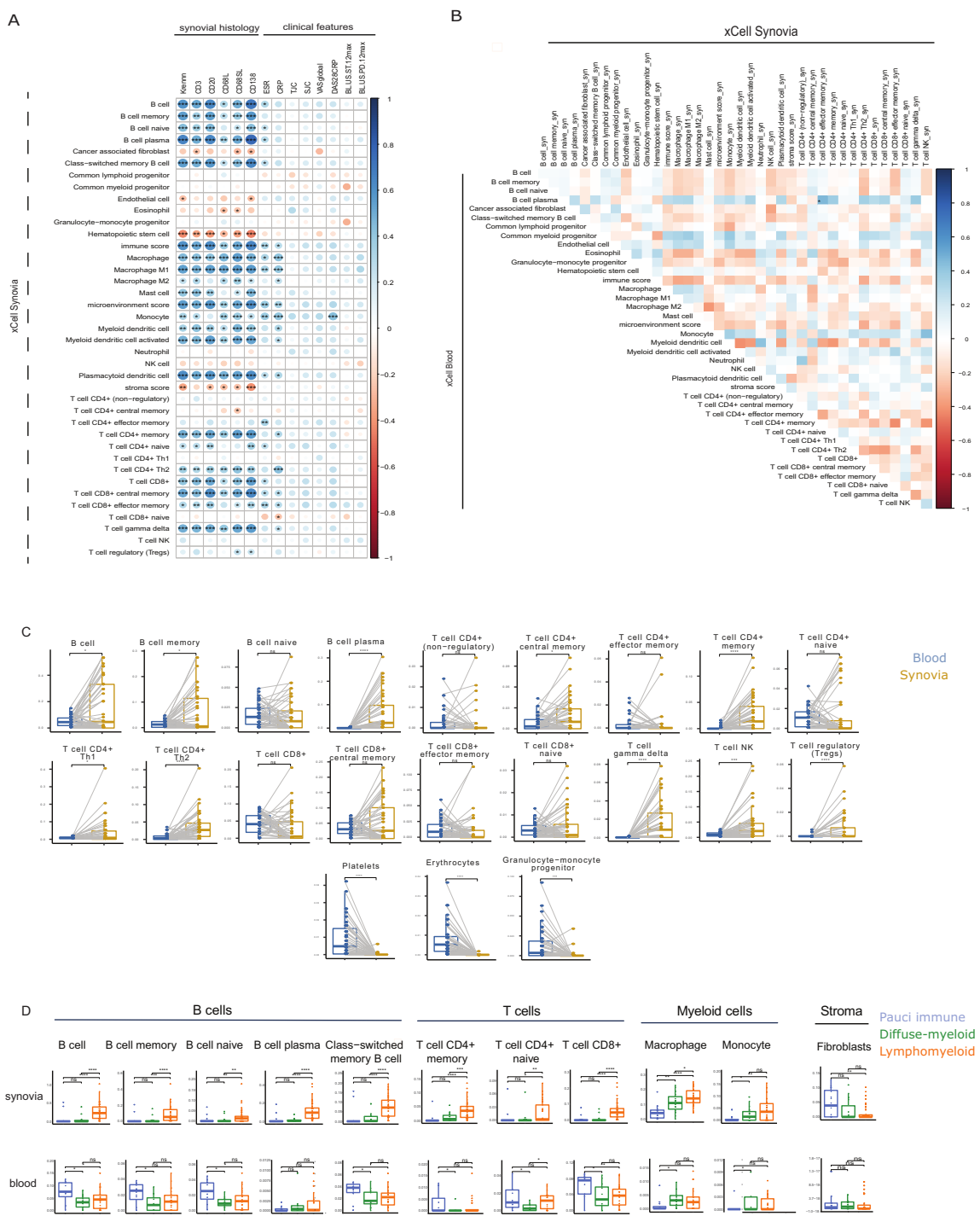
Figure 3. Deconvolution of synovial and peripheral blood RNA sequencing. Deconvolution applied to RNA sequencing of RNA extracted from synovial tissue biopsies (n = 49) and peripheral blood (n = 36). (A) Matrix showing the correlation between xCell signatures in synovial tissue and synovial histology/clinical features. Dot size corresponds to Spearman correlation coefficients (–1/+1), shown in a color scale, with positive correlations in blue and negative correlations in red. Spearman correlation was used with correction for multiple comparison by false discovery rate. (B) Matrix showing the correlation between peripheral blood and synovial tissue signatures; color-coded Spearman correlation coefficients were used, as in A. (C) xCell immune cell signatures in matched peripheral blood (blue) and synovial samples (yellow). Mann-Whitney test was used, n = 36. (D) Immune cell signatures in patients stratified according to synovial pathotypes in synovia (top) and peripheral blood (bottom). Kruskal-Wallis with Dunn's post hoc test was used with 49 synovial tissue samples and 36 peripheral blood samples. Individual dots represent individual patients, boxplots show median and first and third quartiles, and whiskers extend to the highest and lowest values. *$P < 0.05$; **$P < 0.01$; ***$P < 0.001$. CRP, C-reactive protein; DAS28, Disease Activity Score in 28 joints; ESR, erythrocyte sedimentation rate; NK, natural killer; SJC, swollen joint count; Th, T helper; TJC, tender joint count; US-PD 12, ultrasound power doppler score in 12 joints; US-ST 12, ultrasound synovial thickening score in 12 joints; VAS-GH, visual analog scale global health (patient-reported). Color figure can be viewed in the online issue, which is available at http://onlinelibrary.wiley.com/doi/10.1002/art.43194/abstract.
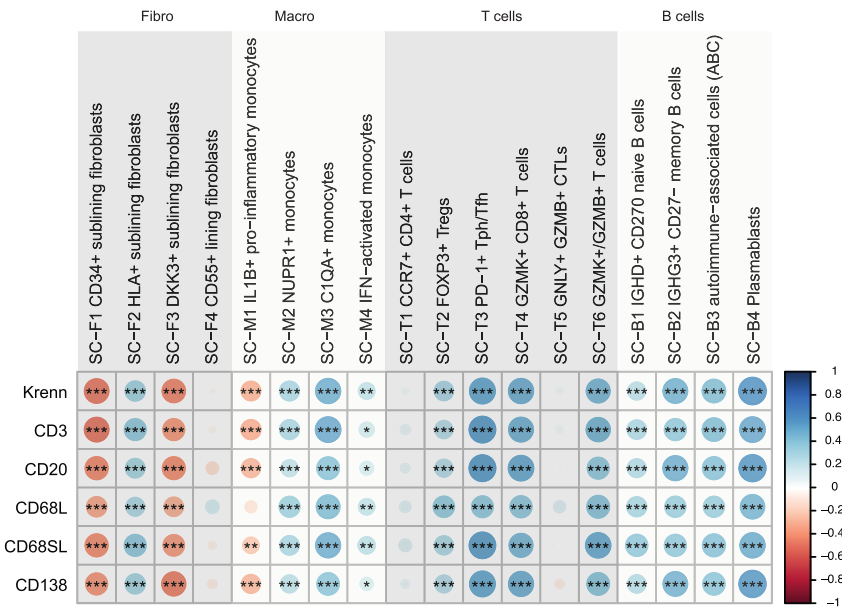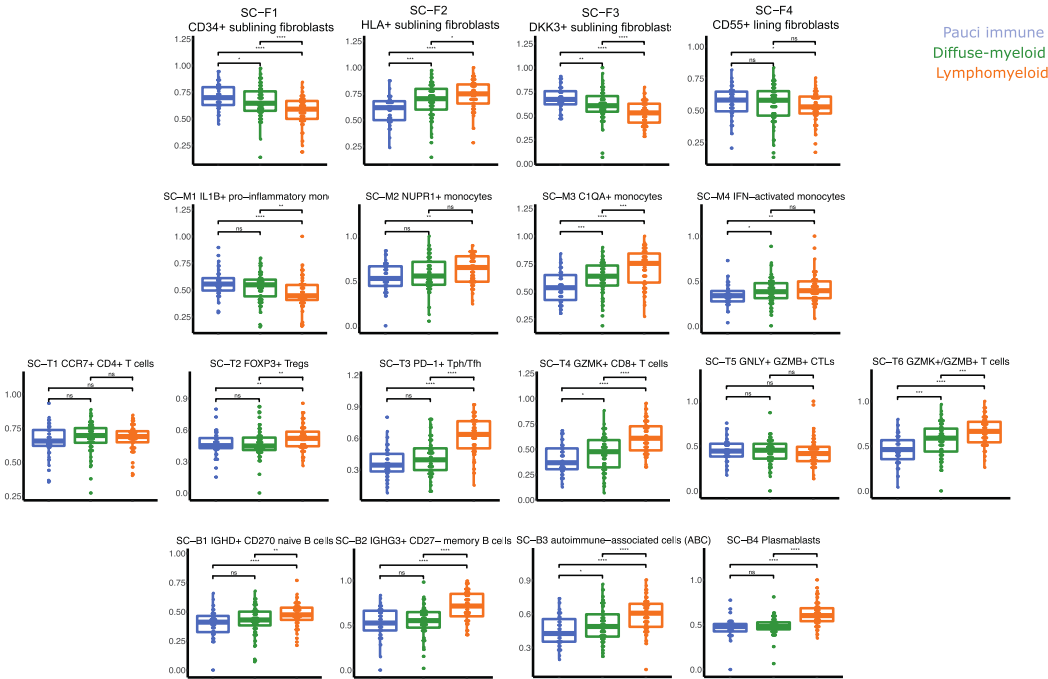
Figure 4. Single cell state signatures and synovial inflammation. (A) Matrix showing the correlation of single cell (SC) state signatures with synovial inflammation. Dot size corresponds to Spearman correlation coefficients as shown in color scale, with positive correlations in blue and negative correlations in red (–1/+1), n = 49. Spearman correlation with correction for multiple comparison by false discovery rate was used. (B) Single cell state signatures in patients stratified according to synovial pathotypes. Kruskal-Wallis with Dunn's post hoc test was used with 49 synovial tissue samples and 36 peripheral blood samples. Individual dots represent individual patients, boxplots show median and first and third quartiles, and whiskers extend to the highest and lowest values. *$P < 0.05$, **$P < 0.01$, ***$P < 0.001$ CRP, C-reactive protein; DAS28, Disease Activity Score in 28 joints; DKK, Dickkopf-related protein; ESR, erythrocyte sedimentation rate; GZMB, granzyme B; GZMK, granzyme K; HLA, human leukocyte antigen; IFN, interferon; IL, interleukin; SJC, swollen joint count; Tfh, T follicular helper; TJC, tender joint count; Tph, T peripheral helper. Color figure can be viewed in the online issue, which is available at http://onlinelibrary.wiley.com/doi/10.1002/art.43194/abstract.
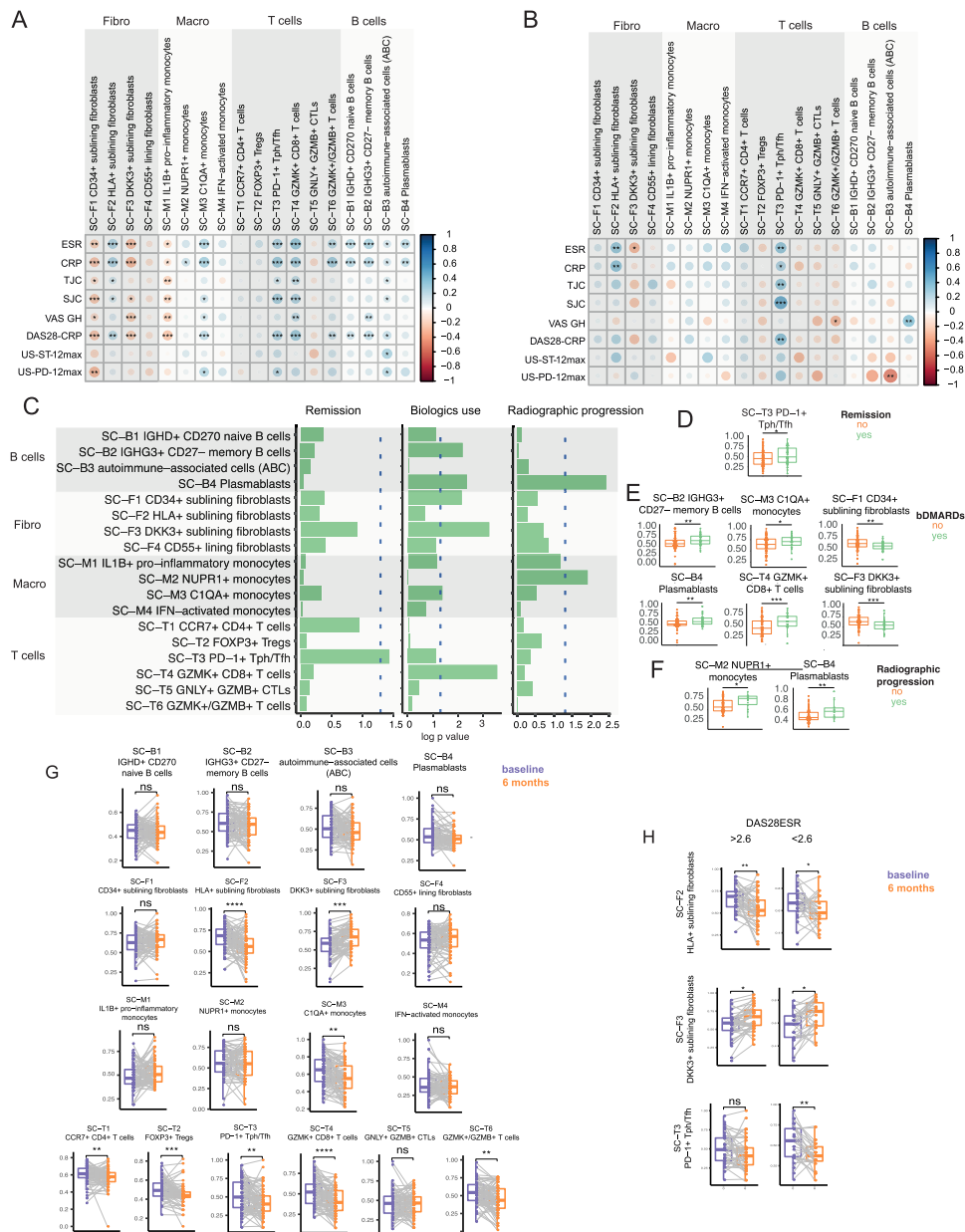
Figure 5. Single cell state signatures and disease outcomes. Matrix showing the correlation of single cell state signatures in (A) synovial tissue and (B) peripheral blood with DAS and their components and ultrasound scores. Dot size corresponds to Spearman correlation coefficients (−1/+1), as shown in color scale, with positive correlations in blue and negative correlations in red. Spearman correlation was used with correction for multiple comparison by false discovery rate. (C) Comparison of baseline synovial immune cell signatures in patients stratified according to remission at six months (DAS28 CRP <2.6), biologic treatment at 12 months, and radiographic progression at 12 months (delta van der Heijde-modified total Sharp score (mTSS) ≥ 1). Lines show P values, with dotted line corresponding to P < 0.05, Mann-Whitney. n = 121 for DAS28 at six months, n =107 for treatment with biologic drugs at 12 months, and n = 96 for radiographic progression at 12 months. (D–F) Individual dot plots showing baseline synovial immune cell signatures significantly different as in C. Mann-Whitney test was used. The values for n are as in Figure 5C. Individual dots represent individual patients, boxplots show median and first and third quartiles, and whiskers extend to the highest and lowest values. (G) Single cell scores in matched baseline (before treatment) and synovial biopsies at six months (after treatment with csDMARDs). (H) Significantly different single cell scores in patients stratified according to DAS28 at six months less than or greater than 2.6. The Mann-Whitney test was used. *P < 0.05, **P < 0.01, ***P < 0.001. bDMARD, biologic disease-modifying antirheumatic drug; CCR, C-C chemokine receptor type; CRP, C-reactive protein; csDMARD, conventional synthetic disease modifying antirheumatic drug; DAS28, Disease Activity Score in 28 joints; DKK, Dickkopf-related protein; ESR, erythrocyte sedimentation rate; GZMB, granzyme B; GZMK, granzyme K; HLA, human leukocyte antigen; IGHD, immunoglobulin heavy constant delta; IGHG3, immunoglobulin heavy constant gamma 3; IL, interleukin; NUPR, nuclear protein 1; SJC, swollen joint count; Tfh, T follicular helper; Tph, T peripheral helper; TJC, tender joint count; US-ST 12, ultrasound synovial thickening score in 12 joints; US-PD 12, ultrasound power doppler score in 12 joints; VAS-GH, visual analog scale global health (patient-reported). Color figure can be viewed in the online issue, which is available at http://onlinelibrary.wiley.com/doi/10.1002/art.43194/abstract.

The Tph/Tfh signature was uniquely linked to treatment response (Figure 5D). Patients progressing to biologic DMARD treatments exhibited elevated baseline memory B cells, plasmablasts, C1QA+ monocytes, and GZMK+ CD8 T cells, whereas CD34+ and DKK3+ fibroblast signatures were lower (Figure 5E). In addition, patients with signs of radiographic progression (delta mTSS ≥1) had increased baseline plasmablast and nuclear protein 1 positive monocyte (Figure 5F). When examining the changes in repeat synovial biopsies after six months of csDMARD treatment (Figure 5G), significant reductions were observed in C1QA+ monocytes and various T cell subsets, including PD1+ Tph cells. Significant reductions were also observed in proinflammatory human leukocyte antigen-positive fibroblasts, whereas DKK3+ fibroblasts increased posttreatment. Changes in fibroblasts were consistent regardless of six month remission status, whereas Tph reduction occurred only in patients achieving DAS28 remission at 6 months (Figure 5H). Importantly, single cell signatures in blood did not show any significant association with disease outcomes (data not shown), including Tph/Tfh signatures. Overall, these findings suggest that pretreatment synovial single cell modular signatures are linked to disease outcomes, including treatment response, treatment with biologic DMARDs, and structural damage progression.

DISCUSSION

Although numerous associations between circulating immune cells and clinical outcomes have been reported in patients with RA, it has been difficult to consistently relate them to clinical outcomes and treatment response. On the other hand, recent studies analyzing the molecular pathology of synovial biopsies have reported specific signatures linked to prognosis (structural damage) and treatment response.[15–17,30] Therefore, in this study, we aimed to explore the relationship of PB immune cells with the cellular and molecular profile of the synovial tissue in a biopsy-driven cohort with early untreated. We observed inverse correlations between circulating B cells and markers of inflammation, disease activity, and US scores, aligning with previous findings of lower B cell counts in patients with active RA,[31] including patients with very early RA[9,32] and patients with arthralgia.[33] Treatment with biologics has been shown to restore the frequency of circulating memory B cells,[10,11,34] and low levels of pretreatment B cells have been associated with lower chances of response to antitumor necrosis factor.[35] Here, we expanded these observations defining that the low B cell count extends to specific subsets, including memory B cells.[36,37] Although the role of B cells in RA pathogenesis is well established and the effectiveness of B cell-depleting therapies in patients with RA is well-known, the usage of circulating B cells as predictive markers remains limited. Even though pretreatment levels of specific CD27+ memory B cells[11,38] and preplasma cells[39] have been associated with response to rituximab, their use in clinical practice

as predictive markers is inadequate. At least in part, this is probably linked to the uncertainty of whether circulating immune cells reflect the inflammatory burden in the synovial tissue. Our results define the relationship between PB and synovia, highlighting the importance of studying both circulating and synovial immune cells to establish the link between circulatory and synovial cells. Upon studying the synovial tissue, pretreatment levels of B cells and posttreatment changes have been linked to treatment response to B cell depletion [40], emphasizing the potential clinical relevance of understanding these dynamics. Recently, two large multicenter randomized biopsy-driven clinical trials have provided promising insights into the ability of synovial signatures to predict disease outcomes,[15,16] whereas deep molecular phenotyping has identified specific signatures associated with multidrug resistance.[17]

Here, we used matched synovial tissue and PB samples to study the relationship of circulating immune cells, assessed by flow cytometry, and synovial inflammation. Most immune cells, including total CD4 and CD8 T cells, B cells, Treg cells, monocytes, and NK cells, showed no correlations. Notably, on the other hand, Tph cells, previously identified in synovial tissue and circulation,[19,41] emerged as a subset associated with both systemic and synovial inflammation. Circulating Tph cells were elevated in patients with seropositive RA and active disease, particularly in those with a lymphomyeloid synovial pathotype characterized by infiltrating B and T cells. This establishes circulating Tph cells as peripheral biomarkers for lymphomyeloid synovitis, a finding particularly relevant given the scarcity of peripheral biomarkers associated with this subtype of synovial inflammation because the only other circulating biomarker ever found in association with lymphomyeloid synovial inflammation and ELS formation is CXCL13,[42] a chemokine produced mainly by Tph cells and their CXCR5+ counterpart.

Regarding molecular investigations, previous transcriptomic analyses of the PB in patients with early RA identified very few differentially expressed genes compared with the synovial tissue.[14] Leveraging the availability of matched PB and synovial whole transcriptomes, we employed deconvolution tools to analyze both tissues from the same patients. As most of the existing deconvolution tools were developed in cancer tissues and have not been tested or validated in other diseases, we benchmarked the performance of five such tools using flow cytometry in the PB and immunohistochemistry in the synovial tissue as gold standards. xCell was selected for its ability to estimate the infiltration of up to 39 immune cell subsets, expanding our assessment compared to conventional histology. Notably, Cibersort,[43] a widely used tool in oncology, demonstrated relatively poorer performance in both PB and synovial tissue of patients with RA compared with other tools.

By using deconvolution with xCell on matched synovial and PB samples, we uncovered diverging relationships between circulating immune cell subsets and synovial inflammation/pathotypes. Specifically, patients classified as lymphomyeloid, with

abundant lymphoid cell infiltration in synovia, exhibited significantly lower levels of B and T cell signatures in circulation. Conversely, those with myeloid infiltration in the synovia consistently showed higher levels of myeloid cells in both synovial tissue and PB. These results, linked with the flow cytometry data indicating inverse correlations of B cells with disease activity, suggest a possible explanation for why PB analysis often falls short in identifying clinically useful biomarkers, emphasizing the importance of directly studying the diseased tissue.

In recent years, advancements in mass cytometry and single cell transcriptomic analyses have enhanced our understanding of synovial tissue in patients with RA, revealing 18 unique cell subsets/states across fibroblast, monocyte/macrophage, B, and T cell lineages.[20] However, the relevance of these subsets in PB and their associations with clinical outcomes remained unclear. Analyzing single cell signature modules in synovial and PB transcriptomes based on synovial pathotypes, we found up-regulated fibroblast subsets, including the DKK3+ subset, in the synovium of patients with a pauci-immune/fibroid pathotype. The DKK3+ fibroblast signature was also elevated in patients with multidrug resistant or refractory RA.[17] Fibroblast subsets showed negative correlations with disease activity, as did IL-1B+ pro-inflammatory macrophages, previously linked to leukocyte-rich RA. Our study compared three synovial RA pathotypes, revealing lower IL1B+ macrophage signatures in lymphomyeloid compared to diffuse-myeloid and pauci-immune pathotypes, providing further insights into the synovial immune landscape.

When examining single cell module signatures in the PB, we observed significant correlations with synovial inflammation and disease activity scores only for PD1+ Tph cells. This aligns with our flow cytometry findings, reinforcing the notion that PD1+ Tph cells serve as PB markers of synovial inflammation and disease activity.

Finally, our study revealed an association of pretreatment synovial signatures with disease outcomes, including treatment response, use of biologic DMARDs and progression of structural damage. Specifically, PD1+ Tph cells were associated with DMARD response, suggesting their potential as PB predictors for both disease activity and treatment response because this is in line with previous results showing a reduction of Tph levels following treatment with csDMARDs.[19] Additionally, the use of biologic DMARDs correlated with elevated levels of immune cell states, including memory B cells, plasmablasts, C1QA+ monocytes, and GZMK+ CD8 T cells. Conversely, fibroblast states were lower in patients progressing to biologics, consistent with our prior findings associating DKK3+ fibroblasts with refractory RA.[17] Lastly, plasmablasts were linked to radiographic progression, supporting prior observations identifying a plasmablast signature as a predictor of structural damage.[14,22]

This study has some limitations. First, this is a post hoc analysis without a predetermined statistical plan, therefore the study has an exploratory nature. Second, although we analyze a unique cohort of patients with early, treatment-naive RA with matched synovial and PB samples, the sample size is relatively limited, so our findings warrant further investigations in larger cohorts. The relatively limited sample size meant we could not correct for potential confounders such as age, body mass index, and gender. Third, it is crucial to note that deconvolution tools estimate relative cell abundance, not absolute values, and they struggle with heavily overlapping cell signatures, thus performing quite poorly in estimating specific cell subsets, as observed for CD4 T cells. Therefore, when attempting to estimate the presence of synovium-specific cell states, we opted to use the top differentially expressed genes as a proxy to estimate their presence. Even though these signatures do not provide exact subset proportions, they revealed significant associations with disease outcomes that are pathogenetically and clinically relevant, warranting exploration in future studies. Finally, more advanced single cells analyses have recently led to the identification of 77 synovial cell states, with patients then clustered into seven synovial Cell Type Abundance Phenotypes (CTAPs) were associated with disease outcomes, including treatment response/nonresponse.[42] The relevance of these subsets in circulation vs synovia and the possibility of reproducing the CTAP classification using blood signatures remains to be investigated. Even though our results highlight the difficulties in identifying circulating signatures that can accurately mirror synovial inflammation, the pursuit of a liquid biopsy for inflammatory arthritis continues to be an ongoing challenge, which can be hopefully addressed by the combined study of PB and synovia.

In conclusion, our results highlight the importance of synovial tissue analyses in identifying clinically relevant associations between immune cells and disease outcomes, with particular reference to pretreatment cell state signatures among which Tph cells emerge as potential circulating biomarkers of lymphomyeloid synovitis and disease activity and showing promise as predictive markers for treatment response.

AUTHOR CONTRIBUTIONS

REFERENCES

1. Rivellese F, Pitzalis C. Cellular and molecular diversity in rheumatoid arthritis. Semin Immunol 2021;58:101519.

2. Fekete A, Soos L, Szekanecz Z, Szabo Z, Szodoray P, Barath S, et al. Disturbances in B- and T-cell homeostasis in rheumatoid arthritis: suggested relationships with antigen-driven immune responses. J Autoimmun 2007;29(2–3):154–163.

3. Coulthard LR, Geiler J, Mathews RJ, et al. Differential effects of infliximab on absolute circulating blood leucocyte counts of innate immune cells in early and late rheumatoid arthritis patients. Clin Exp Immunol 2012;170:36–46.

4. Jongbloed SL, Lebre MC, Fraser AR, et al. Enumeration and phenotypical analysis of distinct dendritic cell subsets in psoriatic arthritis and rheumatoid arthritis. Arthritis Res Ther 2005;8(1):R15.

5. Richez C, Schaeverbeke T, Dumoulin C, et al. Myeloid dendritic cells correlate with clinical response whereas plasmacytoid dendritic cells impact autoantibody development in rheumatoid arthritis patients treated with infliximab. Arthritis Res Ther 2009;11(3):R100.

6. Chalan P, Bijzet J, Kroesen BJ, et al. Altered natural killer cell subsets in seropositive arthralgia and early rheumatoid arthritis are associated with autoantibody status. J Rheumatol 2016;43(6):1008–1016.

7. Aggarwal A, Sharma A, Bhatnagar A. Role of cytolytic impairment of natural killer and natural killer T-cell populations in rheumatoid arthritis. Clin Rheumatol 2014;33(8):1067–1078.

8. Yamin R, Berhani O, Peleg H, et al. High percentages and activity of synovial fluid NK cells present in patients with advanced stage active rheumatoid arthritis. Sci Rep 2019;9(1):1351.

9. Moura RA, Weinmann P, Pereira PA, et al. Alterations on peripheral blood B-cell subpopulations in very early arthritis patients. Rheumatology (Oxford) 2010;49(6):1082–1092.

10. Moura RA, Quaresma C, Vieira AR, et al. B-cell phenotype and IgD-CD27- memory B cells are affected by TNF-inhibitors and tocilizumab treatment in rheumatoid arthritis. PLoS One 2017;12(9):e0182927.

11. Sellam J, Rouanet S, Hendel-Chavez H, et al. Blood memory B cells are disturbed and predict the response to rituximab in patients with rheumatoid arthritis. Arthritis Rheum 2011;63(12):3692–3701.

12. Marston B, Palanichamy A, Anolik JH. B cells in the pathogenesis and treatment of rheumatoid arthritis. Curr Opin Rheumatol 2010;22(3):307–315.

13. Humby F, Lewis M, Ramamoorthi N, et al. Synovial cellular and molecular signatures stratify clinical response to csDMARD therapy and predict radiographic progression in early rheumatoid arthritis patients. Ann Rheum Dis 2019;78(6):761–772.

14. Lewis MJ, Barnes MR, Blighe K, et al. Molecular portraits of early rheumatoid arthritis identify clinical and treatment response phenotypes. Cell Rep 2019;28(9):2455–2470.e5.

15. Humby F, Durez P, Buch MH, et al. Rituximab versus tocilizumab in anti-TNF inadequate responder patients with rheumatoid arthritis (R4RA): 16-week outcomes of a stratified, biopsy-driven, multicentre, open-label, phase 4 randomised controlled trial. Lancet 2021; 397(10271):305–317.

16. Rivellese F, Nerviani A, Giorli G, et al. Stratification of biological therapies by pathobiology in biologic-naive patients with rheumatoid arthritis (STRAP and STRAP-EU): two parallel, open-label, biopsy-driven, randomised trials. Lancet Rheumatol 2023;5(11):e648–e659.

17. Rivellese F, Surace AEA, Goldmann K, et al. Rituximab versus tocilizumab in rheumatoid arthritis: synovial biopsy-based biomarker analysis of the phase 4 R4RA randomized trial. Nat Med 2022;28(6):1256–1268.

18. Yoshitomi H, Ueno H. Shared and distinct roles of T peripheral helper and T follicular helper cells in human diseases. Cell Mol Immunol 2021;18(3):523–527.

19. Rao DA, Gurish MF, Marshall JL, et al. Pathologically expanded peripheral T helper cell subset drives B cells in rheumatoid arthritis. Nature 2017;542(7639):110–114.

20. Zhang F, Wei K, Slowikowski K, et al. Defining inflammatory cell states in rheumatoid arthritis joint synovial tissues by integrating single-cell transcriptomics and mass cytometry. Nat Immunol 2019;20(7):928–942.

21. Aletaha D, Neogi T, Silman AJ, et al. 2010 rheumatoid arthritis classification criteria: an American College of Rheumatology/European League Against Rheumatism collaborative initiative. Arthritis Rheum 2010;62(9):2569–2581.

22. Humby F, Lewis M, Ramamoorthi N, et al. Synovial cellular and molecular signatures stratify clinical response to csDMARD therapy and predict radiographic progression in early rheumatoid arthritis patients. Ann Rheum Dis 2019;78(6):761–772.

23. Kelly S, Humby F, Filer A, et al. Ultrasound-guided synovial biopsy: a safe, well-tolerated and reliable technique for obtaining high-quality synovial tissue from both large and small joints in early arthritis patients. Ann Rheum Dis 2015;74(3):611–617.

24. Krenn V, Morawietz L, Burmester GR, et al. Synovitis score: discrimination between chronic low-grade and high-grade synovitis. Histopathology 2006;49(4):358–364.

25. Sturm G, Finotello F, List M. Immunedeconv: an R package for unified access to computational methods for estimating immune cell fractions from bulk RNA-sequencing data. Methods Mol Biol 2020;212:223–232.

26. Cubuk C, Hidalgo MR, Amadoz A, et al. Gene expression integration into pathway modules reveals a pan-cancer metabolic landscape. Cancer Res 2018;78(21):6059–6072.

27. Decoene I, Herpelinck T, Geris L, et al. Engineering bone-forming callus organoid implants in a xenogeneic-free differentiation medium. Front Chem Eng 2022;4:892190.

28. Hao Y, Hao S, Andersen-Nissen E, et al. Integrated analysis of multimodal single-cell data. Cell 2021;184(13):3573–3587.e29.

29. Gu Z, Eils R, Schlesner M. Complex heatmaps reveal patterns and correlations in multidimensional genomic data. Bioinformatics 2016; 32(18):2847–2849.

30. Zhang F, Jonsson AH, Nathan A, et al. Deconstruction of rheumatoid arthritis synovium defines inflammatory subtypes. Nature 2023; 623(7987):616–624.

31. Wagner U, Kaltenhäuser S, Pierer M, et al. B lymphocytopenia in rheumatoid arthritis is associated with the DRB1 shared epitope and increased acute phase response. Arthritis Res 2002;4(4):R1.

32. Fedele AL, Tolusso B, Gremese E, et al. Memory B cell subsets and plasmablasts are lower in early than in long-standing rheumatoid arthritis. BMC Immunol 2014;15:28.

33. Lübbers J, van Beers-Tas MH, Vosslamber S, et al. Changes in peripheral blood lymphocyte subsets during arthritis development in arthralgia patients. Arthritis Res Ther 2016;18(1):205.

34. Souto-Carneiro MM, Mahadevan V, Takada K, et al. Alterations in peripheral blood memory B cells in patients with active rheumatoid arthritis are dependent on the action of tumour necrosis factor. Arthritis Res Ther 2009;11(3):R84.

35. Rodríguez-Martín E, Nieto-Gañán I, Hernández-Breijo B, et al. Blood lymphocyte subsets for early identification of non-remission to TNF Inhibitors in rheumatoid arthritis. Front Immunol 2020;11:1913.

36. Mahmood Z, Schmalzing M, Dörner T, et al. Therapeutic cytokine inhibition modulates activation and homing receptors of peripheral memory B cell subsets in rheumatoid arthritis patients. Front Immunol 2020;11:572475.

37. Fedele AL, Tolusso B, Gremese E, et al. Memory B cell subsets and plasmablasts are lower in early than in long-standing rheumatoid arthritis. BMC Immunol 2014;15:28.

38. Roll P, Dörner T, Tony HP. Anti-CD20 therapy in patients with rheumatoid arthritis: Predictors of response and b cell subset

regeneration after repeated treatment. Arthritis Rheum 2008; 58(6):1566–1575.

39. Vital EM, Dass S, Rawstron AC, et al. Management of nonresponse to rituximab in rheumatoid arthritis: predictors and outcome of re-treatment. Arthritis Rheum 2010;62(5):1273–1279.

40. Giacomelli R, Afeltra A, Bartoloni E, et al. The growing role of precision medicine for the treatment of autoimmune diseases; results of a systematic review of literature and experts' consensus. Autoimmun Rev 2021;20:102738.

41. Manzo A, Vitolo B, Humby F, et al. Mature antigen-experienced T helper cells synthesize and secrete the B cell chemoattractant CXCL13 in the inflammatory environment of the rheumatoid joint. Arthritis Rheum 2008;58(11):3377–3387.

42. Dennis G Jr, Holweg CTJ, Kummerfeld SK, et al. Synovial phenotypes in rheumatoid arthritis correlate with response to biologic therapeutics. Arthritis Res Ther 2014;16(2):R90.

43. Newman AM, Liu CL, Green MR, et al. Robust enumeration of cell subsets from tissue expression profiles. Nat Methods 2015;12(5):453–457.

AMERICAN COLLEGE
of RHEUMATOLOGY
Empowering Rheumatology Professionals

Longitudinal Associations Between Baseline Sarcopenia and Knee Osteoarthritis Progression and Risk of Knee Replacement

Tianxing Wu,[1] Xiaoshuai Wang,[2] Zhuojian Cai,[3] Peihua Cao,[2] Qin Dang,[2] Weijie Zhou,[4] Jiawei Xie,[4] Jie Chen,[4] Taiwei Wang,[4] Gaochenzi Tao,[5] Weiyu Han,[6] Zhaohua Zhu,[2] Jian Wang,[3] David J. Hunter,[7] ID Rocco Barazzoni,[8] Changhai Ding,[9] ID and Jia Li[3] ID

Objective. Sarcopenia and knee osteoarthritis (KOA) are common conditions in older adults, but their relationship is controversial. We aimed to examine the potential role of sarcopenia in KOA progression and subsequent knee replacement (KR).

Methods. Using data from the Osteoarthritis Initiative, baseline sarcopenia was first screened according to the EWGSOP2 algorithm using the SARC-F (Strength, Assistance with walking, Rise from a chair, Climb stairs, and Falls) questionnaire (screened sarcopenia [Scre-S]), then further assessed combined with the five times chair-stand-test (probable sarcopenia [Prob-S]). Radiographic KOA progression was evaluated by changes in Kellgren-Lawrence Grade and Osteoarthritis Research Society International atlas scores from baseline to the 24- and 48-month follow-ups. Symptomatic progression was evaluated similarly using the Western Ontario McMaster Osteoarthritis Index. The associations of sarcopenia with radiographic or symptomatic progression and subsequent KR were analyzed before and after adjusting for potential confounders and propensity score (PS) matching.

Results. A total of 4,316 participants were included; 27.2% were Scre-S and 16.8% were Prob-S. Baseline Scre-S and Prob-S were positively associated with both radiographic and symptomatic progression in KOA over 24 and 48 months. Both Scre-S and Prob-S were associated with a higher risk of subsequent KR (Scre-S: hazard ratio [HR] 3.84, 95% confidence interval [CI] 3.18 to 4.62; Prob-S: HR 2.29, 95% CI 1.87 to 2.81). These results remained significant in the PS-matched cohort.

Conclusion. Scre-S and Prob-S were significantly and longitudinally associated with both radiographic and symptomatic progression in KOA and subsequent KR. Our findings indicated a potential causal role of sarcopenia in KOA progression and highlighted its potentially therapeutic effect in KOA management.

[1]Tianxing Wu, BM: Division of Orthopaedic Surgery, Department of Orthopedics, Nanfang Hospital, Southern Medical University and Clinical Research Centre and The Second School of Clinical Medicine, Zhujiang Hospital, Southern Medical University, Guangzhou, China; [2]Xiaoshuai Wang, PhD, Peihua Cao, PhD, Qin Dang, PhD, Zhaohua Zhu, PhD: Clinical Research Centre, Zhujiang Hospital, Southern Medical University, Guangzhou, China; [3]Zhuojian Cai, MM, Jian Wang, PhD, Jia Li, PhD: Division of Orthopaedic Surgery, Department of Orthopedics, Nanfang Hospital, Southern Medical University, Guangzhou, China; [4]Weijie Zhou, MM, Jiawei Xie, MM, Jie Chen, MM, Taiwei Wang, MM: The First School of Clinical Medicine, Nanfang Hospital, Southern Medical University, Guangzhou, China; [5]Gaochenzi Tao, MM: Department of Gynecology, Guangzhou Haizhu District

Changgang Street Community Service Center, Guangzhou, China; [6]Weiyu Han, PhD: Department of Orthopaedics, The Tenth Affiliated Hospital, Southern Medical University (Dongguan People's Hospital), Dongguan, China; [7]David J. Hunter, MD: Clinical Research Centre, Zhujiang Hospital, Southern Medical University, Guangzhou, China, and Department of Rheumatology, Royal North Shore Hospital and Sydney Musculoskeletal Health, Kolling Institute, University of Sydney, Sydney, New South Wales, Australia; [8]Rocco Barazzoni, MD: Department of Medical, Surgical and Health Sciences, University of Trieste, Trieste, Italy; [9]Changhai Ding, PhD: Clinical Research Centre, Zhujiang Hospital, Southern Medical University, Guangzhou, China, and Menzies Institute for Medical Research, University of Tasmania, Hobart, Tasmania, Australia.

Drs Wu, X Wang, and Cai are co-first authors and contributed equally to this work.

INTRODUCTION

Knee osteoarthritis (KOA) is one of the most common musculoskeletal disorders in the elderly and leads to chronic pain and disability.[1] However, there have been no disease-modifying treatments demonstrated to slow KOA progression or delay knee replacement (KR).[1] Although the pathologic mechanisms underlying KOA are complex and not yet fully elucidated, sarcopenia has been acknowledged to be closely associated with KOA.[2]

Sarcopenia is defined as a decline in skeletal muscle strength and mass and has a fundamental role in low muscle strength and dysfunction.[2,3] Most importantly, sarcopenia is found to be common in KOA, thereby representing a potentially modifiable risk factor.[4] However, the potential causal role of sarcopenia in the pathogenesis and progression of KOA remains to be determined. Previous studies have indeed shown a concurrent relationship between KOA and sarcopenia-related traits, such as a decline in muscle strength or muscle mass.[5,6] Several cross-sectional studies demonstrated a significantly higher prevalence of sarcopenia in individuals with KOA.[7,8] Patients with radiographic joint damage were also likely to develop sarcopenia more quickly.[9] However, because of the limitations of cross-sectional design, these findings cannot provide strong evidence on a causal relationship between these two diseases. Therefore, whether sarcopenia precedes the progression of KOA with a potential causal role or occurs because of KOA is still a matter of debate.

The biomechanical and biochemical interactions between muscle and joint might be responsible for the mechanisms by which sarcopenia impacts the pathophysiology of KOA.[10,11] Biomechanically, muscle controls force generation for locomotion and prevents joint dislocation.[12] In addition, active muscle contraction absorbs a great deal of the shock transmitted to the joint and thus plays a beneficial role in KOA progression.[13] Biochemically, it is currently known that skeletal muscle can produce myokines, including cytokines, peptides, and growth factors.[14] These myokines have been shown to possibly diffuse to the adjacent cartilage or subchondral bone, which influences their metabolic homeostasis and remodeling processes.[15] Moreover, research has demonstrated that myoblasts and chondrocytes share similar pathologic targets and pathways, and their close anatomic location suggests a likelihood of paracrine communication.[11] The intricate interplay between muscle and joint therefore supports a potential relationship between sarcopenia and KOA progression.

Recently, a Mendelian randomization study indicated that sarcopenia-related traits might have a causal impact on KOA.[16] Given the lack of large-scale genome-wide association studies on sarcopenia, the genetic explanatory power of instrumental variables may still be limited, potentially leading to biased results.[17] Meanwhile, available longitudinal studies are scarce and inconclusive. Veronese et al reported the association of sarcopenia with incident symptomatic KOA, rather than radiographic KOA.[18]

Mohajer et al reported that decreased quadriceps size and increased intramuscular fat were associated with subsequent symptomatic worsening and KR in patients with KOA.[19] In contrast, Misra et al used whole-body dual x-ray absorptiometry to determine muscle mass and reported that sarcopenia was not associated with the risk of KOA.[20] Turkiewicz et al even found that individuals with higher knee extensor strength in early life had an increased risk of KOA in middle age.[21] These findings highlight the need for well-designed studies to comprehensively explore the temporal and causal relationships between sarcopenia and KOA progression. In the present study, we used a multicenter and propensity score (PS)-matched cohort of Osteoarthritis Initiative (OAI) participants to investigate the longitudinal associations of baseline sarcopenia with KOA progression and subsequent KR.

PATIENTS AND METHODS

Study design and participants. Data for the present longitudinal study were obtained from the publicly accessible data sets of the OAI, which is an ongoing multicenter prospective cohort study aimed at identifying biomarkers for KOA. All participants diagnosed with or at risk for KOA were enrolled and observed (ClinicalTrials.gov identifier: NCT00080171). The Health Insurance Portability and Accountability Act (HIPAA)-compliant protocol was approved, and all participants signed informed consent.[22]

In the OAI study population (aged 45–79 years), complete data for sarcopenia screening and probable sarcopenia diagnosis through functional measurement of muscle strength are available along with knee radiographic readings and symptomatic scores at the baseline visit. Notably, participants with advanced KOA (Kellgren-Lawrence Grade [KLG] 4), the highest symptomatic scores (Western Ontario McMaster Osteoarthritis Index [WOMAC] 16–20), or KR surgery history at baseline were excluded.[7] Participants were also excluded if subsequent KR was uncertain. The selection process is depicted in Figure 1.

Evaluation of sarcopenia. In the current study, baseline sarcopenia was evaluated stepwise according to an adapted algorithm by the EWGSOP2 that is based on available OAI data.[23] Details are as follows.

Step 1: screened sarcopenia. The 5-item SARC-F questionnaire is a validated tool recommended by the EWGSOP2 algorithm for screening and case-finding. Items include self-reported strength (S), assistance with walking (A), rising from a chair (R), climbing stairs (C), and history of falls (F). For the current analyses, we developed a conversion method for SARC-F based on the WOMAC function questionnaires (Supplementary Figure 1). The cutoff threshold for screened sarcopenia (Scre-S) was set as SARC-F score of 4 or greater, with SARC-F (+) as positive screening for high sarcopenia risk.
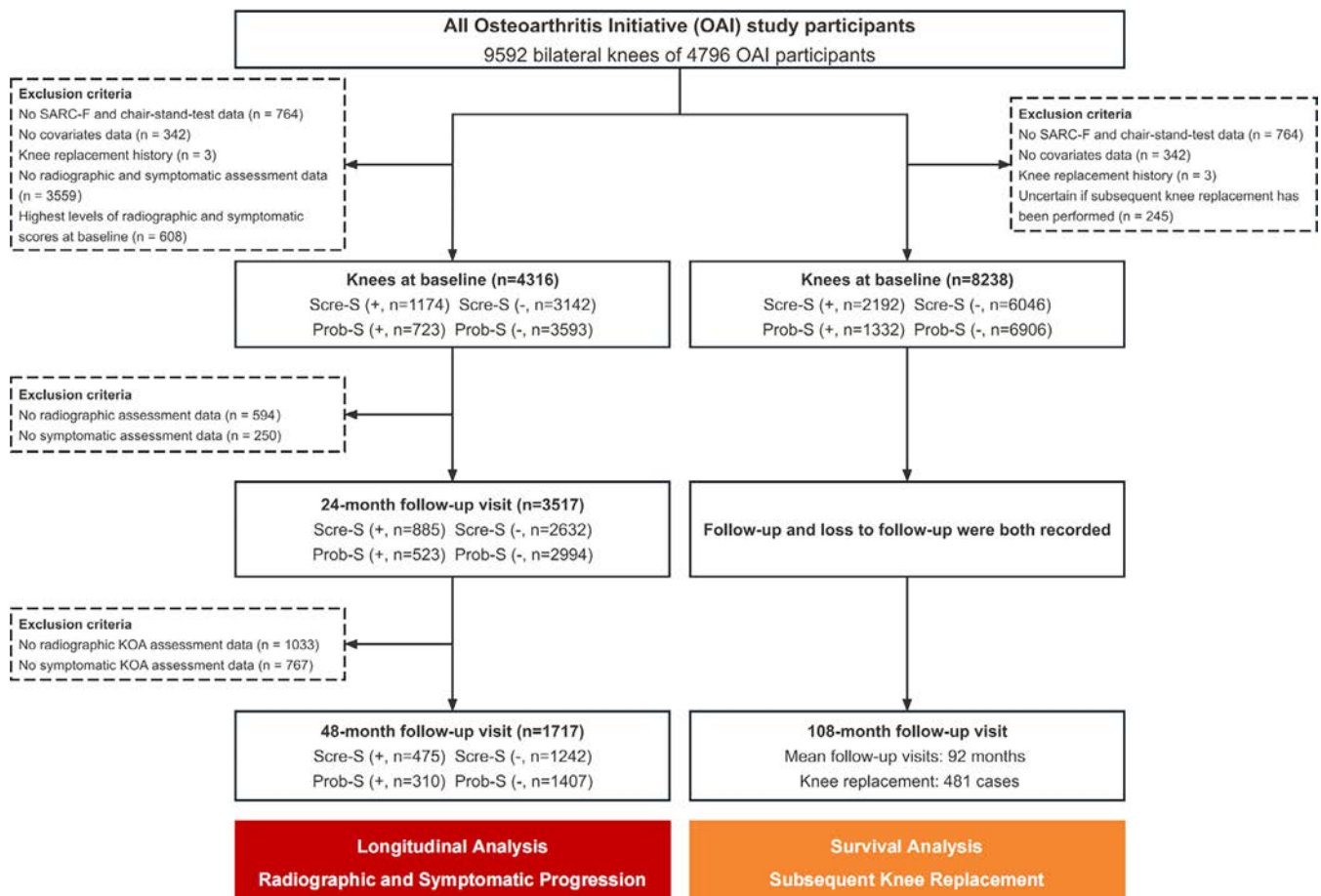
Figure 1. Flowchart of the study. Scre-S, screened sarcopenia; Prob-S, probable sarcopenia. Color figure can be viewed in the online issue, which is available at http://onlinelibrary.wiley.com/doi/10.1002/art.43213/abstract.

Step 2: probable sarcopenia. Skeletal muscle strength is the commonly employed functional parameter for sarcopenia diagnosis according to the widely accepted EWGSOP2 algorithm. Most importantly, low muscle function per se following positive screening leads to the diagnosis of probable sarcopenia (Prob-S) and justifies clinical action. The five times chair-stand-test can be used as a proxy for evaluating the strength of lower limbs. Therefore, the cutoff threshold for Prob-S was set as five times chair-stand-test of at least 12 seconds based on Scre-S.[24] Lower extremity strength, assessed by maximal isometric extensor and flexor strength, was further included to validate the effectiveness of the aforementioned grouping for Scre-S and Prob-S. The Good Strength Chair (Metitur Oy) was applied, and the lever arm length (Newton-meters per body mass [Nm/kg]) was used to calculate the torque. After two warm-up tests, the best of three maximal effort tries for both knee extensor and flexor strengths were recorded, respectively.[6]

Evaluation of radiographic progression in KOA. The radiographic KOA features were evaluated using posteroanterior radiographs with a fixed flexion (15°) protocol, which were subsequently analyzed at one OAI center and scored using semiquantitative KLG and the Osteoarthritis Research Society International (OARSI) atlas grades. Specifically, knee radiographs were evaluated through joint space narrowing (JSN), osteophytes, and sclerosis for the OARSI atlas grades, with every subgrade in the medial tibiofemoral compartment ranging from 0 (none) to 3 (severe).[25] The changes in grades from baseline to 24 or 48 months were calculated as indicators of radiographic progression, respectively.

Evaluation of symptomatic progression in KOA. The assessment of knee pain (including walking on a flat surface, going up/down stairs, at night while in bed, when sitting/lying, and when standing upright) was conducted using the WOMAC items from 0 (no pain) to 5 (most severe pain).[26] The Knee Injury and Osteoarthritis Outcome Score (KOOS) was developed as a tool for evaluating the patient's opinion on their knee and related problems.[27] Three subscales were used in this study, including pain, other symptoms, and knee-related quality of life (QoL). The previous week is the time period that was considered when answering the questions. Standardized answer options were given (five Likert boxes) and each question was assigned a score from 0 (extreme symptoms) to 4 (no symptoms). The changes

from baseline to 24 or 48 months were calculated as indicators of symptomatic progression, respectively.

Evaluation of subsequent KR. Given that KR is a hallmark event of end-stage KOA, it was chosen as the long-term outcome to investigate the impact of baseline sarcopenia.[27] The survival analyses over 108 months follow-up were conducted. At baseline, we excluded participants with missing covariate data and those who had previously undergone KR. KR events were confirmed based on medical records and self-reports.

Confounding factors. Age and obesity are the most prominent risk factors for KOA, with a clear female predominance observed.[28,29] The prevalence of KOA has also been observed to vary across different racial groups.[30] Additionally, insufficient physical activity is a risk factor for both the radiographic and symptomatic progression of KOA.[31,32] Unhealthy lifestyles, such as smoking and excessive alcohol consumption, further exacerbate the progression of KOA.[33] Finally, varus or valgus alignment of the knee can accelerate the radiographic progression of KOA.[34] Based on previous epidemiologic studies on KOA and existing literature, this study identified age, sex, race, body mass index (BMI), Physical Activity Scale for the Elderly (PASE), smoking status, drinking status, and knee alignment (normal, varus, and valgus) as confounding factors, which were adjusted in the models before PS matching.

Statistical analysis. Continuous variables are presented as mean ± SD and were compared by Student's *t*-test, whereas categorical variables are presented as frequency (percentage). Because of the inclusion of bilateral knees, the potential correlation between two observations on each participant, namely the within-subject similarities, should be considered. Thus, the generalized estimating equation (GEE) model, as previously described in the OAI study involving knees of both sides,[35] was conducted to examine the association between baseline sarcopenia and radiographic and symptomatic progression. The longitudinal analyses were adjusted for the covariates and baseline radiographic or symptomatic scores, respectively.

The Kaplan–Meier method was used to estimate survival curves to detect the differences in the risk of KR between the two groups. The Cox proportional hazards model was used to determine hazard ratios (HRs) and their corresponding 95% confidence intervals (CIs). The Breslow test is used to assess short-term differences between groups, whereas the log-rank test is used to investigate disparities in long-term differences. Before PS matching, analyses were adjusted for the covariates. The E-value was calculated to evaluate the evidence for causality in an observational study that confounding factors could potentially influence.[36] A large E-value implies that a considerable amount of unmeasured confounding is needed to explain an effect estimate.

To further validate the results, sensitivity analysis was conducted. The 1:1 PS-matching method was applied between groups with or without Scre-S and Prob-S based on confounding factors (age, sex, racial disparities, BMI, physical activity, smoking, alcohol consumption, and varus or valgus alignment), and the nearest-neighbor method with a caliper was set at 0.01. The associations between baseline sarcopenia and KOA progression (radiographic and symptomatic) were examined in each PS-matched cohort using the GEE model. After PS matching, the analyses were adjusted for additional baseline radiographic or symptomatic scores, respectively.

Restricted cubic splines (RCS) analysis was used to evaluate the exposure-response relationships between the severity of sarcopenia and radiographic, symptomatic progression and subsequent KR with three knots at the 10th, 50th, and 90th percentiles. Cubic spline analyses nonparametrically examine the association of the SARC-F score with the odds ratio of KLG, β of total WOMAC knee pain, and HR of the KR. Analyses were adjusted for the covariates and baseline radiographic or symptomatic scores, respectively.

The statistical analyses were performed using SPSS (version 25.0, SPSS Inc.), and R (version 4.1.2, R Foundation for Statistical Computing). All statistical tests conducted in this study were two-sided, and *P* values less than 0.05 were considered to be statistically significant.

All de-identified patient-level clinical data, outcome data, and radiographic data in our study were obtained from the OAI, an ongoing, multicenter, prospective cohort study designed to identify biomarkers for KOA. The HIPAA-compliant protocol of the OAI study has been received and approved by the ethics committee.

RESULTS

Baseline characteristics and sarcopenia. A total of 4,316 participants were included, with 1,174 participants (27.2%) having positive screening (Scre-S+) based on the SARC-F questionnaire (Table 1). Compared with those without positive screening, individuals in the Scre-S (+) group had a higher proportion of women (67.1% vs 55.9%), exhibited a higher BMI (30.72 vs 28.72), and engaged in less daily physical activity (mean PASE score of 154.46 vs 162.36). Among those with Scre-S (+), 723 participants (16.8% of the total cohort) were further classified as Prob-S based on the further chair-stand-test. Prob-S also had a higher proportion of women, a greater BMI, and less physical activity, compared with Prob-S (–) participants. Maximum extensor strength was significantly lower in individuals with Scre-S (+) (mean force, 307.47 Nm/kg vs 358.95 Nm/kg) and Prob-S (+) (mean force, 294.38 Nm/kg vs 341.10 Nm/kg) compared with the corresponding negative groups (Table 1). Maximum flexor strength also showed consistent differences, which indicated the effectiveness of our grouping for Scre-S and Prob-S.

Table 1. Baseline clinical characteristics of the participants*

Clinical characteristics	Scre-S (+) N = 1,174	Scre-S (−) N = 3,142	P value	Prob-S (+) N = 723	Prob-S (−) N = 3,593	P value
Age, mean ± SD, y	61.51 ± 8.86	62.48 ± 9.01	**0.002**	62.54 ± 8.86	62.15 ± 9.00	0.290
Female, n (%)	788 (67.1)	1,757 (55.9)	**<0.001**	534 (73.9)	2011 (56.0)	**<0.001**
Race, n (%)			**<0.001**			**<0.001**
White	797 (67.9)	2,654 (84.5)		450 (62.2)	3,001 (83.5)	
Black	347 (29.6)	412 (13.1)		255 (35.3)	504 (14.0)	
BMI, mean ± SD	30.72 ± 4.98	28.72 ± 4.47	**<0.001**	30.97 ± 4.89	28.92 ± 4.59	**<0.001**
PASE, mean ± SD	154.46 ± 83.08	162.36 ± 79.11	**0.004**	143.98 ± 79.20	163.48 ± 80.10	**<0.001**
Smoking history, n (%)	203 (17.3)	684 (21.8)	**0.001**	105 (14.5)	782 (21.8)	**<0.001**
Drinking history, n (%)	893 (76.1)	2,591 (82.5)	**<0.001**	529 (73.2)	2,955 (82.2)	**<0.001**
Knee alignment, n (%)			0.353			**0.037**
Normal	323 (27.5)	900 (28.6)		217 (30.0)	1,006 (28.0)	
Varus	319 (27.2)	895 (28.5)		175 (24.2)	1,039 (28.9)	
Valgus	532 (45.3)	1,347 (42.9)		331 (43.5)	1,548 (43.1)	
SARC-F, mean ± SD	5.66 ± 1.51	1.01 ± 1.04	**<0.001**	5.84 ± 1.58	1.55 ± 1.80	**<0.001**
Five times chair-stand-test, mean ± SD	13.88 ± 4.58	11.57 ± 3.19	**<0.001**	16.31 ± 4.18	11.37 ± 3.07	**<0.001**
Max thigh extensor strength	307.47 ± 117.45	358.95 ± 131.93	**<0.001**	294.38 ± 112.40	341.10 ± 126.60	**<0.001**
Max thigh flexor strength	123.63 ± 62.32	151.11 ± 70.57	**<0.001**	121.12 ± 60.71	139.68 ± 66.80	**<0.001**
KLG, n (%)			**<0.001**			**<0.001**
Grade 0	89 (7.6)	584 (18.6)		46 (6.4)	627 (17.5)	
Grade 1	168 (14.3)	567 (18.0)		104 (14.4)	631 (17.6)	
Grade 2	566 (48.2)	1,414 (45.0)		369 (51.0)	1,611 (44.8)	
Grade 3	351 (29.9)	577 (18.4)		204 (28.2)	724 (20.2)	
OARSI JSN, n (%)			**<0.001**			**<0.001**
Grade 0	533 (45.4)	1,644 (52.3)		323 (44.7)	1,854 (51.6)	
Grade 1	368 (31.3)	1,027 (32.7)		242 (33.5)	1,153 (32.1)	
Grade 2	273 (23.3)	471 (15.0)		158 (21.9)	586 (16.3)	
OARSI osteophytes, n (%)			**<0.001**			**<0.001**
Grade 0	398 (33.9)	1,447 (46.1)		249 (34.4)	1,596 (44.4)	
Grade 1	637 (54.3)	1,489 (47.4)		395 (54.6)	1,731 (48.2)	
Grade 2	139 (11.8)	206 (6.6)		79 (10.9)	266 (7.4)	
OARSI sclerosis, n (%)			**<0.001**			**<0.001**
Grade 0	741 (63.1)	2,318 (73.8)		467 (64.6)	2,592 (72.1)	
Grade 1	272 (23.2)	578 (18.4)		157 (21.7)	693 (19.3)	
Grade 2	161 (13.7)	246 (7.8)		99 (13.7)	308 (8.6)	
Total WOMAC pain, mean ± SD	5.48 ± 3.28	0.97 ± 1.55	**<0.001**	5.74 ± 3.32	1.49 ± 2.28	**<0.001**
Pain when walking on flat surface	1.11 ± 0.84	0.18 ± 0.43	**<0.001**	1.13 ± 0.85	0.29 ± 0.58	**<0.001**
Pain when going up/down stairs	1.75 ± 0.81	0.43 ± 0.63	**<0.001**	1.80 ± 0.82	0.58 ± 0.77	**<0.001**
Pain when in bed	0.78 ± 0.95	0.11 ± 0.40	**<0.001**	0.83 ± 0.96	0.18 ± 0.53	**<0.001**
Pain when sitting/lying	0.80 ± 0.82	0.11 ± 0.37	**<0.001**	0.87 ± 0.83	0.19 ± 0.49	**<0.001**
Pain when standing	1.04 ± 0.81	0.14 ± 0.39	**<0.001**	1.10 ± 0.83	0.24 ± 0.53	**<0.001**

* Age range was 45 to 79 years in all study groups. KLG is scored from 0 (no radiographic evidence) to 4 (extreme structure). All OARSI atlas grade subscales are scored from 0 (no evidence) to 3 (most severe). WOMAC total knee pain is scored from 0 (no pain) to 20 (extreme pain). All WOMAC pain subscales are scored from 0 (no pain) to 5 (extreme pain). Statistically significant ($P < 0.05$) results are bolded. BMI, body mass index; JSN, joint space narrowing; KLG, Kellgren-Lawrence Grade; OARSI, the Osteoarthritis Research Society International; PASE, Physical Activity Scale for the Elderly; Prob-S, probable sarcopenia; SARC-F (Strength, Assistance with walking, Rise from a chair, Climb stairs, and Falls); Scre-S, screened sarcopenia; WOMAC, Western Ontario McMaster Osteoarthritis Index.

Associations between baseline sarcopenia and progression in KOA. In cross-sectional analyses, significant associations of Scre-S and Prob-S were observed with both radiographic scores (Supplementary Table 1) and symptomatic scores (Supplementary Tables 2 and 3) at baseline. Longitudinally, baseline sarcopenia was associated with radiographic progression in KOA (including KLG, JSN, and sclerosis) over 48 months (Table 2). Meanwhile, baseline sarcopenia was significantly associated with the progressions of total WOMAC pain, and each subscales over 24 months and 48 months (Table 3). Similar results were also found in KOOS pain, other symptoms,

and QoL (Supplementary Table 3). The multiple-adjusted RCS analysis revealed positive exposure-response correlations between baseline SARC-F score and the risk of radiographic or symptomatic progression in KOA (all P for trend <0.001) (Supplementary Figure 2).

Associations between baseline sarcopenia and KR. Survival analyses were applied to verify the robustness of predicting effect of sarcopenia on subsequent KR. Baseline characteristics of participants in the survival analysis are presented in Supplementary Table 4. During the follow-up period (mean

Table 2. Association between baseline sarcopenia and radiographic progression in KOA*

Radiographic progression	Scre-S		Prob-S	
	OR (95% CI)	P value	OR (95% CI)	P value
Over 24 months				
KLG	1.66 (1.32–2.10)	**<0.001**	1.28 (0.97–1.69)	0.079
OARSI atlas classification				
JSN	1.76 (1.40–2.20)	**<0.001**	1.35 (1.03–1.76)	**0.029**
Osteophytes	1.60 (1.29–1.97)	**<0.001**	1.49 (1.16–1.92)	**0.002**
Sclerosis	2.07 (1.60–2.66)	**<0.001**	1.54 (1.14–2.07)	**0.005**
Over 48 months				
KLG	1.51 (1.23–1.86)	**<0.001**	1.34 (1.04–1.74)	**0.026**
OARSI atlas classification				
JSN	1.62 (1.30–2.01)	**<0.001**	1.59 (1.21–2.09)	**0.001**
Osteophytes	1.32 (1.07–1.63)	**0.010**	1.22 (0.93–1.59)	0.153
Sclerosis	1.96 (1.52–2.54)	**<0.001**	1.69 (1.24–2.30)	**0.001**

* Data are adjusted ORs (95% CIs) based on GEE. Statistically significant (*P* value <0.05) results are bolded. Model adjusted for age, sex, race, BMI, PASE, smoking history, drinking history, knee alignment (normal, varus, and valgus), and baseline radiographic scores. 95% CI, 95% confidence interval; BMI, body mass index; GEE, generalized estimating equation; JSN, joint space narrowing; KLG, Kellgren-Lawrence Grade; KOA, knee osteoarthritis; PASE, Physical Activity Scale for the Elderly; Prob-S, probable sarcopenia; OR, odds ratio; OARSI, the Osteoarthritis Research Society International; Scre-S, screened sarcopenia.

92 months, 108-month follow-up visit), 481 participants with KR were observed. Compared with the negative groups, significantly higher risks of KR were found both in the Scre-S (+) and Prob-S (+) groups (Breslow test, *P* < 0.001; Log-rank test, *P* < 0.001). The HR of KR was 3.84 (95% CI 3.18–4.62) in the Scre-S group and 2.29 (95% CI 1.87–2.81) in the Prob-S group after adjusting for covariates (Figure 2). The E-value for the Scre-S group was 7.14 (95% CI 5.81–8.71), and the E-value for the Prob-S group was 4.01 (95% CI 3.15–5.07), which indicates the independence and higher strength of sarcopenia in promoting the progression of KR (Figure 2). The multiple-adjusted RCS analysis revealed positive exposure-response correlations between baseline SARC-F score and the risk of KR (*P* for trend <0.001) (Supplementary Figure 2).

Replication of associations between baseline sarcopenia and KOA progression in matched cohorts. We generated two matched cohorts using the PS-matching method: In the Scre-S cohort, there were 1,067 matched pairs of negative and positive participants, whereas there were 661 matched pairs in the Prob-S cohort (Figure 3A and E). The baseline characteristics of participants in two cohorts are presented in Supplementary Table 5. Compared with the unmatched cohort, the eight confounding factors in the matched cohort were balanced at baseline among Scre-S (+, −) and Prob-S (+, −), respectively (all *P* values >0.05). In cross-sectional analyses, significant associations of Scre-S and Prob-S were also observed with both radiographic scores (Supplementary Table 6) and

Table 3. Association between baseline sarcopenia and symptomatic progression in KOA*

Symptomatic progression	Scre-S		Prob-S	
	Beta (95% CI)	P value	Beta (95% CI)	P value
Over 24 months				
Total WOMAC pain	0.92 (0.62–1.22)	**<0.001**	0.91 (0.54–1.28)	**<0.001**
Pain when walking on flat surface	0.30 (0.24–0.37)	**<0.001**	0.27 (0.19–0.36)	**<0.001**
Pain when going up/down stairs	0.30 (0.22–0.39)	**<0.001**	0.32 (0.22–0.42)	**<0.001**
Pain when in bed	0.24 (0.17–0.30)	**<0.001**	0.24 (0.16–0.33)	**<0.001**
Pain when sitting/lying	0.20 (0.15–0.26)	**<0.001**	0.23 (0.15–0.30)	**<0.001**
Pain when standing	0.27 (0.20–0.34)	**<0.001**	0.23 (0.14–0.32)	**<0.001**
Over 48 months				
Total WOMAC pain	1.04 (0.57–1.42)	**<0.001**	1.06 (0.64–1.48)	**<0.001**
Pain when walking on flat surface	0.28 (0.20–0.35)	**<0.001**	0.28 (0.18–0.37)	**<0.001**
Pain when going up/downstairs	0.31 (0.21–0.42)	**<0.001**	0.35 (0.23–0.48)	**<0.001**
Pain when in bed	0.19 (0.12–0.26)	**<0.001**	0.22 (0.12–0.32)	**<0.001**
Pain when sitting/lying	0.19 (0.13–0.26)	**<0.001**	0.28 (0.19–0.37)	**<0.001**
Pain when standing	0.23 (0.16–0.30)	**<0.001**	0.26 (0.16–0.36)	**<0.001**

* Data are adjusted β (95% CI) based on GEEs. Statistically significant (*P* < 0.05) results are bolded. Model adjusted for age, sex, race, BMI, PASE, smoking history, drinking history, knee alignment (normal, varus, and valgus), and baseline symptomatic scores. 95% CI, 95% confidence interval; BMI, body mass index; GEE, generalized estimating equation; KOA, knee osteoarthritis; PASE, Physical Activity Scale for the Elderly; Prob-S, probable sarcopenia; Scre-S, screened sarcopenia; WOMAC, Western Ontario McMaster Osteoarthritis Index.
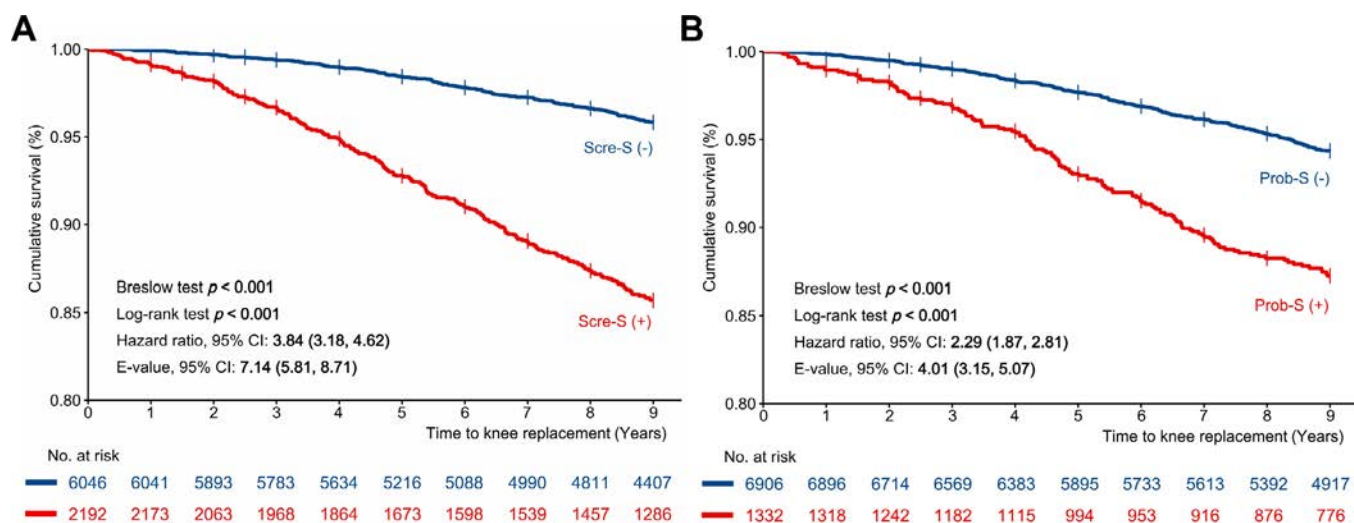
Figure 2. Association of baseline Scre-S (A) and Prob-S (B) with subsequent KR. Data are adjusted HRs (95% CIs) based on multivariable Cox proportional hazard model before PS matching. Model adjusted for age, sex, race, BMI, PASE, smoking, drinking, and knee alignment (normal, varus, and valgus). 95% CI, 95% confidence interval; BMI, body mass index; HR, hazard ratio; KR, knee replacement; PASE, Physical Activity Scale for the Elderly; Prob-S, probable sarcopenia; PS, propensity score; Scre-S, screened sarcopenia. Color figure can be viewed in the online issue, which is available at http://onlinelibrary.wiley.com/doi/10.1002/art.43213/abstract.

symptomatic scores (Supplementary Tables 7 and 8) in the matched cohort, which are consistent with the results in the unmatched cohort. The analyses performed in the matched cohort showed that results were consistent in direction and magnitude of associations of those from the main analyses in the unmatched cohort. Specifically, the relationships between baseline sarcopenia and the progression of KLG, JSN, and sclerosis over 48 months showed significant associations in both the matched and unmatched cohorts rather than with the progression of osteophytes in the matched cohort (Figure 3B and F; Supplementary Table 9). Additionally, baseline sarcopenia was significantly associated with all symptomatic progressions (WOMAC pain and its subscales, KOOS pain, and QoL) in both matched and unmatched cohorts, except for KOOS other symptoms in the matched cohort (Figure 3C and G; Supplementary Tables 8 and 10). The baseline characteristics of participants for survival analysis in the two groups are presented in Supplementary Table 11. The HR of KR was 3.87 (95% CI 2.97–5.04) in the Scre-S group, and 2.24 (95% CI 1.66–3.02) in the Prob-S group (Figure 3D and H).

DISCUSSION

To the best of our knowledge, our study is the first to determine the associations of baseline sarcopenia with KOA progression and subsequent KR in a large-scale, prospective cohort. Both baseline Scre-S and Prob-S were significantly associated with increased risk of radiographic and symptomatic progression of KOA. Importantly, there was a significant and strong increase in the risk for KR in the Scre-S and Prob-S groups compared with

the control groups. These findings were confirmed after adjustment and PS matching, which implies a potential causal role of sarcopenia in KOA progression.

Though expert consensus has indicated that muscle weakness is likely a risk factor for KOA,[29] the existing research remains controversial. Misra et al reported that body composition-based sarcopenia was not associated with incident KOA.[20] It is important to recognize the limitation on the definition of sarcopenia in this paper, which was based on a modified residual method and is no longer consistent with sarcopenia diagnosis according to the EWGSOP2 algorithm.[23,37] Additionally, the selection of outcomes could be somewhat limited, as it defined radiographic KOA solely based on KLG and did not account for symptomatic KOA. Mohajer et al assessed muscle mass on thigh MRI with quantitative markers and found that longitudinal changes of quadriceps size and intramuscular fat could predict subsequent symptomatic worsening and KR, which provided valuable insights regarding its long-term impact on KOA progression.[19] Veronese et al confirmed the association between sarcopenia and incident symptomatic KOA, rather than radiographic KOA.[18] They used the estimation equations to diagnose sarcopenia, which was only validated for adults without obesity.[38] Additionally, they did not further adjust BMI in the analysis, a relevant potential confounding factor. Together with the absence of additional sensitivity analyses, the robustness and reproducibility of the findings would be limited.

In the current analyses, we based our detection of Scre-S on the most accepted and validated diagnostic algorithm EWGSOP2 in the context of available parameters included in the OAI database. Moreover, the EWGSOP2 approach indicates the importance of muscle strength as a functional parameter in the
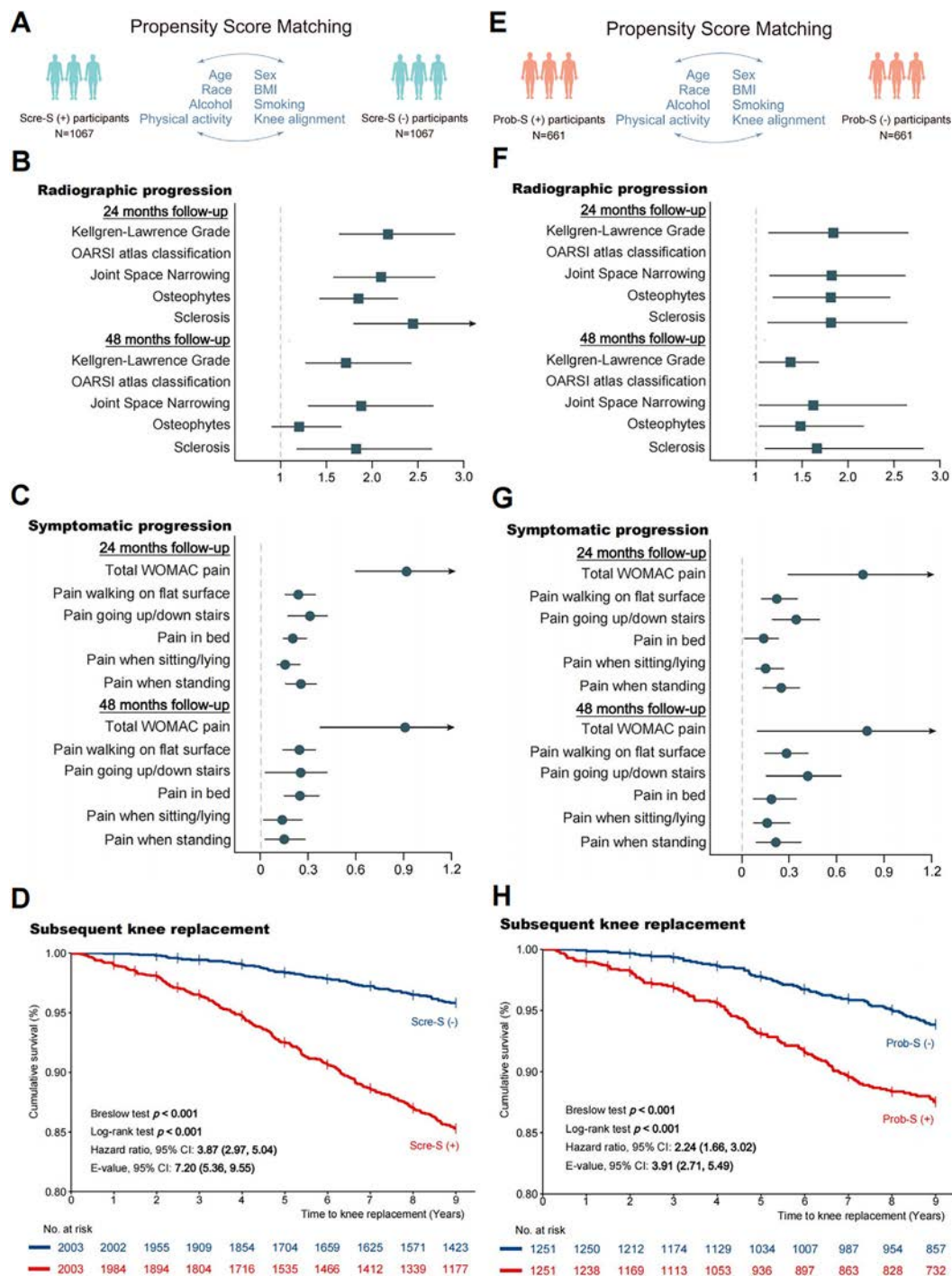
Figure 3. Associations between sarcopenia and progression in KOA and subsequent KR in the matched cohort. (A) The PS-matched procedure generated paired groups of 1,067 Scre-S participants and controls. (B) Association between baseline Scre-S and radiographic progression in KOA after PS matching. Data are adjusted ORs based on the GEE model adjusted for baseline radiographic scores. (C) Association between baseline Scre-S and symptomatic progression in KOA after PS matching. Data are adjusted ORs based on the GEE model adjusted for baseline symptomatic scores. (D) Association of baseline Scre-S with subsequent KR after PS matching based on the Cox proportional hazards model. (E) The PS-matched procedure generated paired groups of 661 Prob-S (+) participants and controls. (F) Association between baseline Prob-S and radiographic progression in KOA after PS matching. Data are adjusted ORs based on the GEE model adjusted for baseline radiographic scores. (G) Association between baseline Prob-S and symptomatic progression in KOA after PS matching. Data are adjusted ORs based on the GEE model adjusted for baseline symptomatic scores. (H) Association of baseline Prob-S with subsequent KR after PS matching based on the Cox proportional hazards model. 95% CI, 95% confidence interval; BMI, body mass index; GEE, generalized estimating equation; KOA, knee osteoarthritis; KR, knee replacement; OARSI, Osteoarthritis Research Society International; OR, odds ratio; Scre-S, screened sarcopenia; Prob-S, probable sarcopenia; PS, propensity score; WOMAC, Western Ontario McMaster Osteoarthritis Index.

diagnostic process after case-finding, and low muscle strength is proposed as a prerequisite for sarcopenia diagnosis and a sufficient parameter to diagnose Prob-S.[23] In this way, we found both Scre-S and Prob-S were strong and independent predictors of KOA progression and KR, which for the first time indicates a longitudinal association between pre-existing sarcopenia and subsequent KOA progression. Specifically, baseline Scre-S and Prob-S were found to be associated with increased pain and decreased QoL in both matched and unmatched cohorts. However, the associations of baseline sarcopenia with the progression of other symptoms (KOOS) were no longer statistically significant after PS matching, although point estimation values suggested a potentially positive correlation (point estimation values of β greater than 0). Considering that the KOOS focuses more on therapeutic effects after knee injury, its usefulness in our observational cohort could be relatively limited. Further studies are required to determine the association between sarcopenia and other symptoms. Based on these findings, clinical sarcopenia is supported to be an important contributor to KOA pathogenesis, leading to KOA progression and negative prognosis with indication for KR. Importantly, from a clinical standpoint, sarcopenia from this study represents new, potentially modifiable risk factors for KOA progression that should therefore be introduced in the clinical management of KOA. It is important to point out that SARC-F and the chair-stand-test as surrogates of direct leg muscle strength measurement are easily available in any clinical setting and could therefore be widely implemented with limited resources.[39]

Regarding potential underlying mechanisms, biomechanical disruptions may not fully explain the role of skeletal muscle alterations in the pathophysiology of KOA.[11] Although quadriceps weakness has been reported to be associated with patellofemoral pathology and pain in KOA, this association has been found inconclusive in a recent systematic review.[40] Similarly, sarcopenia in KOA was previously proposed to result from disuse atrophy caused by knee pain and reduced physical activity.[41] Lower knee extensor strength was, however, reported also in the absence of knee pain.[42] In our study, associations between baseline sarcopenia and KOA progression, both radiographically and symptomatically, generally remained significant after adjusting for baseline knee pain and other potential confounders and addressing the PS-matched method. Therefore, the biochemical and molecular interactions between altered skeletal muscle and the knee joint may be a plausible explanation.[43]

First, adipose tissue infiltration within the muscle is frequently observed in the elderly, and it can secrete not only inflammatory cytokines such as TNF-α and IL-1β, but also adipokines such as resistin or adiponectin, all of which may induce inflammation in KOA.[44,45] Furthermore, skeletal muscle itself can also release inflammatory cytokines such as monocyte chemotactic protein 1, which may subsequently attract mononuclear cells, drive the immune response, and elicit knee symptoms.[46] Last, advanced

approaches have depicted the sarcopenic microenvironment at the single-cell level, which may provide preliminary evidence for micro changes in skeletal composition and be a potential source of interacting molecules or factors.[47,48]

Our study has potential limitations. First, although we employed a prospective design, used the PS-matching method, and used the E-value to measure residual confounding to control for the risk of bias as much as possible, it is important to acknowledge that selection bias may still exist in observational studies. Considering other potential confounders that could not be controlled, further Mendelian randomization studies or randomized controlled trials are needed in the future to verify the causal role of sarcopenia in the progression of KOA. Second, we acknowledged that a full diagnosis of sarcopenia is not available because of a lack of measurement of muscle mass or even its surrogates in the OAI database. We chose to use Scre-S and Prob-S to represent pre-existing sarcopenia, and their confirmed longitudinal associations with KOA progression support a primary role of sarcopenia. Nevertheless, direct sarcopenia diagnosis with measured muscle mass should further confirm the current associations for full sarcopenia with low muscle mass. On the other hand, we believe that our new findings linking key sarcopenia components and important indicators of muscle dysfunction to KOA progression are important in providing the first demonstration of a pathogenetic involvement of sarcopenia in the KOA progression. Last, all participants in this study were of middle to older age, and it remains unclear whether our findings would hold true in young adults.

In summary, our study revealed longitudinal associations between baseline sarcopenia, KOA progression, and subsequent KR. This study provides new insight into the potential causality of sarcopenia to KOA progression. Such a temporal relationship highlights the need for more attention to sarcopenia screening and diagnosis, and potentially to sarcopenia treatment in KOA management.

AUTHOR CONTRIBUTIONS

REFERENCES

1. Duong V, Oo WM, Ding C, et al. Evaluation and treatment of knee pain: a review. JAMA 2023;330(16):1568–1580.

2. Pegreffi F, Balestra A, De Lucia O, et al. Prevalence of sarcopenia in knee osteoarthritis: a systematic review and meta-analysis. J Clin Med 2023;12(4):1532.

3. Donini LM, Busetto L, Bischoff SC, et al. Definition and diagnostic criteria for sarcopenic obesity: ESPEN and EASO consensus statement. Clin Nutr 2022;41(4):990–1000.

4. Cruz-Jentoft AJ, Sayer AA. Sarcopenia. Lancet 2019;393(10191): 2636–2646.

5. Chen S, Han H, Jin J, et al. Osteoarthritis and sarcopenia-related traits: the cross-sectional study from NHANES 2011–2014 and Mendelian randomization study. J Orthop Surg Res 2023;18(1):502.

6. Kemnitz J, Wirth W, Eckstein F, et al. Longitudinal change in thigh muscle strength prior to and concurrent with symptomatic and radiographic knee osteoarthritis progression: data from the Osteoarthritis Initiative. Osteoarthritis Cartilage 2017;25(10):1633–1640.

7. Kiss N, Abbott G, Daly RM, et al. Multimorbidity and the risk of malnutrition, frailty and sarcopenia in adults with cancer in the UK Biobank. J Cachexia Sarcopenia Muscle 2024;15(5):1696–1707.

8. Liu J, Zhu Y, Tan JK, et al. Factors Associated with sarcopenia among elderly individuals residing in community and nursing home settings: a systematic review with a meta-analysis. Nutrients 2023;15(20):4335.

9. Lin JZ, Liang JJ, Ma JD, et al. Myopenia is associated with joint damage in rheumatoid arthritis: a cross-sectional study. J Cachexia Sarcopenia Muscle 2019;10(2):355–367.

10. Yang D, Chen Y, Guo J, et al. The organ-joint axes in osteoarthritis: significant pathogenesis and therapeutic targets. Aging Dis 2024. https://doi.org/10.14336/AD.2024.1223

11. De Ceuninck F, Fradin A, Pastoureau P. Bearing arms against osteoarthritis and sarcopenia: when cartilage and skeletal muscle find common interest in talking together. Drug Discov Today 2014;19(3):305–311.

12. Maniar N, Cole MH, Bryant AL, et al. Muscle force contributions to anterior cruciate ligament loading. Sports Med 2022;52(8):1737–1750.

13. Hollville E, Nordez A, Guilhem G, et al. Interactions between fascicles and tendinous tissues in gastrocnemius medialis and vastus lateralis during drop landing. Scand J Med Sci Sports 2019;29(1):55–70.

14. Chow LS, Gerszten RE, Taylor JM, et al. Exerkines in health, resilience and disease. Nat Rev Endocrinol 2022;18(5):273–289.

15. Mao Y, Jin Z, Yang J, et al. Muscle-bone cross-talk through the FNIP1-TFEB-IGF2 axis is associated with bone metabolism in human and mouse. Sci Transl Med 2024;16(750):eadk9811.

16. Yang J, Liu P, Wang S, et al. Causal relationship between sarcopenia and osteoarthritis: a bi-directional two-sample Mendelian randomized study. Eur J Med Res 2023;28(1):327.

17. Liu JC, Dong SS, Shen H, et al. Multi-omics research in sarcopenia: current progress and future prospects. Ageing Res Rev 2022;76:101576.

18. Veronese N, Stefanac S, Koyanagi A, et al. Lower limb muscle strength and muscle mass are associated with incident symptomatic knee osteoarthritis: a longitudinal cohort study. Front Endocrinol (Lausanne) 2021;12:804560.

19. Mohajer B, Dolatshahi M, Moradi K, et al. Role of thigh muscle changes in knee osteoarthritis outcomes: Osteoarthritis Initiative data. Radiology 2022;305(1):169–178.

20. Misra D, Fielding RA, Felson DT, et al; MOST study. Risk of knee osteoarthritis with obesity, sarcopenic obesity, and sarcopenia. Arthritis Rheumatol 2019;71(2):232–237.

21. Turkiewicz A, Timpka S, Thorlund JB, et al. Knee extensor strength and body weight in adolescent men and the risk of knee osteoarthritis by middle age. Ann Rheum Dis 2017;76(10):1657–1661.

22. Lester G. The Osteoarthritis Initiative: a NIH public-private partnership. HSS J 2012;8(1):62–63.

23. Cruz-Jentoft AJ, Bahat G, Bauer J, et al; Writing Group for the European Working Group on Sarcopenia in Older People 2 (EWGSOP2), and the Extended Group for EWGSOP2. Sarcopenia: revised European consensus on definition and diagnosis. Age Ageing 2019;48(1):16–31.

24. Nishimura T, Arima K, Okabe T, et al. Usefulness of chair stand time as a surrogate of gait speed in diagnosing sarcopenia. Geriatr Gerontol Int 2017;17(4):659–661.

25. Zeng C, Lane NE, Hunter DJ, et al. Intra-articular corticosteroids and the risk of knee osteoarthritis progression: results from the Osteoarthritis Initiative. Osteoarthritis Cartilage 2019;27(6):855–862.

26. Paz-González R, Balboa-Barreiro V, Lourido L, et al. Prognostic model to predict the incidence of radiographic knee osteoarthritis. Ann Rheum Dis 2024;83(5):661–668.

27. Ferket BS, Feldman Z, Zhou J, et al. Impact of total knee replacement practice: cost effectiveness analysis of data from the Osteoarthritis Initiative. BMJ 2017;356:j1131.

28. Binvignat M, Sellam J, Berenbaum F, et al. The role of obesity and adipose tissue dysfunction in osteoarthritis pain. Nat Rev Rheumatol 2024;20(9):565–584.

29. Hunter DJ, Bierma-Zeinstra S. Osteoarthritis. Lancet 2019; 393(10182):1745–1759.

30. Steinmetz JD, Culbreth GT, Haile LM, et al; GBD 2021 Osteoarthritis Collaborators. Global, regional, and national burden of osteoarthritis, 1990–2020 and projections to 2050: a systematic analysis for the Global Burden of Disease Study 2021. Lancet Rheumatol 2023;5(9): e508–e522.

31. Costello KE, Felson DT, Jafarzadeh SR, et al. Gait, physical activity and tibiofemoral cartilage damage: a longitudinal machine learning analysis in the Multicenter Osteoarthritis Study. Br J Sports Med 2023;57(16):1018–1024.

32. Nelligan RK, Hinman RS, Kasza J, et al. Effects of a self-directed web-based strengthening exercise and physical activity program supported by automated text messages for people with knee osteoarthritis: a randomized clinical trial. JAMA Intern Med 2021;181(6): 776–785.

33. Moseng T, Vliet Vlieland TPM, Battista S, et al. EULAR recommendations for the non-pharmacological core management of hip and knee osteoarthritis: 2023 update. Ann Rheum Dis 2024;83(6):730–740.

34. Yoshida S, Nishitani K, Yoshitomi H, et al. Knee alignment correction by high tibial osteotomy reduces symptoms and synovial inflammation in knee osteoarthritis accompanied by macrophage phenotypic change from M1 to M2. Arthritis Rheumatol 2023;75(6):950–960.

35. Atukorala I, Kwoh CK, Guermazi A, et al. Synovitis in knee osteoarthritis: a precursor of disease? Ann Rheum Dis 2016;75(2):390–395.

36. VanderWeele TJ, Ding P. Sensitivity analysis in observational research: introducing the E-value. Ann Intern Med 2017;167(4): 268–274.

37. Newman AB, Kupelian V, Visser M, et al; Health ABC Study Investigators. Sarcopenia: alternative definitions and associations with lower extremity function. J Am Geriatr Soc 2003;51(11):1602–1609.

38. Lee RC, Wang Z, Heo M, et al. Total-body skeletal muscle mass: development and cross-validation of anthropometric prediction models. Am J Clin Nutr 2000;72(3):796–803.

39. Gortan Cappellari G, Guillet C, Poggiogalle E, et al; SOGLI Expert Panel. Sarcopenic obesity research perspectives outlined by the sarcopenic obesity global leadership initiative (SOGLI) - Proceedings from the SOGLI consortium meeting in Rome November 2022. Clin Nutr 2023;42(5):687–699.

40. Bazett-Jones DM, Neal BS, Legg C, et al. Kinematic and kinetic gait characteristics in people with patellofemoral pain: a systematic review and meta-analysis. Sports Med 2023;53(2):519–547.

41. Veronese N, Koyanagi A, Barbagallo M, et al. Pain increases the risk for sarcopenia in community-dwelling adults: results from the English

Longitudinal Study of Ageing. J Gerontol A Biol Sci Med Sci 2023; 78(6):1013–1019.

42. Øiestad BE, Juhl CB, Culvenor AG, et al. Knee extensor muscle weakness is a risk factor for the development of knee osteoarthritis: an updated systematic review and meta-analysis including 46 819 men and women. Br J Sports Med 2022;56(6):349–355.

43. Yao Q, Wu X, Tao C, et al. Osteoarthritis: pathogenic signaling pathways and therapeutic targets. Signal Transduct Target Ther 2023;8(1):56.

44. Li CW, Yu K, Shyh-Chang N, et al. Pathogenesis of sarcopenia and the relationship with fat mass: descriptive review. J Cachexia Sarcopenia Muscle 2022;13(2):781–794.

45. Li Y, Onodera T, Scherer PE. Adiponectin. Trends Endocrinol Metab 2024;35(7):674–675.

46. Singh S, Anshita D, Ravichandiran V. MCP-1: Function, regulation, and involvement in disease. Int Immunopharmacol 2021;101(Part B):107598.

47. Kedlian VR, Wang Y, Liu T, et al. Human skeletal muscle aging atlas. Nat Aging 2024;4(5):727–744.

48. Lai Y, Ramírez-Pardo I, Isern J, et al. Multimodal cell atlas of the ageing human skeletal muscle. Nature 2024;629(8010): 154–164.

Paradoxical Activation of Entheseal Myeloid Cells by JAK1 and Tyk2 Inhibitors via Interleukin-10 Antagonism

Sami Giryes,[1] [ID] Chi Wong,[2] Charlie Bridgewood,[2] Mark Harland,[2] Ala Altaie,[2] [ID] Nicole McDermott,[2] Kerem Abacar,[2] Abhay Rao,[3] Almas Khan,[3] Tristan McMillan,[3] Peter Loughenbury,[3] Robert Dunsmuir,[3] Vishal Borse,[3] Tom Macleod,[2] and Dennis McGonagle[4]

Objective. JAK inhibition (JAKi) is effective in seronegative spondyloarthropathy (SpA) spectrum disorders, but Tyk2 inhibition failed in SpA spectrum ulcerative colitis, and tofacitinib showed minimal benefit in Crohn disease, which highlights the complex role for JAK/STAT signaling in different inflammatory processes. In this study, we investigated whether JAKi might paradoxically activate entheseal innate immunity and aimed to identify the key regulatory cytokines involved in this process.

Methods. Spinal entheseal tissue was activated with Toll-like receptor (TLR) agonists, including TLR4 and interleukin-1 (IL-1) family proteins, and entheseal T cells were activated with anti-CD3/anti-CD28 with IL-23/IL-1β. JAKi via upadacitinib (JAK1/JAK2), deucravacitinib (Tyk2), and ritlecitinib (JAK3) inhibition was evaluated using multiplex cytokine assays, intracellular flow, and bulk RNA sequencing (RNAseq) and cytokine blocking or stimulation.

Results. Following interferon γ stimulation, JAK1 inhibition blocked STAT1 phosphorylation in entheseal cells and strongly blocked activated entheseal T cell tumor necrosis factor α (TNFα), IL-17A, and IL-17F production. The opposite effect was evident in entheseal myeloid cell with exaggerated TLR4 and other adjuvant-mediated cytokine production including IL-23 (∼10-fold increase; $P < 0.001$) or TNFα (∼10-fold increase; $P < 0.0001$). This myeloid effect was induced by upadacitinib and deucravacitinib but not ritlecitinib, suggesting IL-10R JAK1/Tyk2 signaling. Bulk RNAseq showed a multifaceted impact of JAKi on myeloid activation with strong M1 type monocyte polarization under TLR4 stimulation and JAK1 inhibition confirmed by flow cytometry. Direct IL-10 inhibition recapitulated inflammatory cytokine elevations and IL-10R agonist largely, but not completely, rescued this phenotype.

Conclusion. These findings help explain the emergent efficacy of Tyk2 blockade in SpA spectrum–related arthritis that is not IL-10 dependent but indicates why such strategies may not be a panacea for SpA spectrum disorder–related intestinal inflammation.

INTRODUCTION

Spondyloarthropathy (SpA) encompasses ankylosing spondylitis (AS), psoriatic arthropathy (PsA), and related psoriasis; reactive arthritis; and inflammatory bowel disease (IBD)–associated arthritis evident in Crohn disease (CD) and ulcerative colitis (UC). These disorders are associated with enthesitis, which is the cardinal SpA lesion, and associated with both tumor necrosis factor (TNF) and interleukin-23 (IL-23)/IL-17 pathway dysregulation at the synovio-entheseal complex leading to joint inflammation.[1–3]

Cytokine signaling through the JAK-STAT pathway activates more than 50 soluble factors including cytokines, interferons (IFNs), and endocrine factors.[3–5] The JAK and STAT families include four JAK members (JAK1, JAK2, JAK3, and Tyk2) and seven STAT members.[5] IL-23 is a critical cytokine in the

pathogenesis of SpA, being immunogenetically linked to all SpA spectrum manifestations[2,6,7] and to type-17 T cell production pathogenic disease driver cytokines including IL-17A, IL-17F, TNF, and others.[2,8]

Currently, three JAK inhibitors (JAKi) are licensed or soon to be adopted in SpA-associated arthropathy including tofacitinib (considered a pan-JAKi), upadacitinib (predominantly JAK1 inhibition, with reports of JAK2 inhibition in certain assays ranging from 2- to 60-fold less selectivity than JAK1) and deucravacitinib (highly selective Tyk2 inhibition).[9–14] The exact mechanism of JAKi efficacy in SpA is unclear because the pivotal IL-17A, IL-17F, and TNF cytokines do not signal directly via the JAK pathway.[15,16] The IL-23 signaling is mediated by JAK2-Tyk2 and subsequent STAT3 phosphorylation veering lymphoid cells toward IL-17 production.[17,18] A proposed mechanisms JAKi efficacy in SpA is blocking IL-23–dependent JAK2-Tyk2 signaling.[4,19]

However, JAKi is not a panacea for all SpA-related, spectrum-associated inflammation including IBD, which contrasts to TNF monoclonal antibody inhibition that treats all joint and intestinal manifestations. For example, tofacitinib has minimal CD efficacy and consequently is not licensed for that indication.[20] Furthermore, in contrast to IL-23 blockers, Tyk2 inhibition with deucravacitinib failed to show efficacy in UC despite good efficacy for both psoriasis and PsA,[21] although JAK1 inhibition that blocks the common γ chain needed for T cell proliferation and activation is license in IBD. Of note, IL-10 is a key cytokine linked to inborn errors of innate immunity with early onset IBD but is not linked to SpA spectrum skeletal inflammation.[22] Furthermore, IL-10 signals via JAK1 and[23] Tyk2 and could thus be a pivotal cytokine in potential differences between enthesis and intestinal immunology across the SpA spectrum.

Upadacitinib, a JAK1 inhibitor (2- to 60-fold selective over JAK2, >100-fold selective over JAK3, and does not inhibit Tyk2),[12,14,24] has proven efficacy in AS, PsA, UC, and, recently, CD.[25–29] Given the differential efficacy for JAKi across SpA spectrum disorders and IBD, we explored the impact of JAKi on both enthesis innate and adaptive immune responses to better understand the emerging reverse translational immunology pertaining to JAKi in SpA spectrum disorders.

MATERIALS AND METHODS

Peripheral blood and normal spinous process enthesis were obtained from 32 donors with no systemic autoimmune or inflammatory diseases who were undergoing spinal decompression or surgery for scoliosis correction of thoracic or lumbar vertebrae using methodology previously described.[30] Written informed consent to participate was given by all patients before taking part, and research was conducted in compliance with the Helsinki Declaration. Entheseal sample collection was approved by the Northwest-Greater Manchester West Research Ethics Committee (REC:16/NW/0797). Patients

and/or the public were not involved in the design, conduct, reporting, or dissemination plans of this research. Data are available on reasonable request.

The collected enthesis samples were separated into soft tissue and peri-entheseal bone (PEB) with subsequent PEB minced into small fragments ≤5 mm^2, followed by mechanical digestion with cells collected after phosphate buffered saline (PBS) washing. Thereafter, cells were strained and red cells lysis was performed using the ammonium chloride method with two PBS washing steps and resuspension in RPMI 1640 (10% fetal bovine serum, 10 U/mL of penicillin and streptomycin). T cells were further enriched from entheseal cells with pan T cell isolation kit (Miltenyi). Peripheral blood leukocytes were isolated using red cell lysis with ammonium chloride. Three PBS washes were performed before resuspension in RPMI 1640.

Isolated cells were plated at 5×10^5 cells per well in 96 well plates in RPMI 1640. For T cell stimulation, 96 well plates were coated with 1 μg/mL of anti-CD3 (Life Technologies, orthoclone T 3) before cell seeding and stimulation with 2.5 μg/mL of anti-CD28 with or without the addition of 25 ng/mL of IL-1β and IL-23. For upadacitinib inhibition of T cell activation, cells were pretreated with varying upadacitinib (indicated in the Results section) concentrations in a separate well for one hour before transfer to an anti-CD3–coated 96 well plate and subsequent stimulation. For myeloid activation, cells were pretreated with or without upadacitinib (concentration indicated in the Results section) for one hour before stimulation with either lipopolysaccharide (LPS) (10 ng/mL), IL-1β (25 ng/mL), IL-36α (100 ng/mL), mannan (10 μg/mL), zymosan (10 μg/mL), or IL-10 (concentration indicated in the Results section). THP-1 cell lines were cultured in RPMI 1640 and plated at 2×10^5 cells per well in 96 well plates before stimulation.

For cytokine blocking experiments, neutralizing antibodies anti–IL-10Rα, anti–IL-19, and anti-IFN α/β Receptor 1 (IFNAR1) (Supplementary Table S1) were added to cells at the concentrations, indicated in the Results section, one hour before stimulation. NF-κB inhibition experiments conducted on peripheral blood leukocytes used the specific inhibitor caffeic acid phenethyl ester at 1 μM added to cells three hours after LPS stimulation.[31] Following stimulation, cells were pelleted by centrifugation and supernatants collected for cytokine analysis. Cells were collected for further analysis by flow cytometry or isolation of RNA.

Luciferase assay. THP-1 cells stably transduced with an NF-κB–driven luciferase reporter were pretreated with 1 μM of upadacitinib one hour before stimulation with 10 ng/mL LPS. Luciferase activity was then measured each hour after LPS stimulation (0–5 hours). Luciferase activity was measured by the addition of Dual-Glo substrate and buffer solution (Promega) according to the manufacturer's instructions, allowing 20 minutes of incubation time (room temperature), followed by measurement

of luminosity by a Cytation 5 multimode plate reader (Agilent BioTek).

Flow cytometry. For intracellular analysis of cytokines, cells were treated with GolgiPlug (BD Biosciences; 1 μL per 10^6 cells) eight hours before analysis. Cells were stained for cell viability (Zombie Fixable Dyes, BioLegend, 1:1,000, 20-minute incubation) before blocking with 10% mouse serum and 1% human IgG for 10 minutes. Cells were then stained with surface marker antibodies (Supplementary Table S1) at concentrations indicated by the manufacturers for 30 minutes in staining buffer (PBS, 1 mM EDTA, 2% bovine serum albumin with BD brilliant stain buffer). For analysis of intracellular cytokines, after surface staining cells were fixed and permeabilized using a BD Cytofix/Cytoperm fixation/permeabilization kit according to the manufacturer's instructions and then stained with intracellular cytokine antibodies for 30 minutes (Supplementary Table S1). Stained cells were analyzed on a Beckman-Coulter Cytoflex LX cytometer.

For analysis of phosphorylated STAT1, cells were fixed in 4% paraformaldehyde for 10 minutes at 37°C immediately after stimulation. Cells were then permeabilized using BD Phosflow Perm Buffer III for 30 minutes on ice. After fixation, cells were resuspended in staining buffer and anti-pSTAT1 (Supplementary Table S1) for one hour. Cells were analyzed on a Beckman-Coulter Cytoflex LX cytometer.

Bulk RNA sequencing and analysis. RNA was extracted from cell pellets (∼5 × 10^5 cells) using the Total RNA Purification Kit (Norgen Biotek). Sequencing libraries were prepared, and sequenced (PE150, 9 Gb per sample) on the Illumina NovaSeq X plus at Novogene (Novogene). Following quality control (removal of low-quality reads and reads containing adapters and poly-N), reads were aligned to the reference genome using Hisat 2 version 2.0.5. featureCounts version 1.5.0-p3 was used to count reads and calculate fragments per Kb of transcript per million bp sequenced. Differential expression analysis was performed with DESeq2 (DESeq2RPackage 1.20.0), and adjusted P values calculated using the Benjamin and Hochberg's approach. Genes with a adjusted P value ≤0.05 were assigned as differentially expressed. The clusterProfiler R package was used to test the statistical enrichment of differentially expressed genes in Kyoto Encyclopedia of Genes and Genomes (KEGG) pathways, with pathways with corrected P values <0.05 considered significantly enriched. Gene set enrichment analysis (GSEA) for KEGG pathways was performed using the GSEA analysis tool (http://broadinstitute.org/gsea/index.jsp).

Cytokine measurement and statistical analysis. Cytokines were measured either by enzyme-linked immunosorbent assay (ELISA) (IL-23, TNFα; Thermofisher) or by bead-based multiplexed immunoassay (LEGENDplexTM, BioLegend) according to the manufacturer's instructions. GraphPad Prism software

was employed with analysis of variance employment to calculate significance and Dunnet's test used for multiple comparisons. Specific statistical tests are described in the corresponding figure legends. Significant differences between control and test with P values less than 0.05 were denoted with an asterisk, as indicated in the figure legends, or labeled with the exact P value when they were greater than 0.05 but there were trends evident. Any specific statistical tests are outlined in the figure legends.

RESULTS

JAKi strongly inhibiting entheseal T cell activity. We initially evaluated upadacitinib as an exemplar of JAKi with broad efficacy across SpA and IBD. Entheseal leukocytes were pretreated with upadacitinib and then stimulated with IFNγ for 15 minutes. IFNγ signaling requires activation of JAK1 and JAK2 to facilitate STAT1 phosphorylation, which allows translocation to the nucleus and subsequent gene transcription.[32] Analysis by intracellular flow cytometry demonstrated upadacitinib effectively prevented phosphorylation of STAT1 (Figure 1A).

To evaluate upadacitinib effects on T cell–derived SpA-driving cytokines TNFα and IL-17, entheseal leukocytes were pretreated with upadacitinib at concentrations representative of patient sera levels over the course of a dose (0.1–10 μM),[33] then stimulated for 48 hours with type-17-driving cytokines (IL-23 and IL-1β) and anti-CD3/CD28 antibodies for T cell receptor (TCR)–dependent activation of T cells with upadacitinib significantly down-regulating TNFα, IL-17A, and IL-17F production from activated T cells, thus showing how JAKi block activation of entheseal derived T cells (Figure 1B). Intracellular flow cytometry on CD3-enriched entheseal T cells treated in the same conditions showed reduction in TNFα$^+$ and IL-17A$^+$ CD3$^+$ cells after TCR activation when pretreated with upadacitinib (Figure 1C; gating strategy shown in Supplementary Figure S1).

Upadacitinib up-regulating CD14$^+$ entheseal cell IL-23 and TNFα induced via Toll-like receptor activation. Entheseal leukocytes were pretreated with upadacitinib (0.1–10 μM) before stimulation with LPS (10 ng/mL) to evaluate the impact of JAKi on IL-23 and TNF production. Following 24-hour stimulation, IL-23 and TNFα supernatants were measured using ELISA. Upadacitinib addition strongly up-regulated LPS-induced IL-23 and TNFα production, with approximately 10- to 20-fold increased levels observed at 1 μM upadacitinib pretreatment (Figure 2A and B). Because these results showed an increase in cytokine production even at 0.1 μM, we extended the range of upadacitinib down to 100 pM. As shown in Figure 2C and D, the effect is strongest at 1 μM, yet it is still evident at 10 nM.

To determine whether IL-23 and TNFα up-regulation was unique to LPS stimulation, we tested other pathogen-associated molecular patterns and inflammatory cytokines. Zymosan and 1 μM of upadacitinib also further increased IL-23 production (P <

0.01), and a nonsignificant increased trend when stimulated with IL-36γ, demonstrating this effect is beyond LPS (Figure 2E). All stimuli tested that exhibit this effect (Figure 2E) signal via NF-κB suggesting a common mechanism for myeloid cell activation.

We have previously shown entheseal monocytes are important producers of IL-23 following LPS stimulation and therefore performed isolation and depletion of CD14^{+} monocytes from entheseal isolates.[34] As shown in Figure 2F, depletion of CD14^{+} monocytes
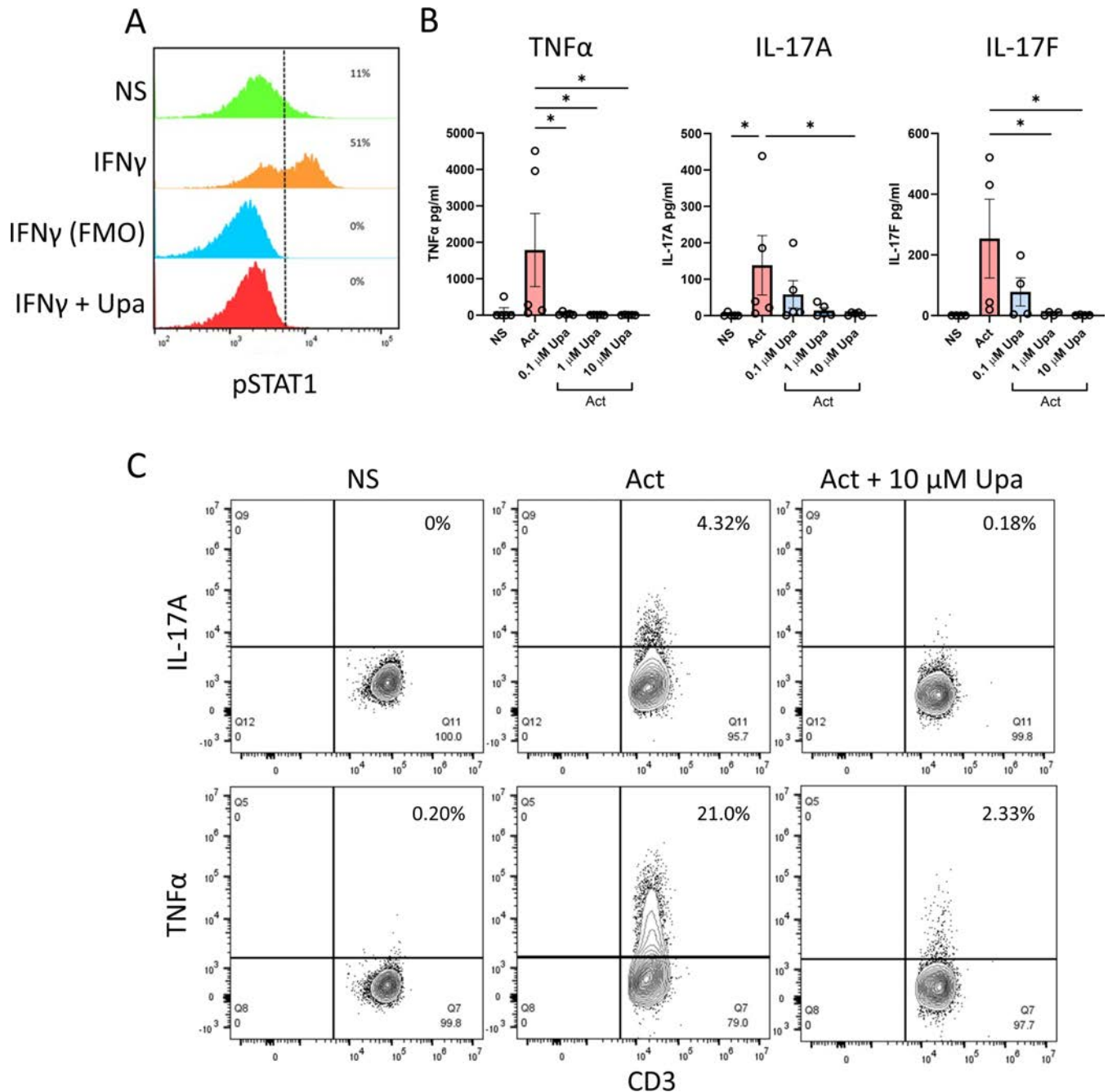

Figure 1. JAK1 inhibition strongly inhibits entheseal T cell activity. (A) Isolated entheseal cells untreated or stimulated with IFNγ (20 ng/mL; 15 minutes) with or without Upa (10 μM) and pSTAT1 measured by flow cytometry. (B) Isolated entheseal cells stimulated with anti-CD3 (1 μg/mL), anti-CD28 (2.5 μg/mL), IL-1β, and IL-23 (25 ng/mL each) for 48 hours for T cell activation with and without indicated concentrations of upadacitinib. Secreted cytokines TNFα (n = 5), IL-17A (n = 5), and IL-17F (n = 4) were measured by enzyme-linked immunosorbent assay. (C) Enriched CD3^{+} entheseal cells were treated as in panel B and analyzed for intracellular IL-17A and TNFα by flow cytometry. Gating strategy is shown in Supplementary Figure S1. Dot plots show CD45^{+}CD3^{+} gated population (gating strategy Supplementary Figure S1). Flow cytometry (A and C) is representative of three independent experiments. *P < 0.05 (statistical test), data are presented as means with SEMs (B). Act, activation; FMO, fluorescence minus one; IFNγ, interferon γ; IL-17A, interleukin 17A; NS, untreated entheseal cells; pSTAT1, phosphorylated STAT1; TNFα, tumor necrosis factor α; Upa, upadacitinib.

ablated the upadacitinib-induced IL-23 level enhancement, and isolated CD14^{+} cells strongly exhibited IL-23 up-regulation after LPS stimulation following pretreatment with upadacitinib (Figure 2F), suggesting that upadacitinib-induced up-regulation of IL-23 and TNFα production was monocyte lineage cells.

Transcriptional analysis implicating IL-10 signaling in JAKi-induced myeloid activation. Given that JAKs are not directly involved in pathogen recognition receptor or IL-1 family receptor signaling pathways, it seems likely that upadacitinib is impacting JAK-dependent secondary responses downstream of myeloid differentiation factor 88 (MyD88) or NF-κB signaling. We therefore leveraged bulk RNA sequencing (RNAseq) to observe transcriptional changes between untreated, LPS-treated, and LPS with upadacitinib-treated entheseal cells to determine how JAKi increased inflammatory myeloid responses. Isolated entheseal leukocytes were treated with LPS with or without 1 μM of upadacitinib for 12 hours to allow for secondary response to cytokines downstream of MyD88/NF-κB signaling before RNA isolation. Bulk RNAseq analysis highlighted increased expression of numerous proinflammatory cytokines following upadacitinib and LPS treatment (Figure 3A), confirming findings observed in Figure 2. *IL23A* (encoding IL-23 p19) was the most significantly up-regulated gene identified with a 10.5-fold increase. Other key genes involved in enthesitis were up-regulated including *CSF2* (encoding granulocyte–macrophage CSF), *IL12B*, *IL6*, and notably *CD80* and *CD83* encoding the M1-associated costimulatory receptors. Numerous IFN-stimulated genes (ISGs) were strongly down-regulated by the addition of upadacitinib (Figure 3A).

KEGG pathway enrichment analysis of upadacitinib-treated samples showed the 20 most significantly enriched pathways (Figure 3B) contained NF-κB, JAK-STAT, and IL-17 signaling pathways in addition to cytokine-cytokine receptor interaction (Figure 3B). GSEA gave normalized enrichment scores of 1.36 (adjusted $P = 0.104$), 1.24 (adjusted $P = 0.281$), 1.51 (adjusted $P = 0.102$), and 1.41 (adjusted $P = 0.104$), respectively, for each pathway (Figure 3C). Transcript levels for NF-κB core enriched genes signaling pathways showed increased expression of inflammatory mediators and NF-κB signaling components following upadacitinib and LPS treatment, suggesting JAK1/JAK2 inhibition may result in loss of negative regulation of NF-κB signaling (Figure 3C).

The role of NF-κB in driving the upadacitinib-induced increase in IL-23 was investigated using both THP-1 monocytic cell line (n = 3) and peripheral blood leukocytes (n = 6). Although THP-1 cells did not show as strong of an LPS plus upadacitinib-dependent effect as primary cells, increased TNFα secretion when pretreated with upadacitinib was evident (Supplementary Figure S2A). An increase in NF-κB activity via an NF-κB–driven luciferase reporter with upadacitinib was noted (Supplementary Figure S2C). Furthermore, NF-κB inhibition in peripheral blood leukocytes treated with a specific NF-κB inhibitor caffeic acid

phenethyl ester three hours after LPS stimulation significantly reduced secretion of IL-23 in cells pretreated with upadacitinib (Supplementary Figure S3).

The anti-inflammatory cytokine IL-10 is a major regulator of NF-κB signaling via JAK1/Tyk2 signaling, and previous reports have shown JAK1 inhibition of IL-10 signaling may increase peripheral blood myeloid cell activity.[35] Examination of our RNA-seq data showed many IL-10–induced regulators of NF-κB activity were down-regulated in the LPS with upadacitinib condition including suppressor of cytokine signaling 1 (SOCS1), SOCS3, strawberry notch homolog 2, and TNFAIP3 interacting protein 3 (TNIP3) (Figure 3D).

A recent transcriptomics report by Aschenbrenner et al[36] identified IL-10 as a key IL-23 regulator in the gut. The authors treated monocytes with LPS with or without an IL-10R–blocking antibody and used transcriptomics to identify key IL-10 regulated genes. Examining the expression IL-10–regulated genes in our data set compared to the data set from Aschenbrenner et al[36] revealed a similar expression patterns with a few notable exceptions (Figure 3E). Of the 52 genes identified as significantly regulated by IL-10 blockade in the data set from Aschenbrenner et al,[36] 30 genes were regulated in the same direction by upadacitinib in our data set, whereas only 4 genes were oppositely regulated, suggesting a considerable amount of overlap in data sets of LPS with IL-10 blockade and LPS with upadacitinib (Figure 3E). Those genes regulated in the opposite direction as in the data set from Aschenbrenner et al[36] (*GBP1*, *GBP4* [encoding guanylate binding protein 1 and 4 respectively], *CXCL9*, and *CXCL10*) are known ISGs and would therefore be expected to be down-regulated by JAK1 inhibition.

Interrupted IL-10 signaling as a primary driver of JAKi-induced entheseal myeloid cell activation. To assess the role of upadacitinib-induced IL-10 blockade in inducing increased myeloid activity, we treated entheseal cells with an IL-10R–neutralizing antibody before stimulation with LPS and compared secretion of IL-23 to that induced by pretreatment with upadacitinib. The addition of an IL-10R–neutralizing antibody increased secretion of IL-23 in a dose-dependent manner (Figure 4A). Conversely, addition of increasing concentrations of recombinant human IL-10 (1–100 ng/mL) to LPS-stimulated cells pretreated with a low dose of upadacitinib (10 nM) reduced secretion of IL-23 (Figure 4B). Intriguingly, blockade of IL-10 signaling did not replicate the same levels of upadacitinib-induced IL-23 and showed a larger impact in peripheral blood cells than in entheseal cells. A total of 25 μg/mL of IL-10Rα blocking antibody increased IL-23 secretion to 50% of that induced by upadacitinib addition in peripheral blood leukocytes, yet only achieved 25% of upadacitinib-induced IL-23 in donor-matched PEB leukocytes, suggesting other mechanisms play a role in the observed upadacitinib-induced inflammation (Figure 4C).
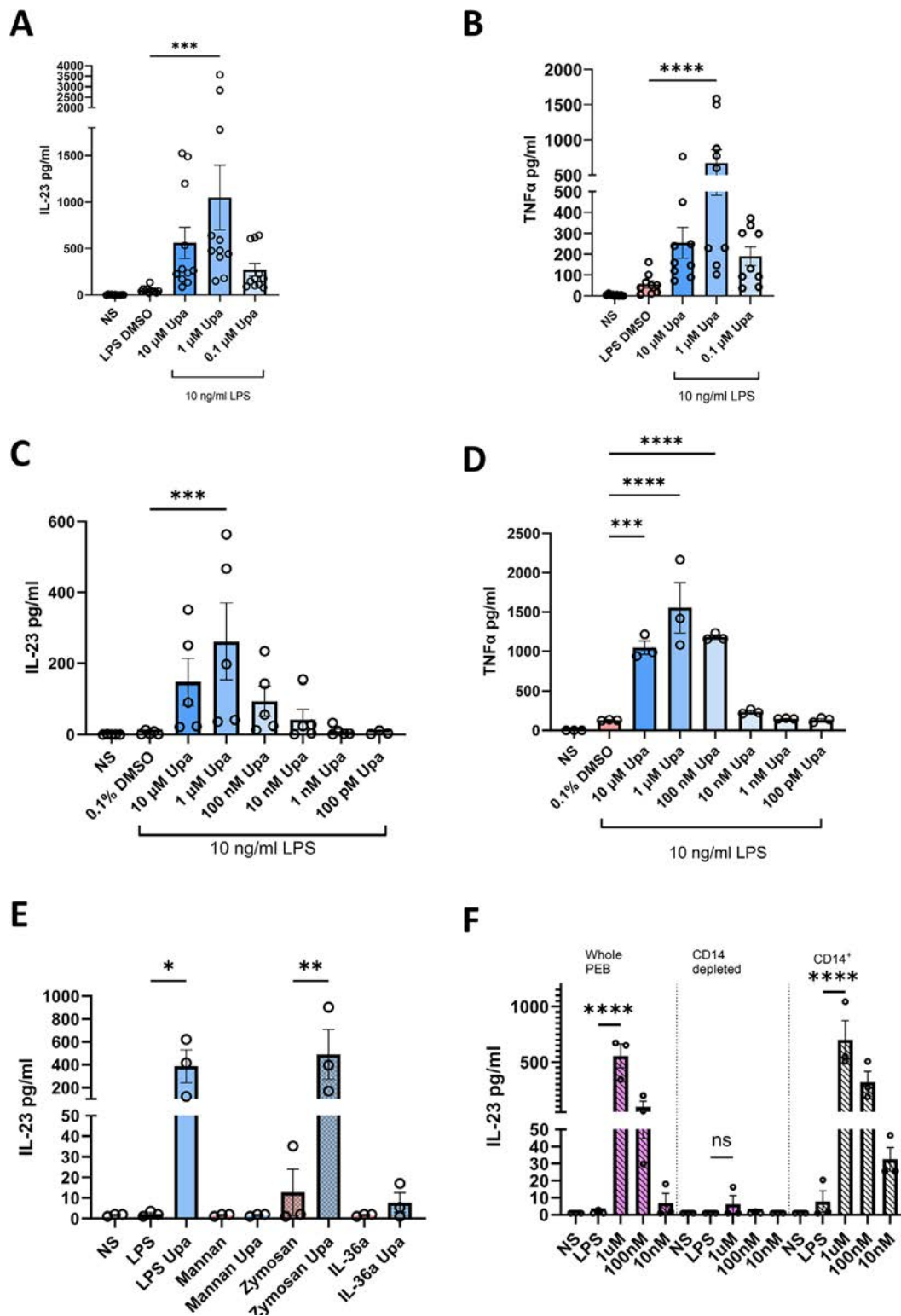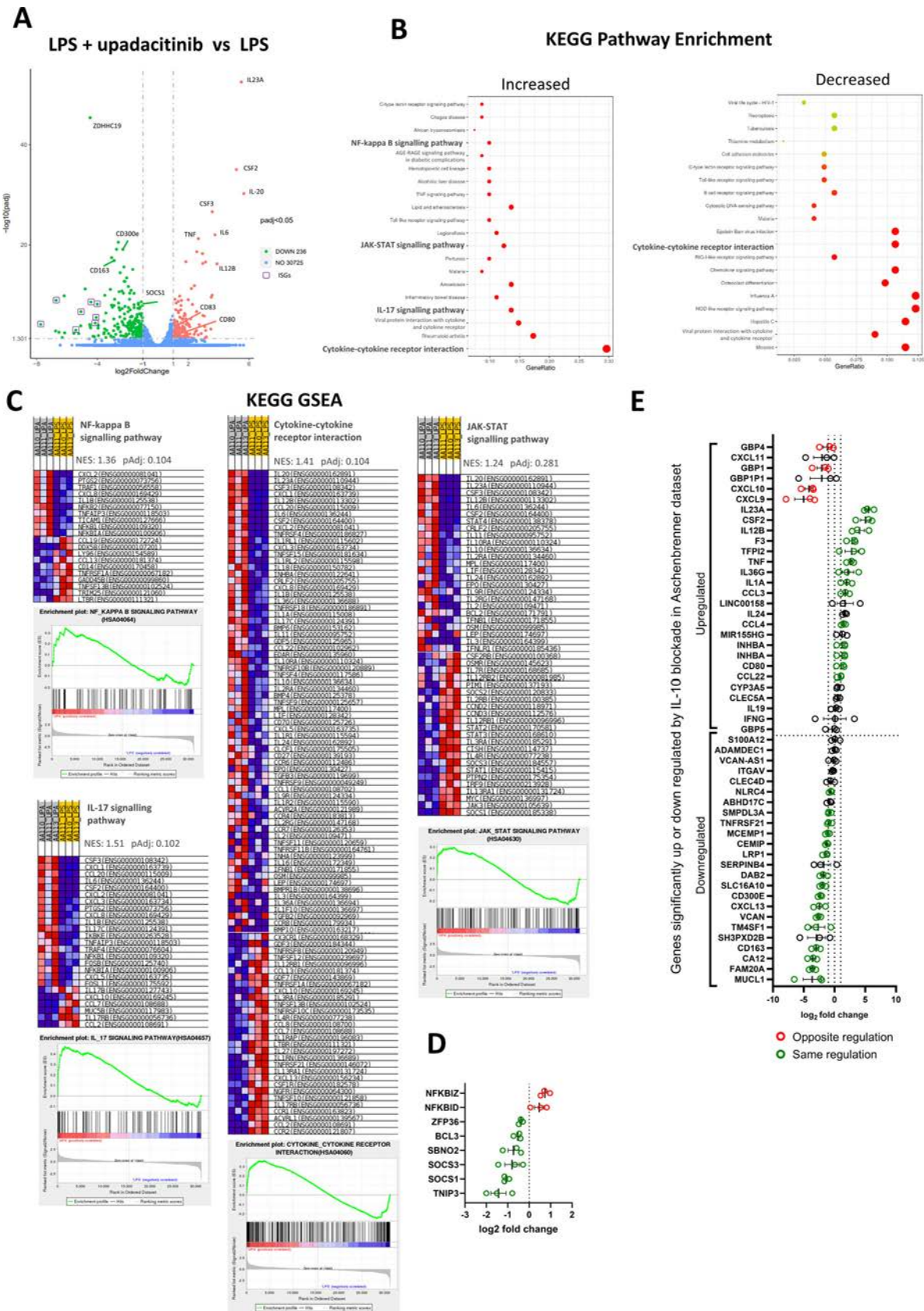
Figure 2. JAK1 inhibition increases NF-κB–driven IL-23 and TNFα from CD14⁺ entheseal cells. Entheseal cells untreated or stimulated with LPS (10 ng/mL) with an indicated concentration of Upa for 24 hours and (A and C) IL-23 and (B and D) TNFα measured by enzyme-linked immunosorbent assay (ELISA). (E) Entheseal cells stimulated with LPS, mannan, zymosan, IL-1β, IL-36α with and without 1 μ*M* Upa, and IL-23 measured by ELISA. (F) Peripheral blood leukocytes, CD14⁺ depleted peripheral blood leukocytes, or isolated CD14⁺ cells were treated with 10 ng/mL LPS with or without Upa. Figures are representative of (A) 11, (B) 9, (C) 5, or (D–E) 3 independent experiments. *P < 0.05, **P < 0.01, ***P < 0.001, ****P < 0.0001 (statistical test). Data are presented as means with SEMs. IL-23, interleukin 23; LPS, lipopolysaccharide; NS, untreated entheseal cells; PEB, peri-entheseal bone; TNFα, tumor necrosis factor α; Upa, upadacitinib. Color figure can be viewed in the online issue, which is available at http://onlinelibrary.wiley.com/doi/10.1002/art.43210/abstract.

Figure 3. Legend on next page.

Although RNAseq data implicated IL-19 signaling as an up-regulated anti-inflammatory pathway following LPS stimulation (Supplementary Figure S4), blockade of IL-19 did not impact IL-23 levels (Figure 4D). Similarly, RNAseq data highlighted a down-regulation of ISGs known to regulate MyD88 and NF-κB driven pathways following upadacitinib addition; however, type I IFN receptor blockade did not impact IL-23 production (Figure 4D).

JAK1/Tyk2 pathway importance in driving JAKi-induced myeloid inflammation. These results suggest that increased IL-23 and other proinflammatory mediator secretion following addition of upadacitinib to LPS-stimulated cells is largely dependent on IL-10 signaling, and therefore JAK1/Tyk2 pathways. Therefore, we tested whether the upadacitinib-induced increase in IL-23 can be replicated by the use of a Tyk2 inhibitor and avoided selective JAK3 inhibition. PEB isolated cells were pretreated with pharmacologically relevant concentrations of either deucravacitinib (Tyk2 inhibitor) or ritlecitinib (JAK3 inhibitor) before stimulation with LPS. Addition of deucravacitinib to LPS-treated PEB cells strongly induced IL-23 (Figure 4E) and TNFα (Figure 4F) secretion in analogy to upadacitinib-treated cells. In contrast, ritlecitinib had no significant impact on either IL-23 or TNFα secretion, indicating the disrupted negative feedback loop is JAK1/Tyk2-dependent further implicating IL-10 signaling (Figure 4E and F).
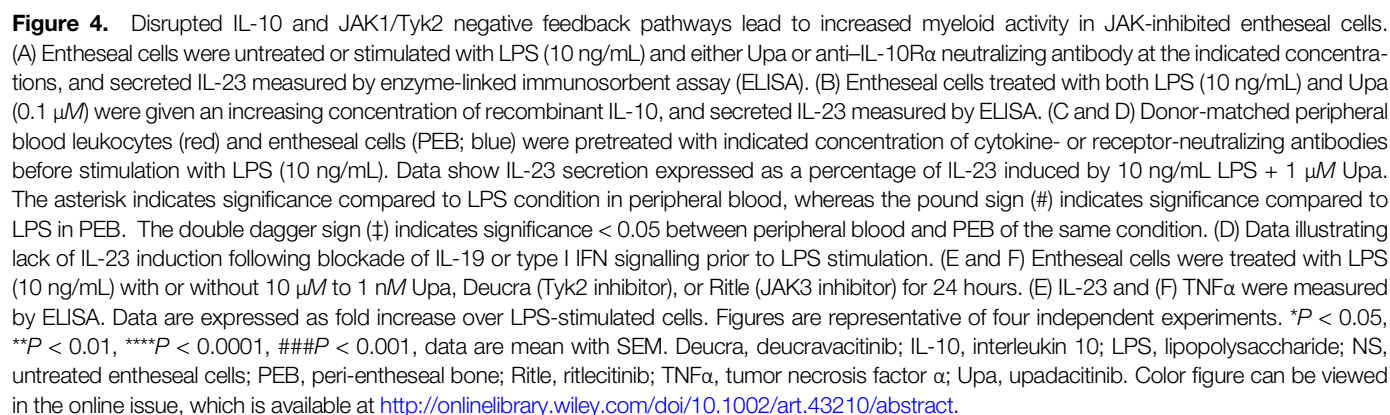
Upadacitinib promoting M1 development in LPS-activated entheseal monocytes. In addition to highlighting the importance of JAK1/TYK2 signaling in controlling IL-23 production, our RNAseq data showed the upadacitinib with LPS group had reduced expression of several M2-associated genes compared to the LPS-treated group. Previous work has also suggested JAKi can promote M1 development in peripheral blood mononuclear cells.[37] We therefore explored whether upadacitinib treatment favored the development of entheseal M1 phenotype monocytes.

LPS-stimulated PEB cells pretreated with upadacitinib for 24 hours were cytometrically analyzed for monocyte CD163, CD209, and CD80 expression. Reduced CD163 and CD209 expressions and increased CD80 expression were noted compared to LPS stimulation alone (Figure 5A and B), indicating that upadacitinib promoted M1 phenotype.

JAK mediating T cell inhibition retained in face of JAK-mediated increased myeloid activity. Our results indicated upadacitinib activated and promoted the production of critical SpA-driving cytokines from entheseal myeloid cells. Furthermore, KEGG pathway enrichment analysis of upadacitinib-treated, LPS-stimulated cells highlighted the IL-17 signaling pathway as one of the most significantly enriched pathways (Figure 3B and C), suggesting an increased potential to drive pathologic T cell responses. These observations, however, are at odds with the clinical observation and aforementioned findings (Figure 1) that upadacitinib is an effective therapeutic in enthesitis and SpA disease. Therefore, we tested whether upadacitinib remains an effective inhibitor of T cell activity in the context of LPS and JAKi-induced increased myeloid activity.

Isolated entheseal cells were stimulated with both LPS and anti-CD3 for 48 hours to activate both myeloid and lymphoid compartments, with or without upadacitinib pretreatment. Anti-CD28 was not used to capture the effect of the myeloid-dependent costimulatory signal. Supernatants were collected and measured for IL-23, IL-6, TNFα, IL-17A, IL-17F, and IL-22. Despite the observation that the addition of upadacitinib, again, increased Th17-driving cytokines and proinflammatory cytokines when stimulated with LPS, T cell–derived IL-17A, IL-17F, and IL-22 induced by LPS with anti-CD3 remained significantly down-regulated when pretreated with upadacitinib (Figure 6A–F) indicating that upadacitinib effectively prevented type-17 T cell activation in the face of LPS-mediated increased myeloid entheseal immune cells activation.

Figure 3. RNA sequencing (RNAseq) highlights extensive innate immune activity and indicates disrupted negative feedback. (A) Volcano plot displaying differentially expressed genes from RNAseq data between entheseal cells treated with LPS (10 ng/mL) and upadacitinib (Upa) (1 μM) and entheseal cells treated with LPS alone for 12 hours. Genes of interest and interferon stimulated genes are annotated. Green indicates down-regulated in LPS + Upa versus LPS alone. Red indicates up-regulated in LPS + Upa versus LPS alone. (B) Dot plots of 20 most significantly up-regulated and down-regulated KEGG pathways enriched in LPS + Upa condition vs LPS alone. Dot size indicates counts of genes enriched in the pathway; color indicates significance. Pathways of interest are emboldened. (C) GSEA of KEGG pathways of interest highlighted in B showing normalized enrichment scores, expression heatmaps for leading edge genes in the gene set, and GSEA plots. (D) Log2 fold-change in genes known to regulate NF-κB activity. Green indicates down-regulated in LPS + Upa versus LPS alone. Red indicates up-regulated in LPS + Upa versus LPS alone. (E) Comparison of Log2 fold-change in gene expression of our LPS + Upa versus LPS alone data set to a gene set of significantly regulated genes identified by Aschenbrenner et al[36] comparing LPS + IL-10R blockade to LPS alone. Colored points signify genes are significantly differentially expressed (adjusted $P < 0.05$). Green points indicate genes are regulated in the same direction in both our data set and the data set from Aschenbrenner et al[36]; red points indicate genes are regulated in the opposite direction in each data set. Data are representative of three independent experiments. Adjusted P values calculated using Benjamin and Hochberg's approach. GSEA, gene set enrichment analysis; IL-10R, interleukin 10R; KEGG, Kyoto Encyclopedia of Genes and Genomes; LPS, lipopolysaccharide; *NFKBIZ*, NF-κB inhibitor zeta; *SBNO2*, Strawberry notch homolog 2; *SOCS1*, suppressor of cytokine signaling 1; Upa, upadacitinib; *ZFP36*, zinc-finger protein 36. Color figure can be viewed in the online issue, which is available at http://onlinelibrary.wiley.com/doi/10.1002/art.43210/abstract.

Figure 4. Disrupted IL-10 and JAK1/Tyk2 negative feedback pathways lead to increased myeloid activity in JAK-inhibited entheseal cells. (A) Entheseal cells were untreated or stimulated with LPS (10 ng/mL) and either Upa or anti–IL-10Rα neutralizing antibody at the indicated concentrations, and secreted IL-23 measured by enzyme-linked immunosorbent assay (ELISA). (B) Entheseal cells treated with both LPS (10 ng/mL) and Upa (0.1 μ*M*) were given an increasing concentration of recombinant IL-10, and secreted IL-23 measured by ELISA. (C and D) Donor-matched peripheral blood leukocytes (red) and entheseal cells (PEB; blue) were pretreated with indicated concentration of cytokine- or receptor-neutralizing antibodies before stimulation with LPS (10 ng/mL). Data show IL-23 secretion expressed as a percentage of IL-23 induced by 10 ng/mL LPS + 1 μ*M* Upa. The asterisk indicates significance compared to LPS condition in peripheral blood, whereas the pound sign (#) indicates significance compared to LPS in PEB. The double dagger sign (‡) indicates significance < 0.05 between peripheral blood and PEB of the same condition. (D) Data illustrating lack of IL-23 induction following blockade of IL-19 or type I IFN signalling prior to LPS stimulation. (E and F) Entheseal cells were treated with LPS (10 ng/mL) with or without 10 μ*M* to 1 n*M* Upa, Deucra (Tyk2 inhibitor), or Ritle (JAK3 inhibitor) for 24 hours. (E) IL-23 and (F) TNFα were measured by ELISA. Data are expressed as fold increase over LPS-stimulated cells. Figures are representative of four independent experiments. *$P < 0.05$, **$P < 0.01$, ****$P < 0.0001$, ###$P < 0.001$, data are mean with SEM. Deucra, deucravacitinib; IL-10, interleukin 10; LPS, lipopolysaccharide; NS, untreated entheseal cells; PEB, peri-entheseal bone; Ritle, ritlecitinib; TNFα, tumor necrosis factor α; Upa, upadacitinib. Color figure can be viewed in the online issue, which is available at http://onlinelibrary.wiley.com/doi/10.1002/art.43210/abstract.

DISCUSSION

Several cytokine-targeted therapies have shown variable efficacy in AS and other SpA domains.[38,39] For example, despite efficacy in axial and peripheral SpA, anti–IL-17A therapy is not effective in IBD.[40] Another example is anti–IL-23 therapy, which is very effective in treating psoriasis and peripheral arthritis but was inefficacious in AS.[41] Although JAKi blocks a multitude of cytokines either directly or indirectly, a Tyk2 inhibitor that antagonizes the IL-23 pathway has failed in UC.[21] In the present work, we offer a molecular explanation for why JAKi may not be a panacea for SpA spectrum disorders, namely in innate immune-driven inflammation that typically occurs in the intestine in SpA and IBD.

Although IL-10 antagonism is not an issue for skeletal immunobiology, it may be very important for intestinal immunobiology because humans with loss-of-function mutations in IL-10 or the IL-10R are prone to early onset IBD,[22] and IL-10 single-nucleotide polymorphisms are also linked to IBD.[42] Blockade of IL-10 by the Tyk2 class of drugs may thus not be beneficial in the intestinal environment, whereas the broader immune inhibition afforded by upadacitinib may protect against this effect in vivo in humans, perhaps via an effect on the common γ chain cytokine receptor that strongly regulates both innate and adaptive T cells.[43] Our findings suggest that SpA spectrum disorders that are immunologically heterogeneous with predominant innate immune involvement may respond less well to JAKi therapy. In that regard, CD is
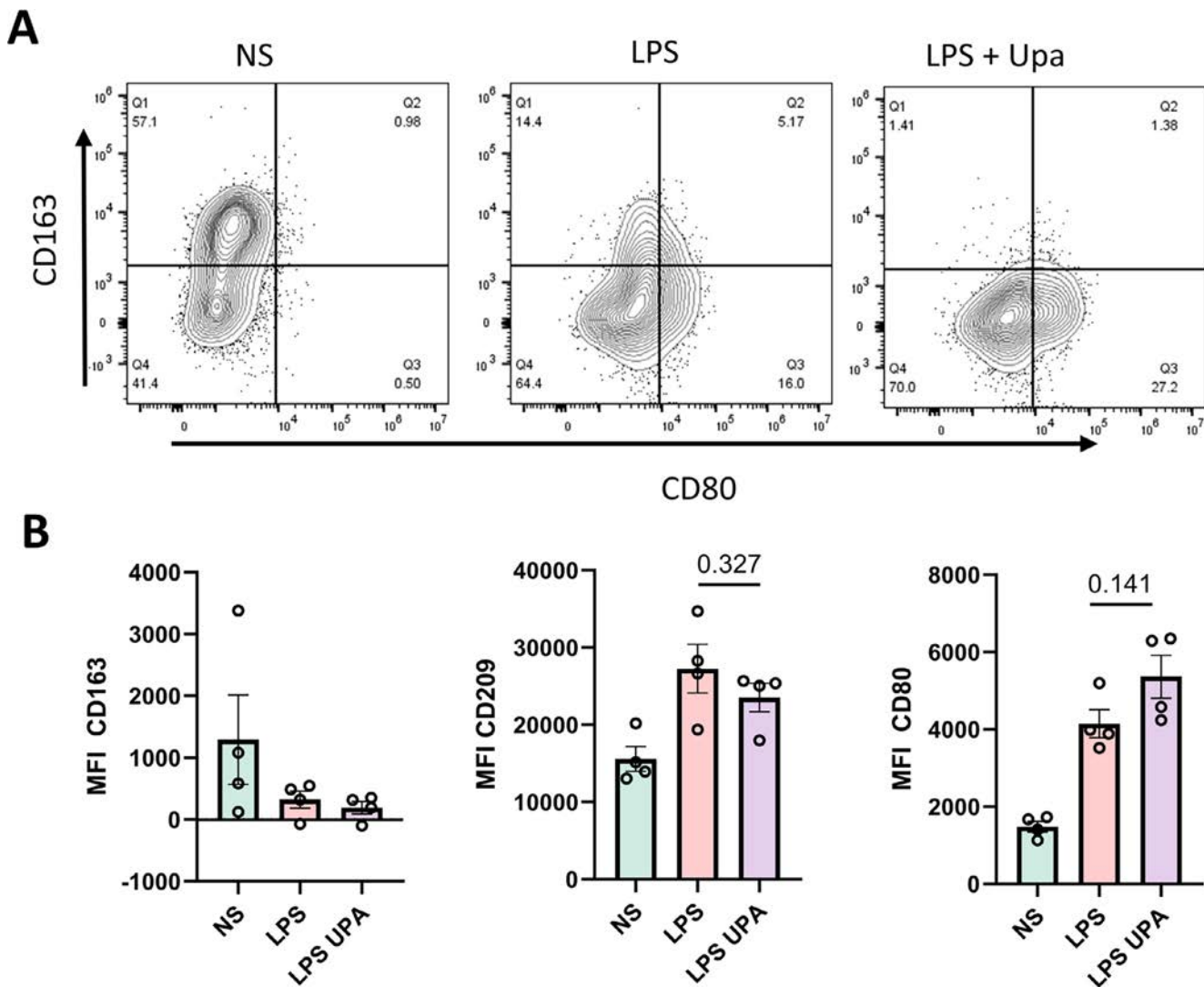
Figure 5. JAK1 inhibition favors M1 phenotype development in entheseal monocytes. (A) Expression of CD163, CD80, and CD209 in entheseal CD14$^+$ monocytes (CD45$^+$CD3$^-$CD19$^-$CD14$^+$HLA-DR$^+$). Entheseal cells were stimulated with LPS (10 ng/mL) with or without Upa (1 μ*M*) for 24 hours and expression of M1-phenotype marker (CD80) and M2-phenotype markers (CD163 and CD209) were assessed by (A and B) flow cytometry. Gating strategy is shown in Supplementary Figure S1. (B) MFI was calculated for quantification of expression levels. *P* values are displayed on figures. Figures are representative of four independent experiments. Data are presented as means with SEMs. LPS, lipopolysaccharide; MFI, median fluorescence intensity; NS, untreated entheseal cells; Upa, upadacitinib. Color figure can be viewed in the online issue, which is available at http://onlinelibrary.wiley.com/doi/10.1002/art.43210/abstract.
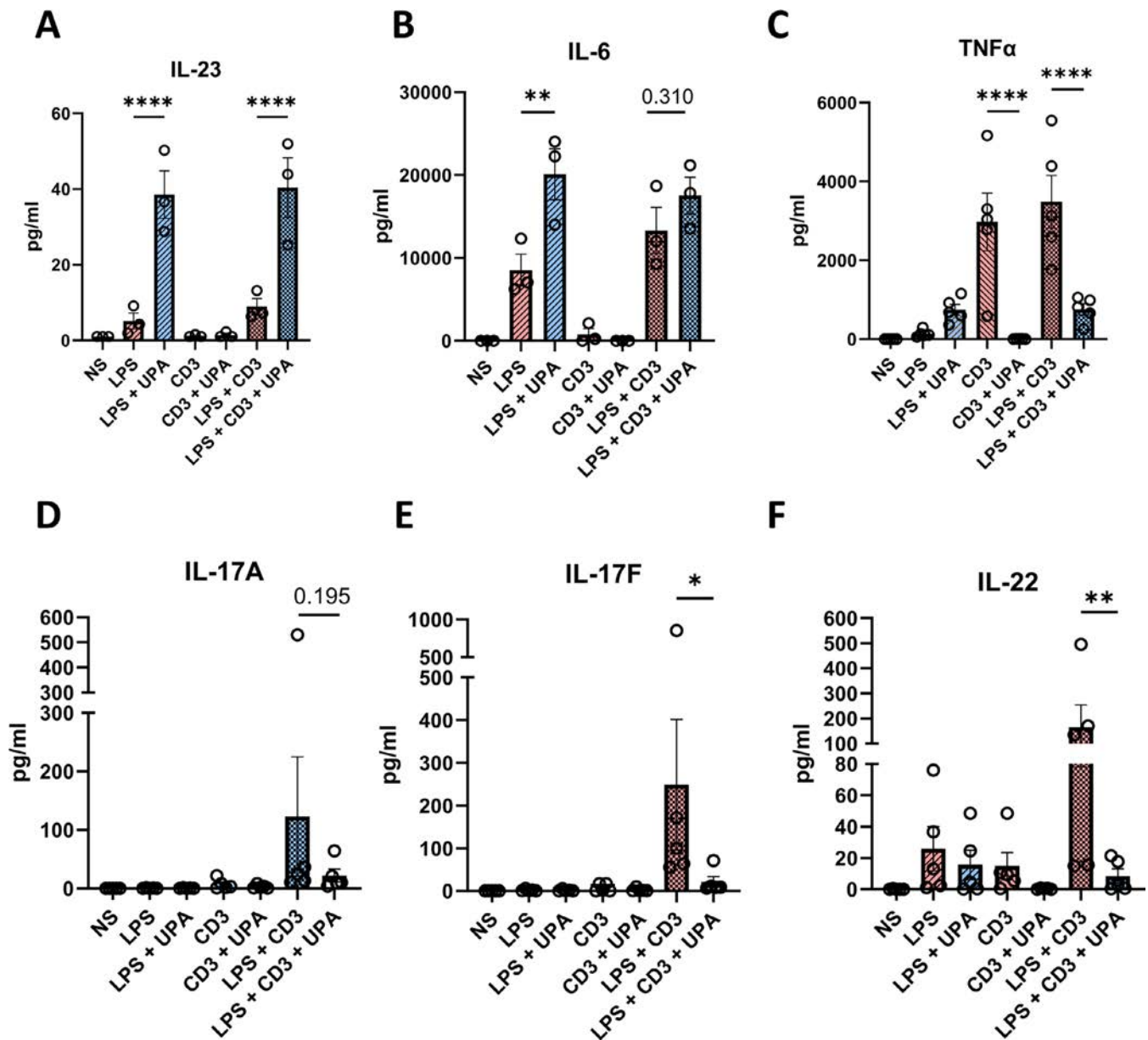
Figure 6. JAK1 inhibition blocks type-17 cytokine production despite increased myeloid-derived Th17-driving cytokines. Entheseal cells treated with LPS (10 ng/mL) with or without Upa (1 μM), anti-CD3 (CD3) with or without upadacitinib, or LPS + anti-CD3 with and without Upa for 48 hours. Secreted (A) IL-23, (B) IL-6, (C) TNFα, (D) IL-17A, (E) IL-17F, and (F) IL-22 were measured by bead-based immunoassays. Figures are representative of three (A and B) and five (C–F) independent experiments. *$P < 0.05$, **$P < 0.01$, **$P < 0.001$, ****$P < 0.0001$. Data are presented as means with SEMs. IL-23, interleukin 23; LPS, lipopolysaccharide; NS, untreated entheseal cells; TNFα, tumor necrosis factor α; Upa, upadacitinib. Color figure can be viewed in the online issue, which is available at http://onlinelibrary.wiley.com/doi/10.1002/art.43210/abstract.

strongly linked to innate immunity and barrier dysfunction via the nucleotide-binding oligomerization domain–containing protein 2 (NOD2) pattern recognition receptor (primarily expressed by monocytes) along with other genes associated with innate immune-driven inflammation.[44,45] Furthermore, patients with IBD have weaker major histocompatibility complex class I (MHC-I) associations compared to the SpA spectrum disorders, but the magnitude of MHC-I associations is greater in

UC than in CD.[46,47] The efficacy of drugs that impact T cell function, such as cyclosporine and vedolizumab, is much greater in UC than CD, implying stronger population level T cell dysregulation in UC.[48] In the light of our findings on LPS and JAKi-mediated activation of myeloid cells, it is possible the lack of robust and consistent JAKi efficacy in CD may represent the failure to suppress a more innate immune-centered pathology.

The enthesis is the key target tissue in SpA and PsA and the normal enthesis has a resident immune cell population in both the soft tissue immediately adjacent to the fibrocartilage and the anchoring bone. Emergent translational immunology suggests that pan-JAKi, JAK1 inhibition, or Tyk2 inhibition works for SpA-related arthropathy, and our current findings suggest that JAKi blocked entheseal lymphocytes key proinflammatory cytokines including TNFα, IL-17A, and IL-17F in keeping with the known robust efficacy of JAKi in SpA-related arthropathy.[4,8]

However, conversely, entheseal myeloid cell activation increased in LPS-stimulated macrophage populations treated with JAKi. Yet, despite the increased activation, JAK-mediated lymphocyte function suppression was unaffected. Given the importance of the IL-23 pathway in the SpA-related diseases with its abundant entheseal and intestinal myeloid cell production, our findings suggest the efficacy of JAKi in SpA is mediated via the adaptive immune system in the face of potential increased activity within the myeloid compartment. This appears to be clinically relevant in the context of Tyk2 inhibition that has failed in UC (thus far reported in a press release).[21]

Our findings at first glance seem counterintuitive, in other words, why would the elevation of several myeloid-related cytokines be associated with good arthritis disease control? As shown in the summary schematic diagram of the mechanisms at play (see the graphical abstract), we traced such cytokine elevations to entheseal myeloid cell IL-10 pathway inhibition and subsequent failure to initiate negative feedback to control drivers of proinflammatory cytokine production such as NF-κB. Indeed, IL-10–specific blockade emulated the results seen in upadacitinib-treated cells and specific inhibition of NF-κB three hours after stimulation with LPS in peripheral blood leukocytes that had been pretreated with upadacitinib significantly reduced the secretion of IL-23 (Supplementary Figure S3). The importance of paracrine IL-10 in controlling gut monocyte IL-23 expression has been reported previously by Aschenbrenner et al,[36] and the transcriptional changes measured in cells treated with LPS and anti–IL-10Rα antibody closely resembles that of entheseal cells treated with LPS and upadacitinib in our work (Figure 3C). Although they did not elucidate the mechanisms by which IL-10 induced the negative feedback, we noted a decrease in the expression of several IL-10-regulated genes known to regulate NF-κB activity, most notably SOCS1 and SOCS3 (Figure 3D); however, further work is required to understand their impact on entheseal monocyte-derived IL-23.

Previous studies have shown that blood myeloid cell JAKi was associated with increased cytokine production.[35,37,49] Although strongly IL-10–dependent, blockade of IL-10 did not completely replicate the increased levels of cytokines observed by upadacitinib addition. This may, in part, be due to the high receptor density of IL-10R on human monocytes, making complete inhibition of signaling using receptor-specific antibodies challenging.[50] This difference was particularly notable in the entheseal leukocytes compared to peripheral blood, in which IL-23 was only up-regulated to 25% of

upadacitinib-induced levels versus 50% in blood by blockade of IL-10 (Figure 4C). The failure of JAK3 inhibition to replicate the observed increases in IL-23 and TNFα following JAK1 and Tyk2 inhibition strongly implicates JAK1/Tyk2 pathways in this mechanism, yet blockade of IFN signaling and IL-19 (both implicated in transcriptomic data) did not impact cytokine production (Figure 4D). These results suggest, in addition to IL-10, other unknown mechanisms are also contributing to the observed increase in proinflammatory cytokines and may be more important in entheseal biology than in peripheral blood.

One of the study's limitations is that upadacitinib also has efficacy against JAK2 signaling. We were unable to rule out JAK2 involvement because of the lack of highly specific JAK2 inhibitors, therefore the observed effect of using upadacitinib and deucravacitinib may not only be due to a JAK1/Tyk2-dependent manner but also may involve JAK2 signaling. Although previous work has suggested JAK3 inhibition to promote myeloid production of proinflammatory cytokines,[49] these experiments were performed with low-dose tofacitinib, which is now known not to be JAK3 specific. Furthermore, in our hands, addition of the highly selective JAK3 inhibitor ritlecitinib to LPS-stimulated entheseal cells did not promote secretion of SpA-driving cytokines, namely IL-23 or TNFα. Interestingly, TNFα, which is produced by both myeloid and T cells, was up-regulated by addition of upadacitinib to LPS-treated cells, yet only to approximately 25% of the output induced from T cells by TCR activation alone. Furthermore, as previously observed, the addition of upadacitinib to TCR-activated T cells completely ablated TNFα production. Yet, when cells are stimulated with both LPS and anti-CD3 and pretreated with upadacitinib, TNFα can only be reduced to the levels observed in LPS- and upadacitinib-treated myeloid cells, indicating that upadacitinib may independently increase myeloid cells TNFα production while also inhibiting T cell TNFα production, with these findings pointing to a key role of conventional T cells in vivo in SpA pathogenesis rather than TNFα from other sources.

In conclusion, JAKi in an in vitro enthesitis model system was associated with disparate impacts of the myeloid and lymphoid compartments and suggested that although upadacitinib effectively blocked the adaptive immune system, LPS-mediated innate immunity was preserved or even up-regulated following JAKi. Given the pervasive gut barrier dysfunction in SpA, bacterial molecules including LPS seem clinically relevant. Given the immunologic heterogeneity in SpA spectrum disorders and allied conditions, these findings provide a map toward therapy in SpA spectrum disease and why JAKi, especially with Tyk2 blockade in IBD, may not be a SpA disease spectrum panacea. In essence, the blockade of IL-10 by JAKi, especially Tyk2 inhibition, may lead to a differential effect of therapy across SpA spectrum joint and intestinal disease. One limitation of our work is the lack of data from IBD tissues, but the work from Aschenbrenner et al[36] strongly demonstrates the importance of IL-10 in the control of IL-23 in gut monocytes, which suggests identical mechanism are also operational in IBD. Additionally, genome-wide association studies

clearly show the importance of innate immune dysregulation in CD.[45] Our findings offer an explanation as to why Tyk2 antagonism and potential detrimental impacts on IL-10 signaling may account for divergent therapy landscape between intestinal and skeletal immunotherapy under the more restricted cytokine antagonism via Tyk2 blockade compared to other JAKs.

ACKNOWLEDGMENTS

AUTHOR CONTRIBUTIONS

All authors contributed to at least one of the following manuscript preparation roles: conceptualization AND/OR methodology, software, investigation, formal analysis, data curation, visualization, and validation AND drafting or reviewing/editing the final draft. As corresponding author, Dr McGonagle confirms that all authors have provided the final approval of the version to be published and takes responsibility for the affirmations regarding article submission (eg, not under consideration by another journal), the integrity of the data presented, and the statements regarding compliance with institutional review board/Declaration of Helsinki requirements.

ROLE OF THE STUDY SPONSOR

AbbVie Inc had no role in the study design or in the collection, analysis, or interpretation of the data, the writing of the manuscript, or the decision to submit the manuscript for publication. Publication of this article was not contingent upon approval by AbbVie Inc.

REFERENCES

1. Sherlock JP, Joyce-Shaikh B, Turner SP, et al. IL-23 induces spondyloarthropathy by acting on ROR-γt+ CD3+CD4–CD8– entheseal resident T cells. Nat Med 2012;18(7):1069–1076.
2. Bridgewood C, Sharif K, Sherlock J, et al. Interleukin-23 pathway at the enthesis: the emerging story of enthesitis in spondyloarthropathy. Immunol Rev 2020;294(1):27–47.
3. Russell T, Bridgewood C, Rowe H, et al. Cytokine "fine tuning" of enthesis tissue homeostasis as a pointer to spondyloarthritis pathogenesis with a focus on relevant TNF and IL-17 targeted therapies. Semin Immunopathol 2021;43(2):193–206.
4. McInnes IB, Szekanecz Z, McGonagle D, et al. A review of JAK-STAT signalling in the pathogenesis of spondyloarthritis and the role of JAK inhibition. Rheumatology (Oxford) 2021;61(5):1783–1794.
5. Hu X, Li J, Fu M, et al. The JAK/STAT signaling pathway: from bench to clinic. Signal Transduct Target Ther 2021;6(1):402.
6. McGonagle D, Tan AL, Watad A, et al. Pathophysiology, assessment and treatment of psoriatic dactylitis. Nat Rev Rheumatol 2019;15(2):113–122.
7. Schett G, Lories RJ, D'Agostino MA, et al. Enthesitis: from pathophysiology to treatment. Nat Rev Rheumatol 2017;13(12):731–741.
8. Fouser LA, Wright JF, Dunussi-Joannopoulos K, et al. Th17 cytokines and their emerging roles in inflammation and autoimmunity. Immunol Rev 2008;226(1):87–102.
9. Kubo S, Nakayamada S, Sakata K, et al. Janus kinase inhibitor baricitinib modulates human innate and adaptive immune system. Front Immunol 2018;9:1510.
10. McInnes IB, Byers NL, Higgs RE, et al. Comparison of baricitinib, upadacitinib, and tofacitinib mediated regulation of cytokine signaling in human leukocyte subpopulations. Arthritis Res Ther 2019;21(1):183.
11. Kubo S, Yamaoka K, Kondo M, et al. The JAK inhibitor, tofacitinib, reduces the T cell stimulatory capacity of human monocyte-derived dendritic cells. Ann Rheum Dis 2014;73(12):2192–2198.
12. Traves PG, Murray B, Campigotto F, et al. JAK selectivity and the implications for clinical inhibition of pharmacodynamic cytokine signalling by filgotinib, upadacitinib, tofacitinib and baricitinib. Ann Rheum Dis 2021;80(7):865–875.
13. Virtanen A, Palmroth M, Liukkonen S, et al. Differences in JAK isoform selectivity among different types of JAK inhibitors evaluated for rheumatic diseases through in vitro profiling. Arthritis Rheumatol 2023;75(11):2054–2061.
14. Parmentier JM, Voss J, Graff C, et al. In vitro and in vivo characterization of the JAK1 selectivity of upadacitinib (ABT-494). BMC Rheumatol 2018;2(1):23.
15. Bouwmeester T, Bauch A, Ruffner H, et al. A physical and functional map of the human TNF-α/NF-kappa B signal transduction pathway. Nat Cell Biol 2004;6(2):97–105.
16. Gravallese EM, Schett G. Effects of the IL-23-IL-17 pathway on bone in spondyloarthritis. Nat Rev Rheumatol 2018;14(11):631–640.
17. Parham C, Chirica M, Timans J, et al. A receptor for the heterodimeric cytokine IL-23 is composed of IL-12Rbeta1 and a novel cytokine receptor subunit, IL-23R. J Immunol 2002;168(11):5699–5708.
18. Teng MWL, Bowman EP, McElwee JJ, et al. IL-12 and IL-23 cytokines: from discovery to targeted therapies for immune-mediated inflammatory diseases. Nat Med 2015;21(7):719–729.
19. Tanaka Y, Luo Y, O'Shea JJ, et al. Janus kinase-targeting therapies in rheumatology: a mechanisms-based approach. Nat Rev Rheumatol 2022;18(3):133–145.
20. Panés J, Sandborn WJ, Schreiber S, et al. Tofacitinib for induction and maintenance therapy of Crohn's disease: results of two phase IIb randomised placebo-controlled trials. Gut 2017;66(6):1049–1059.
21. Danese S, Panaccione R, D'Haens G, et al. DOP42 Efficacy and safety of deucravacitinib, an oral, selective tyrosine kinase 2 inhibitor, in patients with moderately-to-severely active ulcerative colitis: 12-week results from the phase 2 LATTICE-UC study. J Crohns Colitis 2022;16(suppl 1):i091–i092.
22. Sharifinejad N, Zaki-Dizaji M, Sepahvandi R, et al. The clinical, molecular, and therapeutic features of patients with IL10/IL10R deficiency: a systematic review. Clin Exp Immunol 2022;208(3):281–291.
23. Finbloom DS, Winestock KD. IL-10 induces the tyrosine phosphorylation of tyk2 and Jak1 and the differential assembly of STAT1 alpha and STAT3 complexes in human T cells and monocytes. J Immunol 1995;155(3):1079–1090.
24. Chimalakonda A, Burke J, Cheng L, et al. Selectivity profile of the tyrosine kinase 2 inhibitor deucravacitinib compared with Janus kinase 1/2/3 inhibitors. Dermatol Ther (Heidelb) 2021;11(5):1763–1776.
25. van der Heijde D, Song IH, Pangan AL, et al. Efficacy and safety of upadacitinib in patients with active ankylosing spondylitis (SELECT-AXIS 1): a multicentre, randomised, double-blind, placebo-controlled, phase 2/3 trial. Lancet 2019;394(10214):2108–2117.
26. Mease PJ, Lertratanakul A, Anderson JK, et al. Upadacitinib for psoriatic arthritis refractory to biologics: SELECT-PsA 2. Ann Rheum Dis 2021;80(3):312–320.
27. McInnes IB, Anderson JK, Magrey M, et al. Trial of Upadacitinib and Adalimumab for Psoriatic Arthritis. N Engl J Med 2021;384(13):1227–1239.

28. Danese S, Vermeire S, Zhou W, et al. Upadacitinib as induction and maintenance therapy for moderately to severely active ulcerative colitis: results from three phase 3, multicentre, double-blind, randomised trials. Lancet 2022;399(10341):2113–2128.

29. Loftus EV Jr, Panés J, Lacerda AP, et al. Upadacitinib induction and maintenance therapy for Crohn's disease. N Engl J Med 2023; 388(21):1966–1980.

30. Cuthbert RJ, Watad A, Fragkakis EM, et al. Evidence that tissue resident human enthesis γδT-cells can produce IL-17A independently of IL-23R transcript expression. Ann Rheum Dis 2019;78(11):1559–1565.

31. Takakura K, Takatou S, Tomiyama R, et al. Inhibition of nuclear factor-κB p65 phosphorylation by 3,4-dihydroxybenzalacetone and caffeic acid phenethyl ester. J Pharmacol Sci 2018;137(3):248–255.

32. Castro F, Cardoso AP, Gonçalves RM, et al Interferon-gamma at the crossroads of tumor immune surveillance or evasion. Front Immunol 2018;9:847.

33. Klünder B, Mittapalli RK, Mohamed MF, et al. Population pharmacokinetics of upadacitinib using the immediate-release and extended-release formulations in healthy subjects and subjects with rheumatoid arthritis: analyses of phase I-III clinical trials. Clin Pharmacokinet 2019; 58(8):1045–1058.

34. Bridgewood C, Watad A, Russell T, et al. Identification of myeloid cells in the human enthesis as the main source of local IL-23 production. Ann Rheum Dis 2019;78(7):929–933.

35. Pattison MJ, Mackenzie KF, Arthur JSC. Inhibition of JAKs in macrophages increases lipopolysaccharide-induced cytokine production by blocking IL-10–mediated feedback. J Immunol 2012;189(6): 2784–2792.

36. Aschenbrenner D, Quaranta M, Banerjee S, et al. Deconvolution of monocyte responses in inflammatory bowel disease reveals an IL-1 cytokine network that regulates IL-23 in genetic and acquired IL-10 resistance. Gut 2021;70(6):1023–1036.

37. Stalder R, Zhang B, Jean Wrobel L, et al. The Janus kinase inhibitor tofacitinib impacts human dendritic cell differentiation and favours M1 macrophage development. Exp Dermatol 2020;29(1):71–78.

38. Danve A, Deodhar A. Treatment of axial spondyloarthritis: an update. Nat Rev Rheumatol 2022;18(4):205–216.

39. Ramiro S, Nikiphorou E, Sepriano A, et al. ASAS-EULAR recommendations for the management of axial spondyloarthritis: 2022 update. Ann Rheum Dis 2023;82(1):19–34.

40. Fauny M, Moulin D, D'Amico F, et al. Paradoxical gastrointestinal effects of interleukin-17 blockers. Ann Rheum Dis 2020;79(9):1132–1138.

41. McGonagle D, Watad A, Sharif K, et al. Why inhibition of IL-23 lacked efficacy in ankylosing spondylitis. Front Immunol 2021;12:614255.

42. Jostins L, Ripke S, Weersma RK, et al; International IBD Genetics Consortium (IIBDGC). Host-microbe interactions have shaped the genetic architecture of inflammatory bowel disease. Nature 2012; 491(7422):119–124.

43. Rochman Y, Spolski R, Leonard WJ. New insights into the regulation of T cells by gamma(c) family cytokines. Nat Rev Immunol 2009;9(7): 480–490.

44. Hugot JP, Chamaillard M, Zouali H, et al. Association of NOD2 leucine-rich repeat variants with susceptibility to Crohn's disease. Nature 2001;411(6837):599–603.

45. Barrett JC, Hansoul S, Nicolae DL, et al; NIDDK IBD Genetics Consortium; Belgian-French IBD Consortium; Wellcome Trust Case Control Consortium. Genome-wide association defines more than 30 distinct susceptibility loci for Crohn's disease. Nat Genet 2008;40(8): 955–962.

46. Goyette P, Boucher G, Mallon D, et al; International Inflammatory Bowel Disease Genetics Consortium; Australia and New Zealand IBDGC; Belgium IBD Genetics Consortium; Italian Group for IBD Genetic Consortium; NIDDK Inflammatory Bowel Disease Genetics Consortium; United Kingdom IBDGC; Wellcome Trust Case Control Consortium; Quebec IBD Genetics Consortium. High-density mapping of the MHC identifies a shared role for HLA-DRB1*01:03 in inflammatory bowel diseases and heterozygous advantage in ulcerative colitis. Nat Genet 2015;47(2):172–179.

47. Kuiper JJ, Prinz JC, Stratikos E, et al; EULAR studygroup MHC-I-opathies. EULAR study group on 'MHC-I-opathy': identifying disease-overarching mechanisms across disciplines and borders. Ann Rheum Dis 2023;82(7):887–896.

48. Vasudevan A, Gibson PR, van Langenberg DR. Time to clinical response and remission for therapeutics in inflammatory bowel diseases: what should the clinician expect, what should patients be told? World J Gastroenterol 2017;23(35):6385–6402.

49. Wang H, Brown J, Gao S, et al. The role of JAK-3 in regulating TLR-mediated inflammatory cytokine production in innate immune cells. J Immunol 2013;191(3):1164–1174.

50. Monaco G, Lee B, Xu W, et al. RNA-seq signatures normalized by mRNA abundance Allow absolute deconvolution of human immune cell types. Cell Rep 2019;26(6):1627–1640.e7.

AMERICAN COLLEGE
of RHEUMATOLOGY
Empowering Rheumatology Professionals

BRIEF REPORT

Effect of Long-Term Voclosporin Treatment on Renal Histology in Patients With Active Lupus Nephritis With Repeat Renal Biopsies

Brad H. Rovin,[1] (ID) Clarissa Cassol,[2] Samir V. Parikh,[1] (ID) Amit Saxena,[3] (ID) Neil Solomons,[4] Vanessa Birardi,[5] (ID) Ernie Yap,[5] Clint W. Abner,[6] David R. W. Jayne,[7] (ID) and Robert B. Huizinga[8] (ID)

Objective. This study characterized the impact of voclosporin on kidney histology in patients with lupus nephritis (LN) who had protocolized repeat kidney biopsies in the AURORA clinical trials.

Methods. Patients were randomized to voclosporin or placebo treatment for up to 3 years; all patients received mycophenolate mofetil and low-dose glucocorticoids. Patients had baseline kidney biopsies within 6 months before study start and repeat biopsies after approximately 18 months of study treatment. The revised National Institutes of Health indices for LN activity and chronicity (CI) were calculated in addition to a semiquantitative assessment of vascular and tubular lesions.

Results. Sixteen patients in the voclosporin group and 10 patients in the control group had both baseline and repeat kidney biopsies. Patient clinical characteristics were similar at baseline. In the voclosporin group, most (n = 13) patients had pure class IV lesions (pure class V, n = 1; mixed, n = 2). In the control group, three patients had pure class IV (pure class III, n = 3; pure class V, n = 1; mixed, n = 3). Most of the voclosporin-treated patients had no change in CI (n = 8) or a change no greater than 2 (n = 6); control-treated patients also had no change in CI (n = 3) or a change no greater than 2 (n = 6). No trends in vascular lesions or tubular compartment changes were observed.

Conclusion. Outcomes from this small subgroup show that exposure to study treatment was not associated with nephrotoxicity based on histopathologic evaluation after 18 months. These data are reassuring and further contribute to the safety profile of voclosporin for the treatment of adults with active LN.

INTRODUCTION

Lupus nephritis (LN) can lead to loss of kidney function and is associated with a high risk of end-stage kidney disease and death.[1,2] Response to treatment can be slow, and treatment regimens are associated with considerable toxicity.[3] LN is characterized by proteinuria, which is damaging to kidneys and is independently associated with cardiovascular morbidity, thrombosis, chronic kidney disease, and an increased mortality risk.[4] Decline in proteinuria is a marker of treatment response and overall prognosis.[5,6]

Immunosuppressants, including calcineurin inhibitors (CNIs), are used in the treatment of LN, as recommended by recent treatment guidelines.[5–7] CNIs work through inhibition of T cell function, resulting in disease modification and inhibition of synaptopodin degradation, stabilizing the podocyte cytoskeleton.[8] Additionally, CNIs have a hemodynamic effect associated with reversible vasoconstriction of the afferent arterioles that can acutely decrease proteinuria.[9]

A factor limiting chronic use of CNIs is the potential for nephrotoxicity. First-generation CNIs cyclosporine A (CsA) and tacrolimus (Tac) have been implicated in the development of irreversible

chronic lesions in the kidney, particularly when used at higher doses in the solid organ transplant setting.[10–13]

Voclosporin, a second-generation CNI, is indicated for the treatment of adults with active LN and has a distinct pharmacological and clinical profile compared with CsA and Tac.[14] In the AURORA clinical program, a voclosporin-based triple therapy regimen with mycophenolate mofetil (MMF) and low-dose glucocorticoids (GCs) resulted in rapid and sustained proteinuria reductions in patients with active LN with an acceptable long-term safety profile.[15,16] Based on these results, recent American College of Rheumatology guidelines recommend voclosporin as part of a triple immunosuppressive regimen as a first-line treatment option for all LN classes.[7]

To assess the impact of voclosporin on kidney histopathology in patients with LN, the AURORA clinical program included a protocolized repeat kidney biopsy substudy. Results from patients enrolled in this substudy are reported here.

PATIENTS AND METHODS

Study design. The AURORA clinical program was composed of two phase 3 clinical trials: the pivotal 1-year AURORA 1 study and the follow-up 2-year AURORA 2 study. The study designs of AURORA 1 and AURORA 2 have been reported.[15,16] Briefly, patients in AURORA 1 were randomized to receive double-blind voclosporin (23.7 mg twice daily), or matching placebo, with MMF (target 2 g/day) and GCs.[14] Patients in AURORA 2 continued on the same double-blind study drug (voclosporin or placebo), MMF, and GCs at the doses used at the end of AURORA 1 (Figure 1).[15,16] The AURORA 1 inclusion criteria required patients to have a locally read baseline kidney biopsy with evidence of active LN requiring treatment and International

Society of Nephrology/Renal Pathology Society (ISN/RPS) 2003 classification of III, IV, and/or V disease.[17] AURORA 2 inclusion criteria required patients to complete study treatment in AURORA 1, and, in the opinion of the investigator, required continued immunosuppressive therapy.

AURORA 2 patients had an opportunity for a kidney biopsy to be performed at approximately 6 months into AURORA 2 as part of an elective repeat kidney biopsy substudy. Additional inclusion criteria specific for the biopsy substudy required that the locally read kidney biopsy at baseline had been performed within 6 months of screening for AURORA 1 and investigator confirmation that biopsy sample requirements could be met, including staining of samples and transfer of slide images to a central laboratory, as well as substudy-specific, patient-signed, informed consent.

The protocol was approved by an institutional review board or independent ethics committee at each trial site; all participants provided informed consent in accordance with the Declaration of Helsinki and International Council for Harmonisation of Technical Requirements for Pharmaceuticals for Human Use and Good Clinical Practice guideline. The aggregated data underlying this article, the study protocol, and statistical analysis plan will be shared with researchers on reasonable request to the corresponding author.

Kidney biopsy sample preparation. Baseline and repeat kidney biopsies were processed by local laboratories to prepare slides for the central reads using recuts of the original biopsy blocks. Slides were prepared for routine light microscopy and stained with hematoxylin and eosin, periodic acid-Schiff (PAS), Masson's trichrome, and Jones' methenamine silver-PAS. Once processed, four whole-slide scanned images,
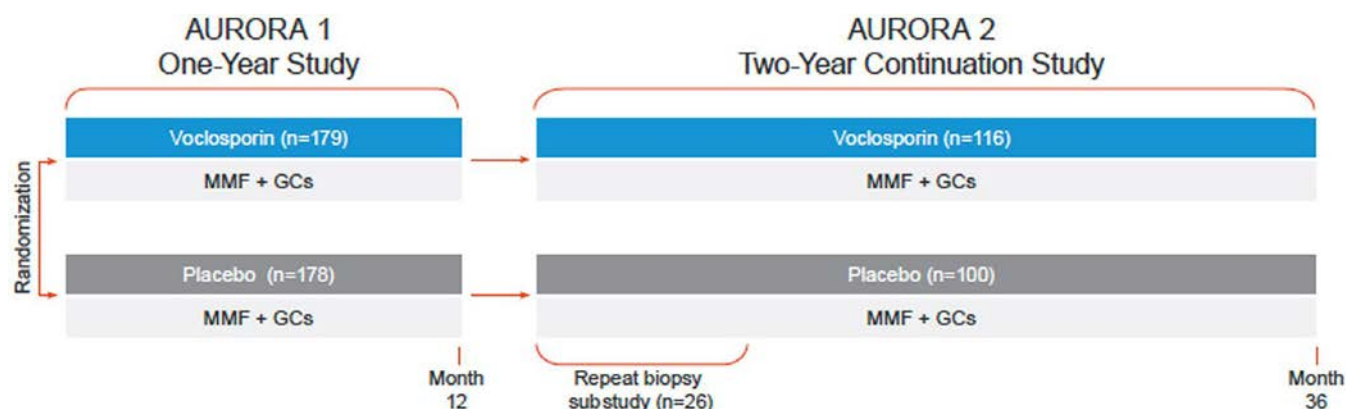

Figure 1. AURORA 1 and AURORA 2 study designs. AURORA 1 enrolled patients with active lupus nephritis, urine protein-creatinine ratio greater than or equal to 1.5 g/g (≥2 g/g for class V) and estimated glomerular filtration rate greater than 45 mL/min/1.73 m^2; patients were randomized to receive double-blind voclosporin (23.7 mg twice daily) or matching placebo, with MMF (target 2 g/day) and low-dose oral GCs. A protocol-defined GC taper included intravenous methylprednisolone on days 1 and 2. Oral GC was initiated on day 3 with 20 to 25 mg/day prednisone or equivalent and tapered to a target dose of 2.5 mg/day by week 16. Patients in AURORA 2 continued on the same double-blind study drug (voclosporin or placebo), MMF, and GCs at the doses used at the end of AURORA 1. GC, glucocorticoid; MMF, mycophenolate mofetil.

corresponding to each of these four stains, were captured and transferred electronically to a central United States–based College of American Pathologists–accredited laboratory (Arkana Laboratories, Arkansas, USA). Histopathologic grading and assessment were conducted by one reader from a panel of seven nephropathologists; the same reader reviewed both the baseline and repeat kidney biopsies obtained from the same patient. Nephropathologists were blinded to treatment arm, biopsy sequence (baseline or repeat), clinical parameters of patients, and initial biopsy reports from the local pathologists.

Histologic assessments. A total of 37 patients from the AURORA 2 study enrolled in the kidney biopsy substudy; 16 in the voclosporin group and 10 in the control group had sufficient kidney biopsy samples at both baseline and repeat to allow activity indices (AIs) and chronicity indices (CIs) to be assessed. Grading of baseline and repeat biopsies was based on the revised National Institutes of Health (NIH) indices for LN activity and chronicity, following the 2018 update to the ISN/RPS AI and CI scoring system.[18,19]

Additional manifestations associated with CNI nephrotoxicity were assessed in vascular and tubular compartments. Vascular assessment included arterial sclerosis, thrombotic microangiopathy, and arteriolar hyalinosis. Tubular compartment assessment focused on the presence of isometric tubular vacuolization, a nonspecific morphologic finding often seen with CNI-induced toxicity.[20]

Clinical parameters. Assessed clinical outcomes included complete renal response (CRR, defined as a urine protein-creatinine ratio [UPCR] ≤0.5 g/g; stable estimated glomerular filtration rate [eGFR]; low-dose GCs [<10 mg prednisone per day for ≥3 consecutive days or for ≥7 days during the 8 weeks before assessment], and no rescue medication), partial renal response (PRR; defined as a reduction in UPCR of ≥50% from baseline), blood pressure, UPCR, laboratory assessments and adverse events (AEs). Kidney function was assessed with corrected eGFR (Chronic Kidney Disease Epidemiology Collaboration equation) using a prespecified ceiling of 90 mL/min/1.73 m^2 and compared with the results of the overall AURORA population.

RESULTS

Baseline demographics and disease characteristics for biopsy substudy patients were generally like those of the overall AURORA 1 population. For instance, mean UPCR at baseline in the substudy was 4.59 g/g in the voclosporin group and 4.71 g/g in the control group compared with the overall AURORA 1 population that had 4.14 g/g in the voclosporin group and 3.87 g/g in the control group.[15] The biopsy substudy population represented seven countries with the largest number from Peru, and most patients were of Hispanic or Latino ethnicity (Table 1).

The median time between the baseline kidney biopsy and start of AURORA 1 was 0.99 months (range 0.3–4.8 months) for the voclosporin group and 1.49 months (range 0.3–1.7 months) for the control group of the biopsy substudy. The repeat kidney biopsy occurred after a median of 17.8 months (range 15.2–23.6 months) of study treatment for the voclosporin group and 16.5 months (range 13.6–21.4 months) for the control group. Of the patients in the biopsy substudy, all but three completed 36 months of study treatment; one patient in the voclosporin group and two in the control group discontinued study drug early because of AEs.

The median dose of study drug (voclosporin or placebo) in the biopsy substudy was 42.5 mg/day in the voclosporin group and 47.2 mg/day in the control group, consistent with the overall AURORA 1 population reporting 41.3 mg/day study drug in the voclosporin group and 45.5 mg/day in the control group. Exposure to GCs and MMF was also similar between substudy groups during the AURORA 1 and AURORA 2 studies. Before the baseline kidney biopsy in AURORA 1, several patients in the voclosporin group and in the control group reported GC and MMF use (Table S1).

Clinical findings. Higher rates of CRR and PRR were observed in the voclosporin group of the biopsy substudy. In biopsy substudy patients, the early mean reductions in UPCR observed in AURORA 1 were maintained out to 3 years in AURORA 2, with no increase in UPCR at the follow-up visit taking place 4 weeks after study drug discontinuation, consistent with the results of the overall AURORA study population (Tables S2 and S3; Figure S1).

Over the 3-year study period, corrected mean eGFR remained stable and within the normal range in both groups of the biopsy substudy, consistent with findings from the overall AURORA population (Table S2; Figures S2 and S3).[15,16] Mean blood pressure and levels of electrolytes, glucose, and serum creatinine were stable over time in the substudy, consistent with previous reports.[15,16]

There were no unexpected AEs related to treatment; the safety profile and frequency of AEs in the substudy were similar to the overall AURORA 1 and AURORA 2 populations.[15,16] In the substudy patients treated with voclosporin, the AE of "glomerular filtration rate (GFR) decreased" by MedDRA preferred term was reported in six (37.5%) patients in year 1 and two (12.5%) patients in year 2, with no reports in year 3; no AEs of GFR decreased were reported in the control group. AEs led to permanent discontinuation of study treatment in two patients (renal impairment and disseminated tuberculosis both considered by the investigator as related to the study drug) in the control group and in one patient in the voclosporin group who experienced worsening systemic lupus erythematosus considered by the investigator as unrelated to voclosporin.

Table 1. Baseline demographics and disease characteristics of patients in the voclosporin and control groups of the kidney biopsy substudy*

Characteristics	Voclosporin (n = 16)	Control (n = 10)
Age, years		
Median (IQR)	27.0 (24–33)	33.5 (27–43)
Sex, n (%)		
Female	15 (93.8)	9 (90.0)
Race,[a] n (%)		
Mestizo	9 (56.3)	4 (40.0)
White	4 (25.0)	3 (30.0)
Asian	3 (18.8)	3 (30.0)
Ethnicity,[a] n (%)		
Hispanic or Latino	9 (56.3)	6 (60.0)
Non-Hispanic or non-Latino	7 (43.8)	4 (40.0)
Region, n (%)		
North America	0 (0.0)	3 (30.0)
Latin America	9 (56.3)	4 (40.0)
Europe	4 (25.0)	2 (20.0)
Asia	3 (18.8)	1 (10.0)
Country, n (%)		
Belarus	1 (6.3)	2 (20.0)
Mexico	1 (6.3)	2 (20.0)
Peru	8 (50.0)	2 (20.0)
Philippines	3 (18.8)	1 (10.0)
Russia	2 (12.5)	0 (0.0)
Ukraine	1 (6.3)	0 (0.0)
USA	0 (0.0)	3 (20.0)
Time since LN diagnosis, years		
Median (IQR)	3.5 (1.0–5.0)	4.0 (1.0–10.0)
Time since SLE diagnosis, years		
Median (IQR)	3.5 (1.0–5.5)	6.0 (1.0–14.0)
Biopsy class, n (%)		
Pure class III	0 (0.0)	3 (30.0)
Pure class IV	13 (81.3)	3 (30.0)
Pure class V	1 (6.3)	1 (10.0)
Mixed class III/V or IV/V	2 (12.6)	3 (30.0)
eGFR, mL/min/1.73 m^2		
Corrected, mean (SD)	80.3 (16.4)	82.6 (12.3)
UPCR, g/g		
Mean (SD)	4.59 (2.5)	4.7 (2.6)
≥2 g/g, n (%)	13 (81.3)	9 (90.0)
C3, mg/dL		
Mean (SD)	78.1 (37.36)	90.9 (39.74)
Median (min, max)	71.5 (29, 149)	97.5 (39, 158)
Low, n (%)[b]	10 (62.5)	4 (40.0)
C4, mg/dL		
Mean (SD)	15.6 (8.93)	17.1 (10.77)
Median (min, max)	12.0 (8, 41)	14.0 (6, 37)
Low, n (%)[c]	10 (62.5)	6 (60.0)
Anti-dsDNA antibodies, IU/mL		
Mean (SD)	55.7 (70.2)	86.2 (107.9)
Median (min, max)	25.0 (2, 238)	52.0 (2, 339)
High dsDNA, n (%)[d]	7 (43.8)	6 (60.0)
Missing	1 (6.3)	0 (0.0)
SLEDAI total score		
Mean (SD)	13.9 (5.68)	10.9 (3.73)
Median (min, max)	14.0 (4, 24)	12.0 (6, 17)

(Continued)

Table 1. (Cont'd)

Characteristics	Voclosporin (n = 16)	Control (n = 10)
SLEDAI nonrenal score		
Mean (SD)	6.4 (4.01)	4.1 (2.33)
Median (min, max)	6.0 (0, 12)	4.0 (2, 8)
Prior use of ACEi/ARBs, n (%)	13 (81.3)	8 (80.0)

* Data from pretreatment baseline in AURORA 1 for 10 patients in the control group and 16 patients in the voclosporin group of the biopsy substudy. Kidney function assessed with corrected eGFR (Chronic Kidney Disease Epidemiology Collaboration equation) using a prespecified ceiling of 90 mL/min/1.73 m^2. ACEi, angiotensin-converting enzyme inhibitor; ARB, angiotensin II receptor blocker; C3, complement 3; C4, complement 4; dsDNA, double-stranded DNA; eGFR, estimated glomerular filtration rate; IQR, interquartile range; LN, lupus nephritis; max, maximum; min, minimum; SD, standard deviation; SLE, systemic lupus erythematosus; SLEDAI, Systemic Lupus Erythematosus Disease Activity Index; UPCR, urine protein-creatinine ratio.
[a] Race and ethnicity of patients in AURORA 1 were self-reported using a fixed set of predefined categories.
[b] Low C3 was defined as less than 90 mg/dL.
[c] Low C4 was defined as less than 16 mg/dL.
[d] High anti-dsDNA was defined as greater than 25 IU/mL.

Activity and chronicity scoring. Median CI and AI were similar between treatment groups of the substudy at baseline and remained stable over time (Table 2; Table S4). Individual CIs over time were variable between patients, with increases, decreases, and no change in score observed in both groups. Most patients in the voclosporin group had no change in CI (n = 8) or a change of ≤2 (n = 6); one patient had a decrease from 7 to 4 and another had an increase from 6 to 10. The latter patient discontinued the study because of an AE of worsening systemic lupus erythematosus. In the control group, most patients had a score change ≤2 (n = 6); three patients had no change in CI, and one had a decrease from 5 to 1 (Figure S4).

Baseline AI of 0 was reported for 69% of the patients in the voclosporin group and 30% of the control group of the substudy population; three patients with an AI of 0 had a component of class V LN. Of the 11 patients classified with only proliferative LN (class III or IV) and an AI of 0, 7 had chronic damage with CIs ranging from 3 to 10, and the remaining 4 patients had no chronic damage at baseline. All patients with baseline histologic activity had resolution at repeat biopsy with an AI of 0 or a large decline, apart from one patient in the control group that had an AI of 4 at baseline and 3 at the repeat biopsy (Table 2; Figure S4).

Vascular and tubular evaluation. Vascular and tubular examination and scoring was performed in both baseline and repeat kidney biopsies. No trends in vascular changes were observed. One patient in the voclosporin group and three patients in the control group had arteriolar hyalinosis on repeat biopsy that was not present on the baseline biopsy. Two patients in the voclosporin group and one patient in the control group had arterial sclerosis on repeat biopsy not apparent on the baseline biopsy (Table 2).

Table 2. Patient-level histology data in the voclosporin group[*]

Patient no.	AURORA 1 baseline				Biopsy scores, baseline/repeat[b]						Renal response at month 18[c]
	Biopsy class[a]	sCr, mg/dL	UPCR, g/g	Time from biopsy to enrollment, days	AI	CI	AS	TMA	AH	ITV	
Voclosporin											
1	IV	1.30	1.9	146	0/0	6/10	NA/3	1/0	1/1	0/0	PRR
2	IV	1.26	3.5	10	0/0	10/9	1/1	0/0	0/0	0/0	CRR
3	IV	1.24	8.7	31	9/1	8/9	2/0	0/0	1/1	1/1	PRR
4	IV	0.37	5.7	36	0/4	10/8	NA/0	0/0	0/0	0/0	CRR
5	IV	0.92	3.9	43	0/0	5/5	NA/0	0/0	0/0	0/0	PRR
6	IV	0.48	2.0	37	4/0	4/5	3/3	0/0	1/1	1/0	CRR
7	IV	0.45	2.8	58	0/0	7/4	0/1	0/0	1/0	0/1	CRR
8	IV	0.80	6.5	7	0/0	3/3	0/0	0/0	1/1	0/0	CRR
9	IV	0.69	8.7	27	6/1	3/3	NA/0	0/0	0/0	0/0	PRR
10	III/V	1.19	4.2	15	4/0	3/3	2/2	0/0	0/0	0/0	CRR
11	IV	0.77	7.1	83	6/0	2/2	0/2	0/0	0/0	0/0	CRR
12	IV	0.37	2.5	15	0/0	0/2	0/0	0/0	0/0	0/0	PRR
13	IV	0.69	1.5	7	0/0	0/2	0/1	0/0	0/1	0/0	CRR
14	IV	0.55	7.3	41	0/0	0/0	0/0	0/0	0/0	0/0	PRR
15	IV/V	1.09	4.9	20	0/0	0/0	NA/NA	0/0	0/0	0/0	CRR
16	V	0.69	2.1	14	0/0	0/0	1/1	0/0	0/0	0/0	No response
Control											
17	III/V	1.09	9.1	52	0/0	7/9	3/3	0/0	0/0	0/0	PRR
18	IV	0.60	7.0	9	1/0	4/4	3/3	0/0	0/1	0/0	No response
19	IV/V	0.99	5.4	47	10/1	4/4	0/1	0/0	1/1	0/0	CRR
20	IV	1.13	2.1	49	6/0	3/4	1/0	0/0	0/1	0/0	CRR
21	III/V	0.77	2.2	42	5/0	1/3	2/2	0/0	0/0	0/0	CRR
22	V	0.43	1.7	13	1/0	4/2	2/2	0/0	0/0	0/0	No response
23	IV	0.57	4.0	7	0/0	5/1	2/NA	0/0	1/0	0/0	PRR
24	III	0.76	7.7	48	0/0	0/1	2/0	0/0	0/0	0/0	No response
25	III	0.77	3.3	51	4/3	1/0	3/3	0/0	0/1	0/0	CRR
26	III	0.67	4.5	30	3/0	0/0	0/0	0/0	0/0	0/0	CRR

* Analysis includes data from before treatment in AURORA 1 (baseline) to month 18 of AURORA 2 for 26 patients in the kidney biopsy substudy. AH, arteriolar hyalinosis; AI, activity index; AS, arterial sclerosis; CI, chronicity index; CRR, complete renal response; ITV, isometric tubular vacuolization; NA, no arteries available for assessment; PRR, partial renal response; sCr, serum creatinine; TMA, thrombotic microangiopathy; UPCR, urine protein-creatinine ratio.
[a] Biopsy class was assigned at baseline based on local pathology read according to the 2003 Nephrology/Renal Pathology Society classification.[17]
[b] Histopathologic grading based on the National Institutes of Health indices for lupus nephritis activity (scale 0–24) and chronicity (scale 0–12).[18]
[c] All patients who achieved CRR at month 18 also had PRR. Vascular assessment included AS (0 = absent, 1 = mild, 2 = moderate, and 3 = severe), TMA (0 = absent and 1 = present), AH (0 = absent and 1 = present), and ITV (0 = absent and 1 = present).

DISCUSSION

This is the first study to assess histologic changes in the kidneys of patients with active LN enrolled in a randomized, blinded clinical trial and treated with voclosporin or placebo in combination with MMF and low-dose GCs. Exposure to voclosporin for a median of 18 months was not associated with onset or progression of nephrotoxicity based on evaluation of histologic compartments and vascular lesions.

CIs, histologic measurements of chronic kidney injury, remained stable at follow-up in both treatment groups.[21] Given that injury patterns may not be comprehensively captured by the NIH AI and CI scoring system, we also evaluated the vascular and tubular compartments for arterial sclerosis, arteriolar hyalinosis, isometric tubular vacuolization, and thrombotic microangiopathy, lesions that are commonly associated with CNI nephrotoxicity.[11,12] Notably, our data did not indicate any significant trends or signals of CNI nephrotoxicity in either treatment group.

For most patients, AI, a histologic measure of kidney inflammation, decreased or remained unchanged between baseline and repeat biopsies. Of patients with an AI ≥1 at baseline, all but two patients in the control arm achieved a clinically important decline in AI at the repeat biopsy, consistent with their clinical outcome as complete or partial renal responders. However, two patients with significant residual activity on repeat biopsy, including a placebo-treated patient with an AI of 3 and a voclosporin-treated patient with an AI of 4, were also considered complete renal responders at repeat biopsy. This may represent the known discordance between clinical and histologic response seen in patients with LN.[22–26] Alvarado et al reported on 25 patients with LN with repeat biopsies and found that, despite achieving clinical CRR (n = 16), nine patients had an AI >0 and five had an AI ≥2.[26]

Unexpectedly, and of potential concern, were the substudy patients enrolled into the AURORA 1 trial with an AI of 0. Eight of these 14 patients had moderate to severe chronic kidney damage based on CI scores that could contribute to the clinically relevant levels of proteinuria at trial entry. The remaining six patients

demonstrating no activity or chronic damage at baseline had elevated proteinuria that decreased demonstrably with treatment. Two of the six patients had a class V component on biopsy that likely accounted for their proteinuria at baseline. Proteinuria in the remaining four patients is more difficult to explain. This may reflect the known discordance of proteinuria with histologic findings, variations in determining the AIs and CIs among nephropathologists, and limitations of these tools to capture all clinically relevant histologic lesions.[22–29] Finally, study enrollment was based on the local investigator's judgment and local pathology readings without adjudication or verification by the study sponsor. From this experience, we propose that future studies in LN include protocolized central verification of LN activity to adjudicate results for all LN trials.

The AURORA clinical program provided a unique opportunity to evaluate repeat kidney biopsies following extended treatment with voclosporin compared with placebo. Clinical efficacy results in this substudy were consistent with outcomes reported in the larger studies demonstrating that voclosporin was effective at reducing or resolving proteinuria.[15,16] Given the toxicity of proteinuria to the kidney, the ability of voclosporin to lower proteinuria even in patients with chronic kidney damage, resulting from its impact on glomerular hemodynamics and podocyte structure, provides an additional tangible example of the benefit of voclosporin in LN.

Interpretation of this analysis is preliminary, limited by small sample size and selection bias of including AURORA 2 patients, who found treatment in AURORA 1 (either voclosporin or placebo) acceptable and who elected to continue the same blinded therapy in AURORA 2. The repeat biopsy substudy of AURORA 2 overlapped with the COVID-19 pandemic; pandemic-related restrictions likely limited the ability to participate. Additionally, although findings reported here after 18 months of treatment are reassuring, evaluating repeat kidney biopsies after longer exposure periods and in larger patient subgroups representative of the global LN population (eg, patients with impaired renal function or patients of African ancestry) is necessary to better understand the safety of voclosporin in a real-world setting. Finally, the NIH indices used for histologic assessments in this study are established as a semiquantitative tool in LN and are used clinically and in research for both initial and repeat biopsy evaluation. In addition to the use of molecular diagnostics and noninvasive biomarkers, ongoing work promises to expand the clinical value of the NIH indices as classification and prognostic tools to optimize the evaluation and management of LN.[27,30]

These data demonstrate that treatment with voclosporin for approximately 18 months, in combination with low-dose MMF and GCs, is not associated with increased risk of kidney injury. The lack of histologic evidence of nephrotoxicity in this small subgroup, in addition to the positive clinical outcomes demonstrated, further our understanding of the safety and efficacy of long-term voclosporin use in LN.

REFERENCES

1. Maroz N, Segal MS. Lupus nephritis and end-stage kidney disease. Am J Med Sci 2013;346(4):319–323.

2. Hanly JG, O'Keeffe AG, Su L, et al. The frequency and outcome of lupus nephritis: results from an international inception cohort study. Rheumatology (Oxford) 2016;55(2):252–262.

3. Almaani S, Meara A, Rovin BH. Update on lupus nephritis. Clin J Am Soc Nephrol 2017;12(5):825–835.

4. Hemmelgarn BR, Manns BJ, Lloyd A, et al; Alberta Kidney Disease Network. Relation between kidney function, proteinuria, and adverse outcomes. JAMA 2010;303(5):423–429.

5. Fanouriakis A, Kostopoulou M, Andersen J, et al. EULAR recommendations for the management of systemic lupus erythematosus: 2023 update. Ann Rheum Dis 2024;83(1):15–29.

6. Rovin BH, Ayoub IM, Chan TM, et al; Kidney Disease: Improving Global Outcomes (KDIGO) Lupus Nephritis Work Group. KDIGO 2024 Clinical Practice Guideline for the management of LUPUS NEPHRITIS. Kidney Int 2024;105(1S):S1–S69.

7. Sammaritano LR, Askanase A, Bermas BL, et al. 2024 American College of Rheumatology (ACR) Guideline for the Screening, Treatment, and Management of Lupus Nephritis. Arthritis Rheumatol 2025; 77(9):1115–1135. https://doi.org/10.1002/art.43212

8. Ponticelli C, Podestà MA. Calcineurin inhibitors in lupus nephritis. J Nephrol 2021;34(2):399–402.

9. Hošková L, Málek I, Kopkan L, et al. Pathophysiological mechanisms of calcineurin inhibitor-induced nephrotoxicity and arterial hypertension. Physiol Res 2017;66(2):167–180.

10. Gallagher M, Jardine M, Perkovic V, et al. Cyclosporine withdrawal improves long-term graft survival in renal transplantation. Transplantation 2009;87(12):1877–1883.

11. Naesens M, Kuypers DR, Sarwal M. Calcineurin inhibitor nephrotoxicity. Clin J Am Soc Nephrol 2009;4(2):481–508.

12. Nankivell BJ, Borrows RJ, Fung CL, et al. Calcineurin inhibitor nephrotoxicity: longitudinal assessment by protocol histology. Transplantation 2004;78(4):557–565.

13. Karolin A, Genitsch V, Sidler D. Calcineurin inhibitor toxicity in solid organ transplantation. Pharmacology 2021;106(7-8):347–355.

14. Ponticelli C, Reggiani F, Moroni G. Old and new calcineurin inhibitors in lupus nephritis. J Clin Med 2021;10(21):4832.

15. Rovin BH, Teng YKO, Ginzler EM, et al. Efficacy and safety of voclosporin versus placebo for lupus nephritis (AURORA 1): a double-blind, randomised, multicentre, placebo-controlled, phase 3 trial. Lancet 2021;397(10289):2070–2080.

16. Saxena A, Ginzler EM, Gibson K, et al. Safety and efficacy of long-term voclosporin treatment for lupus nephritis in the phase 3 AURORA 2 clinical trial. Arthritis Rheumatol 2024;76(1):59–67.

17. Markowitz GS, D'Agati VD. The ISN/RPS 2003 classification of lupus nephritis: an assessment at 3 years. Kidney Int. 2007;71(6):491-495. doi:10.1038/sj.ki.5002118.

18. Bajema IM, Wilhelmus S, Alpers CE, et al. Revision of the International Society of Nephrology/Renal Pathology Society classification for lupus nephritis: clarification of definitions, and modified National Institutes of Health activity and chronicity indices. Kidney Int 2018;93(4): 789–796.

19. Austin HA III, Muenz LR, Joyce KM, et al. Diffuse proliferative lupus nephritis: identification of specific pathologic features affecting renal outcome. Kidney Int 1984;25(4):689–695.

20. Lusco MA, Fogo AB, Najafian B, et al. AJKD Atlas of Renal Pathology: calcineurin inhibitor nephrotoxicity. Am J Kidney Dis 2017;69(5): e21–e22.

21. Moroni G, Porata G, Raffiotta F, et al. Beyond ISN/RPS lupus nephritis classification: adding chronicity index to clinical variables predicts kidney survival. Kidney360 2021;3(1):122–132.

22. Malvar A, Pirruccio P, Alberton V, et al. Histologic versus clinical remission in proliferative lupus nephritis. Nephrol Dial Transplant 2017; 32(8):1338–1344.

23. Dasari S, Chakraborty A, Truong L, et al. A systematic review of inter-pathologist agreement in histologic classification of lupus nephritis. Kidney Int Rep 2019;4(10):1420–1425.

24. Grootscholten C, Bajema IM, Florquin S, et al. Interobserver agreement of scoring of histopathological characteristics and classification of lupus nephritis. Nephrol Dial Transplant 2008;23(1):223–230.

25. Wernick RM, Smith DL, Houghton DC, et al. Reliability of histologic scoring for lupus nephritis: a community-based evaluation. Ann Intern Med 1993;119(8):805–811.

26. Alvarado AS, Malvar A, Lococo B, et al. The value of repeat kidney biopsy in quiescent Argentinian lupus nephritis patients. Lupus 2014;23(8):840–847.

27. Choi SE, Fogo AB, Lim BJ. Histologic evaluation of activity and chronicity of lupus nephritis and its clinical significance. Kidney Res Clin Pract 2023;42(2):166–173.

28. Furness PN, Taub N. Interobserver reproducibility and application of the ISN/RPS classification of lupus nephritis-a UK-wide study. Am J Surg Pathol 2006;30(8):1030–1035.

29. Rao K, Ferrario F, Cook T, et al. OP0062 Lupus nephritis histopathology interobserver agreement between local pathologists and an expert panel of nephropathologists in belong. Ann Rheum Dis 2013; 71(suppl 3):74. https://doi.org/10.1136/annrheumdis-2012-eular. 1745

30. Bajema IM, Balow JE, Haas M, et al. Update on scoring and providing evidence basis for assessing pathology in lupus nephritis. Kidney Int 2023;103(5):813–816.

Deep Immunophenotyping and Clustering Identifies Biomarkers Predictive of Lymphoma in Primary Sjögren Disease

Cindy Marques,[1] Paul Régnier,[1] (ID) Anna Maciejewski-Duval,[1] Clara Richard de Vesvrotte,[2] Thomas Vazquez,[3] Camille Montardi,[4] Bénédicte Manoury,[5] Karim Dorgham,[6] Cloé Comarmond,[7] Arsène Mekinian,[8] (ID) Michelle Rosenzwajg,[9] Alexandre Le Joncour,[10] (ID) Matheus Vieira,[1] Georgina Maalouf,[10] (ID) Gaëlle Leroux,[10] Fanny Domont,[10] Anne-Claire Desbois,[10] Adrien Mirouse,[1] (ID) David Klatzmann,[3] (ID) J. E. Gottenberg,[11] Patrice Cacoub,[1] (ID) and David Saadoun[1]

Objective. Patients with primary Sjögren disease (pSD) are prone to develop non-Hodgkin lymphoma (NHL), but relevant biomarkers are lacking. We aimed to determine new biomarkers predictive of NHL in patients with pSD.

Methods. Two hundred six patients with pSD fulfilling American College of Rheumatology/EULAR 2016 criteria were included and divided into three groups: pSD, lymphoproliferative pSD (Arl-pSD), and NHL-pSD. Deep flow cytometry immunophenotyping of B and T cell compartments as well as serum interferon-α (IFNα) quantification were coupled to clinical, biologic, and histopathologic data analysis.

Results. We identified CD11c$^+$ FcRL5$^+$ tissue-like memory B cells and IFNγ$^+$ TNFα$^+$ conventional T cells as significantly associated with NHL in pSD. These clusters showed progressive enrichment in Arl-pSD and NHL-pSD as compared to pSD. The combination of these two population abundances discriminates patients with NHL-pSD with a sensitivity of 78.9% and a specificity of 76.8%, thus overcoming alone the performance of the sum of conventional clinical and biologic markers such as cryoglobulinemia vasculitis, parotid enlargement, adapted clinical EULAR Sjögren's Syndrome Disease Activity Index, rheumatoid factor antibodies, low C4 and elevated serum IFNα levels (68.4% and 78.0%, respectively). CD11c$^+$ FcRL5$^+$ tissue-like memory B cells were associated with occurrence of mucosa-associated lymphoid tissue (MALT) marginal-zone NHL, whereas IFNγ$^+$ TNFα$^+$ conventional T cells were more indicative of non-MALT B cell NHL.

Conclusion. We unveil novel biomarkers of NHL in pSD based on an integrative analysis coupling deep immunophenotyping and clinical, biologic, and histopathologic data. Furthermore, these markers allow distinguishing B cell NHL subtypes in pSD.

INTRODUCTION

Primary Sjögren disease (pSD) is a systemic autoimmune disease characterized by lymphoid infiltration of salivary and lacrimal glands. The most severe systemic complication concerning patients with pSD is the development of B cell lymphoma, which occurs in 5% to 10% of patients. The risk is estimated to be 15 to 20 times higher than that of the general population.[1–3] pSD is then one of the most relevant models for studying the links between autoimmunity and lymphomagenesis. The subtypes of pSD-related lymphoma include non-Hodgkin B cell lymphoma (NHL), with a predominance of marginal-zone lymphoma (MZL),

which arises in mucosa-associated lymphoid tissue (MALT) primarily involving extranodal sites, such as salivary glands and parotid glands.[4–7] Diffuse large cell B cell lymphoma (DLBCL), an aggressive B cell lymphoma, represents the second most common subtype develop by patients with pSD. DLBCL might occur either as de novo or by transformation of an indolent MZL, given the clonal relationship identified between these two types.[8,9]

Current pathophysiologic models describe abnormal activation of mucosal epithelial cells by a trigger not yet identified. Such persistent innate and adaptive immune system stimulation leads to the dysregulated production of antinuclear, anti-Ro/SSA, anti-La/SSB, and rheumatoid factor (RF) autoantibodies, resulting in the formation and accumulation of immune complexes (ICs). These ICs amplify the production of interferon-α (IFNα), a crucial cytokine in the pathophysiology, via endogenous activation of plasmacytoid dendritic cells[10] that could cause the chronic stimulation of autoreactive clonal RF B cells, which are enriched within the infiltrated tissues and are a potential source of prelymphomatous B cells.[11–13] Such a clonal B cell population is thought to represent a key component in the complex process leading to tumor escape. A correlation has been established between NHL-pSD and the presence of anergic, clonal, and autoreactive CD21$^{-/low}$ B cells. These B cells mainly produce autoantibodies and display somatic hypermutation profiles, which is characteristic of a strong and long-lasting selection by autoantigens, suggesting that they can represent the actual source of prelymphomatous B cells in pSD.[14,15]

Risk factors for NHL-pSD include a combination of clinical, biologic, and pathologic features mainly reflecting the B cell hyperactivation. These markers include permanent swelling of salivary glands, lymphadenopathy, splenomegaly, cryoglobulinemia vasculitis (CryoVas), elevated EULAR Sjögren's Syndrome Disease Activity Index (ESSDAI), CD4 T cell lymphopenia reflected by a CD4/CD8 T cell ratio ≤0.8, C4 consumption, hypergammaglobulinemia, monoclonal gammopathy, and RF autoantibodies, as well as pathologic evidence of a high focus score and local organizations in tertiary lymphoid structures in minor salivary gland biopsy samples.[16–21] These elements are neither sensitive nor specific enough, alone or in combination, for the detection of patients with pSD at a higher risk of lymphoma. Patients with pSD presenting one or more of these markers are numerous, forming a very heterogeneous group from which it is tremendously difficult to distinguish those at risk for developing lymphoma.

Only a few studies have evaluated the relevance of deep immunophenotyping for the prediction of NHL in patients with pSD. To determine new biomarkers predictive of NHL in pSD, we initiated the generation of this study involving 206 patients with pSD fulfilling American College of Rheumatology (ACR)/EULAR 2016 criteria,[22] which was divided into three groups: pSD, lymphoproliferative pSD (Arl-pSD), and NHL-pSD. Deep flow cytometry immunophenotyping of B and T cell compartments, coupled with clinical, biologic, and histopathologic data analysis, was performed systematically. We also quantified IFNα because of its important role in the pathophysiology of pSD, which is supported by previous work focusing on lymphoma and Sjögren disease showing up-regulation of IFN genes in Sjögren patients with lymphoma. although this associationhas not been specifically proven yet.[23] Unsupervised and supervised analyses were conducted in this work with the purpose of (1) identifying clusters of NHL-pSD patients along with their shared and specific cell parameters and (2) characterizing potential biomarkers of NHL in pSD.

MATERIALS AND METHODS

Patients. We successively included patients with pSD observed at the Department of Internal Medicine at Pitié-Salpêtrière Hospital, Paris, France, between April 2007 and September 2022. All patients met the ACR/EULAR 2016 criteria[22] for pSD. Clinical, biologic, histopathologic and therapeutic regimen data were collected. The items of the ESSDAI score, the reference score for rating disease activity, were collected at inclusion. We established an adapted clinESSDAI, corresponding to a clinESSDAI as defined by Seror et al (which features removal of the biologic domain and modification of weighting of certain domains[24]), without the "lymphadenopathy" domain. Patients with pSD were divided into three groups based on their lymphoproliferative status. The nonlymphoproliferative pSD group (named pSD) included patients with pSD without clinical or biologic features of lymphoproliferation. The at risk of lymphoma pSD (Arl-pSD) group consisted of patients with at least one clinical or biologic feature of lymphoproliferation on the day of inclusion and/or at any time

Immunopathology-Biotherapy Department, Groupe Hospitalier de la Pitié-Salpêtrière, AP-HP, Paris, France; [10]Alexandre Le Joncour, MD, PhD, Georgina Maalouf, MD, Gaëlle Leroux, MD, Fanny Domont, MD, Anne-Claire Desbois, MD, PhD: Department of Internal Medicine and Clinical Immunology, Groupe Hospitalier Pitié-Salpêtrière, AP-HP, Sorbonne Université and Centre de Référence des Maladies Auto-Immunes Systémiques Rares, Centre de Référence des Maladies Auto-Inflammatoires et de l'Amylose inflammatoire, Paris, France; [11]J. E. Gottenberg, MD, PhD: Rheumatology Department, EA 3432, Hôpitaux Universitaires de Strasbourg, Université de Strasbourg, Strasbourg, France.

Drs Marques and Régnier contributed equally to this work.
Cindy Marques and Paul Régnier are co first authors.

during the course of the disease as follows: clinical features included parotid enlargement, lymphadenopathy, splenomegaly, and CryoVas; biologic features included hypergammaglobulinemia (>20 g/L), monoclonal gammopathy, cryoglobulinemia, RF antibodies (>15 IU/mL), and C4 consumption (<0.16 g/L). The lymphoma-associated pSD (NHL-pSD) group included patients with histologically confirmed previous or current lymphoma associated with pSD. At inclusion, patients were randomly assigned to two distinct cohorts defined as the "discovery" set and the "validation" set. Patient characteristics were compared using Fisher's exact test for qualitative variables and Student's *t*-test for quantitative values. The study was approved by the local ethics committee of Pitié-Salpêtrière Hospital – CPP-IV Ile de France and was conducted in accordance with the Declaration of Helsinki. All participants provided written informed consent. Patients and the public were not involved in this research. Deidentified patients' data and statistical analysis are available upon reasonable request to the corresponding author.

Mouse G6 antibody production and labeling. Mouse G6 antibody is an anti-idiotypic monoclonal antibody discovered in a screen against RFs that selectively binds to IGHV1-69 heavy-chain germline gene 51p1 alleles and is highly expressed in several B cell malignancies and autoimmune diseases.[25,26] IGHV1-69 was recently shown to be expressed by extranodal MZL clonotypes in pSD.[13] It was produced in the Monoclonal Antibody Production Unit of the Clinical Immunology Service of University of Birmingham and conjugated to Qdot 655 fluorochrome using the SiteClick Antibody Labeling Kit (ThermoFisher Scientific) according to the manufacturer's instructions.

Flow cytometry data acquisition. Peripheral blood mononuclear cells were obtained by Ficoll separation and were stained for 30 minutes at 4°C with monoclonal antibodies listed in Supplementary Table 1. Cells were stained for cell surface markers, then permeabilized with the Intracellular Fixation & Permeabilization Buffer Set (eBioscience, 88-8824-00) and then stained with intracellular markers according to the manufacturer's instructions for 30 minutes at 4°C. Sample acquisitions were performed on a BD LSR Fortessa SORP (BD Biosciences) and a CytoFLEX LX (Beckman Coulter) flow cytometer. To make the staining and acquisition protocols feasible and reproducible, samples were independently processed in 19 different batches on the same cytometer using the same acquisition template (which includes channel gains and compensations) that was created for the first batch.

IFNα quantification. Serum IFNα was quantified using the SIMOA IFNα Advantage Kit on an HD-1 analyzer (Quanterix) following the manufacturer's instructions. The IFNα concentration in the samples was interpolated from the calibration curve by multiplying it by the dilution factor. Final concentrations were then expressed in pg/mL. Samples with nondetectable values were evaluated according to the limit of detection value; samples above the detection range were replaced by the upper limit of quantification as previously described.[27]

Statistical analysis. *Flow cytometry data.* Flow cytometry data (flow cytometry standard [FCS] format) from all groups were first imported into FlowJo version 10.9, in which compensations were optimally adjusted, and lymphocyte-shaped single cells were exported to facilitate the subsequent analysis. Then newly exported FCS files for both T and B panels were opened, processed, and analyzed using the *PICAFlow* R package, which we had previously developed for the unsupervised and semiautomated analysis of flow/mass cytometry data.[28] The package allows one to control/correct the compensation matrix, to transform each channel of the data set, and to remove batch/run effects for each channel of the data set using the *GaussNorm* method. As the frequency of NHL-pSD among all patients with Sjögren disease was rather low, a full randomized cohort generation would have led to severe disbalance of the patients with NHL-pSD between the cohorts, which would have impaired the precision and robustness of our unsupervised analysis. To avoid this problem, the two generated subcohorts (discovery and validation) were constructed to be identical in size (n = 103 for each), to contain the same number of patients from each group (pSD, Arl-pSD, and NHL-pSD), and to present similar clinical features, as shown in Table 1. Of note, the whole flow cytometry data processing and analysis through *PICAFlow* was performed independently on these two subcohorts. Results are presented as scatter plots showing the median with the 95% confidence interval, and differences between groups of interest (pSD, Arl-pSD, and/or NHL-pSD) were assessed with either Kruskal-Wallis or Dunn tests.

Other statistical analyses. Receiver operating characteristic (ROC) curves were calculated using the *ROCit* R package with the *empirical* method and default parameters. Log2 fold change (Log2FC) values were computed using the median of the associated series as metric. We used either Fisher's exact test for categorical values (the first six items of the subfigure) or the Mann-Whitney test for the continuous values (the last four items of the subfigure). *P* values were corrected using the Benjamini-Hochberg methodology. Adjusted *P* values <0.05 were deemed significant.

RESULTS

Characteristics of patients with pSD. Two hundred six patients with pSD were included, comprising 88 with pSD, 99 with Arl-pSD, and 19 with NHL-pSD (Table 1); 185 (89.8%) were women, the median age was 58 years (interquartile range 20 years), and 125 (62.8%) were White. Two independent cohorts were formed simultaneously, with no statistically significant differences in clinical, biologic, pathologic, and therapeutic data (Supplementary Table 2). The discovery set

Table 1. Characteristics of patients with pSD*

	pSD (n = 88)	Arl-pSD (n = 99)	NHL-pSD (n = 19)	Total (n = 206)
General features				
Age, median (IQR), y	58.0 (21)	54 (20.5)	60 (17)	58 (20)
Female, n (%)	81 (93.1)	89 (89.9)	14 (73.7)	185 (89.8)
Ethnic group, n (%)				
White	68 (79.1)	46 (47.4)	11 (57.9)	125 (62.8)
Other	18 (20.9)	51 (52.6)	8 (42.1)	74 (37.2)
Body mass index, median (IQR)	25.1 (7.5)	23.9 (7.9)	23 (6.5)	24.6 (7.8)
Tobacco chronic exposure, n (%)	13 (15.9)	31 (13.8)	7 (41.2)	42 (21.8)
Prolonged alcohol exposure, n (%)	4 (4.9)	3 (3.2)	1 (5.9)	8 (4.1)
Sjögren features				
Disease duration, median (IQR), mo	49 (104)	48.5 (107.5)	40 (171)	48 (108.5)
Oral dryness, n (%)	73 (85.9)	72 (83.7)	15 (88.2)	172 (86)
Ocular dryness, n (%)	75 (88.2)	73 (84.9)	15 (88.2)	175 (87.5)
Anti-SSA antibodies, n (%)	37 (45.1)	73 (75.3)	14 (82.4)	124 (63.3)
Anti-SSB antibodies, n (%)	13 (15.9)	45 (46.4)	7 (41.2)	65 (33.2)
Salivary gland Chisholm stage III or IV, n (%)	45 (71.4)	48 (66.7)	13 (92.9)	106 (71.1)
Salivary gland focus score, median (IQR)	1.0 (0.89)	1.0 (1.03)	2.4 (2)	1 (1.1)
Organ involvement, n (%)				
Constitutional symptoms	10 (11.9)	27 (27.6)	13 (76.5)	50 (25.1)
Enlarged parotid	0 (0)	24 (24.5)	4 (23.5)	28 (14)
Lymphadenopathy	1 (1.2)	22 (22.5)	4 (23.5)	27 (13.5)
Splenomegaly	0 (0)	4 (4.1)	1 (5.9)	5 (2.5)
Articular	43 (50.6)	65 (66.3)	9 (52.9)	117 (58.5)
Cutaneous and/or vascular	0 (0)	47 (48.0)	13 (76.5)	81 (40.5)
Pulmonary	7 (8.2)	22 (22.5)	2 (11.8)	31 (15.5)
Renal	0 (0)	5 (5.1)	2 (11.8)	7 (3.5)
Muscular	3 (3.5)	8 (8.2)	1 (5.9)	12 (6)
Peripheral nervous system	27 (31.8)	20 (20.4)	10 (58.8)	57 (28.5)
Central nervous system	5 (5.9)	8 (8.2)	2 (11.8)	15 (7.5)
Hematologic	2 (2.4)	17 (17.4)	7 (41.2)	26 (13)
Lymphoma	0 (0)	0 (0)	19 (100)	19 (9.4)
Adapted clinESSDAI score at visit, median (IQR)	3.0 (5)	6.0 (12)	15.0 (12)	5 (11.8)
Biologic features				
Hemoglobin, median (IQR), g/dL	13.5 (1.2)	12.8 (1.3)	11.5 (1.6)	13 (2)
Platelet count, median (IQR), 10^9/L	253 (71)	250 (79)	262 (78)	252 (80)
Lymphocyte count, median (IQR), 10^9/L	1.6 (0.8)	1.4 (0.9)	1.2 (0.8)	1.5 (9.2)
Serum creatinine level, median (IQR), μmol/L	66 (17)	68 (17)	68 (23)	68 (18)
Rheumatoid factor > 15 IU/mL, n (%)	1 (1.4)	45 (51.7)	11 (73.3)	63 (36.6)
C3 < 0.82 g/L, n (%)	4 (5.5)	15 (17.2)	3 (21.4)	22 (12.6)
C4 < 0.16 g/L, n (%)	10 (13.7)	21 (24.1)	10 (62.5)	41 (23.4)
Cryoglobulinemia, n (%)	0 (0)	13 (14.3)	4 (26.7)	17 (9.4)
Gamma globulins, median (IQR), g/L	10.5 (3.3)	13.8 (6.7)	18.0 (5)	12 (5.6)
Previous treatments, n (%)				
Plaquenil	41 (49.4)	49 (50.5)	10 (62.5)	100 (51)
Glucocorticoids	26 (31.0)	36 (37.1)	14 (82.4)	76 (38.4)
Immunosuppressors	21 (24.1)	23 (23.7)	9 (52.9)	55 (27.9)
Rituximab	1 (1.2)	6 (6.1)	8 (47.1)	15 (7.6)
Treatments at visit				
Plaquenil, n (%)	32 (38.1)	34 (35.8)	8 (47.1)	74 (37.8)
Glucocorticoids, n (%)	19 (22.6)	28 (29.2)	8 (47.1)	55 (27.9)
Glucocorticoids dose (equivalent prednisone), median (IQR), mg/L	5.5 (2)	10 (8.5)	10 (9)	8 (5)
Immunosuppressors, n (%)	6 (7.1)	21 (21.9)	5 (29.4)	26 (13.2)
Rituximab, n (%)	0 (0)	0 (0)	3 (17.6)	3 (1.5)
Time since last rituximab infusion, median (IQR), mo	NA	NA	1 (1–25)	1 (1–25)

* Arl-pSD, lymphoproliferative pSD; clinESSDAI, clinical EULAR Sjögren's Syndrome Disease Activity Index; IQR, interquartile range; NA, nonapplicable; NHL, non-Hodgkin lymphoma; pSD, primary Sjögren disease.

included 44 patients with pSD, 49 with Arl-pSD, and 10 with NHL-pSD, and the validation set included 44 patients with pSD, 50 with Arl-pSD, and 9 with NHL-pSD. We used clinical (ie, parotid enlargement, lymphadenopathy, splenomegaly, CryoVas) and biologic (ie, hypergammaglobulinemia, RF positivity, low C4 level, and cryoglobulinemia) well-described markers of lymphoproliferation in pSD to perform the clustering of the whole cohort using the Uniform Manifold Approximation and Projection (UMAP) dimensionality reduction method (Figure 1A). The overlays of logarithm-transformed IFNα levels and a focus score greater than 1 are represented in Figure 1B.

Supervised and unsupervised analysis of B lymphocytes panel. We first analyzed the sets in a supervised manner to focus on 10 well-described B cell populations

(Figure 2A). We extracted the median percentage of each cell population among the total B cells and then represented the differences as Log2FC for the Arl-pSD and NHL-pSD groups, considering pSD as the reference (Figure 2B). We observed that only atypical memory B cells (AtMs) and tissue-like memory B cells (TLMs), two B cell populations well described in autoimmune and lymphoproliferative diseases, presented a linear and continuous accumulation through the Arl-pSD and NHL-pSD groups in both the discovery and validation data sets (Supplementary Figure 1A). Then, to confirm and explore further the phenotype observed in the supervised approach based on "classical gating," we proceeded with unsupervised analyses of the FCS files obtained from the cytometer using the *PICAFlow* R package.[28] We used UMAP dimensionality reduction as well as hierarchical clustering to establish a finite number of B cell clusters for
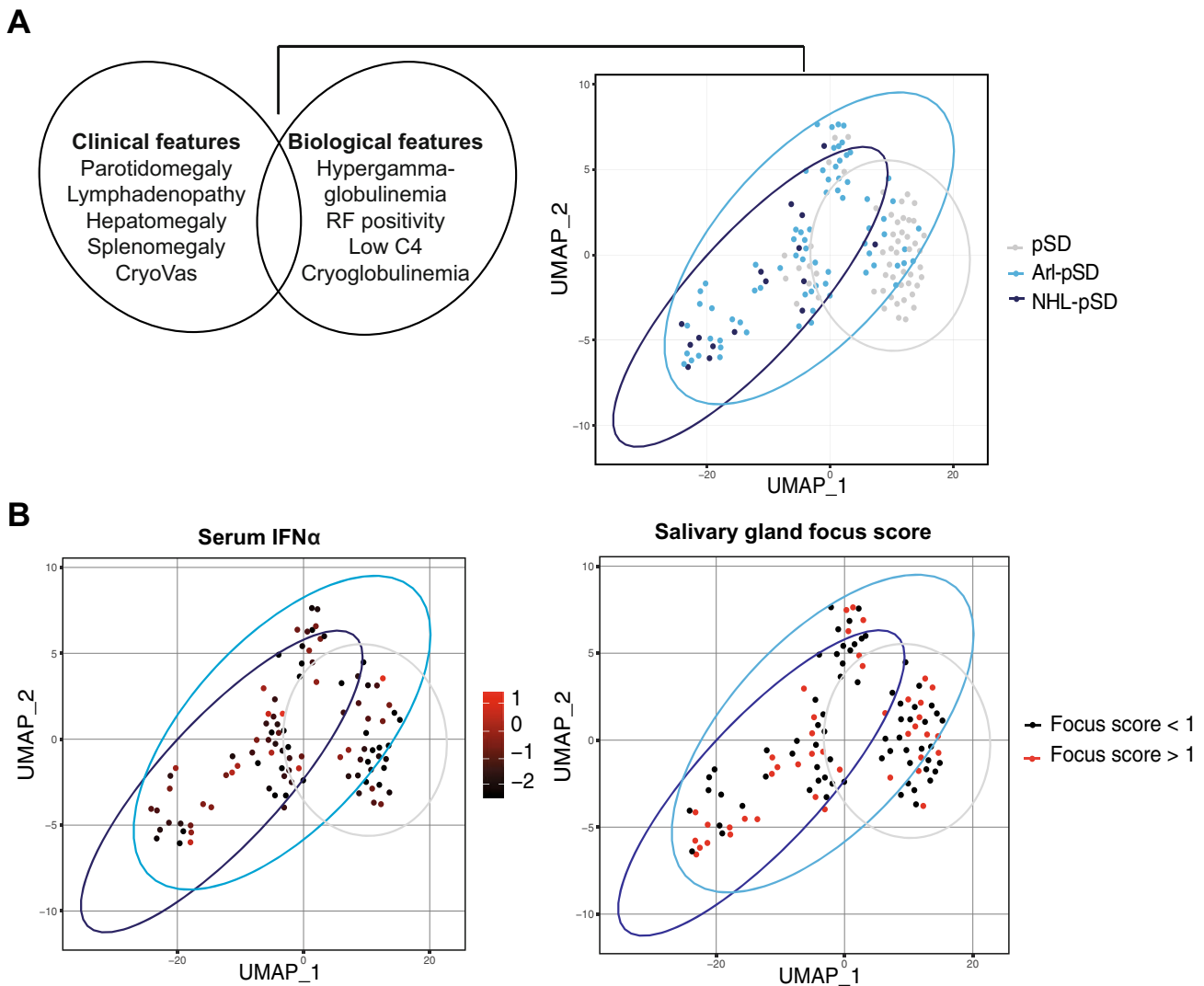
Figure 1. Clustering analysis in a cohort with pSD. (A) Clustering of the entire cohort using the UMAP) dimensionality reduction method, incorporating clinical and biologic markers of lymphoproliferation in pSD. (B) Overlays of logarithm-transformed IFNα levels and a focus score greater than 1. Arl-pSD, lymphoproliferative pSD; CryoVas, cryoglobulinemia vasculitis; IFNα, interferon-α; NHL, non-Hodgkin lymphoma; pSD, primary Sjögren disease; RF, rheumatoid factor; UMAP, uniform manifold approximation and projection.
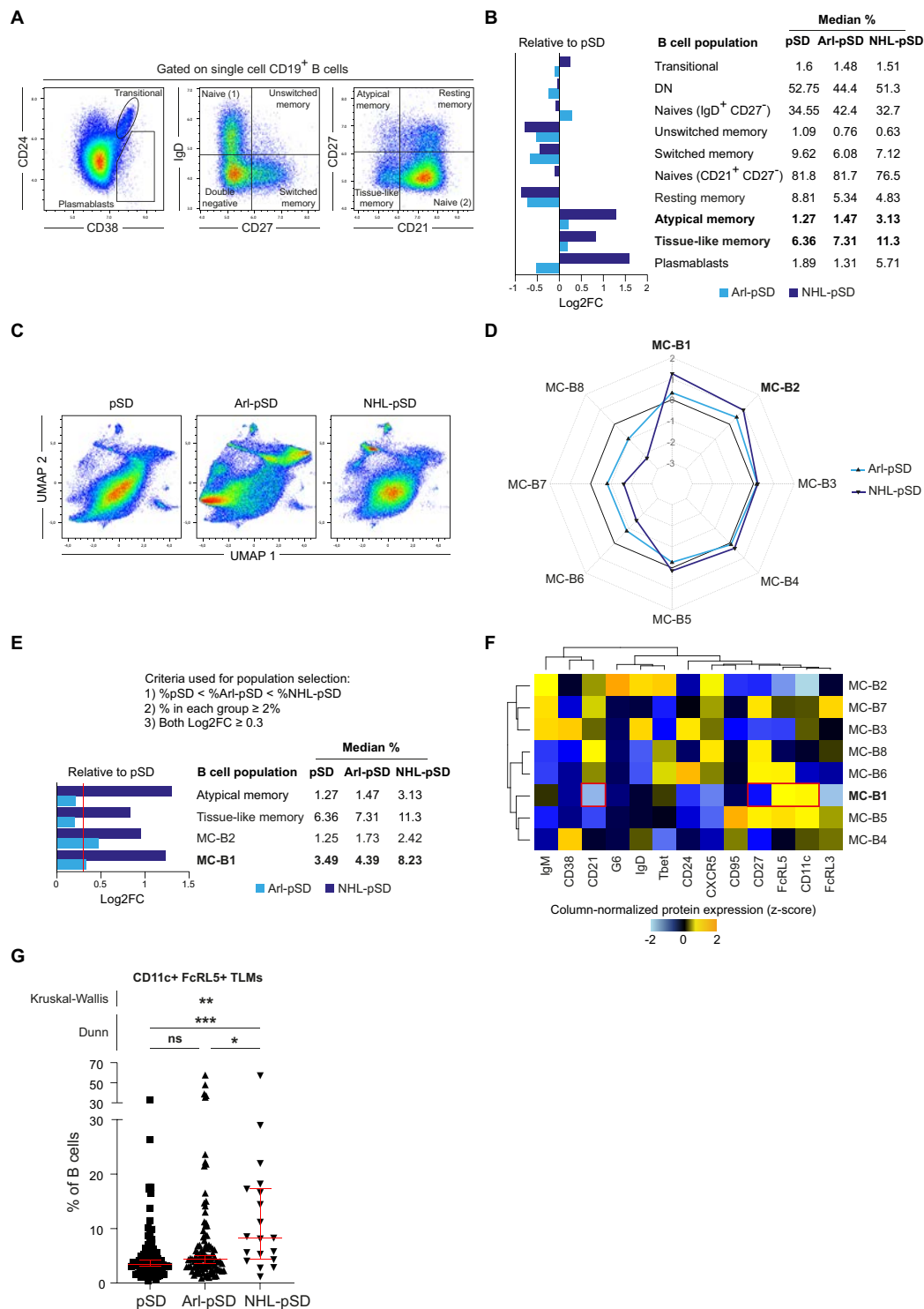
Figure 2. B cell populations analysis in pSD. (A) Supervised analysis of 10 well-described B cell populations. (B) Median percentage of each B cell population among total B cells, presented as Log2FC for Arl-pSD and NHL-pSD, using pSD as the baseline. (C) Unsupervised analysis of flow cytometry standard files using in-house developed R scripts, applying UMAP dimensionality reduction and hierarchical clustering to define B cell clusters in pSD, Arl-pSD, and NHL-pSD groups. (D) Identification of eight distinct B cell clusters (MC-B1 to MC-B8), with Log2FC computation between the reference group (pSD) and others (Arl-pSD or NHL-pSD). (E) Comparison of identified B cell populations according to criteria for defining relevant populations in discriminating pSD, Arl-pSD, and NHL-pSD. (F) Characterization of MC-B1 phenotype, identifying CD21$^-$ CD27$^-$ CD11c$^+$ FcRL5$^+$ B cells, defined as CD11c$^+$ FcRL5$^+$ TLMs. (G) Progressive increase of CD11c$^+$ FcRL5$^+$ TLMs through lymphoproliferative stages. *$P < 0.05$; **$P < 0.01$; ***$P < 0.001$. Arl-pSD, lymphoproliferative pSD; DN, CD21 CD27 Double Negative B cells; Log2FC, log2 fold change; NHL, non-Hodgkin lymphoma; pSD, primary Sjögren disease; TLM, tissue-like memory B cell; UMAP, uniform manifold approximation and projection. Color figure can be viewed in the online issue, which is available at http://onlinelibrary.wiley.com/doi/10.1002/art.43207/abstract.

the pSD, Arl-pSD, and NHL-pSD groups (Figure 2C). We finally obtained eight distinct B cells clusters (labeled from MC-B1 to MC-B8) for which we computed the Log2FC between the reference group (pSD) and the others (either Arl-pSD or NHL-pSD) (Figure 2D).

We performed the analysis workflow separately on the discovery and the validation sets and only kept the clusters that had matching phenotypes in these two data sets. Among these eight clusters, MC-B1 and MC-B2 showed a progressive enrichment through lymphoproliferation. Then we decided to compare the performance of AtMs, TLMs, MC-B1, and MC-B2. We applied three criteria to define a population as relevant in discriminating pSD, Arl-pSD, and NHL-pSD (Figure 2E): (1) the abundance of the cluster should linearly progress through lymphoproliferation (percentage pSD < percentage Arl-pSD < percentage NHL-pSD); (2) the abundance of the cluster in each group should be at least 2%; and (3) the Log2FC between pSD and Arl-pSD and between pSD and NHL-pSD should be at least 0.3, thus representing an ≈23% to 24% increase. MC-B1 was the only cluster to meet all these criteria and was thus considered as the most potent parameter in discriminating pSD, Arl-pSD, and NHL-pSD. The MC-B1 cluster phenotype corresponded to $CD21^-$ $CD27^-$ $CD11c^+$ $FcRL5^+$ B cells, defined as $CD11c^+$ $FcRL5^+$ TLMs (Figure 2F, Supplementary Figure 2C and 2E). Thus, the unsupervised clustering confirmed the expansion of TLMs in NHL-pSD observed in the supervised analysis and refined the phenotype of these TLMs by identifying CD11c and FcRL5 as positive membranous markers. The proportion of $CD11c^+$ $FcRL5^+$ TLMs gradually increased through lymphoproliferation, representing a median of 3.49% of B cells in pSD, 4.39% of B cells in Arl-pSD, and 8.23% of B cells in NHL (Figure 2G and Supplementary Figure 2G).

Supervised and unsupervised analysis of T lymphocytes panel. The same workflow was then performed on the T panel. We first analyzed 10 different T cell populations (Figure 3A and B). We observed that Th1, Th2, Th17, and Th17.1 cells presented a linear and progressive accumulation through the Arl-pSD and NHL-pSD groups in both the discovery and validation data sets (Supplementary Figure 1B). Again using the *PICAFlow* R package,[27] we extracted the two UMAP dimensions for the pSD, Arl-pSD, and NHL-pSD groups (Figure 3C) and obtained six distinct T cells clusters (labeled from MC-T1 to MC-T6) for which we computed the Log2FC between the reference group (pSD) and the other ones (either Arl-pSD or NHL-pSD) (Figure 3D). Among these six clusters, only MC-T1 and MC-T2 showed a progressive enrichment through lymphoproliferation. Hereafter, we decided to compare the performance of Th1, Th2, Th17, Th17.1, MC-T1, and MC-T2 clusters. We applied the same three previously described criteria to define a population as relevant (Figure 3E). MC-T1, defined as $IFN\gamma^+$ $TNF\alpha^+$ conventional T cells, was the only cluster to meet all these criteria

(Figure 3F, Supplementary Figures 3D and 2D). The proportion of $IFN\gamma^+$ $TNF\alpha^+$ conventional T cells progressively increases through lymphoproliferation, representing a median of 2.58% of T cells in pSD, 3.47% of T cells in Arl-pSD, and 6.55% of T cells in NHL-pSD (Figure 3G and Supplementary Figure 2H).

ROC analysis. We compared the performance of $CD11c^+$ $FcRL5^+$ TLMs and $IFN\gamma^+$ $TNF\alpha^+$ conventional T cells with previously known markers for identifying NHL-pSD among patients with pSD in the whole cohort. We established ROC curves for clinical (ie, parotid enlargement, splenomegaly, lymphadenopathy, CryoVas, adapted clinESSDAI) and biologic (ie, hypergammaglobulinemia, RF antibodies, low C4 level, cryoglobulinemia) items, analyzed as qualitative variables, as well as for salivary gland biopsy focus scores and the serum IFNα levels, analyzed as quantitative variables. The sum of all those items reached a sensitivity of 68.4% and a specificity of 78.0% (Figure 4A). The $CD11c^+$ $FcRL5^+$ TLM abundance reached a sensitivity of 73.7% and a specificity of 67.3%, and the $IFN\gamma^+$ $TNF\alpha^+$ conventional T cell abundance shown a sensitivity of 73.7% and a specificity of 68.5%. Thus, the isolated sum of both biomarkers alone led to a sensitivity of 78.9% and a specificity of 76.8% (Figure 4B). Similarly, we generated the ROC curve of the sum of clinical, biologic, and histopathologic items (Figure 4A) in addition to $CD11c^+$ $FcRL5^+$ TLM and $IFN\gamma^+$ $TNF\alpha^+$ conventional T cell abundances (Figure 4B), ultimately reaching a sensitivity of 89.5% and a specificity of 72.0% (Figure 4C).

Clustering of patients with NHL-pSD. Next, we assessed the performance of $CD11c^+$ $FcRL5^+$ TLM and $IFN\gamma^+$ $TNF\alpha^+$ conventional T cell abundances alone by stratifying patients. We computed UMAP dimensional reduction using only $CD11c^+$ $FcRL5^+$ TLM and $IFN\gamma^+$ $TNF\alpha^+$ conventional T cell abundances for each patient of our cohort and plotted the resulting two UMAP dimensions (Figure 5A). Unexpectedly, three different clusters emerged: C1, which showed low abundance of $CD11c^+$ $FcRL5^+$ TLMs and $IFN\gamma^+$ $TNF\alpha^+$ conventional T cells (Figure 5B, left); C2, which showed high abundance of $CD11c^+$ $FcRL5^+$ TLMs but low abundance of $IFN\gamma^+$ $TNF\alpha^+$ conventional T cells; and C3, which showed low abundance of $CD11c^+$ $FcRL5^+$ TLMs but high abundance of $IFN\gamma^+$ $TNF\alpha^+$ conventional T cells. Fourteen of the 19 patients with NHL-pSD (73.7%) clustered in C2 (n = 7) or C3 (n = 7). Interestingly, biologic, clinical, and histopathologic features of C2 and C3 patients highly differed (Figure 5C). C2 was enriched in patients with "classical" B cell proliferation clinical (ie, CryoVas, lymphadenopathy, parotid enlargement) and biologic (ie, low C4 level, RF positivity) markers. C2 patients also presented higher ESSDAI scores, higher salivary gland focus scores, and higher IFNα serum levels than C3 patients.

We then focused our analysis on patients with NHL-pSD across C2 and C3 clusters. The proportion of them having MALT NHL was higher in the C2 NHL-pSD group than in the C3 NHL-pSD group (85.7% vs 14.3%; $P \approx 0.087$). In comparison to C3 patients with
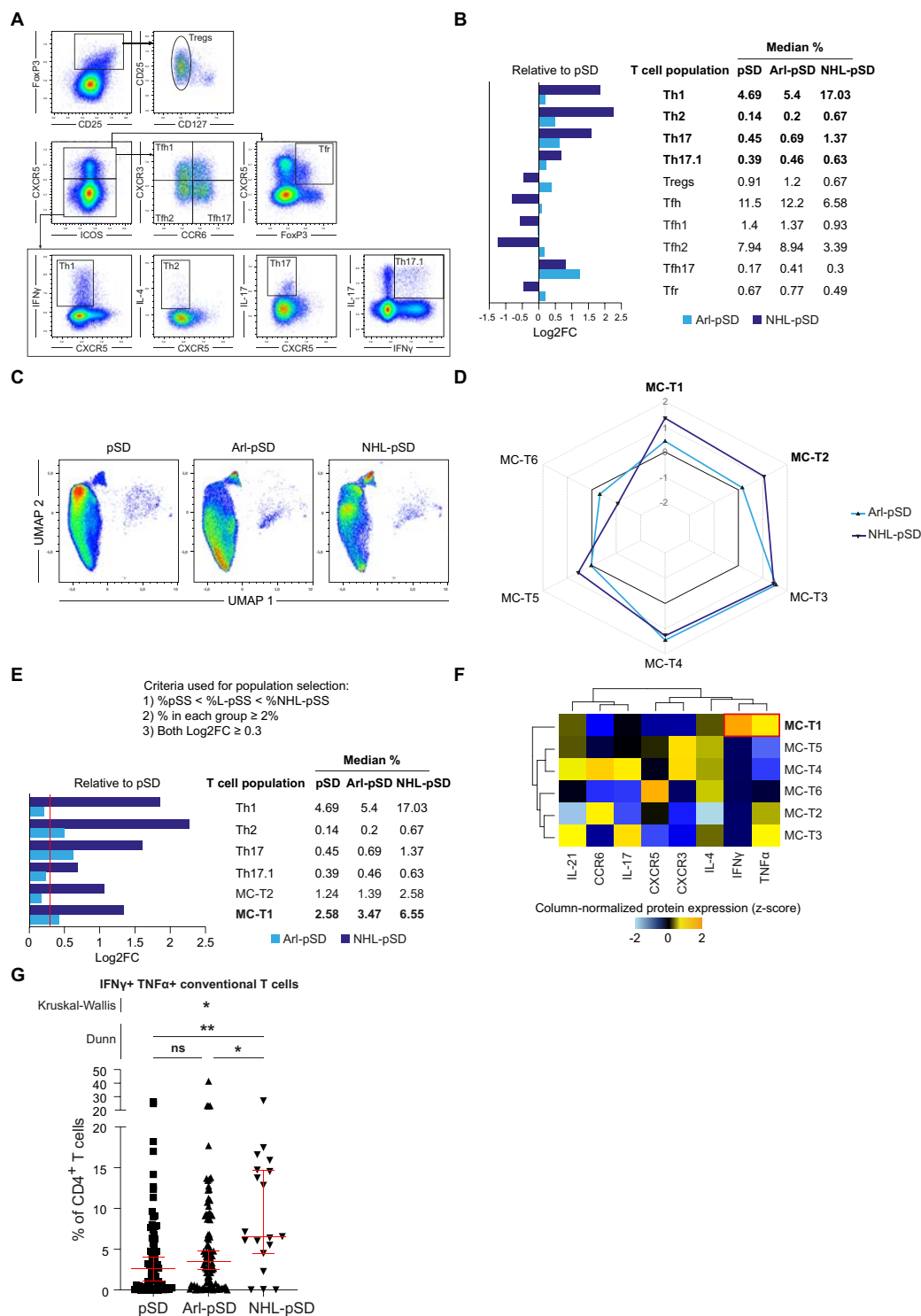
Figure 3. T cell populations analysis in pSD. (A) Supervised analysis of 10 different T cell populations. (B) Median percentage of each T cell population among total T cells, presented as Log2FC for Arl-pSD and NHL-pSD, using pSD as the baseline. (C) Unsupervised analysis of flow cytometry standard files using in-house developed R scripts, applying UMAP dimensionality reduction and hierarchical clustering to define B cell clusters in pSD, Arl-pSD, and NHL-pSD groups. (D) Identification of six distinct T cell clusters (MC-T1 to MC-T6), with Log2FC computation between the reference group (pSD) and others (Arl-pSD or NHL-pSD). (E) Comparison of identified T cell populations according to criteria for defining relevant populations in discriminating pSD, Arl-pSD, and NHL-pSD. (F) Characterization of MC-T1 phenotype, defined as IFNγ⁺ TNFα⁺ conventional T cells, meeting all set criteria. (G) Progressive increase of IFNγ⁺ TNFα⁺ conventional T cells through lymphoproliferation stages. *$P < 0.05$; **$P < 0.01$. Arl-pSD, lymphoproliferative pSD; Log2FC, log2 fold change; L-pSD, lymphoproliferative primary Sjögren's disease; pSD, primary Sjögren's disease; UMAP, uniform manifold approximation and projection. Color figure can be viewed in the online issue, which is available at http://onlinelibrary.wiley.com/doi/10.1002/art.43207/abstract.
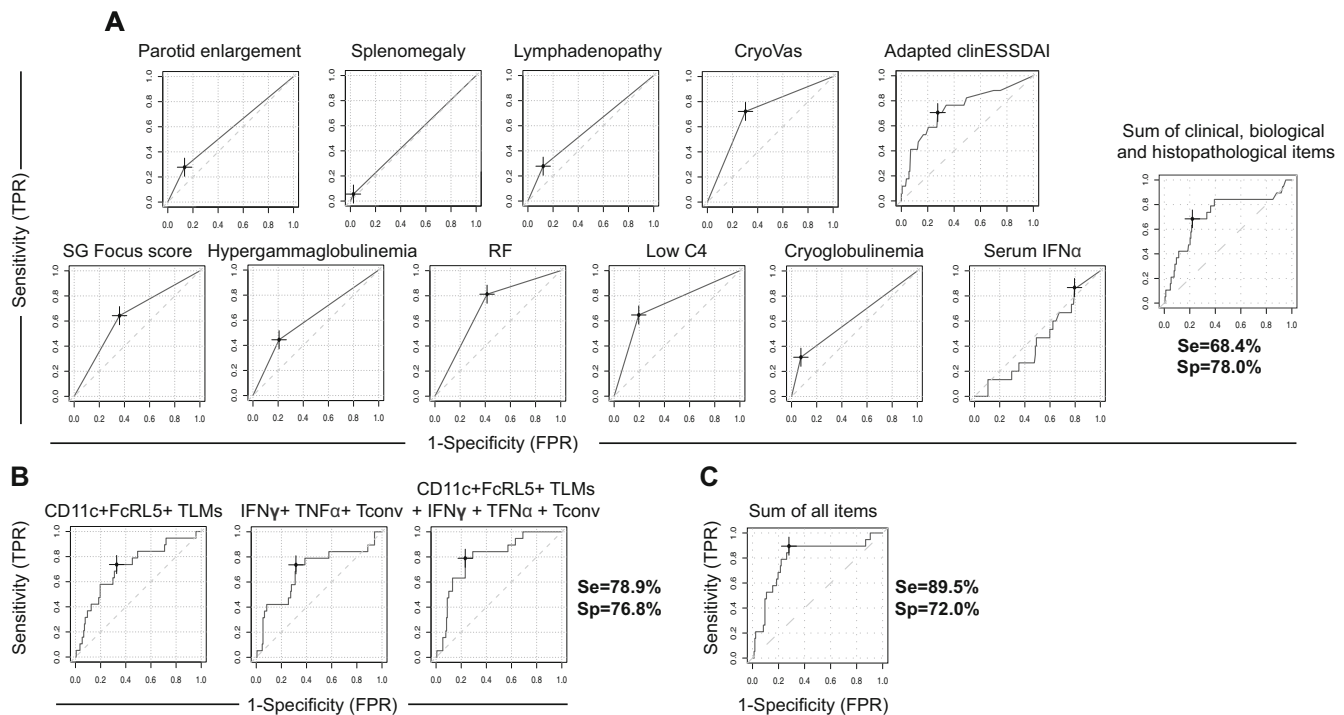
Figure 4. Evaluation of biomarkers in distinguishing patients with NHL-pSD from those with pSD. (A) ROC curves established for clinical and biologic markers. (B) Analysis of the cumulative abundance of CD11c⁺ FcRL5⁺ TLMs and IFNγ⁺ TNFα⁺ Tconv. (C) ROC curve for the sum of clinical, biologic, histopathologic items and the identified biomarkers. clinESSDAI, clinical EULAR Sjögren's Syndrome Disease Activity Index; CryoVas, cryoglobulinemia vasculitis; FPR, False Positive Rate; IFNα, interferon-α; NHL, non-Hodgkin lymphoma; pSD, primary Sjögren disease; RF, rheumatoid factor; ROC, receiver operating characteristic; Se, sensitivity; SG, salivary gland; Sp, specificity; Tconv, conventional T cells; TLM, tissue-like memory B cell; TPR, true positive rate.

NHL-pSD, C2 patients with NHL-pSD presented with more CryoVas (100% vs 57.1%; $P \approx 0.385$) and RF antibodies (100% vs 71.4%; $P \approx 0.592$) (Figure 5D). On the other hand, the patients with NHL-pSD from the C3 cluster were more prone to be male (42.9% vs 14.3%; $P \approx 0.592$) and more frequently showed anti-SSB antibody positivity (57.1% vs 28.6%; $P = 0.592$). C3 NHL-pSD included a center-like large B cell lymphoma, an Epstein-Barr virus–associated aggressive lymphoma, Waldenstrom's disease, a lymphoplasmacytic lymphoma, and two low-grade lymphomas. However, patients with NHL-pSD from both clusters seem to share some features, such as overall age, anti-SSA antibody positivity, and C4 consumption. Of note, patients with NHL-pSD from cluster C2 showed increased median abundance of CD11c⁺ FcRL5⁺ TLMs (18.2% vs 5.6%; $P = 0.0024$) and decreased median abundance of IFNγ⁺ TNFα⁺ conventional T cells (6.1% vs 15.9%; $P = 0.0024$) as compared to C3 patients with NHL-pSD. Also, C2 patients with NHL-pSD had increased median levels of serum IFNα as compared to C3 patients with NHL-pSD (0.037 vs 0.007 pg/mL; $P = 0.473$).

DISCUSSION

In this study, we described a large cohort of 206 patients with pSD, along with their demographic, clinical, biologic,

histopathologic, and immunologic data. First, we used the combination of several markers of lymphoproliferation traditionally described in the literature (ie, parotid enlargement, lymphadenopathy, splenomegaly, CryoVas, hypergammaglobulinemia, low C4 level, RF antibodies, cryoglobulinemia, and minor salivary gland biopsy focus score) to cluster patients with pSD. The association of each of these markers with lymphoma has been well described over the last decade in large series.[18,19,29,30] We also investigated serum IFNα level in our cohort, as literature already highlighted the IFN signature as a potential biomarker.[31] Although all the previously mentioned features were able to identify nonproliferative pSD, they were insufficient, even in combination, to delineate patients with NHL.

We aimed to use deep immunophenotyping of blood samples from patients with pSD to determine new biomarkers of NHL. We identified CD11c⁺ FcRL5⁺ TLMs and IFNγ⁺ TNFα⁺ conventional T cells as significantly associated with NHL in pSD. These two lymphocyte populations increased gradually and significantly during transition to lymphoma, representing a median of 8.23% of B lymphocytes and 6.55% of T lymphocytes in NHL (ie, 2.5 times more than in pSD without lymphoproliferation). The enrichment of these two populations was correlated with the conventional aforementioned clinical, biologic, and histopathologic markers predictive of lymphoma in pSD. Interestingly, the
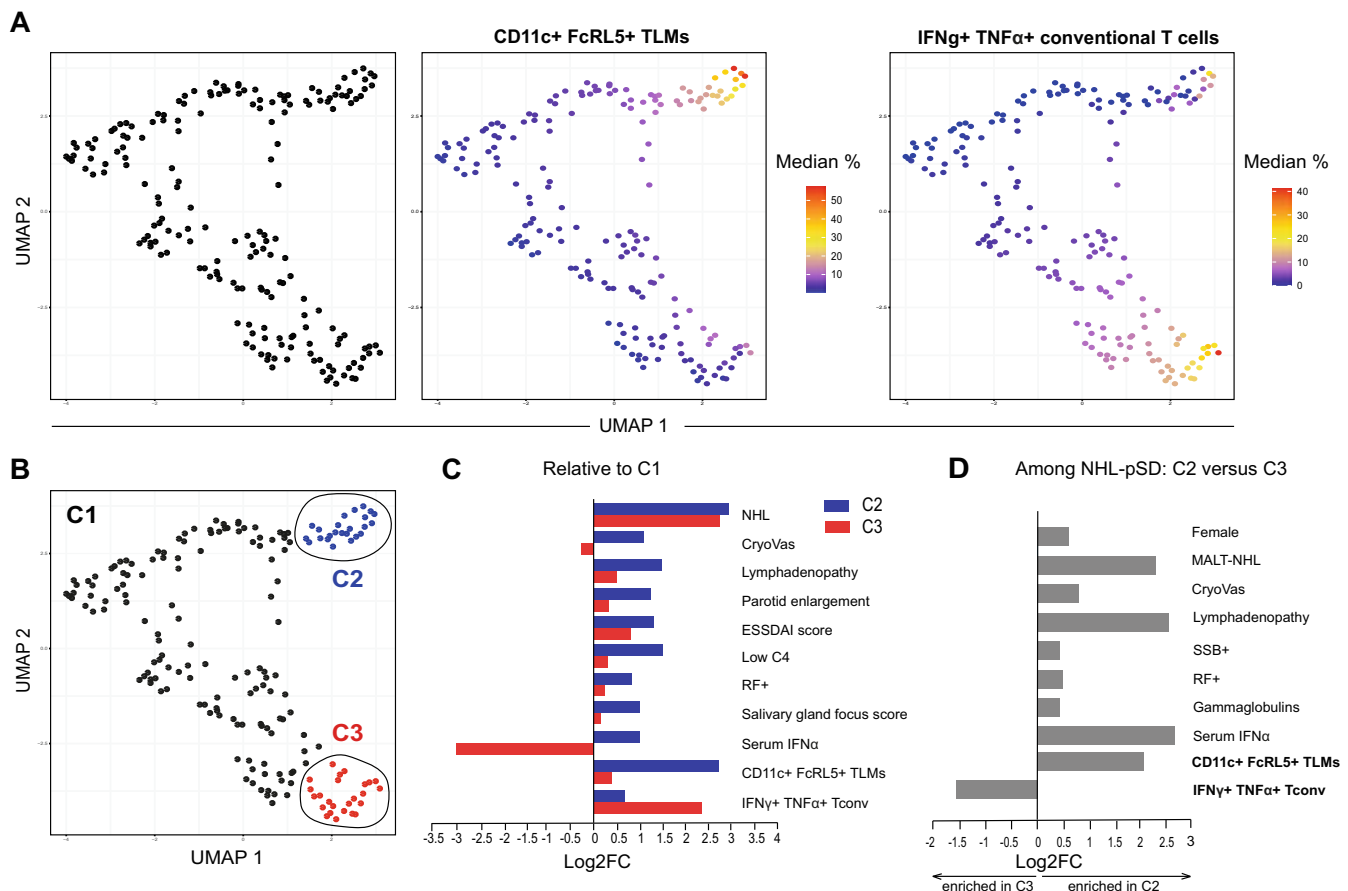
Figure 5. Stratification of patients using CD11c$^+$ FcRL5$^+$ TLMs and IFNγ$^+$ TNFα$^+$ Tconv. (A) UMAP dimensional reduction computed on CD11c$^+$ FcRL5$^+$ TLMs and IFNγ$^+$ TNFα$^+$ Tconv abundances for each patient, resulting in the identification of three distinct clusters. (B) Cluster C1 with low abundances of both CD11c$^+$ FcRL5$^+$ TLMs and IFNγ$^+$ TNFα$^+$ Tconv, cluster C2 with high abundance of CD11c$^+$ FcRL5$^+$ TLMs but low abundance of IFNγ$^+$ TNFα$^+$ Tconv, and cluster C3 with the opposite pattern. (C) Clinical, biologic, and histopathologic characteristics of patients in clusters C2 and C3 in comparison to C1. (D) Comparative analysis of patients with NHL-pSD within clusters C2 and C3. CryoVas, cryoglobulinemia vasculitis; ESSDAI, EULAR Sjögren's Syndrome Disease Activity Index; IFNα, interferon-α; Log2FC, log2 fold change; MALT, mucosa-associated lymphoid tissue; NHL, non-Hodgkin lymphoma; pSD, primary Sjögren disease; RF, rheumatoid factor; Tconv, conventional T cells; TLM, tissue-like memory B cell; UMAP, uniform manifold approximation and projection. Color figure can be viewed in the online issue, which is available at http://onlinelibrary.wiley.com/doi/10.1002/art.43207/abstract.

combination of these two populations alone allowed a significant gain in sensitivity in the prediction of lymphoma compared to the sum of all conventional clinical and biologic markers, reaching a sensitivity of 78.9% (vs 68.4%) for a slight decrease in specificity (76.8% vs 78%). The combination of all the markers allows for a supplementary gain in sensitivity (89.5%) at the expense of a loss in specificity (72.0%). These two populations, not yet described in the literature to our knowledge, therefore represent an innovative biomarker to identify patients who are more prone to develop lymphoma during their disease course.

Remarkably, we were able to identify two clusters of NHL-pSD along with their shared and specific cell parameters. CD11c$^+$ FcRL5$^+$ TLMs enabled the detection of a homogeneous group of patients with MALT NHL exhibiting known clinical and biologic characteristics found in classic NHL-pSD, such as lymphadenopathy, CryoVas, RF antibodies, and a high level of circulating IFNα. Conversely, the C3 cluster isolated thanks to IFNγ$^+$

TNFα$^+$ conventional T cells contained highly distinct B cell NHL-pSD, including three low-grade NHLs but only one MALT NHL. The clinical and biologic data of these patients show significantly less B cell hyperactivation markers than in C2 patients, and their serum IFNα levels did not differ from those in the overall cohort of patients with pSD. In summary, these patients may have gone unnoticed by clinicians because they would not have been detected by the current known biomarkers in the disease. Clusters C2 and C3 also included patients without a diagnosis of lymphoma. Longitudinal monitoring of these patients will be crucial to identify progression of certain individuals from the Arl-pSD group to the NHL-pSD group and monitor the evolution of their CD11c$^+$ FcRL5$^+$ TLMs and IFNγ$^+$ TNFα$^+$ conventional T cells.

We refined for the first time the phenotype of CD21$^-$ cells in pSD by identifying them as TLMs expressing CD11c and FcRL5. This phenotype corroborates a growing literature that has been studying the phenotype and functionality of nonclassic memory

B cells (MBCs) across various other autoimmune diseases prone to lymphomagenesis, such as rheumatoid arthritis, systemic lupus erythematosus, or hepatitis C virus–associated cryoglobulinemic vasculitis.[32–36] Although heterogeneous, these B cell populations share several features, including low expression of CD21 and CD27 and high expression of genes not usually expressed by classic MBCs, including T-bet, CD11c, and a variety of inhibitory receptors, notably members of the FcRLs. They have a maturation profile mediated by the antigen and are enriched in autoreactive clones. Of note, we previously established a correlation between lymphoproliferation and the expansion of anergic, clonal, autoreactive, and strongly antigen-selected CD27$^-$CD21$^-$ TLMs in Arl-pSD.[14,15] By studying patients with pSD who presented at least 30% of CD21$^{-/low}$ B cells in their peripheral B cell compartment, we identified three patients with monoclonal expansions in their blood. All three showed the highest frequency of expanded clones in CD21$^{-/low}$ B cells, suggesting that these monoclonal expansions may originate from this compartment.

Determining whether the CD11c$^+$ FcRL5$^+$ TLM population could indeed represent the prelymphomatous B cell source in pSD is a central and crucial question to assess. Growing data from the literature suggest that "B cell maturation and evolution towards lymphoma likely take place in ectopic lymphoid structures, particularly those displaying a fully organized architecture with segregated T and B cell areas and germinal center (GC)-like structures, collectively termed tertiary lymphoid organs (TLOs).[32–36]" Ectopic GCs are detected by microscopy in one-third of the salivary glands from patients with pSD. They are the site of the maturation of B lymphocytes via the process of locally driven somatic Ig variable heavy- and light-chain gene hypermutation (SHM).[37,38] In addition, serum levels of CXCL13 and CCL11, two cytokines involved in the development of GC-like structures, are associated with the occurrence of lymphoma in pSD.[39–41] We can hypothesize that in a chronic inflammatory environment, such as pSD salivary glands, ICs may accumulate. These would then be presented by dendritic cells (DCs) to CD4$^+$ T cells in the T cell zone and differentiate into IFNγ-expressing Th1 and Tfh1 cells. In the B cell zone, DCs present ICs to naive B lymphocytes. At the B–T border, Tfh1 cells could induce the differentiation of CD11c$^+$ FcRL5$^+$ TLMs that enter the GC, where they clonally expand by proliferation and undergo Ig class switching and SHM, leading to RF-positive clones and ultimately lymphoma.[11,12,33]

Interestingly, we also highlighted for the first time the correlation between lymphoproliferation and a CD4$^+$ T cell population (named MC-T1) whose phenotype is close to Th1 lymphocytes. They are conventional T cells expressing both IFNγ$^+$ and TNFα$^+$. Over the past decade, IFNs have emerged as key cytokines in the pathophysiology of the disease. A strong IFNα signature has been clearly demonstrated in the peripheral blood and salivary glands from patients with pSD.[42,43] Further evidence for a role of IFNs comes from genome-wide association studies suggesting pre-existing genetic anomalies along with up-regulation of IFN-associated genes in the blood and salivary glands of patients with pSD.[43–46] Interestingly, specific type I–related transcript (IFIT-3) was localized in salivary duct epithelial cells, whereas type II–related transcript (GBP-2) was found in both lymphoid aggregates and duct epithelial cells localized in the site of inflammatory cell infiltration, suggesting a specific role of type II IFN in lymphomageneis.[47] Of note, both IFNα and IFNγ induce BAFF production in monocytes, which in turn stimulates B cells proliferation and survival. Importantly, BAFF levels are correlated with disease activity, clonal B cell expansion in salivary glands, and lymphoma occurrence in pSD.[48,49]

One of the main limitations of our study is the small number of patients with NHL and its cross-sectional, nonlongitudinal nature. It will be essential to prospectively evaluate an even larger cohort of patients with pSD to determine whether there is a progressive enrichment of CD11c$^+$ FcRL5$^+$ TLMs or other B cell subsets in patients with Arl-pSD who ultimately develop lymphoma during follow-up.

The methodology used combined an unsupervised approach, data normalization, and deep cluster analysis to identify the populations of interest as accurately as possible. Notably, the relevance of the two identified biomarkers in the discovery set was assessed in a validation cohort. Nevertheless, it would be necessary to assess identified B and T cell populations in a large independent series of patients with pSD including a large number of patients with NHL-pSD to validate our results. Another limitation was the absence of analysis conducted within the salivary glands of the patients. It appears necessary to perform the same experiments within the inflamed and infiltrated tissue to verify their involvement in the maturation processes described earlier. Future research should also be conducted to characterize these cells at the molecular and functional levels.

Finally, our work opens up interesting prospects both clinically and therapeutically. The identification of CD11c$^+$ FcRL5$^+$ TLMs and IFNγ$^+$ TNFα$^+$ conventional T cells using flow cytometry could be routinely conducted to assist clinicians in managing patients at risk of developing pSD-NHL. Although the pathophysiology of the disease involves activation of the innate and adaptive immune systems, most immunosuppressive or immunomodulatory treatments successfully used in other autoimmune models have failed in pSD.[50,51] Therefore, the identification of new cellular and molecular targets such as CD11c$^+$ FcRL5$^+$ TLMs and IFNγ$^+$ TNFα$^+$conventional T cells brings new therapeutic perspectives.

In conclusion, this study enhances our knowledge of pSD-associated lymphomagenesis and provides promising biomarkers, namely CD11c$^+$ FcRL5$^+$ TLMs and IFNγ$^+$ TNFα$^+$ conventional T cells, for identifying patients at higher risk of developing lymphoma in pSD. These findings could have significant clinical implications for early detection of high-risk patients with pSD and improved patient management. Further research

is needed to confirm and expand these results, potentially leading to targeted therapeutic strategies in the future.

AUTHOR CONTRIBUTIONS

All authors contributed to at least one of the following manuscript preparation roles: conceptualization AND/OR methodology, software, investigation, formal analysis, data curation, visualization, validation, AND drafting or reviewing/editing the final draft. As corresponding author, Dr Saadoun confirms that all authors have provided the final approval of the version to be published and takes responsibility for the affirmations regarding article submission (eg, not under consideration by another journal), the integrity of the data presented, and the statements regarding compliance with institutional review board/Declaration of Helsinki requirements.

REFERENCES

1. Nocturne G, Mariette X. Sjögren syndrome-associated lymphomas: an update on pathogenesis and management. Br J Haematol 2015; 168(3):317–327.

2. Zhong H, Liu S, Wang Y, et al. Primary Sjögren's syndrome is associated with increased risk of malignancies besides lymphoma: a systematic review and meta-analysis. Autoimmun Rev 2022;21(5): 103084.

3. Zintzaras E, Voulgarelis M, Moutsopoulos HM. The risk of lymphoma development in autoimmune diseases: a meta-analysis. Arch Intern Med 2005;165(20):2337–2344.

4. Royer B, Cazals-Hatem D, Sibilia J, et al. Lymphomas in patients with Sjogren's syndrome are marginal zone B-cell neoplasms, arise in diverse extranodal and nodal sites, and are not associated with viruses. Blood 1997;90(2):766–775.

5. Parreau S, Nocturne G, Mariette X, et al. Features of non-Hodgkin's lymphoma diagnosed in minor salivary gland biopsies from primary Sjögren's syndrome patients. Rheumatology (Oxford) 2022;61(9): 3818–3823.

6. Vasaitis L, Nordmark G, Theander E, et al. Population-based study of patients with primary Sjögren's syndrome and lymphoma: lymphoma subtypes, clinical characteristics, and gender differences. Scand J Rheumatol 2020;49(3):225–232.

7. Chatzis LG, Stergiou IE, Goules AV, et al. Clinical picture, outcome and predictive factors of lymphoma in primary Sjögren's syndrome: results from a harmonized dataset (1981-2021). Rheumatology (Oxford) 2022;61(9):3576–3585.

8. Gorodetskiy VR, Probatova NA, Radenska-Lopovok SG, et al. Clonal relationship of marginal zone lymphoma and diffuse large B-cell lymphoma in Sjogren's syndrome patients: case series study and review of the literature. Rheumatol Int 2020;40(3):499–506.

9. Bende RJ, Slot LM, Kwakkenbos MJ, et al. Lymphoma-associated mutations in autoreactive memory B cells of patients with Sjögren's syndrome. J Pathol 2023;259(3):264–275.

10. Båve U, Nordmark G, Lövgren T, et al. Activation of the type I interferon system in primary Sjögren's syndrome: a possible etiopathogenic mechanism. Arthritis Rheum 2005;52(4):1185–1195.

11. Bende RJ, Aarts WM, Riedl RG, et al. Among B cell non-Hodgkin's lymphomas, MALT lymphomas express a unique antibody repertoire with frequent rheumatoid factor reactivity. J Exp Med 2005;201(8): 1229–1241.

12. Bende RJ, Janssen J, Beentjes A, et al. Salivary gland mucosa-associated lymphoid tissue-type lymphoma from Sjögren's syndrome patients in the majority express rheumatoid factors affinity-selected for IgG. Arthritis Rheumatol 2020;72(8):1330–1340.

13. Kolijn PM, Huijser E, Wahadat MJ, et al. Extranodal marginal zone lymphoma clonotypes are detectable prior to eMZL diagnosis in tissue biopsies and peripheral blood of Sjögren's syndrome patients through immunogenetics. Front Oncol 2023;13:1130686.

14. Saadoun D, Terrier B, Bannock J, et al. Expansion of autoreactive unresponsive CD21-/low B cells in Sjögren's syndrome-associated lymphoproliferation. Arthritis Rheum 2013;65(4):1085–1096.

15. Glauzy S, Boccitto M, Bannock JM, et al. Accumulation of antigen-driven lymphoproliferations in complement receptor 2/CD21$^{-/low}$ B cells from patients with Sjögren's syndrome. Arthritis Rheumatol 2018;70(2):298–307.

16. Nishishinya MB, Pereda CA, Muñoz-Fernández S, et al. Identification of lymphoma predictors in patients with primary Sjögren's syndrome: a systematic literature review and meta-analysis. Rheumatol Int 2015; 35(1):17–26.

17. Papageorgiou A, Voulgarelis M, Tzioufas AG. Clinical picture, outcome and predictive factors of lymphoma in Sjögren syndrome. Autoimmun Rev 2015;14(7):641–649.

18. Goules AV, Tzioufas AG. Lymphomagenesis in Sjögren's syndrome: predictive biomarkers towards precision medicine. Autoimmun Rev 2019;18(2):137–143.

19. Chatzis L, Goules AV, Pezoulas V, et al. A biomarker for lymphoma development in Sjogren's syndrome: salivary gland focus score. J Autoimmun 2021;121:102648.

20. Stergiou IE, Bakasis AD, Giannouli S, et al. Biomarkers of lymphoma in Sjögren's syndrome: what's the latest? Expert Rev Clin Immunol 2022;18(11):1155–1171.

21. De Vita S, Gandolfo S. Predicting lymphoma development in patients with Sjögren's syndrome. Expert Rev Clin Immunol 2019;15(9): 929–938.

22. Shoboski C, Shoboski S, Seror R, et al. 2016 ACR-EULAR classification criteria for primary Sjögren's Syndrome: a consensus and data-driven methodology involving three international patient cohorts. Arthritis Rheumatol 2016; 69(1):35–45.

23. Duret PM, Schleiss C, Kawka L, et al. Association between Bruton's tyrosine kinase gene overexpression and risk of lymphoma in primary Sjögren's syndrome. Arthritis Rheumatol 2023;75(10):1798–1811.

24. Seror R, Meiners P, Baron G, et al; EULAR Sjögren Task Force. Development of the ClinESSDAI: a clinical score without biological domain. A tool for biological studies. Ann Rheum Dis 2016;75(11):1945–1950.

25. Avnir Y, Prachanronarong KL, Zhang Z, et al. Structural determination of the broadly reactive anti-IGHV1-69 anti-idiotypic antibody G6 and its idiotope. Cell Rep 2017;21(11):3243–3255.

26. Tucci FA, Kitanovski S, Johansson P, et al. Biased IGH VDJ gene repertoire and clonal expansions in B cells of chronically hepatitis C virus-infected individuals. Blood 2018;131(5):546–557.

27. Mathian A, Mouries-Martin S, Dorgham K, et al. Monitoring disease activity in systemic lupus erythematosus with single-molecule array digital enzyme-linked immunosorbent assay quantification of serum interferon-α. Arthritis Rheumatol 2019;71(5):756–765.

28. Régnier P, Marques C, Saadoun D. *PICAFlow*: a complete R workflow dedicated to flow/mass cytometry data, from pre-processing to deep and comprehensive analysis. Bioinform Adv 2023;3(1):vbad177.

29. Mariette X, Criswell LA. Primary Sjögren's syndrome. N Engl J Med 2018;378(10):931–939.

30. Kapsogeorgou EK, Voulgarelis M, Tzioufas AG. Predictive markers of lymphomagenesis in Sjögren's syndrome: from clinical data to molecular stratification. J Autoimmun 2019;104:102316.

31. Rodríguez-Carrio J, Burska A, Conaghan PG, et al. Association between type I interferon pathway activation and clinical outcomes in rheumatic and musculoskeletal diseases: a systematic literature review informing EULAR points to consider. RMD Open 2023;9(1):e002864.

32. Isnardi I, Ng YS, Menard L, et al. Complement receptor 2/CD21- human naive B cells contain mostly autoreactive unresponsive clones. Blood 2010;115(24):5026–5036.

33. Portugal S, Obeng-Adjei N, Moir S, et al. Atypical memory B cells in human chronic infectious diseases: an interim report. Cell Immunol 2017;321:18–25.

34. Jenks SA, Cashman KS, Zumaquero E, et al. Distinct effector B cells induced by unregulated Toll-like receptor 7 contribute to pathogenic responses in systemic lupus erythematosus. Immunity 2018;49(4):725–739.e6.

35. Rubtsova K, Rubtsov AV, Cancro MP, et al. Age-associated B cells: a T-bet-dependent effector with roles in protective and pathogenic immunity. J Immunol 2015;195(5):1933–1937.

36. Wang S, Wang J, Kumar V, et al. IL-21 drives expansion and plasma cell differentiation of autoreactive CD11chiT-bet+ B cells in SLE. Nat Commun 2018;9(1):1758.

37. Bombardieri M, Lewis M, Pitzalis C. Ectopic lymphoid neogenesis in rheumatic autoimmune diseases. Nat Rev Rheumatol 2017;13(3):141–154.

38. Nocturne G, Pontarini E, Bombardieri M, et al. Lymphomas complicating primary Sjögren's syndrome: from autoimmunity to lymphoma. Rheumatology (Oxford) 2021;60(8):3513–3521.

39. Nocturne G, Seror R, Fogel O, et al. CXCL13 and CCL11 serum levels and lymphoma and disease activity in primary Sjögren's syndrome. Arthritis Rheumatol 2015;67(12):3226–3233.

40. Traianos EY, Locke J, Lendrem D, et al; UK primary Sjögren's syndrome registry. Serum CXCL13 levels are associated with lymphoma risk and lymphoma occurrence in primary Sjögren's syndrome. Rheumatol Int 2020;40(4):541–548.

41. Badarinza M, Serban O, Maghear L, et al. Diagnostic role of CXCL13 biomarker in primary Sjogren's syndrome patients with parotid non-Hodgkin's lymphoma complication. Med Clin (Barc) 2023;160(11):484–488.

42. Nezos A, Gravani F, Tassidou A, et al. Type I and II interferon signatures in Sjogren's syndrome pathogenesis: contributions in distinct clinical phenotypes and Sjogren's related lymphomagenesis. J Autoimmun 2015;63:47–58.

43. Trutschel D, Bost P, Mariette X, et al; Milieu Intérieur Consortium, ASSESS study investigators, and NECESSITY Consortium. Variability of primary Sjögren's syndrome is driven by interferon-α and interferon-α blood levels are associated with the class II HLA-DQ locus. Arthritis Rheumatol 2022;74(12):1991–2002.

44. Lessard CJ, Li H, Adrianto I, et al; UK Primary Sjögren's Syndrome Registry. Variants at multiple loci implicated in both innate and adaptive immune responses are associated with Sjögren's syndrome. Nat Genet 2013;45(11):1284–1292.

45. Li Y, Zhang K, Chen H, et al. A genome-wide association study in Han Chinese identifies a susceptibility locus for primary Sjögren's syndrome at 7q11.23. Nat Genet 2013;45(11):1361–1365.

46. Nezos A, Makri P, Gandolfo S, et al. TREX1 variants in Sjogren's syndrome related lymphomagenesis. Cytokine 2020;132:154781.

47. Hall JC, Baer AN, Shah AA, et al. Molecular subsetting of interferon pathways in Sjögren's syndrome. Arthritis Rheumatol 2015;67(9):2437–2446.

48. Gottenberg JE, Seror R, Miceli-Richard C, et al; Data at Enrollment in the Prospective ASSESS Cohort. Serum levels of beta2-microglobulin and free light chains of immunoglobulins are associated with systemic disease activity in primary Sjögren's syndrome. Data at enrollment in the prospective ASSESS cohort. PLoS One 2013;8(5):e59868.

49. Quartuccio L, Salvin S, Fabris M, et al. BLyS upregulation in Sjogren's syndrome associated with lymphoproliferative disorders, higher ESSDAI score and B-cell clonal expansion in the salivary glands. Rheumatology (Oxford) 2013;52(2):276–281.

50. Price EJ, Baer AN. How to treat Sjögren's syndrome. Rheumatology (Oxford) 2021;60(6):2574–2587.

51. Mavragani CP, Moutsopoulos HM. Sjögren's syndrome: old and new therapeutic targets. J Autoimmun 2020;110:102364.

AMERICAN COLLEGE
of RHEUMATOLOGY
Empowering Rheumatology Professionals

Time-Dependent Effect of Prophylactic Trimethoprim-Sulfamethoxazole on the Incidence of Serious Infections in Antineutrophil Cytoplasmic Antibody–Associated Vasculitis: A Target Trial Emulation Study

Yun Kyu Kim,[1] Jeffrey R. Curtis,[2] (ID) Se Rim Choi,[3] Jina Yeo,[4] Min Jung Kim,[5] Yun Jong Lee,[6] (ID) Eun Bong Lee,[7] (ID) and Jun Won Park[1] (ID)

Objective. The objective of this study was to investigate the effect of prophylactic trimethoprim-sulfamethoxazole (TMP-SMX) on the incidence of serious infections in patients with antineutrophil cytoplasmic antibody–associated vasculitis (AAV).

Methods. This multicenter cohort study was designed to emulate a target trial that studied 296 patients with AAV who were treated with rituximab (RTX) or cyclophosphamide (CYC) as induction therapy. Patients were grouped based on the administration of TMP-SMX within 14 days following induction therapy (n = 240 and 56 patients in prophylaxis and control groups, respectively) (intention-to-treat) and also as a time-dependent exposure (time-varying). Inverse probability weighting was applied to minimize the baseline imbalance between the two groups. The primary outcome was one-year incidence of serious infection.

Results. During the 252.1 person-years of observation, 77 cases of serious infections were recorded in 65 patients with a fatality rate of 18.5%. Most serious infections (n = 66, 85.7%) occurred within the first 180 days of observation. The prophylaxis group showed a significantly lower incidence of serious infections than the control group (hazard ratio [HR] 0.48 [95% confidence interval (CI) 0.32–0.72]). However, this beneficial effect of TMP-SMX was only significant during the first 180 days (HR 0.41 [95% CI 0.22–0.76]) and not thereafter (HR 3.67 [95% CI 0.46–29.43]) (interaction P = 0.044). This result was also consistent with the time-varying analysis result. Based on one case of severe adverse drug reaction related to TMP-SMX, the number needed to harm was 127.4, whereas the number needed to treat to prevent one serious infection was 8.0.

Conclusion. Prophylactic TMP-SMX significantly reduced the risk of serious infections in patients with AAV, particularly during the first six months of induction therapy with RTX or CYC.

INTRODUCTION

Antineutrophil cytoplasmic antibody–associated vasculitis (AAV) is a group of autoimmune diseases characterized by the severe inflammation of small blood vessels and the development of autoantibodies to the proteinase 3 or myeloperoxidase.[1] AAV poses significant clinical challenges because of potential major organ involvement, especially the respiratory tract and kidney.[2, 3] To achieve remission of life-threatening AAV, glucocorticoids (GCs) combined with either rituximab (RTX) or cyclophosphamide (CYC) have been recommended.[4] However, these intensive immunosuppressive therapies increase the risk of infection, which is the most frequent cause of death, especially in the early phase of the disease.[5–8] Hence, preventing serious infection-related complications is crucial to improve the treatment outcome of AAV.

Trimethoprim-sulfamethoxazole (TMP-SMX) is widely used as primary prophylaxis against *Pneumocystis jirovecii* pneumonia (PJP) in patients who are immunocompromised, including those with rheumatic diseases receiving immunosuppressive treatment.[9,10] Notably, a few observational studies recently suggested that prophylactic TMP-SMX could reduce the risk of serious infections, as well as PJP.[11,12] Based on these findings, the EULAR recommended the prophylactic use of TMP-SMX against PJP and other infections in patients with AAV.[13] However, the effect of TMP-SMX on the incidence of non-PJP–related infection has not been confirmed in other studies. Furthermore, the risk of serious infections could be influenced by various patient-specific factors, including disease activity, comorbidities, and immunosuppressive treatment. Moreover, the interaction between these factors and the efficacy of prophylactic TMP-SMX against serious infections has not been thoroughly investigated. Using a target trial emulation framework, this observational study aimed to investigate the effect of prophylactic TMP-SMX on serious infections and the clinical factors influencing its effectiveness in a large-scale cohort of patients with AAV.

PATIENTS AND METHODS

Patients. This study was designed to emulate a hypothetical target trial in which patients with AAV received or did not receive prophylactic TMP-SMX (Supplementary Table 1).[14] Detailed description of our study design is provided in Supplementary Text 1. We included patients with AAV from four tertiary referral hospitals in South Korea. From the electronic medical database of each institution, we identified patients with new onset or relapsing AAV who received RTX or intravenous CYC as induction therapy between 2005 and 2023. All patients were diagnosed with either granulomatosis with polyangiitis (GPA), microscopic polyangiitis (MPA), or eosinophilic granulomatosis with polyangiitis (EGPA) according to the 2022 American College of Rheumatology/EULAR classification criteria for AAV.[15–17]

Patients were excluded from the study if they were <18 years of age at the time of induction with RTX or CYC, had concomitant malignancy or history of solid organ transplantation, or started the induction therapy at another hospital. The flow chart of patient inclusion is shown in Supplementary Figure 1.

This study was conducted in accordance with the Declaration of Helsinki and approved by the institutional review board of each center. The requirement for patient consent was waived because of the retrospective nature of the study.

Exposure to prophylactic TMP-SMX. In this study, physicians at each institution determined the selection process of patients for prophylactic TMP-SMX. In addition, because there were no established guidelines for discontinuing TMP-SMX, the decision about when or whether to discontinue was also made at the physician's discretion. The TMP/SMX dosage was either one single-strength tablet (TMP 80 mg and SMX 400 mg) daily or one double-strength tablet (TMP 160 mg and SMX 800 mg) every other day, adjusted according to the patient's renal function. No patients received alternative prophylactic agents, such as dapsone or aerosolized pentamidine.

In this study, the index date (day 0) was defined as 14 days after the initiation of RTX or CYC as induction therapy. This 14-day lead-in period was established to ensure a stable study population and sufficient time for evaluating the prophylactic efficacy of TMP-SMX. Patients who developed serious infection or censored during the lead-in period were excluded. Exposure to TMP-SMX was determined using two approaches (Supplementary Figure 2). First, an intention-to-treat (ITT) design was used in which each patient was classified into the prophylaxis group if he/she received the prophylactic TMP-SMX at the index date. In the ITT analysis, classified patients remained in their original group regardless of later treatment changes. Second, a time-varying analysis (ie, as-treated) was performed in which each person-day observation was classified according to whether the patient received prophylactic TMP-SMX. In this approach, patients were able to dynamically transit between exposed and unexposed categories without restriction, defining consecutive periods of exposure or nonexposure as episodes. In both analyses, observation for all patients started on the index date and continued until either death, loss to follow-up (defined as no visit for more than 6 months since the last visit), or 52 weeks from the index date, whichever occurred first.

Data collection. Clinical information on the demographics, comorbidities, laboratory and radiologic findings, prescribed medications, and history of infection was collected from the electronic health record database (EHR) of each hospital. At each enrolled hospital, prescription data—covering all medications, their prescribed duration, and dosages for both inpatients and outpatients—were systematically documented in an integrated

database. This comprehensive recording allowed us to verify the prescription details of medications, including TMP-SMX.

Data on baseline characteristics were collected during the 14-day lead-in period. The Birmingham Vasculitis Activity Score (BVAS) was calculated using BVAS version 3.[18] Severe anemia was defined as a hemoglobin level of <8.0 g/dL, lymphopenia as a lymphocyte count of <800/μL, and azotemia as a glomerular filtration rate (GFR) of <60 mL/min/1.73 m². Baseline GC dose was defined as the mean daily prednisone-equivalent dose during the lead-in period, and GCs pulse was defined as the administration of intravenous methylprednisolone (250–1,000 mg/day) or an equivalent dose for 1 to 5 days. High-dose GCs was defined as a mean dose of GCs ≥30 mg/day of prednisone or its equivalent.[10] For the time-varying analysis, data on time-varying confounders were collected. These included laboratory values such as hemoglobin level, lymphocyte count and GFR, and GCs dose at each patient visit, which occurred every two to eight weeks.

Outcome. The primary outcome was the occurrence of serious infections, which were defined as any infection requiring intravenous antimicrobial treatment, hospitalization, or extended hospital stay. An extended hospital stay was defined as a prolonged hospitalization due to infection treatment, such as when a patient developed an infection during hospitalization for induction therapy that necessitated an extended stay for infection management. To identify all serious infections, we collected data on hospitalization and prescribed intravenous antimicrobial agents to the study population at each center. Also, we reviewed all medical records from the enrolled hospitals to capture serious infection cases that occurred outside of them. Based on these data, suspicious cases of serious infection were initially identified. Subsequently, two independent authors (YKK and JWP) reviewed the medical records to confirm the presence of severe infection.

Secondary outcomes included infection-related death and the occurrence of severe adverse drug reactions (ADR) related to TMP-SMX. All adverse events (AEs) were evaluated by two independent authors (YKK and JWP) and assigned a likelihood of causation based on their timing and recognized patterns. The severity of each AE was evaluated using the Common Terminology Criteria for Adverse Events version 5.0.[19] A severe AE was defined as having a grade 3 or higher severity. Cases with probable/likely or certain causation were considered ADRs.[20] We performed a risk-benefit analysis of prophylactic TMP-SMX by comparing the number needed to treat (NNT) for one year to prevent a serious infection with the number needed to harm (NNH) due to a severe ADR.

Statistical analysis. There were no missing values for clinical factors, laboratory findings, or prescription information; therefore, there was no imputation of missing values. Comparison of clinical factors between the two groups was performed using the chi-square test for categorical variables and Student's *t*-test for continuous variables. Differences in one-year incidence rates between the two groups were compared using Poisson regression.

In the target trial emulation framework, we emulated randomization by adjusting for baseline covariates using inverse probability weighting (IPW) (Supplementary Text 1).[21] The prophylactic efficacy of TMP-SMX was estimated using a Cox proportional hazards model with adjustment using robust standard errors accounting for the clustering effect of the participating institutions. The proportional hazards assumption was assessed using scaled Schoenfeld residuals. Because the incidence of serious infection could be influenced by time from the induction therapy, it was anticipated that the prophylactic effect of TMP-SMX could be dependent on the interval of time since induction with RTX or CYC was initiated. Therefore, we performed a prespecified analysis using piecewise Cox regression to investigate the time point at which TMP-SMX significantly influenced the risk of serious infection.[22,23] This method segments the observation period into predefined time intervals and enables hazard ratios (HRs) to vary across these intervals.

To determine explanatory risk factors for serious infection, we also conducted Cox regression on the unweighted population. The baseline clinical factors showing a relevant association (*P* < 0.1) in the univariable Cox regression analysis were entered into the multivariable analysis. The effect of prophylactic TMP-SMX on outcomes was estimated in various subgroups stratified by these factors.

We also conducted several sensitivity analyses. First, the prophylactic efficacy of TMP-SMX was estimated adjusting for the risk factors for serious infection rather than applying IPW. Second, the effect of prophylactic TMP-SMX on outcomes was estimated using the Anderson and Gill model to consider recurrent events of serious infection.[24] Third, AAV relapse was added to the censoring criteria. Finally, to address the potential for misclassification when defining patient group based on TMP-SMX administration on the index date, we redefined the lead-in period as the 28 days after induction therapy and re-classified patients based on whether they received prophylaxis for at least 14 days during this period. In this sensitivity analysis, follow-up for all patients began 28 days after induction with RTX or CYC. All statistical analyses were performed using R version 4.3.2, and statistical significance was set at *P* < 0.05.

RESULTS

Baseline characteristics. This study included 296 patients with AAV who received either RTX or CYC as induction therapy. Of these, 240 were in the prophylaxis group, and 56 were in the control group. In the prophylaxis group, the mean ± SD duration of using prophylactic TMP-SMX was 168.5 ± 136.7 days. Approximately 45.8% of patients (n = 110) in the prophylaxis group discontinued the use of

Table 1. Baseline characteristics of the study population*

Baseline characteristics	Prophylaxis group (n = 240)	Control group (n = 56)	SMD before IPW	SMD after IPW
Age, mean ± SD, y	63.7 ± 13.4	61.5 ± 15.9	0.149	0.051
Female, n (%)	134 (55.8)	34 (60.7)	0.099	0.034
Weight, mean ± SD, kg	58.8 ± 11.2	58.0 ± 13.1	0.058	0.008
Hypertension, n (%)	71 (29.6)	22 (39.3)	0.205	0.007
Diabetes, n (%)	47 (19.6)	11 (19.6)	0.001	0.017
Chronic hepatitis B, n (%)	2 (3.6)	6 (2.5)	0.062	0.024
Severe anemia,[a] n (%)	14 (5.8)	3 (5.4)	0.021	0.093
Lymphopenia,[b] n (%)	60 (25.0)	14 (25.0)	<0.001	0.028
GFR, mean ± SD, mL/min/1.73 m^2	52.7 ± 40.7	59.9 ± 39.4	0.179	0.064
ANCA positivity, n (%)	207 (86.2)	41 (73.2)	0.329	0.076
PR3-ANCA/c-ANCA	22 (9.2)	11 (19.6)		
MPO-ANCA/p-ANCA	185 (77.1)	30 (53.6)		
Underlying AAV, n (%)			0.432	0.040
GPA	69 (28.7)	25 (44.6)		
MPA	161 (67.1)	26 (46.4)		
EGPA	10 (4.2)	5 (8.9)		
New onset AAV, n (%)	213 (88.8)	49 (87.5)	0.039	0.010
BVAS, mean ± SD,	16.9 ± 6.4	14.9 ± 6.5	0.304	0.065
Lung involvement, n (%)	160 (66.7)	37 (66.1)	0.013	0.006
RTX, n (%)	165(68.8)	36 (64.3)	0.095	0.038
GCs pulse, n (%)	106 (44.2)	21 (37.5)	0.136	0.072
Mean GCs dose, mean ± SD, mg[c]	45.9 ± 19.6	39.2 ± 23.0	0.314	0.072

* AAV, ANCA-associated vasculitis; ANCA, antineutrophil cytoplasmic antibody; BVAS, Birmingham Vasculitis Activity Score; EGPA, eosinophilic granulomatosis with polyangiitis; GCs, glucocorticoids; GFR, glomerular filtration rate; GPA, granulomatosis with polyangiitis; IPW, inverse probability weighting; MPA, microscopic polyangiitis; MPO, myeloperoxidase; PR3, proteinase 3; RTX, rituximab; SMD, standardized mean difference.
[a] Defined as hemoglobin <8g/dL.
[b] Defined as <800 lymphocytes/μL.
[c] Mean daily dose of GCs were measured within 14 days before the index date.

prophylactic TMP-SMX within the first 180 days of observation. Of these, 19 patients discontinued because of AEs, whereas the remaining 91 patients discontinued based on physician discretion. Among the 56 patients in the control group, 11 (19.6%) initiated TMP-SMX at some point after the index date but remained classified in the control group in the ITT analysis. The mean ± SD daily dose of GC at baseline was 44.6 ± 20.4 mg of prednisone equivalent, which decreased to 6.9 ± 5.7 mg by day 180 (Figure 1).

The baseline characteristics of the study population are shown in Table 1. MPA was predominant in the study population (63.2%), followed by GPA (31.8%) and EGPA (5.1%). Compared with GPA, patients with MPA had lower GFR (39.6 vs 76.7 mL/min/1.73 m^2; P < 0.001), higher BVAS (17.3 vs 15.3; P = 0.022), and comparable proportion of pulmonary involvement (68.4% vs 70.2%; P = 0.869). Most patients (n = 262, 88.5%) were newly diagnosed with AAV and had undergone an initial induction therapy. A total of 201 patients (67.9%) received RTX (rather than CYC) to induce remission. Patients in the prophylaxis group had a higher BVAS score (16.9 vs 14.9; P = 0.040), received a higher GC dose, and were more likely to have MPA than those in the control group. After applying IPW, all measured covariates were well-balanced (standardized mean difference <0.1). In time-varying analysis, 445 episodes (251 with TMP-SMX and 194 without TMP-SMX) were analyzed and all

measured covariates including time-dependent confounders were well-balanced after weighting (Supplementary Table 2).

Incidence of serious infection. During the 252.1 person-years of observation (mean ± SD of follow-up duration = 310.9 ± 109.7 days per patient), 77 cases of serious infections occurred, with an incidence rate of 30.5 [95% confidence interval (95% CI) 24.2–37.9] per 100 person-years. This included three cases of hospitalization at other hospitals due to serious infections. The clinical features of the observed serious infections are described in Supplementary Table 3. There were 35 bacterial infections, 7 viral infections, 7 non-PJP-related fungal infections, 5 PJP cases, and 23 clinically diagnosed bacterial infections without microbiologic confirmation. The most common anatomic site of infection was the respiratory tract (54.5%), followed by the gastrointestinal tract (13.0%), urinary tract (11.7%), and skin and soft tissues (10.4%). In patients who experienced recurrent infections (n = 11), the mean ± SD interval between infections was 47.3 ± 32.0 days. Most serious infections (n = 66, 85.7%) occurred within the first 180 days (incidence rate 49.9 of 100 person-years), with a significantly higher incidence than in the period after 180 days (incidence rate 9.2 of 100 person-years; and incidence rate ratio (IRR) 5.43 [95% CI 2.87–10.28]) (Figure 1). Regarding the GC dose, in 32 (41.6%) cases, patients were receiving <15mg/day of prednisone or its equivalent at the time of serious
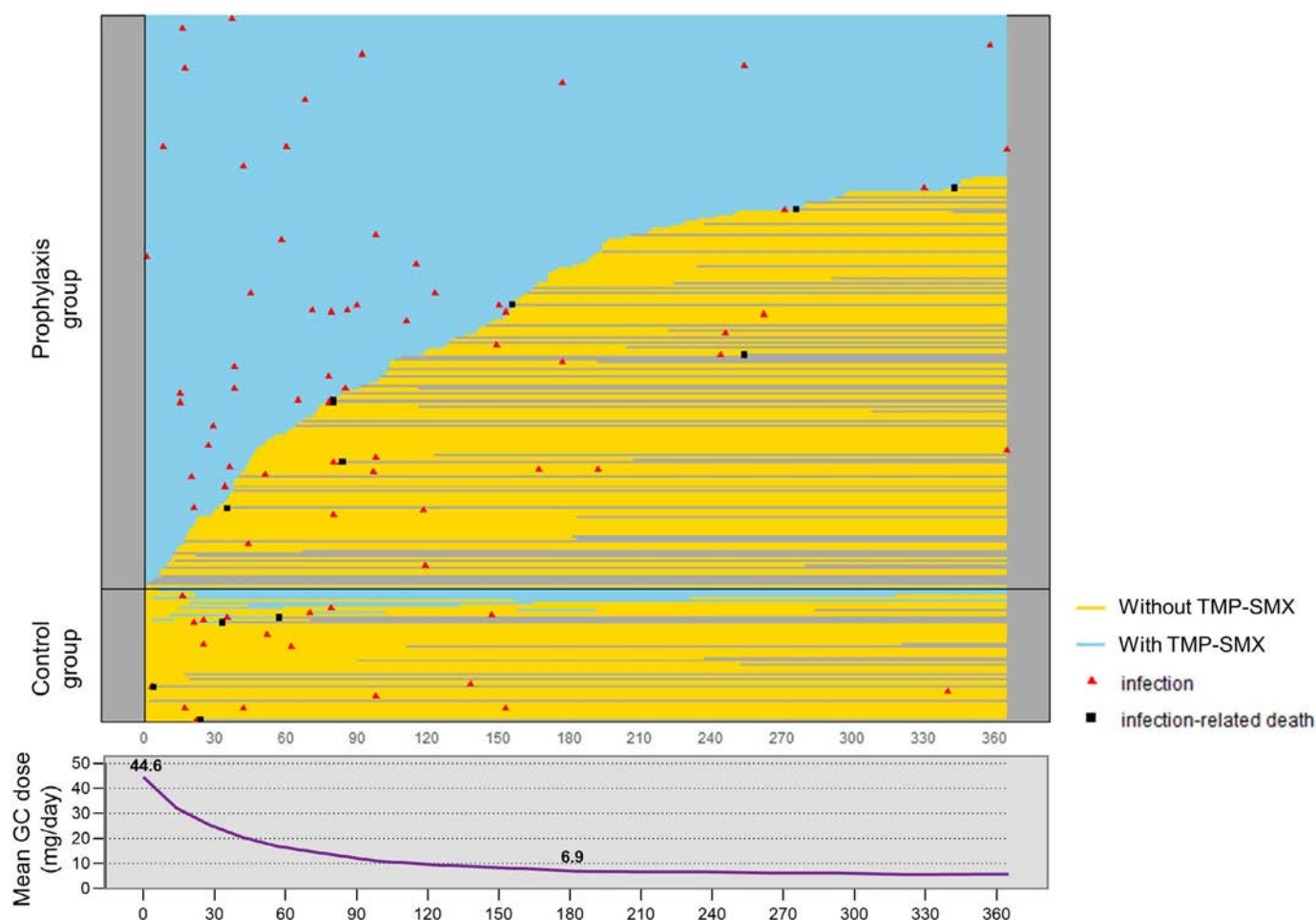
Figure 1. Pattern of the prophylactic use of TMP-SMX and incidence of serious infection in the study population. Each horizontal line indicates the follow-up period of each patient. Blue and yellow lines indicate follow-up with and without prophylactic TMP-SMX. TMP-SMX, trimethoprim-sulfamethoxazole.

infection. Among 65 patients who experienced serious infections, 12 (18.5%) died from these infections during the observation period.

The efficacy of prophylactic TMP-SMX. The crude incidence rate (per 100 person-years) of serious infections was numerically lower in the prophylaxis group than in the control group (28.6 vs 39.0; $P = 0.252$) (Supplementary Table 4). Five cases of PJP were observed with a significantly higher incidence in the control group (1.0 vs 6.5; $P = 0.037$).

After applying IPW, we plotted Kaplan–Meier curve for time to serious infection in both the ITT analysis and time-varying analysis (Figure 2). In the ITT analysis, prophylactic TMP-SMX significantly reduced the one-year incidence of serious infection with an overall HR of 0.48 [95% CI 0.32–0.72]. This effect remained consistent after excluding PJP and viral infections (HR 0.63 [95% CI 0.44–0.90]). In addition, infection-related mortality in the prophylaxis group was significantly lower than that in the control group (HR 0.23 [95% CI 0.10–0.53]). This result was consistent

with that obtained in the time-varying analysis of the effect of prophylactic TMP-SMX (Table 2).

Time-dependent effect of prophylactic TMP-SMX on the risk of serious infection. For the primary outcome, the examination of the Schoenfeld residuals provided some evidence for violation of the proportional hazards assumption ($P = 0.051$ for ITT analysis). The efficacy of prophylactic TMP-SMX was more evident during the first 180 days (Figure 2). The time-dependent HR plot indicated that the HR in the prophylactic group approached the null at this time point (Supplementary Figure 3). Piecewise Cox regression at fixed change points on day 180 showed that the prophylactic effect of TMP-SMX was prominent in the initial period but was not significant thereafter in either ITT or time-varying analyses (Table 3). Compared with the alternative time point at day 120, the difference in the effect of prophylactic TMP-SMX was more pronounced at day 180, during which the treatment-by-period interaction showed a lower P value. This result was consistent with that obtained from the measurement of time-stratified IRR for overall serious infections in the IPW-
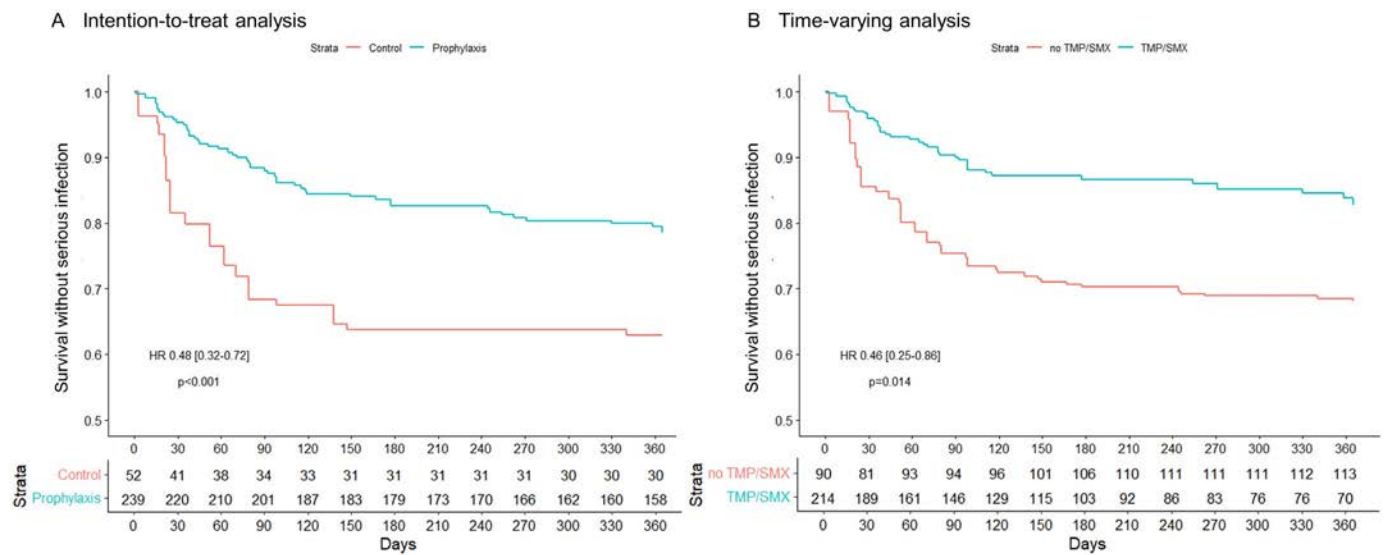
Figure 2. Kaplan–Meier curve showing one-year incidence of serious infection based on (A) ITT analysis and (B) time-varying analysis. HR, hazard ratio; ITT, intention-to-treat; TMP/SMX, trimethoprim-sulfamethoxazole. Color figure can be viewed in the online issue, which is available at http://onlinelibrary.wiley.com/doi/10.1002/art.43185/abstract.

applied pseudopopulation. During the first 180 days of observation, the IRR of the prophylaxis group was initially 0.48 [95% CI 0.26–0.87] (P = 0.016) and afterward was 4.56 [95% CI 0.58–35.73] (P = 0.149).

Risk factors for serious infection. In the unweighted univariable Cox regression, old age (age ≥ 60), hypertension, lymphopenia, azotemia, MPA, new onset AAV, high BVAS (BVAS ≥16), lung involvement, GCs pulse, and high-dose GCs were associated with increased frequency of serious infections (Supplementary Table 5). There was no significant difference in the risk of serious infections between the patients receiving RTX and those receiving CYC (P = 0.837). In the multivariable analysis, old age, lymphopenia, azotemia, and lung involvement significantly increased the risk of serious infection.

The effect of TMP-SMX was evaluated in various subgroups to identify the clinical factors affecting its prophylactic efficacy (Figure 3). The effect of prophylactic TMP-SMX was more prominent in patients with baseline lymphopenia (P value for interaction <0.001), azotemia (P = 0.005), MPA (P = 0.013), or relapsed AAV (P = 0.067). Other clinical factors, such as old age, hypertension, high BVAS score, lung involvement, GCs pulse, and high-dose GCs, did not significantly affect the effect of prophylactic TMP-SMX.

Safety of TMP-SMX. During the 127.4 person-years of TMP-SMX prophylaxis, 35 cases of AE occurred (Supplementary Table 6), 8 of which were ADRs related to prophylactic TMP-SMX (incidence rate 6.28 [95% CI 2.87–11.68] per 100 person-years) (Supplementary Table 7). However, among these AE cases, 27 (77.1%) patients discontinued TMP-SMX. There was only one case of severe ADR, which was a liver function test abnormality. This was resolved shortly after the discontinuation of TMP-SMX. Based on the safety assessment, the NNH for severe ADR was 127.4, whereas the NNT for preventing one case of serious infection was 8.0.

Sensitivity analysis. First, prophylactic TMP-SMX showed similar efficacy in the unweighted study population based on the conventional multivariable Cox regression (adjusted HR 0.42 [95% CI 0.32–0.56]). The prophylactic efficacy of TMP-SMX was evident during the initial 180 days of follow-up (Supplementary Figure 4). Second, to consider recurrent events of serious infection, we used the Andersen and Gill model to allow for recurrent events in the survival analysis. In the Andersen and Gill model, TMP-SMX showed a significant impact during the first 180 days

Table 2. Prophylactic efficacy of TMP-SMX based on ITT analysis and time-varying analysis*

	ITT analysis[a]		Time-varying analysis[a,b]	
	HR (95% CI)	P value	HR (95% CI)	P value
Serious infection	0.48 (0.32–0.72)	<0.001	0.46 (0.25–0.86)	0.014
Serious infection except PJP and viral infection	0.63 (0.44–0.90)	0.011	0.60 (0.30–1.21)	0.155
Infection-related mortality	0.23 (0.10–0.53)	<0.001	0.22 (0.05–0.94)	0.041

* CI, confidence interval; HR, hazard ratio; IPW, inverse probability weighting; ITT, intention-to-treat; PJP, *Pneumocystis jirovecii* pneumonia; TMP-SMX, trimethoprim-sulfamethoxazole.
[a] Analysis was performed after applying IPW.
[b] The intracluster effect caused by multiple episodes in the same patient was accounted for.

Table 3. Piecewise HR (95% CI) of prophylactic TMP-SMX for serious infection at fixed change points of day 120 and day 180 based on ITT analysis and time-varying analysis[*]

	Day 120			Day 180		
Change-point	Baseline to day 120, HR (95% CI)	Day 120 onward, HR (95% CI)	Treatment-by-period interaction, P value	Baseline to day 180, HR (95% CI)	Day 180 onward, HR (95% CI)	Treatment-by-period interaction, P value
ITT analysis[a]	0.41 (0.21–0.80)	0.97 (0.22–4.32)	0.301	0.41 (0.22–0.76)	3.67 (0.46–29.43)	0.044
Time-varying analysis[a,b]	0.42 (0.21–0.82)	0.78 (0.26–2.38)	0.337	0.40 (0.21–0.77)	1.48 (0.40–5.48)	0.074

[*] CI, confidence interval; HR, hazard ratio; IPW, inverse probability weighting; ITT, intention-to-treat; TMP-SMX, trimethoprim-sulfamethoxazole.
[a] Analysis was performed after applying IPW.
[b] The intracluster effect caused by multiple episodes in the same patient was accounted for.

(HR 0.48 [95% CI 0.27–0.87]) but insignificant afterward (Supplementary Figure 5), which was consistent with our main result. Furthermore, the effect of prophylactic TMP-SMX did not change when AAV relapse (n = 22) was included in the censoring criteria (Supplementary Figure 6) or when the lead-in period was extended to 28 days (Supplementary Figure 7).

DISCUSSION

In this study, we demonstrated that the prophylactic use of TMP-SMX significantly lowered the risk of serious infection in patients with AAV with the greatest impact observed during the initial 180 days of the observation period. The benefits were more evident in patients with additional risk factors for serious
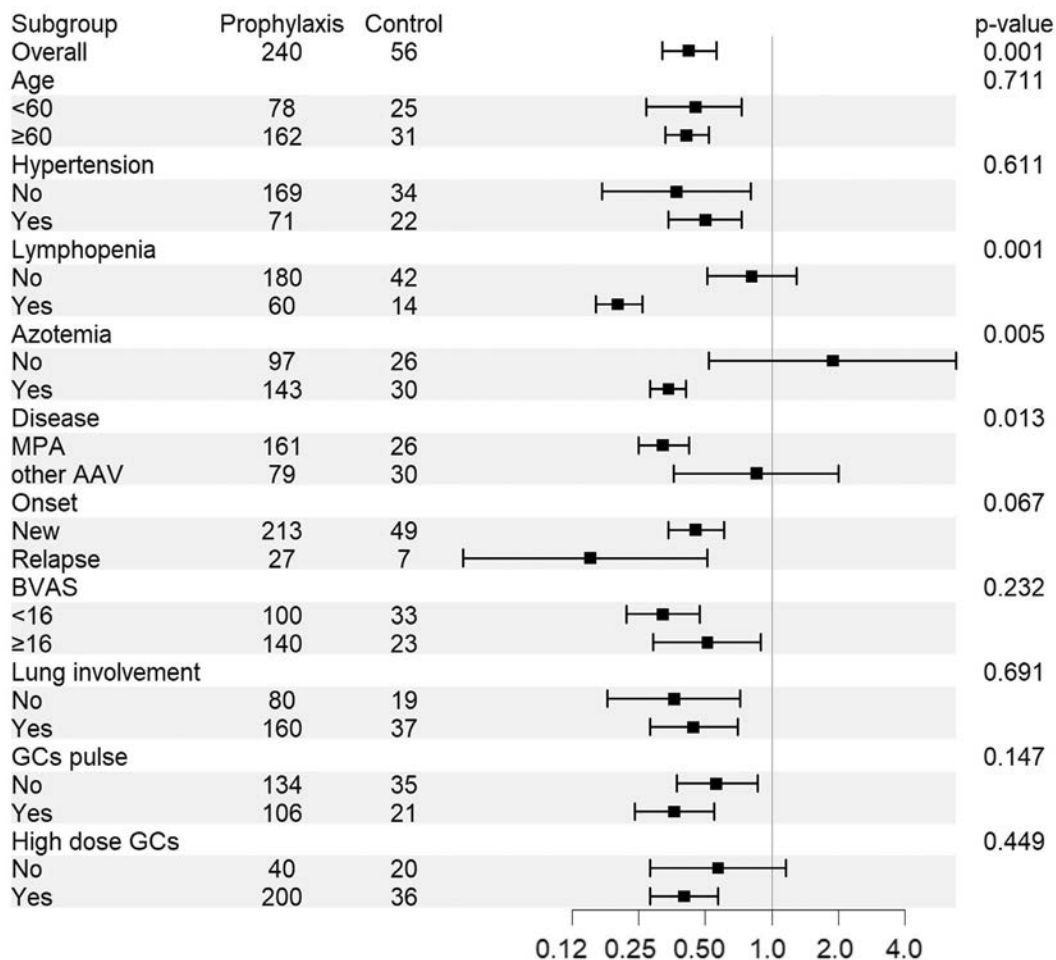
Figure 3. Clinical factors affecting the prophylactic efficacy of TMP-SMX. AAV, antineutrophil cytoplasmic antibody–associated vasculitis; BVAS, Birmingham Vasculitis Activity Score; GC, glucocorticoid; MPA, microscopic polyangiitis; TMP-SMX, trimethoprim-sulfamethoxazole.

infections. To the best of our knowledge, this is the first large-scale cohort study to focus on factors affecting the prophylactic effect of TMP-SMX.

Patients with AAV are more susceptible to serious infections than the general population because of disease-specific organ damage, potential long-term effects of widespread inflammation, and medications used to treat AAV.[6] The increased susceptibility to infection is most significant in the early phase because of intensive immunosuppressive treatment; thus, infection is one of the common causes of early mortality in patients with AAV.[7,8,25] This study confirmed these reports, as indicated by the 1-year incidence of serious infection after induction therapy using RTX or CYC of 30.5 per 100 person-years, with a significant fatality rate, which suggests that decreasing the risk of serious infections is crucial for improving treatment outcomes in patients with AAV.

Despite its significant impact on the prognosis of patients with AAV, there have been few studies on optimal management to minimize the risk of infection. Notably, some recent studies have suggested that prophylactic TMP-SMX could prevent serious infections in patients with AAV as well as PJP,[11,12,26] which is consistent with the results of this study, in which the prophylaxis group was associated with an approximately 50% reduction in serious infections compared with the control group. The mechanisms underlying the reduced incidence of serious infections in patients receiving prophylactic TMP-SMX remain unclear. However, TMP-SMX has broad-spectrum antimicrobial effects against bacteria, fungi, and protozoa,[27] which may allow the removal of pathogens in patients with AAV. A recent meta-analysis demonstrated that prophylactic TMP-SMX was associated with a lower incidence of bacterial infections in patients with HIV infection.[28] Although the antimicrobial effect of TMP-SMX has not been thoroughly investigated in patients without HIV, our results strongly suggest that prophylactic TMP-SMX provides additional benefits in patients with AAV beyond reducing the risk of PJP. Furthermore, we demonstrated a favorable safety profile of prophylactic TMP-SMX, with the NNH for serious ADR being significantly higher than the NNT to prevent one case of serious infection. This risk-benefit assessment indicates that prophylactic TMP-SMX should be administered to patients with AAV receiving induction immunosuppressive treatment.

Although we have demonstrated the beneficial effects of prophylactic TMP-SMX on the risk of serious infection, the optimal duration remains uncertain. Because the risk of serious infection is influenced by disease activity and degree of immunosuppression, the risk likely varies according to the interval from the start of induction treatment. Interestingly, this study showed that approximately 86% of serious infections occurred during the first 180 days of the observation period, and the preventive effect of TMP-SMX was evident only during this period. Because the effect of prophylaxis is dependent on the incidence of the target disease, stable disease activity and tapering of GC 180 days after baseline could have contributed to the observed result. Previous studies on the effect of prophylactic TMP-SMX on PJP risk showed that tapering prednisone dose to <15 mg/day might be a relevant threshold for considering its withdrawal.[9,29] However, in this study, patients received a lower dose of GC (mean ± SD: 6.9 ± 5.7 mg/day of prednisone) on day 180, and approximately 40% of the serious infections occurred when patients were receiving less than 15 mg/day of prednisone or its equivalent. These findings suggest that prolonged use of TMP-SMX, for at least six months from the initiation of induction therapy, may be necessary to ensure a better outcome in patients with AAV.

This study had some limitations. First, the baseline characteristics of the patients in the prophylaxis and control groups were significantly different because of the retrospective nature of our study. Although we attempted to minimize selection bias by applying IPW, unmeasured confounders such as compliance to prophylactic TMP-SMX could have affected our results. Second, although we thoroughly reviewed the EHR data to capture all relevant information on hospitalization at other institutions, some external hospitalizations may not have been recorded in our database. However, we would not expect differential reporting according to whether patients received concomitant TMP-SMX or not, thus biasing toward the null. Third, the duration of TMP-SMX use in the prophylaxis group was heterogeneous, and approximately 50% of the patients discontinued it within 180 days, which could have led to a biased estimate of the effect of TMP-SMX. We showed consistent results in the time-varying analysis performed to determine exposure to TMP-SMX. However, its effect on serious infection other than PJP and viral infection was less significant in time-varying analysis. Because time-varying analysis accounts for changes in TMP-SMX use over time, it inherently divides each patient's observation period into smaller time segments, which substantially increases the variance of treatment effect. Therefore, we believe that our finding should be further validated in future larger scale studies with a more homogeneous pattern of prophylactic TMP-SMX prescription. Finally, because patients with an index date before 2018 could not have contracted COVID-19, the impact of prophylactic TMP-SMX on the incidence of COVID-19 and related infectious complications could not be fully estimated in this study.

In conclusion, we showed that prophylactic TMP-SMX significantly reduced the overall incidence of serious infections beyond just PJP in patients with AAV undergoing induction therapy with CYC or RTX. The prophylactic effect is most pronounced in the initial period following induction therapy when the risk of serious infection peaks. Although the additional benefits of TMP-SMX should be confirmed in future randomized studies, it may impact clinical practice for better treatment outcomes in patients with AAV.

AUTHOR CONTRIBUTIONS

All authors contributed to at least one of the following manuscript preparation roles: conceptualization AND/OR methodology, software,

investigation, formal analysis, data curation, visualization, and validation AND drafting or reviewing/editing the final draft. As corresponding author, Dr Park confirms that all authors have provided the final approval of the version to be published and takes responsibility for the affirmations regarding article submission (eg, not under consideration by another journal), the integrity of the data presented, and the statements regarding compliance with institutional review board/Declaration of Helsinki requirements.

REFERENCES

1. Jennette JC, Falk RJ, Bacon PA, et al. 2012 revised international Chapel Hill Consensus Conference nomenclature of vasculitides. Arthritis Rheum 2013;65(1):1–11.

2. Sánchez-Álamo B, Moi L, Bajema I, et al; EUVAS. Long-term outcomes and prognostic factors for survival of patients with ANCA-associated vasculitis. Nephrol Dial Transplant 2023;38(7):1655–1665.

3. Robson J, Doll H, Suppiah R, et al. Damage in the anca-associated vasculitides: long-term data from the European Vasculitis Study Group (EUVAS) therapeutic trials. Ann Rheum Dis 2015;74(1): 177–184.

4. Yates M, Watts RA, Bajema IM, et al. EULAR/ERA-EDTA recommendations for the management of ANCA-associated vasculitis. Ann Rheum Dis 2016;75(9):1583–1594.

5. Kronbichler A, Jayne DR, Mayer G. Frequency, risk factors and prophylaxis of infection in ANCA-associated vasculitis. Eur J Clin Invest 2015;45(3):346–368.

6. Mohammad AJ, Segelmark M, Smith R, et al. Severe infection in antineutrophil cytoplasmic antibody-associated vasculitis. J Rheumatol 2017;44(10):1468–1475.

7. Flossmann O, Berden A, de Groot K, et al; European Vasculitis Study Group. Long-term patient survival in ANCA-associated vasculitis. Ann Rheum Dis 2011;70(3):488–494.

8. Little MA, Nightingale P, Verburgh CA, et al; European Vasculitis Study (EUVAS) Group. Early mortality in systemic vasculitis: relative contribution of adverse events and active vasculitis. Ann Rheum Dis 2010; 69(6):1036–1043.

9. Park JW, Curtis JR, Moon J, et al. Prophylactic effect of trimethoprim-sulfamethoxazole for pneumocystis pneumonia in patients with rheumatic diseases exposed to prolonged high-dose glucocorticoids. Ann Rheum Dis 2018;77(5):644–649.

10. Park JW, Curtis JR, Choi SR, et al. Risk-benefit analysis of primary prophylaxis against Pneumocystis jirovecii pneumonia in patients with rheumatic diseases receiving rituximab. Arthritis Rheumatol 2023; 75(11):2036–2044.

11. Kronbichler A, Kerschbaum J, Gopaluni S, et al. Trimethoprim-sulfamethoxazole prophylaxis prevents severe/life-threatening infections following rituximab in antineutrophil cytoplasm antibody-associated vasculitis. Ann Rheum Dis 2018; 77(10):1440–1447.

12. Waki D, Nishimura K, Yoshida T, et al. Protective effect of different doses of trimethoprim-sulfamethoxazole prophylaxis for early severe infections among patients with antineutrophil cytoplasmic autoantibody-associated vasculitis. Clin Exp Rheumatol 2021;39(2) (suppl 129):142–148.

13. Hellmich B, Sánchez-Álamo B, Schirmer JH, et al. EULAR recommendations for the management of ANCA-associated vasculitis: 2022 update. Ann Rheum Dis. 2024;83(1):30–47.

14. Hubbard RA, Gatsonis CA, Hogan JW, et al. "Target trial emulation" for observational studies - potential and pitfalls. N Engl J Med 2024; 391(21):1975–1977.

15. Grayson PC, Ponte C, Suppiah R, et al; DCVAS Study Group. 2022 American College of Rheumatology/European Alliance of Associations for Rheumatology classification criteria for eosinophilic granulomatosis with polyangiitis. Ann Rheum Dis 2022;81(3):309–314.

16. Robson JC, Grayson PC, Ponte C, et al; DCVAS Investigators. 2022 American College of Rheumatology/European Alliance of Associations for Rheumatology classification criteria for granulomatosis with polyangiitis. Ann Rheum Dis 2022;81(3):315–320.

17. Suppiah R, Robson JC, Grayson PC, et al; DCVAS INVESTIGATORS. 2022 American College of Rheumatology/European Alliance of Associations for Rheumatology classification criteria for microscopic polyangiitis. Ann Rheum Dis 2022;81(3):321–326.

18. Mukhtyar C, Lee R, Brown D, et al. Modification and validation of the Birmingham Vasculitis Activity Score (version 3). Ann Rheum Dis 2009;68(12):1827–1832.

19. Freites-Martinez A, Santana N, Arias-Santiago S, et al. Using the Common Terminology Criteria for Adverse Events (CTCAE - version 5.0) to evaluate the severity of adverse events of anticancer therapies. Actas Dermosifiliogr (Engl Ed) 2021;112(1):90–92.

20. Edwards IR, Aronson JK. Adverse drug reactions: definitions, diagnosis, and management. Lancet 2000;356(9237):1255–1259.

21. Austin PC, Stuart EA. Moving towards best practice when using inverse probability of treatment weighting (IPTW) using the propensity score to estimate causal treatment effects in observational studies. Stat Med 2015;34(28):3661–3679.

22. Friedman M. Piecewise exponential models for survival data with covariates. Ann Statist 1982;10(1):101–113.

23. Curtis JR, Yamaoka K, Chen YH, et al. Malignancy risk with tofacitinib versus TNF inhibitors in rheumatoid arthritis: results from the open-label, randomised controlled ORAL Surveillance trial. Ann Rheum Dis 2023;82(3):331–343.

24. Amorim LD, Cai J. Modelling recurrent events: a tutorial for analysis in epidemiology. Int J Epidemiol 2015;44(1):324–333.

25. Rathmann J, Jayne D, Segelmark M, et al. Incidence and predictors of severe infections in ANCA-associated vasculitis: a population-based cohort study. Rheumatology (Oxford) 2021;60(6):2745–2754.

26. Odler B, Riedl R, Gauckler P, et al; RAVE–ITN Research Group. Risk factors for serious infections in ANCA-associated vasculitis. Ann Rheum Dis 2023;82(5):681–687.

27. Kemnic TR, Coleman M. Trimethoprim Sulfamethoxazole. Statpearls; 2024.

28. Prosty C, Katergi K, Sorin M, et al. Comparative efficacy and safety of Pneumocystis jirovecii pneumonia prophylaxis regimens for people living with HIV: a systematic review and network meta-analysis of randomized controlled trials. Clin Microbiol Infect 2024;30(7):866–876.

29. Suryaprasad A, Stone JH. When is it safe to stop Pneumocystis jiroveci pneumonia prophylaxis? Insights from three cases complicating autoimmune diseases. Arthritis Rheum 2008;59(7):1034–1039.

AMERICAN COLLEGE
of RHEUMATOLOGY
Empowering Rheumatology Professionals

BRIEF REPORT

Maintenance of Remission After Tocilizumab Withdrawal in Patients With Glucocorticoid-Dependent Polymyalgia Rheumatica

Baptiste Chevet,[1] Aghiles Souki,[2] Emmanuel Nowak,[2] Guillermo Carvajal-Alegria,[1] Emmanuelle Dernis,[3] Christophe Richez,[4] Marie-Elise Truchetet,[4] Daniel Wendling,[5] Eric Toussirot,[6] Aleth Perdriger,[7] Jacques-Eric Gottenberg,[8] Renaud Felten,[8] Bruno Fautrel,[9] Anne Lohse,[10] Laurent Chiche,[11] Pascal Hilliquin,[12] Catherine Le Henaff,[13] Benjamin Dervieux,[14] Guillaume Direz,[3] Isabelle Chary-Valckenaere,[15] Divi Cornec,[1] Dewi Guellec,[16] Thierry Marhadour,[17] Alain Saraux,[17] and Valérie Devauchelle-Pensec[1]

Objective. The SEMAPHORE trial evaluated the efficacy and safety of tocilizumab (TCZ) treatment in patients with glucocorticoid (GC)-dependent polymyalgia rheumatica (PMR). TCZ reduced GC dose and disease activity at week 24. This study aimed to assess relapse rates after stopping TCZ treatment in patients achieving remission at week 24.

Methods. In the randomized study, 101 patients received intravenous TCZ (8 mg/kg) or placebo for 24 weeks. Of the 49 patients treated with TCZ, 33 achieved the primary outcome (PMR activity score <10 and GC dose reduction of ≤5 mg/day or ≥10 mg). All 33 patients except one stopped TCZ treatment at week 24 and completed a visit at week 32, with optional follow-up visits every eight weeks until week 48. Relapse was defined as the failure of the primary composite outcome during follow-up or the need for one or more TCZ infusion. Results were analyzed using Kaplan-Meier curves.

Results. Among the 33 patients who received TCZ in remission at week 24, seven stopped follow-ups before week 48, and two of the remaining 26 patients (7.7%) sustained remission in the following six months. 24 (92.3%) of the total patients experienced a relapse. The median time to relapse was 15 weeks (interquartile range, 8–25 weeks).

Conclusion. Among patients with GC-dependent PMR in remission after a six-month TCZ treatment, only a minority of the patients remained relapse-free after TCZ discontinuation. This study suggests that a six-month treatment course is not long enough to withdraw the TCZ. Further studies are needed to determine the optimal TCZ treatment duration and strategies for cessation to prevent relapses.

INTRODUCTION

Polymyalgia rheumatica (PMR) is an inflammatory condition characterized by pain and stiffness in the shoulders and pelvis experienced by people after 50 years of age. Glucocorticoids (GCs) are the first-line treatment,[1,2] and patients are expected to be weaned off GCs after a 12 month taper. However, a quarter of all patients with PMR continue treatment with GCs five years after PMR diagnosis.[3]

In the SEMAPHORE trial,[4] tocilizumab (TCZ), an anti-interleukin 6 receptor, reduced both disease activity and GC usage in patients with GC-dependent PMR. One hundred patients were randomized into two groups, one to receive TCZ and one to receive a placebo during a 24-week course. The primary outcome was the composite score, which was defined as a PMR activity score (PMR-AS)[5] <10 when the GC concentration decreases by ≤5 mg per day or when the decrease of the GC concentration was ≥10 mg compared with that of the inclusion. Thirty-three patients (67%) in the cohort treated with TCZ completed the primary outcome, which was significantly greater than that of the placebo arm, 16 out of 51 (31%), and 24 out of 49 (49.0%; $P < 0.001$), had low disease activity without steroids.

Nevertheless, as of today, no strategy for TCZ withdrawal has been evaluated, and no prospective study has assessed relapses after TCZ discontinuation. In the current observational prospective extension study, we aimed to assess sustained remission after a six-month treatment with TCZ in the patients with GC-dependent PMR included in the SEMAPHORE trial, who achieved the primary endpoint.

PATIENTS AND METHODS

Study design and patient population. The inclusion criteria for the SEMAPHORE trial, a randomized parallel-group placebo-controlled, double-blinded study, were previously thoroughly detailed.[4] In summary, patients were ≥50 years old, fulfilled Chuang's classification criteria for PMR[6] and experienced disease relapse when the prednisone-equivalent (GC) dose was decreased to less than 10 mg/day, which was the SEMAPHORE definition of GC-dependency. Patients with manifestations of giant cell arteritis (GCA) were excluded. All participants were randomly assigned a ratio of 1:1 to receive intravenous 8 mg/kg of TCZ every four weeks or a corresponding placebo for 24 weeks. The GCs were tapered in accordance with the disease activity (PMR-AS), following a protocol previously described.[4] The final TCZ infusion was at week 20, the SEMAPHORE primary outcome was assessed at week 24, and the extension study lasted from week 24 to week 48. The investigators were advised to stop TCZ at week 24 if patients were in remission. No procedure was required beyond week 24 if patients were not in remission.

In this follow-up phase of the SEMAPHORE trial, all patients who achieved the primary endpoint at week 24 had a visit at week

32. Further follow-up visits were optional and planned every eight weeks until week 48 (Supplementary Figure 1). Additionally, follow-up stopped at the time of PMR relapse. Relapse was defined in the current extension study as the cessation of sustained remission. This included patients requiring a new infusion of TCZ, those with a PMR score of at least 10, or those needing an increase in GC dosage by ≥5 mg/day or more than 10 mg per day compared with baseline were considered to be relapsing. Anonymization regarding the original treatment group was maintained throughout the entire follow-up phase. During the follow-up phase, the patient could receive or not receive an open-label TCZ dose at each visit, according to the clinician's decision.

The trial was conducted in accordance with the Declaration of Helsinki and International Conference on Harmonisation guidelines for Good Clinical Practice. The trial protocol was approved by the appropriate ethics committee (CPP Ouest VI). Patients provided written informed consent.

Outcomes. The primary outcome of the current follow-up study was sustained remission, defined as the maintenance of the primary outcome of the SEMAPHORE trial (sustained low disease activity level, PMR-AS < 10) and a conserved low GC dose) with no TCZ treatment among patients who completed the composite endpoint of the treatment phase at week 24.

PMR-AS is a composite score for monitoring treatment in clinical practice and for use in therapeutic trials. The core set comprises five parameters, including a biologic factor (C-reactive protein [CRP] levels), a patient-reported outcome (pain intensity on a visual activity scale from 0 to 10), morning stiffness duration (in minutes, × 0.1), a physician's assessment of global activity (0–10), and a clinical examination (upper limb elevation 0–3).[5]

Among the secondary outcomes, we assessed the time to relapse, patient features at the time of relapse, TCZ reports, and safety of TCZ from week 24 to week 48 of follow-up. Furthermore, we evaluated the efficacy of TCZ among patients who were not in remission after six months of therapy.

Statistics. Patient characteristics at inclusion for patients in remission at week 24 and for patients who relapsed during the following weeks were recorded. Data are presented as frequencies and percentages for qualitative variables and as headcounts, means, SDs, medians, quartiles, minimums, and maximums for quantitative variables.

A Kaplan-Meier analysis was performed to describe the time to relapse from week 24 while censoring for patients lost to follow-up or by the end of the study. Adverse events during the extension phase were recorded and described accordingly.

RESULTS

Among the 33 patients who completed the primary outcome in the SEMAPHORE study and were considered in remission at

week 24, the mean age was 67.6 ± 8.3 years. The median GC dose at inclusion in the SEMAPHORE trial was 10.0 mg/day (interquartile range [IQR] 10.0–15.0), and 0 mg at week 24 after six doses of TCZ (IQR 0.0–3.0). Eighty-eight percent of the patients did not have GC treatment (Table 1). After week 24, all 33 patients considered in remission discontinued TCZ treatment except one (Supplementary Figure 2). The median PMR-AS at inclusion was 20.3 and was 3.7 (IQR 1.7–6.7) at week 24. The median follow-up time was 50.0 weeks (IQR 48.9–52.3), or 26 weeks after week 24.

At week 48, seven out of 33 patients did not complete the optional follow-up. Two of the remaining 26 patients experienced remission within the following six months, whereas 24 patients relapsed. At week 48, the relapse-free remission rate was 27.3% (95% confidence interval [CI] 11.9–45.4), as estimated by the Kaplan-Meier analysis. The median time to relapse was 15 weeks (95% CI 8.7–24) after TCZ discontinuation (Figure 1).

Table 1. Characteristics of 33 patients who achieved the primary outcome in the SEMAPHORE trial at week 24*

Characteristics	Value
At inclusion in the SEMAPHORE trial	
Demographics	
Age, mean ± SD, y	67.6 ± 8.3
Women, n (%)	23 (69.7)
PMR characteristics	
Disease duration, month, median (IQR)	19.0 (9.0–42.0)
CRP PMR-AS, median (IQR)	20.3 (15.1–29.0)
Ongoing treatments	
GC dosage, median (IQR)	10.0 (10.0–15.0)
GC dosage ≤5 mg/day, n (%)	3 (9.1)
GC dosage >5 mg/day, n (%)	30 (90.9)
Methotrexate use, n (%)	
Current	10 (30.3)
Never	16 (48.5)
Prior	7 (21.2)
Follow-up duration, median (IQR), weeks	50.0 (48.9–52.3)
At week 24 of the SEMAPHORE trial	
PMR characteristics	
CRP PMR-AS, median (IQR)	3.7 (1.7–6.7)
Patient VAS score, median (IQR)	2.0 (0.4–3.0)
Physician VAS score, median (IQR)	0.5 (0.0–1.0)
Elevation of the upper limbs, n (%)	
0	0
<90	0
90	1 (3.0)
>90	32 (97.0)
Morning stiffness, median (IQR), min	5.0 (0.0–15.0)
CRP level, median (IQR), mg/dL	0.0 (0.0–0.4)
Ongoing treatments	
GC dosage, median (IQR), mg/day	0.0 (0.0–3.0)
No GC, n (%)	22 (66.7)
GC dosage ≤5 mg/day, n (%)	29 (87.9)
GC dosage >5 mg/day, n (%)	4 (12.1)

* Primary outcome was defined as in remission with a decrease in GC (PMR-AS < 10 and GCs ≤5 mg/day or a decrease in GCs ≥10 mg compared to the baseline). CRP, C-reactive protein; GC, glucocorticoid; IQR, interquartile range; PMR, polymyalgia rheumatica; PMR-AS, polymyalgia rheumatica activity score; TCZ, tocilizumab; VAS, visual analog scale.

The earliest relapse occurred 76 days after the last TCZ infusion. In other words, TCZ prevented clinical relapses or increased CRP levels for a minimum of 11 weeks.

At the time of relapse, 13 out of 24 relapsing patients had no GC treatment, and the median GC dose for the 24 relapsing patients was 0 mg/day (IQR 0–10, range 0–25). The median CRP level was 5.2 mg/L (IQR 1.2–16.0, range 0–44), and the median PMR-AS was 12.0 (IQR 5.0–22.9). The increase in the PMR-AS was driven mainly by the increase in the median (IQR) patient visual analog scale (VAS) score, 6.0 (2.8–7.2). The other patients' characteristics at the time of relapse are displayed in Supplementary Table 1. Among the patients who did not experience any relapse, an increase of GC dose below 5 mg/day was observed in two of them (Supplementary Table 2). This minimal increase is not clinically relevant, therefore was not considered to be a relapse.

Among the 16 patients treated with TCZ but not in remission at week 24, four (25%) achieved remission after continuing TCZ treatment for another 24 weeks. The other 12 patients with GC-dependent PMR did not achieve remission but achieved decreased GC treatment during the follow-up extension.

Infections were reported in 45% of patients after a six-month course of TCZ. No major other side effects arose, as depicted in Supplementary Table 3.

DISCUSSION

In this extension of the SEMAPHORE trial, among the patients with GC-dependent PMR in remission after 24 weeks of treatment with TCZ, more than 90% relapsed in the following six months. Relapse occurred approximately 15 weeks after treatment discontinuation. This finding suggests that a six-month treatment plan in patients with GC-dependent PMR is not sufficient to achieve long-lasting treatment-free remission.

Seven patients did not complete the thorough six-month follow-up and quit the study before any relapse was noted, as allowed in the study design. Together with the two patients who did not relapse at week 48, nine patients did not relapse at the end of the follow-up period. This short follow-up time among the former seven patients could drastically impact the rate of remission maintenance. Because few patients did not relapse at week 48, analyses to determine predictive factors of relapse could not be performed.

To the best of our knowledge, no other prospective study has focused on strategies to discontinue TCZ in patients with GC-dependent PMR. In a retrospective study[7] including 53 patients with PMR who were mostly GC-dependent, TCZ was administered for 12 months, and strategies for discontinuation were analyzed. Although 48% of the attempts to abruptly stop TCZ failed and led to a relapse, significantly more patients with progressive dose tapering or time spacing (79% and 87%, respectively) achieved TCZ-free remission.
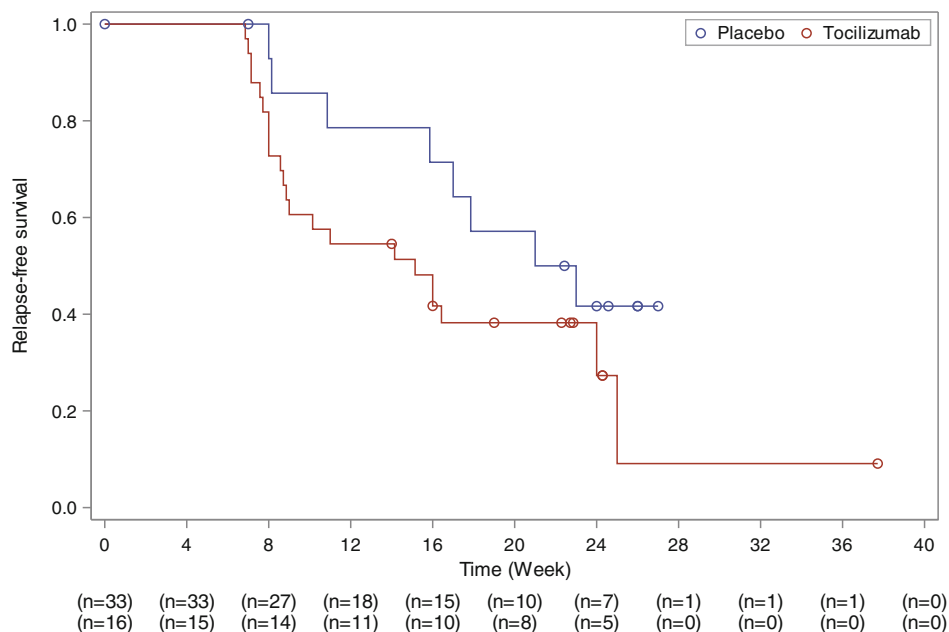
Figure 1. Relapse-free survival among patients with GC-dependent PMR in remission after six months of treatment with tocilizumab. Remission was defined as a PMR-AS <10 and daily GC dose of ≤5 mg/day or a daily GC dose decreased by ≥10 mg. Day 0 was the visit at week 24 in the SEMAPHORE trial. The last tocilizumab infusion was at week 20 in the SEMAPHORE study. GC, glucocorticoid, PMR, polymyalgia rheumatica; PMR-AS, polymyalgia rheumatica activity score. Color figure can be viewed in the online issue, which is available at http://onlinelibrary.wiley.com/doi/10.1002/art.43221/abstract.

Conversely, in the TENOR trial,[8] which included patients with new onset PMR, 20 patients received only three monthly TCZ infusion treatments and no GCs at the start of the trial. After three months, all patients were in remission and received tapered GC treatment starting at 7.5 mg per day. TCZ-free remission was sustained for all patients at six months. Among the 14 patients retrospectively retrieved two years after the start of the TENOR trial,[9] 12 experienced no relapse. Similarly, two other trials included only patients with new onset PMR. In the PMR-SPARE study by Bonelli et al,[10] subcutaneous TCZ was administered for 16 weeks, with the last assessment conducted eight weeks later (at week 24). In a study by Lally et al,[11] intravenous TCZ was administered for 12 weeks, with the final assessment conducted three months later. In both studies, TCZ was shown to reduce PMR activity in patients with new onset PMR. Therefore, these data suggest that patients with GC-dependent PMR and patients with GC-naive PMR present different characteristics and might benefit from different treatment strategies.

PMR and GCA are closely associated; 40% to 60% of patients with GCA present with PMR symptoms, and 14% to 20% of patients with PMR suffer from GCA.[12] Hence, treatment studies in patients with GCA are interesting to consider in PMR care. A few studies have investigated the decrease of TCZ treatment in patients with GCA. The Giant Cell Arteritis Actemra randomized trial evaluated the efficacy in patients who were GC-naive and patients with relapsing GCA who were placed into four different arms, including one arm given TCZ treatment weekly,

one arm given TCZ treatment every other week, and two placebo groups.[13] In a two-year extension after week 52, physicians were able to withdraw TCZ treatment from patients in remission.[14] Among the 125 patients included in the groups treated with TCZ who thoroughly completed the two-year extension, 90% to 95% were in remission. At the end, only 25 out of 81 (30.9%) patients who received a weekly TCZ dose and eight out of 36 (22.2%) patients who received a dose every other week were in remission after a one-year course of TCZ and could discontinue GC and TCZ treatments while maintaining two-year remission. Thus, together with smaller or retrospective studies,[15] this study highlights the high rates of relapse in patients who were diagnosed with GC-dependent GCA, as we observed in patients with GC-dependent PMR.

At the time of relapse in our study, the median CRP level was 5.2 mg/L (IQR 0–16), despite an expected normalized CRP level when patients received TCZ. In a retrospective study of GCA patients, 59% of patients treated with TCZ displayed an increase in CRP levels at the time of relapse,[15] but this record of elevation remains sparse and inconsistent.[16] Nevertheless, the different PMR activity scores presented excellent correlations (κ = 0.90), although no CRP levels were analyzed.[17]

At the time of relapse, the PMR-AS was increased to 12.0, whereas it was 3.7 at week 24. The increase in the PMR-AS score was driven mainly by the patient's VAS score, despite a short duration of morning stiffness and a low physician-determined VAS score. Therefore, we can hypothesize that a

different relapse definition, which is based solely on objective features rather than patient-reported outcomes, would result in a lower relapse rate.

Our study has numerous strengths. The prospective design of the study allows comprehensive and thorough data collection. Moreover, the study focuses on patients who were GC-dependent with long disease durations, which is relevant from different perspectives. TCZ tends to be indicated in patients who were GC-dependent with several relapses, as described in the latest French Rheumatology Society guidelines.[1] GCs remain the first-line treatment with an interesting cost–effectiveness ratio. Therefore, the inclusion of patients who are GC-dependent is consistent with the current use of TCZ in therapeutic strategies. The cost-effectiveness of TCZ in the treatment of patients with PMR remains to be debated.

However, our study is not without limitations. This study is only an extension, and despite its prospective design, the population depended on the few patients whose primary outcome was successful in the SEMAPHORE trial. Additionally, seven of the patients quit the follow-up before week 48. Hence, only a limited number of patients were included in our analysis.

Among patients with GC-dependent PMR in remission after a six-month TCZ treatment, only a minor portion of patients remained relapse-free after treatment discontinuation. Further investigations with a controlled design are needed to evaluate different strategies for TCZ discontinuation. PMR might be considered a chronic disease among patients with GC-dependent PMR, and further cost-efficacy studies for TCZ should be conducted. Additionally, TCZ tapering strategies are under evaluation in dedicated studies among patients with GCA,[18] and similar works need to be conducted in patients with PMR.

AUTHOR CONTRIBUTIONS

ROLE OF THE STUDY SPONSOR

REFERENCES

1. Wendling D, Al Tabaa O, Chevet B, et al. Recommendations of the French Society of Rheumatology for the management in current practice of patients with polymyalgia rheumatica. Joint Bone Spine 2024; 91(4):105730.

2. Dejaco C, Singh YP, Perel P, et al. European League Against Rheumatism; American College of Rheumatology. 2015 Recommendations for the management of polymyalgia rheumatica: a European League Against Rheumatism/American College of Rheumatology collaborative initiative. Ann Rheum Dis. 2015;74(10):1799–1807.

3. Floris A, Piga M, Chessa E, et al. Long-term glucocorticoid treatment and high relapse rate remain unresolved issues in the real-life management of polymyalgia rheumatica: a systematic literature review and meta-analysis. Clin Rheumatol 2022;41(1):19–31.

4. Devauchelle-Pensec V, Carvajal-Alegria G, Dernis E, et al. Effect of tocilizumab on disease activity in patients with active polymyalgia rheumatica receiving glucocorticoid therapy: a randomized clinical trial. JAMA 2022;328(11):1053–1062.

5. Leeb BF, Bird HA. A disease activity score for polymyalgia rheumatica. Ann Rheum Dis 2004;63(10):1279–1283.

6. Chuang TY, Hunder GG, Ilstrup DM, Kurland LT. Polymyalgia rheumatica: a 10-year epidemiologic and clinical study. Ann Intern Med 1982; 97(5):672–680.

7. Assaraf M, Chevet B, Wendling D, et al. Efficacy and management of tocilizumab in polymyalgia rheumatica: results of a multicenter retrospective observational study. Rheumatology (Oxford) 2024;63(8): 2065–2073.

8. Devauchelle-Pensec V, Berthelot JM, Cornec D, et al. Efficacy of first-line tocilizumab therapy in early polymyalgia rheumatica: a prospective longitudinal study. Ann Rheum Dis 2016;75(8):1506–1510.

9. Carvajal Alegria G, Saraux A, Devauchelle-Pensec V. Is tocilizumab as efficient as steroids early in polymyalgia rheumatica? Semin Arthritis Rheum 2020;50(4):582.

10. Bonelli M, Radner H, Kerschbaumer A, et al. Tocilizumab in patients with new onset polymyalgia rheumatica (PMR-SPARE): a phase 2/3 randomised controlled trial. Ann Rheum Dis 2022;81(6):838–844.

11. Lally L, Forbess L, Hatzis C, et al. Brief report: a prospective open-label phase IIa trial of tocilizumab in the treatment of polymyalgia rheumatica. Arthritis Rheumatol 2016;68(10):2550–2554.

12. Buttgereit F, Dejaco C, Matteson EL, et al. Polymyalgia rheumatica and giant cell arteritis: a systematic review. JAMA 2016;315(22): 2442–2458.

13. Stone JH, Tuckwell K, Dimonaco S, et al. Trial of tocilizumab in giant-cell arteritis. N Engl J Med 2017;377(4):317–328.

14. Stone JH, Han J, Aringer M, et al; GiACTA investigators. Long-term effect of tocilizumab in patients with giant cell arteritis: open-label extension phase of the Giant Cell Arteritis Actemra (GiACTA) trial. Lancet Rheumatol 2021;3(5):e328–e336.

15. Samec MJ, Rakholiya J, Langenfeld H, et al. Relapse risk and safety of long-term tocilizumab use among patients with giant cell arteritis: a single-enterprise cohort study. J Rheumatol 2023;50(10):1310–1317.

16. Matza MA, Dagincourt N, Mohan SV, et al. Outcomes during and after long-term tocilizumab treatment in patients with giant cell arteritis. RMD Open 2023;9(2):e002923.

17. D'Agostino J, Souki A, Lohse A, et al. Concordance and agreement between different activity scores in polymyalgia rheumatica. RMD Open 2024;10(1):e003741.

18. Tocilizumab discontinuation in giant cell arteritis (MAGICA). ClinicalTrials.gov identifier: NCT06037460. Updated May 28, 2025. Accessed June 26, 2025. https://clinicaltrials.gov/study/NCT06037460

AMERICAN COLLEGE
of RHEUMATOLOGY
Empowering Rheumatology Professionals

Aberrant Glycosylation of IgG in Children With Active Lupus Nephritis Alters Podocyte Metabolism and Causes Podocyte Injury

Rhea Bhargava,[1] Rohit Upadhyay,[1] Cong Zhao,[2] Prasad Katakam,[1] Scott Wenderfer,[3] Jing Chen,[1] Hua He,[2] Richard Cummings,[4] Maria G. Tsokos,[4] and George C. Tsokos[4]

Objective. Podocytes are integral to the maintenance of the glomerular filtration barrier. Their injury results in proteinuria and disease progression in lupus nephritis (LN). Aberrant IgG glycosylation drives podocyte injury in LN and leads to cytoskeletal rearrangement, motility changes, and decreased nephrin production. Based on these findings, we hypothesized that IgG glycosylation patterns differentiate systemic lupus erythematosus (SLE) with and without LN and that this aberrant glycosylation reprograms podocyte metabolism.

Methods. IgG was isolated from 40 pediatric SLE and from 7 healthy control samples. N-glycan analysis was performed using mass spectrometry. IgG deglycosylation was performed through enzymatic treatment by Peptide N-Glycosidase F for functional studies in podocytes. Untargeted metabolomics was performed in cultured podocytes after exposure to healthy IgG, LN-derived IgG, or deglycosylated LN-IgG and analyzed by metabolite set enrichment analysis. Digital droplet polymerase chain reaction was used to evaluate urine cells and podocytes in culture for *pyruvate kinase* expression.

Results. The glycosylation pattern of IgG from children with LN was different from that in children with SLE without kidney involvement. Successful treatment led to normalization of IgG glycosylation. Cultured podocytes treated with LN-derived IgG had a lower rate of glycolysis compared to podocytes incubated with deglycosylated LN-IgG or IgG from healthy volunteers. Untargeted metabolomics of podocytes revealed glycolysis as the most enriched pathway in LN and identified five key metabolites (pyruvic acid, phosphoenolpyruvic acid, 2-phosoglycerate, 3 phosphoglycerate, and fructose 1,6 bisphosphate) in which their levels significantly differed among podocytes exposed to LN-derived IgG (LN-IgG) compared to healthy IgG and deglycosylated LN-IgG. This analysis also revealed clustering around a rate limiting step of glycolysis catalyzed by PKM (Pyruvate Kinase M). Urine analyses revealed elevated pyruvic acid and greater expression of pyruvate kinase in podocytes shed in urine in patients with LN compared to levels in patients with SLE without kidney involvement. Podocytes in culture had elevated PKM levels when exposed to LN-IgG compared to IgG from patients with nonrenal SLE and LN in remission.

Conclusion. Aberrant IgG glycosylation develops in children with LN and adversely alters podocyte metabolism, rendering these cells vulnerable to injury. Successful treatment reverses IgG glycosylation to patterns comparable to those in patients with nonrenal SLE. These data lay a strong foundation for larger translational studies evaluating the potential of IgG glycosylation as a predictive and pharmacodynamic biomarker for LN. This work also supports a need for the development of approaches to control the aberrant glycosylation of self-targeting IgG in patients with LN as a mechanism to minimize podocytopathy.

INTRODUCTION

Systemic lupus erythematosus (SLE) is a chronic autoinflammatory disease, with significant kidney involvement in roughly 50% of cases.[1] One of the defining features of lupus nephritis (LN) is autoimmune injury of podocytes, the epithelial cells resting on the outer surface of glomerular capillaries that secrete and maintain the glomerular basement membrane and are

responsible for removing adhered IgG and albumin.[2,3] Podocyte injury is the main cause of proteinuria in LN, and low podocyte count (podocytopenia) leads to irreversible glomerular damage.[4–7] We and others have previously demonstrated that LN in adult patients is characterized by aberrantly glycosylated circulating IgG (LN-derived IgG [LN-IgG]) that is injurious to podocytes. Our work has further illustrated that LN-IgG injures podocytes at least in part by upregulating the expression of calcium [Ca^{2+}]/calmodulin-dependent kinase IV (CaMK4) and subsequently its downstream signaling pathways, with the sequelae of cytoskeletal dysfunction and repressed expression of the key glomerular slit diaphragm protein nephrin.[8–10]

Although as yet unproven, this mechanism of renal injury is likely to be especially prominent in children. SLE in children tends to be more aggressive, with more major organ involvement than in adults.[11] LN is not only the primary manifestation in 60% to 80% of childhood-onset SLE but also the most important determinant of morbidity and mortality in this population.[12] Because immunosuppressive treatment protocols are only able to achieve complete remission in less than 50% of patients with LN, up to 40% of patients with SLE go on to develop irreversible chronic kidney disease. The high frequency of SLE progression from no kidney involvement to irreversible kidney injury highlights a paramount need for identification of early blood and urinary biomarkers that precede observable changes in clinical parameters such as glomerular filtration rate (GFR) and/or creatinine clearance.[13–15] The appearance of aberrantly glycosylated IgG has great potential as one such an early biomarker because results in adults indicate it is likely to be one of the precipitating events of LN.[8–10]

The composition of IgG glycan chains in patients with LN is also important because the quantity and nature of these (ie, the glycome) can determine whether a given antibody may have a harmful or beneficial effect.[15–22] For example, our work has shown that the presence of galactose in IgG glycosyl chains protects against podocyte injury, but the presence of fucose promotes podocyte injury through the CaMK4 signaling pathway.[8] Consistent with our work, another study has shown that the presence of fucose at the IgG N-linkage site can affect IgG binding to several receptors and is associated with greater antibody-dependent cellular cytotoxicity than when glycan chains lack a core fucose.[17] The combination of a terminal sialic acid with galactose in the penultimate position has been reported to be associated with decreased inflammation, a reduction in the binding of the antibody to its Fc receptor, and the regulation of other cell interactions.[17,21,22]

The role played by IgG glycosylation in mediating the cytoskeletal alterations associated with podocyte injury in LN remains incompletely understood. Our earlier mechanistic studies identified CaMK4 up-regulation as being central to this process.[8–10] However, these studies have left open the question of whether the aberrant IgG glycosylation in patients with LN could also affect cytoskeletal function by modulating intracellular Ca^{2+} ([Ca^{2+}]i) concentrations. Ca^{2+} is the activating cofactor for CaMK4 (and thus signaling pathways downstream of it), and is also well established to regulate cellular cytoskeleton shape and cell motility through its allosteric activation of key metabolic enzymes and metabolite shuttles and its interactions with actin binding proteins that modulate actin polymerization and depolymerization.[23–25] The potential importance of Ca^{2+} in LN is illustrated by work showing that elevation of Ca^{2+}i levels by a variety of stimuli can cause podocyte, which, if unchecked, can lead to increased glomerular permeability and albuminuria.[24] There is also evidence that LN may lead to impairments in energy generating metabolic pathways such as glycolysis and lipid oxidation.[26] Podocytes require robust ATP synthesis to maintain their cytoskeleton and glomerular filtration barrier proteins,[27] and further, ATP energy is required for the active process of clearing basement membranes of adhered albumin and immune complexes. Some studies have highlighted a primary role for mitochondria in normal podocyte ATP generation, whereas others have found anaerobic glycolysis as the predominant metabolic pathway.[27–29] 29 As a result, any adverse effects of LN-IgG on either aerobic or anaerobic ATP production would render the podocyte less able to conduct these functions and could contribute to the proteinuria associated with LN.

In this study, we evaluated the IgG glycome in a pediatric SLE cohort and found that the composition and amount of IgG glycosylation changes toward a phenotype that is more harmful to podocytes over the course of the disease. These compositional changes can distinguish renal from nonrenal SLE and treatment-responsive from treatment-resistant disease. Further, we demonstrate that IgG glycosylation can change podocyte calcium handling and induce potentially harmful reprogramming of the glycolytic pathway in podocytes, presenting novel mechanistic pathways for LN-associated renal injury and offering potential therapeutic targets for LN.

MATERIALS AND METHODS

Mass spectrometry analysis of IgG N-glycans. N-glycans were released from 100 μg of purified IgG samples. Samples were resuspended in 40 μL of lysis buffer (5% sodium dodecyl sulfate, 50 mM triethylammonium bicarbonate [TEAB], pH 7.1). Homogenized samples were then treated with dithiothreitol at a final concentration of 10 mM and incubated at 95°C for 10 minutes to reduce disulfide bonds. After cooling to room

temperature, samples were acidified with 1.2% phosphoric acid and mixed by vortex. Acidified samples were diluted in 310 uL of binding buffer (90% methanol, 100 m*M* TEAB, pH 7.1) before applying to S-trap plate and processed according to manufacturer's protocol with some modifications (ProtiFi, LLC). Samples were then incubated with 1 µL of Peptide:N-glycosidase F (PNGase F) in 20 m*M* ammonium bicarbonate overnight at 37°C. Released N-glycans were cleaned with a hypercarb column and eluted with 50% acetonitrile and 0.1% trifluoroacetic acid. Released N-glycans were dried by Speedvac, then resuspended in 0.1% piperidine. Samples were analyzed on a Thermo Fisher Orbitrap Fusion Lumos Mass Spectrometer coupled to a Dionex Ultimate 3000 LC-MS (Liquid Chromatography/Mass Spectrometry) system. Samples were directly injected into the MS via the loading pump of the LC system. Data were analyzed using Skyline, Thermo Fisher Freestyle, and GlycoWorkBench software.

Immortalized human podocyte cell line.

The immortalized human podocyte cell line was cultured as previously described.[8–10] In short, cells were cultured in RPMI 1640 containing 10% fetal bovine serum, insulin, transferrin, and selenium. They proliferated at 33°C and differentiated into mature podocytes within 7 to 10 days when transferred to 37°C, due to the temperature-sensitive SV40-T gene and a telomerase gene. After being transferred to 37°C for 10 days, the cells were treated with IgG (10 µg/mL) from patients with SLE and active LN, patients with SLE without kidney involvement, or healthy controls. The cells were collected 24 to 72 hours after stimulation.

Measurement of intracellular calcium.

Podocytes were cultured and differentiated in 96 well plates to near confluence. Fluo-4, AM (Invitrogen, Catalog no. F14201) stock (1 m*M*) was dissolved in the cell media to achieve a final concentration of 4 µ*M* for use in the experiments. Cells were loaded with Fluo-4 for 30 minutes, and then IgGs (10 µg/mL) were added to the cells for different time points up to 60 minutes at 10-minute time intervals. Cells were washed with phosphate buffered saline (PBS) before fluorescence measurements. Fluorescence was measured using a BioTek Synergy HT Multi-Detection Microplate Reader (BioTek) through excitation at 494 nm and emission at 506 nm wavelength.

Quantitative polymerase chain reaction.

Purified total RNA (0.2–1 µg) was used to prepare complementary DNA (cDNA) through high-capacity RNA to cDNA kit (Applied Biosystems, catalog no. 4368814). Candidate gene expressions were estimated using the fluorescent dye SYBR Green methodology and CFX96 Touch Real-Time polymerase chain reaction (PCR) (Bio-Rad). Bioinformatically validated primer sets (QuantiTect Primer Assays, Qiagen, or Integrated DNA Technologies) were purchased for use in SYBR Green-based reverse transcriptase PCR. Real-time fluorescence from SYBR Green (Applied Biosystems) was measured by the Bio-Rad CFX Manager 3.1 System Software. Gene expression was normalized to the endogenous controls (β-actin or GAPDH) and comparative C(T) (2–[ΔΔCT]) values were estimated. Relative gene expression was calculated through the 2–(ΔΔCT) method and expressed in arbitrary units relative to paired controls.

Scratch or wound-healing assay.

Human podocytes were plated in six-well plates and treated after reaching 70% to 80% confluency. Scratches were created using a sterile 200 µL pipette tip. Following scratch formation, cells were immediately treated with vehicle, LN-IgG, or deglycosylated LN-IgG for 72 hours. Areas covered by cells were quantified and subjected to statistical analysis. Areas covered by cells were imaged between 0 and 72 hours for quantification.

Phalloidin staining.

Briefly, human podocytes were exposed to healthy IgG, LN-IgGs, or deglycosylated LN-IgGs, and cells were washed with PBS at the end of incubation and fixed with 4% paraformaldehyde. Fixed cells were washed three times with PBS, and permeabilized cells were washed with Triton X-100 (0.1%) and bovine serum albumin (2%) in PBS. Permeabilized cells were incubated with normal goat serum (Cell Signaling Technology, catalog no. 5425S) plus 0.1% Triton X-100 (PBS with Tween 20) for one hour to block nonspecific binding and subsequently with Phalloidin DyLight 488 (green; catalog no. 21,833) to visualize their cytoskeletal architecture. Stained cells were mounted with coverslips using UltraCruz Aqueous Mounting Medium (Santa Cruz Biotechnology, catalog no. sc-24,941). We captured images on original magnification, ×20, or ×40 using a fluorescent microscope (M5000, Thermo Fisher Scientific). We used ImageJ software to quantitate and analyze Immunofluorescence (IF) images.

IgG isolation and tagging and metabolomics sample preparation and analysis.

Ig were isolated using Melon Gel IgG Spin Purification Kit (Thermo Scientific; catalog no. 45206),[15] following manufacturer instructions. For untargeted metabolomics (endogenous metabolites), cells were grown in a 10-cm (or 60-cm) dish. After aspirating the culture media from the dish, adherent cells were washed with 5 mL of cold PBS and immediately harvested with 1 mL of cold 80:20 Methanol (EMD Millipore catalog no. MX0486-6) to water (volume/volume) harvest solution. Snap-frozen vials containing the pellet were stored at −80°C in a sample box until analysis was performed by Gigantest. Metabolite set enrichment analysis (MSEA) was performed to identify the biologically meaningful patterns using the MetaboAnalyst 6.0 software (https://www.metaboanalyst.ca).

Seahorse glycolytic rate assay.

Glycolytic parameters were determined in the Agilent Seahorse XFe24 analyzer using a Glycolytic Rate Assay Kit available from the manufacturer. Human podocytes were seeded in Seahorse XF24 cell culture microplates

and then pretreated with healthy IgG, LN-IgG, or deglycosylated LN-IgG for either 4 or 24 hours.

Droplet digital PCR. All reagents were purchased for use with the reverse transcriptase droplet digital PCR (RT-ddPCR) system (Bio-Rad). Predesigned primer and probe sets for human *PKM (pyruvate kinase), NPHS1(nephrin), and NPHS2(podocin)* were acquired from Thermo Scientific. A primer and probe set for human GAPDH were designed and synthesized by Thermo Scientific. For each target gene, the amount of total RNA in a PCR reaction was determined by a pilot ddPCR using serial diluted total RNA, in which the determined amount is in a linear range. Following droplet generation and PCR amplification, droplets were analyzed on the QX200 droplet reader, and target gene copy numbers were determined using the QuantaSoft analysis software (Bio-Rad). The data were normalized based on the copy number of the human GAPDH messenger RNA (mRNA) in each sample.

Direct ATP measurement. The total amount of ATP in cells (intracellular) and in cell media (extracellular) was determined by using the ATP determination kit from Thermo fisher scientific (catalog no. A22066). Differentiated podocytes in 96 well plates were exposed with healthy IgGs, LN-IgGs, and deglycosylated LN-IgGs for up to 48 hours. Cell lysate and cell supernatant was used for ATP determination as indicated by the manufacturer. The amount of ATP was determined by comparison with a curve obtained by using known amounts of ATP. FLUOstar Optima (BMG Labtech) multidetection microplate luminometer was used to quantify luminescence produced by the ATP assay.

Ethics, approval, and statistics. Data collection was approved by the institutional review board at Baylor College of Medicine. Informed assent and consent were obtained from the patients and caregivers before enrolling in the study, in accordance with principles of the Declaration of Helsinki.

Paired *t*-tests were employed to assess the association within six months for the type of glycan biomarkers between baseline and follow-up, as well as for features of chain and complex types. The generalized estimating equation (GEE) models were applied to analyze the association of LN with glycan markers, LN with features of chain, and LN with complex type among all baseline participants. Moreover, Spearman correlation coefficients and the Wilcoxon rank test were used to compare clinical features associated with the type of glycan biomarkers, features of the chain, and complex types among all participants at baseline.

RESULTS

Description of the patient cohort. We studied 30 children with a diagnosis of SLE who enrolled into the study from a single center in Houston, Texas, between 2015 and 2021. Inclusion criteria in the cohort included age 2 to 18 years and having at least 4 of 11 classification criteria from the 1997 revised American College of Rheumatology system for SLE. Deidentified clinical and pathologic information was extracted from patient records. Systemic Lupus Erythematosus Disease Activity Index (SLEDAI) 2000 scores were used to assess disease activity and severity,[30] and renal SLEDAI (rSLEDAI) scores were calculated using the four urinary metrics of the SLEDAI[31,32] (Table 1).

We also analyzed 10 paired samples from children with LN, collected before and six months after initiation of immunosuppressive treatment for LN. Immunosuppressive therapy consisted of hydroxychloroquine and glucocorticoids along with various combinations of mycophenolate, cyclophosphamide, anti-CD20, and intravenous IgG (IVIG).

Description of the IgG glycome. We detected 28 distinct glycan chains on IgG, all of which shared a (Mannose)3(N-acetylglucosamine)2 stem. Nine of the 28 chains lacked core fucosylation, whereas 1 chain had both a core and a terminal fucose residue. The remaining chains exhibited a single core fucose residue on their stems. Sixteen chains had terminal sialylation, whereas only three chains displayed terminal galactosylation.

Table 1. Demographics and characteristics of the individuals in the study cohort*

Baseline characteristic	SLE without LN	LN	Quiescent SLE	LN after treatment
Sex, n (%)				
Female	9 (90)	8 (80)	7 (70)	8 (80)
Male	1 (10)	2 (20)	3 (30)	2 (20)
SLEDAI, range	9–17	10–33	0–3	4–25
Renal SELDAI, range	0	8–16	0	0–16
UPCR, range, mg/mg	0.06–0.26	0.3–15	0.02–0.11	0.08–5.8
Serum Cr, range, mg/dL	0.4–0.7	0.4–2.0	0.5–0.7	0.4–1.4
eGFR, range, mL/1.73m^2/min	82–137	31–186	73–124	46–132
Anti-dsDNA, range, IU	0–1,280	0–2,560	0–1,280	0–1,280
C3,[a] range, mg/dL	14–126	5–51	89–151	5–118

* anti-dsDNA, anti–double-stranded DNA titers; Cr, creatinine; eGFR, estimated glomerular filtration rate; LN, lupus nephritis; SLE, systemic lupus erythematosus; SLEDAI, Systemic Lupus Erythematosus Disease Activity Index; UPCR, urinary protein-creatinine ratio.
[a] C3 complement levels.

Terminal sialic acid residues had a penultimate galactose in all chains. Among the 16 chains with terminal sialic acid residues, 6 chains had incomplete sialylation with an exposed terminal galactose. Eight glycan chains lacked any terminal galactose or sialic acid. The detected glycan chains along with their ion name and structure are displayed in Supplementary Figure 1.

Association of response to immunosuppressive therapy in LN with IgG glycomic alterations. We sought to determine whether treatment of LN with immunosuppressive induction therapy brought any changes to the IgG glycome. Accordingly, we compared the IgG glycan composition of 20 paired LN samples collected at diagnosis and six months after immunosuppression therapy. In this cohort, seven patients received oral mycophenolate as induction therapy, whereas three patients received intravenous cyclophosphamide. There was one child who received both mycophenolate and cyclophosphamide during the six-month follow-up period. Overall glycosylation of IgG was reduced after immunosuppression (Figure 1A). Notably, two chains characterized by the presence of terminal galactose and absence of sialylation (G9 and G10), were significantly up-regulated following induction therapy (Figure 1B and C). Conversely, 11 glycan chains showed significant decrease after treatment (G5, G11, G14, G19–G22, and G25–G27), 9 of which are characterized by terminally capped sialylated glycans (Figure 1D–N). Consistent with the findings of changes in the prevalence of specific chains, we observed a decrease in overall sialylation, an increase in overall neutral (uncharged) glycans, and an increase in overall terminal galactosylation after patients with LN underwent induction therapy (Figure 1O–Q). Statistical details for these analyses are shown in Supplementary Table 1.

To address the effects of pharmacotherapy, we compared the IgG glycome of children who experienced complete remission after immunosuppressive induction therapy (responders) to those who had persistent LN activity (nonresponders). Response to therapy was defined as rSLEDAI returning to 0 after six months of treatment. We found that glycan chain G9 was up-regulated in nonresponders but unchanged in responders, whereas the opposite effect was observed with glycan G1. The pattern of G9 up-regulation and G1 down-regulation was a differential characteristic between responders and nonresponders (Figure 2A and B). A similar observation showing G9 as a differentiator for responders and nonresponders had previously been observed in our study in adults.[8] Further examination of the overall IgG glycome characteristics revealed that levels of mono-antennary undecorated glycans, and biantennary galactosylated glycans were also differentiators of responders from nonresponders (Figure 2C and D).

Taken together, data from these experiments show that although levels of most glycans decreased after treatment, glycans with terminal galactose residues increased. Moreover G1, G9, and monoantennary complex chains emerged as potential biomarkers for monitoring how well a patient responds to induction therapy.

Distinct signature of IgG glycosylation in active LN compared to nonrenal SLE. Because the IgG glycosylation "signature" in patients with LN can be altered by SLE treatment, an obvious next question was whether there were specific glycosylation signatures associated with the progression from quiescent SLE to active SLE without renal involvement and subsequently from active SLE without renal involvement to LN. To answer this question, we evaluated the IgG glycome of children with active LN, active nonrenal SLE, and quiescent SLE and used GEE models to examine the association between IgG glycosyl chain composition and rSLEDAI, adjusting for age, sex, and race. Our data identified four chains (G20, G22, G23, and G26) elevated in patients with LN relative to levels in patients with quiescent disease, three of which (G20, G22, and G23) also increased with rSLEDAI (Figure 2E–G, Supplementary Tables 2 and 3). All three were characterized by terminal sialic acid residues with penultimate galactose. Of these, G20 was also statistically greater in patients with LN than in patients with nonrenal SLE (Figure 2E). Because this chain had also been found to decrease significantly after successful LN treatment (Figure 1H), our data would indicate that it might be particularly relevant to renal injury. Stepping back for a broader perspective, we also examined how the overall IgG glycan composition correlates with key clinical and serologic features indicative of active LN, such as low or declining GFR, elevated rSLEDAI scores, double-stranded DNA antibodies, low complement levels, hematuria, and proteinuria. We found that tri-antennary glycans capped with sialic acid and a penultimate galactose were in fact associated with all of the foregoing parameters (declining GFR in particular), whereas neutral glycans negatively correlated with GFR. In contrast, biantennary complex glycans were associated with better renal health as defined by higher GFR (Supplementary Tables 4 and 5).

In our comparison between active SLE without renal involvement and quiescent disease, we noted increased levels of three chains (G4, G5, and G6) lacking galactosylation and sialylation (Figure 2I–K). Conversely, the chain G18, distinguished by a terminal fucose, showed reduced levels in active SLE compared to the quiescent state. Notably, G18 also exhibited decreased levels in active LN relative to quiescent disease (Figure 2L).

In summary, the previously mentioned data suggest that IgG glycosylation may potentially be a tool for monitoring LN activity and differentiating SLE with and without LN. The G20:G18 ratio may have particularly good potential as a biomarker for LN because G20 was significantly greater and G18 was significantly lower in LN compared to both active SLE without renal involvement and quiescent SLE. Triantennary glycans capped with terminal sialic acid and penultimate galactose were associated with features that signify LN and rSLEDAI, making this pattern also characteristic of LN.
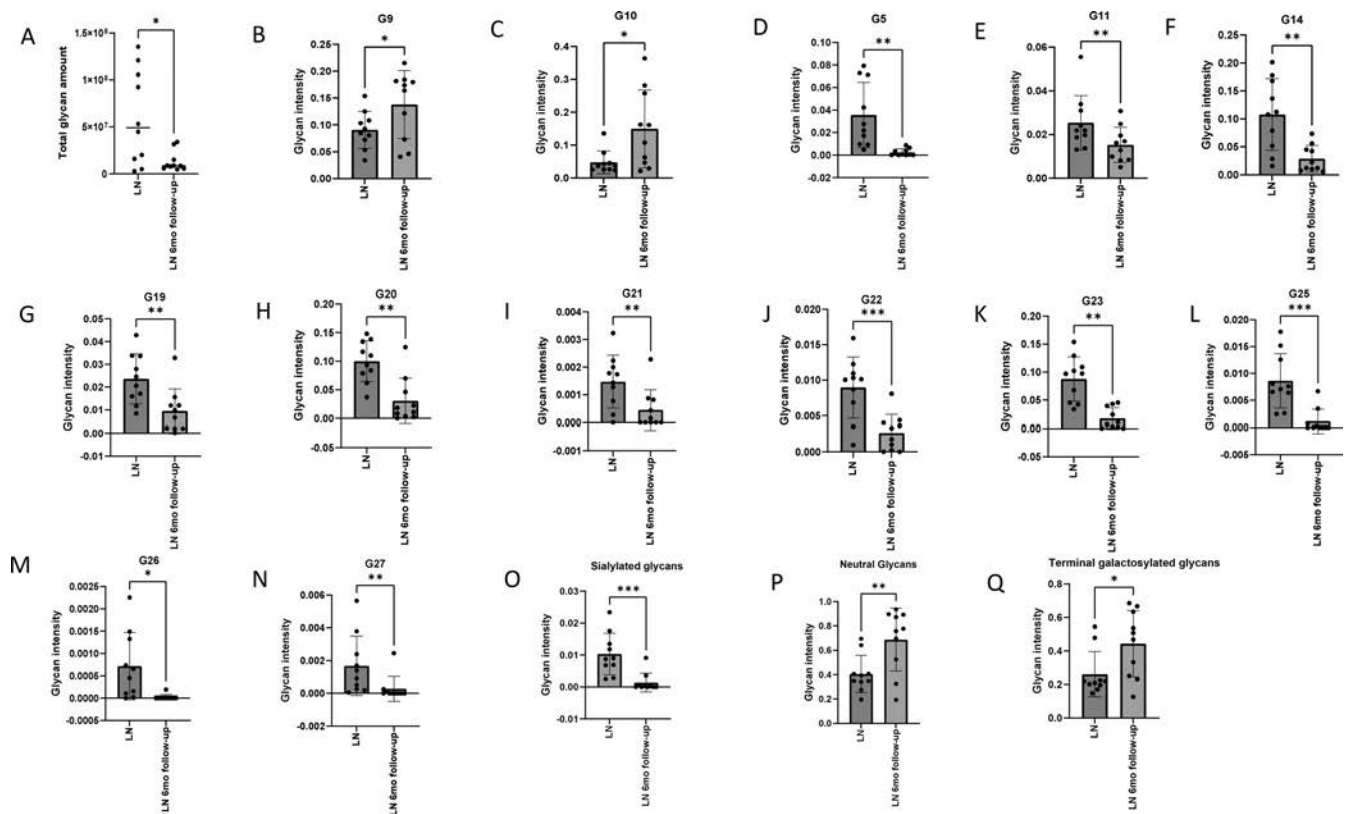
Figure 1. Induction therapy alters the IgG glycome in LN. (A) Overall glycosylation of IgG in paired samples before and six months after induction therapy in LN. (B–N) Levels of specific IgG glycan chains in paired samples with LN at diagnosis and six months after induction therapy. (O) Sialylated glycans decreased six months after induction therapy. (P) Neutral glycans and (Q) terminally galactosylated glycans increased six months after induction therapy in LN. Paired t-tests and false discovery rates were calculated to account for multiple tests over the markers studied (n = 10). *$P < 0.05$, **$P < 0.01$, ***$P < 0.001$. LN, lupus nephritis.

Glycosylation of IgG in LN causing cytoskeletal injury, altered calcium handling, and reduced metabolism in podocytes. Although data in this and earlier reports[8–10,33] indicate that IgG glycosylation changes during the course of LN and is associated with kidney injury, the role that the attached glycans may play in the pathogenesis of LN remains only partially elucidated. To explore this question further, we treated IgG isolated from patients with LN with PNGase F (deglycosylated LN-IgG) to remove glycan residues from the protein elements and conducted a series of experiment in which we incubated cultured podocytes for up to 72 hours with either LN-IgG, deglycosylated LN-IgG, or IgG isolated from untreated control patients without SLE. Consistent with our earlier results, podocytes exposed to native LN-IgG had disorganized cytoskeletons and lower motility compared to those exposed to control IgG or deglycosylated IgG (Figure 3A and B). Given the central role of Ca^{2+} in cytoskeletal organization, we evaluated calcium flux in podocytes exposed to LN-IgG in the presence and absence of glycans. LN-IgG exhibited a pronounced elevation in $(Ca^{2+})i$, exceeding the comparable increases observed with deglycosylated LN-IgG and control IgG (Figure 3C). LN-IgG also repressed the expression of

nephrin mRNA and protein relative to levels seen with both deglycosylated LN-IgG and control Ig-G (Figure 3D).

Because podocytes require a substantial level of ATP to maintain their cytoskeletal structure and function,[34] we hypothesized that aberrant IgG glycosylation may cause metabolic reprogramming of these cells toward a phenotype with a reduced metabolic capacity, and that this could be contributory to the etiology of LN. To explore this hypothesis in cultured podocytes, we first analyzed their real-time ATP production, oxygen consumption, and lactic acid release using the Agilent Seahorse XFe24 Metabolic Analyzer and determined that they derive more than 90% of their ATP production from glycolysis (Figure 4A). We also noted that ATP was decreased in podocytes exposed to LN-IgG compared to healthy IgG. This decline was abrogated when these cells were exposed to deglycosylated LN-IgG (Supplementary Figure 2). Based on this knowledge, we next used a glycolytic rate assay to evaluate the change in multiple glycolytic parameters after exposure of cultured podocytes to LN-IgG for either 4 or 24 hours. We found that cultured podocytes incubated with either native or deglycosylated LN-IgG for four hours had lower rates of basal and compensatory glycolysis compared to cells exposed to IgG
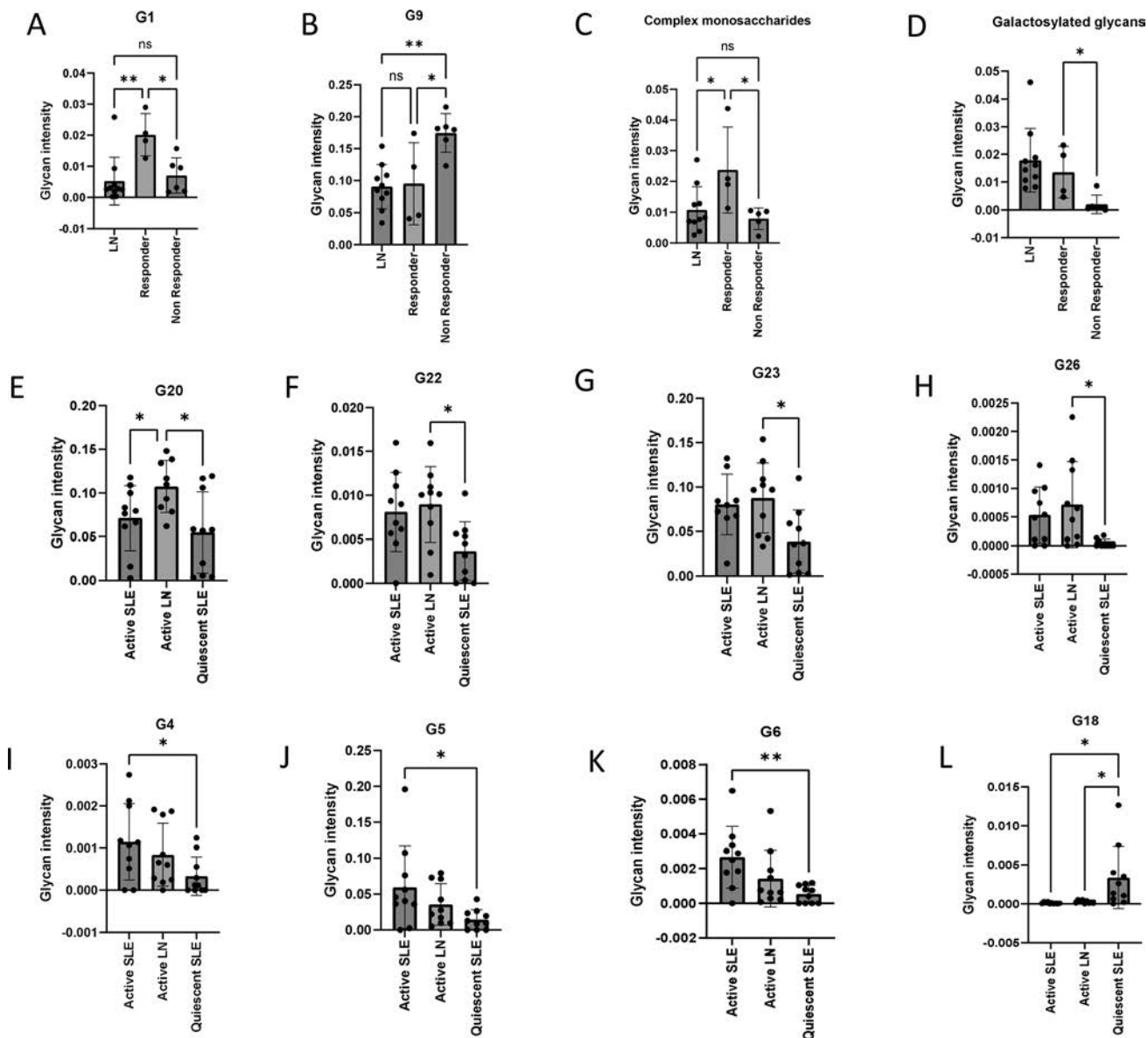
Figure 2. IgG glycomic alterations can differentiate responders from nonresponders to induction therapy among patients with LN and distinguish LN from quiescent SLE and active nonrenal SLE. Chains (A) G1 and (B) G9 changed in opposite directions in responders and nonresponders. (C) Complex monosaccharides and (D) galactosylated glycans also changed in opposite directions in these two groups. (E) G20 was higher in active LN compared to active SLE without LN, and quiescent LN (F–H) G22, G23, and G26 were higher in LN compared to quiescent LN. (I–K) G4, G5, and G6 were elevated in SLE without LN compared to quiescent SLE. (L) G18 was higher in quiescent SLE compared to active SLE with and without LN. Data are presented as means ± SEMs (n = 10). Statistical differences were determined using one-way analysis of variance with Tukey's post hoc test. *$P < 0.05$, **$P < 0.01$. LN, lupus nephritis; SLE, systemic lupus erythematosus.

from healthy volunteers (Figure 4B). This depressed glycolytic effect persisted out to 24 hours in podocytes incubated with native LN-IgG but disappeared in podocytes exposed to deglycosylated LN-IgG, in which glycolysis was found comparable to the controls (Figure 4C). We also explored the cellular energy phenotype of podocytes under these three conditions by plotting oxygen consumption rate (an index of aerobic metabolism) against the extracellular acidification rate (an index of anerobic metabolism). Podocytes exposed to deglycosylated LN-IgG appeared more energetic than

those exposed to native LN-IgG, suggesting that IgG glycosylation impeded the ability of podocytes to use both glycolysis and mitochondrial respiration to generate ATP for repair and maintenance of their cytoskeletal structure under autoimmune stress (Figure 4D).

Characterization of podocyte metabolic reprogramming by glycosylated IgG from patients with LN. We performed untargeted intracellular metabolomics in podocytes after treatment with healthy IgG, native LN-IgG, or
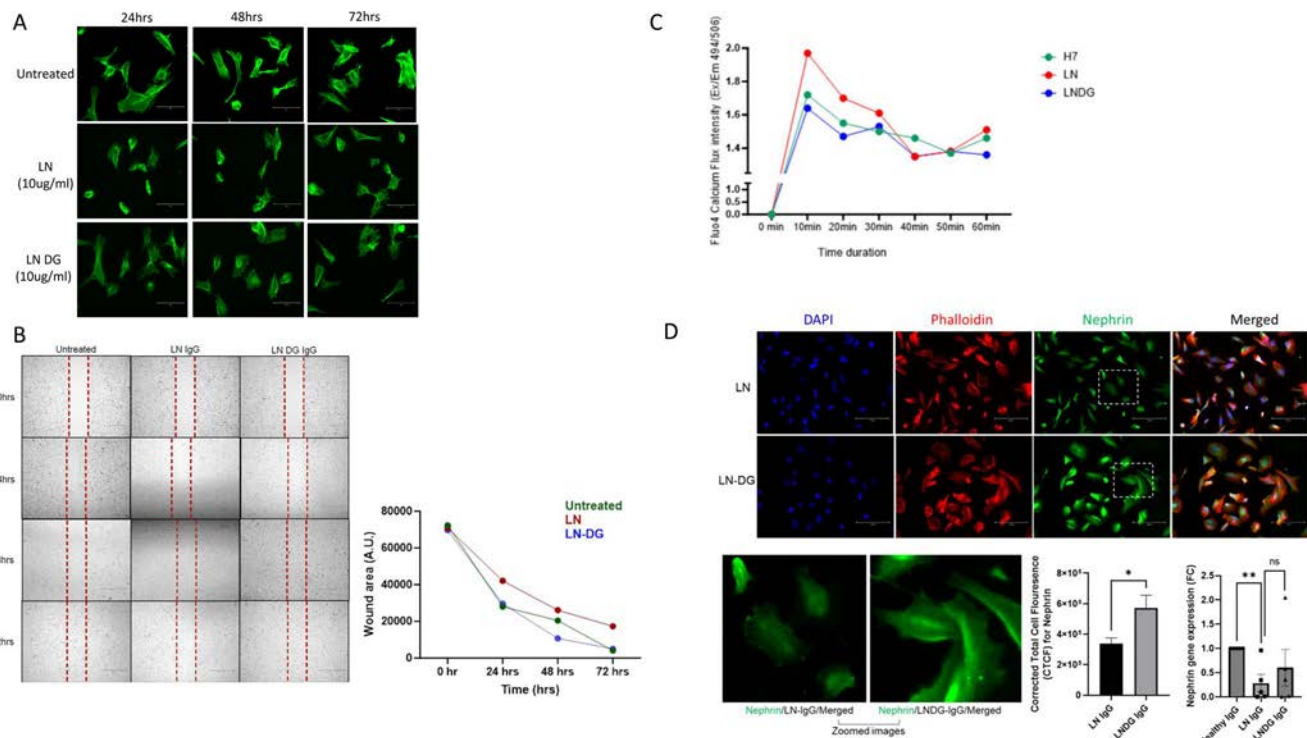
Figure 3. Deglycosylation of LN-IgG prevents podocyte injury. (A) Representative results of phalloidin staining of human podocytes after treatment with LN-IgG and deglycosylated LN-IgG. (B) Representative images and quantification (n = 5) of wound-healing assay 0, 24, 48, and 72 hours after wounding. Results show that IgG glycosylation renders podocytes hypomotile. (C) Increased calcium flux is noted in podocytes exposed to LN-derived IgG compared to deglycosylated LN-IgG and healthy IgG. (D) Depressed nephrin protein and messenger RNA (mRNA) expression in podocytes exposed to LN-derived IgG compared to deglycosylated LN-Ig. Protein expression was monitored by immunofluorescence, and mRNA expression was monitored by quantitative polymerase chain reaction showing depressed nephrin expression and transcription in podocytes exposed to LN-derived IgG compared to deglycosylated LN-IgG. Protein and mRNA expression data are means ± SEMs (n = 5). Statistical differences were calculated via one-way analysis of variance with Tukey's post hoc test. *$P < 0.05$, **$P < 0.01$. A.U., arbitrary units; CTCF, corrected total cell fluorescence; DAPI, 4',6-diamidino-2-phenylindole; DG, deglycosylated; Em, Emission; Ex, Excitation; LN, lupus nephritis; LNDG, Deglycoylated LN-IgG; ns, not significant.

deglycosylated LN-IgG to clarify specific metabolic pathways involved in podocyte injury in LN. Overall, 332 metabolites were identified across nine samples, 56 of which were significantly different between cells treated with native and deglycosylated LN-IgG (Supplementary Table 6). We subsequently conducted MSEA using the database of pathway-associated metabolite sets (Small Molecule Pathway Database) to compare the metabolomes of podocytes incubated with native and deglycosylated IgG. The top 20 metabolic pathways affected by LN-IgG glycosylation (glycosylated or deglycosylated) were identified (Figure 5A). Metabolites in the glycolytic pathway were among the most affected by IgG deglycosylation, with an overall 8.4-fold enrichment when the IgG glycosyl chains were removed. Within this pathway, levels of five glycolytic intermediates (fructose 1,6 biphosphate, pyruvic acid, 2-phosphoglycerate, 3-phosphoglycerate, and phosphoenolpyruvic acid) proved to be highly sensitive to IgG deglycosylation. Interestingly, IgG-deglycosylation–dependent increases consistent with the overall enrichment in this pathway were seen in only three of these five glycolytic intermediates (2-phosphoglycerate, 3-phosphoglycerate, and phosphoenolpyruvic acid), whereas deglycosylation-dependent decreases were

seen in the other two (fructose 1,6 biphosphate and pyruvic acid) (Figure 5B). These differential changes of metabolite levels within the same major pathway provide powerful evidence of podocyte metabolic reprogramming in LN that is dependent on IgG glycosylation.

We next sought to determine whether there was evidence of this type of metabolic reprogramming in human LN. Active LN has been associated with significantly changed levels of a large number of metabolic intermediates, including pyruvate,[35] in conjunction with the appearance of viable podocytes[36] in the urine. These observations, in combination with our cultured podocyte data showing increased podocyte pyruvate in response to native LN-IgG, led us to focus on urinary pyruvate and its potential sources in our cohort of patients with LN. Consistent with the metabolic reprogramming observed in cultured podocytes, we found increased urinary pyruvic acid levels in patients with active LN compared to patients with non-renal SLE (Figure 5C), and this was accompanied by an equally significant increase in the expression of pyruvate kinase mRNA in podocytes isolated from urine (PKM) (Figure 5D). To validate this increase in pyruvate kinase mRNA in our cultured podocyte model, we compared PKM expression in cultured podocytes incubated
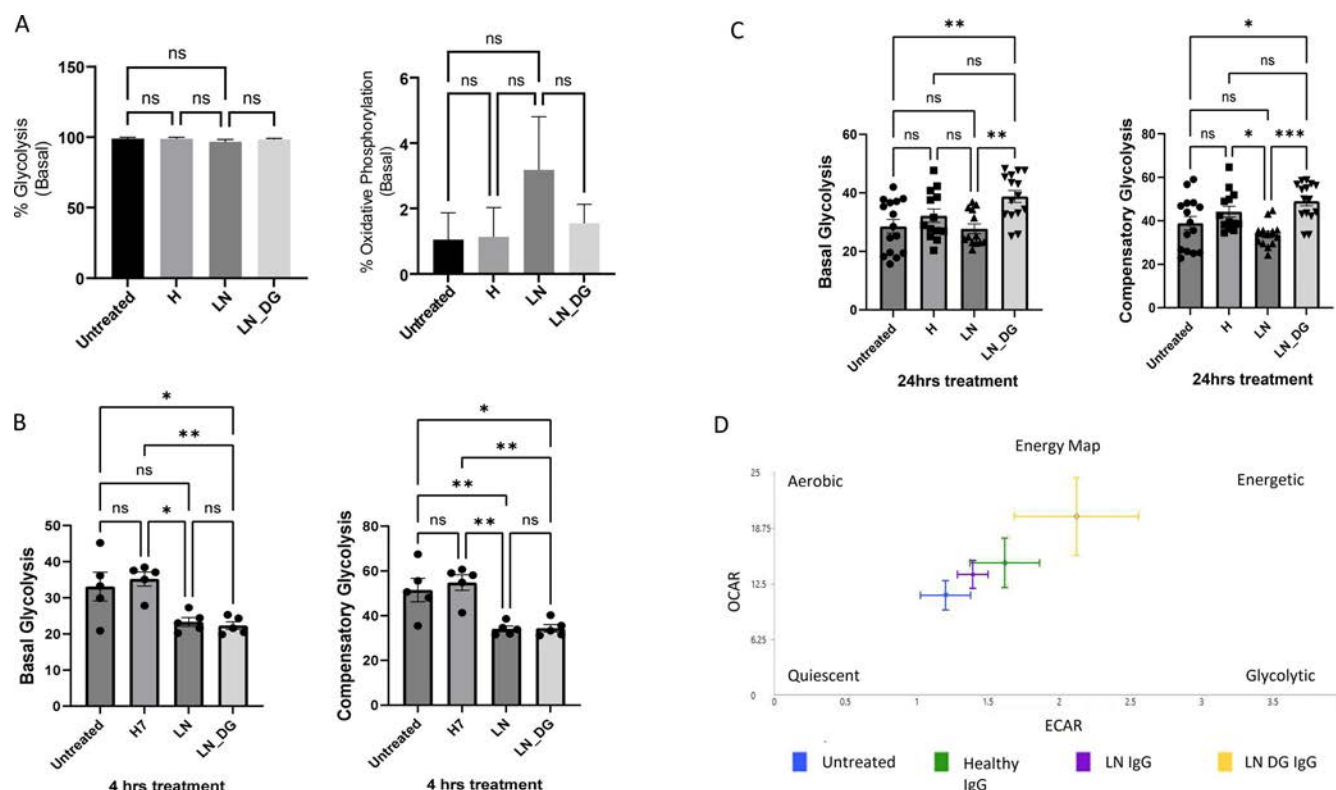
Figure 4. IgG glycans can alter podocyte metabolism and energy profile. (A) Podocytes in culture rely primarily on glycolysis for ATP production. Untreated: No IgG; H: IgG from healthy controls; LN: IgG from patients with LN; LN_DG: deglycosylated IgG from patients with LN. (B) Incubation of podocytes with LN-IgG for four hours suppresses both basal and complementary glycolysis regardless of IgG glycosylation status. (C) Only glycosylated IgG suppresses basal and compensatory glycolysis in 24-hour incubations. (D) Energy profile of podocytes was mapped by plotting OCAR against ECAR for podocytes exposed to control media, native IgG from healthy controls, native IgG from LN-IgG, and deglycosylated LN-IgG. Podocytes incubated with deglycosylated LN-IgG were more energetic than cells incubated with native LN-IgG. All results are expressed as means ± SEMs (n = 5). Statistical differences were calculated using one-way analysis of variance with Tukey's post hoc test. *$P < 0.05$, **$P < 0.01$. ECAR, Extra Cellular Acidification Rate; LN, lupus nephritis; ns, not significant; OCR, Oxygen consumption rate. Color figure can be viewed in the online issue, which is available at http://onlinelibrary.wiley.com/doi/10.1002/art.43200/abstract.

with either IgG isolated from patients with LN, patients with SLE without renal involvement, or IgG from patients whose LN was in remission. Consistent with our in vivo urinary data, we found that PKM expression was elevated in podocytes exposed to LN-IgG compared to both IgG derived from LN in remission and SLE without renal involvement (Figure 5E).

Taken together, these metabolic data suggest that IgG glycosylation can impair ATP production through glycolytic reprogramming in podocytes (Supplementary Figure 2), leaving them vulnerable to stress and susceptible to injury. Further, data from human urine confirm that pyruvic acid is a potential biomarker for LN and suggest that PKM may have potential as a therapeutic target within the glycolytic pathway.

DISCUSSION

We present evidence that the glycosylation profile of IgG undergoes significant changes during the course of SLE in children, exhibiting distinct patterns in children with active LN compared to those in remission. These findings suggest that the IgG

glycosylation profile holds promise as a secondary pharmacodynamic and disease activity biomarker in LN. Mechanistically, we discovered that glycosylation plays a critical role in the injurious effects of IgG on podocytes in pediatric patients with LN, potentially impairing podocyte metabolism and leaving these terminally differentiated cells less capable of adapting to stress and injury. LN is the most common critical organ complication of SLE that affects approximately 60% of patients with SLE.[37] The mortality rate in LN is 6-fold higher than in those with SLE without kidney involvement and 26-fold higher in those who progress to end-stage kidney disease.[38–42] The significant morbidity associated with LN highlights the need for novel early biomarkers defined by biologic vulnerabilities that can identify individuals at the greatest risk for LN in SLE and potentially allow treatment paradigms to shift to a proactive approach.

Podocyte injury is an early event in the pathogenesis of LN, and protecting podocyte integrity can ameliorate LN in mice.[43] We have previously demonstrated that aberrant IgG glycosylation drives podocyte injury in adult LN,[8–10] leading to the overarching hypothesis that delineation of the evolution of aberrant glycosylation
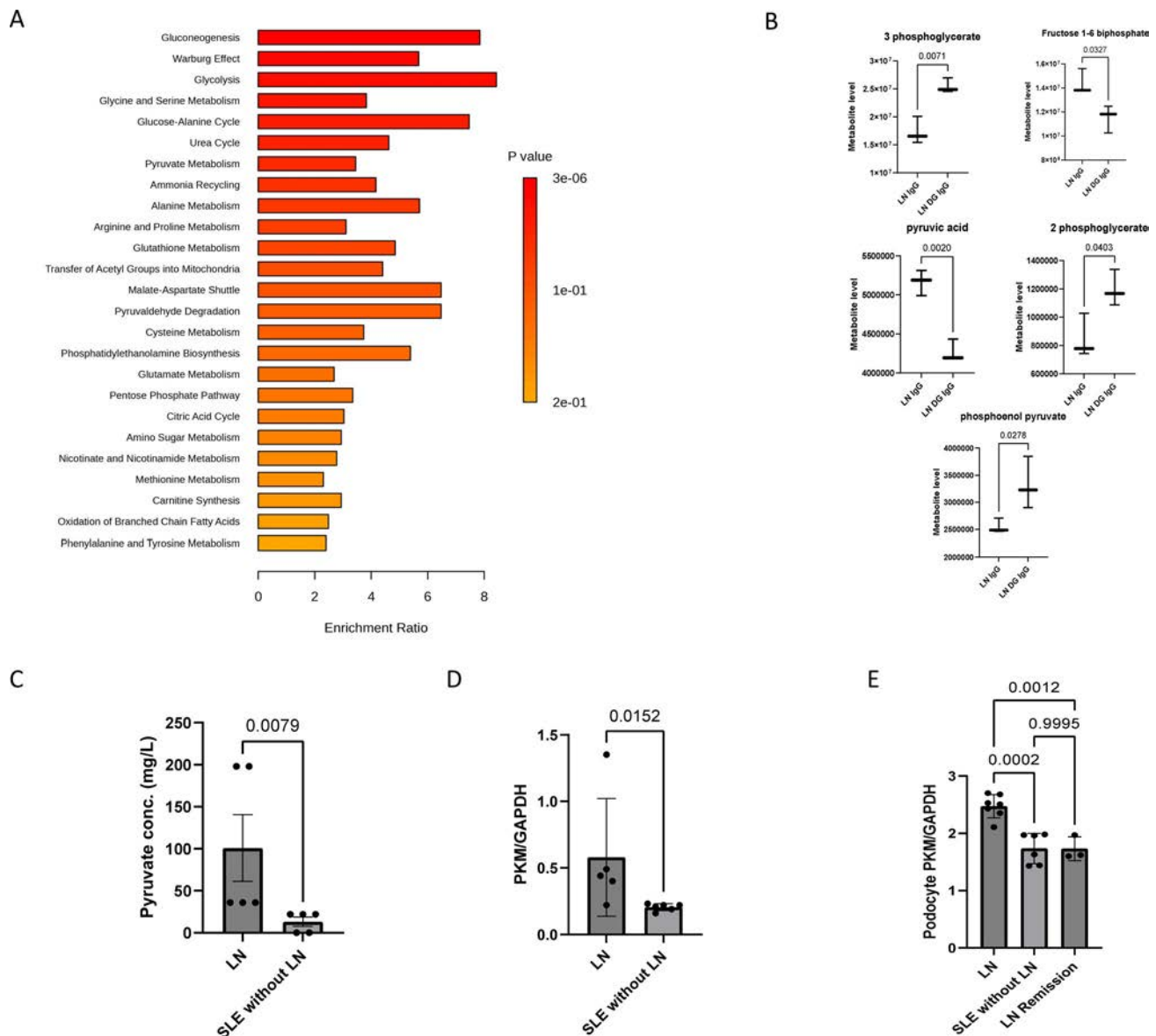
Figure 5. Glycans on IgG can alter podocyte metabolism. Untargeted metabolomics was performed in podocytes exposed to LN-IgG and deglycosylated LN-IgG. Overall, 332 metabolites were identified across nine samples, 56 of which were significantly different between cells treated with native and deglycosylated LN-derived IgG. (A) Top 25 enriched pathways enriched by deglycosylation are presented according to the results of metabolite set enrichment analysis. (B) Aberrantly regulated metabolites with P value < 0.05, fold change >2, or reciprocal of fold change value >2. All data were presented as means ± SEMs (n = 3). *P < 0.05; **P < 0.01. (C) Urine pyruvic acid levels were increased in LN. **P < 0.01, Mann-Whitney U-test. (D) Urine derived cells had higher PKM (pyruvate kinase M) transcription in LN compared to SLE without LN. **P < 0.01, two-tailed t-test. (E) Cultured podocytes were exposed to IgG from individuals with SLE with and without LN. Podocyte PKM levels were higher in podocytes exposed to LN-derived IgG compared to SLE without kidney involvement and LN in remission. Results are expressed as means ± SEMs (n = 3 in each group for metabolomic studies, n = 5 in each group for urine data), and statistical differences were calculated using one-way analysis of variance with Tukey's post hoc test. **P < 0.01, ***P < 0.001. conc., concentration; DG, deglycosylated; LN, lupus nephritis; SLE, systemic lupus erythematosus. Color figure can be viewed in the online issue, which is available at http://onlinelibrary.wiley.com/doi/10.1002/art.43200/abstract.

during the natural course of SLE may yield key data to explain the onset of kidney involvement in SLE. In this study, we evaluated a pediatric SLE cohort and found distinct differences in the IgG glycan signature present in SLE with and without LN and that specific IgG glycan patterns could also distinguish active LN from those in remission. Interestingly, we were also able to identify IgG glycan patterns that were able to differentiate children with LN who responded to

treatment compared to nonresponders. Although our findings require confirmation in a larger cohort involving both adult and pediatric patients, this study lays the foundation for the development of IgG glycans as noninvasive, potentially early biomarkers for LN.

Several studies have demonstrated that the effector function of IgG is dependent on the Fc-glycan chain attached to it, largely, the modulation of antibody binding to Fcγ receptors.[44] Our

findings are of special interest because podocytes do not express traditional Fcγ receptors but instead they express the neonatal Fc receptor (FcRn).[3] We have previously demonstrated that monomeric IgG, regardless of its glycosylation status, can bind to FcRn and enter the podocyte.[8,10]

Podocytes play an active role in removing proteins including IgG from the glomerular basement membrane, and an impairment of the clearance machinery is likely to be a common mechanism promoting glomerular disease.[3] To sustain their function, podocytes rely on a constant energy supply.[27–29] Here, we illustrate that IgG glycans can detrimentally impact podocyte bioenergetics by potentially inducing metabolic reprogramming and that podocytes may process or adapt to nonpathogenic IgG but undergo considerable stress when exposed to the pathogenic IgG present in LN and, in turn, may also fail to adapt to the increased energy requirements of the repair process. Untargeted metabolomics identified key glycolytic metabolites that were differentially regulated in podocytes dependent on whether they were exposed to pathogenic native LN-IgG or nonpathogenic deglycosylated LN-IgG. To our knowledge, this is the first study that evaluates podocyte metabolic pathways in a model of LN and that demonstrates the ability of glycans to alter metabolic processes. More importantly, we were able to demonstrate that at least one of these metabolic changes, an increase in urinary pyruvate, could plausibly translate to human LN as a novel completely noninvasive monitoring strategy for kidney involvement in SLE.

Our data from adults with LN revealed that IgG fucose was associated with podocyte pathogenicity, whereas the presence of terminal galactose was found to be protective against podocyte injury. Although the changes in galactosylation noted in the current pediatric cohort corroborated our initial findings in adults, here, we also found a correlation between the presence of sialic acid in IgG glycans and the clinical severity of LN. Sialylation has been shown to decrease with age,[45,46] and this may explain these differences. Genome-wide association studies in autoimmune disease have identified loci linked to N-glycosylation (ST6GAL1, B4GALT1, and FUT8) encoding glycosyltransferases that are associated with the addition of fucose and galactose or the transfer of sialic acid residues to galactose.[47] Our findings may suggest accelerated aging in lupus, but the overall significance of these differences requires further confirmation in a larger comparative adult and pediatric cohort. The anti-inflammatory effect of IVIG has been in part attributed to its glycosylation status.[20] In this cohort, only five children received IVIG during their disease course, whereas only one child received it as part of their induction therapy for LN. Given the small number of patients who received IVIG and the samples not being collected at the time of IVIG administration, this is less likely to be a confounder in our analysis. The small sample size is also a limitation; however, the data do support the need for larger studies to evaluate glycans as biomarkers for SLE.

The triggers for aberrant glycosylation in SLE have not been fully elucidated. Abnormally elevated cytokines can modulate IgG glycan patterns probably by regulating intracellular glycosyltransferases in human B cells. Cytokine-mediated, T cell–dependent activation of B cells may also alter IgG N-glycosylation.[48] Additionally, metabolites may account for the observed differences in glycosylation patterns between SLE with and without LN.[49]

In summary, we demonstrate that IgG glycosylation changes with SLE disease activity, exhibits a distinct signature in LN, and can differentiate responders from nonresponders to induction therapy. Data in this report also confirm that aberrant IgG glycosylation can lead to podocyte injury in childhood-onset LN in addition to the previously reported podocyte injury in adult LN.[8] Mechanistically we demonstrate that aberrant IgG glycosylation may alter the metabolome of podocytes, possibly lowering their capacity for compensatory increases in ATP production to repair injury due to autoimmune stimuli. More importantly, we provide a solid foundation for a larger biomarker study to determine the potential of the glycome to distinguish LN from nonrenal SLE, which, if successful, could improve our ability to monitor disease activity and identify patients with SLE more likely to develop kidney disease.

AUTHOR CONTRIBUTIONS

REFERENCES

1. Tsokos GC. Systemic lupus erythematosus. N Engl J Med 2011; 365(22):2110–2121.

2. Korbet SM, Lewis EJ; Collaborative Study Group. Severe lupus nephritis: the predictive value of a ≥ 50% reduction in proteinuria at 6 months. Nephrol Dial Transplant 2013;28(9):2313–2318.

3. Akilesh S, Huber TB, Wu H, et al. Podocytes use FcRn to clear IgG from the glomerular basement membrane. Proc Natl Acad Sci USA 2008;105(3):967–972.

4. Tian Y, Guo H, Miao X, et al. Nestin protects podocyte from injury in lupus nephritis by mitophagy and oxidative stress. Cell Death Dis 2020;11(5):319.

5. Nagata M. Podocyte injury and its consequences. Kidney Int 2016; 89(6):1221–1230.

6. Giardino L, Armelloni S, Corbelli A, et al. Podocyte glutamatergic signaling contributes to the function of the glomerular filtration barrier. J Am Soc Nephrol 2009;20(9):1929–1940.

7. Müller-Deile J, Schiffer M. The podocyte power-plant disaster and its contribution to glomerulopathy. Front Endocrinol (Lausanne) 2014;5:209.

8. Bhargava R, Lehoux S, Maeda K, et al. Aberrantly glycosylated IgG elicits pathogenic signaling in podocytes and signifies lupus nephritis. JCI Insight 2021;6(9):e147789.

9. Maeda K, Otomo K, Yoshida N, et al. CaMK4 compromises podocyte function in autoimmune and nonautoimmune kidney disease. J Clin Invest 2018;128(8):3445–3459.

10. Bhargava R, Maeda K, Tsokos MG, et al. N-glycosylated IgG in patients with kidney transplants increases calcium/calmodulin kinase IV in podocytes and causes injury. Am J Transplant 2021;21(1):148–160.

11. Baqi N, Moazami S, Singh A, et al Lupus nephritis in children. A longitudinal study of prognostic factors and therapy. J Am Soc Nephrol 1996;7(6):924–929.

12. Wenderfer SE, Chang JC, Davies AG, et al. Using a multi-institutional pediatric learning health system to identify systemic lupus erythematosus and lupus nephritis: development and validation of computable phenotypes. Clin J Am Soc Nephrol 2022;17(1):65–74.

13. Hanly JG, O'Keeffe AG, Su L, et al. The frequency and outcome of lupus nephritis: results from an international inception cohort study. Rheumatology (Oxford) 2016;55(2):252–262.

14. El Hadidi KT, Medhat BM, Abdel Baki NM, et al. Characteristics of systemic lupus erythematosus in a sample of the Egyptian population: a retrospective cohort of 1109 patients from a single center. Lupus 2018;27(6):1030–1038.

15. Gergianaki I, Fanouriakis A, Repa A, et al. Epidemiology and burden of systemic lupus erythematosus in a Southern European population: data from the community-based lupus Registry of Crete, Greece. Ann Rheum Dis 2017;76:1992–2000.

16. Reily C, Stewart TJ, Renfrow MB, et al. Glycosylation in health and disease. Nat Rev Nephrol 2019;15(6):346–366.

17. Shinkawa T, Nakamura K, Yamane N, et al. The absence of fucose but not the presence of galactose or bisecting N-acetylglucosamine of human IgG1 complex-type oligosaccharides shows the critical role of enhancing antibody-dependent cellular cytotoxicity. J Biol Chem 2003;278(5):3466–3473.

18. Fiebiger BM, Maamary J, Pincetic A, et al. Protection in antibody- and T cell-mediated autoimmune diseases by antiinflammatory IgG Fcs requires type II FcRs. Proc Natl Acad Sci USA 2015; 112(18):E2385–E2394.

19. Reusch D, Tejada ML. Fc glycans of therapeutic antibodies as critical quality attributes. Glycobiology 2015;25(12):1325–1334.

20. Anthony RM, Nimmerjahn F, Ashline DJ, et al. Recapitulation of IVIG anti-inflammatory activity with a recombinant IgG Fc. Science 2008; 320(5874):373–376.

21. Zhang Q, Joubert MK, Polozova A, et al. Glycan engineering reveals interrelated effects of terminal galactose and core fucose on antibody-dependent cell-mediated cytotoxicity. Biotechnol Prog 2020;36(6):e3045.

22. Ohmi Y, Ise W, Harazono A, et al. Sialylation converts arthritogenic IgG into inhibitors of collagen-induced arthritis. Nat Commun 2016; 7(1):11205.

23. dos Remedios CG, Chhabra D, Kekic M, et al. Actin binding proteins: regulation of cytoskeletal microfilaments. Physiol Rev 2003;83(2): 433–473.

24. Wieder N, Greka A. Calcium, TRPC channels, and regulation of the actin cytoskeleton in podocytes: towards a future of targeted therapies. Pediatr Nephrol 2016;31(7):1047–1054.

25. Brini M, Carafoli E. The plasma membrane Ca^2+ ATPase and the plasma membrane sodium calcium exchanger cooperate in the regulation of cell calcium. Cold Spring Harb Perspect Biol 2011;3(2):a004168.

26. Li W, Sivakumar R, Titov AA, et al. Metabolic factors that contribute to lupus pathogenesis. Crit Rev Immunol 2016;36(1):75–98.

27. Imasawa T, Rossignol R. Podocyte energy metabolism and glomerular diseases. Int J Biochem Cell Biol 2013;45(9):2109–2118.

28. Gujarati NA, Vasquez JM, Bogenhagen DF, et al. The complicated role of mitochondria in the podocyte. Am J Physiol Renal Physiol 2020;319(6):F955–F965.

29. Brinkkoetter PT, Bork T, Salou S, et al. Anaerobic glycolysis maintains the glomerular filtration barrier independent of mitochondrial metabolism and dynamics. Cell Rep 2019;27(5):1551–1566.e5.

30. Gladman DD, Ibañez D, Urowitz MB. Systemic Lupus Erythematosus Disease Activity Index 2000. J Rheumatol 2002;29(2):288–291.

31. Bajema IM, Wilhelmus S, Alpers CE, et al. Revision of the International Society of Nephrology/Renal Pathology Society classification for lupus nephritis: clarification of definitions, and modified National Institutes of Health activity and chronicity indices. Kidney Int 2018;93(4):789–796.

32. Petri M, Orbai AM, Alarcon GS, et al. Derivation and validation of the systemic lupus international collaborating clinics classification criteria for systemic lupus erythematosus. Arthritis Rheum 2012; 64: 2677–2686.

33. Lu X, Wang L, Wang M, et al. Association between immunoglobulin G N-glycosylation and lupus nephritis in female patients with systemic lupus erythematosus: a case-control study. Front Immunol 2023;14: 1257906.

34. Ozawa S, Ueda S, Imamura H, et al. Glycolysis, but not Mitochondria, responsible for intracellular ATP distribution in cortical area of podocytes. Sci Rep 2015;5(1):18575.

35. Omer MH, Shafqat A, Ahmad O, et al. Urinary biomarkers for lupus nephritis: a systems biology approach. J Clin Med 2024;13(8):2339.

36. Vogelmann SU, Nelson WJ, Myers BD, et al. Urinary excretion of viable podocytes in health and renal disease. Am J Physiol Renal Physiol 2003;285(1):F40–F48.

37. Rojas-Rivera JE, García-Carro C, Ávila AI, et al. Diagnosis and treatment of lupus nephritis: a summary of the Consensus Document of the Spanish Group for the Study of Glomerular Diseases (GLOSEN). Clin Kidney J 2023;16(9):1384–1402.

38. Yap DY, Tang CS, Ma MK, et al. Survival analysis and causes of mortality in patients with lupus nephritis. Nephrol Dial Transplant 2012; 27(8):3248–3254.

39. Lerang K, Gilboe IM, Steinar Thelle D, et al. Mortality and years of potential life loss in systemic lupus erythematosus: a population-based cohort study. Lupus 2014;23(14):1546–1552.

40. Bernatsky S, Boivin JF, Joseph L, et al. Mortality in systemic lupus erythematosus. Arthritis Rheum 2006;54(8):2550–2557.

41. Faurschou M, Dreyer L, Kamper AL, et al. Long-term mortality and renal outcome in a cohort of 100 patients with lupus nephritis. Arthritis Care Res (Hoboken) 2010;62(6):873–880.

42. Tektonidou MG, Dasgupta A, Ward MM. Risk of end-stage renal disease in patients with lupus nephritis, 1971-2015: a systematic review and Bayesian meta-analysis. Arthritis Rheumatol 2016;68(6):1432–1441.

43. Bhargava R, Tsokos GC. The immune podocyte. Curr Opin Rheumatol 2019;31(2):167–174.

44. Lutz HU, Fehr J. Total sialic acid content of glycophorins during senescence of human red blood cells. J Biol Chem 1979;254(22): 11177–11180.

45. Yanofsky SM, Dugas CM, Katsurada A, et al. Angiotensin II biphasically regulates cell differentiation in human iPSC-derived kidney organoids. Am J Physiol Renal Physiol 2021;321(5):F559–F571.

46. Tadokoro T, Yamamoto K, Kuwahara I, et al. Preferential reduction of the α-2-6-sialylation from cell surface N-glycans of human diploid fibroblastic cells by in vitro aging. Glycoconjugate J 2006;23(5–6): 443–452.

47. Lauc G, Huffman JE, Pučić M, et al. Loci associated with N-glycosylation of human immunoglobulin G show pleiotropy with autoimmune diseases and haematological cancers. PLoS Genet 2013;9(1):e1003225.

48. Radovani B, Nimmerjahn F. IgG glycosylation: biomarker, functional modulator, and structural component. J Immunol 2024;213(11): 1573–1584.

49. Scheper AF, Schofield J, Bohara R, et al. Understanding glycosylation: regulation through the metabolic flux of precursor pathways. Biotechnol Adv 2023;67:108184.

AMERICAN COLLEGE
of RHEUMATOLOGY
Empowering Rheumatology Professionals

Three-Year Outcomes and Latent Class Trajectory Analysis of the Childhood Arthritis and Rheumatology Research Alliance Polyarticular JIA Consensus Treatment Plans Study

Sarah Ringold,[1] Mei-Sing Ong,[2] George Tomlinson,[3] Marc D. Natter,[2] Laura E. Schanberg,[4] Vincent Del Gaizo,[5] Brian M. Feldman,[6] Katherine L. Murphy,[5] and Yukiko Kimura,[7] the CARRA Registry STOP-JIA Investigators

Objective. To assess the impact of differences in the timing of initial biologic disease-modifying antirheumatic drug (bDMARD) therapy using the Childhood Arthritis and Rheumatology Research Alliance (CARRA) Start Time Optimization of biologics in Polyarticular Juvenile Idiopathic Arthritis (JIA) (STOP-JIA) – consensus treatment plans study on outcomes through three years.

Methods. Start Time Optimization of biologics in Polyarticular-JIA participants with CARRA Registry follow-up through three years were eligible. Outcomes included American College of Rheumatology clinically inactive disease (CID) off glucocorticoids, clinical Juvenile Arthritis Disease Activity Score based on 10 joints inactive disease (cJADAS-10-ID) (cJADAS-10-ID: cJADAS-10 ≤ 2.5), clinical remission on medication (CRM), and proportion of time in CID and/or cJADAS-10-ID. Latent class trajectory modeling (LCTM) was applied to identify participant subgroups sharing similar disease courses over this period.

Results. A total of 297 participants were included (n = 190 step-up [SU], 76 early combination [EC], and 31 biologic first). At the three-year visit, CID was achieved by 35%, 42%, and 44%, respectively (P = 0.35 for SU versus EC). EC was superior to SU in achieving CRM (59.9% vs 40.6%; P = 0.012), time spent in CID (38% versus 30%; P = 0.04), and cJADAS-10-ID (51% versus 41%; P = 0.02). Slow, moderate, and rapid improvement trajectories were identified by LCTM; bDMARD initiation within the first (odds ratio [OR] 5.33) or second (OR 2.67) month from baseline was associated with the rapid improvement trajectory.

Conclusion. EC was superior to SU across three years for outcomes reflecting time spent in lower disease activity. Starting bDMARD within two months predicted rapid improvement and maintenance of inactive disease. These results support the hypothesis that early bDMARD initiation reduces overall disease burden in pJIA.

INTRODUCTION

Juvenile idiopathic arthritis (JIA) is the most common pediatric rheumatic disease and has been found to be an important cause of childhood-onset disability. The polyarticular forms of JIA (pJIA) are defined by involvement of at least five joints and are associated with a particularly high risk of persistently active disease that may result in joint damage and permanent disability.

Timely treatment with systemic therapies, including conventional synthetic disease modifying antirheumatic drugs (csDMARDs) and biologic disease-modifying antirheumatic drugs (bDMARDs), has been shown to reduce the risk of joint damage and improve quality of life and functional outcomes.[1,2] Recent studies show that the majority of patients with pJIA can achieve inactive disease (ID), but the actual percentages differ between studies, and the optimal strategy to attain ID is unknown.[3–5] This remains an active

area of research to further improve outcomes for children with pJIA.

The primary objective of the Start Time Optimization of biologics in Polyarticular-JIA (STOP-JIA) study was to compare the effectiveness of the Childhood Arthritis and Rheumatology Research Alliance (CARRA) consensus treatment plans (CTPs) for untreated pJIA in achieving American College of Rheumatology (ACR) clinically inactive disease (CID)[3] off of glucocorticoids (GC) at 12 months. The CTPs differed in the timing of bDMARD introduction: step-up (SU) (initial treatment with csDMARD monotherapy and adding a bDMARD at or after three months if needed); early combination (EC) (initial treatment with both a csDMARD and a bDMARD); and biologic first (BF) (initial treatment with bDMARD monotherapy). Although there were no significant differences between the CTPs in the achievement of CID off of GCs at 12 months in the primary study, a significantly higher proportion of children in the EC group achieved inactive disease at 12 months as assessed by the clinical Juvenile Arthritis Disease Activity Score using a maximum of 10 joints (cJADAS-10) (cJADAS-10-ID ≤2.5) and the pediatric ACR70 as compared with the SU group.[5] Latent class trajectory modeling (LCTM) of the participants' disease course (as defined by cJADAS-10-ID) identified three distinct disease trajectories through the 12 months, which was characterized by slow, moderate, or rapid disease activity improvement over time. The odds of being in the rapid improvement trajectory increased by more than threefold for patients treated with bDMARDs within three months from baseline.[6] Together, these analyses suggested a potential benefit at 12 months of earlier bDMARDs introduction in the treatment of children with pJIA.

However, because pJIA is a chronic disease, it is particularly important to measure the impact of initial therapies on longer-term outcomes that may ultimately be more significant and relevant in reducing overall disease burden. Therefore, the objective of the current study was to measure the impact of initial CTP and the timing of bDMARD introduction on disease outcomes for the STOP-JIA cohort through the three-year study period. Outcomes "through three years" are defined as those that occurred at any time during the entire period from the baseline visit until the three-year visit, whereas "at the three-year visit" is limited to an outcome at the three-year time point.

PATIENTS AND METHODS

Patients. Patients with untreated pJIA who were age ≤19 years at diagnosis and presented to 1 of 56 CARRA Registry sites participating in STOP-JIA were enrolled between December 2015 and August 2018. CARRA Registry data, including disease activity assessments, medication start and stop dates, and Serious Adverse Events/Events of Special Interest reporting were collected for STOP-JIA participants at 3, 6, 9, and 12 months and every 6 months (±3 months) thereafter at routine clinical care

visits. To capture as many patients as possible who had follow-up at around the three-year time point, the study cohort included those with a registry visit at 30 (±3) months, 36 (±3) months, or 42 (±3) months. The analysis cohort for disease trajectory using LCTM included participants with at least one calculable cJADAS-10 measurement in every year of study enrollment through three years to ensure that the analyses adequately captured the longitudinal disease course of study participants. The primary STOP-JIA study was approved by the Duke University Medical Center institutional review board (Pro00054616) and used the same consent as the CARRA Registry. See Appendix A for CARRA registry site principal investigators, subinvestigators, and research coordinators.

Treatment strategies. Development and descriptions of the CTPs have been previously published.[7,8] Because validated cJADAS-10 cutoffs for disease activity were available at the time of the STOP-JIA study,[8] attaining a score of ≤2.5 was used as a goal for disease activity status and used to guide shared decision-making about treatment at 3, 6, 9, and 12 months and every 6 months (±3 months) thereafter.

Outcomes. The following outcomes were assessed at Registry visits for each participant: 1) the individual ACR pediatric core set components[9]; 2) ACR criteria for CID off GCs[3]; 3) ACR clinical remission on medication (CRM), which was defined as CID at ≥2 consecutive CARRA Registry visits spanning at least 6 months[10]; and 4) the cJADAS-10 disease activity states.[11] To capture disease burden over time, time-weighted measures of CID and cJADAS-10-ID were calculated for each patient that represented the percentages of follow-up time spent in these states. When a patient was in the same disease activity state at two consecutive visits, the full duration between those visits was attributed to that state. If a patient's disease activity state changed between visits (eg, from inactive to active disease), half of the duration between visits was assigned to each state (Supplementary Table 1). Patient-reported outcomes (PROs) were captured every 3 months for the first 12 months of treatment and then every 6 months. These included the patient global assessment of overall well-being (patient/parent global assessment score), the Childhood Health Assessment Questionnaire, and the following Patient Reported Outcome Measurement Information Systems outcome measures: global health assessment, pain interference, mobility, and upper extremity. Medication safety was assessed through adverse event reporting mechanisms in place for the Registry.

Statistical analyses. A score was calculated for all participants that captured the propensity for each participant to be on the assigned CTP.[8] The propensity scores were used in regression models to compute inverse-probability-of-treatment-weighted (IPTW) comparisons of outcomes between CTP groups, with further adjustment by a small number of covariates

with residual imbalance. We computed differences in proportions with CID, cJADAS-10-ID, and ACR70 at the three-year time point, differences in proportions ever achieving CRM (CID for six or more months) during the three years, and differences in mean percentages during the three-year period spent in CID and cJADAS-10-ID. Missing outcome values at each time point during follow-up were imputed from a model that included all available outcome data (both at the same time and other times), CTP group, and baseline values of the physician global score, the patient/parent global score and the active joint count. All IPTW comparisons between CTPs were pooled across 30 imputed datasets. Analyses were performed in R 4.3.2 using the packages twang for calculating propensity scores and mice for imputation.[12–14]

LCTM. We applied LCTM to identify subgroups of participants sharing similar disease courses within the 36 months following STOP-JIA baseline, and to evaluate whether the timing of receiving a bDMARD was associated with a participant's trajectory class. Longitudinal disease activity, measured by cJADAS-10, was considered the class-defining variable in the model. Models were fitted for each of three definitions of early receipt of a bDMARD: by one, two, or three months from enrollment. Each model also included a propensity score (PS), represented by PS quintile, to adjust for differences in patient mix between those that did and did not receive a bDMARD early. Details of the modeling approach are described in Supplementary Methods.

RESULTS

A total of 297 patients had at least one CARRA Registry visit 30 to 42 months after enrollment, including 190 patients (64%) originally started on SU, 76 (36%) on EC, and 31 (10%) on BF (Table 1). When compared with patients who did not have a follow-up visit 30 to 42 months after enrollment, patients who had follow-up tended to be younger at baseline, less likely to be Black, and more likely to be White (as determined by a larger standardized mean difference (Supplementary Table 2). There were no other large differences between patients with and without follow-up at baseline.

Comparisons between CTPs for three-year outcomes. There were no significant differences between CTPs in the proportion of participants who achieved CID off GCs at the three-year time point for either the observed values or the PS adjusted and imputed estimates (EC 42.6%, BF 44.3%, SU 34.9) (Table 2). There were also no significant differences between CTPs in cJA-DAS10 ID at the three-year visit (adjusted estimates 61.3% EC, 58.6% BF, and 46.8% SU).

A higher proportion of patients in the EC group achieved CRM during the three-year follow-up as compared with the SU group (59.9% versus 40.6%; difference 19%, 95% CI 4.2–34.3, $P = 0.012$) (Table 3); there was no significant difference in achievement of CRM between EC and BF groups ($P = 0.316$). Comparing the percentage of time spent in CID through three years between CTPs, patients receiving EC treatment spent a statistically significantly higher proportion of time in CID (37.7%) compared with SU treated patients (29.5%; $P = 0.041$; Table 3). The proportion of time spent in cJADAS-10-ID, was also higher for the EC versus SU group (51.2% versus 41.1%; $P = 0.018$). Figure 1, which shows the percentages of participants in each cJADAS-10 disease activity state over time by CTP, represents this finding graphically; more patients in the EC CTP achieved inactive and low disease activity states than in the other two CTP groups during the 3 years. Seventeen participants experienced 22 SAEs, and 36 patients experienced 40 events of special interest that were not classified as SAEs (Supplementary Tables S23–6). No deaths were reported.

Latent trajectory classes. A total of 259 patients had at least one cJADAS-10 measurement in each year of follow-up. The best-fitting model identified three distinct disease trajectories in the cohort, characterized by rapid, moderate, and slow improvement in disease activity over time (Figure 2 and Supplementary Figure 1). Patients in the rapid improvement group experienced the fastest improvement in disease activity, achieving cJADAS-10-ID (cJADAS-10 ≤ 2.5) within the first year of study enrollment, and remained inactive throughout years 2 and 3. Patients in the moderate and slow improvement groups had higher disease activity at baseline, compared with the rapid improvement group. Moderate and slow improvement groups also exhibited improved cJADAS-10 scores within the first year, although the moderate improvement group achieved this at a faster rate. While patients in the moderate improvement group continued to improve in years 2 and 3 and had mean scores in the minimal disease activity range (cJADAS-10 >2.5–5) by year 3, mean scores for patients in the slow improvement group continued in the moderate disease activity range (cJADAS-10 >5–16) throughout years 2 and 3. Of 259 patients in the total cohort, 20 (7.7%) were classified as slow improvement, with no variation by model. The number of patients classified as rapid and moderate improvement varied by model, ranging from 165 (63.7%) to 176 (68%) for rapid, and 63 (24.3%) to 74 (28.6%) for moderate improvement groups (Supplementary Table 7). Seventy-four of the 171 patients (43.3%) who had the rapid improvement trajectory received bDMARDs within 2 months of enrollment (Supplementary Table 8). In all models, the mean posterior class-membership probabilities exceeded 0.80 for all three classes, indicating clear separation of class membership (Supplementary Table 7). With the exception of similar disease activity at baseline for the moderate and slow improvement groups, mean predicted trajectories and 95% predicted intervals for the three classes did not intersect (Figure 2), indicating clear separation of class membership. We also did not observe statistically significant differences in disease duration among children in different latent trajectory classes.

Table 1. Baseline characteristics of patients included in the three-year analysis*

Baseline characteristics	SU (n = 190)	EC (n = 76)	BF (n = 31)	P value	SMD
Age, median (IQR), y	10.6 (5.8–13.5)	11.3 (8.7–15.0)	11.7 (5.1–14.0)	0.070	0.213
Female, n (%)	142 (74.7)	59 (77.6)	16 (51.6)	0.016	0.376
Race, n (%)				0.935	0.075
Black	11 (5.8)	5 (6.6)	2 (6.5)		
Other	35 (18.4)	17 (22.4)	7 (22.6)		
White	144 (75.8)	54 (71.1)	22 (71.0)		
Months since symptom onset, median (IQR)	5.8 (2.9–16.5)	6.9 (3.4–17.2)	4.5 (2.3–17.3)	0.459	0.071
Months since diagnosis, median (IQR)	0.0 (0.0–0.9)	0.0 (0.0–0.4)	0.6 (0.0–2.1)	0.039	0.198
Disease course, n (%)				0.018	0.571
Enthesitis related	11 (5.8)	6 (7.9)	6 (19.4)		
Extended oligoarticular	11 (5.8)	0 (0.0)	2 (6.5)		
Poly (RF−)	123 (64.7)	41 (53.9)	12 (38.7)		
Poly (RF+)	32 (16.8)	21 (27.6)	6 (19.4)		
Psoriatic	10 (5.3)	5 (6.6)	3 (9.7)		
Undifferentiated	3 (1.6)	3 (3.9)	2 (6.5)		
Physician global assessment, median (IQR)	5.0 (3.5–6.5)	6.0 (5.0–8.0)	6.0 (5.0–8.0)	<0.001	0.389
Patient/parent global, median (IQR)	4.0 (1.5–6.0)	5.0 (3.0–7.0)	5.0 (3.0–7.0)	0.015	0.307
cJADAS-10, median (IQR)	17.0 (14.0–20.5)	21.0 (18.0–23.0)	19.0 (16.0–22.0)	<0.001	0.452
Number of joints with active arthritis, median (IQR)	9.0 (6.0–15.0)	14.5 (9.0–22.2)	8.0 (6.0–16.0)	<0.001	0.329
CHAQ, median (IQR)	0.6 (0.2–1.3)	1.0 (0.5–1.5)	0.9 (0.6–1.8)	0.027	0.261

* Visit within the following window: −30 to 42 months. The P values and SMDs compare the three CTP groups for the 297 patients in the three-year cohort. P values are from chi-squared tests for categorical variables and Kruskal-Wallis tests for continuous variables. BF, biologic first; CHAQ, Childhood Health Assessment Questionnaire; cJADAS-10, clinical Juvenile Arthritis Disease Activity Score based on 10 joints; CTP, consensus treatment plans; EC, early combination; IQR, interquartile range; Poly, polyarticular; RF, rheumatoid factor; SMD, standardized mean difference; SU, step-up.

The timing of bDMARD initiation was assessed as a predictor of trajectory membership using slow improvement as the reference (Table 4). Odds ratios (ORs) listed for being in the rapid or moderate improvement groups therefore represent the relative odds of being in the respective group rather than the slow improvement group when a bDMARD is started early. These analyses showed that timing of bDMARD initiation was a significant predictor of disease trajectory. Specifically, those treated with bDMARDs within the first month after baseline assessment were much more likely to follow the rapid improvement trajectory (OR 5.33; 95% confidence interval [CI] 1.35–21.1; P = 0.017) than

the slow improvement trajectory. Similarly, initiation of bDMARDs within the first 2 months was associated with the rapid improvement trajectory (OR 2.67; 95% CI 1.09–6.53; P = 0.032). Of note, 34 patients (19.7%) in the rapid improvement group and 7 patients (10.4%) in the moderate improvement group did not receive a bDMARD during the 3 years, and all patients in the slow improvement group received bDMARDs at some time during the 3 year follow-up. PROs improved in all CTP groups over the three-year timeframe, with the EC patients improving most. However, the differences between CTPs were small, and the small sample size and low response rates make interpretation

Table 2. Differences between CTPs in achievement of ACR CID off GCs or ACR remission at three years*

	Unadjusted estimate, %	Adjusted estimate, % (95% CI)	IPTW difference between CTPs, % difference (95% CI)	
			Versus biologic first	Versus SU
CID off of GCs at three years				
Early combination	34.9	42.6 (28.2–57.0)	−1.7 (−25.1 to 21.7; P = 0.887)	7.7 (−8.6 to 24.0; P = 0.353)
Biologic first	40.7	44.3 (25.3–63.3)	–	9.4 (−11.9 to 30.7; P = 0.387)
SU	34.2	34.9 (25.7–44.1)	–	–
cJADAS-10 inactive disease at three years				
Early combination	60.7	61.3 (47.6–74.9)	2.6 (−20.6 to 25.9; P = 0.824)	14.5 (−1.4 to 30.3; P = 0.073)
Biologic first	63.6	58.6 (39.2–78.0)	–	11.8 (−9.3 to 33.0; P = 0.273)
SU	56.6	46.8 (37.7–55.8)	–	–

* Estimates at three years for patients who had a visit in the 30 to 42 month window; unadjusted estimates are based on observed data, and adjusted estimates are based on the imputed datasets with both IPTW and regression adjustment. A total of 242 participants had observed data at three years for CID and 226 for cJADAS-10. All 297 contributed to the adjusted estimates at three years. cJADAS-10 inactive disease is cJADAS-10 ≤ 2.5. ACR, American College of Rheumatology; CID, clinically inactive disease; cJADAS-10, clinical Juvenile Arthritis Disease Activity Score based on 10 joints; CI, confidence interval; CTP, consensus treatment plans; GC, glucocorticoid; IPTW, inverse-probability-of-treatment-weighted; PS, propensity score; SU, step-up.

Table 3. Differences between CTPs in achievement of ACR Clinical Remission, percentage of time spent in CID or cJADAS-10 through three years[*]

	Unadjusted estimate, %	Adjusted estimate, % (95% CI)	IPTW difference between CTPs, % difference (95% CI)	
			Versus BF	Versus SU
ACR clinical remission at any time through three years				
EC	50.0	59.9 (47.1–72.7)	12.3 (−11.7 to 36.3; $P = 0.316$)	19.2 (4.2–34.3; $P = 0.012$)
BF	32.3	47.6 (26.7–68.5)	–	6.9 (−15.7 to 29.6; $P = 0.547$)
SU	36.3	40.6 (32.9–48.3)	–	–
Percentage of time spent in ACR CID through three years				
EC	41.3	37.7 (31.0–44.5)	−0.6 (−13.7 to 12.6; $P = 0.934$)	8.2 (0.3–16.1; $P = 0.041$)
BF	35.5	38.3 (26.9–49.7)	–	8.8 (−3.3 to 20.8; $P = 0.154$)
SU	31.8	29.5 (25.7–33.3)	–	–
Percentage of time spent in cJADAS-10 inactive disease				
EC	55.9	51.2 (43.9–58.4)	4.0 (−9.6 to 17.6; $P = 0.565$)	10.1 (1.7–18.4; $P = 0.018$)
BF	48.6	47.2 (35.8–58.5)	–	6.1 (−6.4 to 18.5; $P = 0.338$)
SU	44.8	41.1 (36.9–45.3)	–	–

* Estimates at three years for patients who had a visit in the 30 to 42 month window; unadjusted estimates are based on observed data, and adjusted estimates are based on the imputed datasets with both IPTW and regression adjustment. cJADAS-10 inactive disease is cJADAS-10 ≤ 2.5. ACR, American College of Rheumatology; BF, biologic first; CID, clinically inactive disease; cJADAS-10, clinical Juvenile Arthritis Disease Activity Score based on 10 joints; CI, confidence interval; CTP, consensus treatment plans; EC, early combination; IPTW, inverse-probability-of-treatment-weighting; SU, step-up.

difficult (see Supplementary PROs section: Supplementary Figure 2 and Supplementary Tables 9–16).

DISCUSSION

JIA is a chronic disease associated with ongoing disease burden, with both short and long-term outcomes of particular importance to patients, caregivers, and clinicians. Our previously published results of the STOP-JIA study outcomes at 12 months[5] found no significant differences between CTP groups in achieving the primary outcome of CID off GCs at 12 months. However, the study did show that EC treatment led to significantly higher percentages achieving cJADAS-10-ID and pediatric ACR70 than SU treatment. Moreover, the trajectory analysis of the STOP-JIA cohort over 12 months[6] indicated that starting bDMARDs early greatly increased the odds of achieving rapid rather than slow improvement. We therefore sought to determine whether initial CTP treatment was associated with improved outcomes and trajectories over a longer, three-year follow-up period. These new analyses, based upon longer-term data available after completion of the STOP-JIA trial, were made possible by the embedded design of the STOP-JIA trial within the CARRA Registry, which clearly speaks to the scientific value of investments made for such long-term, observational efforts and clinical research infrastructure.[15]

The current STOP-JIA three-year analysis reveals that patients started on the EC CTP spent significantly more time in inactive disease states, as measured by CID and cJADAS-10-ID, than patients started on the SU CTP, despite no differences at the three-year time point between CTP groups in percentage of patients achieving either CID or cJADAS-10-ID off GCs. The EC group also achieved CRM more frequently than those who started the SU CTP. The 8% difference in the percentage of follow-up time spent in CID corresponds to one additional month per year ($0.08 \times 12 = 0.96$ months) in CID. Although numerically small, one month per year in CID may reflect a clinically significant and meaningful difference in disease activity that may also result in reduction of disease burden.

LCTM modeling through three years also indicated that early introduction of bDMARDs greatly increased the odds of membership in the rapid improvement trajectory group compared with the slow improvement group. Interestingly, results of the current, long-term analysis determined that this "window" for early introduction constituted bDMARD introduction within 1 or 2 months from baseline, rather than the 3-month window found in our previous 12-month cohort analysis. Notably, the trajectory analysis demonstrated that the rapid improvement group—the group that achieved cJADAS-10-ID fastest—also went on to sustain a state of inactive disease throughout three years of follow-up, in contrast to the other groups. As in the previous 12-month cohort analysis, a small number of patients attained the rapid improvement trajectory with csDMARDs alone, suggesting again that a subgroup of patients do not require use of bDMARDs. The current analysis did not identify characteristics that predicted which patients could achieve rapid improvement and maintain cJADAS-10-ID with csDMARD monotherapy. Additional research is therefore needed to identify these patients, ideally at initiation of treatment.
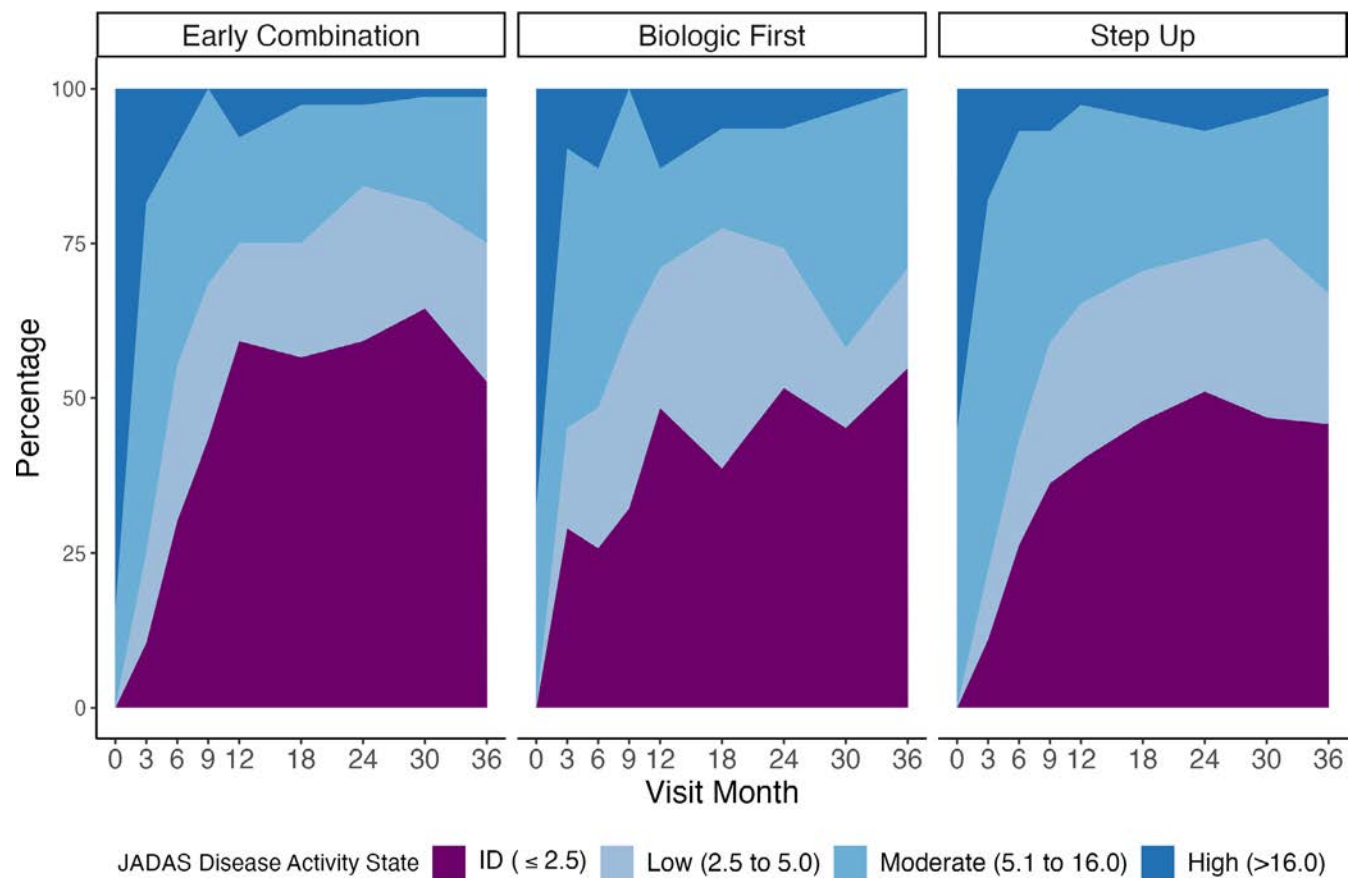
Figure 1. cJADAS-10 disease activity states through three years for each CTP group. Percentages of patients in each disease activity state based on the observed cJADAS-10 at that visit. When a patient had a missing value at that visit, the average imputed cJADAS-10 was used. The imputation model included observations from 0 to 42 months. cJADAS-10, clinical Juvenile Arthritis Disease Activity Score based on 10 joints; CTP, consensus treatment plan.
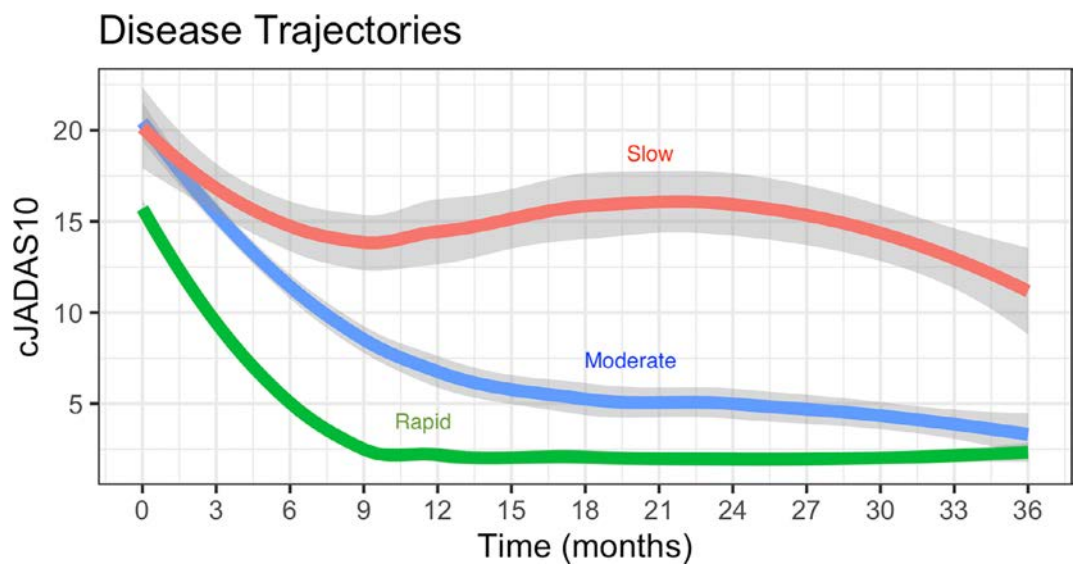

Figure 2. LCTM of cJADAS-10 through three-year period. Each curve shows the estimated mean cJADAS-10 versus time for the corresponding trajectory group, along with a 95% CI band in gray. The horizontal line represents the threshold for definition of cJADAS-10 inactive disease (ie, cJADAS-10 ≤ 2.5). CI, confidence interval; cJADAS-10, clinical Juvenile Arthritis Disease Activity Score based on 10 joints; LCTM, latent class trajectory modeling. Color figure can be viewed in the online issue, which is available at http://onlinelibrary.wiley.com/doi/10.1002/art.43216/abstract.

Table 4. Predictors of latent trajectory class membership, using the slow improvement trajectory as the reference group[*]

Timing of bDMARD initiation from baseline assessment	Rapid improvement		Moderate improvement	
	OR (95% CI)	P value	OR (95% CI)	P value
≤1 month	5.33 (1.35–21.1)	0.017	2.40 (0.57–10.2)	0.235
≤2 months	2.67 (1.09–6.53)	0.032	1.38 (0.41–4.64)	0.610
≤3 months	2.10 (0.68–6.51)	0.198	0.88 (0.27–2.85)	0.826

* bDMARD, biologic disease-modifying antirheumatic drug; CI, confidence interval; OR, odds ratio.

Our results are consistent with previous studies in adult rheumatoid arthritis (RA) and considerably extend and strengthen a previously very limited body of evidence regarding the impact of effective treatment timing on outcomes in JIA. Data from adult RA suggest that earlier introduction of bDMARD may reduce joint damage and improve functional outcomes.[16,17] Previous studies attempting to answer this question for JIA have been limited in number and more equivocal, including several shorter-term clinical trials and observational studies. The "Aggressive combination drug therapy in very early polyarticular juvenile idiopathic arthritis" (ACUTE-JIA) trial randomized patients with pJIA to infliximab/methotrexate combination therapy, methotrexate monotherapy, or triple therapy (sulfasalazine, methotrexate, hydroxychloroquine) and found that a statistically significant higher proportion of patients receiving infliximab/methotrexate achieved pediatric ACR75[9] at 12 months than the other two study arms.[18] Furthermore, ACUTE-JIA found that patients receiving infliximab/methotrexate spent a longer amount of time in inactive disease than the other two arms. However, PROs did not differ between treatment arms, each showing similar improvements.[19] The "TRial of Early Aggressive Therapy in polyarticular JIA "(TREAT-JIA) randomized patients to methotrexate or methotrexate/etanercept/prednisone and found no difference between treatment arms in the achievement of CID at 12 months.[10] Importantly, however, TREAT-JIA showed that the likelihood of CID at six months increased by 30% for each month closer to disease onset that treatment was started. Similarly, data from observational studies, including a report from the "Biologika in der Kinderrheumatologie" and "Juvenile Arthritis Methotrexate/Biologics Long-Term Observation" registries[20] found that patients who received bDMARD within two years of diagnosis were more likely to be in drug-free remission, have lower disease activity, and report better overall well-being and improved functional status as compared with patients who started these medications later. These results suggested that the impact of bDMARD start time may become more apparent over time and play a role in modulation of disease course. More recently, the "Behandel-Strategieen (BeSt)-for-Kids" study randomized patients to three initial treatment arms—bDMARD and csDMARD (EC), csDMARD alone (SU), and csDMARD plus GC therapy—using a treat-to-target approach.[21] Treat-to-target is a therapeutic strategy in which stricter disease control is achieved through treatment escalation when needed to maintain low disease activity goals and is currently recommended in both JIA and RA to improve disease outcomes.[22,23] BeSt-for-Kids showed that although patients who started on EC therapy improved more quickly and were better able to maintain low disease activity, approximately 70% of patients in all treatment groups achieved CID at 24 months after baseline. Although the numbers were small (30 in each arm), and occurrence of disease flares upon treatment withdrawal during the trial complicated the analysis, the BeSt-for-Kids results, together with those of STOP-JIA, suggest that a strategy that combines early bDMARD initiation with treat-to-target could be even more effective, and this paradigm needs to be tested. The "Comparison of STep-up and step-down therapeutic strategies in childhood ARthritiS" (STARS) is a step toward this goal: it is a randomized controlled clinical trial that will study SU treatment intensification coupled with treat-to-target in oligo and polyarticular JIA, compared with "step down," in which EC is initiated without additional treat-to-target[24] and has a planned enrollment of 260 participants and long-term follow-up of five years.

A limitation of the current study is that not all STOP-JIA participants had sufficient longitudinal data for inclusion in this three-year outcomes analysis, and we therefore assessed for potentially meaningful differences in characteristics between included and excluded participants. However, differences in baseline characteristics between these groups were small; the largest difference was that of demographics: included patients were younger, possibly because of older patients transitioning to adult providers, and there were fewer Black participants who had three-year follow-ups. Multiple imputation was used to reduce bias from missing data, but this method assumes missing values can be predicted from observed values. Regarding baseline disease characteristics, although we found differences in JIA categories and disease severity measures between CTP groups, these differences (higher severity and activity scores in the EC and BF CTP groups) were similar to those reported between the groups in our earlier, 12-month analysis.[8] Although statistical methods were used to reduce confounding by indication through PS weighting and adjustments for disease severity, all such bias may not have been eliminated. Because initial CTP choices reflected patient and physician preferences, there was an unequal number of patients who started on each CTP; this limited comparisons involving the BF group, which had the fewest patients.

In summary, the three-year results from the STOP-JIA study clearly demonstrate that EC treatment increases the duration of time spent in inactive disease and likelihood of achieving remission on medications. Furthermore, early introduction of bDMARD markedly increases the likelihood of achieving rapid improvement and maintaining CID for most patients with polyarticular JIA. These improved outcomes are likely to meaningfully reduce overall disease damage and the long-term burden of disease. Nonetheless, achievement of sustained inactive disease remains elusive, with more than half of patients continuing to experience active disease at the time of the three-year visit. It is possible that adding treat-to-target to EC treatment may improve outcomes further and is an important topic for future research. Furthermore, the identification of a small subgroup of patients with favorable outcomes on csDMARD monotherapy, ie, without bDMARD use, suggests the importance of additional research to identify early disease course predictors of response to csDMARDs alone. Future studies of the STOP-JIA cohort, which will incorporate combined analyses of clinical and multiomics factors, including important long-term radiographic, physical function, social achievement status, as well as other PROs, will improve understanding of the impact of early bDMARD therapy and enhance future treatment decision-making by patients, parents, and clinicians.

In conclusion, the results of this long-term, three-year STOP-JIA analysis now provide convincing evidence that very early introduction of bDMARDs, specifically as part of EC therapy for pJIA, is warranted for the vast majority of patients with pJIA, and that the traditional SU "pyramid" paradigm should be reconsidered in the current bDMARD era.

AUTHOR CONTRIBUTIONS

All authors contributed to at least one of the following manuscript preparation roles: conceptualization AND/OR methodology, software, investigation, formal analysis, data curation, visualization, and validation AND drafting or reviewing/editing the final draft. As corresponding author, Dr Kimura confirms that all authors have provided the final approval of the version to be published, and takes responsibility for the affirmations regarding article submission (eg, not under consideration by another journal), the integrity of the data presented, and the statements regarding compliance with institutional review board/Declaration of Helsinki requirements.

ACKNOWLEDGMENTS

APPENDIX A: CARRA REGISTRY SITE PRINCIPAL INVESTIGATORS, SUBINVESTIGATORS, AND RESEARCH COORDINATORS

The CARRA Registry principal investigators, subinvestigators, and research coordinators are listed as follows: R. Amir, K. Abulaban, A. Adams, R. Agbayani, C. Aguiar Lapsia, H. Ahmed, S. Akoghlanian, A. AlBijadi, E. Allenspach, M. Alpizar, G. Amarilyo, W. Ambler, M. Amoruso, E. Anderson, S. Angeles-Hahn, S. Ardoin, S. Armendariz, N. Aviran Dagan, I. Balboni, S. Balevic, L. Ballenger, S. Ballinger, N. Balmuri, S. Baluta, F. Barbar-Smiley, L. Barillas-Arias, M. Basiaga, K. Baszis, M. Becker, A. Begezda, E. Beil, H. Bell-Brunson, H. Benham, S. Benseler, L. Bermudez-Santiago, W. Bernal, T. Beukelman, T. Bigley, C. Bingham, B. Binstadt, C. Black, B. Blackmon, M. Blakley, J. Bohnsack, A. Boneparth, H. Bradfield, J. Bridges, E. Brooks, M. Brothers, A. Brown, D. Brown, H. Brunner, L. Buckley, Mary Buckley, Meredith Buckley, H. Bukulmez, D. Bullock, A. Cancino, B. Cameron, S. Canna, L. Cannon, S. Canny, V. Cartwright, E. Cassidy, E. Chalom, I. Chang, Johanna Chang, Joyce Chang, M. Chang, A. Chang-Hoftman, V. Chauhan, A. Chen, T. Chinn, P. Chiraseveenuprapund, K. Ciaglia, M. Cidon, D. Co, E. Cohen, R. Connor, K. Cook, A. Cooper, J. Cooper, K. Corbin, C. Correll, R. Cron, L. Curiel-Duran, M. Curry, A. Dagci, A. Dalrymple, E. Datyner, A. Davis, T. Davis, D. De Ranieri, J. Dean, C. DeCoste, F. Dedeoglu, M. DeGuzman, N. Delnay, V. Dempsey, E. DeSantis, R. Devine, M. Dhalla, A. Dhanrajani, J. Dingle, D. Dissanayake, B. Dizon, J. Dowling, J. Drew, K. Driest, Q. Du, D. Durkee, J. Dvergsten, A. Eberhard, M. Eckert, K. Ede, B. Edelheit, C. Edens, M. Elder, Y. Elzaki, S. Fadrhonc, C. Failing, D. Fair, L. Favier, B. Feldman, J. Fennell, I. Ferguson, P. Ferguson, K. Fields, C. Figuerosa, E. Flanagan, C. Fleming, L. Fogel, E. Fox, M. Fox, L. Franklin, R. Fuhlbrigge, J. Fuller, T. Futch-West, S. Gagne, M. Geiszler, D. Gerstbacher, M. Gilbert, M. Gillispie-Taylor, A.C. Gironella, D. Glaser, I. Goh, S. Gorry, N. Goswami, A. Gotte, B. Gottlieb, T. Graham, S. Grevich, T. Griffin, A. Grim, A. Grom, M. Guevara, P. Guittar, L. Guzman, M. Guzman, M. Hager, T. Hahn, O. Halyabar, E. Hammelev, T. Hammond, M. Hance, S. Haro, J. Harris, O. Harry, J. Hausmann, A. Hay, K. Hays, K. Hayward, J. Heiart, L. Henderson, M. Henrickson, A. Hersh, L. Hiraki, M. Hiskey, P. Hobday, C. Hoffart, M. Holland, M. Hollander, S. Hong, D. Horton, M. Horwitz, J. Hsu, A. Huber, J. Huggins, J. Hui-Yuen, A. Huttenlocher, M. Ibarra, A. Imlay, L. Imundo, C. Inman, A. Jackson, H. Jackson, S. Jackson, K. James, G. Janow, J. Jaquith, S. Jared, Y. Jiang, N. Johnson, J. Jones, K. Jones, S. Jones, S. Joshi, C. Justice, D. Kafisheh, K. Kaidar, S. Kasinathan, K. Kaufman, R. Kaur, U. Khalsa, E. Kessler, B. Kienzle, S. Kim, Y. Kimura, D. Kingsbury, M. Kitcharoensakkul, T. Klausmeier, J. Klauss, K. Klein, M. Klein-Gitelman, A. Knight, L. Kovalick, D. Krajewski, S. Kramer, C. Kremer, T. LaFlam, J. Lai, B. Lang, S. Lapidus, B. Lapin, A. Lasky, E. Lawson, R. Laxer, A. Lee, Patricia Lee, Pui Lee, T. Lee, E. Leisinger, L. Lentini, M. Lerman, Y. Levinsky, D. Levy, S. Li, S. Lieberman, L. Lim, E. Limenis, C. Lin, N. Ling, G. Lionetti, R. Livny, M. Lo, A. Long, M. Lopez-Peña, D. Lovell, N. Luca, S. Lvovich, A. Lytch, M. Ma, A. Machado, J. MacMahon, J. Madison, B. Malla, J. Maller, M. Mannion, C. Manos, L. Mansfield, B. Marston, A. Martyniuk, K. Marzan, T. Mason, S. Matossian, K. Mcallister, L. McAllister, K. McBrearty, K. McConnell, D. McCurdy, K. McDaniels, J. McDonald, I. McHale, L. McIntosh, E. Meidan, E. Mellins, Zi. Mian, P. Miettunen, M. Miller, D. Milojevic, R. Mitacek, M. Mitchell, R. Modica, S. Mohan, K. Moore, T. Moore, L. Moorthy, J. Moreno, E. Morgan, E. Morgan Dewitt, T. Moussa, A. Moyer, V. Mruk, B. Murante, A. Murphy, E. Muscal, O. Mwizerwa, A. Najafi, K. Nanda, L. Nassi, S. Nativ, M. Natter, J. Neely, B. Nelson, L. Newhall, A. Nguyen, P. Nigrovic, J. Nocton, B. Nolan, A. Nowakowski, K. Nowicki, R. Oakes, E. Oberle, S. Ogbonnaya-Whittesley, E. Ogbu, O. Okeke, M. Oliver, R. Olveda, K. O'Neil, K. Onel, A. Orandi, M. Orlando, R. Oz, J. Padam, E. Pagano, A. Paller, N. Pan, J. Pandya, S. Panupattanapong, A. Pappo Toledano, J. Patel, P. Patel, A. Patrick, S. Patrizi, S. Paul, P. Pepmueller, J. Perfetto, M. Perron, M. Peskin, C. Pinnoti, L. Ponder, R. Pooni, S. Prahalad, S. Protopapas, B. Puplava, J. Quach, M. Quinlan-Waters, C. Rabinovich, S. Radhakrishna, J. Rafko, H. Rahimi, S. Ramsey, R. Randell, L. Ray, Ann

Reed, Annelle Reed, H. Reid, D. Reiff, I. Reyhan, B. Richard, A. Richmond, M. Riebschleger, E. Rife, S. Ringold, M. Riordan, M. Riskalla, M. Ritter, A. Robinson, L. Robinson, L. Rodgers, M. Rodriquez, D. Rogers, K. Rojas, T. Ronis, A. Rosado, M. Rosenkranz, N. Rosenwasser, H. Rothermel, D. Rothman, E. Rothschild, K. Rouster-Stevens, T. Rubinstein, N. Ruth, S. Sabbagh, N. Saad, R. Sadun, L. Santiago, A.C. Sandborg, V. Saper, A. Sarkissian, L. Scalzi, J. Schahn, L. Schanberg, K. Schikler, A. Schlefman, B. Schlichting, H. Schmeling, K. Schmidt, E. Schmitt, R. Schneider, G. Schulert, C. Schutt, T. Seay, C. Seper, B. Shaham, J. Shalen, R. Sheets, A. Shehab, S. Shenoi, M. Sherman, J. Shirley, M. Shishov, E. Silverman, N. Singer, V. Sivaraman, E. Sloan, C. Smith, J. Smith, E. Smitherman, J. Soep, M. Son, S. Spence, C. Spencer, L. Spiegel, J. Spitznagle, H. Srinivasalu, H. Stapp, K. Steigerwald, A. Stephens, Y. Sterba Rokovchik, S. Stern, A. Stevens, B. Stevens, R. Stevenson, K. Stewart, C. Stingl, M. Stoll, E. Stringer, S. Sule, J. Sullivan, J. Sumner, R. Sundel, M. Sutter, C. Swafar, N. Swayne, T. Symington, R. Syed, G. Syverson, A.M. Szymanski, S. Taber, R. Tal, A. Tambralli, A. Taneja, T. Tanner, G. Tarshish, S. Tarvin, A. Taxter, J. Taylor, M. Tesher, T. Thakurdeen, A. Thatayatikom, A. Theisen, G. Thieroff, B. Thomas, L. Thomas, N. Thomas, L. Timmerman, T. Ting, C. Todd, D. Toib, K. Torok, C. Toruner, H. Tory, M. Toth, E. Treemarcki, S. Tse, T. Tse, C. Tsin, J. Twatchman-Basset, M. Twilt, T. Valcarcel, R. Valdovinos, A. Vallee, H. Van Mater, S. Vandenbergen, C. Varghese, N. Vasquez, P. Vega-Fernandez, R. Vehe, K. Veiga, J. Velez, J. Verbsky, R. Verstegen, N. Volpe, E. von Scheven, S. Vora, L. Wagner-Weiner, D. Wahezi, S. Wakefield, B. Walker, S. Wallgren, H. Walters, M. Waterfield, A. Watts, P. Weiser, J. Weiss, P. Weiss, E. Wershba, V. Westheuser, A. White, K. Widrick, C. Williams, S. Wong, S. Wooldridge, L. Woolnough, T. Wright, E. Wu, A. Yalcindag, M. Yee, R. Yeung, K. Yomogida, A. Zeft, Y. Zhang, Y. Zhao, Z. Zheng, A. Zhu, and C. Zic.

REFERENCES

1. Wallace CA, Huang B, Bandeira M, et al. Patterns of clinical remission in select categories of juvenile idiopathic arthritis. Arthritis Rheum 2005;52(11):3554–3562.

2. Ringold S, Seidel KD, Koepsell TD, et al. Inactive disease in polyarticular juvenile idiopathic arthritis: current patterns and associations. Rheumatology (Oxford) 2009;48(8):972–977.

3. Wallace CA, Giannini EH, Huang B, et al; Childhood Arthritis Rheumatology Research Alliance; Pediatric Rheumatology Collaborative Study Group; Paediatric Rheumatology International Trials Organisation. American College of Rheumatology provisional criteria for defining clinical inactive disease in select categories of juvenile idiopathic arthritis. Arthritis Care Res (Hoboken) 2011;63(7):929–936.

4. Mannion ML, Xie F, Beukelman T; CARRA Registry Investigators. Investigation of inactive disease states among patients with juvenile idiopathic arthritis in the Childhood Arthritis and Rheumatology Research Alliance registry. ACR Open Rheumatol 2022;4(9):825–831.

5. Kimura Y, Schanberg LE, Tomlinson GA, et al; CARRA STOP-JIA Investigators. Optimizing the start time of biologics in polyarticular juvenile idiopathic arthritis: a comparative effectiveness study of Childhood Arthritis and Rheumatology Research Alliance consensus treatment plans. Arthritis Rheumatol 2021;73(10):1898–1909.

6. Ong MS, Ringold S, Kimura Y, et al; CARRA Registry Investigators. Improved disease course associated with early initiation of biologics in polyarticular juvenile idiopathic arthritis: trajectory analysis of a Childhood Arthritis and Rheumatology Research Alliance consensus treatment plans study. Arthritis Rheumatol 2021;73(10):1910–1920.

7. Ringold S, Weiss PF, Colbert RA, et al; Juvenile Idiopathic Arthritis Research Committee of the Childhood Arthritis and Rheumatology Research Alliance. Childhood Arthritis and Rheumatology Research Alliance consensus treatment plans for new-onset polyarticular juvenile idiopathic arthritis. Arthritis Care Res (Hoboken) 2014;66(7): 1063–1072.

8. Kimura Y, Schanberg LE, Tomlinson G, et al; CARRA STOP-JIA Investigators. Optimizing the start time of biologics in polyarticular

juvenile idiopathic arthritis: a comparative effectiveness study of CARRA consensus treatment plans for untreated polyarticular JIA. Arthritis Rheumatol 2021;73(10):1898–1909.

9. Giannini EH, Ruperto N, Ravelli A, et al. Preliminary definition of improvement in juvenile arthritis. Arthritis Rheum 1997;40(7):1202–1209.

10. Wallace CA, Giannini EH, Spalding SJ, et al; Childhood Arthritis and Rheumatology Research Alliance. Trial of early aggressive therapy in polyarticular juvenile idiopathic arthritis. Arthritis Rheum 2012;64(6): 2012–2021.

11. Trincianti C, Van Dijkhuizen EHP, Alongi A, et al; Paediatric Rheumatology International Trials Organisation. Definition and validation of the American College of Rheumatology 2021 juvenile arthritis disease activity score cutoffs for disease activity states in juvenile idiopathic arthritis. Arthritis Rheumatol 2021;73(11):1966–1975.

12. Cefalu M. Ridgeway G, McCaffrey D, et al. twang: Toolkit for Weighting and Analysis of Nonequivalent Groups. R package version 2.6.1. The Comprehensive R Archive Network (CRAN) 2024. Accessed July 22, 2024. https://cran.r-project.org/web/packages/twang/

13. van Buuren S, Groothuis-Oudshoorn K. mice: Multivariate imputation by chained equations in R. J Stat Softw 2011;45(3):1–67.

14. R Core Team. R: A Language and Environment for Statistical Computing. R Foundation for Statistical Computing 2024. Accessed June 15, 2024. https://cran.r-project.org/

15. Beukelman T, Kimura Y, Ilowite NT, et al; CARRA Registry Investigators. The new Childhood Arthritis and Rheumatology Research Alliance (CARRA) registry: design, rationale, and characteristics of patients enrolled in the first 12 months. Pediatr Rheumatol Online J 2017;15(1):30.

16. Donahue KE, Schulman ER, Gartlehner G, et al. Comparative effectiveness of combining MTX with biologic drug therapy versus either MTX or biologics alone for early rheumatoid arthritis in adults: a systematic review and network meta-analysis. J Gen Intern Med 2019; 34(10):2232–2245.

17. Burgers LE, Raza K, van der Helm-van Mil AH. Window of opportunity in rheumatoid arthritis - definitions and supporting evidence: from old to new perspectives. RMD Open 2019;5(1):e000870.

18. Tynjälä P, Vähäsalo P, Tarkiainen M, et al. Aggressive combination drug therapy in very early polyarticular juvenile idiopathic arthritis (ACUTE-JIA): a multicentre randomised open-label clinical trial. Ann Rheum Dis 2011;70(9):1605–1612.

19. Tarkiainen M, Tynjälä P, Vähäsalo P, et al. Health-related quality of life during early aggressive treatment in patients with polyarticular juvenile idiopathic arthritis: results from randomized controlled trial. Pediatr Rheumatol Online J 2019;17(1):80.

20. Minden K, Horneff G, Niewerth M, et al. Time of disease-modifying antirheumatic drug start in juvenile idiopathic arthritis and the likelihood of a drug-free remission in young adulthood. Arthritis Care Res (Hoboken) 2019;71(4):471–481.

21. Hissink Muller PCE, Brinkman DMC, Schonenberg D, et al. A comparison of three treatment strategies in recent onset non-systemic juvenile idiopathic arthritis: initial 3-months results of the BeSt for Kids-study. Pediatr Rheumatol Online J 2017;15(1):11.

22. Smolen JS, Aletaha D, Bijlsma JWJ, et al; T2T Expert Committee. Treating rheumatoid arthritis to target: recommendations of an international task force. Ann Rheum Dis 2010;69(4):631–637.

23. Ravelli A, Consolaro A, Horneff G, et al. Treating juvenile idiopathic arthritis to target: recommendations of an international task force. Ann Rheum Dis 2018;77(6):819–828.

24. Burrone M, Mazzoni M, Naddei R, et al; Paediatric Rheumatology International Trials Organisation (PRINTO). Looking for the best strategy to treat children with new onset juvenile idiopathic arthritis: presentation of the "comparison of STep-up and step-down therapeutic strategies in childhood ARthritiS" (STARS) trial. Pediatr Rheumatol Online J 2022;20(1):80.

AMERICAN COLLEGE
of RHEUMATOLOGY
Empowering Rheumatology Professionals

BRIEF REPORT

Innate Lymphoid Cell Phenotypic and Functional Alterations in Patients With Systemic Juvenile Idiopathic Arthritis

Linda Quatrini,[1] Cecilia Ciancaglini,[2] Ivan Caiello,[3] Silvia Santopolo,[1] Manuela Pardeo,[4] Valentina Matteo,[3] Elena Loricchio,[3] Donato Amodio,[5] Elena Morrocchi,[5] Giulio Olivieri,[6] Paolo Palma,[5] Antonella Insalaco,[4] Marco Francesco Natale,[4] Arianna De Matteis,[4] Nicola Tumino,[1] Claudia Bracaglia,[4] Paola Vacca,[1] Lorenzo Moretta,[2] Fabrizio De Benedetti,[7] and Giusi Prencipe[3]

Objective. Systemic juvenile idiopathic arthritis (sJIA) is a chronic childhood disease classically attributed to innate immune cell dysregulation. This study aimed to elucidate the role of innate lymphoid cells (ILCs), including natural killer (NK) cells and helper-ILCs (hILCs), in sJIA during clinically inactive disease (CID) through phenotypic and functional analysis.

Methods. Peripheral ILCs from children with sJIA during CID receiving interleukin-1 (IL-1) inhibitors (n = 40) were analyzed by flow cytometry and compared to 23 healthy children (HC) and 22 patients with unrelated autoinflammatory diseases taking IL-1 inhibitors. Plasma proteomic profiling was also performed.

Results. Patients with sJIA showed a significant reduction in circulating NK cell frequencies compared to HC, with an increased proportion of CD56^{bright} NK cells. Although overall hILC frequencies were comparable to HC, ILC1s were increased, whereas ILC precursors were reduced. ILC1 frequency correlated positively with IL-18 plasma levels, whereas ILC2 frequency correlated negatively. Functional assessments revealed that NK cells from patients with sJIA had variable interferon γ (IFNγ) production upon IL-18/IL-12 stimulation, inversely correlating with IL-18 levels. Additionally, hILCs from these patients showed a specific impairment in IFNγ production despite normal IL-13 production, potentially linked to decreased IL-18 receptor α expression in ILC1s. Proteomic analysis confirmed IL-18 as the most up-regulated cytokine in sJIA plasma.

Conclusion. Patients with sJIA in CID exhibit significant innate immune abnormalities, including altered ILC subset distribution and impaired IFNγ production, strongly associated with IL-18 levels. These findings suggest ongoing immune dysregulation despite clinical remission, underscoring a potential role for ILCs and cytokine interaction in sJIA pathogenesis.

INTRODUCTION

Systemic juvenile idiopathic arthritis (sJIA), or Still disease, is a chronic childhood disorder of unknown cause, characterized by arthritis and systemic inflammatory features, including rash and spiking fever.[1] The pathogenesis of sJIA is complex and dysregulation of innate immune cells is prominent, supporting the classification of sJIA as an autoinflammatory disorder. Approximately 10%

[1]Linda Quatrini, PhD, Silvia Santopolo, PhD, Nicola Tumino, PhD, Paola Vacca, PhD: Innate Lymphoid Cells Unit, Bambino Gesù Children's Hospital, IRCCS, Rome, Italy; [2]Cecilia Ciancaglini, PhD, Lorenzo Moretta, MD: Tumor Immunology Unit, Bambino Gesù Children's Hospital, IRCCS, Rome, Italy; [3]Ivan Caiello, BSc, Valentina Matteo, BSc, Elena Loricchio, PhD, Giusi Prencipe, PhD: Laboratory of Immuno-Rheumatology, Bambino Gesù Children's Hospital, IRCCS, Rome, Italy; [4]Manuela Pardeo, MD, Antonella Insalaco, MD, Marco Francesco Natale, MD, Arianna De Matteis, MD, Claudia Bracaglia, MD: Division of Rheumatology, ERN RITA Center, Bambino Gesù Children's Hospital, IRCCS, Rome, Italy; [5]Donato Amodio, MD, PhD, Elena Morrocchi, PhD, Paolo

Palma, MD, PhD: Clinical and Research Unit of Clinical Immunology and Vaccinology, Bambino Gesù Children's Hospital, IRCCS and Department of Systems Medicine, University of Rome "Tor Vergata," Rome, Italy; [6]Giulio Olivieri, MD: Clinical and Research Unit of Clinical Immunology and Vaccinology, Bambino Gesù Children's Hospital, IRCCS and PhD Program in Immunology, Molecular Medicine and Applied Biotechnology, University of Rome "Tor Vergata," Rome, Italy; [7]Fabrizio De Benedetti, MD, PhD: Laboratory of Immuno-Rheumatology and Division of Rheumatology, ERN RITA Center, Bambino Gesù Children's Hospital, IRCCS, Rome, Italy.

Drs Quatrini and Ciancaglini are co-first authors and contributed equally to this work.

to 15% of patients develop macrophage activation syndrome (MAS), a potentially fatal hyperinflammatory syndrome classified among the secondary hemophagocytic lymphohistiocytosis.[2] The effect of the innate proinflammatory cytokines interleukin-1β (IL-1β), IL-6, and IL-18 may explain many features of the disease. On the other hand, the contribution of interferon γ (IFNγ) seems to be more relevant for MAS development. Indeed, increased circulating concentrations of IFNγ and IFNγ-induced chemokines CXCL9 and CXCL10 have been found in patients with sJIA with MAS as compared to patients with active sJIA without MAS.[3]

Innate lymphoid cells (ILCs), including natural killer (NK) cells and helper-ILCs (hILCs), are important cellular sources of IFNγ. hILCs serve as the innate counterpart of T helper cells and are specialized in the secretion of cytokines. In peripheral blood (PB), hILCs include ILC1s, ILC2s, and ILC precursors (ILCPs), whereas mature ILC3s are present only in tissues. ILC1s express the transcription factor T bet and produce IFNγ. ILC2 express GATA3 and produce IL-13, whereas ILCPs consist of precursors capable of differentiating into mature ILC subsets in response to specific inflammatory signals. Because of their shared ability to produce IFNγ as a signature cytokine, NK cells and ILC1s were initially collectively referred to as "group 1 ILCs."[4,5]

Patients with active sJIA display an NK cell dysfunction, characterized by decreased number and reduced IFNγ production and cytotoxicity, possibly due to hyporesponsiveness[6,7] to IL-18. Although a growing body of evidence in recent years has implicated ILCs in the pathogenesis of inflammatory arthritis, including JIA, rheumatoid arthritis, and spondyloarthritis,[8,9] the role and phenotype of hILCs in sJIA remain largely unexplored.

The main goal of treatment in sJIA is to rapidly achieve clinically inactive disease (CID).[10] Given the central role of IL-1 and IL-6 in its pathogenesis, inhibitors targeting these cytokines have become standard therapies over the past decades. Nevertheless, despite favorable responses to IL-1 and IL-6 blockade, particularly with early treatments, a subset of patients (15–30%) remains nonresponsive.[11] Moreover, several observations suggest that abnormalities of innate immunity persist in patients with sJIA and CID. These abnormalities involve circulating myeloid cells[12] and elevated IL-18 circulating levels.[7,13] In fact, IL-18 levels often remain high in patients with sJIA and CID, normalizing only after prolonged remission.[12] In the present study, we aimed to investigate the presence and function of ILCs in the PB of patients with sJIA during CID, focusing on their potential role in persistent immune dysregulation and disease pathogenesis.

PATIENTS AND METHODS

Patients and samples. Forty patients with sJIA, as defined by the International League of Associations for Rheumatology criteria,[14] were enrolled in this study (Supplementary Table 1). All patients had CID, as defined according to the Wallace criteria,[10] were off glucocorticoids, and were receiving IL-1 inhibitors (anakinra [n = 31] or canakinumab [n = 9]). Among the 31 patients treated with anakinra, 19 patients were on a daily regimen, whereas 12 patients were on a tapered schedule (decalage), with 9 patients following step 1 (alternate-day regimen) and 3 patients following step 2 (once every three days). Of the nine patients receiving canakinumab, five patients were on full-dose therapy, whereas four patients were on a tapered regimen (three patients receiving doses every 8 weeks and one patient receiving doses every 10 weeks).

Additionally, 22 patients, receiving IL-1 inhibitors (anakinra [n = 11] or canakinumab [n = 11]), with unrelated autoinflammatory diseases (AIDs) were also enrolled (Supplementary Table 1). A control group of 23 healthy children (HC) (12 of 23 were female [53%]; median age 11.0 years, interquartile range [IQR] 5.0–15.0 years) was recruited from the division of Rheumatology at Bambino Gesù Children's Hospital. These children were evaluated for joint pain but were found to have noninflammatory conditions. Biologic samples (plasma and PB mononuclear cells [PBMCs]) were collected. PBMCs were isolated by density gradient centrifugation and cells were used for both phenotypic analysis by flow cytometry and cytokine production assays. Because limited blood volumes were available from pediatric patients, not all analyses were performed on every sample. The study was approved by the Ethics Committee of Bambino Gesù Children's Hospital (1683 OPBG 2018), and written informed consent was obtained from patients and/or their parents.

Cell stimulation, flow cytometry analysis, and cytokine detection. Freshly isolated PBMCs were left unstimulated or stimulated with phorbol 12–myristate 13–acetate (PMA) (Sigma) (10 ng/mL) plus ionomycin (Sigma) (1 μg/mL) in the presence of Golgi Plug (BD Biosciences) for three hours at 37°C. Alternatively, cells were stimulated overnight with IL-12 (Miltenyi) (10 ng/mL) and IL-18 (R&D) (100 ng/mL) at 37°C, and Golgi Plug was added for the last four hours of stimulation. At the end of the stimulation, cells were stained for flow cytometry analysis. PBMCs were analyzed by flow cytometry using directly conjugated monoclonal antibodies. The following antibodies were used for cell surface staining: CD3-FITC, CD19-FITC, CD14-FITC, CD127-APC, CD218 (IL-18 receptor α [IL-18RA])-APC (Miltenyi), CD56-PECy7, CD127-PE, CD45-KrO, CD3-APC-A700, CD14-APC-A700, CD19-APC-A700, CD94-APC, CD117-ECD, CRTH2-FITC (from DURAClone dry preformulated custom antibody panel, Beckman Coulter), and CD7-PECF594 (BD Biosciences). Dead cells were excluded using LIVE/DEAD Fixable Blue Dead Cell Stain Kit (Invitrogen).

After surface staining, stimulated cells were fixed and permeabilized using Fixation/Permeabilization Solution Kit (BD Biosciences) to detect intracellular cytokines with the following antibodies: IFNγ-APCeFluor780 (eBioscience) and IL-13-PE (Miltenyi). For the analysis of freshly isolated PBMCs, lymphocytes were first gated, then dead cells, doublets, CD45$^-$, and lin(CD3, CD14, CD19)$^+$ cells were excluded. NK cells were gated as CD94$^+$ cells, whereas hILCs were gated as CD94$^-$CD127$^+$ cells. Among hILCs, ILC1s were gated as CD117$^-$CRTH2$^-$, ILC2s were gated as CRTH2$^+$, and ILCPs were gated as CD117$^+$CRTH2$^-$.

For the analysis of stimulated PBMCs, lymphocytes were first gated, then dead cells, doublets, CD7$^-$ and lin(CD3, CD14, CD19)$^+$ cells were excluded. NK cells were gated as CD56$^+$ cells, whereas hILCs were gated as CD127$^+$ cells.

Data were acquired with a Cytoflex LX flow cytometer (Beckman Coulter) and analyzed using FlowJo software version 10.8.1 (BD Biosciences). Plasma levels of IL-18 were measured by enzyme-linked immunosorbent assay using a commercial kit (R&D), according to the manufacturer's instructions.

Ex vivo culture of HC PBMCs and NK cells. NK cells were isolated from HC PBMCs by negative selection using the RosetteSep Human NK Cell Enrichment Cocktail (Stemcell Technologies). Total PBMCs were cultured in 10% fetal bovine serum–supplemented RPMI 1640 medium with the indicated concentrations of IL-18 (R&D) and, in addition to IL-18, NK cells were cultured with IL-2, IL-1β, and IL-6 (R&D, 10 ng/mL each). After six days, total PBMCs or NK cells were stimulated with IL-18/IL-12 as described in the previous paragraph for subsequent cytofluorimetric analysis.

Proteomic assay. Plasma samples were analyzed using the Olink Target 48 cytokine panel based on the highly sensitive and specific proximity extension assay technology as previously described.[15] Briefly, each target protein was recognized by double antibodies linked to complementary DNA tags that hybridize when in proximity, subsequently quantified using a high throughput microfluidic real-time polymerase chain reaction instrument, Olink Signature Q100. Proteins exhibiting values below the limit of detection in over 80% of samples were excluded from the dataset. The data were preprocessed using the NPX Manager Software (version 1.16.0). Data were analyzed with R and Olink Analyze R package (version 1.3.0).

Statistical analysis. Statistical analysis was performed using GraphPad Prism software version 8.0.1. Data are shown as medians and IQR. To compare two groups, the Mann-Whitney U-test was used. To compare two groups in the proteomics analysis we used multiple *t*-tests with Welch correction. To compare more than two groups Kruskal-Wallis test was used, followed by

uncorrected Dunn's test. For correlation analyses, the Spearman test was used. *P* values less than 0.05 were considered significant.

RESULTS

Composition of the circulating ILC compartment in patients with sJIA. We analyzed the composition of the circulating ILC compartment in patients with sJIA receiving IL-1 inhibitors during CID. NK cells and hILCs were compared to those observed in HC. Additionally, to evaluate the potential effects of IL-1 inhibitors in modulating the number of ILCs in patients with sJIA, NK cells and hILCs were also assessed in the PB of patients with unrelated AIDs, who were receiving IL-1 inhibitors. NK cells were gated among live lymphocytes as lin-CD94$^+$ cells, whereas hILCs were gated as lin$^-$CD94$^-$CD127$^+$ (Supplementary Figure 1A). The frequency of NK cells within lymphocytes and their absolute number were significantly lower in patients with sJIA compared to HC (Figure 1A and B). Among NK cells, the frequency of CD56^{bright} cells was significantly higher in patients with sJIA compared to HC and patients with AID (Figure 1C). The frequency and absolute numbers of hILCs were instead comparable among patients with sJIA, patients with AID, and HC (Figure 1D and E). In patients with sJIA, the frequencies of hILCs, but not of NK cells, correlated with the duration of therapy with IL-1 inhibitors (Supplementary Figure 1B and C). Altogether, our data show that patients with sJIA during CID are characterized by a marked reduction of circulating NK cells, accompanied by an increase in the percentage of CD56^{bright} cells, whereas no significant abnormalities are observed in the percentage and number of hILCs.

Abnormal hILC subset proportions in patients with sJIA and CID correlating with IL-18 plasma concentration. We next investigated the composition of the hILC compartment by measuring the frequency of each subset among lymphocytes in patients with sJIA during CID. ILC1s were identified as CD117$^-$CRTH2$^-$, ILC2s as CRTH2$^+$ and ILCPs as CD117$^+$CRTH2$^-$ (Supplementary Figure 1A). Compared to HC, patients with sJIA showed a significant increase in both the frequency and absolute number of ILC1s (Figure 2A and D), and a reduction in both the frequency and absolute number of ILCPs (Figure 2C and F). Although the frequency of ILC2 was comparable between the two groups (Figure 2B), patients with sJIA had significantly reduced absolute numbers of ILC2s (Figure 2E).

Furthermore, we analyzed the proportion of each subset within hILCs. In line with the data on the frequency among total lymphocytes and cell numbers (Figure 2A–F), we found a significantly higher proportion of ILC1s and a lower proportion of ILCPs in patients with sJIA (Figure 2G–I). Of note, these abnormalities were specific to sJIA because they were not observed in patients with AID similarly receiving the same IL-1 inhibitor treatment.
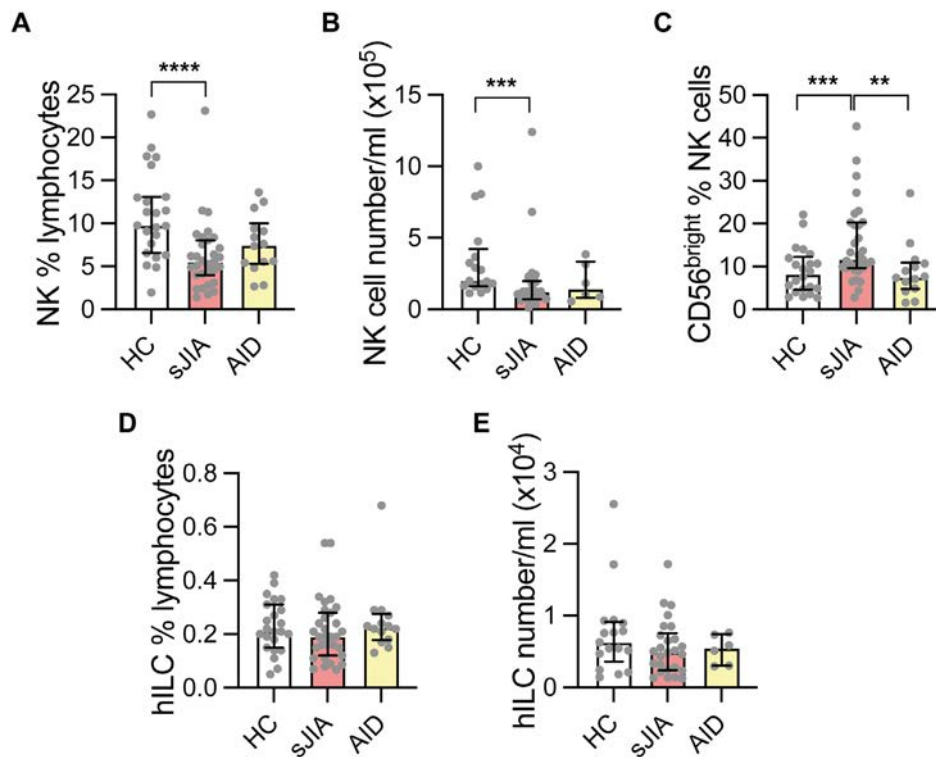
Figure 1. NK cell frequency and number in the peripheral blood of patients with sJIA are decreased compared to HC. (A–C) Scatter dot plots and bars showing the medians and interquartile ranges (IQR) of (A) NK cell frequency within live lymphocytes, (B) their absolute number, (C) and the frequency of CD56^{bright} NK cells among total NK cells. D and E, Scatter dot plots and bars showing the medians and IQR of (D) hILC frequency within live lymphocytes and (E) their absolute number. Symbols represent individual patients. A, C, and D n = 23 HC; n = 31 sJIA; n = 14 AID. B and E n = 17 HC; n =26 sJIA; n =7 AID. Kruskal-Wallis test was used, followed by uncorrected Dunn's test. (**P < 0.01; ***P < 0.005; ****P < 0.001). AID, autoinflammatory disease; HC, healthy children; hILC, helper innate lymphoid cell; NK, natural killer; sJIA, systemic juvenile idiopathic arthritis.

Given the observed changes in NK cell numbers and in hILC subset proportions in patients with sJIA, we next investigated whether these abnormalities were linked to the circulating levels of IL-18, which is the signature inflammatory cytokine in sJIA. We found a significant positive correlation between ILC1 proportion among hILCs and IL-18 plasma concentration (Figure 2L). Consistently, a significant negative correlation between ILC2 proportion and IL-18 levels was also found (Figure 2L). ILC2 (but not ILC1) cell number/mL negatively correlated with IL-18 plasma concentration (r = −0.4017, *P* = 0.0419). These abnormalities were not linked to surface expression levels of the IL-18 receptor, as we observed that ILC1 from patients with sJIA expressed significantly lower levels of IL-18RA compared to HC and patients with AID (Figure 2M and Supplementary Figure 2A and B). To further explore the role of IL-18, we stimulated HC PBMCs with IL-18, and we found a reduction in ILCP and an increase in ILC1 proportions among hILC, suggesting that IL-18 drives ILCP differentiation toward ILC1 (Supplementary Figure 2C and D). Collectively, our data show that patients with sJIA during CID exhibit an abnormality in the hILC subset proportions, characterized by an increase in the ILC1 subset that is associated with circulating levels of IL-18 and a decrease in the ILCP subset.

Dysfunctional IFNγ production in response to IL-18 stimulation by NK cells and hILCs. To assess the capacity of NK cells and hILCs to produce IFNγ in patients with sJIA as compared to HC, we stimulated PBMCs and measured intracellular IFNγ in these subsets by flow cytometry (Figure 3A–D, Supplementary Figure 3, and Supplementary Figure 4A–D). To evaluate the intrinsic cellular potential to synthesize cytokines, we used PMA/ionomycin as a nonspecific stimulus (Supplementary Figure 3A). Alternatively, we stimulated cells with IL-18 in the presence of IL-12 (Supplementary Figure 3B). We found that in patients with sJIA, the frequency of NK cells capable of producing IFNγ in response to both PMA/ionomycin and IL-18/IL-12 was comparable to that of HC (Figure 3A). However, we found that, on ex vivo cell stimulation with IL-18 and IL-12, patients with sJIA clustered into two distinct subgroups: 5 of 14 patients were hyperresponders (% IFNγ + median = 62.8), whereas the remaining 9 of 14 patients were hypo- or null responders (% IFNγ + median = 3.4) (Figure 3A). The median treatment duration did not differ significantly between hyperresponsive and hyporesponsive patients. Interestingly, we found a negative correlation between the percentage of IFNγ + NK cells and the circulating levels of IL-18 (Figure 3 B). In line with these data, we observed
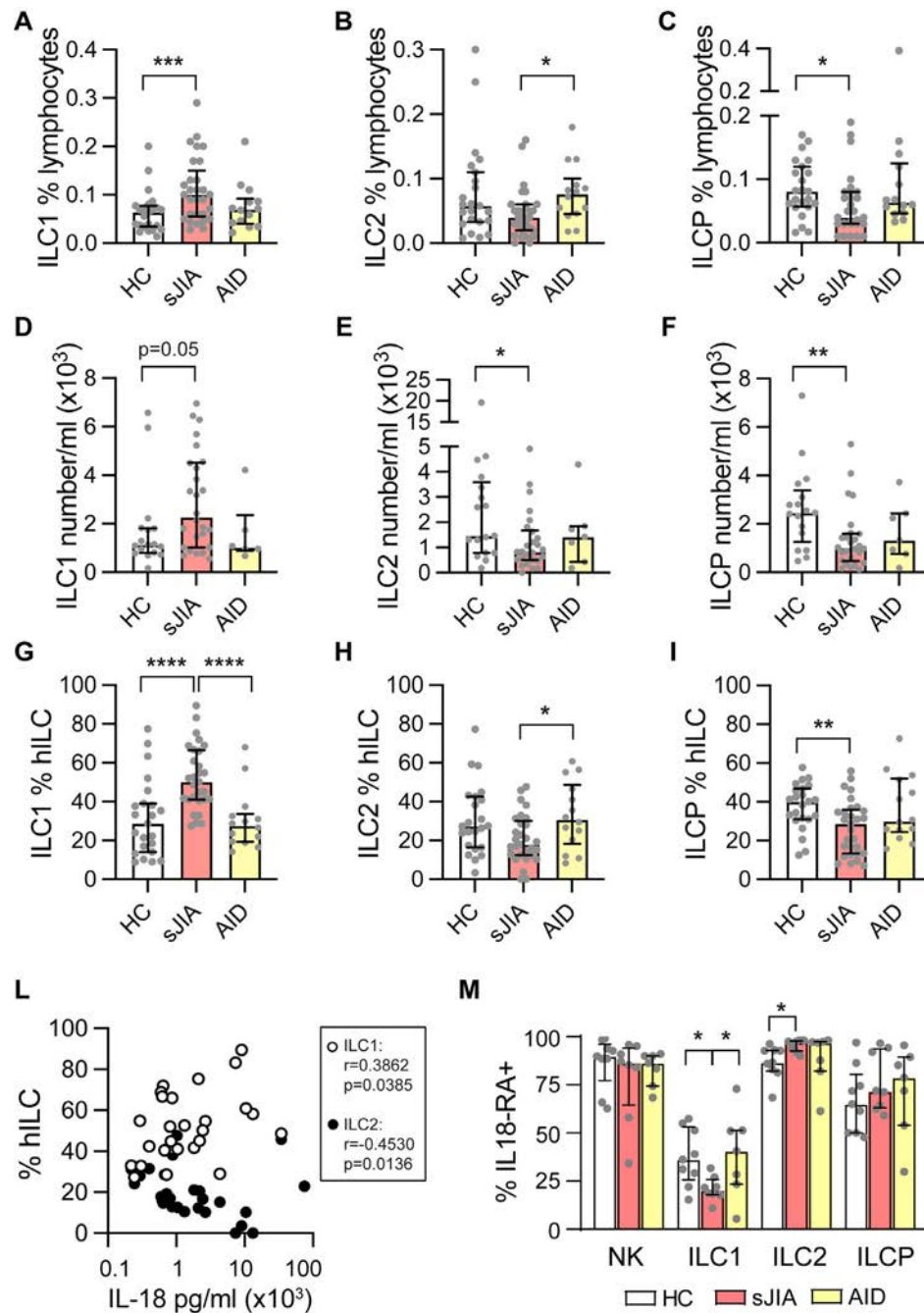
Figure 2. Changes in ILC subset frequencies are associated with IL-18 plasma concentration. (A–I) Scatter dot plots and bars showing for each hILC subsets the medians and interquartile ranges (IQR) of (A–C) cell frequency within live lymphocytes, (D–F) of cell number, and (G–I) cell frequency within total hILCs. A–C and G–I n = 23 HC; n = 29 sJIA, n = 14 AID. D–F n = 17 HC; n = 26 sJIA, n = 7 AID. (L) Scatterplots showing the correlation between IL-18 plasma concentration and ILC1 (empty dots) and ILC2 (black plots) frequency within hILCs. n = 29. r and *P* values were determined by the Spearman correlation test. Symbols represent individual patients. (M) Scatter dot plots and bars showing for each ILC subsets the median and IQR of IL-18RA$^+$ cell frequency within each ILC subset. n = 9 HC; n = 8 sJIA; n = 7 AID. In A–I and M, Kruskal-Wallis test was used, followed by uncorrected Dunn's test (*$P < 0.05$; **$P < 0.01$; ***$P < 0.005$; ****$P < 0.001$). AID, autoinflammatory disease; HC, healthy children; hILC, helper innate lymphoid cell; ICL, innate lymphoid cell; IL-18, interleukin 18; IL-18RA, interleukin 18 receptor α; NK, natural killer; sJIA, systemic juvenile idiopathic arthritis.

that preincubating ex vivo NK cells from HC with increasing IL-18 concentrations reduced their subsequent ability to produce IFNγ in response to IL-18/IL-12 stimulation in a dose-dependent manner (Supplementary Figure 4E and F). This desensitization was

independent of the presence of IL-1β and IL-6, other cytokines that characterize sJIA milieu (Supplementary Figure 4E and F).

Regarding hILCs, despite a significantly higher proportion of ILC1s in patients with sJIA (Figure 2G), the frequency of IFNγ +
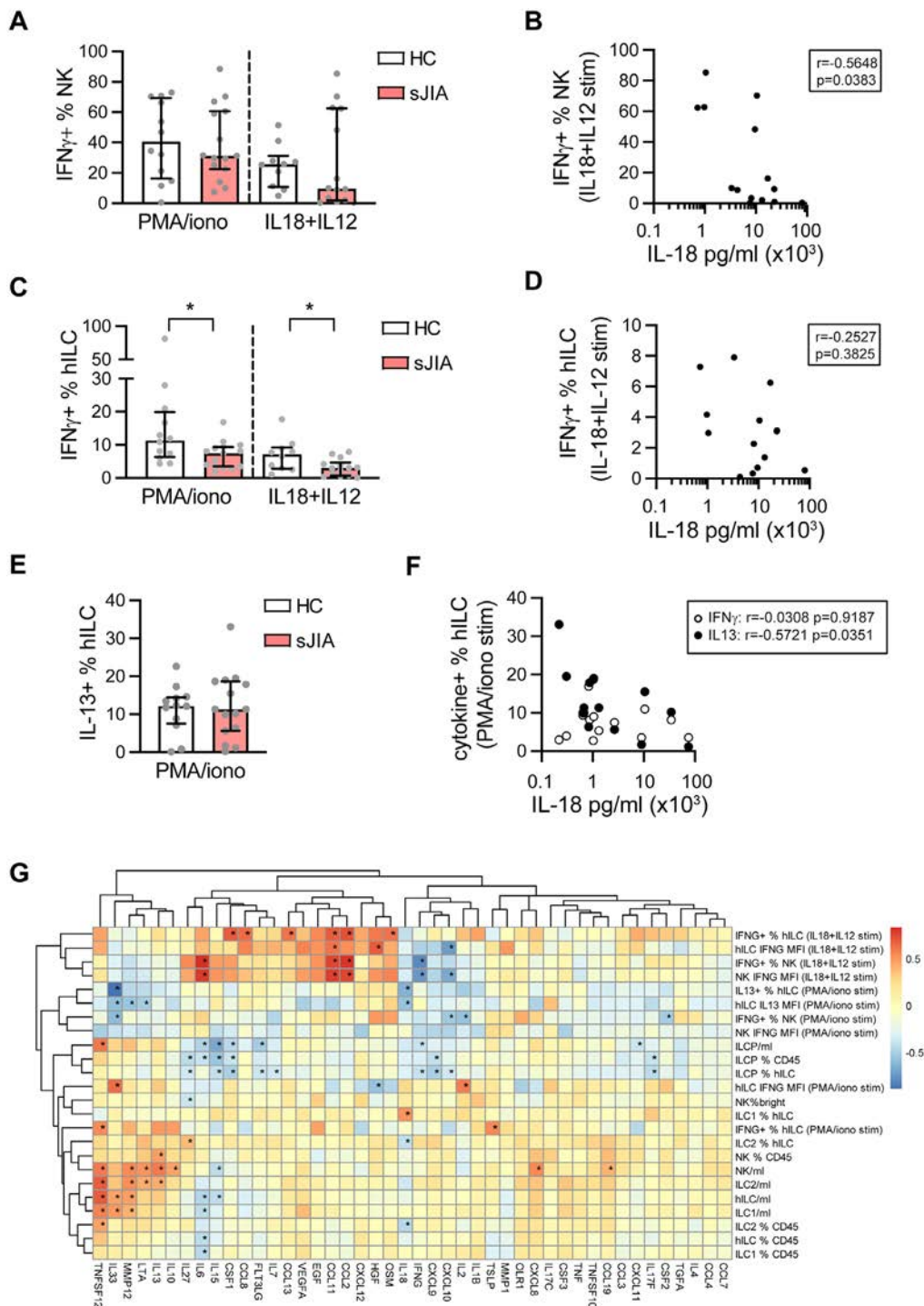
Figure 3. Dysfunctional IFNγ production by ILCs in patient with sJIA. (A, C, and E) Scatter dot plots and bars showing the median and IQR of (A and C) IFNγ+ and (E) IL-13+ cell frequency for cells stimulated as indicated. (B and D) Scatterplots showing the correlation between IL-18 plasma concentration and IFNγ+ cell frequency for (B) NK cells and (D) hILCs stimulated with IL-18 and IL-12. (F) Scatterplot showing the correlation between IL-18 plasma concentration and IFNγ+ (empty dots) or IL-13+ (black dots) cell frequency for hILCs stimulated with PMA/iono. (G) Heatmap of correlations calculated between proteins in sJIA plasma samples and phenotypic/functional ILC data. r values are represented by color, and P values <0.05 are represented by an asterisk. Dendrograms represent hierarchical clustering between rows and columns. A, C, and E n = 12 PMA/iono HC; n = 15 PMA/iono sJIA; n = 10 IL-18 and IL-12 HC; n =14 IL-18 and IL-12 sJIA. B, D, and F n = 14. In C, significance was determined by Mann-Whitney U-tests (*P < 0.05). In B, D, F, and G, r and P values were determined by the Spearman correlation test. Symbols represent individual patients. HC, healthy children; hILC, helper innate lymphoid cell; ILC, helper innate lymphoid cell; IFNγ, interferon γ; IL-18, interleukin 18; iono, ionomycin; IQR, interquartile range; NK, natural killer; PMA, phorbol 12–myristate 13–acetate; sJIA, systemic juvenile idiopathic arthritis.

hILCs following both PMA/ionomycin or IL-18/IL-12 stimulations was significantly lower in patients with sJIA compared to HC (Figure 3C). Differently from NK cells, no significant correlation between the percentage of IFNγ and hILCs, and the circulating levels of IL-18 was found in IL-18/IL-12 stimulation (Figure 3D). As expected, IL-13 was not produced by hILCs in response to IL-18 with IL-12 (data not shown). In PMA/ionomycin stimulation, the frequency of hILCs positive for IL-13, the signature cytokine for ILC2, was comparable between sJIA and HC (Figure 3E). Given the opposite correlation of ILC1 and ILC2 frequencies among hILCs with IL-18 plasma concentration (Figure 2L), we investigated whether there was any association with hILC ability to produce the ILC1 and ILC2 signature cytokines IFNγ and IL-13, respectively. Consistently, IL-18 plasma concentration negatively correlated with the frequency of IL-13 and hILCs, whereas no correlation was observed with the frequency of IFNγ and hILCs (Figure 3F).

Overall, these findings indicate that in patients with sJIA during CID, hILCs display a specific functional impairment in IFNγ production. Conversely, in patients with sJIA, the responsiveness of NK cells to ex vivo stimulation with IL-18 and IL-12, in terms of IFNγ production, is associated with in vivo IL-18 plasma levels.

Proteomic profile of patients with sJIA during CID. To explore the plasma proteomic profile of children with sJIA during CID while receiving IL-1 inhibitors, we quantified the concentrations of 44 proteins in 35 patients and 5 HC. These data confirmed that IL-18 levels were the highest among all the proteins assessed in sJIA samples, and we observed that samples clustered according to IL-18 concentration rather than diagnosis (Supplementary Figure 5A). Indeed, patients with lower plasma levels of IL-18 clustered together with HC and displayed increased expression of tumor necrosis factor superfamily 10 (TNFSF10) and TNFSF12 compared to patients with higher IL-18 levels (Supplementary Figure 5A). Principal component analysis of the protein data set confirmed that patients could not be distinguished from HC (Supplementary Figure 5B), suggesting a similar inflammatory profile between the two groups. Indeed, except for IL-18, which was the top up-regulated cytokine in patients with sJIA, differential analysis between sJIA and HC samples revealed that only IL-15 and colony stimulating factor 3 (CSF3) (also known as G-CSF) were significantly up-regulated in patients with sJIA (Supplementary Figure 5C). Correlation analysis between the expression of pairs of proteins allowed to identify a disease-associated pattern during CID, consisting of 12 proteins including the IFNγ-CXCL9/CXCL10 axis (Supplementary Figure 6). Additionally, we integrated proteomics with the phenotypic and functional ILC analysis data. This comprehensive approach allowed to identify additional correlations and confirmed that ILC

phenotypes and functions were primarily linked to IL-18 levels during CID in patients with sJIA (Figure 3G).

DISCUSSION

In this study, we performed immunophenotyping of the ILC compartment in the PB of patients with sJIA during CID receiving IL-1 inhibitors. Similar to what has been shown in active disease,[16] we found a decreased frequency and number of NK cells in patients during CID compared to HC. Notably, we also observed that these patients exhibited an increase in the percentage of NK CD56^{bright} cells compared to HC. This subset of NK cells is typically associated with IFNγ production rather than cytotoxic activity. These data expand on what is already known and suggest that a reduced NK cell frequency may represent a persistent dysfunctional feature of sJIA, even during the inactive phase of the disease.

In contrast to NK cells, we found that in patients with sJIA during CID the frequency and number of hILCs were comparable to HC. Furthermore, in these patients, the hILC frequency positively correlated with the duration of IL-1 inhibitor treatments, suggesting that prolonged control of disease activity may facilitate the recovery of circulating hILCs. Within the hILC compartment, patients with sJIA exhibited a significant increase in ILC1 and a decrease in ILCP frequencies and absolute numbers compared to HC. Importantly, these changes were specific to sJIA and not observed in patients with other autoinflammatory diseases receiving IL-1 inhibitors, suggesting a unique pattern of hILC dysregulation in sJIA. Additionally, we found that both ILC1 and ILC2 proportions among hILCs correlated with plasma IL-18 levels, further supporting the pivotal role of IL-18 in sJIA pathogenesis. The positive correlation between IL-18 levels and the proportion of ILC1s, alongside the negative correlation with the ILC2 proportion, highlights the influence of IL-18 on the hILC landscape. The high IL-18 plasma levels may be responsible for the IL18-driven ILC1 expansion observed, as suggested by the ILCP-ILC1 conversion induced by stimulating HC PBMCs with IL-18 ex vivo. Furthermore, the negative correlation between IL-18 levels and the frequency of IL-13^{+} hILCs underscores the IL-18's role in skewing the balance away from ILC2-driven responses, which could have anti-inflammatory effects. Consistent with our results, hILCs respond to IL-18 during inflammation, with IL-18 driving preferential ILCP differentiation toward ILC1s and production of IFNγ.[17]

Regarding the functional capability of ILCs, we found that both NK cells and hILCs from patients with sJIA exhibited functional abnormalities. Despite the higher frequency of CD56^{bright} cells, NK cells from patients with sJIA displayed a heterogeneous response to IL-18/IL-12 stimulation, with some patients being hyperresponders and others hypo- or nonresponders. This variability in NK cell response was inversely correlated with circulating IL-18 levels, suggesting a potential desensitization mechanism induced by prolonged exposure to high IL-18 concentrations.

Similar findings have been reported in patients with sJIA during active disease and at disease onset.[6,7] This IL-18 desensitization mechanism is also supported by our data on HC NK cells, showing a dose-dependent loss of responsivity to further IL-18 stimulation on preincubation with this cytokine. These findings suggest that prolonged IL-18 exposure may induce a refractory state in NK cells, potentially impairing their ability to mount an appropriate immune response in inflammatory conditions. Reduced IFNγ production by NK cells in response to IL-18 may represent a protective mechanism aimed at preventing excessive IFNγ production and, consequently, the development of MAS during active sJIA. However, in patients with sJIA with low IL-18 plasma levels, despite proteomic data indicating a similarity with HC cytokine expression patterns, NK cells were hyperresponsive to this cytokine in terms of IFNγ production, therefore suggesting that a decrease in IL-18 plasma concentration during CID may not be associated with a recovery of physiologic NK cell function. This hypothesis aligns with data demonstrating that leukocytes from patients with inactive sJIA exhibit underlying alterations in Toll-like receptor signaling and a skewed monocyte phenotype, even in patients who are clinically and transcriptionally comparable to healthy individuals.[12]

Conversely, despite the increased proportion of ILC1s in patients with sJIA and CID, hILCs demonstrated significant functional impairment in their ability to produce IFNγ on stimulation with PMA/ionomycin or IL-18/IL-12, while maintaining normal IL-13 production. This impairment may be due to reduced IL-18RA expression on ILC1s in patients with sJIA and could represent a protective mechanism to avoid excessive IFNγ production.

Proteomic integration analysis confirmed that ILC phenotypes and functions were predominantly associated with IL-18 levels, further emphasizing its role as a key driver of immune dysregulation in sJIA. Additionally, hierarchical clustering revealed distinct groups of highly correlated cytokines, indicating shared biologic pathways. Notably, a very well-defined cluster, including CXCL9, CXCL10, and IFNγ, along with nine other proteins, was identified, suggesting a distinct inflammatory signature driven by IFNγ in patients with sJIA, even during CID.

Because of the low frequency of ILCs in the PB, a limitation of this study is that the number of cells obtained from children's samples was insufficient to perform all analyses in parallel for each patient. To avoid potential alterations in cell subset proportions and function because of cell thawing, we conducted our analyses on freshly isolated PBMCs. This approach limited the number of patients we could enroll, particularly those with treatment-naïve sJIA at disease onset.

Despite these limitations, our study provides the first phenotypic and functional characterization of ILCs in patients with sJIA during CID. Our findings underscore the persistent dysregulation of innate immune cells in patients with sJIA, even in the absence of active disease symptoms, and highlight the potential pathogenic role of specific immune cell subsets and cytokine interactions. We demonstrate that NK cells and hILCs in patients with sJIA during CID exhibit opposite dysfunctional features, with NK cells being more responsive to IL-18 stimulation and hILCs showing an intrinsic impairment in IFNγ production, compared to the respective subsets in HC. These findings further contribute to the definition of recovery from active disease as a state of compensation[2] or adaptation to an altered inflammatory environment, rather than a reversion to an initial normal state.

ACKNOWLEDGMENT

AUTHOR CONTRIBUTIONS

All authors contributed to at least one of the following manuscript preparation roles: conceptualization AND/OR methodology, software, investigation, formal analysis, data curation, visualization, and validation AND drafting or reviewing/editing the final draft. As corresponding author, Dr Quatrini confirms that all authors have provided the final approval of the version to be published and takes responsibility for the affirmations regarding article submission (eg, not under consideration by another journal), the integrity of the data presented, and the statements regarding compliance with institutional review board/Declaration of Helsinki requirements.

REFERENCES

1. Fautrel B, Mitrovic S, De Matteis A, et al. EULAR/PReS recommendations for the diagnosis and management of Still's disease, comprising systemic juvenile idiopathic arthritis and adult-onset Still's disease. Ann Rheum Dis 2024;83(12):1614–1627.

2. Mellins ED, Macaubas C, Grom AA. Pathogenesis of systemic juvenile idiopathic arthritis: some answers, more questions. Nat Rev Rheumatol 2011;7(7):4164–4126.

3. Bracaglia C, Prencipe G, De Benedetti F. Macrophage activation syndrome: different mechanisms leading to a one clinical syndrome. Pediatr Rheumatol Online J 2017;15(1):5.

4. Vivier E, Artis D, Colonna M, et al. Innate lymphoid cells: 10 years on. Cell 2018;174(5):1054–1066.

5. Quatrini L, Della Chiesa M, Sivori S, et al. Human NK cells, their receptors and function. Eur J Immunol 2021;51(7):1566–1579.

6. Put K, Vandenhaute J, Avau A, et al. Inflammatory gene expression profile and defective interferon-γ and granzyme K in natural killer cells from systemic juvenile idiopathic arthritis patients. Arthritis Rheumatol 2017;69(1):213–224.

7. de Jager W, Vastert SJ, Beekman JM, et al. Defective phosphorylation of interleukin-18 receptor β causes impaired natural killer cell function in systemic-onset juvenile idiopathic arthritis. Arthritis Rheum 2009;60(9):2782–2793.

8. Rosser EC, Lom H, Bending D, et al. Innate lymphoid cells and T cells contribute to the interleukin-17A signature detected in the synovial fluid of patients with juvenile idiopathic arthritis. Arthritis Rheumatol 2019;71(3):460–467.

9. Fang W, Zhang Y, Chen Z. Innate lymphoid cells in inflammatory arthritis. Arthritis Res Ther 2020;22(1):25.

10. Wallace CA, Ruperto N, Giannini EH; Childhood Arthritis and Rheumatology Research Alliance; Pediatric Rheumatology International Trials Organization; Pediatric Rheumatology Collaborative Study Group. Preliminary criteria for clinical remission for select categories of juvenile idiopathic arthritis. J Rheumatol 2004;31(11):2290–2294.

11. Hinze CH, Foell D, Kessel C. Treatment of systemic juvenile idiopathic arthritis. Nat Rev Rheumatol 2023;19(12):778–789.

12. Cepika AM, Banchereau R, Segura E, et al. A multidimensional blood stimulation assay reveals immune alterations underlying systemic juvenile idiopathic arthritis. J Exp Med 2017;214(11):3449–3466.

13. Shimizu M, Yokoyama T, Yamada K, et al. Distinct cytokine profiles of systemic-onset juvenile idiopathic arthritis-associated macrophage activation syndrome with particular emphasis on the role of interleukin-18 in its pathogenesis. Rheumatology (Oxford) 2010;49(9):1645–1653.

14. Petty RE, Southwood TR, Manners P, et al. International League of Associations for Rheumatology classification of juvenile idiopathic arthritis: second revision, Edmonton, 2001. J Rheumatol 2004;31(2):390–392.

15. Cotugno N, Olivieri G, Pascucci GR, et al. Multi-modal immune dynamics of pre-COVID-19 Kawasaki Disease following intravenous immunoglobulin. Clin Immunol 2024;267:110349.

16. Vandenhaute J, Wouters CH, Matthys P. Natural killer cells in systemic autoinflammatory diseases: a focus on systemic juvenile idiopathic arthritis and macrophage activation syndrome. Front Immunol 2020;10:3089.

17. Lim AI, Li Y, Lopez-Lastra S, et al. Systemic human ILC precursors provide a substrate for tissue ILC differentiation. Cell 2017;168:1086–1100.e10.

AMERICAN COLLEGE
of RHEUMATOLOGY
Empowering Rheumatology Professionals

Clinical Images: Subacromial bursitis with rice bodies as an initial solo presentation of rheumatoid arthritis
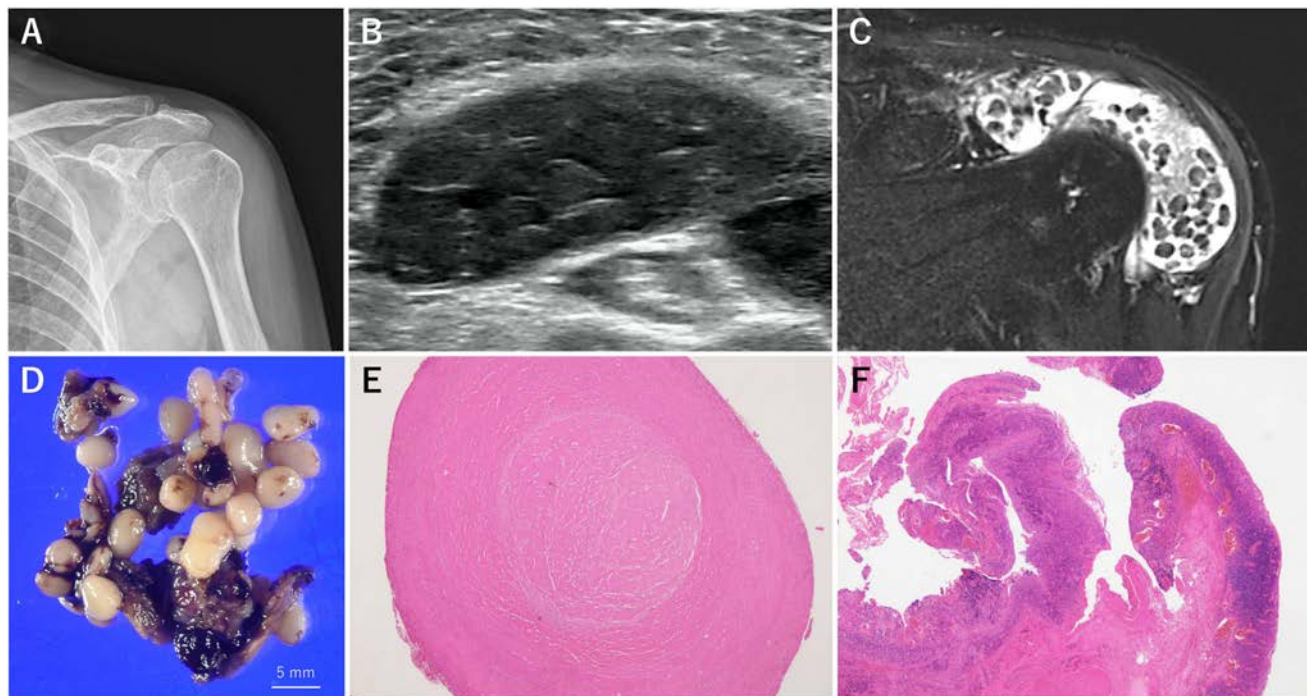
The patient, a 69-year-old woman with chronic polyarthritis, was referred to our department. She had visited an orthopedic clinic a year before this referral for a three-month history of left shoulder pain. Tenderness and swelling were detected only in the left shoulder and not in the other joints. (A) Radiography showed no calcification or bone erosions, (B) whereas ultrasonography revealed an effusion in the subacromial bursa with multiple hypoechoic to hyperechoic nodules. (C) T2-weighted magnetic resonance imaging showed multiple nodules of low-signal intensity in the distended fluid-filled subacromial bursa. Tan nodules were arthroscopically extracted, revealing typical rice bodies. (D) The brown component comprised the bursal lining with old blood and iron pigmentation (formalin fixed). Pathologic examination revealed that typical rice bodies consist of an amorphous acidophilic core surrounded by fibrin. Bursal lining showed synovial villous hypertrophy, a band-like zone of chronic inflammation, and perivascular aggregates. (E and F) No cartilaginous or chondrocyte proliferation was detected (hematoxylin and eosin stain, ×20). No evidence of malignancy or infection was detected. Arthroscopic bursectomy resulted in complete improvement. However, eight months after surgery, polyarthritis occurred in the fingers, hands, knees, and right shoulder, which persisted for two months. At our department, ultrasonography revealed joint synovitis. Serum rheumatoid factor and anti–cyclic citrullinated peptide antibodies were highly positive. The patient was diagnosed with rheumatoid arthritis (RA) and treated with methotrexate. Rice bodies can develop at any time and are not associated with disease activity in RA.[1] However, patients who develop only subacromial bursitis with rice bodies as an initial manifestation of RA are extremely rare.[2] These cases should be carefully followed up, even after surgical improvement, because polyarthritis may develop later in the course of RA.

1. Popert AJ, Scott DL, Wainwright AC, et al. Frequency of occurrence, mode of development, and significance or rice bodies in rheumatoid joints. Ann Rheum Dis 1982;41(2):109–117.
2. Subramaniam R, Tan JW, Chau CY, et al. Subacromial bursitis with giant rice bodies as initial presentation of rheumatoid arthritis. J Clin Rheumatol 2012;18(7):352–355.

Takeshi Zoshima, MD, PhD
takeshiz1983@yahoo.co.jp
*Department of Nephrology and Rheumatology, Kanazawa University Hospital
and Department of Internal Medicine, Asanogawa General Hospital
Kanazawa, Japan*

Clinical Images: Acute vision loss due to granulomatosis with polyangiitis
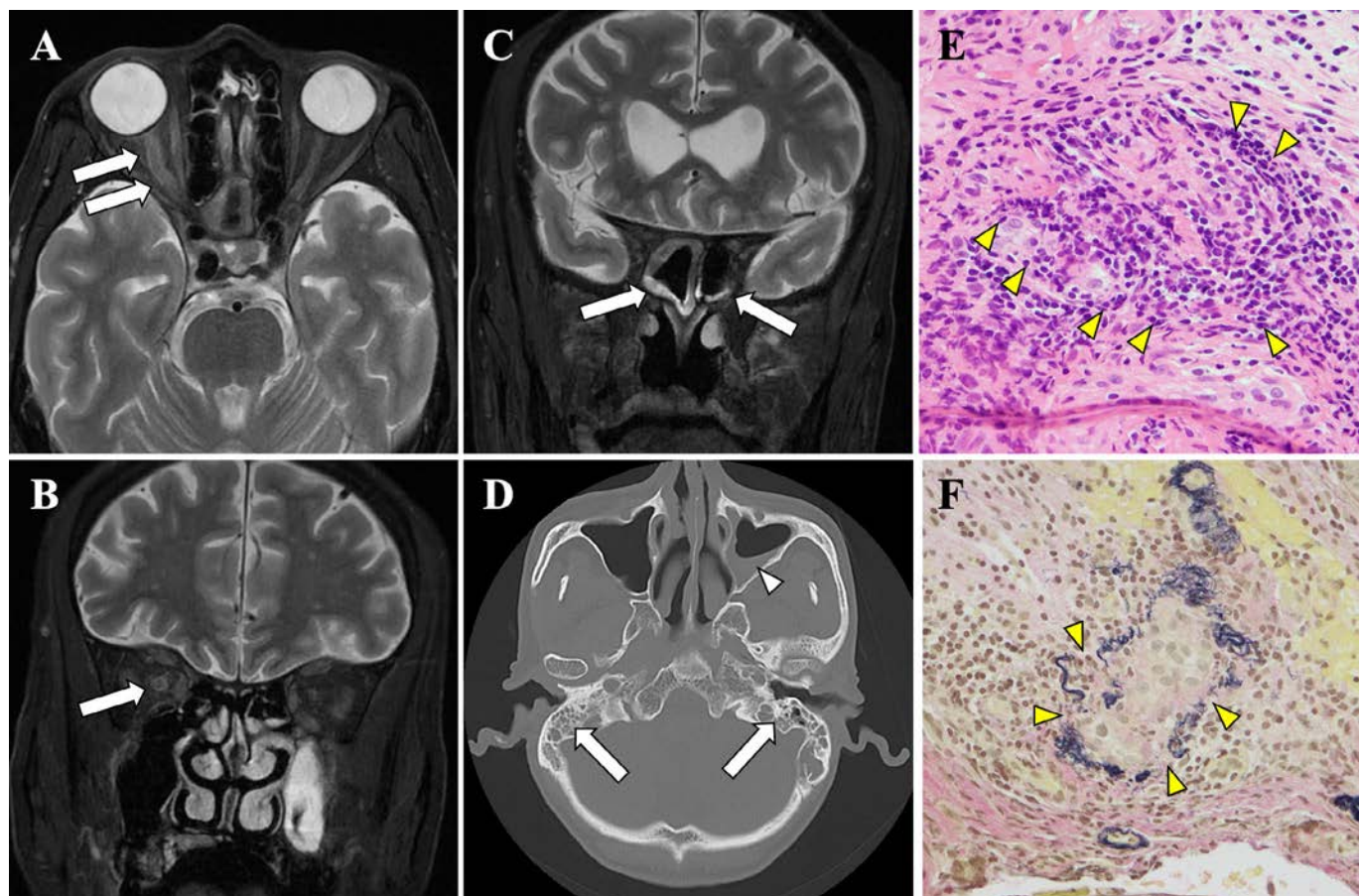
A 70-year-old man presented with progressive hearing loss and persistent postnasal drip for five months. Despite starting antibiotics, the patient's condition remained refractory. The patient suddenly experienced vision loss two weeks before presentation. Physical examination revealed complete blindness, positive relative afferent pupillary defect in the right eye, and hearing loss. Ophthalmoscopy revealed no abnormalities. Audiometry demonstrated severe bilateral mixed hearing loss. Laboratory findings showed elevated C-reactive protein level (5.94 mg/dL), erythrocyte sedimentation rate (115 mm/h), and positive proteinase 3 antineutrophil cytoplasmic antibody level (89.7 IU/L). Antinuclear antibody, T-SPOT.TB test, and blood culture results were negative. Angiotensin-converting enzyme, lysozyme, serum IgG4, interleukin-2 receptor, and all tumor marker levels were normal. Axial (A, arrows) and coronal (B, arrow) T2-weighted enhanced magnetic resonance imaging showed high intensity and contrast effect around the right optic nerve, the so-called "tram track sign" and "donut sign," which indicated optic perineuritis. Furthermore, sinusitis was detected (C, arrows). Computed tomography showed poor air-containing and soft shadows in the bilateral mastoid antrums (D, arrows) and fluid accumulation in left maxillary sinus (D, arrowhead) that suggested otitis media and sinusitis. A biopsy specimen from the right maxillary sinus revealed lymphocyte and plasma cell infiltration around the capillaries in hematoxylin and eosin staining (E, arrowheads), and Elastica-van Gieson staining showed elastic fiber disruption in the vessel wall (F, arrowheads), which indicated small-vessel vasculitis. Thus, granulomatosis with polyangiitis (GPA) was diagnosed. Methylprednisolone at 1,000 mg was initiated, followed by intravenous administration of rituximab at 500 mg weekly and gradual tapering of prednisolone. Symptoms and laboratory and imaging findings gradually improved. Therefore, optic perineuritis due to GPA should be considered a cause of sudden vision loss.

Hirotaka Yamamoto, MD
hr413055@gmail.com
Yoshinori Taniguchi, MD
*Kochi Medical School Hospital, Kochi University,
Nankoku, Kochi, Japan*

AMERICAN COLLEGE
of RHEUMATOLOGY
Empowering Rheumatology Professionals

Arthritis & Rheumatology
Vol. 77, No. 10, October 2025, pp 1454–1459
© 2025 American College of Rheumatology

LETTER

Granulomatosis with polyangiitis presenting as strawberry gingivitis: methodologic aspects: comment on the article by Liu et al

To the Editor:

With interest, we read the report by Liu et al[1] describing a patient with strawberry gingivitis, attributed to granulomatosis with polyangiitis (GPA). The authors state "…co-localization staining for proteinase 3 (PR3) and IgG revealed specific PR3-ANCA [anti-neutrophil cytoplasmic antibody] positivity… (Figure C, D)" and "This case underscores the diagnostic challenge of GPA, especially in ANCA-negative presentations by [indirect immunofluorescence] IIF, necessitating reliance on histopathology and targeted immunologic testing to establish a diagnosis." Unfortunately, the presented histopathology and immunologic testing results have substantial inadequacies. Central to their argument is their interpretation of stainings of PR3 and IgG in approximately the same location as conclusive evidence of specific presence of PR3-ANCA. We respectfully disagree with this conclusion because it is not proven by the evidence provided.

PR3, the target of PR3-ANCA, is expressed mainly by neutrophils. Upon neutrophil priming by inflammatory cytokines, PR3 expression on the cell surface is up-regulated by binding to NB1 (also known as CD177), and it can also be released by activated neutrophils into the extracellular environment during the process of NETosis or other forms of inflammatory neutrophil cell death.[2,3] Detection of PR3 in inflamed tissue is therefore not specific for GPA. Furthermore, colocalization with IgG in immunohistochemistry does not demonstrate that IgG is bound to a colocalized protein in a specific antibody–antigen binding manner. Thus, the statement that colocalization staining for PR3 and IgG would reveal specific PR3-ANCA positivity appears to be a misconception. Furthermore, Figure 1C and 1D are uninterpretable because the underlying anatomic structures cannot be identified, the images do not seem to represent serial sections, and Figure 1C seems to show only stained PR3 and 1D shows only stained IgG, without clear red-green overlap anywhere.

The serologic diagnosis of GPA could also be challenged. The patient first tested negative for ANCA by IIF but was nonetheless classified as having GPA after a low-positive PR3-ANCA enzyme-linked immunosorbent assay (ELISA) result. This testing sequence is not consistent with the latest ANCA-testing consensus guidelines, which recommend the use of a high-quality antigen-specific immunoassay as the preferred first screening method. If this test reveals low antibody levels (as in this case), a second, different immunoassay or IIF is advised for confirmation.[4] Therefore, the PR3-ANCA test result reported here (weakly positive ELISA with negative IIF) is not conclusively supportive of GPA.

In summary, although strawberry gingivitis is considered pathognomonic for GPA, and the follow-up with persistently elevated cytoplasmic ANCA and PR3-ANCA levels makes the diagnosis of GPA plausible, we would like to add a word of caution regarding the diagnostic methods employed here. GPA can be difficult to diagnose, and it is important to only embrace diagnostic methods with validated sensitivity and specificity to avoid overdiagnosis and possibly overtreatment.

Diane van der Woude, MD, PhD iD
dvanderwoude@lumc.nl
Department of Rheumatology
Leiden University Medical Center
Leiden, The Netherlands
Ingeborg M. Bajema, MD, PhD
Department of Pathology and Medical Biology
University Medical Center Groningen
Groningen, The Netherlands
Ulrich Specks, MD iD
Division of Pulmonary and Critical Care Medicine
Department of Internal Medicine
Mayo Clinic
Rochester, Minnesota

1. Liu H, Qi W, Han Q, et al. Clinical images: granulomatosis with polyangiitis presenting as strawberry gingivitis: diagnostic challenges with negative antineutrophil cytoplasmic antibody. Arthritis Rheumatol 2025;77(8):1106–1107. https://doi.org/10.1002/art.43119.

2. Falde SD, Fussner LA, Tazelaar HD, et al. Proteinase 3-specific antineutrophil cytoplasmic antibody-associated vasculitis. Lancet Rheumatol 2024;6(5):e314–e27.

3. von Vietinghoff S, Tunnemann G, Eulenberg C, et al. NB1 mediates surface expression of the ANCA antigen proteinase 3 on human neutrophils. Blood 2007;109(10):4487–4493.

4. Bossuyt X, Cohen Tervaert JW, Arimura Y, et al. Position paper: Revised 2017 international consensus on testing of ANCAs in granulomatosis with polyangiitis and microscopic polyangiitis. Nat Rev Rheumatol 2017;13(11):683–692.

Reply

To the Editor:

We sincerely appreciate the interest in our report[1] and the detailed comments made by van der Woude et al. We would like to address the concerns as follows:

1. Clarification on Figures 1C and 1D

Because of journal requirements, figure legends were not included, which may have led to some misunderstandings regarding Figure 1C and 1D, which depict IgG and proteinase 3 (PR3) costaining in healthy human gingiva and strawberry gingivitis, respectively. To clarify, we provide more detailed staining images in Figure 1.

2. Colocalization of IgG and PR3

We acknowledge that IgG and PR3 colocalization staining alone does not confirm specific immune binding between PR3 and IgG. However, given the available immunodetection methods at the time, we were unable to use more precise immunologic techniques to determine the exact tissue localization of PR3-specific antineutrophil cytoplasmic antibodies (ANCAs).

Despite this limitation, the observed colocalization of IgG and PR3 in the patient sample, compared to the control, still suggests the potential presence of PR3-ANCA–specific antibodies, which remains meaningful for the diagnosis of granulomatosis with polyangiitis (GPA).

3. Diagnostic workflow limitations

As oral medicine specialists, we recognize that there were limitations in our adherence to the latest GPA diagnostic guidelines. In our case, we followed the 1999 ANCA-testing consensus guidelines[2], using indirect immunofluorescence (IIF) for initial screening, followed by PR3-ANCA enzyme-linked immunosorbent assay (ELISA) for further assessment. We acknowledge that the most recent consensus guidelines recommend using specific PR3-ELISA as the first-line screening method, followed by a confirmatory test if the result is weakly positive. However, even under the latest guidelines[3], a combination of IIF and PR3-ELISA results should be considered to improve diagnostic accuracy. Given that our patient showed negative IIF and weakly positive PR3-ELISA, additional laboratory tests would indeed be required to confirm a GPA diagnosis. Thus, we maintain that local tissue biopsy remains a valuable diagnostic tool for helping confirm GPA. IgG and PR3 colocalization analysis may aid in GPA diagnosis,
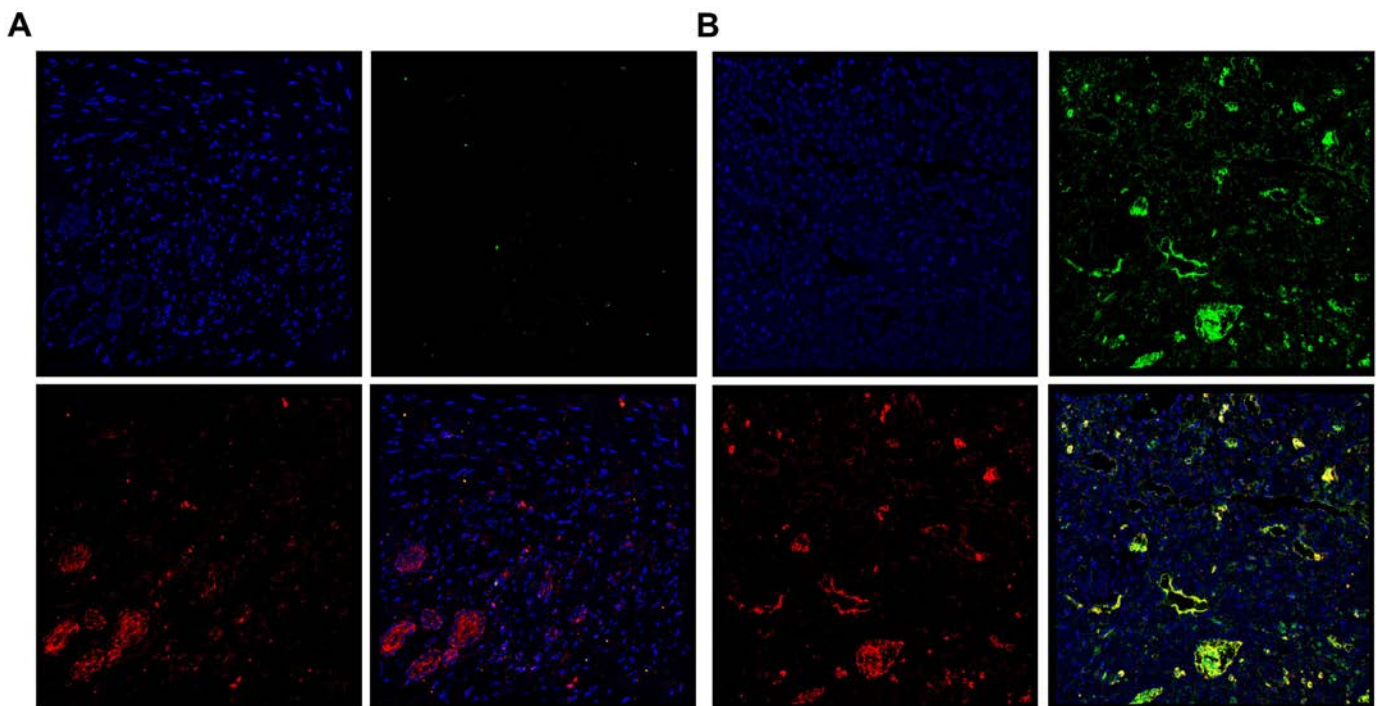

Figure 1. (A) IgG and proteinase 3 (PR3) costaining in gingival samples from a healthy control (top left: DAPI; top right: IgG-FITC; fluorescein isothiocyanate: bottom left: PR3-Cy3; cyanine 3 bottom right: merged image). (B) Corresponding staining in the patient's gingival sample.

particularly in cases in which conventional ANCA testing yields inconclusive results. However, we acknowledge that this approach has not been validated in the literature and recognize the limitations of our immunodetection method, including the absence of more advanced techniques such as confocal microscopy–based antibody affinity assays or bimolecular fluorescence complementation.

We appreciate your insightful comments and the opportunity to clarify these points. We hope that our responses adequately address your concerns and contribute to a constructive discussion.

Hanghang Liu [ID]
Xian Liu [ID]
Jssyliuxian@163.com
State Key Laboratory of Oral Diseases & National Center for Stomatology & National Clinical Research Center for Oral Diseases, West China Hospital of Stomatology
Sichuan University
Chengdu, Sichuan, China

1. Liu H, Qi W, Han Q, et al. Clinical images: granulomatosis with polyangiitis presenting as strawberry gingivitis: diagnostic challenges with negative antineutrophil cytoplasmic antibody. Arthritis Rheumatol 2025;77(8):1106–1107. https://doi.org/10.1002/art.43119.

2. Savige J, Gillis D, Benson E, et al. International consensus statement on testing and reporting of antineutrophil cytoplasmic antibodies (ANCA). *Am J Clinn Pathol* 1999;111(4):507–513.

3. Bossuyt X, Cohen Tervaert JW, Arimura Y, et al. Revised 2017 international consensus on testing of ANCAs in granulomatosis with polyangiitis and microscopic polyangiitis. *Nat Rev Rheumatol* 2017;13(11):683–692.

DOI 10.1002/art.43176

Methodological considerations for "Proinflammatory dietary pattern and the risk of female gout": comment on the article by Rai et al

To the Editor:

We read with great interest the article by Rai et al titled "*Proinflammatory Dietary Pattern and the Risk of Female Gout: Sex-Specific Findings From Three Prospective Cohort Studies.*"[1] Although the authors provided a detailed discussion of the study's limitations, we wish to highlight additional methodological considerations that could further refine the interpretation and generalizability of these findings.

First, the study predominantly enrolled US White health care professionals— a population with socioeconomic status, health literacy, and health care access markedly higher than the general population. This selection bias may limit the external validity of conclusions when extrapolated to other racial and ethnic groups (e.g., African American, Hispanic individuals) and low-and middle-income countries,[2] particularly given well-documented racial disparities in gout incidence.[3]

Second, although validated food frequency questionnaires (FFQs) were used to calculate empirical dietary inflammatory pattern (EDIP) scores, inherent recall bias and classification errors in FFQs likely attenuated true diet-gout associations.[4] The exclusive reliance on EDIP as a proinflammatory diet metric, without concurrent measurement of inflammatory biomarkers such as C-reactive protein or interleukin-6, precludes validation of its biological plausibility. Furthermore, prolonged EDIP update intervals fail to capture short-term dietary fluctuations that may dynamically influence gout risk, and discontinuing EDIP assessments following metabolic disease diagnoses (e.g., diabetes) introduces information truncation bias by neglecting reverse causation between disease progression and dietary modifications.

Third, the Cox proportional hazards models incorporated time-varying adjustments for covariates (e.g., body mass index [BMI], smoking status) but relied solely on stratification and covariate adjustment to address confounding. This approach may inadequately control for unmeasured time-varying confounders, such as temporal shifts in medication use (e.g., urate-lowering therapies) and socioeconomic status. Treating BMI as a causal mediator through stratification risks overadjustment bias, potentially obscuring the direct effect of dietary patterns on gout pathogenesis mediated via adiposity-independent inflammatory pathways.

Finally, although most alcoholic beverages were classified as "anti-inflammatory" components, this categorization may conflate risks in subgroups with alcohol misuse or impaired hepatic and/or renal function. Although sex-specific differences were emphasized, the analysis omitted exploration of estrogen levels, oral contraceptive use, or hormone replacement therapies— all factors known to modulate both inflammatory pathways and uric acid metabolism.[5]

Despite these limitations, the study provides compelling epidemiological evidence for sexually dimorphic associations between proinflammatory diets and gout risk. Future research should prioritize diverse populations, validate dietary indices against clinical biomarkers, employ time-dependent EDIP metrics or machine learning algorithms (e.g., random forests) to capture nonlinear dietary effects, and utilize causal mediation models or Mendelian randomization analyses to elucidate sex-specific biological mechanisms. Such advancements would substantially enhance the translational relevance of dietary interventions in gout prevention.

Fusen Chen and Jiatao Li contributed equally to this work.

Fusen Chen, MM
Jiatao Li, MM
Tiejuan Shao, PhD
tiejuanshao@zcmu.edu.cn
*College of Basic Medical Sciences,
Zhejiang Chinese Medical University
Hangzhou, China*

1. Rai SK, Choi HK, Lu N, et al. Proinflammatory dietary pattern and the risk of female gout: sex-specific findings from three prospective cohort studies. Arthritis Rheumatol 2025;77(8):1077–1086. https://doi.org/10.1002/art.43127

2. Singh JA. Racial and gender disparities among patients with gout. Curr Rheumatol Rep 2013;15(2):307.

3. McCormick N, Lu N, Yokose C, et al. Racial and sex disparities in gout prevalence among US adults. JAMA Netw Open 2022;5(8):e2226804.

4. Looman M, Boshuizen HC, Feskens EJ, et al. Using enhanced regression calibration to combine dietary intake estimates from 24 h recall and FFQ reduces bias in diet-disease associations. Public Health Nutr 2019;22(15):2738–2746.

5. Eun Y, Kim IY, Han K, et al. Association between female reproductive factors and gout: a nationwide population-based cohort study of 1 million postmenopausal women. Arthritis Res Ther 2021;23(1):304.

Reply

To the Editor:

We read with interest the comments by Dr Chen et al regarding our article[1] and appreciate the opportunity to address the methodologic considerations raised. First, we acknowledge our study population was not representative of the US general population, and, as mentioned in our article, replication in diverse populations will be valuable. Moreover, despite the homogeneity of our cohorts in terms of health literacy and health care access, they offer many strengths to longitudinally evaluate diet–disease associations, including the availability of repeated measures and well-characterized physician-diagnosed gout cases. Still, although the absolute rates of gout and distribution of dietary intake in this study are more readily generalizable to White US health professionals, the underlying biologic effects of the empirical dietary inflammatory pattern (EDIP) (reflected by the hazard ratios) are likely to be similar among other Americans, as has been shown when comparing risk factor levels and risk factor associations between the more selected UK Biobank cohort and more representative UK populations.[2]

Second, the prospective nature of our study (wherein disease-free participants are routinely surveyed about their diets before disease onset) minimizes the possibility of recall bias. Moreover, one key strength of using the validated food frequency questionnaire (FFQ) is its lack of reliance on participants' memory, as usual intake is typically easier to describe versus recalling what specific foods were eaten at any given meal in the past.[3] Any remaining misclassification is expected to be nondifferential with respect to our outcome and would likely simply attenuate the observed association toward the null. Chen et al further postulated that the EDIP lacks concurrent biomarker measurement and validation; we noted the EDIP was indeed developed and validated using biomarker data (C-reactive protein, interleukin-6, and tumor necrosis factor α receptor 2) in our three cohorts as well as the Women's Health Initiative.[4] Next, although Chen et al are correct that our use of cumulatively averaged repeated measures of EDIP will not capture short-term dietary fluctuations, the current study focused on the public health–related question of long-term diet and new-onset gout rather than recurrent flare risk among those with gout. Indeed, another key strength of using the FFQ is minimization of within-person variation (generated by short-term dietary fluctuations), which may dampen observed associations between habitual diet and disease risk.[3] Regarding the possibility of reverse causation introduced by our modeling approach, we note that our approach is actually intended to minimize potential bias resulting from a change in diet following the diagnosis of another condition.[5]

Third, Chen et al remarked that our modeling approach "may inadequately control for unmeasured time-varying confounders, such as temporal shifts in medication use (eg, urate-lowering therapies)." As in all observational studies (and acknowledged in our article), unmeasured confounding remains possible. Importantly, this is a gout-free population, and therefore participants are highly unlikely to be using urate-lowering therapy; however, we did adjust for available medications known to be associated with gout risk, including diuretics and postmenopausal hormone therapy. With respect to body mass index (BMI) overadjustment, we presented estimates before and after BMI adjustment (with the latter representing the association independent of adiposity).

Finally, as mentioned in our Methods section, we note that we adjusted for alcohol intake because of its established positive association with gout, which is likely to be even higher among those with impaired hepatic and/or renal function. Although our cohort did not have data on estrogen levels for all participants, we did adjust for menopausal status and postmenopausal hormone use.

In summary, we appreciate the comments but wish the readers to take away our article's principal finding: consuming a more anti-inflammatory diet may modulate systemic and metabolic inflammation, potentially reducing gout risk and its life-threatening comorbidities, particularly for women.

Sharan K. Rai, PhD
Hyon K. Choi, MD, DrPH
Natalie McCormick, PhD 🔗
nmccormick@mgh.harvard.edu
Massachusetts General Hospital,
 Harvard Medical School,
 Channing Division of Network Medicine,
 and The Mongan Institute, General Hospital,
Boston,
 and Arthritis Research Canada
 Vancouver, British Columbia, Canada
Chio Yokose, MD, MS 🔗
Massachusetts General Hospital
 and Harvard Medical School
Boston, MA

1. Rai SK, Choi HK, Lu N, et al. Proinflammatory dietary pattern and the risk of female gout: sex-specific findings from three prospective cohort studies. Arthritis Rheumatol 2025;77(8):1077–1086. https://doi.org/10.1002/art.43127

2. Batty GD, Gale CR, Kivimäki M, et al. Comparison of risk factor associations in UK Biobank against representative, general population based studies with conventional response rates: prospective cohort study and individual participant meta-analysis. BMJ 2020;368:m131.

3. Willett WC. Nutritional Epidemiology. 3rd ed. Oxford University Press; 2012. https://doi.org/10.1093/acprof:oso/9780199754038.001.0001

4. Tabung FK, Smith-Warner SA, Chavarro JE, et al. Development and validation of an empirical dietary inflammatory index. J Nutr 2016; 146(8):1560–1570.

5. Bernstein AM, Rosner BA, Willett WC. Cereal fiber and coronary heart disease: a comparison of modeling approaches for repeated dietary measurements, intermediate outcomes, and long follow-up. Eur J Epidemiol 2011;26(11):877–886.

DOI 10.1002/art.43187

Enhancing predictive biomarkers in limited cutaneous systemic sclerosis: the role of type I interferon score and sex considerations: comment on the article by Di Donato et al

To the Editor:

I sincerely thank Di Donato et al for their valuable insights and detailed analysis.[1] Their study effectively highlights the important role of the serum type I interferon (IFN) score as a predictive biomarker for disease progression in limited cutaneous systemic sclerosis (lcSSc), which has significant clinical relevance. This is an innovative approach that could improve personalized treatment for patients with lcSSc. However, although the conclusions of this study are valuable, I would like to offer a few suggestions to deepen the understanding of these associations.

The first concern is that the study cohort consists primarily of female patients (96%), which is much higher than the sex distribution of systemic sclerosis (SSc) in the real world (about 80% female).[2] This raises concerns about the generalizability of the results. Although male patients with SSc are less common, they generally have worse prognoses.[2] The study did not include enough male participants, which may obscure the specific predictive value of the IFN score in sex subgroups. Future studies should consider a more balanced sex representation or expand the male cohort to verify the predictive value of the IFN score across the sexes.

Another limitation is the reliance on the baseline IFN score to predict disease progression without considering changes in the IFN score over time. Using a single time point measurement does not capture the dynamic nature of lcSSc disease progression. Longitudinal measurements of the IFN score could provide a more accurate understanding of how fluctuations in type I IFN activity are related to disease flares or improvements. This would offer a more comprehensive understanding of the role of IFN signaling throughout the disease course, especially when patients receive treatments that may affect these scores.

Although the study reports excellent performance metrics (area under the curve and C-index) for its predictive model, the generalizability of the findings is limited by the lack of external validation. It remains unclear how the model would apply to other lcSSc cohorts or perform in real-world settings. There are significant ethnic differences in the clinical phenotype and antibody profile of SSc,[3] with Asian patients having higher rates of anti-Scl70 antibody positivity and African American patients at greater risk for interstitial lung disease.[3] I suggest that future research include independent validation cohorts from different clinical environments or regions to ensure the predictive value of the IFN score.

In conclusion, I hope that the authors will take these issues into account to further improve the robustness of their study, and we look forward to more insightful studies of IFN scores in the future.

Sheng Li, MD 🔗
449040479@qq.com
Ningbo No.2 Hospital
Ningbo, Zhejiang, China

1. Di Donato S, Ross R, Karanth R, et al. Serum type I interferon score for prediction of clinically meaningful disease progression in limited cutaneous systemic sclerosis. Arthritis Rheumatol 2025;77(7):929–941. https://doi.org/10.1002/art.43120

2. Hughes M, Pauling JD, Armstrong-James L, et al. Gender-related differences in systemic sclerosis. Autoimmun Rev 2020;19(4):102494.

3. Jaeger VK, Tikly M, Xu D, et al; and EUSTAR co-authors. Racial differences in systemic sclerosis disease presentation: a European Scleroderma Trials and Research group study. Rheumatology (Oxford) 2020;59(7):1684–1694.

Reply

To the Editor:

We appreciate the interest of Dr Li in our study on the role of the type I interferon (IFN) score in predicting disease progression in limited cutaneous systemic sclerosis (lcSSc).[1] Their comments provide valuable feedback, and we take this opportunity to expand on the highlighted aspects of our work.

The first point raised is on the sex distribution in our cohort being reportedly higher than the one observed in systemic sclerosis. We recruited consecutive patients with lcSSc. The higher proportion of female patients is consistent with the well-documented sex distribution in lcSSc. Multiple studies, including the largest analysis of patients with lcSSc from the European Scleroderma Trials and Research (EUSTAR) database,[2] have reported a higher proportion of female patients within this subset, with women accounting for approximately 90% of cases, a significantly greater prevalence compared to diffuse cutaneous systemic sclerosis (dcSSc). Notably, male patients tend to present with more severe disease phenotypes, including a faster progression of skin involvement, with up to 60% developing dcSSc within the first year of symptom onset.[3] Therefore, our cohort reflects real-world data, and its generalizability should be considered in this context.

As to the second point raised, it is important to clarify that our study does not rely on a baseline IFN score measured at disease onset. Rather, we studied a prevalent cohort with a median disease duration of 8 (interquartile range 10) years. This would rather underscore the notion that the predictive value of the IFN score for future outcomes remains valid at any time point. Nonetheless, we fully acknowledge the importance of evaluating longitudinal changes in the IFN score in relation to both disease events and treatment. This aspect is currently under investigation, and our ongoing analysis will provide insights into the temporal dynamics of the IFN score and the proportion and clinical features of patients who have a significant change in their IFN status over time. These data, once available, will contribute to a deeper understanding of the role of type I IFN activation in disease progression and response to therapy.

The third point raised relates to an external validation of our data. We agree independent validation will be crucial to assess its generalizability, and we encourage further efforts in this direction, including testing across different ethnic backgrounds. Specifically, in our current data set, the majority of are of White European background (93.3%), with only a small representation of East Asian and Middle Eastern participants. Given this imbalance, our sample size is not sufficient to draw meaningful comparisons across ethnic groups. Nonetheless, exploring potential racial differences remains an important avenue for future research in larger and more diverse populations.

Stefano Di Donato, MD
Christopher P. Denton, MD, PhD
Leeds Institute of Rheumatic and Musculoskeletal Medicine
    University of Leeds
    and NIHR Leeds Biomedical Research
    Centre, Leeds Teaching Hospitals NHS Trust
Leeds, United Kingdom
Francesco Del Galdo, MD, PhD
F.delgaldo@leeds.ac.uk
Centre for Rheumatology, Division of Medicine
University College London
London, United Kingdom

1. Di Donato S, Ross R, Karanth R, et al. Serum type I interferon score for prediction of clinically meaningful disease progression in limited cutaneous systemic sclerosis. Arthritis Rheumatol 2025;77(7):929–941. https://doi.org/10.1002/art.43120

2. Frantz C, Huscher D, Avouac J, et al; EUSTAR co-authors. Outcomes of limited cutaneous systemic sclerosis patients: results on more than 12,000 patients from the EUSTAR database. Autoimmun Rev 2020; 19(2):102452.

3. Carreira PE, Carmona L, Joven BE, et al; the EUSTAR co-authors. Gender differences in early systemic sclerosis patients: a report from the EULAR scleroderma trials and research group (EUSTAR) database. Clin Exp Rheumatol 2018;36(4 suppl 113):68–75.